

12-1-2018

Shorter and Improved Access to the Key Tetracyclic Core of Sarpagine-Macroline-Ajmaline Indole Alkaloids: the Total Synthesis of Alkaloids Macrocarpines A-g, Talcarpine, N(4)-methyl-n(4),21-secotalpinine, Deoxyperaksine, Dihydroperaksine, Talpinine, O-acetylalpinine, and N(4)-methylalpinine

Md Toufiqur Rahman
University of Wisconsin-Milwaukee

Follow this and additional works at: <https://dc.uwm.edu/etd>

 Part of the [Organic Chemistry Commons](#)

Recommended Citation

Rahman, Md Toufiqur, "Shorter and Improved Access to the Key Tetracyclic Core of Sarpagine-Macroline-Ajmaline Indole Alkaloids: the Total Synthesis of Alkaloids Macrocarpines A-g, Talcarpine, N(4)-methyl-n(4),21-secotalpinine, Deoxyperaksine, Dihydroperaksine, Talpinine, O-acetylalpinine, and N(4)-methylalpinine" (2018). *Theses and Dissertations*. 2007.
<https://dc.uwm.edu/etd/2007>

This Dissertation is brought to you for free and open access by UWM Digital Commons. It has been accepted for inclusion in Theses and Dissertations by an authorized administrator of UWM Digital Commons. For more information, please contact open-access@uwm.edu.

Part I

SHORTER AND IMPROVED ACCESS TO THE KEY TETRACYCLIC CORE OF C-19 METHYL SUBSTITUTED BIOACTIVE SARPAGINE-MACROLINE-AJMALINE INDOLE ALKALOIDS VIA A NEW AMBIDEXTROUS ASYMMETRIC PICTET-SPENGLER REACTION BEGINNING FROM EITHER D-(+)- OR L-(-)-TRYPTOPHAN

Part II

THE TOTAL SYNTHESIS OF A NUMBER OF BIOACTIVE C-19 METHYL SUBSTITUTED MACROLINE-SARPAGINE INDOLE ALKALOIDS INCLUDING MACROCARPINES A-G, TALCARPINE, *N*(4)-METHYL-*N*(4),21-SECOTALPININE, DEOXYPERAKSINE, DIHYDROPERAKSINE, TALPININE, *O*-ACETYLTALPININE, AS WELL AS *N*(4)-METHYLTALPININE

by

Md Toufiqur Rahman

A Dissertation Submitted in

Partial Fulfillment of the

Requirements for the Degree of

Doctor of Philosophy

in Chemistry

at

The University of Wisconsin-Milwaukee

December 2018

ABSTRACT

Part I

SHORTER AND IMPROVED ACCESS TO THE KEY TETRACYCLIC CORE OF C-19 METHYL SUBSTITUTED BIOACTIVE SARPAGINE-MACROLINE-AJMALINE INDOLE ALKALOIDS VIA A NEW AMBIDEXTROUS ASYMMETRIC PICTET-SPENGLER REACTION BEGINNING FROM EITHER D-(+)- OR L-(-)-TRYPTOPHAN

Part II

THE TOTAL SYNTHESIS OF A NUMBER OF BIOACTIVE C-19 METHYL SUBSTITUTED MACROLINE-SARPAGINE INDOLE ALKALOIDS INCLUDING MACROCARPINES A-G, TALCARPINE, *N*(4)-METHYL-*N*(4),21-SECOTALPININE, DEOXYPERAKSINE, DIHYDROPERAKSINE, TALPININE, *O*-ACETYLTALPININE, AS WELL AS *N*(4)-METHYLTALPININE

by

Md Toufiqur Rahman

The University of Wisconsin-Milwaukee, 2018
Under the Supervision of Professor James M. Cook

Abstract-Part I

Chapter 1. A Shorter and Improved Access to the Bicyclo[3.3.1]nonane core of Sarpagine/Macroline/Ajmaline Alkaloids

Extension of the asymmetric Pictet-Spengler (P-S) reaction to bulkier *N*_b-alkylated tryptophan derivatives resulted in a shorter and improved stereospecific access to the key bicyclo[3.3.1]nonane framework of bioactive C-19 methyl substituted sarpagine/macroline/ajmaline indole alkaloids with excellent diastereoselectivity *via* internal asymmetric induction. The asymmetric Pictet-Spengler/Dieckmann protocol with bulky *N*_b-alkyl substituted

systems enabled a more direct and two-step shorter route to this key architecture. Complete stereocontrol of the C-19 methyl function in either the α - or β -configuration was achieved which would enable one to gain rapid access to the crucial intermediates for the total synthesis of any member of this group of seventy alkaloids.

Chapter 2. Unprecedented Stereocontrol in the Synthesis of 1,2,3-Trisubstituted Tetrahydro- β -carbolines: The Ambidextrous Pictet-Spengler Reaction

The asymmetric Pictet-Spengler (P-S) reaction of chiral N_b -ethynyl substituted tryptophan methyl ester derivatives (from both D- and L-tryptophan) with a simple aliphatic aldehyde, exhibited unprecedented stereoselectivity toward either of the diastereomeric products. A simple variation of conditions altered the outcome of the cyclization from either 100% *trans*-selective to 100% *cis*-selective originating entirely from internal asymmetric induction under mild conditions. This resulted in the highly efficient access to both 1,3-*cis*-(1,2,3-trisubstituted tetrahydro- β -carbolines, TH β Cs) and 1,3-*trans*-(1,2,3-trisubstituted TH β Cs). By exploiting this very useful ambidextrous-diastereoselectivity, one can set the crucial C-3 and C-5 stereocenters of the C-19 methyl substituted sarpagine-macroline-ajmaline alkaloids beginning either with the DNA-encoded and cheaper L-(-)-tryptophan, as well as optionally from commercially available D-(+)-tryptophan.

Chapter 3. Access to the (+)- or (-)-Enantiomers of the Bioactive C-19 Methyl Substituted Sarpagine/Macroline/Ajmaline Alkaloids from Either D- or L-Tryptophan via the Ambidextrous Pictet-Spengler Reaction

The unnatural enantiomers of bioactive natural alkaloids are potential drug candidates. The unnatural enantiomer of alkaloids may have similar drug-like properties or even better than the natural counterpart depending on the rate of metabolism. The ambidextrous Pictet-Spengler reaction has enabled one to access the key intermediates with the bicyclo[3.3.1] framework starting

from either the natural L-tryptophan or the commercially available D-tryptophan. Logically, the ambidextrous nature of this P-S process would allow one ready access to the unnatural enantiomers of the alkaloids from this subgroup. As the proof of concept, which is important to illustrate the full potential of the ambidextrous P-S reaction, both D-tryptophan and L-tryptophan were employed to synthesize the key intermediates toward the natural enantiomers of alkaloids. Now the enantiomeric series of the same key intermediates could also be synthesized from both D- and L-tryptophan in high yield and optical purity via this P-S/Dieckmann protocol. One can make either the natural or the unnatural alkaloids from either starting amino acid ester, stereo and enantiospecifically at will.

Abstract-Part II

Chapter 4. The Total Synthesis of Macroparpines D and E via an Efficient Copper-Mediated Cross-Coupling Process

After gaining access to the bicyclo[3.3.1] framework via the ambidextrous Pictet-Spengler reaction, the focus turned to the completion of the total synthesis of a number of C-19 methyl substituted sarpagine/macroline/ajmaline indole alkaloids. As a step towards that, alkaloids with N_a -H, N_b -CH₃ substitution patterns were both of interest via the same route. An enolate driven copper-mediated cross-coupling process enabled a cheaper and greener access to the key pentacyclic intermediates required for the enantiospecific total synthesis of a number of C-19 methyl substituted sarpagine/macroline indole alkaloids. Replacement of palladium (**60-68%** yields) with copper iodide (**82-89%** yields) resulted in a much cleaner process in high yield. The formation of an unusual seven-membered cross-coupling product was completely inhibited by using TEMPO as a radical scavenger. Further functionalization led to the first enantiospecific total synthesis of macroparpines D and E.

Chapter 5. The Total Synthesis of Talcarpine, *N*₄-Methyl-*N*_{4,21}-secotalpinine, Dihydroperaksine, Deoxyperaksine, and Macrocarpines A-C

After the successful completion of the total synthesis of several C(19)-methyl *N*_a-H, *N*_b-CH₃ substituted alkaloids, focus turned toward the total synthesis of a number of alkaloids bearing the *N*_a-CH₃, *N*_b-CH₃ substitution pattern. In addition, a pair of sarpagine alkaloids, termed dihydroperaksine and deoxyperaksine bore the C-19 (*S*)-methyl substitution; this was opposite to the chirality in many of the alkaloids of this group. Access to these alkaloids in high yields illustrated the versatility of the strategy developed here to access alkaloids with either C-19 (*S*)- or (*R*)-methyl substituents. This effort resulted in the successful total synthesis of several bioactive alkaloids, as well as correction of the literature values for macrocarpine A and *N*₄-methyl-*N*_{4,21}-secotalpinine.

Chapter 6. The Total Synthesis of Macrocarpines F and G, Talpinine, *O*-Acetyltalpinine, as well as *N*₄-Methyltalpinine

A late stage *N*_b-demethylation of macrocarpines A and C afforded the *N*_b-H bearing alkaloids macrocarpines F and G, respectively. A similar transformation enabled access to the bioactive alkaloid talpinine from both talcarpine and *N*₄-methyl-*N*_{4,21}-secotalpinine. The other bioactive alkaloid *O*-acetyltalpinine was also prepared from synthetic talpinine in high yield. Finally, the unusual quaternary *N*_b-nitrogen function containing alkaloid *N*₄-methyltalpinine that exhibited potent NFκB inhibitory activity was completed via facile transformations in excellent yield.

To
my parents,
my brothers and sisters,
my wife,
and especially my son Reon

4.2.1. Partial Synthesis of Peraksine 77 by Sakai et al.....	43
4.2.2. Partial Synthesis of Talcarpine 21 from Ajmaline 113 by Sakai	44
4.2.3. Partial Synthesis of Talcarpine 21 and Related Alkaloids from Talpinine 37 by Schmid et al.....	45
4.2.4. Biomimetic Transformations Between Alkaloids by LeQuesne.....	48
4.3. Total and Formal Synthesis	50
4.3.1. Total Synthesis of Talpinine 37 and Talcarpine 21 by Yu et al.....	50
4.3.2. Total Synthesis of the Alkaloids Isolated from Rauvolfia serpentina Hairy Root Culture by Edwankar et al.....	53
4.3.3. Total Synthesis of Peraksine 41 and Attempted Total Synthesis of Macrosalpine 53 by Edwankar et al.....	54
4.3.4. Formal Synthesis of Talcarpine 21 by Edwankar et al.....	58
5. Conclusion.....	59
6. References.....	59

Part I. Improved and Shorter Access to the Key Tetracyclic Core of C-19 Methyl Substituted Bioactive Sarpagine-Macroline-Ajmaline Indole Alkaloids via a New Asymmetric Pictet-Spengler Reaction Starting from Either D-(+)- or L-(-)-Tryptophan

Chapter 1. A Shorter and Improved Access to the Bicyclo[3.3.1]nonane Core of Sarpagine/-Macroline/Ajmaline Alkaloids

1. Introduction.....	73
2. Results and Discussion.....	76
3. Conclusion.....	87

4. Experimental Section.....	88
5. References.....	103

Chapter 2. Unprecedented Stereocontrol in the Synthesis of 1,2,3-Trisubstituted Tetrahydro- β -carbolines: The Ambidextrous Pictet-Spengler Reaction

1. Introduction.....	107
2. Results and Discussion.....	113
3. Conclusion.....	126
4. Experimental Section.....	127
5. References.....	150

Chapter 3. Access to the (+)- or (-)-Enantiomers of the Bioactive C-19 Methyl Substituted Sarpagine/Macroline/Ajmaline Alkaloids from Either D- or L-Tryptophan via the Ambidextrous Pictet-Spengler Reaction

1. Introduction.....	156
2. Results and Discussion.....	159
3. Conclusion.....	164
4. Experimental Section.....	165
5. References.....	177

Part II. The Total Synthesis of a Number of Bioactive C-19 Methyl Substituted Macroline-Sarpagine Indole Alkaloids Including Macrocarpines A-G, Talcarpine, *N*(4)-Methyl-*N*(4),21-Secotalpinine, Deoxyperaksine, Dihydroperaksine, Talpinine, *O*-Acetyltalpinine, as well as *N*(4)-Methyltalpinine

Chapter 4. The Total Synthesis of Macrocarpines D and E via an Efficient Copper-Mediated Cross-Coupling Process

1. Introduction.....	183
2. Results and Discussion.....	186
3. Conclusion.....	196
4. Experimental Section.....	197
4.1. Biogenetic Numbering for Macrocarpine D and Macrocarpine E.....	220
4.2. Comparison Tables 2 and 3 for Natural and Synthetic Macrocarpine D.....	221
4.3. Comparison Tables 4 and 4 for Natural and Synthetic Macrocarpine E.....	223
5. Spectra and X-ray Data.....	225
6. References.....	225

Chapter 5. The Total Synthesis of Talcarpine, *N*₄-Methyl-*N*_{4,21}-Secotalpinine, Dihydroperaksine, Deoxyperaksine, and Macrocarpines A-C

1. Introduction.....	228
2. Results and Discussion.....	231
3. Conclusion.....	237
4. Experimental Section.....	238
5. Spectra and X-ray Data.....	272

6. References.....	272
Chapter 6. The Total Synthesis of Macroparpines F and G, Talpinine, <i>O</i>-Acetyltalpinine, as well as <i>N</i>₄-Methyltalpinine	
1. Introduction.....	275
2. Results and Discussion.....	275
2.1. Synthesis of Macroparpine F (1) and Macroparpine G (2).....	277
2.1.1 Macroparpine F (1).....	280
2.1.2. Macroparpine G (2).....	283
2.3. Talpinine (8).....	285
2.4. Synthesis of <i>O</i> -Acetyltalpinine (14).....	288
2.5. Synthesis of <i>N</i> ₄ -Methyltalpinine (15).....	293
3. Conclusion.....	304
4. Experimental Section.....	304
5. Spectra Section.....	307
6. References.....	307
General Conclusion and Future Direction.....	309
Appendices	
III. Appendix A (Chapter 1).....	313

IV. Appendix B (chapter 4).....	350
V. Appendix C (Chapter 4: NMR and Mass Spectra of the Synthetic Macrocarpined D (4) and E (5)).....	374
VI. Appendix D (Chapter 5: X-ray Data for compound 16b).....	385
VII. Appendix E (Chapter 5: NMR Spectra of Alkaloids 1-3, 8, and 9).....	394
VIII. Appendix F (Chapter 6: NMR spectra of Alkaloids 1,2,8,14, and 15).....	439
IX. Appendix G (Chapter 3: Comparisons between the NMR spectra of the enantiomeric pairs (15 vs 24), (16 vs 25), (17 vs 26), (18 vs 27), (19 vs 29), (20 vs 28), (21 vs 30), (22 vs 31), and (23 vs 32)).....	462
X. Curriculum Vitae	481

LIST OF FIGURES

General Introduction

Figure 1. Sarpagine/macroline/ajmaline framework (1-11).....	6
Figure 2. Plausible biosynthetic pathway for rauvovertine C 60 proposed by Gao et al..	35
Figure 3. Possible origin of the rauvoloids A-E 68-72 from a common intermediate perakine 77 proposed by Liu	36

Figure 4. Plausible biosynthesis of rauvomines A (61) and B (62) proposed by Zeng et al.....	37
Figure 5. Equilibrium between <i>E</i> -vomilenine and <i>Z</i> -vomilenine via their ring-opened (<i>Chano</i>) forms.....	40
Figure 6. Plausible pathways for the formation of “artifact alkaloids” proposed by Lounasmaa	41
Figure 7. Putative biosynthetic formation of the alkaloids 47 , 48 , and 49 from raucaffrinoline 76 in <i>R. serpentina</i> hairy root culture by Stöckigt et al.....	43

Part I.

Chapter 1.

Figure 1. Representative examples of chiral C-19 methyl substituted macroline/sarpagine alkaloids.....	74
Figure 2. ORTEP representation of 13a •HCl.....	81
Figure 3. ORTEP representation of 13b •HCl	81
Figure 4. ORTEP representation of 25	84
Figure 5. ORTEP representation of 12b	86

Chapter 2.

Figure 1. Representative examples of C-19 methyl substituted sarpagine/ ajmaline indole alkaloids 8-13	111
Figure 1A. Representative examples of C-19 methyl substituted macroline, sarpagine, and ajmaline-type indole alkaloids.....	112
Figure 2. Comparison between the (a) ^1H and (b) ^{13}C NMR spectra of (+)- 28 from L-tryptophan (red) and D-tryptophan (blue) as shown in Scheme 7.....	122
Figure 3a: Comparison between ^1H of (-)- 30 prepared from L-tryptophan (red) and D-tryptophan (blue).....	124
Figure 3b: Comparison between ^{13}C of (-)- 30 prepared from L-tryptophan (red) and D-tryptophan (blue).....	125

Chapter 3.

Figure 1. Representative examples of bioactive C-19 methyl substituted sarpagine/ macroline-/ajmaline alkaloids.....	159
Figure 2. Access to both the natural and unnatural series of intermediates from D- and L- tryptophan.....	161

Part II.

Chapter 4.

Figure 1. Examples of some C-19 methyl substituted sarpagine/macroline indole alkaloids	184
Figure 2. ORTEP representation of 22	187

Figure 3. Figure 3. ORTEP representation of 23	188
Figure 4. ORTEP representation of 23'	189
Figure 5. ORTEP representation of 19	193
Chapter 5.	
Figure 1. Representative examples of chiral C-19 methyl substituted macroline/ sarpagine alkaloids.....	229
Figure 2. ORTEP representation of 16b	235
Chapter 6.	
Figure 1. LC-MS analysis of the ACE-Cl mediated <i>N</i> _b -demethylation of macrocarpine A (1).....	278
Figure 2. Selected NOE that confirms C-20 stereochemistry of macrocarpine G.....	285
Figure 3. <i>N</i> _b -demethylation of 10 using ACE-Cl.....	287
Figure 4. ¹ H NMR of the crude Rx and alkaloid 10 in CD ₃ OD.....	295
Figure 5. Comparison between the ¹ H NMR spectra of talcarpine 13 and <i>N</i> ₄ -methyl- <i>N</i> _{4,21} -secotalpinine in CD ₃ OD and CDCl ₃	297
Figure 6. Temperature dependence of the broadness of aldehyde peak of 10	298
Figure 7. Epimerization of talcarpine 13 into <i>N</i> ₄ -methyl- <i>N</i> _{4,21} -secotalpinine 10 under basic conditions.....	299
Figure 8. Epimerization of 13 in the presence of triethylamine forming 16 via 10	299
Figure 9. Progress of the reaction of dry HCl with indole base 10	301

LIST OF TABLES

General Introduction

Table 1. Macroline-related C-19 methyl substituted alkaloids.....13

Table 2. Sarpagine-related C-19 substituted alkaloids.....15

Table 3. Ajmaline-related C-19 methyl substituted alkaloids20

Table 4. Plant source(s) and plant morphology of the C-19 methyl substituted
sarpagine-/macroline/ajmaline alkaloids (**12-80**)22

Table 5. Biologically active alkaloids from the C-19 methyl substituted subgroup
and their activity32

Part I.

Chapter 1.

Table 1. Pictet-Spengler reaction of **13a** or **13b** with **21** or **27** under different
conditions79

Chapter 2.

Table 1. P-S reaction of amines **4a-i** with aldehyde **5**119

Chapter 3.

Table 1. Comparison between the natural and unnatural enantiomers of intermediates towards C-19 methyl substituted sarpagine/macroline/ajmaline alkaloids.....	164
--	-----

Part II.

Chapter 4.

Table 1: Optimization of reaction conditions for the Cu-mediated cross-coupling reaction of 22	192
Table 2. Comparison of the ^1H NMR Spectral Data for Natural and Synthetic Macrocarpine D (4) in CDCl_3	221
Table 3. Comparison of the ^{13}C NMR Spectral Data for Natural and Synthetic macrocarpine D (4) in CDCl_3	222
Table 4. Comparison of the ^1H NMR Spectral Data for Natural and Synthetic macrocarpine E (5) in CDCl_3	223
Table 5. Comparison of the ^{13}C NMR Spectral Data for Natural and Synthetic macrocarpine E (5) in CDCl_3	224
Chapter 5.	
Table 1. ^1H NMR Spectral Data for Natural and Synthetic (-)-Talcarpine (4) in CDCl_3	245

Table 2. Comparison of the ^{13}C NMR Spectral Data for Natural and Synthetic (-)-Talcarpine	
--	--

(4) in CDCl ₃	246
Table 3. ¹ H NMR Spectral Data for Natural and Synthetic (+)- <i>N</i> (4)-Methyl- <i>N</i> (4), 21- <i>secotalpinine</i> (5) in CDCl ₃	248
Table 4: Comparison of the ¹³ C NMR Spectral Data for Natural and Synthetic (+)- <i>N</i> (4)-Methyl- <i>N</i> (4), 21- <i>secotalpinine</i> (5) in CDCl ₃	249
Table 5. Comparison of the ¹ H NMR Spectral Data for Natural and Synthetic (-)- <i>Macrocarpine A</i> (1) in CDCl ₃	251
Table 6. Comparison of the ¹³ C NMR Spectral Data for Natural and Synthetic (-)- <i>Macrocarpine A</i> (1) in CDCl ₃	252
Table 7. Comparison of the ¹ H NMR Spectral Data for Natural and Synthetic (-)- <i>Macrocarpine B</i> (2) in CDCl ₃	255
Table 8. Comparison of the ¹ H NMR Spectral Data for Natural and Synthetic (-)- <i>Macrocarpine B</i> (2) in CDCl ₃	256
Table 9. Comparison of the ¹ H NMR Spectral Data for Natural and Synthetic <i>Macrocarpine C</i> (3) in CDCl ₃	259
Table 10. Comparison of the ¹³ C NMR Spectral Data for Natural and Synthetic <i>Macrocarpine C</i> (3) in CDCl ₃	260

Chapter 6.

Table 1. Comparison between the ¹H NMR of natural and synthetic

macrocarpine F (1).....	281
Table 2. Comparison between the ¹³ C NMR of natural and synthetic	
macrocarpine F (1).....	282
Table 3. Comparison between the ¹ H NMR of natural and synthetic	
macrocarpine G (2).....	284
Table 4. Comparison between the ¹ H NMR of natural and synthetic	
<i>O</i> -acetyltalpinine 14	290
Table 5. Comparison between the ¹³ C NMR of natural and synthetic	
<i>O</i> -acetyltalpinine 14	291
Table 6. Comparison between the ¹ H NMRs of the natural and the synthetic	
<i>N</i> ₄ -methyltalpinine (15) in CD ₃ OD.....	302
Table 7. Comparison between the ¹³ C NMR of the synthetic and natural	
<i>N</i> ₄ -methyltalpinine (15) in CD ₃ OD.....	303
 Appendices	
Appendix A: Tables A1-A26.....	315-349
Appendix B: Tables B1-B24.....	350-373
Appendix D: Tables D1-D7	386-393

ACKNOWLEDGEMENTS

First and foremost, I would like to express my sincere gratitude to my advisor Professor James M. Cook, for his outstanding supervision throughout the years. His extraordinary enthusiasm for natural products chemistry and organic chemistry in general has motivated me tremendously in pursuing my research in the total synthesis of natural products. I will always be grateful for his in-depth knowledge of the field, as well as his guidance during crucial turning points in my research career. I am also grateful for Dr. Cook's patience and encouragement during the tough times in my Ph. D. research. Thanks also to my advisor for his pro-chemistry stance throughout and allowing me to work in my own way, independently.

I would like to thank my doctoral committee, Professors Hossain, Indig, Pacheco, and Schwabacher, for their suggestions and fruitful discussions during the course of my graduate studies, not only during research but also during graduate courses. I express my special thank to Dr. Arnold for his support and helpful suggestions during the course of my doctoral research. I am also very grateful to Dr. Föersterling for his instruction and helpful discussions of the NMR studies on many occasions. I greatly appreciate Mr. Neal Korfhage for his expertise in scientific glassblowing, which allowed me to customize glassware to set up special reactions that may have otherwise be impossible. I sincerely thank Dr. Mark Wang for performing the LRMS and HRMS analysis. I greatly appreciate Dr. Anna Benko for her outstanding expertise and support during the last couple of years for help with mass spectroscopy. I would also like to thank Dr. Shama Mirza for her help in analysis of mass spectra. I acknowledge the expertise and support form Dr. Jeffrey R. Deschamps for his outstanding help in X-ray analysis, which has been essential for confirmation of the structure of many crucial compounds during my doctoral research.

I am thankful to the past and present members of the Cook group. It has really been a pleasure to be a part of this group. I thank Dr. Mohd. Shahjahan Kabir, Dr. Ojas Namjoshi, Dr. Wenyuan Yin, Dr. German Fonseca, Dr. Sundari Rallapalli, Dr. Ranjit Verma, Dr. Michael Rajesh, Dr. Kashi Reddy Methuku, Dr. Ashwini Verma, and Dr. Lalit Golani, for their wise guidance during my time in the Cook group. I sincerely thank Dr. V. V. N. Phani Babu Tiruveedhula for the training and orientation during my first year in Dr. Cook's group. Thanks to Kamal Pandey for proof-reading this manuscript.

I am grateful to my fellow lab members Michael Poe, Chris Witzigmann, Poonam Biawat, Phani Babu, Guanguan Li, Zubair Ahmed, Daniel Knutson, Farjana Rashid, Yeunus Mian, Taukir Ahmed, Kamal Pandey, and Prithu Mondal for creating such an amicable atmosphere in this group. I would like to acknowledge the financial and academic support of the Department of Chemistry at UW-Milwaukee, UW-Milwaukee Graduate School, and the National Institutes of Health (NIH). I gratefully acknowledge the Sosnovsky Award for Excellence in Graduate Research, which boosted my confidence and inspired me to work harder. I thank the Late Professor George Sosnovsky for sponsoring the Sosnovsky Award. I would like to thank Ms. Elise D. Nicks, Ms. Mary Eckert, Ms. Wendy Grober, Ms. Shelley Hagen, and Ms. Goldie Gibbs for being there for me whenever I needed help.

My late parents have always been my source of strength and motivation throughout my life and in the long eventful journey of doctoral studies. My siblings have always been there for me. Without their love and support, it would be impossible for me to go forward with my goals. I am especially grateful to my elder brother and guardian Mr. Md Bulbul Hossain for his unwavering determination throughout his life to support our family, especially my education. My lovely nieces

and nephews have always brought joy and happiness in my life. I am grateful to my entire family for their love and support.

I would also like to acknowledge personal and family friends Dr. Mohammad Rezaul Karim, Ms. Afsana Alam Mahim, Dr. Anik Iqbal, Ms. Farjana Rashid, Mr. Md Yeunus Mian, Ms. Dishary Sharmin, Mr. Reaz Ahmed Chowdhury, Ms. Samia Islam, and my lovely niece Anuva and nephew Zohan for their company and support during my time in the United States.

Lastly, Rajwana Jahan, my wife and co-worker both in the laboratory and at home has provided invaluable support and help during this time which helped me tremendously to achieve my goals. My son Reon has brought us immense joy and pleasure. A loving family is what one needs at the end of a stressful day and I cannot be luckier in this respect. My in-laws residing in the United States have also been a great support. I am especially grateful to my uncle-in-law Dr. Anwar A. Bhuiyan for his support and wise advice.

GENERAL INTRODUCTION

1. Introduction

1.1 The Sarpagine-Macroline-Ajmaline Family of Alkaloids

The sarpagine, macroline, and ajmaline group of alkaloids are a family of structurally and biosynthetically related alkaloids.¹⁻⁴ Collectively, they form a major class of indole alkaloids termed here sarpagine/macroline/ajmaline alkaloids. Over the years numerous alkaloids that belong to this group have been isolated from various medicinal plants of *Alstonia* and *Rauwolfia* genera (*Apocynaceae*) worldwide.⁵⁻¹⁰ Many of these alkaloids possess useful biological activity ranging from anti-hypertensive to anticancer activity and many of these activities correlate well with their traditional uses.^{8,11-14} As a result there has been a significant interest in the isolation, biosynthesis, total synthesis, as well as the determination of their biological activity over the years. This is evident from the increased number of novel alkaloids reported recently, as well as new useful bioactivities.^{5-8,15} Diversity arises due to variation in configurations, substitution patterns and the rearrangement of functional groups around the core-structure of these alkaloids. Often, it is observed that a number of alkaloids that belong to the greater sarpagine/macroline/ajmaline family can be categorized into smaller subgroups by considering common structural features of interest, as expected. Such sub-classification is often quite useful in discussion of their biosynthetic origin, structural analysis both in identification and in stereochemical assignments, as well as elucidation of a general synthetic strategy to access most of the alkaloids in that subclass. In addition, the synthetic and biological studies of the unnatural enantiomers of the bioactive alkaloids are widely unexplored. The unnatural enantiomers of natural products may in fact have important biological activity or even less toxicity and metabolic properties that are much longer-lived in vivo than their natural counterparts. Furthermore, natural products have always played a

major role in drug-discovery and have been a great source of new drugs.¹⁶ The optimization of the already bioactive natural products by the synthesis of analogs for better drug-related properties has resulted in many clinical candidates which have superior bioactivity, as compared to the parent natural products. The discovery of the anti-HIV drugs lamivudine and emtricitabine by Professor Liotta has saved millions of lives and helped to ameliorate the global HIV situation by subduing it from a death sentence to a manageable chronic disease.¹⁷ Both of these anti-HIV drugs were developed from unnatural L-nucleoside enantiomers.^{17,18} On the other hand, structure-activity studies on vinblastine analogs by Professor Boger have resulted in better and more-potent drug-candidates than the natural vinblastine.^{19,20} Understandably, the exploration of the bioactivity of unnatural enantiomers, as well as the optimization of native bioactive natural products can be possible only after robust and practical synthetic strategies are developed to avail the alkaloid of interest in reasonable quantities.

1.2 The C-19 Methyl Substituted Sarpagine Macroline-Ajmaline Alkaloids

The C-19 methyl substituted sarpagine/macroline/ajmaline group of alkaloids is an emerging group of alkaloids, which have been populated by an increasing number of members over the recent years.⁶⁻⁸ This subgroup was first discussed by Lounasmaa,^{6,21} which has since been referred to as the C-19 methyl substituted sarpagine/-macroline/ajmaline alkaloids, by many.²²⁻²⁷ However, a broader definition and collective discussion have not been reported until now. Of course, the bioactivity of some of these alkaloids has increased their importance, as well as interest in their total synthesis.²⁸⁻³¹ In fact, the common structural feature of the C-19 methyl function renders these alkaloids distinct from their original family and also makes them accessible via a common

synthetic strategy. As a matter of convenience, discussion of their isolation, bioactivity, and synthesis has now become important. This chapter is a compilation of the monomeric alkaloids which possess the C-19 methyl substituent (as a part of the core ring system) which belongs to either the sarpagine, macroline, or ajmaline alkaloid series reported recently. An up to date discussion of their isolation from various plant sources (and corresponding plant morphology), proposed biosynthetic studies, as well as reported biosynthesis are included. In addition, the partial or formal, as well as the total syntheses have also been included. The core-structures of each of these subclasses are illustrated in Figure 1.

1.3 The C-19 Methyl Substituted Sarpagine-Macroline-Ajmaline Frameworks

The general structures are numbered according to the biogenetic numbering system proposed by Le Men and Taylor and the same numbering system has been followed throughout this chapter.^{32,33} Sarpagine alkaloids possess the characteristic C(21)-N₄ bond, as well as the C-16 configuration as shown in **1-3** where, the C(17) group occupies the α -position at C(16) and the corresponding H-atom is β . In the sarpagine-type alkaloids, when there is no substitution on the carbon atom adjacent to the N₄ nitrogen atom (i.e., C-21 in **1**), the biogenetic numbering system according to Le Men and Taylor is shown in structure **1**.³² Even though the ethylidene function contains a methyl group at C-19 in **1**, it is not considered as a C-19 methyl substituted alkaloid since the methyl function is not a substituent on the core-ring system. Similarly, when there is a heteroatom (commonly, O) attached at the C(α) position of N₄, it does not alter the biogenetic numbering (see **2**). However, when there is a C-atom substituent (i.e., CH₃) on the carbon atom alpha to N₄, it alters the biogenetic numbering, as shown in structure **3**. As a result, these structures are considered to belong to this C-19 methyl substituted subclass of alkaloids. The absolute stereochemistry at C-

3(*S*), C-5(*S*), C-15(β -H), and C-16(β -H) is the same (as depicted in **2**) throughout the sarpagine group, while the stereochemistry of the C-19 methyl function can either be the β [i.e., (*S*)], or α [i.e., (*R*)] configuration (see Figure 1).

The general structure and biogenetic numbering of macroline alkaloids are depicted in Figure 1 (see **4-6**). Configurations at C(3), C(5), C(15), and C(16) are the same as the sarpagine alkaloids, except for the absence of the C(21)-N₄ bond in the case of the macroline series. Similarly, in the case of macroline (or macroline-derived) alkaloids, the type-A macroline (**4**) alkaloids (including the ring-open macroline alkaloids) are not considered as the C-19 methyl substituted variant since the methyl function is not directly connected to the core architecture. On the contrary, the type-B (see **5**) macroline bases contain the methyl function at the C-19 position of the ring system and, therefore, are regarded as belonging to this group. In addition to these simple types of sarpagine alkaloids, there are a number of macroline alkaloids which possess both the macroline-type core with a C-19 methyl substituent, as well as the C(21)-N₄ linkage found in those alkaloids represented by compound **6**. These alkaloids can be considered as the macroline-derived sarpagine-type (or simply, sarpagine-macroline) alkaloids. One well-known example of this type of alkaloid is talpinine **37** (*vide infra*).

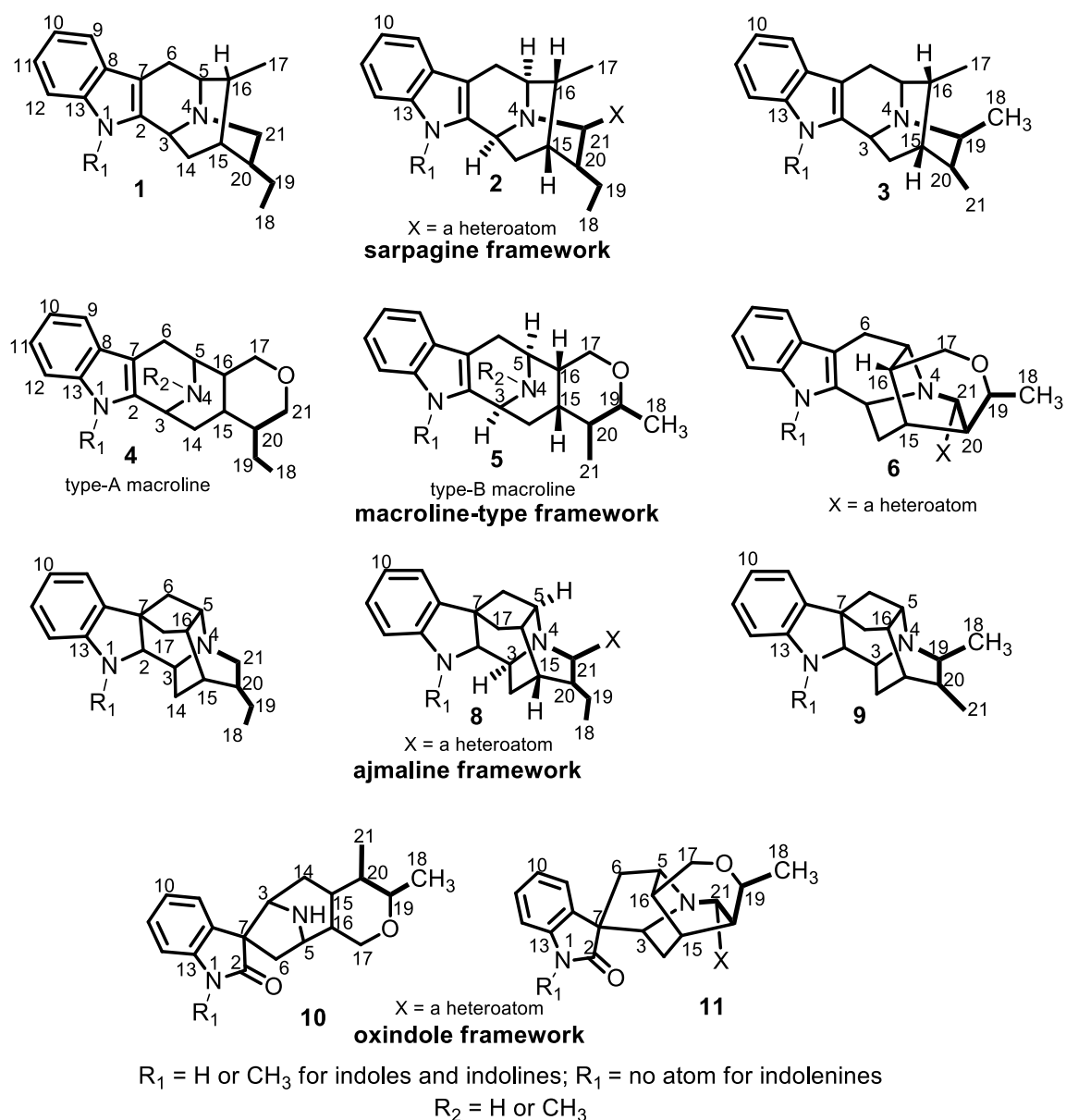


Figure 1. sarpagine/macroline/ajmaline framework (1-11)

The ajmaline group of alkaloids is the other major type of alkaloids that are closely related to the sarpagine alkaloids, both structurally and biosynthetically.^{34,35} In the same fashion as both the sarpagine and macroline alkaloids, the ajmaline series bear the same configurations at C(3), C(5), and C(15) whereas the C(16) configuration is antipodal to that of the sarpagine and macroline bases. In addition, in the ajmaline alkaloids, the C(17) carbon atom is necessarily connected to

C(7), see **7-9**. Alkaloids which contain the core-skeleton **7** and **8** are not considered as a C-19 methyl substituted variant, whereas skeleton **9** is considered in the C-19 class for the same reasons, as discussed above.

Additionally, a few oxindole alkaloids with the spirocyclic junction at C-7 (both *R* and *S*) possess the C-19 methyl substituted sarpagine skeleton (**3**) or the type-B macroline skeleton (**5**) or the macroline-derived sarpagine-type skeleton (**6**). They are included in this compilation (see **10** and **11**). These oxindole alkaloids also belong to either the *chitosenine* (*7R*) or the *alstonisine* (*7S*) series of bases.³⁶

2. Occurrence

The sarpagine/macroline/ajmaline family of indole alkaloids are diversely distributed among more than a hundred species of 25 major genera of the *Apocynaceae* family of plants.⁸ Alkaloids that belong to this C(19)-methyl substituted subgroups are listed in this section as “macroline-related” (Table 1), “sarpagine-related” (Table 2), and “ajmaline-related” (Table 3), sub-classifications. Illustrated in Table 4 are the plant sources, plant morphologies and references to the isolation of these series.

2.1 Macroline-Related C-19 Methyl Substituted Alkaloids

Among macroline-related alkaloids (see Table 1), macrocarpines A-H (**12-19**)³⁷⁻³⁹ are primary alcohols which contain a hydroxyl group (*O*-acetyl, in the case of macrocarpine C **14**³⁷) at C(21). All of these alkaloids **12-19** contain the type-B (see structure **5** in Figure 1) macroline framework

with a C-19 β -methyl function, while C-20 can be either α or β . In addition, both of the N_1 and N_4 nitrogen functions can possess either a hydrogen atom or a methyl function. Macrocarpines A (**12**), B(**13**), and C(**14**) were first reported by Kam.³⁷ Later, N_1 -demethyl, N_4 -demethyl, and ring-A oxygenated (10-methoxy) variants (macrocarpines D-H, **15-19**) have also been isolated from various *Alstonia* species.^{38,39} Among these, the optical rotation of **12** has been revised recently (*vide infra*, via stereospecific synthesis).²³ Alstohentine **20**, a C-20 hydroxy macroline alkaloid is also known to occur in *Alstonia macrophylla*.⁴⁰ Talcarpine **21** and N_4 -methyl- $N_4,21$ -secotalpinine **22** are C(20)-formyl variants of macrocarpine A and macrocarpine B, respectively. Talcarpine **21** has been known since 1972⁴¹, while **22** has been isolated as a natural product only recently³⁷ but appeared in reports on partial synthesis in several instances.^{3,41,42} The optical rotation of **22** has also been revised recently (*vide infra*, see the total synthesis of this alkaloid).²³ Both alkaloids **21** and **22** occur in *A. macrophylla* as well as in *A. angustifolia*, while **21** also occurs in *P. talbotii* (see Table 4 for a detailed list). Recently, the C(19)-antipode of talcarpine, 19-epitalcarpine **23** has been isolated from *A. angustifolia*.³⁹

A number of alkaloids from this group contain a C(19)-C(20) site of unsaturation, which forms an enal function (e.g., see alstonerinal, **24**). Alstonerinal **24** is the C(19)-C(20) dehydro variant of talcarpine **21** and has been isolated from *A. macrophylla* and *A. angustifolia*.^{50,43} The 10-methoxy version, 19-20-dehydro-10-methoxytalcarpine **25**^{44,45} occurs in *A. angustifolia* and *T. dichotoma*, while the 11-methoxy variant alstophyllal **29** has been isolated from *A. macrophylla*.^{38,40} In addition, N_4 -demethyl and N_1 -demethyl versions of these types of alkaloids have also been isolated from plant sources. The N_4 -demethylalstonerinal **26**,⁴⁶ N_1 -demethylalstonerinal **27**,³⁹ and N_1 -demethylalstophyllal **30**³⁷ were also found in *Alstonia* species. The oxidized derivative, 6-

oxoalstophyllal **28**⁴⁰ contains a carbonyl group at C(6), while the *N*₄-oxide, alstoniaphylline C **31**,⁴³ is an indolenine-containing macroline alkaloid. Both occur in *A. macrophylla*.

In addition, as mentioned, there are a few alkaloids which contain an oxindole moiety with a spiro-C(7) center (**32-36** in Table 1). Both *N*₄-demethylalstophyllal oxindole **32**⁴⁷ and 16-hydroxy-*N*₄-demethylalstophyllal oxindole **35**⁴⁰ occur in *A. macrophylla*. These two rearranged alstophyllal bases are antipodal to each other at the *spiro*-center at C(7) with (*R*) and (*S*) configurations, respectively. Alstonal **33**,⁴⁷ *N*₁-demethylalstonal **34**⁴⁸ and the 16-hydroxyalstonal **36**⁴⁰ are oxindole alkaloids with the same (*S*) configuration at the C(7)-spiro center. All three of them occur in *A. macrophylla*, while oxindoles **33** and **34** also occur in *T. dichotoma*⁴⁵ and *A. angustifolia*,⁴⁶ respectively.

2.2 Sarpagine-Related C-19 Methyl Substituted Alkaloids

The majority of sarpagine-related alkaloids of this group bear a β -methyl function at C(19) while a few of them contain the opposite configuration (see Table 2). Talpinine **37** is a macroline-derived sarpagine alkaloid with a C(21)-*N*(4) bond. It was first isolated from *P. talbotii*⁴¹ and later from *A. angustifolia*.³⁹ Recently, *O*-acetyltalpinine **39** has also been isolated from *A. angustifolia*.³⁹ A quaternary *N*_b-nitrogen containing talpinine variant, *N*₄-methyltalpinine **38**, and its C(19)-antipode, *N*₄-methyl-19-epitalpinine **40**, have been isolated recently from *A. angustifolia*.^{28,39} Peraksine **41** was first isolated from *R. perakensis*.⁴⁹ Since that time, it has been isolated from more than ten other *Rauwolfia* species (see Table 4). Alstoyunines A (**42**) and B (**43**) are structurally related to base **41** and were isolated from *A. yunnanensis* in 2009.²⁹ Alstoyunine A **42** bears a cyclic acetal group at C(21) and a hemi-acetal substituent at C(17), whereas the related **43** contains a cyclic

hemi-acetal function at C(21) and an acetal group at C(17).²⁹ The N_1 -methyl variant of **42**, termed alstiyunnanenine A **45**, was also isolated from *A. yunnanensis* Diels, recently.⁵⁰ The ring-A oxygenated and N_1 -demethylated version of talpinine, 21-hydroxycyclolochnerine **44**, was isolated from the cell cultures of *Catharanthus roseus*.⁵¹ Verticillatine **46** is a quaternary N_b -nitrogen containing alkaloid with a hydroxyl function at C(10) and a cyclic hemi-acetal function at C(17); it was isolated from *R. verticillata*.^{52,53} The hairy root culture of *R. serpentina* investigated by Stöckigt et al. resulted in the isolation of three alkaloids related to dihydroperaksine (see **47-49**).⁵⁴ These alkaloids are structurally similar to dihydroperaksine **50**, but the configurations at C(19) and C(20) are opposite to **50** and thus they represent a novel subgroup of sarpagine alkaloids that have the 19(*S*),20(*R*) stereochemistry as a common structural feature. Consequently, they were named 19(*S*),20(*R*)-dihydroperaksine **47**, 19(*S*),20(*R*)-dihydroperaksine-17-al **48**, and 10-hydroxy-19(*S*),20(*R*)-dihydroperaksine **49**.⁵⁴ Dihydroperaksine **50** and deoxyperaksine **51** are two sarpagine-related alkaloids with the C-19 α methyl [i.e., (*R*)] function that belong to this group. Both were isolated from *R. perakensis*⁵⁵ while **50** and **51** also occur in *R. caffra*^{56,57} and *R. vomitoria*,⁵⁸ respectively. In several instances, 19(*S*),20(*R*)-dihydroperaksine **47** has been designated as dihydroperaksine in the literature.^{25,26,59,60} The names should not be used interchangeably since they are different alkaloids with opposite configurations at C(19) and C(20). The enantiospecific total synthesis of dihydroperaksine **50** has been reported recently with the 19(*R*),20(*S*) configuration and the optical rotations of the natural and synthetic dihydroperaksine are in excellent agreement (natural: $[\alpha]_D = +40.8^{55}$; synthetic: $[\alpha]_D = +40.0^{23}$), consequently, the structure of dihydroperaksine **50** is most probably correct, as drawn in Table 2. Moreover, the cyclic-ether linkage between C(17) and C(21) in deoxyperaksine **51** was synthesized from the same synthetic dihydroperaksine **50**. Consequently, this confirms the structure of deoxyperaksine

to be correct as drawn in **51** as well. *O*-Acetylpreperakine **52** was isolated from the stem bark of *R. volkensii*.⁶¹ Macrosalpine **53** is an *N*₄-methyl substituted quaternary sarpagine alkaloid, which has been isolated as the chloride and thiocyanate salts from *A. macrophylla*.⁶² It contains a cyclic hemi-acetal bond formed by linking the C(17) hydroxyl function with the C(21) aldehyde function of the sarpagine system. The 7(*S*)-talpinine oxindole **54** is the only macroline-derived sarpagine oxindole alkaloid of this group;³⁹ it was isolated from *A. angustifolia*.³⁹ Vinmajine F **55** was isolated from cultivated *V. major*.³⁰

Rauvovertines A-C (**56**, **58**, and **60**) and 17-*epi*-rauvovertines A **57** and B **59** were isolated from *R. verticillata*.⁵⁹ Rauvovertine A **56** and its 17-*epi* variant **57** were isolated as an inseparable mixture (**56:57** \approx 3:2) while rauvovertine B **58** and its 17-*epi* version **59** were also isolated as an inseparable mixture (**58:59** \approx 2:1). The orientations of the C(17) functional groups were assigned by NMR correlation studies, which also revealed that the C-17 α epimer occupied an equatorial orientation on the pyran ring which had adopted a chair conformation. This helped to rationalize the prevalence of the C-17 α epimers **56** and **58**.⁵⁹ On the other hand, rauvovertine C **60** was isolated as a single epimer which contained an C-17 α methoxy function as determined again by NMR correlation experiments. The base contains an unusual imine bridge connecting the C(17) carbon atom with C(20) and represents a new class of peraksine alkaloid.⁵⁹ Rauvomines A **61** and B **62** are two unusual monoterpene indole alkaloids and were isolated along with peraksine **41** and alstoyunine A **42** from the aerial parts of *R. vomitoria*.⁶³ Rauvomine A **61** is a C₁₈ sarpagine-type alkaloid with a β -chlorine atom at C(20). Rauvomine B **62**, on the other hand, represents a new type of sarpagine indole alkaloid with a substituted cyclopropane ring that results in a 6/5/6/6/3/5-fused hexacyclic sarpagine system (see Table 2). In addition, the C-16 configuration in rauvomine B is antipodal to other macroline and sarpagine alkaloids in this group. The structures and absolute

configurations of both of these alkaloids were determined by spectroscopic analysis, X-ray crystallography, as well as electronic circular dichroism.⁶³ Vinmajorines C-E (**63-65**) were isolated from *V. major*.⁶⁴ All three of these bases contain a methoxy group at C-10 of ring A.

Table 1. Macropine-related C-19 methyl substituted alkaloids

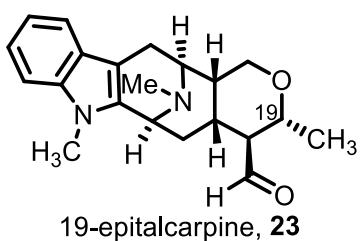
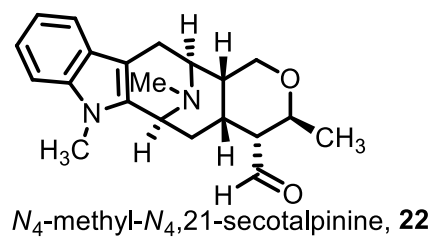
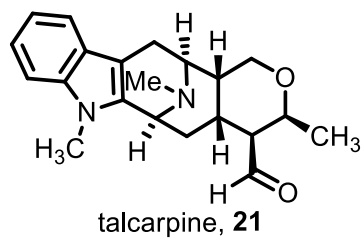
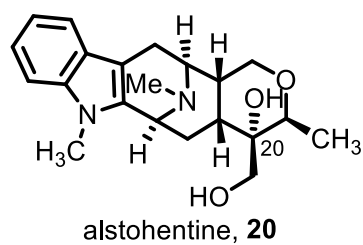
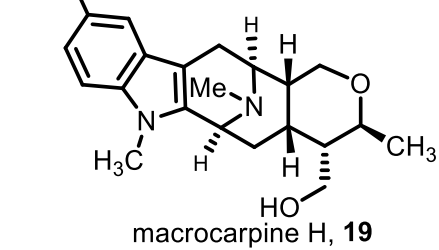
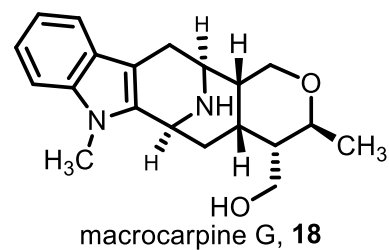
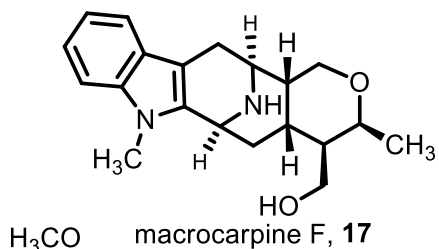
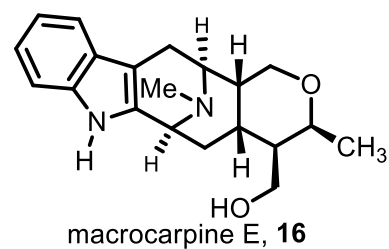
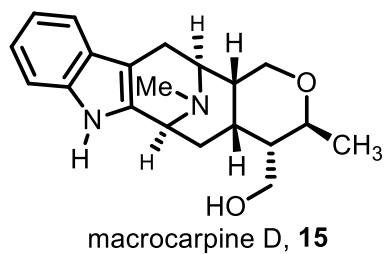
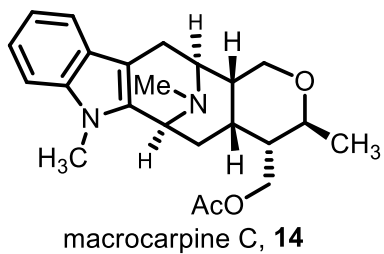
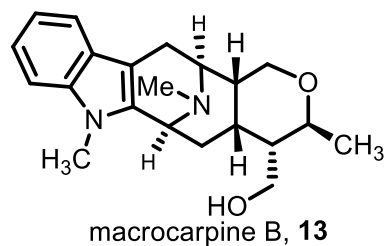
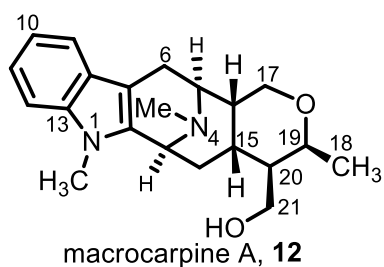


Table 1. Macroline-related C-19 methyl substituted alkaloids: (Continued: 2)

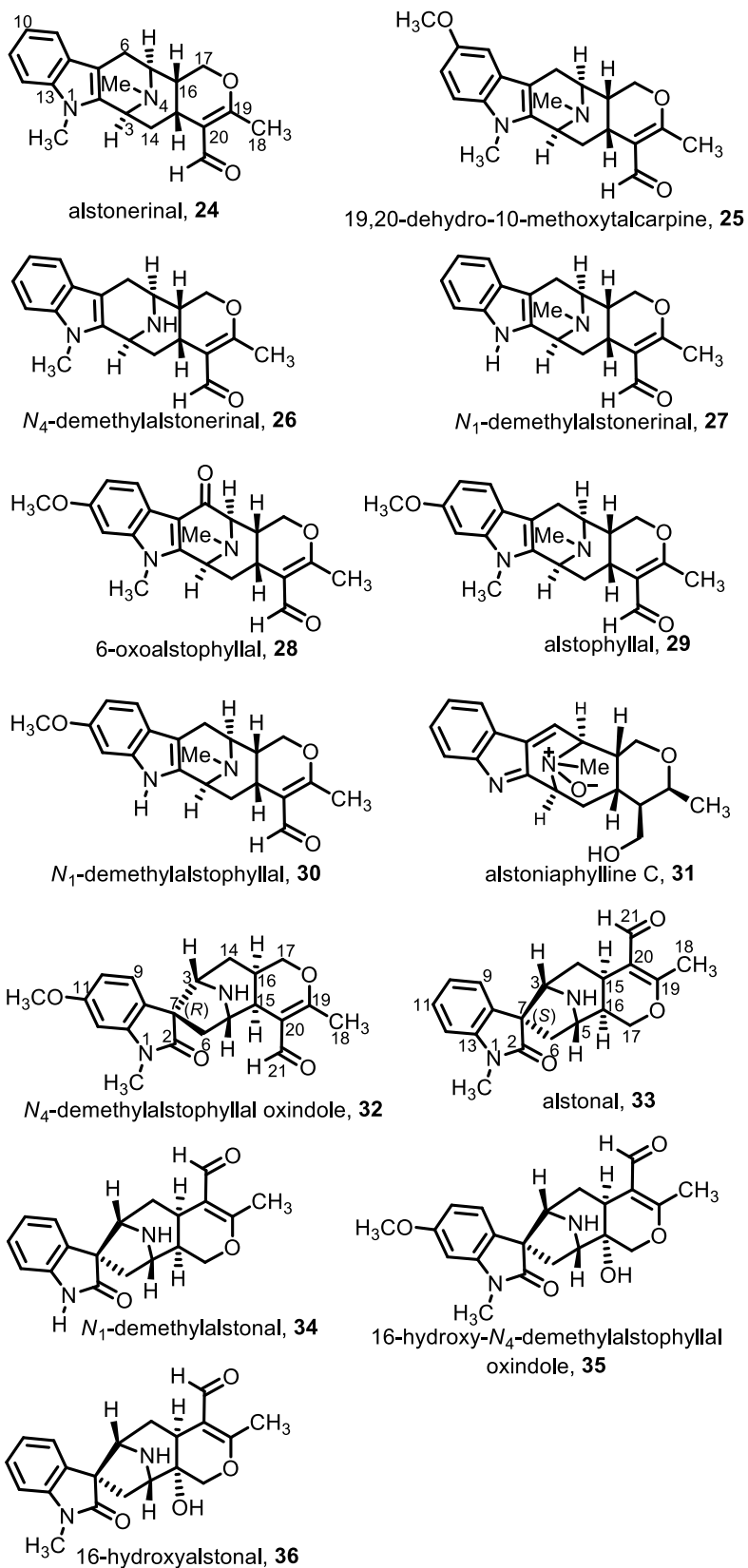
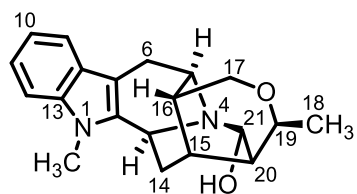
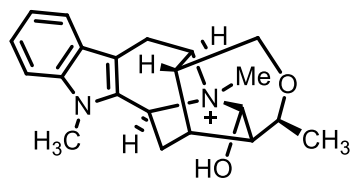


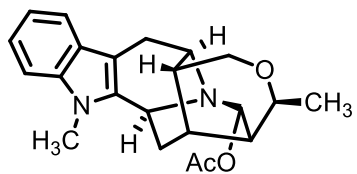
Table 2. Sarpagine-related C-19 substituted alkaloids



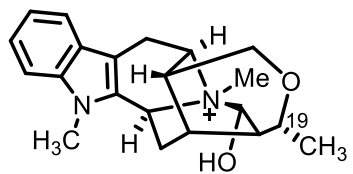
talpinine, **37**



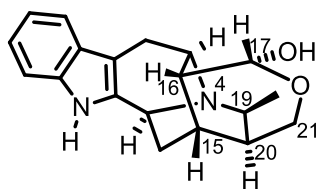
*N*₄-methyltalpinine, **38**



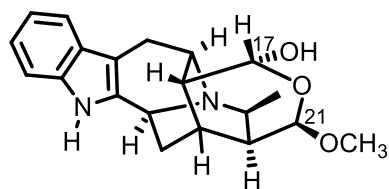
O-acetyltalpinine, **39**



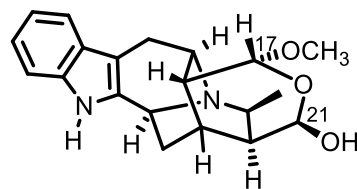
*N*₄-methyl-19-epitalpinine, **40**



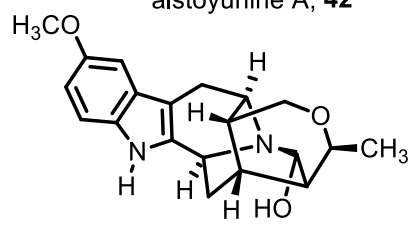
peraksine, **41**



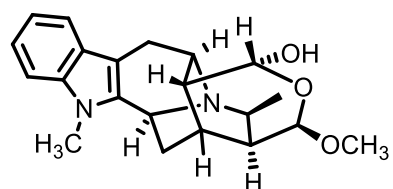
alstoyunine A, **42**



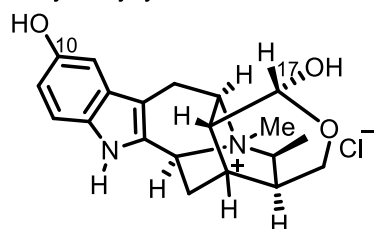
alstoyunine B, **43**



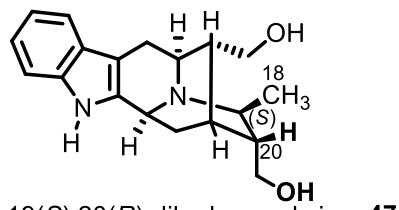
21-hydroxycyclolochnerine, **44**



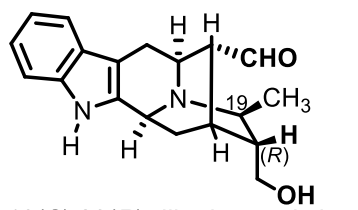
alstiyunnanenine A, **45**



verticillatine, **46**

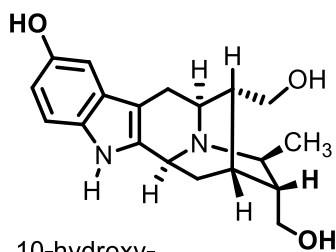


19(*S*),20(*R*)-dihydroperaksine, **47**

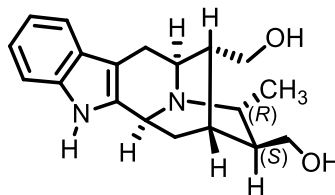


19(*S*),20(*R*)-dihydroperaksine-17-al, **48**

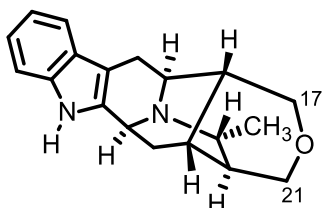
Table 2. Sarpagine-related C-19 methyl substituted alkaloids (continued: 2)



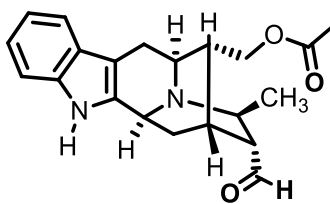
10-hydroxy-
19(*S*),20(*R*)-dihydroperaksine, **49**



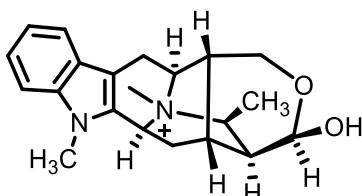
dihydroperaksine, **50**



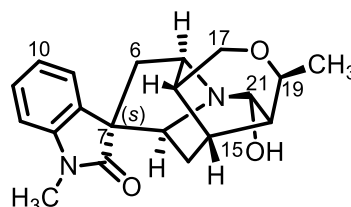
deoxyperaksine, **51**



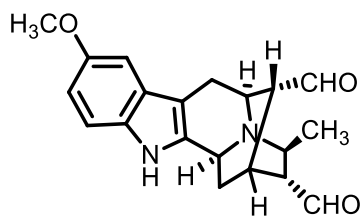
O-acetylpreperakine, **52**



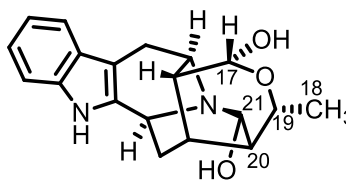
macrosalhinine, **53**



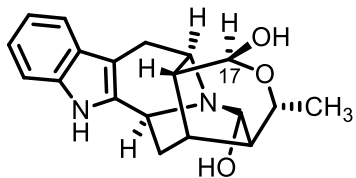
7(*S*)-talpinine oxindole, **54**



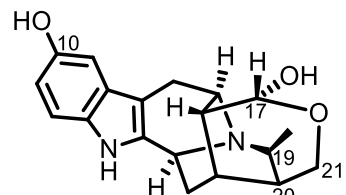
vinmajine F, **55**



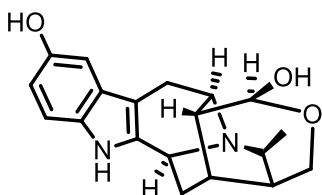
rauvovertine A, **56**



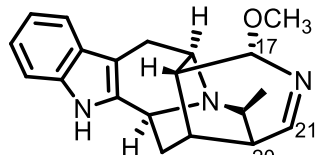
17-*epi*-rauvovertine A, **57**



rauvovertine B, **58**

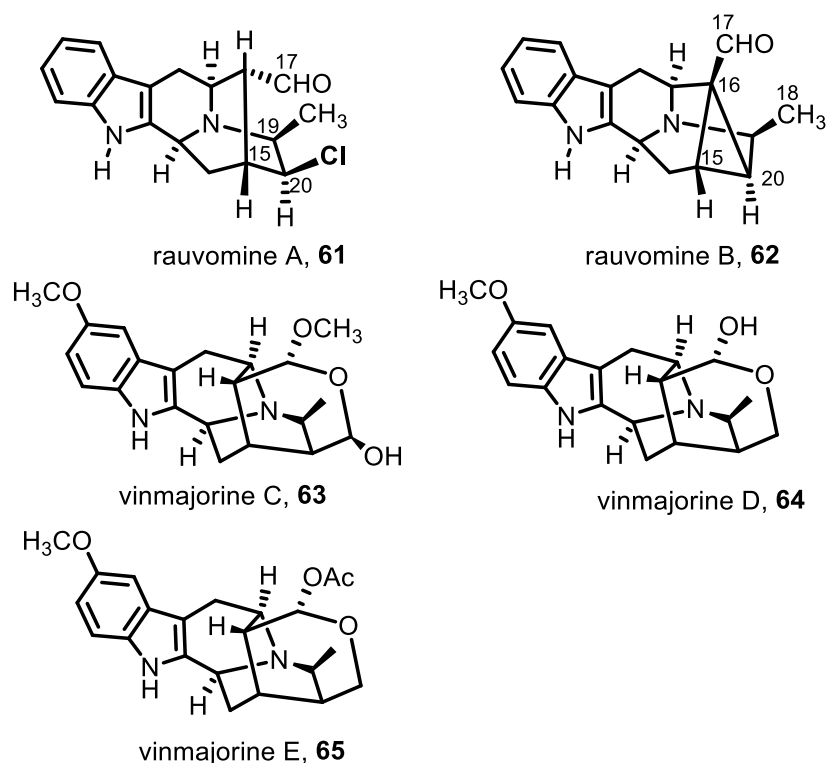


17-*epi*-rauvovertine B, **59**



rauvovertine C, **60**

Table 2. Sarpagine-related C-19 methyl substituted alkaloids (continued: 3)



Vinmajorine C **63** resembles alstoyunine B (*vide supra*, **43**) in substitution and stereochemistry at C-17 and C-21, while vinmajorine D **64** is similar to peraksine **41**. Vinmajorine E **65** is the C-17 *O*-acetate of alkaloid **64**.

2.3 Ajmaline-Related C-19 Methyl Substituted Alkaloids

All of the ajmaline alkaloids that belong to this group bear a β -methyl [i.e., (*S*)] function at C(19) with an indolenine moiety at C(1)-C(2) (see Table 3). Alstoyunines C **66** and D **67** were isolated from *A. yunnanensis*.²⁹ Both of these bear an *N*₄-oxide function and the C(21)-carboxylic acid group. The base **67** contains an *N*₁-oxide function as well. Alstoyunine D **67** has also been isolated from *A. rupestris* and named vinorine *N*₁,*N*₄-dioxide.³¹ The name “vinorine *N*₁,*N*₄-dioxide” is a

misnomer and may be misleading since vinorine⁶⁵ (*vide infra*, **112**) does not resemble **67**. Rauvoloids A-E (**68-72**) were isolated from *R. yunnanensis*⁶⁶ and are perakine-type alkaloids with a C₁₈ skeleton and no formyl function at C(20). Rauvoloid A **68** bears no carbon substituent at C(20), while rauvoloids B **69** and C **70** contain an α - and β -chloro substituents at C(20), respectively. The question remains whether the C(20) chloro substituents **69** and **70** arise on isolation or from an unconventional biosynthesis. As far as the authors know this has not been determined. In rauvoloid D **71** there is a (1*E*)-3-oxo-butenyl group at C(20) which makes it the first perakine-type alkaloid with a C₂₂ skeleton. The base **71** was also isolated previously from *R. tetraphylla* and was named rauvotetraphylline D.⁶⁰ Rauvoloid E **72** is the diethoxy acetal analog of the C(20)-formyl function and has the same skeleton as perakine **77**. The 10-methoxy ajmaline alkaloids, vinmajines A **73** and B **75**, were isolated from cultivated *V. major*.³⁰ Vinmajine A **73** contains a methoxy-acetamido acetal group at the C-20 α formyl group, whereas **75** contains a β -hydroxymethyl group at C(20). Raucaffrinoline **76** was first isolated from *R. caffra*⁶⁷ and later it has also been isolated from various *Rauwolfia* and *Alstonia* species (see Table 4). Examination of the X-ray crystal structure of **76** confirmed its structure as drawn. In the crystal structure it was observed that raucaffrinoline formed an intermolecular OH \cdots O hydrogen bond via the C-21 hydroxyl group with the carbonyl oxygen of the C-17 acetate group which formed an infinite chain along the [100] axis.⁶⁸ Perakine **77** (also known as *raucaffrine*^{33,69}) was first isolated from *R. perakensis*⁵⁷ and later from various other *Rauwolfia*, *Alstonia*, and *Vinca* species (see Table 4 for details). Perakine dimethyl acetal **82** was isolated from *R. sellowii* and is considered to be an artifact of the isolation process.⁷⁰ The ring-A oxygenated perakine variant 10-methoxyperakine **81** was later isolated from *V. major*.^{30,71} Vincawajine **78** was isolated from the aerial parts of *V. major*.⁷¹ Vincawajine **78** and 10-methoxyperakine **81** were reported as C-20 β (acetoxymethyl and

formyl substituted bases, respectively). But these are C-20 α substituted alkaloids according to Lounasmaa, as drawn here in Table 3.^{7,21} Perakine *N*₄-oxide **80** and raucaffrinoline *N*₄-oxide **79** were isolated recently from *A. yunnanensis*.⁷² The biogenetic numbering was incorrectly represented in that report.⁷² The correct numbering is as drawn in structures (**79** and **80**). The base 10-methoxyraucaffrinoline **74** was isolated from *V. herbacea* L. and the biogenetic numbering was shown incorrectly in that report.⁷³ The correct biogenetic numbering is shown here in structure **74**. Perakine *N*₁,*N*₄-dioxide **83** was isolated from the aerial parts of *A. rupestris*.³¹

Table 3. Ajmaline-related C-19 methyl substituted alkaloids

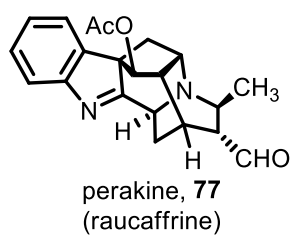
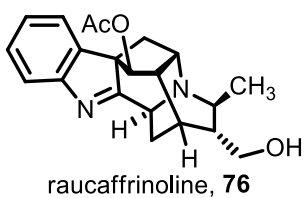
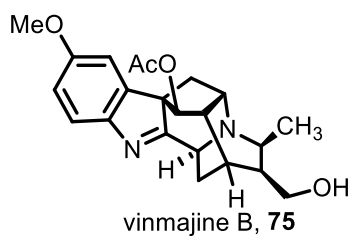
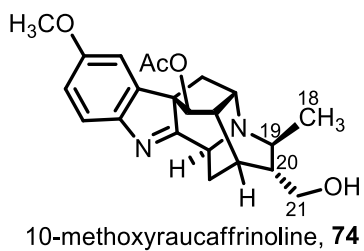
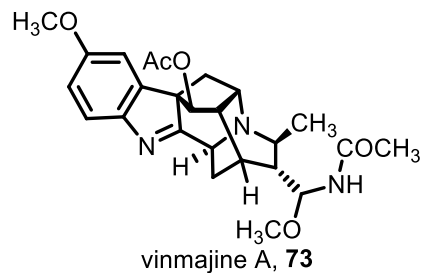
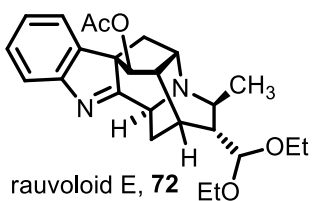
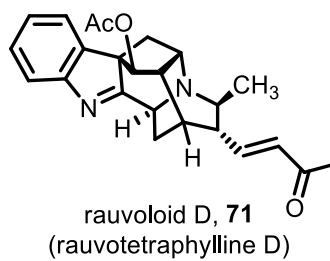
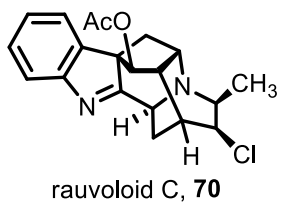
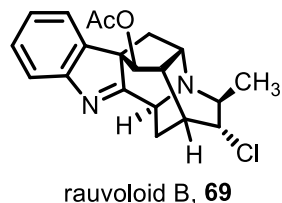
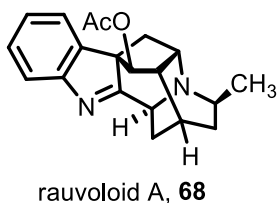
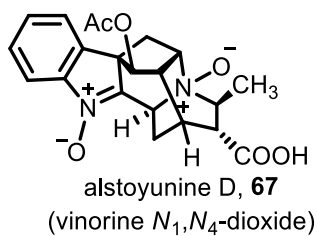
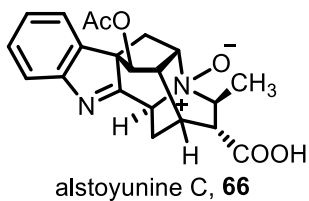


Table 3. Ajmaline-related C-19 methyl substituted alkaloids (continued: 2)

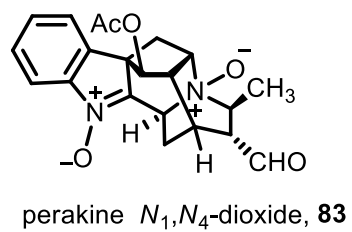
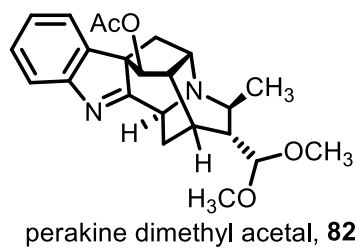
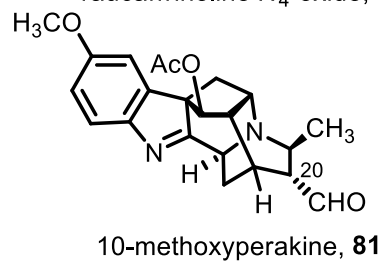
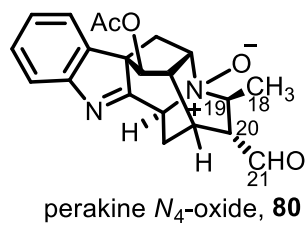
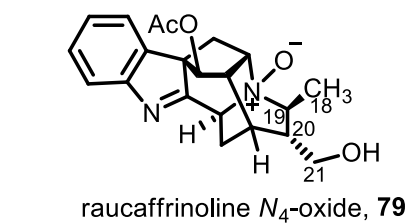
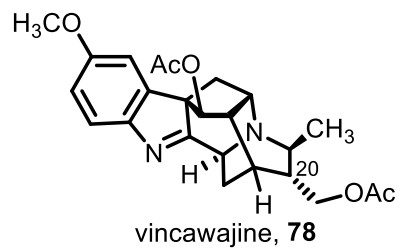


Table 4. Plant source(s) and plant morphology of the C-19 methyl substituted sarpagine-/macroline/ajmaline alkaloids (12-80)

Macroline alkaloids		
Alkaloid	Plant	Morphology (ref)
Macrocarpine A (12)	<i>Alstonia macrophylla</i>	Bark ³⁷ ; Leaves ⁴⁰
Macrocarpine B (13)	<i>Alstonia macrophylla</i> <i>Alstonia angustifolia</i>	Bark ^{37,43} ; Leaves ⁴⁰ Stem bark and leaves ³⁹ ; Stem bark ²⁸
Macrocarpine C (14)	<i>Alstonia macrophylla</i>	Bark ³⁷
Macrocarpine D (15)	<i>Alstonia macrophylla</i> <i>Alstonia angustifolia</i>	Stem bark ^{38,74} Stem bark ³⁸ ; Stem bark and leaves ³⁹
Macrocarpines E-H (16-19)	<i>Alstonia angustifolia</i>	Stem bark and leaves ³⁹
Alstohentine (20)	<i>Alstonia macrophylla</i>	Leaves ⁴⁰
Talcarpine (21)	<i>Pleiocarpa talbotii</i> Wernham <i>Alstonia macrophylla</i> <i>Alstonia angustifolia</i>	Stem bark ⁴¹ Bark ^{37,43,47} ; Leaves ⁷⁵ ; Root bark ^{76,77} Stem bark and leaves ³⁹
<i>N</i> ₄ -Methyl- <i>N</i> ₄ ,21-secotalpinine (22)	<i>Alstonia angustifolia</i> <i>Alstonia macrophylla</i>	Stem bark ²⁸ Bark ³⁷
Sarpagine and macroline-derived sarpagine alkaloids		
Alkaloid	Plant	Morphology (ref)
19-Epitalcarpine (23)	<i>Alstonia angustifolia</i>	Stem bark and leaves ³⁹
Alstonerinal (24)	<i>Alstonia angustifolia</i> <i>Alstonia macrophylla</i>	Stem bark and leaves ³⁹ ; Leaves ⁴⁶ ; Stem bark ^{28,78} Bark ⁴³

Table 4. Continued: 2

Alkaloid	Plant	Morphology (ref)
19,20-Dehydro-10-methoxytalcarpine (25)	<i>Alstonia angustifolia</i>	Leaves ⁴⁴
	<i>Tabernaemontana dichotoma</i>	Bark ⁴⁵
<i>N</i> ₄ -Demethylalstonerinal (26)	<i>Alstonia angustifolia</i> var. <i>latifolia</i>	Leaves ⁴⁶
<i>N</i> ₁ -Demethylalstonerinal (27)	<i>Alstonia angustifolia</i>	Stem bark and leaves ³⁹
6-Oxoalstophyllal (28)	<i>Alstonia macrophylla</i>	Leaves ⁴⁰
Alstophyllal (29)	<i>Alstonia macrophylla</i>	Bark ^{37,43} ; Leaves ⁴⁰
<i>N</i> ₁ -Demethylalstophyllal (30)	<i>Alstonia macrophylla</i>	Bark ³⁷
Alstoniaphylline C (31)	<i>Alstonia macrophylla</i>	Bark ⁴³
<i>N</i> ₄ -Demethylalstophyllal oxindole (32)	<i>Alstonia macrophylla</i>	Bark ⁴⁷
Alstonal (33)	<i>Alstonia macrophylla</i>	Leaves ⁴⁸ ; Bark ⁴⁷ ; Stem bark ⁷⁸
	<i>Tabernaemontana dichotoma</i>	Bark ⁴⁵
<i>N</i> ₁ -Demethylalstonal (34)	<i>Alstonia angustifolia</i> var. <i>latifolia</i>	Leaves
	<i>Alstonia macrophylla</i>	Leaves ⁴⁸
16-Hydroxy- <i>N</i> ₄ -demethylalstophyllal oxindole (35)	<i>Alstonia macrophylla</i>	Leaves ⁴⁰
16-Hydroxyalstonal (36)	<i>Alstonia macrophylla</i>	Leaves ⁴⁰
Talpinine (37)	<i>Alstonia angustifolia</i>	Stem bark and leaves ³⁹
	<i>Pleiocarpa talbotii</i> Wernham	Stem bark ⁴¹

Table 4. Continued: 3

Alkaloid	Plant	Morphology (ref)
<i>N</i> ₄ -Methyltalpine (38)	<i>Alstonia angustifolia</i>	Stem bark ²⁸
<i>O</i> -Acetyltalpinine (39)	<i>Alstonia angustifolia</i>	Stem bark and leaves
<i>N</i> ₄ -Methyl-19-epitalpinine (40)	<i>Alstonia angustifolia</i>	Stem bark and leaves ³⁹
Peraksine (vomifoline) (41)	<i>Rauwolfia caffra</i>	Leaves ^{57,79}
	<i>Rauwolfia perakensis</i>	Leaves ^{49,55,80}
	<i>Rauwolfia vomitoria</i>	Stem bark ⁵⁸ ; Leaves ^{81,82} ; Aerial parts ⁶³
	<i>Rauwolfia volkensii</i>	Stem bark ⁶¹ ; Leaves ⁸³
	<i>Rauwolfia verticillata</i> (Lour.) Bail of Hong Kong	Wood ⁸⁴
	<i>Rauwolfia verticillata</i>	Stem ⁵⁹
	<i>Rauwolfia mombasiana</i> STAPF	Leaves ⁸⁵
	<i>Rauwolfia cumminsii</i>	Stem bark ⁸⁶
	<i>Rauwolfia nitida</i>	Root bark ⁸⁷
	<i>Rauwolfia oreogiton</i>	Leaves ⁸⁸
<i>Rauwolfia sumatrana</i> JACK	Leaves ⁸⁹	
<i>Rauwolfia tetraphylla</i>	Aerial parts ⁶⁰	
Alstoyunine A (42)	<i>Alstonia yunnanensis</i>	Whole plant ²⁹
	<i>Rauwolfia vomitoria</i>	Aerial parts ⁶³
Alstoyunine B (43)	<i>Alstonia yunnanensis</i>	Whole plant ²⁹
21-Hydroxycyclolochnerine (44)	<i>Catharanthus roseus</i>	Cell cultures ^{51,90} ; Root ⁹¹
Alstiyunnanenine A (45)	<i>Alstonia yunnanensis</i> Diels	Aerial parts ⁵⁰

Table 4. Continued: 4

Alkaloid	Plant	Morphology (ref)
Verticillatine (46)	<i>Rauwolfia verticillata</i>	Root ^{52,53}
19(S),20(R)- Dihydroperaksine (47)	<i>Rauwolfia serpentina</i> <i>Rauwolfia verticillata</i> <i>Rauwolfia tetraphylla</i>	Hairy root culture ⁵⁴ Stem ⁵⁹ Aerial parts ⁶⁰
19(S),20(R)- Dihydroperaksine-17-al (48)	<i>Rauwolfia serpentina</i>	Hairy root culture ⁵⁴
10-Hydroxy-19(S),20(R)- dihydroperaksine (49)	<i>Rauwolfia serpentina</i> <i>Rauwolfia tetraphylla</i>	Hairy root culture ⁵⁴ Aerial parts ⁶⁰
Dihydroperaksine (50)	<i>Rauwolfia caffra</i> <i>Rauwolfia perakensis</i>	Leaves ⁵⁷ ; stem bark ⁵⁶ Leaves and stem ⁵⁵
Deoxyperaksine (51)	<i>Rauwolfia vomitoria</i> <i>Rauwolfia perakensis</i>	Stem bark ⁵⁸ Leaves and stem ⁵⁵
<i>O</i> -Acetylpreperakine (52)	<i>Rauwolfia volkensii</i>	Stem bark ⁶¹
Macrosalpine chloride and thiocyanate (53)	<i>Alstonia macrophylla</i> Wall.	Bark ⁶²
7(S)-Talpinine oxindole (54)	<i>Alstonia angustifolia</i>	Stem bark and leaves ³⁹
Vinmajine F (55)	<i>Vinca major</i>	Whole plant ³⁰
Rauvovertine A (56)	<i>Rauwolfia verticillata</i>	Stem ⁵⁹
17-Epi-rauvovertine A (57)	<i>Rauwolfia verticillata</i>	Stem ⁵⁹
Rauvovertine B (58)	<i>Rauwolfia verticillata</i>	Stem ⁵⁹
17-Epi-rauvovertine B (59)	<i>Rauwolfia verticillata</i>	Stem ⁵⁹
Rauvovertine C (60)	<i>Rauwolfia verticillata</i>	Stem ⁵⁹
Rauvomine A (61)	<i>Rauwolfia vomitoria</i>	Aerial parts ⁶³
Rauvomine B (62)	<i>Rauwolfia vomitoria</i>	Aerial parts ⁶³
Vinmajorines C-E (63-65)	<i>Vinca major</i>	Whole plant ⁶⁴

Table 4. Continued: 5

Ajmaline Alkaloids		
Alkaloid	Plant	Morphology (ref)
Alstoyunine C (66)	<i>Alstonia yunnanensis</i>	Whole plant ²⁹
Alstoyunine D (67) (vinorine <i>N</i> ₁ , <i>N</i> ₄ -dioxide)	<i>Alstonia yunnanensis</i> <i>Alstonia rupestris</i>	Whole plant ²⁹ Aerial parts ³¹
Rauvoloid A-C, E (68-70, 72)	<i>Rauwolfia yunnanensis</i>	Leaves ⁶⁶
Rauvoloid D (71) (Rauvotetraphylline D)	<i>Rauwolfia yunnanensis</i> <i>Rauwolfia tetraphylla</i>	Leaves ⁶⁶ Aerial parts ⁶⁰
Vinmajines A-B (73, 75)	<i>Vinca major</i>	Whole plant ³⁰
10-Methoxyraucafrinoline (74)	<i>Vinca major</i> <i>Vinca herbacea</i> Waldst. et. Kit	Whole plant ³⁰ Aerial parts ⁷³
Raucaffrinoline (76)	<i>Rauwolfia caffra</i> <i>Rauwolfia caffra</i> Sonder <i>Rauwolfia yunnanensis</i> <i>Rauwolfia of New Calédonia</i> <i>Rauwolfia vomitoria</i> <i>Rauwolfia serpentina</i> <i>Alstonia venenata</i> <i>Rauwolfia nitida</i> <i>Rauwolfia sellowii</i> <i>Rauwolfia bahiensis</i> A. DC.	Leaves ⁵⁷ Root bark ⁶⁷ Leaves ⁶⁶ Leaves ⁹² Leaves ⁸¹ Hairy root culture ⁵⁴ Leaves ⁹³ Root bark ⁸⁷ Leaves ⁷⁰ Aerial parts ⁶⁸

Table 4: Continued: 6

Alkaloid	Plant	Morphology (ref)
Perakine (77, raucaffrine)	<i>Rauwolfia caffra</i>	Leaves ⁵⁷ ; Stem bark ⁵⁶
	<i>Rauwolfia yunnanensis</i>	Leaves ⁶⁶
	<i>Rauwolfia vomitoria</i>	Leaves ^{81,94}
	<i>Rauwolfia serpentina</i>	Hairy root culture ⁵⁴
	<i>Alstonia yunnanensis</i>	Whole plant ²⁹
	<i>Rauwolfia perakensis</i>	Root and leaves ^{49,80}
	<i>Vinca major</i>	Whole plant ³⁰
	<i>Rauwolfia Caffra</i> Sonder	Root ⁹⁵
	<i>Alstonia mairei</i>	Leaves and twigs ⁹³
	<i>Rauwolfia sumatrana</i> JACK	Leaves ⁸⁹
	<i>Rauwolfia sellowii</i>	Leaves ⁷⁰
	<i>Rauwolfia biauriculata</i>	Leaves, stem and root bark ⁹⁶
<i>Rauwolfia sprucei</i> Muell Arg.	Stems and leaves ⁹⁷ Stem bark ⁹⁸	
Vincawajine (78)	<i>Vinca major</i>	Aerial parts ⁷¹
Raucaffrinoline N ₄ -oxide (79)	<i>Alstonia yunnanensis</i>	Whole plant ⁷²
Perakine N ₄ -oxide (80)	<i>Alstonia yunnanensis</i>	Whole plant ⁷²
10-Methoxyperakine (81)	<i>Vinca major</i>	Aerial parts ⁷¹ ; Whole plant ³⁰
Perakine dimethyl acetal (82)	<i>Rauwolfia sellowii</i>	Leaves ⁷⁰
Perakine N ₁ ,N ₄ -dioxide (83)	<i>Alstonia rupestris</i>	Aerial parts ³¹

3. Bioactivity

The biological activity of the majority of the alkaloids in this chapter has not been reported. We presume this is due to the paucity of isolated alkaloids from botanical sources, which hinders biological screening. In some cases the geographical location of the plants bearing these alkaloids is problematic. Most of the isolated material (if not all of it) is primarily used for isolation and characterization purposes by spectroscopic and optical methods, some of which are destructive. Sometimes the structural and stereochemical confirmation by derivatizing the isolated alkaloid (if required) is the primary focus. For example, some alkaloids, the structures of which have been known for several decades, have not had any biological activity reported until recently. With the availability of better spectroscopic methods and instruments, it is expected that a lower loading of material will be required for characterization and as a result, this will facilitate the studies of biology. Although the role(s) of the C-19 methyl function in these secondary metabolites is not known yet, a number of indole alkaloids that belong to this group have been reported to possess useful and important biological activity ranging from anti-hypertensive to anticancer. These active alkaloids can belong to any of the groups described herein *i.e.*, the sarpagine, macroline, and ajmaline series (see Table 5 for the list of bioactive alkaloids).

Examination of the biological activity of talpinine **37** and *O*-acetyltalpinine **39** has shown moderate to weak cytotoxicity in reversing the multidrug resistance of vincristine resistant human cancer cell line (KB/VJ300).³⁹ Alstoyunines A-D (**42-43**, **66-67**) were screened for anti-inflammatory and cytotoxicity. Among them, alstoyunine C **66** demonstrated selective COX-2 inhibition (94.85%), while none of the bases in this series were cytotoxic against human myeloid leukemia HL-60, hepatocellular carcinoma SMMC-7721, breast cancer SK-BR-3, pancreatic cancer PANC-

1, or lung cancer A-549 cell lines.²⁹ Alstiyunnanenine A **45** was screened against eight human tumor cell lines. It showed weak activity against the osteosarcoma cell lines Saos-2 and M663 with IC₅₀ values of 26.8±4.1 and 27.7±4.0 μM, respectively.⁵⁰ The 19,20-dehydro-10-methoxytalcarpine **25** and alstonal **33** along with a few related alkaloids isolated from the bark of *T. dichotoma* were screened for their vasorelaxant activity on normotensive rat aortic arteries precontracted with phenylephrine. Alstonal **33** showed strong vasorelaxant activity, while **25** did not show much relaxation.⁴⁵

The new quaternary nitrogen alkaloid *N*₄-methyltalpinine **38** and the known alkaloids *N*₄-methyl-*N*₄,21-secotalpinine **22**, alstonerinal **24**, and macrocarpine B **13**, along with a few other alkaloids isolated from *A. angustifolia*, were screened for their leishmanicidal activity against promastigotes of *Leishmania mexicana*, as well as their cytotoxic and NF-κB inhibitory activities.²⁸ The *N*₄-methyl-*N*₄,21-secotalpinine **22** demonstrated potent antileishmanial activity. Alstonerinal **24** exhibited moderate cytotoxicity against a human colon cancer cell line (HT-29) and weak activity against *L. Mexicana*. The *N*₄-methyltalpinine **38**, on the other hand, exhibited very strong NF-κB inhibition.²⁸ This is an important activity.^{99,100}

Perakine *N*₄-oxide **80** and raucaffrinoline *N*₄-oxide **79** along with a few other alkaloids isolated from *A. yunnanensis* were evaluated for their anti-inflammatory (selective COX-2 inhibition) and cytotoxicity activity against seven human cancer cell lines.⁷² Both **79** and **80** showed selective COX-2 inhibition (94.77% and 88.09%, respectively) which supports their anti-inflammatory properties. On the other hand, both alkaloids exhibited cytotoxicity against astrocytoma (CCF-STTG1), gliomas (CHG-5, SHG-44, U251), human skin melanoma (SK-MEL-2) and human breast cancer (MCF-7) cell lines, while none of these were active against the BEN-MEN-1 (meningioma) cell line.⁷²

Talcarpine **21** exhibited weak antimalarial activity against the *Plasmodium falciparum* (K1 strain).⁷⁷ Vinmajines A-B, F (**73**, **75**, **55**) and perakine **77**, along with a few other alkaloids isolated from cultivated *Vinca major*, were screened for cytotoxicity against five human cancer cell lines (HL-6-, SMMC-7721, A-549, MCF-7, SW480).³⁰ Vinmajine F **55** and perakine **77** demonstrated potent cytotoxicity against human lung cancer cell line A-549, while **55** was found more cytotoxic against the A-549 cell line ($IC_{50} = 3.1 \mu M$) than the positive control cisplatin ($IC_{50} = 9.24 \mu M$).³⁰ Perakine *N*₁,*N*₄-dioxide **83** and alstoyunine D **67** were evaluated for their cytotoxic and antimicrobial properties.³¹ In the cytotoxicity screening assay against seven human tumor cell lines both alkaloids did not show any significant cytotoxicity. On the other hand, in the antimicrobial screen using disk diffusion methods against seven different fungi and bacteria, both of them showed potent activity against *Staphylococcus aureus* with MIC values of 0.49 and 0.83 mM, respectively.³¹ Verticillatine **46** was studied for its effect on mean arterial pressure (MAP), cerebral blood flow (CBF), and cerebrovascular resistance (CVR) in pentobarbital anesthetized dogs and cats. Verticillatine **46** significantly reduced MAP and CVR in both animals while CBF increased in dogs and remained unaltered in cats.¹⁰¹ In another study **46** exhibited ganglionic blocking effects.⁵² Rauvovertine A **56**, 17-*epi*-rauvovertine A **57**, rauvovertine B **58**, 17-*epi*-rauvovertine B **59**, and rauvovertine C **60** were screened against five human cancer cell lines by the MTS method using cisplatin and taxol as positive controls.⁵⁹ Among these, only **60** showed moderate cytotoxicity against all of the cancer cell lines (HL-60, SMMC-7721, A-549, MCF-7, and SW-480) with IC_{50} values of 10.76-15.7 μM .⁵⁹ Rauvomines A **61** and B **62** along with peraksine **41** and alstoyunine A **42**, isolated from *R. vomitoria*, were screened for their cytotoxic and anti-inflammatory properties.⁶³ Only alstoyunine A **42** showed weak cytotoxicity against human colon cancer cell lines HT-29 and SW480 while the remaining alkaloids did not show any appreciable

cytotoxicity. The rauvomine B **62** showed significant inhibition of the macrophage RAW 264.7 cell line ($IC_{50} = 39.6 \mu\text{M}$; positive control *celecoxib* $IC_{50} = 34.3 \mu\text{M}$), while other alkaloids exhibited moderate activity.⁶³ Vinmajorines C-E (**63-65**) were screened for their cytotoxicity against five human cancer cell lines (MCF-7, SMMC-7721, HL-60, SW480, and A-549). Vinmajorine C **63** exhibited moderate ($IC_{50} = 19.86 \mu\text{M}$) and vinmajorine E **65** showed weak ($IC_{50} = 34.89 \mu\text{M}$) cytotoxicity only against the human lung cancer cell line A-549 while vinmajorine D **64** was inactive.

The 19(S),20(R)-dihydroperaksine-17,21-al (see **84**), a biosynthetic derivative of perakine by acetylcysteine (AE)¹⁰² was predicted to be an inhibitor of aldose reductase (AR) in a computational docking study of 142 *Rauvolfia serpentina* derived compounds, which would be a potential lead for designing novel compounds for the treatment of diabetes and its complications.¹⁰³

Table 5. Biologically active alkaloids from the C-19 methyl substituted subgroup and their activity

Alkaloid	Bioactivity	Reference
Talpinine (37)	Anticancer: Moderate to weak cytotoxic [IC_{50} = 14-22 μ g/mL) activity in the presence of 0.1 μ g/mL vincristine] activity in reversing multidrug resistance in drug-resistant KB/VJ300 cells	Kam ³⁹
<i>O</i> -acetyltalpinine (39)		
Alstoyunine C (66)	Anti-inflammatory activity: selective inhibition of COX-2 (94.84%) enzyme	Tan ²⁹
Alstiyunnanenine A (45)	Anticancer: weak cytotoxicity against osteosarcoma cell lines Saos-2 and M663, $IC_{50} \leq 30 \mu$ M	Shi and Wu ⁵⁰
<i>N</i> ₄ -methyltalpinine (38)	Anticancer: NF- κ B (p65) inhibitory activity: $ED_{50} = 1.2 \mu$ M	Kinghorn ²⁸
<i>N</i> ₄ -methyl- <i>N</i> _{4,21} -secotalpinine (22)	Antileishmanial: active against promastigotes of <i>Leishmania mexicana</i> ($IC_{50} = 57.8 \mu$ M)	Kinghorn ²⁸
Alstonerinal (24)	Anticancer: active against human colon cancer cell line (HT-29 cells, $ED_{50} = 8.6 \mu$ M) Antileishmanial: active against promastigotes of <i>Leishmania mexicana</i> ($IC_{50} = 145.4 \mu$ M)	Kinghorn ²⁸
Alstonal (33)	Antihypertensive: Potent vasorelaxant activity at 30 μ M in precontracted (phenylephrine) rat aortic rings	Zaima ⁴⁵
Perakine <i>N</i> ₄ -oxide (80)	Anticancer: Cytotoxic (IC_{50}) against glioma (CHG-5, SHG-44, U251: 12.9, 11.8, 12.3 μ M respectively), astrocytoma (CCF-STTG1: 12.3 μ M), human skin cancer (SK-MEL-2: 33.7 μ M), and human breast cancer cells (MCF-7: 28.1 μ M). Anti-inflammatory: selective inhibition of COX-2 (94.77%) enzyme	Liang ⁷²

Table 5. Continued: 2

Alkaloid	Bioactivity	Reference
Raucaffrinoline <i>N</i> ₄ -oxide (79)	Anticancer: Cytotoxic (IC ₅₀) against glioma (CHG-5, SHG-44, U251: 12.1, 9.2, 9.7 μM respectively), astrocytoma (CCF-STTG1: 11.4 μM), human skin cancer (SK-MEL-2: 34.9 μM), and human breast cancer cell (MCF-7: 29.9 μM) lines Anti-inflammatory: selective inhibition of COX-2 (88.09%) enzyme	Liang ⁷²
Talcarpine (21)	Antimalarial: active against multidrug-resistant <i>Plasmodium falciparum</i> (K1 strain), IC ₅₀ = 40.3±2.9 μM	Houghton ⁷⁷
Vinmajine F (55)	Anticancer: Stronger cytotoxicity against human lung cancer cells A-549 than cisplatin (IC ₅₀ = 3.1 μM vs cisplatin IC ₅₀ = 9.24 μM)	Cheng ³⁰
Perakine (77)	Anticancer: Cytotoxic against human lung cancer cells A-549 (IC ₅₀ = 14.5 μM vs cisplatin IC ₅₀ = 9.24 μM)	Cheng ³⁰
Perakine <i>N</i> ₁ , <i>N</i> ₄ -dioxide (83)	Antimicrobial: strong activity against <i>S. aureus</i> , MIC = 0.49 mM	Hua ³¹
Alstoyunine D (67)	Antimicrobial: strong activity against <i>S. aureus</i> , MIC = 0.83 mM	Hua ³¹
Verticillatine (46)	Antihypertensive: Ganglionic blocking effect Antihypertensive: Vasodilation effect (significant reduction in mean arterial pressure) and improved cerebral blood circulation in dogs and cats.	Lin ⁵² Zeng ¹⁰¹
Rauvoverline C (60)	Anticancer: moderate cytotoxicity (IC ₅₀) against human cancer cell lines HL-60 (10.76 μM), SMMC-7721 (15.02 μM), A-549 (15.70 μM), MCF-7 (12.63 μM), and SW-480 (14.02 μM).	Wang ⁵⁹

Table 5: Continued: 3

Alkaloid	Bioactivity	Reference
Rauvomine A (61)	Anti-inflammatory: modest activity in inhibiting macrophage RAW 264.7 cell line, IC ₅₀ = 55.5 μM.	Gao and Chen ⁶³
Rauvomine B (62)	Anti-inflammatory: significant activity in inhibiting macrophage RAW 264.7 cell line, IC ₅₀ = 39.6 μM.	Gao and Chen ⁶³
Alstoyunine A (42)	Anticancer: weak cytotoxicity against human colon cancer cell lines HT-29 (IC ₅₀ = 35.2 μM) and SW480 (IC ₅₀ = 45.3 μM); Anti-inflammatory: weak activity against RAW 264.7 macrophage cell line (IC ₅₀ = 75.3 μM)	Gao and Chen ⁶³
Peraksine (41)	Anti-inflammatory: moderate activity against RAW 264.7 macrophage cell line (IC ₅₀ = 65.2 μM)	Gao and Chen ⁶³
Vinmajorine C (63)	Anticancer: moderate cytotoxicity against A-549 cell line (IC ₅₀ = 19.86 μM)	Li and Zhao ⁶⁴
Vinmajorine E (65)	Anticancer: weak cytotoxicity against A-549 cell line (IC ₅₀ = 34.89 μM)	Li and Zhao ⁶⁴

4. Biosynthesis and Synthesis (Partial, Formal, and Total Synthesis) of the Alkaloids from this Subgroup

4.1 Biosynthesis

For the detailed biosynthetic, structural and chemo-enzymatic significance of sarpagine-ajmaline-type alkaloids see the Chapter by Stöckigt et al.¹⁰⁴

4.1.1 Proposed Biosynthesis of Rauvovertine C (60) by Gao et al.⁵⁹

A plausible biosynthetic pathway was proposed for the formation of the unusual imine bridge containing sarpagine-type alkaloid rauvovertine C **60**⁵⁹ (Figure 2). Although no enzymatic reactions have been carried out to support this mechanism. The C-16 α ,C-20 β -dialdehyde **85** could possibly originate from perakine **77** (which is known to occur in *Rauvolfia* species) via an enzymatic process and this could be followed by the isomerization of the C-20 α aldehyde in **84**.^{54,66} The imine intermediate **86** is proposed to form via an amination reaction of the β -aminoethanol^{105,106} with the aldehyde function at C-21. The reaction of the C-21-imine with the formyl function at C-17 in the base **86** in the presence of acid would form the iminium ion intermediate **87**. Rauvovertine C **60** would possibly be generated from the iminium intermediate via de-alkylation of the iminium ion and this would be followed by methylation of the C-17-hydroxyl function. However, there was NH₃ in the isolation process which could have led to a simple imine, which could cyclize to give **60**.

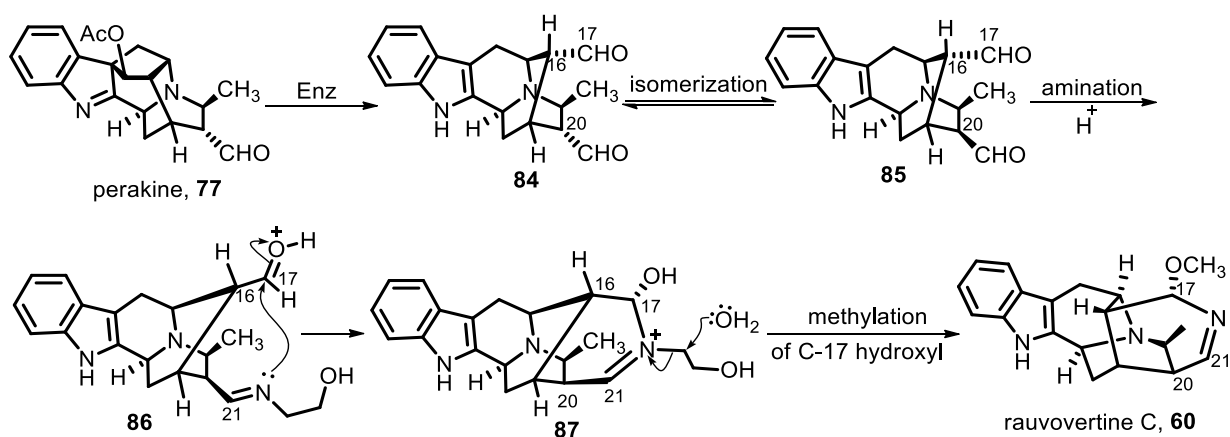


Figure 2. Plausible biosynthetic pathway for rauvovertine C **60** proposed by Gao et al.⁵⁹

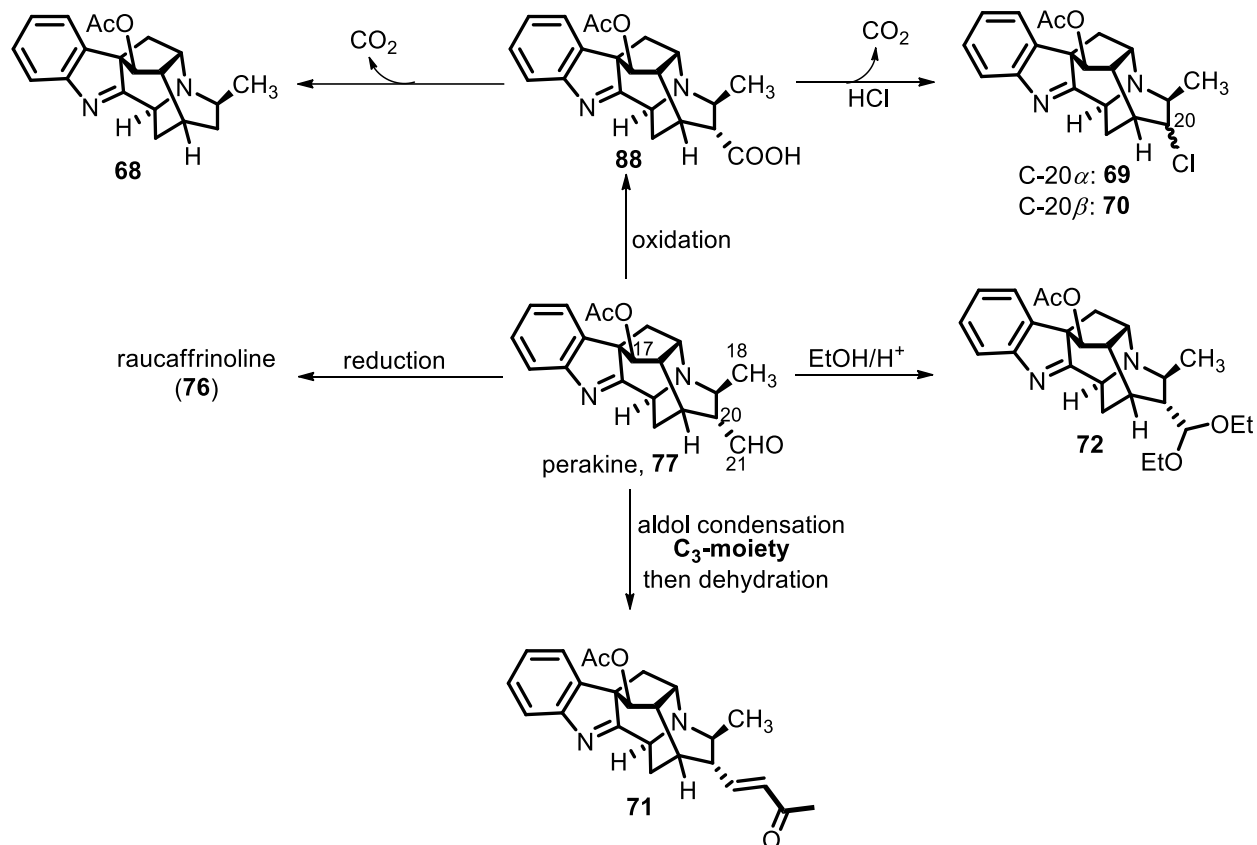


Figure 3. Possible origin of the rauvoloids A-E **68-72** from a common intermediate perakine **77** proposed by Liu⁶⁶

4.1.2 Proposed Biosynthesis of Rauvoloids A-E (68-72) by Liu⁶⁶

Liu proposed the possible origin of five new alkaloids, the rauvoloids A-E **68-72** from a common precursor, perakine **77**⁶⁶ (Figure 3). As hypothesized by Geng and Liu, biogenetically, a sequence of oxidations and decarboxylation of perakine **77** might form rauvolid A **68**. Decarboxylation of the oxidized precursor **88** in the presence of HCl might form the C(20)-Cl epimers, rauvoloids B **69** and C **70**. On the other hand, an aldol condensation of the perakine C(21)-formyl function with a C₃-moiety could be the origin of the C₂₂ skeleton present in rauvolid D **71**. Rauvolid E **72** could form by acetalization of the C(21)-formyl function with ethanol in the presence of acid. No

biosynthetic experiments have been executed in this work, consequently, these could also possibly be considered as artifact alkaloids that formed during the isolation process.^{60,66}

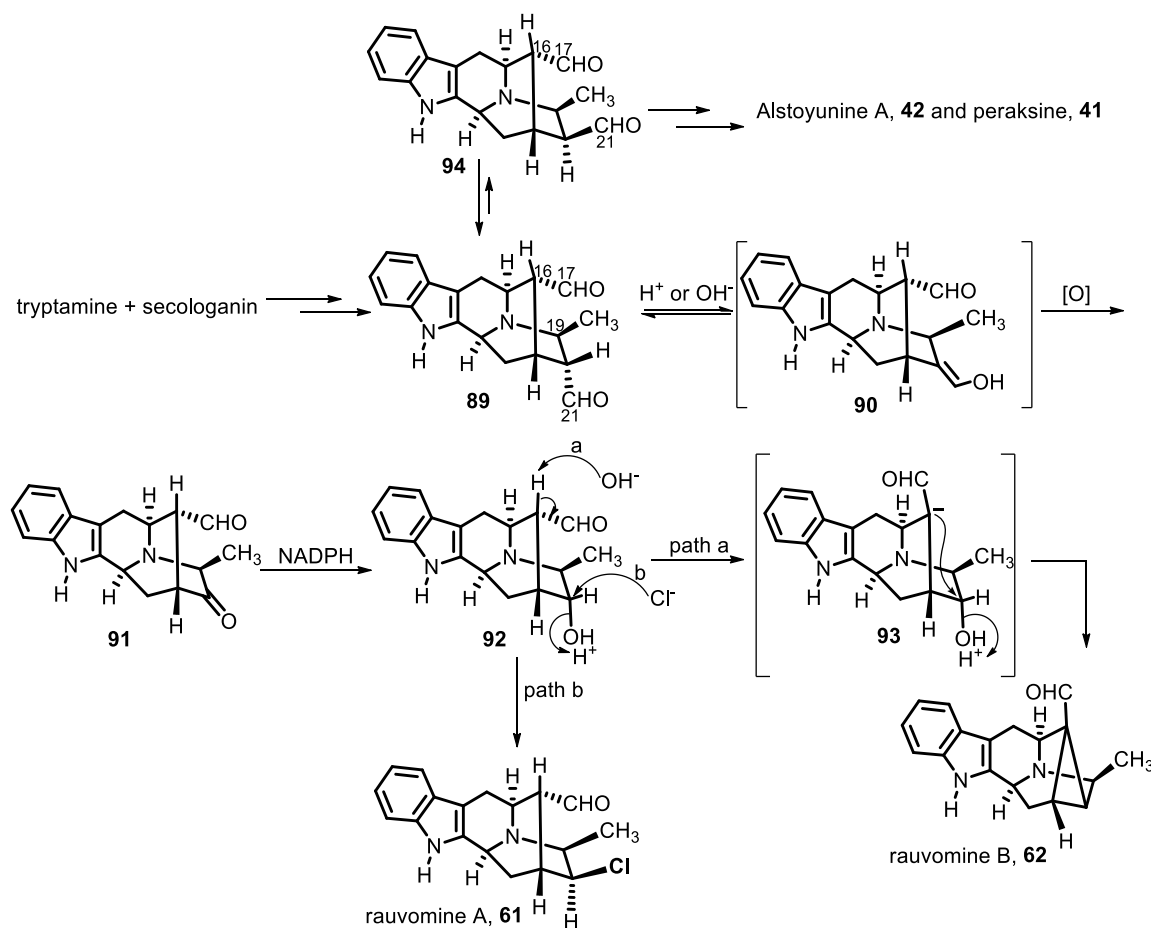


Figure 4. Plausible biosynthesis of rauvomines A (**61**) and B (**62**) proposed by Zeng et al.⁶³

4.1.3 Proposed Biosynthesis of Rauvomines A (**61**) and B (**62**) by Zeng et al.⁶³

A plausible biosynthesis of rauvomines A **61** and B **62** was proposed by Zeng et al. during the report of their isolation and structure determination of **61** and **62**, along with two other known alkaloids peraksine **41** and alstoyunine A **42** from the aerial parts of *R. vomitoria*⁶³ (Figure 4). The C-17,C-21-dialdehyde **89** was known to originate from tryptamine (the authors mentioned

tryptophan, which should be tryptamine) and secologanin.^{59,107} The enolization of aldehyde **89** could lead to intermediate **90**.⁵⁹ The C-20 α hydroxyl function in **92** could form from the enol intermediate **90**, followed by oxidation to **91** and subsequent NADPH mediated reduction. An intramolecular cyclization via the S_N2 substitution of the C(20)-hydroxyl by the enolate carbon atom at C(16) could form the cyclopropane ring present in rauvomine B (path a, via **93**), whereas replacement of the hydroxyl function in **92** with a chlorine atom (path b) might generate rauvomine A **61**. Besides, the C-16(α),C-20(β) dialdehyde **94** could originate from the dialdehyde **89** by isomerization. This dialdehyde could react with methanol to generate alstoyunine A **42** while partial reduction, followed by intramolecular aldol condensation could generate peraksine (**41**, not shown here).^{102,108} Again, whether this is related to the biosynthesis of **41** and **42** remains to be determined.

4.1.4 Interpretation of the Formation of Nine Artifact Alkaloids Proposed by Lounasmaa²¹

Lounasmaa proposed the origin of nine alkaloids that could, in fact, be “artifact alkaloids” formed during the isolation process (see Figures 5 and 6).²¹ In that interesting discussion, logical arguments were put forward to support the artifactual nature of those alkaloids and their possible formation based on organic chemistry. However, it is controversial since no enzymatic studies were carried out to support the hypothesis despite the sensible nature of the arguments from a chemical point of view. Nevertheless, it is worth considering to promote further studies to either confirm or disprove the hypothesis proposed by Lounasmaa. The *O*-acetylpreperakine **52**, macrosalhinine **53**, peraksine **41**, 19(*S*),20(*R*)-dihydroperaksine **47**, perakine **77**, and raucaffrinoline **76** were proposed to form from *E*-vomilenine (via *Z*-vomilenine) during the isolation process. On

the other hand, verticillatine **46** would be formed from the 10-hydroxy related compounds, whereas 10-methoxyperakine **81** and vincawajine **78** would be formed from their 10-methoxy counterparts. The C-21 hydroxy indolenines **95** and **98** could rearrange to their corresponding tautomeric amino-aldehyde ring-opened *Chano* forms **96** and **97** (Figure 5). The *Chano* forms could interconvert to permit the *E*- and *Z*-vomilenines (**95** and **98**) to reach equilibrium favoring the *E*-vomilenine **95** (Figure 5). In addition, acidic or basic conditions during the isolation process might cleave the acetyl function of either the *E*-vomilenine **95** or the *Z*-vomilenine **98** which would ultimately form *Z*-vellosimine **101** via 16-*epi-Z*-vellosimine **100**. It is important to mention that the *Z*-ethylidene moiety is in fact more stable than the *E*-ethylidene in vellosimine or related compounds as suggested by the predominance of the *Z*-ethylidene moiety in studies carried out by Wang *et al.*¹⁰⁹ and Cao *et al.*¹¹⁰ during the synthesis of vellosimine and koumidine, respectively (not shown here). In this regard, another interesting point is that all of these alkaloids form via *Z*-ethylidene derivatives even though the *E*-ethylidenes (in vomilenines) are thermodynamically favored because the *Chano* form derived from *E*-vomilenine would generate 19-*epi*-perakine, which has never been isolated (all of these nine alkaloids bear the C-19 β -CH₃ group). This would mean that the *E*-ethylidenes first isomerize to the corresponding *Z*-ethylidene counterparts before re-cyclization, as shown in Figure 5.

As hypothesized by Lounasmaa, *O*-acetylpreperakine **52** could form from *Z*-vellosimine **101**, which would originate from *E*-vomilenine **95** via *Z*-vomilenine **98**, as shown in Figure 5. Recyclization of the *Chano* forms from β -side attack (in **103**), partial reduction of the C(17)-formyl group (in **89**) and acetylation during isolation could deliver *O*-acetylpreperakine **52** (Figure 6). On the other hand, the recyclization of **103** could yield an equilibrium mixture of α - and β - (**89** and **94**) aldehydes (in favor of the α -aldehyde **89**). Isomerization to the C-20 β -aldehyde, followed

by partial reduction would provide **105**, which after hemiacetal formation, and methylation during isolation could afford macrosalhine **53**.

On the contrary, the diol **47** could form by reduction of both of the formyl functions (C-17 and C-21) of the intermediate **89**. On the other hand, peraksine could form in a manner similar to macrosalhine **53** via partial reduction and subsequent hemiacetal formation from **94**. Similarly, verticillatine **46** could form from the 10-hydroxy counterpart via similar transformations analogous to peraksine. Similarly, perakine **77** could form via *Z*-vomilenine **98** after generation of the *Chano* form and cyclization from the β -side. The partial reduction of the C(21)-formyl function would afford raucaffrinoline **76**. The 10-methoxyperakine **81**, 10-methoxyraucaffrinoline **74**, and vincawajine **78** could form via similar transformations but only from the 10-methoxy variant **110**.²¹

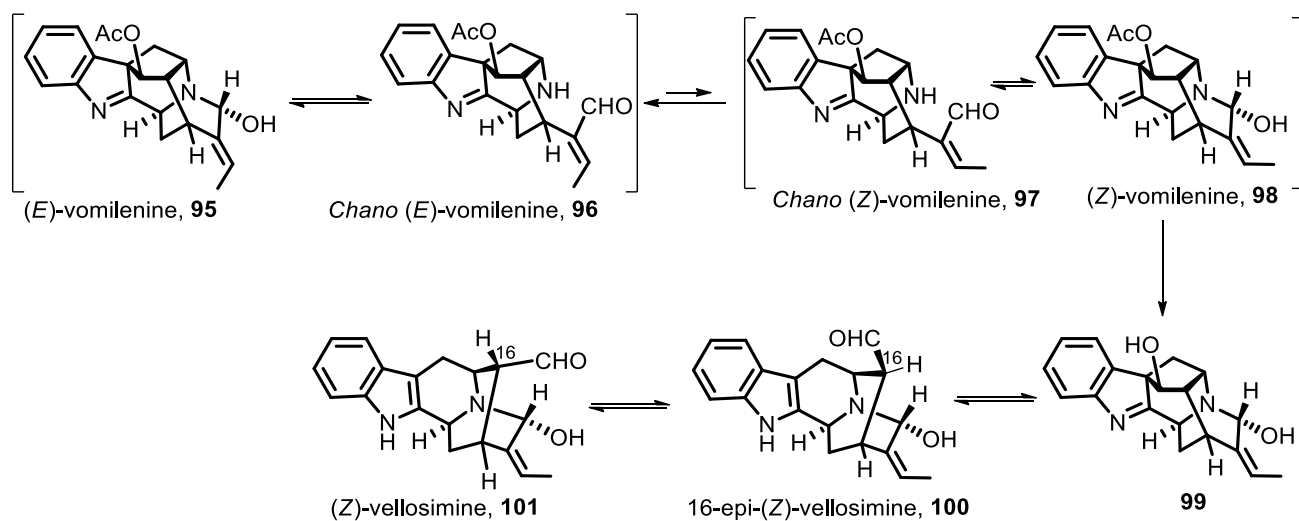


Figure 5. Equilibrium between *E*-vomilenine and *Z*-vomilenine via their ring-opened (*Chano*) forms

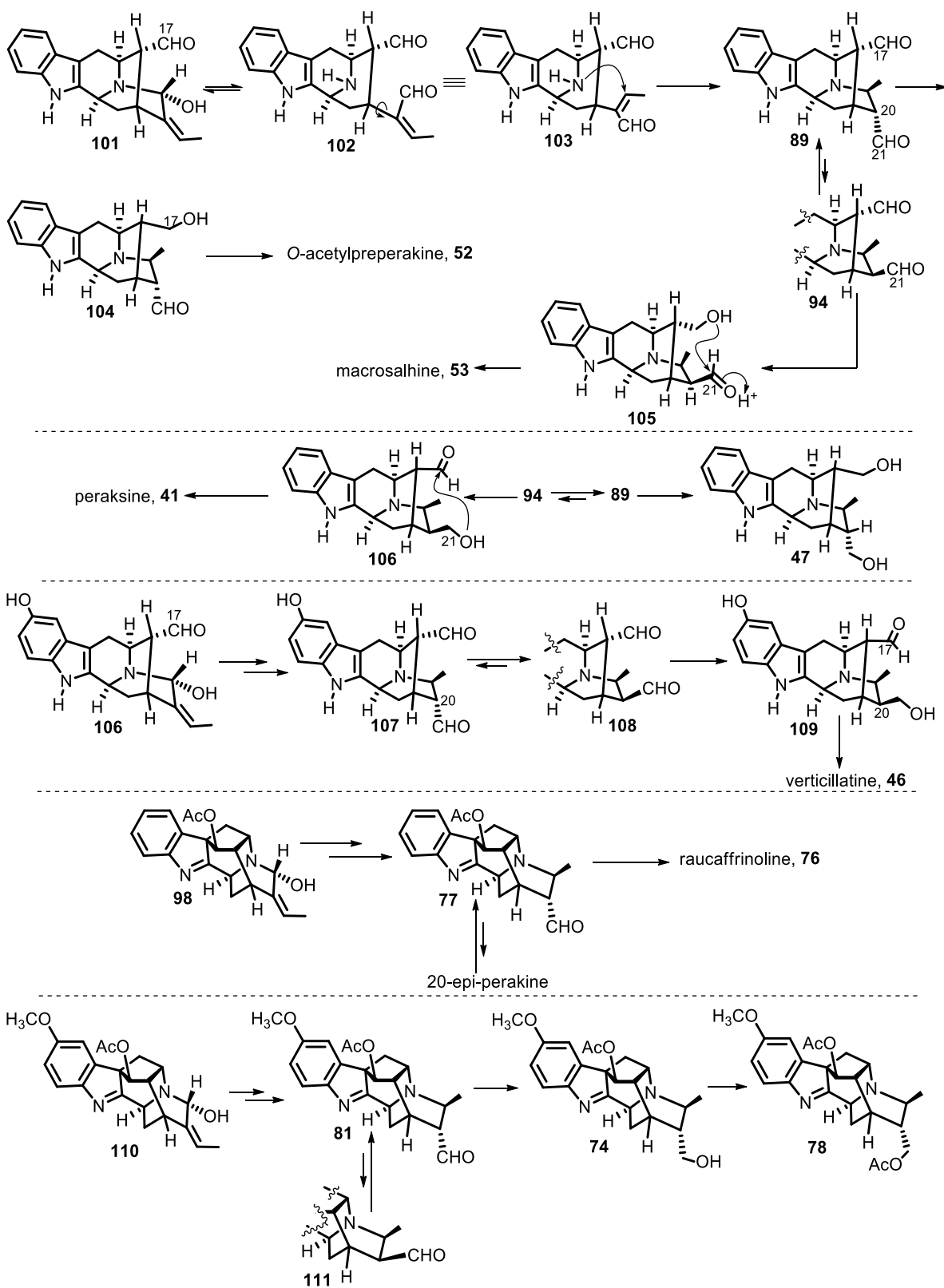


Figure 6. Plausible pathways for the formation of "artifact alkaloids" proposed by Lounasmaa²¹

4.1.5 Putative Biosynthetic Formation of Alkaloids in *Rauvolfia serpentina* Hairy Root Culture Executed by Stöckigt et al.⁵⁴

On the other hand biosynthetic experiments have been carried out by Stöckigt et al.¹⁰⁴ The alkaloids isolated from the hairy root culture of *Rauvolfia serpentina*⁵⁴ were presumed to be derived from perakine **77** or its reduced form raucaffrinoline **76**, both of which were isolated from the *Rauvolfia* hairy root culture by Stöckigt et al. (Figure 7).¹¹¹ Raucaffrinoline **76** could be enzymatically prepared from *E*-vomilenine **95** in the presence of NADPH₂ or from perakine.¹¹¹ In this case, Stöckigt dismissed the possibility of **47** and **48** being artifact alkaloids, which were felt to be artifacts of the isolation process, as proposed by Lounasmaa²¹ since the corresponding precursor for **49** was not detected in *Rauvolfia* plants and cell cultures.^{111,112} To support their hypothesis Stöckigt et al. incubated raucaffrinoline **76** with a crude enzyme preparation from the hairy root culture of *R. serpentina*. A deactivated enzyme mixture (boiled) was used as a negative control. After overnight incubation, the 19(*S*),20(*R*)-dihydroperaksine-17-al **48** was isolated, while in the deactivated enzyme, raucaffrinoline **76** remained unchanged. This suggested that, enzymatic deacetylation facilitated the C(17)-C(7) bond cleavage and the formation of 19(*S*),20(*R*)-dihydroperaksine-17-al **48** took place, which upon reduction would form 19(*S*),20(*R*)-dihydroperaksine **47**. The 10-hydroxy dihydroperaksine derivative **49** was presumed to be formed via a late-stage hydroxylation of **48**. The final proof of this concept remains outstanding until the isolation and characterization of the appropriate enzymes are performed.⁵⁴ However, Stöckigt has provided enzymatic evidence for the generation of **48** and then **47**, which is in agreement with previous studies.^{102,104,113} An enzymatic network is shown in Figure 7 that involves three enzymes; perakine reductase (PR), acetylerase (AE), and an uninvestigated reductase (XR).^{114,102,104} These results seem to support the hypothesis that these alkaloids are not artifacts.⁵⁴

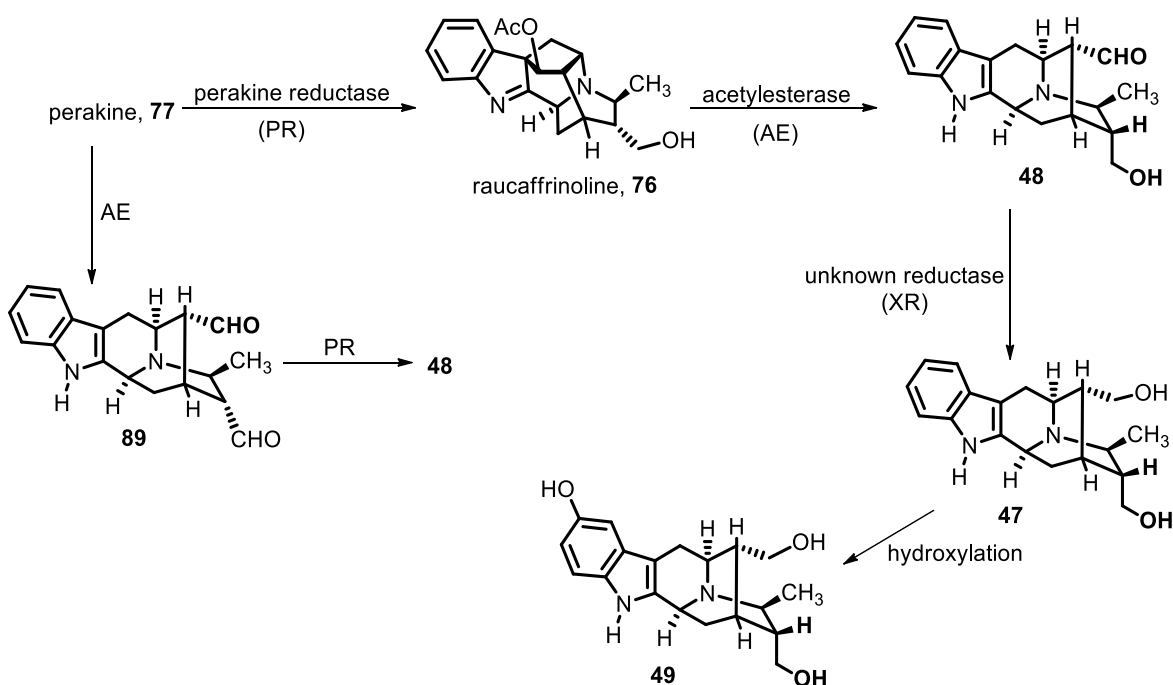


Figure 7. Putative biosynthetic formation of the alkaloids **47**, **48**, and **49** from raucaffrinoline **76** in *R. serpentina* hairy root culture by Stöckigt et al.⁵⁴

4.2 Partial Synthesis

4.2.1 Partial Synthesis of Perakine 77 by Sakai et al.¹¹³

Vomilenine **95** is known to play an important role in the biosynthesis of *Rauwolfia* alkaloids.^{104,115-118} Ajmaline **113**, perakine **77**, raucaffrinoline **76**, and related alkaloids are believed to originate from strictosidine via polyneuridine aldehyde and its conversion into 16-*epi*-vellosimine **100** by PNA-esterase (Scheme 1).^{104,113} Acetyl CoA and vinorine synthase are known to convert 16-*epi*-vellosimine into vinorine **112**, which after the action of a hydroxylase provides vomilenine **95**. Perakine **77** is also considered to be an artifact alkaloid formed by the effect of acetic acid on vomilenine. Sakai et al.¹¹³ synthesized both *Z*- and *E*-vomilenine (**98** and **95**, respectively) from ajmaline **113** to investigate the role of the ethylidene configuration in the transformation. The 19-

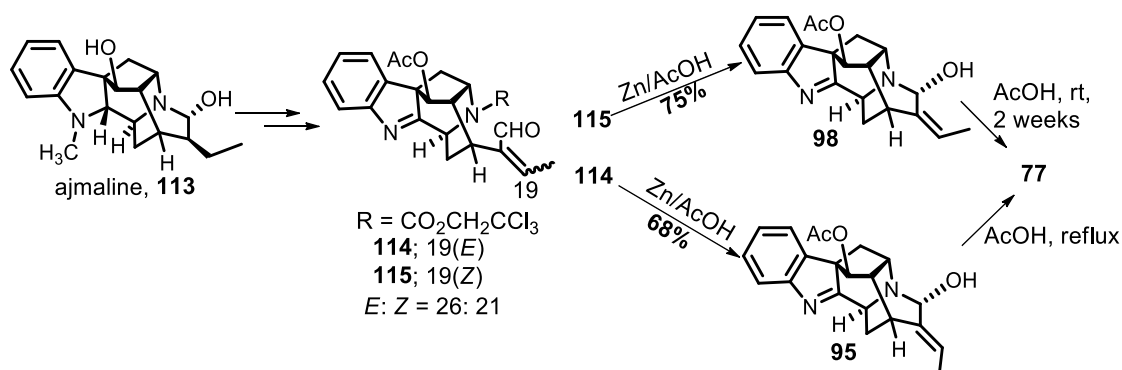
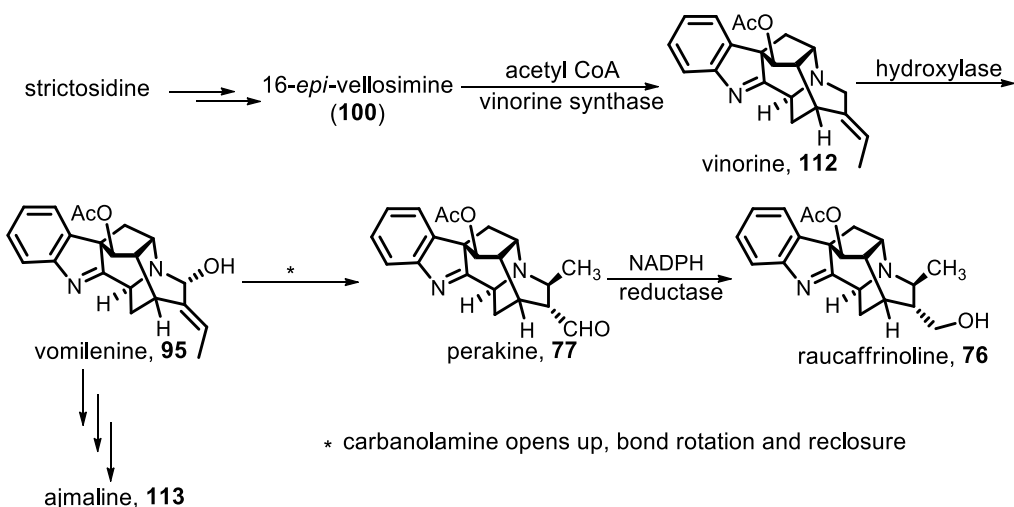
(*Z*) and 19-(*E*) olefins (**114** and **115**, respectively) were prepared by the degradation of ajmaline. Upon removing the carbamate protecting group on the *N*_b nitrogen atom with Zn/AcOH, the (*Z*)-olefin **115** delivered *Z*-vomilenine **98** in 75% yield, whereas the *E*-olefin **114** produced *E*-vomilenine **95** in 68% yield. The *Z*-vomilenine was converted into perakine under mild conditions on treatment with AcOH at room temperature, while it took treatment with hot AcOH¹¹⁹ to transform *E*-vomilenine into perakine **77**. Interestingly, the same material was produced from both transformations which suggested that cleavage of the amino-acetal function in *Z*-vomilenine is more facile than in *E*-vomilenine.¹¹³

4.2.2 Partial Synthesis of Talcarpine **21** from Ajmaline **113** by Sakai et al.⁴²

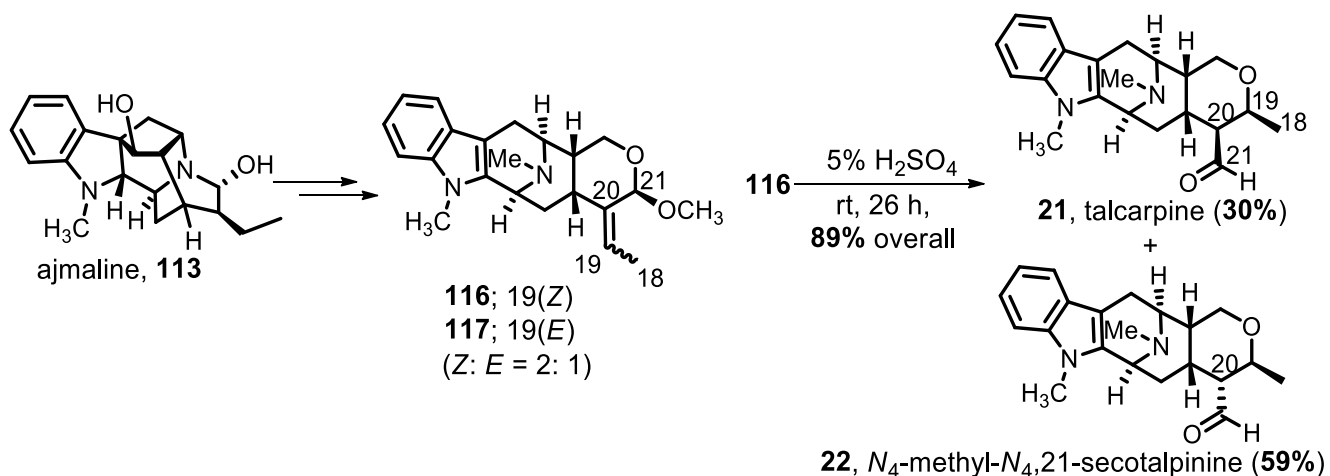
Sakai et al. devised an efficient synthetic route (Scheme 2) to several alkaloids by the degradation of ajmaline and confirmed the C-19 stereochemistry of talcarpine **21** to be β *i.e.*, (*S*).⁴² The 19(*Z*) and 19(*E*) olefins (**116** and **117**) were prepared in a 2 to 1 ratio from ajmaline **113** in several steps. The geometry of the olefin was confirmed by NOE experiments. The major (*Z*) olefin **116** upon treatment with 5% aq H₂SO₄ at room temperature for 26 hours furnished the C-20 β aldehyde **21** as a minor product in 30% yield, accompanied by the C-20 α aldehyde **22** as the major product in 59% yield. The C-19 stereochemistry was concluded to be (*S*) by NOESY analysis after preparation of the C-21-acetyl derivative after reduction of the C-20 aldehyde.

4.2.3 Partial Synthesis of Talcarpine **21** and Related Alkaloids from Talpinine **37** by Schmid et al.⁴¹

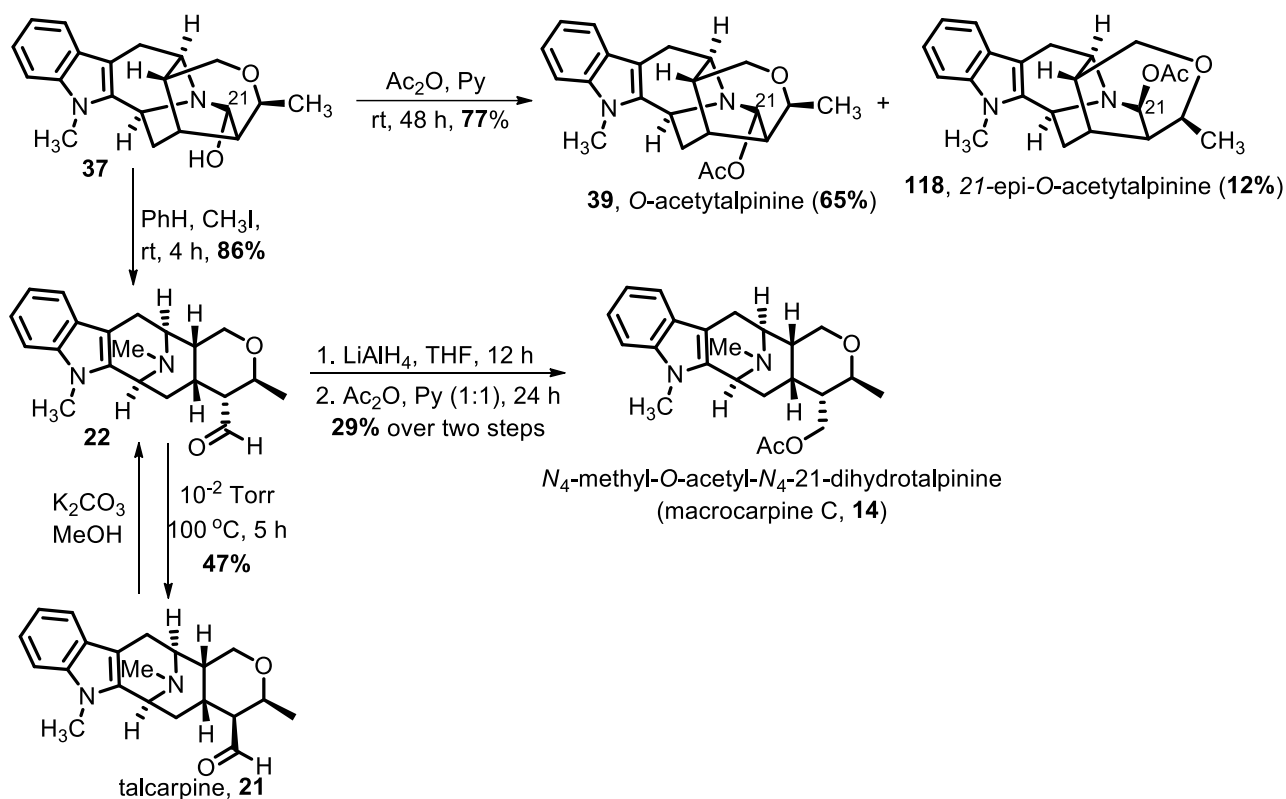
During the structure determination of talpinine **37** by chemical degradation, talcarpine **21** was synthesized (Scheme 3).⁴¹ Talpinine, upon acetylation with acetic anhydride in the presence of pyridine, afforded the C-21-*O*-acetyl derivative **39** (*O*-acetyltalpinine, later isolated as a natural product),³⁹ along with a small amount of its C-21-epimeric derivative 21-*epi-O*-acetyltalpinine **118** in 77% combined yield. On the other hand, treatment of **37** with iodomethane in benzene at room temperature for 4 hours transformed it into the C-20 α aldehyde **22** by the cleavage of *N*₄-C(21) bond. This base was further reduced and acetylated to provide the *N*₄-methyl-*O*-acetyl-*N*₄-21-dihydrotalpinine **14** which was later isolated from *A. macrophylla* and named macrocarpine C.³⁷ The base **22** could be converted into talcarpine **21** by pyrolysis while talcarpine could also be converted into **22** by treatment with K₂CO₃ in methanol.⁴¹



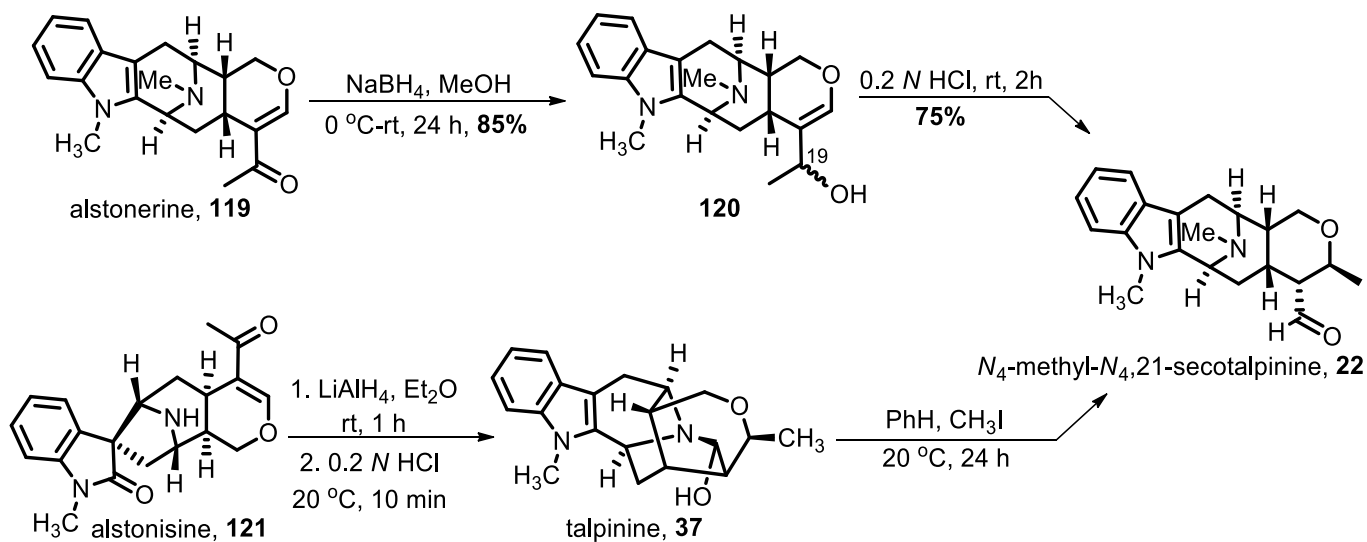
Scheme 1. Partial synthesis of perakine **77** from ajmaline **113** via vomilenine **95** by Sakai et al.¹¹³



Scheme 2. Partial synthesis of talcarpine **21** and *N*₄-methyl-*N*₄,21-secotalpine **22** from ajmaline **113** by Sakai et al.⁴²



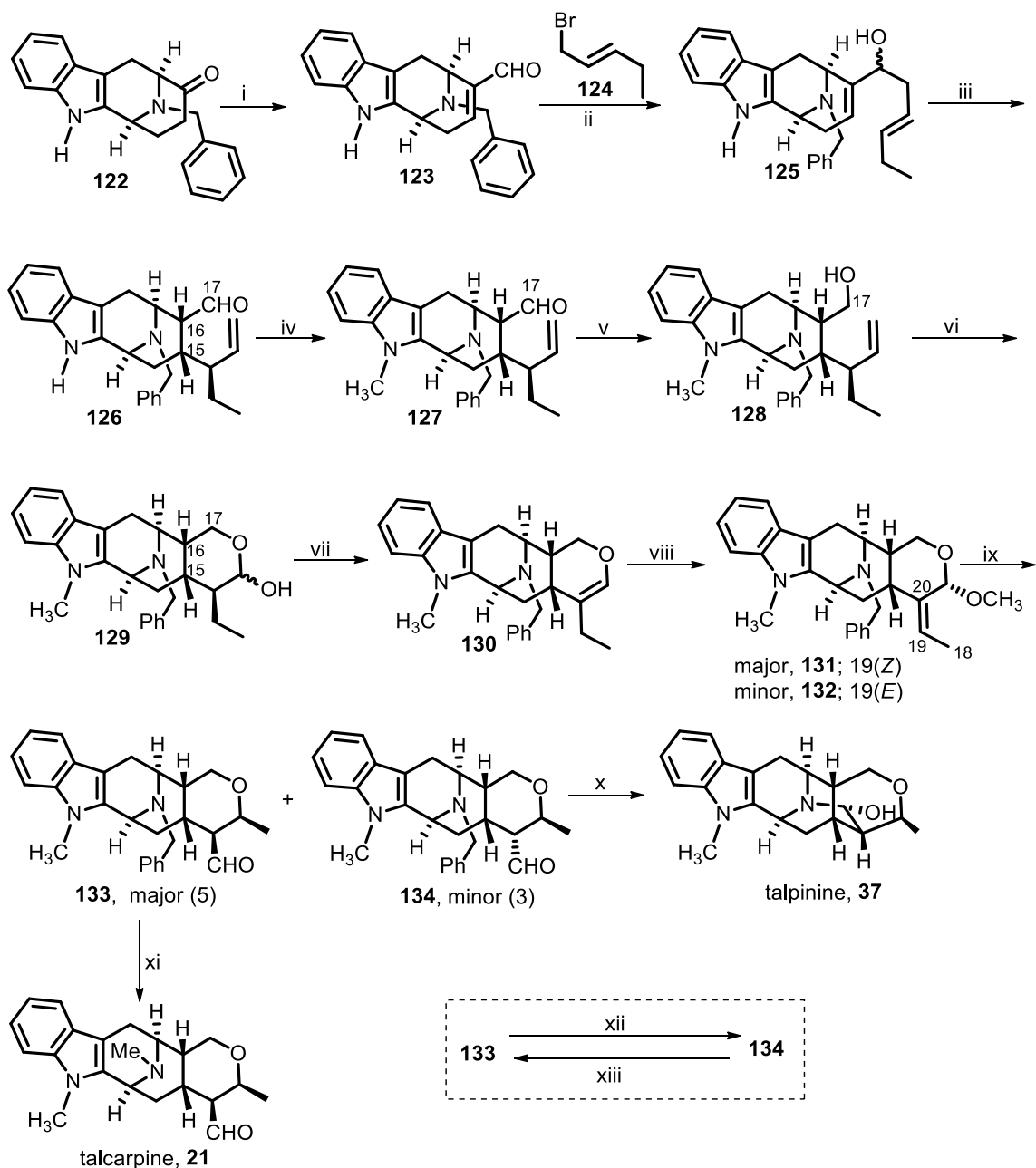
Scheme 3. Partial synthesis of several alkaloids from talpinine by Schmid et al.⁴¹



Scheme 4. Biomimetic transformations between several alkaloids by Le Quesne³

4.2.4 Biomimetic Transformations Between Alkaloids by Le Quesne³

During the biomimetic transformations among several monomeric macroline alkaloids, Le Quesne³ converted known alstonerine **119** into *N*₄-methyl-*N*_{4,21}-secotalpinine **22** (Scheme 4). The reduction of **119** with sodium borohydride in methanol at 0 °C-rt for 24 hours delivered the C-19-hydroxy alstonerines **120** as a mixture of epimers in 85% yield. This was followed by acid catalyzed rearrangement with 0.2 *N* aq HCl at room temperature for 24 hours to furnish *N*₄-methyl-*N*_{4,21}-secotalpinine **22** in 75% yield. In addition, alstonisine **121** upon reduction with LiAlH₄ in ether at room temperature for one hour produced several compounds one of which was **37** (5%). Treatment of talpinine **37** with iodomethane in benzene at 20 °C for 24 hours provided **22** in excellent yield whose properties were identical with the natural product.



Scheme 5. Total synthesis of talcarpine and talpinine by Yu et al.¹²⁰ Reagents and conditions: i) a. PhSOCH₂Cl, LDA, THF; KOH, THF-H₂O, rt, 10 h; b. LiClO₄, dioxane, reflux, 4 h, **90%**; ii) Li/Ph₂/BaI₂, **124**, THF, -78 °C, **90%**; iii) KH, dioxane, 18-crown-6, 100 °C, 14 h; MeOH, rt, 4 h, **88%**; iv) NaH, THF, CH₃I, rt, 6 h, **95%**; v) NaBH₄, MeOH, rt, 1 h, **95%**; vi) OsO₄, Py, NaHSO₃; NaIO₄, H₂O, MeOH, 0 °C, **75%**; vii) benzene, *p*-TSA, DST, reflux, 5 h, **95%**; viii) *p*-TSA, MeOH, *N*-(phenylseleno)phthalimide; NaIO₄, H₂O, MeOH, 0 °C, 20 h, **90%**; ix) 5% aq. H₂SO₄, 3 days,

90% combined yield; x) Pd/C, H₂, EtOH, rt, 5 h, **92%**; xi) Pd/C, H₂, MeOH, rt, 5 h, **90%**; xii) K₂CO₃, EtOH, rt, 2 days, **85%**; xiii) 10⁻¹ torr/100 °C, **75%**.

4.3 Total and Formal Synthesis

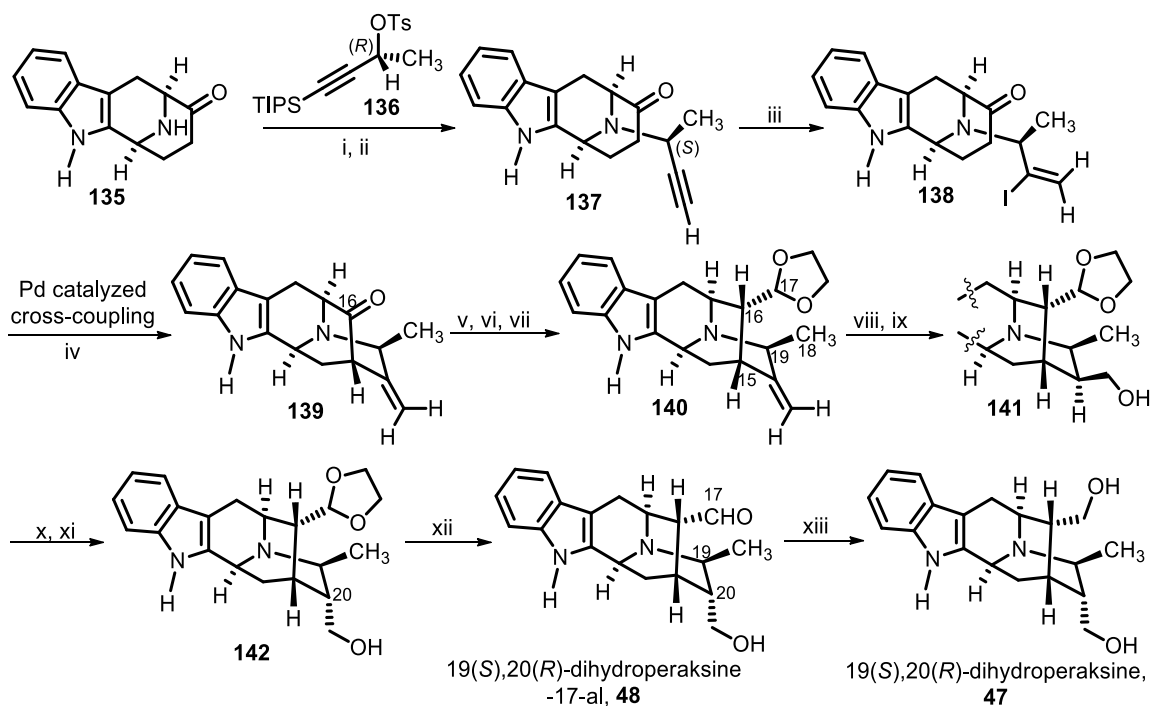
In this chapter the reported total synthesis of the C-19 methyl substituted subgroup of sarpagine/macroline/ajmaline alkaloids have been compiled. The total synthesis of the greater sarpagine/ajmaline-related alkaloids have been enriched by the numerous studies by van Tamelen,^{121,122} Cook,^{109,123-126} Kluge,¹²⁷ Le Quesne,^{3,128} Schmid,⁴¹ Martin,^{129,130} Magnus,¹³¹ Bailey,^{132,133} and more recently impressive work from Gaich^{134,135} and others.¹³⁶⁻¹³⁹ Since the synthesis of the broader sarpagine-macroline-ajmaline group is out of the scope of this chapter, only the synthesis of sarpagine or related alkaloids that bear C-19 methyl functions are described here.

4.3.1 Total Synthesis of Talpinine **37** and Talcarpine **21** by Yu et al.¹²⁰

The first enantiospecific total synthesis of talpinine **37**, as well as talcarpine **21** was executed by Yu et al. (Scheme 5).¹²⁰ The conversion of the ketone **122** into the α,β -unsaturated aldehyde **123** *via* spirooxiranophenylsulfoxide in 87% yield provided the key intermediate for several alkaloids including talcarpine and talpinine. The α,β -unsaturated aldehyde underwent a 1,2-addition upon reaction with the barium Grignard reagent, analogous to the work of Yamamoto,¹⁴⁰ prepared *in situ* from **124** at very low temperature to provide **125**. The allylic alcohol **125** underwent an anionic oxy-Cope rearrangement with KH in dioxane in the presence of 18-crown-6. The rearrangement took place almost exclusively (30:1) from the bottom face of the C(15)-C(16) double bond to

furnish the desired stereochemistry at C(15) and C(16), as shown in aldehyde **126**. The minor diastereomer which contained the epimeric aldehyde function at C(16) was converted completely into the desired aldehyde **126** by stirring the reaction mixture with methanol. This provided the more stable aldehyde in 88% yield from the allylic alcohol **129**. The indole nitrogen atom in **126** was methylated via a regiospecific alkylation with NaH and iodomethane in THF at room temperature to furnish the *N*₁-methylated indole **127** in 95% yield. This process was followed by reduction of the C(17) aldehyde with sodium borohydride in ethanol to provide the alcohol **128** in 95% yield. The oxidative cleavage of the olefinic double bond by treatment of a pre-prepared solution of OsO₄-pyridine in THF at 0 °C for 8 hours, was followed by treatment with NaIO₄ and subsequent cyclization of the so formed aldehyde with the C(17) alcohol to furnish the desired hemiacetal **125**. The hemiacetal underwent dehydration upon heating in refluxing benzene in the presence of *p*-TSA to provide the enol ether **130** as the sole product. The regiospecific oxyseleation of the enol ether **130** was performed with *N*-phenylselenophthalimide in CH₂Cl₂-MeOH at 0 °C in the presence of *p*-TSA to furnish selenoacetals in a 9:1 ratio (not shown). The subsequent treatment of the selenoacetals with NaIO₄ in THF-H₂O-MeOH solution at 0 °C for 10 hours gave the mixture of selenoxide acetals, which underwent the selenoxide elimination to provide the acetals **131** and **132** in a 4:1 ratio in favor of the desired product **131** in 90% yield. The acid catalyzed hydrolysis of the major acetal, which was followed by a Michael-type cyclization of the alcohol with the so formed α,β -unsaturated aldehyde, resulted in a mixture of *N*₄-benzyl-*N*_{4,21}-secotalpinine **134** and *N*₆-benzyltalcarpine **133** in a 3:5 ratio in 90% yield. The catalytic debenylation of the hydrochloride salt of the C-20 α aldehyde **134** went smoothly with 10% Pd/C, H₂ in ethanol to give talpinine **37** in 92% yield. The optical rotation and spectral properties of synthetic **37** were in excellent agreement with talpinine.⁴¹ The debenzylated amine (*N*₆-nitrogen

atom with a lone pair of electrons) had immediately attacked the C(21) aldehyde, as planned, to form the F-ring of **37**. The β -aldehyde, *N*_b-benzyltalcarpine **133** was treated with 1.5 equivalents of Pd/C, H₂ in the presence of MeOH to undergo the *N*_b-benzyl/*N*_b-methyl exchange reaction, which ultimately resulted in the desired alkaloid, talcarpine **21**. The β -aldehyde **133** could be completely converted into the α -aldehyde **134** by treatment of **133** with K₂CO₃ in EtOH for 2 days (85% yield). The reverse transformation could be done by pyrolysis of **134** and recyclization under reduced pressure in 75% yield to give **133**, analogous to the earlier work of Schmid.^{41,120}



Scheme 6. Reagents and conditions: i) **136**, K₂CO₃, CH₃CN, 65-70 °C, **88%**; ii) TBAF. xH₂O, THF, 0 °C-rt, **96%**; iii) I-B(Cy)₂, CH₂Cl₂, 0 °C-rt; AcOH; NaOH/H₂O₂, 0 °C-rt, **74%**; iv) Pd₂(dba)₃, DPEPhos, *t*-BuONa, THF, 70 °C, **60%**; v) Ph₃P(Cl)CH₂OCH₃, *t*-BuOK, benzene, rt, 13 h; vi) 2 *N* aq HCl, THF, 55 °C; vii) ethyleneglycol, *p*TSA.H₂O, benzene, DST, reflux, **90%** over 3 steps; viii) BH₃·DMS, THF, rt; NaBO₃·4H₂O, rt; ix) Na₂CO₃, MeOH, reflux, 5 h, **76%** over two steps; x) NCS/DMS, CH₂Cl₂, -5 °C-10 °C, 30 min, cool to -78 °C; Et₃N (excess), warm to rt,

3 h, **67%**; xi) NaBH₄, EtOH, 0 °C-rt, **94%**; xii) 1.38 N aq HCl, acetone/H₂O, 70 °C, **96%**; xiii) NaBH₄, EtOH, **94%**.

4.3.2 Total Synthesis of the Alkaloids Isolated from *Rauvolfia serpentina* Hairy Root Culture by Edwankar et al.^{25,26}

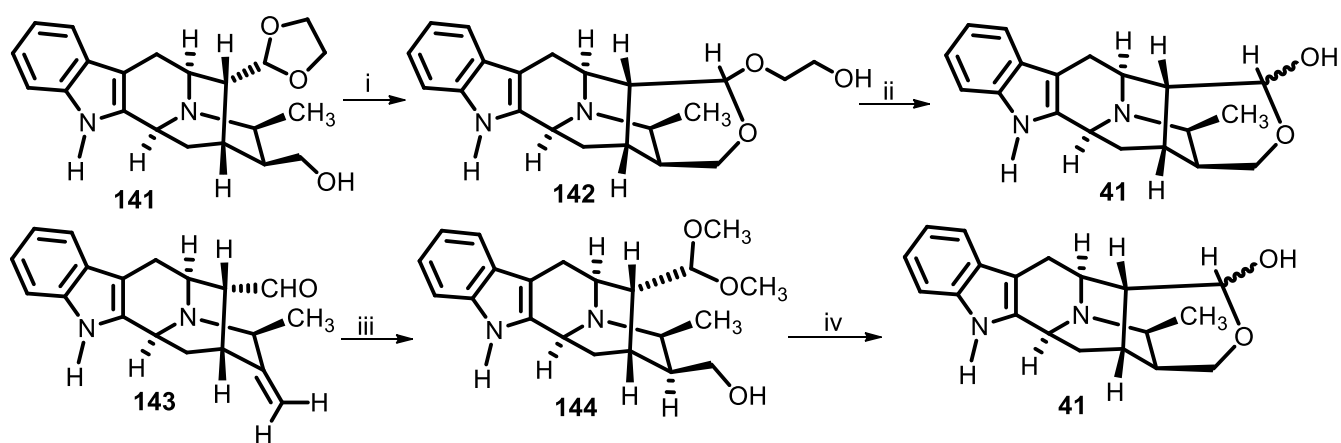
The first regiospecific and enantiospecific total synthesis of 19(*S*),20(*R*)-dihydroper-aksine **47**, and 19(*S*),20(*R*)-dihydroperaksine-17-al **48** was carried out by Edwankar et al.²⁵ In this synthesis (Scheme 6), an S_N2 alkylation of the N_b-nitrogen atom in amine **135** with the optically active (*R*)-tosylate **136** provided the N_b-ethynyl tethered ketone when it was stirred in the presence of K₂CO₃/dry acetonitrile in 88% yield. Subsequent deprotection of the silyl group with tetrabutylammonium fluoride furnished the terminal alkyne **137**. An interesting haloboration of the terminal alkyne in **137** was performed with dicyclohexyl-iodoborane, I-B(Cy)₂, which was the first example of a haloboration of a terminal alkyne with this iodoborane.²⁵ The flexible nature of the two cyclohexyl groups was believed to be responsible for the smooth transformation as opposed to the rigid nature of iodo-9BBN.²⁵ The subsequent protodeboronation of the so formed iodoborane with acetic acid provided the key vinyl iodide intermediate **138** in a reasonable 74% yield with complete regioselectivity. The key pentacyclic ketone **139** was formed via a palladium catalyzed intramolecular α -vinylation¹⁴¹ of the ketone in 60% isolated yield. The ketone **139** was subjected to a one-carbon homologation process at C(16) via a Wittig-hydrolysis sequence. The aldehyde was found to occupy the thermodynamically more stable alpha orientation even in the presence of the β -C(19) methyl function (not shown here, see **151**). The aldehyde was subsequently protected as the cyclic acetal **140** with ethylene glycol in the presence of *p*-TSA·H₂O in refluxing benzene in 90% yield over three steps. The olefin in **140** was subjected to a hydroboration-

oxidation sequence to furnish the required β -primary alcohol **141** in 76% yield over two steps. The primary alcohol was accompanied by a small amount of tertiary alcohol (primary: tertiary = 25:1). The oxidation of the primary alcohol **141** in the presence of an indole N_a -H and N_b -nitrogen atom was found to be problematic. Several oxidation protocols were employed and failed due to the formation of trace amounts of desired aldehyde, accompanied by the N_b -oxide and over oxidized products. A modified Corey-Kim oxidation protocol was employed with a lower reagent loading and lower temperature to circumvent the over oxidized byproducts. This method worked very well. This furnished the C-20 α + β -aldehydes as a mixture of epimers, which was completely converted into the α -epimer in the same vessel by stirring with an excess of triethylamine at room temperature for 3 hours. The α -aldehyde was then reduced to the primary alcohol **142** with sodium borohydride in ethanol in 94% yield. The cyclic acetal in **142** was cleaved under acidic conditions to provide the C(17) aldehyde which was identical to 19(*S*),20(*R*)-dihydroperaksine-17-al **48**. The reduction of the aldehyde with sodium borohydride furnished the desired alkaloid 19(*S*),20(*R*)-dihydroperaksine **47** whose properties were in good agreement with the natural product.²⁵

4.3.3 Total Synthesis of Peraksine 41 and Attempted Total Synthesis of Macrosalhinine 53 by Edwankar et al.²⁶

In 2014, Edwankar et al. published a general strategy to gain access to the C-19 methyl substituted macroline/sarpagine indole alkaloids while reporting the total synthesis of peraksine (Scheme 7).²⁶ This accompanied by the previously reported total syntheses²⁵ of **47** and **48** (*vide supra*), provided a general strategy which would also be useful in the total synthesis of other alkaloids from this subgroup.

To furnish the hemiacetal ring present in peraksine **41**, the cyclic acetal **141** was hydrolyzed under acidic conditions by heating the mixture to reflux for 24 hours in the presence of 1 *N* aq HCl in THF. Under these conditions, only 50% of the acetal cleaved to form the ether **142**. This ether **142** (via the OH group) was in equilibrium with acetal **141** and could not be cleaved to the desired aldehyde.²⁶ Additional heating of the ether with additional amounts of 1 *N* aq HCl for 4 days furnished only a trace amount of peraksine **41**. Alternatively, the olefinic aldehyde **143** was converted into the dimethoxy acetal by refluxing it in the presence of *p*-TSA•H₂O in MeOH for 6 h in 93% yield. The olefin was subsequently subjected to a hydroboration-oxidation sequence to furnish the monol **144** in 35% yield. The dimethoxy acetal **144** was less stable, as compared to the cyclic acetal (in **141**), and consequently was cleaved under acidic conditions with 1 *N* aq HCl in THF, at reflux (for 24 h) to furnish the alkaloid peraksine **41** as an epimeric mixture in 52% yield. It was reported earlier by Arthur et. al., that peraksine was isolated as a mixture of epimers.⁸⁴

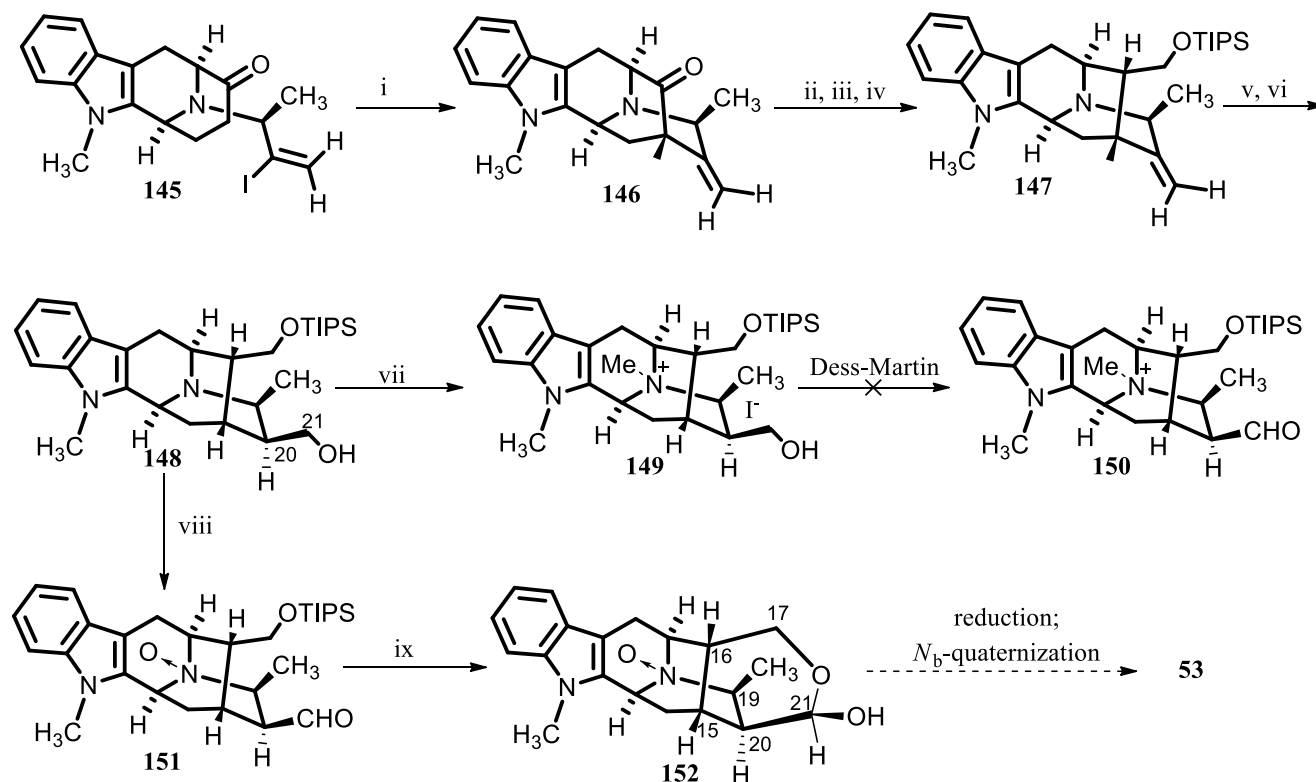


Scheme 7. Reagents and conditions: i) 1 *N* aq HCl (10 equiv), THF, reflux, 1 d, **88%**; ii) 1 *N* HCl (additional 10 equiv), reflux, 4 d, trace amount of **41**; iii) a. *p*-TSA•H₂O, CH₃OH, CHCl₃, reflux, 6

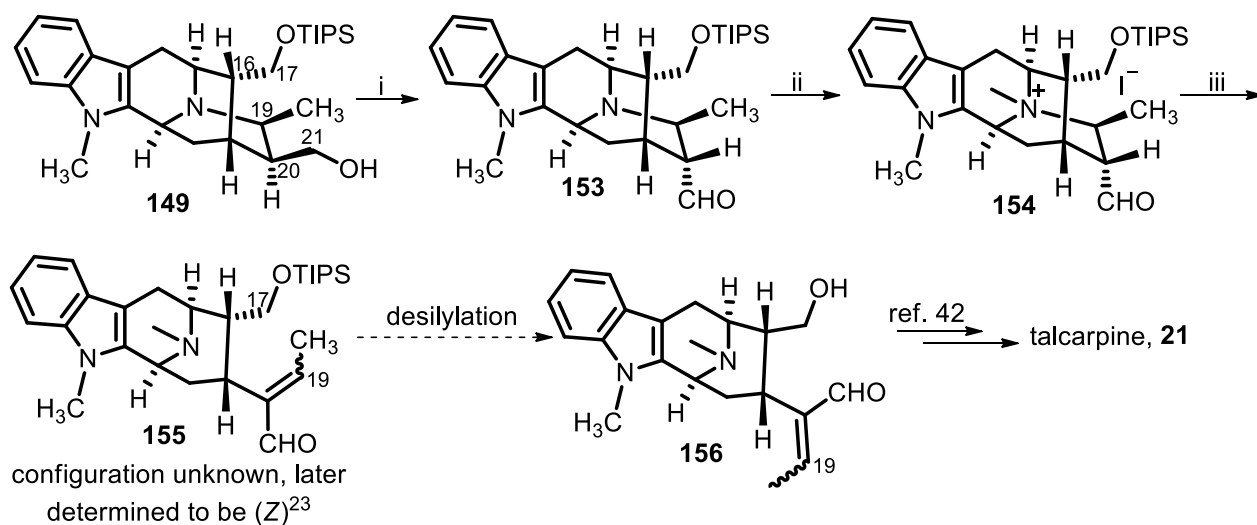
h, **93%**; b. BH_3 . DMS, THF, rt, 2 h, then $\text{NaBO}_3 \cdot 4\text{H}_2\text{O}$; Na_2CO_3 , CH_3OH , reflux, 5 h, **35%**; iv) 1 *N* aq HCl, THF, reflux, 1 d, **52%**.

In the same report,²⁶ Edwankar reported the attempted total synthesis of the quaternary N_b -nitrogen containing sarpagine alkaloid macrosalpine **53** and a formal synthesis of talcarpine **21** (Scheme 8). To access macrosalpine **53**, the N_a -methyl containing vinyl iodide **145** was subjected to a palladium catalyzed α -vinylation to provide the N_a -methylated pentacyclic ketone intermediate **146** in 68% yield. A one-carbon homologation of the ketone was achieved by a Wittig-hydrolysis sequence to furnish the thermodynamically more stable C-16 α -aldehyde in 90% yield. The aldehyde (not shown here) was reduced to a primary alcohol in the presence of sodium borohydride in ethanol in excellent yield. The subsequent protection of the primary alcohol with a triisopropylsilyl group was done in the presence of triisopropylsilyl triflate and 2,6-lutidine in CH_2Cl_2 at rt in 95% yield to furnish indole **147**. The hydroboration-oxidation of the olefin in **147** provided the C-20 β -hydroxymethyl intermediate **148** in 71% yield over two steps. The N_b -nitrogen atom was methylated with iodomethane in THF at 0 °C in the dark to provide the methiodide salt **149** in quantitative yield. The Dess-Martin oxidation of the quaternary ammonium containing primary alcohol was not successful to furnish the C-20 β -aldehyde **150**. Consequently, as an alternative approach, the monol **148** was oxidized with DMP in methylene chloride at rt for 3 hours to provide the C-20 β -aldehyde **151** in 67% yield, while the N_b -nitrogen formed an *N*-oxide. Several other oxidation protocols were also unsuccessful. The TIPS protection was removed under mild acidic conditions and the so formed primary alcohol reacted with the C-20 β -aldehyde to furnish the desired hemiacetal ring of macrosalpine **152**. The last step of the synthesis could not be carried out

due to the lack of material, but it was felt that macrosalphine **53** would be available from this macrosalphine *N*₄-oxide **152** by a reduction/quaternization sequence.²⁶



Scheme 8. Reagents and conditions: i) Pd₂(dba)₃, DPEPhos, *t*-BuONa, THF, 70 °C, **68%**; ii) Ph₃P(Cl)CH₂OCH₃, *t*-BuOK, PhH, rt, 13 h; then 2 *N* aq HCl, THF, 55 °C, 6 h, **90%**; iii) NaBH₄, EtOH, 0 °C-rt, **90%**; iv) TIPSOTf, 2,6-lutidine, CH₂Cl₂, rt, **95%**; v) BH₃.DMS, THF, rt, 2 h, NaBO₃.4H₂O; vi) Na₂CO₃, MeOH, reflux, 5 h, **81%** over two steps; vii) CH₃I, THF, 0 °C, overnight, **99%**; viii) DMP, CH₂Cl₂, 0 °C-rt, 3 h, **67%**; ix) aq 1 *N* HCl, THF, reflux, 2 h, **75%**.



Scheme 9. Reagents and conditions: i) NCS/DMS, CH₂Cl₂, -5 to -10 °C, cool to -78 °C, 2 h, Et₃N, 80%; ii) CH₃I, MeOH, rt, 85%; iii) *t*-BuOK, THF, rt, 60%.

4.3.4 Formal Synthesis of Talcarpine 21 by Edwankar et al.²⁶

In the formal synthesis of talcarpine **21**,²⁶ The Milwaukee group converted the *N*_a-methylated C-20 β-primary alcohol **149** into a mixture of α,β-epimeric aldehydes by Corey-Kim oxidation. This was followed by complete epimerization into the thermodynamically more stable C-20α-aldehyde **153**. This took place by treatment of the mixture with excess triethylamine in methanol at room temperature in 80% yield (Scheme 9). The quaternization of the *N*_b-nitrogen function with iodomethane in methanol at room temperature furnished the methiodide salt **154** in excellent yield. The methiodide salt underwent a *retro*-Michael ring opening to the α,β-unsaturated aldehyde **155** as a single isomer, of which the geometry of the olefin was not determined at that time, but was later determined to be the (*Z*)-geometry by Rahman et al.²³ This olefin provided the *macroline* framework, which upon desilylation would provide the important macroline equivalent **156** which

was used in the partial synthesis of talcarpine **21** by Sakai et al.⁴² by the degradation of ajmaline (*vide supra*). This was a much better route to talcarpine **21** than the previous routes.

5. Conclusion

Contained in this chapter is a compilation of research on approximately 70 alkaloids that could be categorized as C-19 methyl substituted sarpagine-macroline-ajmaline bases. Many of these alkaloids have important bioactivity, while the majority remain unexplored. More than a dozen of these alkaloids have been prepared in the laboratory, to date.²²⁻²⁶ With the increased number of reported C-19 methyl substituted alkaloids and novel bioactivity of the alkaloids, which belong to this group, it is anticipated the interest in the synthesis, biosynthesis, and activity of these alkaloids will grow. Most of the alkaloids await total synthesis and much exploration is required for the in depth bioactivity of these alkaloids including the unnatural enantiomers.

6. References

- (1) Burke, D. E.; DeMarkey, C. A.; Le Quesne, P.; Cook, J. M. *J. Chem. Soc., Chem. Commun.* **1972**, 1346.
- (2) Esmond, R. W.; Le Quesne, P. W. *J. Am. Chem. Soc.* **1980**, *102*, 7116.
- (3) Garnick, R. L.; Le Quesne, P. W. *J. Am. Chem. Soc.* **1978**, *100*, 4213.
- (4) Saxton, J. E. *Indoles, Part 4: The Monoterpenoid Indole Alkaloids*; John Wiley & Sons: Chichester, 1983.

- (5) Hamaker, L. K.; Cook, J. M. In *Alkaloids: Chemical and Biological Perspectives*; Pelletier, S. W., Ed.; Elsevier Science: New York: 1995; Vol. 9, p 23.
- (6) Lounasmaa, M.; Hanhinen, P.; Westersund (née Halonen), M. In *The Alkaloids: Chemistry and Biology*; Cordell, G. A., Ed.; Academic Press: San Diego, CA: 1999; Vol. 52, p 103.
- (7) Lounasmaa, M.; Hanhinen, P. In *The Alkaloids: Chemistry and Biology*; Cordell, G. A., Ed.; Academic Press: San Diego, 2001; Vol. 55, pp 1-90.
- (8) Namjoshi, O. A.; Cook, J. M. In *The Alkaloids: Chemistry and Biology*; Knölker, H.-J., Ed.; Academic Press: San Diego, CA: 2016; Vol. 76, p 63.
- (9) Ban, Y.; Murakami, Y.; Iwasawa, Y.; Tsuchiya, M.; Takano, N. *Med. Res. Rev.* **1988**, 8, 231.
- (10) Koskinen, A.; Lounasmaa, M. The Sarpagine-Ajmaline Group of Indole Alkaloids. In *Progress in the Chemistry of Organic Natural Products*; Herz, W., Grisebach, H., Kirby, G. W., Eds.; Springer-Verlag: New York, 1983; Vol. 43, p 267.
- (11) Cordell, G. A.; Quinn-Beattie, M. L.; Farnsworth, N. R. *Phytother. Res.* **2001**, 15, 183.
- (12) Cordell, G. A.; Colvard, M. D. *J. Nat. Prod.* **2012**, 75, 514.
- (13) Cordell, G. A.; Colvard, M. D. *J. Ethnopharmacol.* **2005**, 100, 5.
- (14) Cordell, G. A. *Phytochem. Rev.* **2002**, 1, 261.

- (15) Bi, Y.; Hamaker, L. K.; Cook, J. M. In *Studies in Natural Products Chemistry, Bioactive Natural Products, Part A*; Basha, F. Z., Rahman, A., Eds.; Elsevier Science: Amsterdam, 1993; Vol. 13, p 383.
- (16) Newman, D. J.; Cragg, G. M. *J. Nat. Prod.* **2012**, *75*, 311.
- (17) Liotta, D. C.; Painter, G. R. *Acc. Chem. Res.* **2016**, *49*, 2091.
- (18) Mathé, C.; Gosselin, G. *Antiviral Res.* **2006**, *71*, 276.
- (19) Sears, J. E.; Boger, D. L. *Acc. Chem. Res.* **2015**, *48*, 653.
- (20) Lukesh III, J. C.; Carney, D. W.; Dong, H.; Cross, R. M.; Shukla, V.; Duncan, K. K.; Yang, S.; Brody, D. M.; Brütsch, M. M.; Radakovic, A.; Boger, D. L. *J. Med. Chem.* **2017**, *60*, 7591.
- (21) Lounasmaa, M.; Hanhinen, P. *J. Nat. Prod.* **2000**, *63*, 1456.
- (22) Rahman, M. T.; Cook, J. M. *Eur. J. Org. Chem.* **2018**, 3224.
- (23) Rahman, M. T.; Deschamps, J. R.; Imler, G. H.; Cook, J. M. *Chem. Eur. J.* **2018**, *24*, 2354.
- (24) Rahman, M. T.; Deschamps, J. R.; Imler, G. H.; Schwabacher, A. W.; Cook, J. M. *Org. Lett.* **2016**, *18*, 4174.
- (25) Edwankar, R. V.; Edwankar, C. R.; Deschamps, J.; Cook, J. M. *Org. Lett.* **2011**, *13*, 5216.
- (26) Edwankar, R. V.; Edwankar, C. R.; Deschamps, J. R.; Cook, J. M. *J. Org. Chem.* **2014**, *79*, 10030.

- (27) M Heravi, M.; Zadsirjan, V.; Malmir, M. *Molecules* **2018**, *23*, 943.
- (28) Pan, L.; Terrazas, C.; Acuña, U. M.; Ninh, T. N.; Chai, H.; De Blanco, E. J. C.; Soejarto, D. D.; Satoskar, A. R.; Kinghorn, A. D. *Phytochem. Lett.* **2014**, *10*, 54.
- (29) Feng, T.; Li, Y.; Cai, X.-H.; Gong, X.; Liu, Y.-P.; Zhang, R.-T.; Zhang, X.-Y.; Tan, Q.-G.; Luo, X.-D. *J. Nat. Prod.* **2009**, *72*, 1836.
- (30) Cheng, G.-G.; Zhao, Y.-L.; Zhang, Y.; Lunga, P.-K.; Hu, D.-B.; Li, Y.; Gu, J.; Song, C.-W.; Sun, W.-B.; Liu, Y.-P. *Tetrahedron* **2014**, *70*, 8723.
- (31) Zhang, L.; Hua, Z.; Song, Y.; Feng, C. *Fitoterapia* **2014**, *97*, 142.
- (32) Le Men, J.; Taylor, W. I. *Experientia* **1965**, *21*, 508.
- (33) Buckingham, J.; Baggaley, K. H.; Roberts, A. D.; Szabo, L. F. *Dictionary of Alkaloids, with CD-ROM*; Taylor & Francis Group: Abington, UK, 2010.
- (34) Woodward, R. *Angew. Chem.* **1956**, *68*, 13.
- (35) Pfitzner, A.; Stöckigt, J. *Tetrahedron Lett.* **1983**, *24*, 5197.
- (36) Stephen, M. R.; Rahman, M. T.; Tiruveedhula, V.; Fonseca, G. O.; Deschamps, J. R.; Cook, J. M. *Chem. Eur. J.* **2017**, *23*, 15805.
- (37) Kam, T.-S.; Choo, Y.-M.; Komiyama, K. *Tetrahedron* **2004**, *60*, 3957.
- (38) Tan, S. J., Ph. D. Dissertation thesis, Department of Chemistry, Faculty of Science, University of Malaya, 2011.
- (39) Tan, S.-J.; Lim, J.-L.; Low, Y.-Y.; Sim, K.-S.; Lim, S.-H.; Kam, T.-S. *J. Nat. Prod.* **2014**, *77*, 2068.

- (40) Kam, T.-S.; Choo, Y.-M. *J. Nat. Prod.* **2004**, *67*, 547.
- (41) Naranjo, J.; Pinar, M.; Hesse, M.; Schmid, H. *Helv. Chim. Acta* **1972**, *55*, 752.
- (42) Takayama, H.; Phisalaphong, C.; Kitajima, M.; Aimi, N.; Sakai, S.-i. *Tetrahedron* **1991**, *47*, 1383.
- (43) Cheenpracha, S.; Ritthiwigrom, T.; Laphookhieo, S. *J. Nat. Prod.* **2013**, *76*, 723.
- (44) Ghedira, K.; Zeches-Hanrot, M.; Richard, B.; Massiot, G.; Le Men-Olivier, L.; Sevenet, T.; Goh, S. *Phytochemistry* **1988**, *27*, 3955.
- (45) Zaima, K.; Koga, I.; Iwasawa, N.; Hosoya, T.; Hirasawa, Y.; Kaneda, T.; Ismail, I. S.; Lajis, N. H.; Morita, H. *J. Nat. Med.* **2013**, *67*, 9.
- (46) Kam, T.-S.; Choo, Y.-M. *Phytochemistry* **2004**, *65*, 603.
- (47) Wong, W.-H.; Lim, P.-B.; Chuah, C.-H. *Phytochemistry* **1996**, *41*, 313.
- (48) Kam, T.-S.; Choo, Y.-M. *Tetrahedron* **2000**, *56*, 6143.
- (49) Kiang, A.; Wan, A. S. *J. Chem. Soc.* **1960**, 1394.
- (50) Li, C.-J.; Chen, S.; Sun, C.; Zhang, L.; Shi, X.; Wu, S.-J. *Fitoterapia* **2017**, *117*, 79.
- (51) Kohl, W.; Witte, B.; Sheldrick, W.; Höfle, G. *Planta Med.* **1984**, *50*, 242.
- (52) Lin, M.; Yang, B.-Q.; Yu, D.-Q. *Acta Pharmacol. Sin.* **1986**, *21*, 114.
- (53) Lin, M.; Yang, B.; Yu, D. In *Chem. Abstr.* **1986**; Vol. 104, p 221983r.

- (54) Sheludko, Y.; Gerasimenko, I.; Kolshorn, H.; Stöckigt, J. *J. Nat. Prod.* **2002**, *65*, 1006.
- (55) Kiang, A.; Loh, S.; Demanczyk, M.; Gemenden, C.; Papariello, G.; Taylor, W. *Tetrahedron* **1966**, *22*, 3293.
- (56) Nasser, A. *J. Ethnopharmacol.* **1984**, *11*, 99.
- (57) Nasser, A. M. *Phytochemistry* **1983**, *22*, 2297.
- (58) Iwu, M. *Planta Med.* **1982**, *45*, 105.
- (59) Gao, Y.; Yu, A.-L.; Li, G.-T.; Hai, P.; Li, Y.; Liu, J.-K.; Wang, F. *Fitoterapia* **2015**, *107*, 44.
- (60) Gao, Y.; Zhou, D.-S.; Kong, L.-M.; Hai, P.; Li, Y.; Wang, F.; Liu, J.-K. *Nat. Prod. Bioprospect.* **2012**, *2*, 65.
- (61) Akinloye, B. *Planta Med.* **1979**, *37*, 361.
- (62) Khan, Z. M.; Hesse, M.; Schmid, H. *Helv. Chim. Acta* **1967**, *50*, 1002.
- (63) Zeng, J.; Zhang, D.-B.; Zhou, P.-P.; Zhang, Q.-L.; Zhao, L.; Chen, J.-J.; Gao, K. *Org. Lett.* **2017**, *19*, 3998.
- (64) Zhang, Z. J.; Du, R. N.; He, J.; Wu, X. D.; Li, Y.; Li, R. T.; Zhao, Q. S. *Helv. Chim. Acta* **2016**, *99*, 157.
- (65) Stöckigt, J.; Pfitzner, A.; Firl, J. *Plant Cell Rep.* **1981**, *1*, 36.
- (66) Geng, C.-A.; Liu, X.-K. *Fitoterapia* **2013**, *89*, 42.
- (67) Atallah Khan, M.; Siddiqui, S. *Cell. Mol. Life Sci.* **1972**, *28*, 127.

- (68) Sabino, J. R.; Kato, L.; Braga, R. M.; Vencato, I. *Acta Cryst. E* **2006**, *62*, o3181.
- (69) Glasby, J. *Encyclopedia of the Alkaloids: Vol. 2*; Plenum Press: New York, 1975.
- (70) Batista, C. V. F.; Schripsema, J.; Verpoorte, R.; Rech, S. B.; Henriques, A. T. *Phytochemistry* **1996**, *41*, 969.
- (71) Sultana, A.; Nighat, F.; Bhatti, M. K.; Kurucu, S.; Kartal, M. *Phytochemistry* **1995**, *38*, 1057.
- (72) Cao, P.; Liang, Y.; Gao, X.; Li, X.-M.; Song, Z.-Q.; Liang, G. *Molecules* **2012**, *17*, 13631.
- (73) Boğa, M.; Kolak, U.; Topçu, G.; Bahadori, F.; Kartal, M.; Farnsworth, N. R. *Phytochem. Lett.* **2011**, *4*, 399.
- (74) Lim, S.-H.; Low, Y.-Y.; Sinniah, S. K.; Yong, K.-T.; Sim, K.-S.; Kam, T.-S. *Phytochemistry* **2014**, *98*, 204.
- (75) Ratnayake, C. K.; Arambewela, L. S.; De Silva, K.; Alvi, K. *Phytochemistry* **1987**, *26*, 868.
- (76) Keawpradub, N.; Houghton, P.; Eno-Amooquaye, E.; Burke, P. *Planta Med.* **1997**, *63*, 97.
- (77) Keawpradub, N.; Kirby, G.; Steele, J.; Houghton, P. *Planta Med.* **1999**, *65*, 690.
- (78) Kam, T.-S.; Iek, H.; Choo, Y.-M. *Phytochemistry* **1999**, *51*, 839.
- (79) Habib, M. S. *Phytochemistry* **1974**, *13*, 661.
- (80) Kiang, A.; Wan, A.; Goh, H. *Lloydia* **1964**, *27*, 220.

- (81) Amer, M. M. *Phytochemistry* **1980**, *19*, 1833.
- (82) Pousset, J.; Poisson, J. In *Annales Pharmaceutiques Francaises* 1965; Vol. 23, p 733.
- (83) Akinloye, B. A. *Phytochemistry* **1980**, *19*, 307.
- (84) Arthur, H.; Johns, S.; Lamberton, J.; Loo, S. *Aust. J. Chem.* **1968**, *21*, 1399.
- (85) Iwu, M. *Planta Med.* **1978**, *33*, 232.
- (86) Iwu, M. M. *Phytochemistry* **1978**, *17*, 1651.
- (87) Amer, M. A. *Phytochemistry* **1981**, *20*, 2569.
- (88) Akinloye, B. A. *Phytochemistry* **1980**, *19*, 2741.
- (89) Subhadhirasakul, S.; Takayama, H.; Aimi, N.; Ponglux, D.; Sakai, S.-i. *Chem. Pharm. Bull.* **1994**, *42*, 1427.
- (90) Peraza-Sánchez, S. R.; Gamboa-Angulo, M. M.; Erosa-López, C.; Ramírez-Erosa, I.; Escalante-Erosa, F.; Peña-Rodríguez, L. M.; Loyola-Vargas, V. M. *Nat. Prod. Lett.* **1998**, *11*, 217.
- (91) Wang, C.-H.; Zhang, Y.; Jiang, M.-M. *Chem. Nat. Comp.* **2014**, *49*, 1177.
- (92) Libot, F.; Kunesch, N.; Poisson, J. *Phytochemistry* **1980**, *19*, 989.
- (93) Cai, X. H.; Zeng, C. X.; Feng, T.; Li, Y.; Luo, X. D. *Helv. Chim. Acta* **2010**, *93*, 2037.
- (94) Ulshafer, P.; Bartlett, M.; Dorfman, L.; Gillen, M.; Schlittler, E.; Wenkert, E. *Tetrahedron Lett.* **1961**, *2*, 363.

- (95) Khan, M. A.; Horn, H.; Voelter, W. *Z. Naturforsch. B* **1982**, *37*, 494.
- (96) Abaul, J.; Philogène, E.; Bourgeois, P.; Mérault, G.; Poupat, C.; Ahond, A.; Potier, P. *J. Nat. Prod.* **1986**, *49*, 829.
- (97) A. Madinaveitia, E. Valencia, J. Bermejo and A. G. Gonzalez, *Biochem. Syst. Ecol.* **1995**, *23*, 877.
- (98) Carlos, L. A.; Mathias, L.; Braz-Filho, R.; Vieira, I. J. C. *Quím. Nova* **2016**, *39*, 156.
- (99) Baldwin, A. S. *J. Clin. Invest.* **2001**, *107*, 241.
- (100) Baeuerle, P. A.; Henkel, T. *Annu. Rev. Immunol.* **1994**, *12*, 141.
- (101) Gui-yun, Z.; Bao-hong, T.; Rong, Z.; Li-fen, D.; Chao, X. *Acta Pharmacol. Sin.* **1991**, *12*, 471.
- (102) Sun, L.; Ruppert, M.; Sheludko, Y.; Warzecha, H.; Zhao, Y.; Stöckigt, J. *Plant Mol. Biol.* **2008**, *67*, 455.
- (103) Pathania, S.; Randhawa, V.; Bagler, G. *PLoS One* **2013**, *8*, e61327.
- (104) Wu, F.; Kerčmar, P.; Zhang, C.; Stöckigt, J. In *The Alkaloids: Chemistry and Biology*; Knölker, H.-J., Ed.; Academic Press: San Diego, CA: 2016; Vol. 76, p 1.
- (105) Zhang, J.; Abdel-Mageed, W. M.; Liu, M.; Huang, P.; He, W.; Li, L.; Song, F.; Dai, H.; Liu, X.; Liang, J. *Org. Lett.* **2013**, *15*, 4726.
- (106) Wang, F.-P.; Liang, X.-T. In *The Alkaloids*; Cordell, G. A., Ed.; Academic Press: San Diego, CA, 2002; Vol. 59, pp 1-280.

- (107) Sun, L.; Chen, Y.; Rajendran, C.; Mueller, U.; Panjikar, S.; Wang, M.; Mindnich, R.; Rosenthal, C.; Penning, T. M.; Stöckigt, J. *J. Biol. Chem.* **2012**, *287*, 11213.
- (108) Rosenthal, C.; Mueller, U.; Panjikar, S.; Sun, L.; Ruppert, M.; Zhao, Y.; Stöckigt, J. *Acta Cryst. F* **2006**, *62*, 1286.
- (109) Wang, T.; Cook, J. M. *Org. Lett.* **2000**, *2*, 2057.
- (110) Cao, H.; Yu, J.; Wearing, X. Z.; Zhang, C.; Liu, X.; Deschamps, J.; Cook, J. M. *Tetrahedron Lett.* **2003**, *44*, 8013.
- (111) Stöckigt, J. In *The Alkaloids*; Cordell G. A., Ed.; Academic: San Diego, 1995; Vol. 47, p 115.
- (112) Court, W. *Planta Med.* **1983**, *48*, 228.
- (113) Takayama, H.; Phisalaphong, C.; Kitajima, M.; Aimi, N.; Sakai, S.-i.; Stöckigt, J. *Chem. Pharm. Bull.* **1991**, *39*, 266.
- (114) Sheludko, Y.; Gerasymenko, I. In *Biotechnology for Medicinal Plants*; Chandra, S., Lata H., Varma A., Eds.; Springer: 2013, p 241.
- (115) Polz, L.; Schübel, H.; Stöckigt, J. *Z. Naturforsch.* **1987**, *42*, 333.
- (116) Ruyter, C. M.; Schübel, H.; Stöckigt, J. *Z. Naturforsch. C Bio. Sci.* **1988**, *43*, 479.
- (117) Schübel, H.; Ruyter, C. M.; Stöckigt, J. *Phytochemistry* **1989**, *28*, 491.
- (118) Stöckigt, J.; Schübel, H. *NATO ASI Series. H* **1988**, *18*, 251.
- (119) Taylor, W.; Frey, A.; Hofmann, A. *Helv. Chim. Acta* **1962**, *45*, 611.
- (120) Yu, P.; Wang, T.; Li, J.; Cook, J. M. *J. Org. Chem.* **2000**, *65*, 3173.

- (121) van Tamelen, E. E.; Oliver, L. *J. Am. Chem. Soc.* **1970**, *92*, 2136.
- (122) van Tamelen, E.; Oliver, L. *Bioorg. Chem.* **1976**, *5*, 309.
- (123) Liao, X.; Zhou, H.; Wearing, X. Z.; Ma, J.; Cook, J. M. *Org. Lett.* **2005**, *7*, 3501.
- (124) Zhao, S.; Liao, X.; Wang, T.; Flippen-Anderson, J.; Cook, J. M. *J. Org. Chem.* **2003**, *68*, 6279.
- (125) Gan, T.; Cook, J. M. *Tetrahedron Lett.* **1996**, *37*, 5033.
- (126) Edwankar, C. R.; Edwankar, R. V.; Deschamps, J. R.; Cook, J. M. *Angew. Chem.* **2012**, *124*, 11932.
- (127) Cloudsdale, I. S.; Kluge, A. F.; McClure, N. L. *J. Org. Chem.* **1982**, *47*, 919.
- (128) Esmond, R. W.; Le Quesne, P. W. *J. Am. Chem. Soc.* **1980**, *102*, 7116.
- (129) Miller, K. A.; Martin, S. F. *Org. Lett.* **2007**, *9*, 1113.
- (130) Deiters, A.; Chen, K.; Eary, C. T.; Martin, S. F. *J. Am. Chem. Soc.* **2003**, *125*, 4541.
- (131) Magnus, P.; Mugrage, B.; DeLuca, M. R.; Cain, G. A. *J. Am. Chem. Soc.* **1990**, *112*, 5220.
- (132) Bailey, P. D.; Clingan, P. D.; Mills, T. J.; Price, R. A.; Pritchard, R. G. *Chem. Commun.* **2003**, 2800.
- (133) Bailey, P. D.; Morgan, K. M. *J. Chem. Soc., Perkin Trans. 1* **2000**, 3578.
- (134) Krüger, S.; Gaich, T. *Angew. Chem. Int. Ed.* **2015**, *54*, 315.

- (135) Krüger, S.; Gaich, T. *Eur. J. Org. Chem.* **2016**, 2016, 4893.
- (136) Kitajima, M.; Watanabe, K.; Maeda, H.; Kogure, N.; Takayama, H. *Org. Lett.* **2016**, 18, 1912.
- (137) Kadam, V. D.; Rao B, S. S.; Mahesh, S.; Chakraborty, M.; Vemulapalli, S. P. B.; Dayaka, S. N.; Sudhakar, G. *Org. Lett.* **2018**, 20, 4782-4786.
- (138) Tran, Y. S.; Kwon, O. *Org. Lett.* **2005**, 7, 4289.
- (139) Ohba, M.; Natsutani, I.; Sakuma, T. *Tetrahedron Lett.* **2004**, 45, 6471.
- (140) Yanagisawa, A.; Habaue, S.; Yamamoto, H. *J. Am. Chem. Soc.* **1991**, 113, 8955.
- (141) Liao, X.; Zhou, H.; Yu, J.; Cook, J. M. *J. Org. Chem.* **2006**, 71, 8884.

PART I. IMPROVED AND SHORTER ACCESS TO THE KEY TETRACYCLIC CORE OF C-19 METHYL SUBSTITUTED BIOACTIVE SARPAGINE-MACROLINE-AJMALINE INDOLE ALKALOIDS VIA A NEW ASYMMETRIC PICTET-SPENGLER REACTION STARTING FROM EITHER D-(+)- OR L-(-)-TRYPTOPHAN

Chapter 1

A Shorter and Improved Access to the Bicyclo[3.3.1]nonane Core of Sarpagine/Macroline/Ajmaline Alkaloids

1. Introduction

Extension of the asymmetric Pictet-Spengler reaction to bulkier N_b -alkylated tryptophan derivatives resulted in an improved stereospecific access to the key azabicyclo[3.3.1]nonane core of bioactive C-19 methyl substituted sarpagine/macroline/ajmaline indole alkaloids with excellent diastereoselectivity *via* internal asymmetric induction. Complete stereocontrol of the C-19 methyl function in either the α - or β -configuration was achieved which enables the total synthesis of any member from this group of seventy alkaloids.

The C-19 methyl substituted macroline/sarpagine and ajmaline alkaloids are an emerging group of biosynthetically related indole alkaloids, some of which have historical significance,¹ and have been primarily isolated from various medicinal plants of the *Apocynaceae* family. Currently, about thirty alkaloids belong to this group. Some of them are depicted in Figure 1. Most of these alkaloids have not been tested for their biological activity, presumably, due to the paucity of isolated material. Yet, some of these alkaloids have been shown to possess important biological activity ranging from anti-hypertensive to anticancer properties. Macrocarpines A-C (**1-3**) have been isolated from the stem bark of *Alstonia macrophylla* by Kam.² Talcarpine (**4**), which was isolated from *Alstonia macrophylla* and *Pleiocarpa talbotii*, exhibited antimalarial activity.³⁻⁵ The $N(4)$ -methyl- $N(4),21$ -secotalpinine **5**, isolated from *Pleiocarpa talbotii* and *Alstonia angustifolia*, demonstrated promising anti-leishmanial activity.^{2,4,6} Talpinine **6**, another related alkaloid, exhibited moderate activity in reversing multidrug resistance in a vincristine-resistant KB/VJ300 cell line in the presence of 0.12 μ M vincristine.^{4,7} The $N(4)$ -methyltalpinine **7**, which contains a quaternary N_b -nitrogen atom, is the N_b -methylated version of talpinine **6**, and has shown potent and important NF κ B inhibition.⁶ While the majority of these alkaloids have the β methyl configuration at C-19, a few contain the α C-19 methyl function (e.g., dihydroperaksine **8**, also

known as dihydrovomifoline and deoxyperaksine **9**).⁸⁻¹¹ All of these alkaloids bear either an N_a -methyl or N_a -hydrogen substituted indole nitrogen atom. Similarly, the N_b -nitrogen atom also varies in the pattern of substitution. In addition, all of these alkaloids contain 6 or 7 quaternary centers with various substitution patterns and configurations, which renders the synthesis of these alkaloids of interest. The challenge to access the complex architecture of these alkaloids and their promising biological activity stimulated our interest in the total synthesis of these natural products *via* a general strategy. To illustrate the feasibility of this strategy to access either the α or β C-19 methyl substituted alkaloids stereospecifically, herein we report the total synthesis of (-)-macrocarpines A-C (**1-3**), (-)-talcarpine (**4**), (+)- $N(4)$ -methyl- $N(4),21$ -secotalpinine (**5**), (+)-dihydroperaksine (**8**) and (-)-deoxyperaksine (**9**) with complete stereocontrol of the methyl function at C-19.

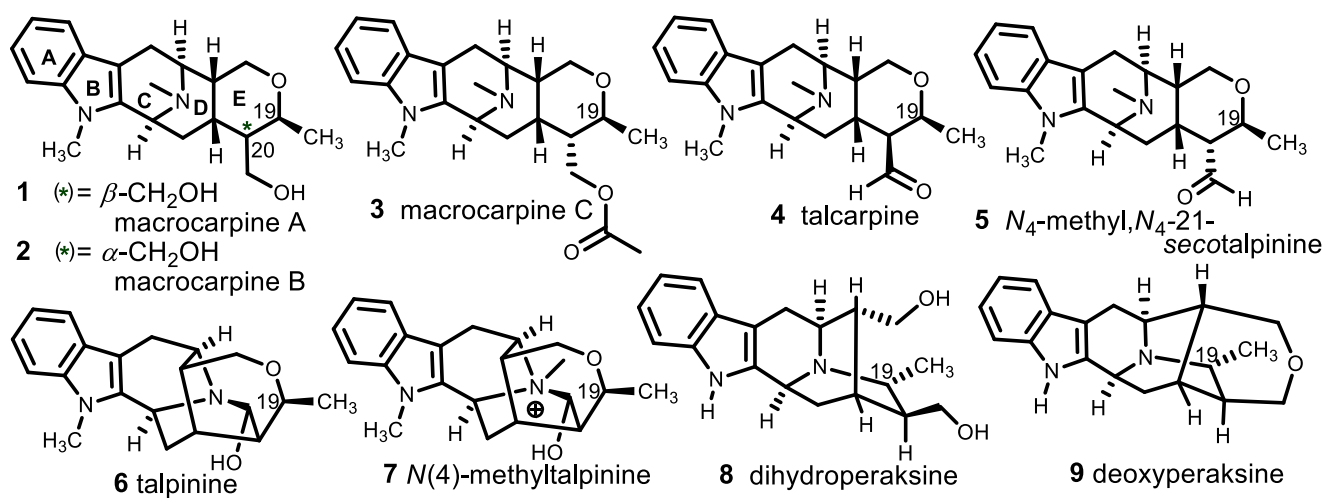
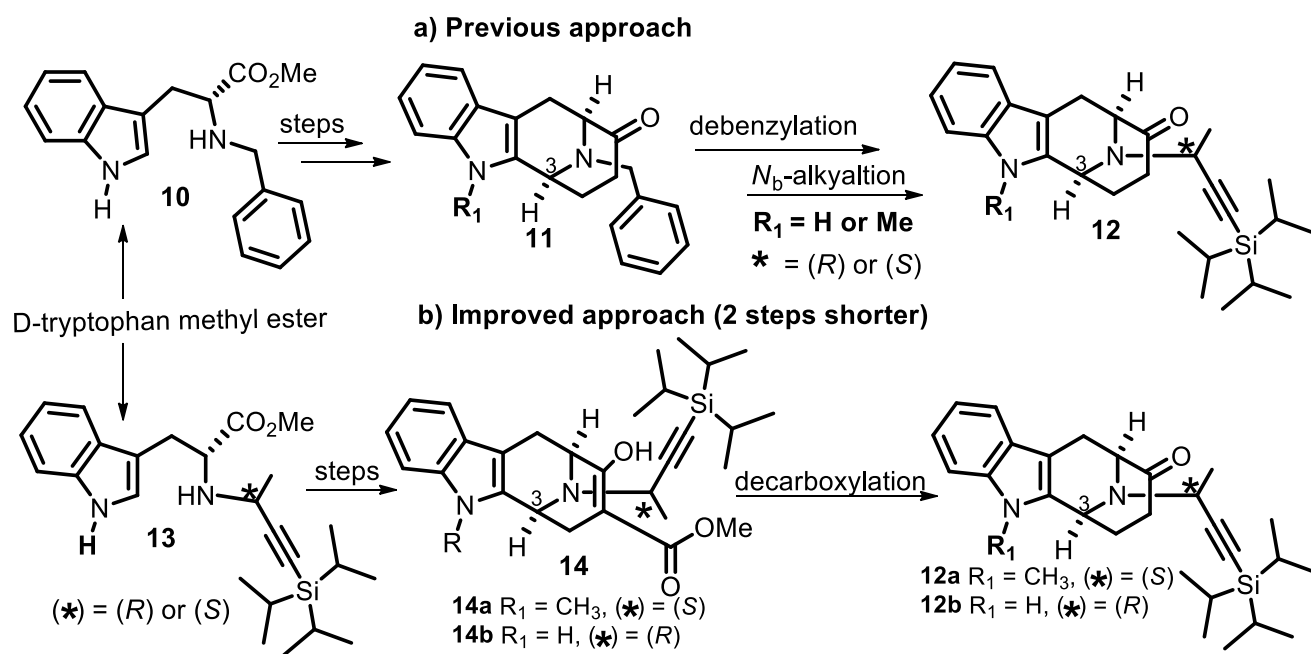


Figure 1. Representative examples of chiral C-19 methyl substituted macroline/sarpagine alkaloids.

The Pictet-Spengler reaction is among the most useful reactions in organic chemistry and probably the best one to access the tetrahydro- β -carboline and tetrahydroisoquinoline systems.¹²⁻¹⁵ The asymmetric version of this reaction has been used in numerous instances for stereospecific access to this system and has been the key to the total synthesis of numerous indole, bisindole, and oxindole alkaloids.¹⁶⁻²³ In this vein, the synthesis of numerous alkaloids of the sarpagine, macroline, and ajmaline group, have been accessed *via* the *trans*-diester/Dieckmann protocol, in excellent yield and with 100% diastereoselectivity.^{13,18,24,25} This diastereospecific cyclization reaction sets the required stereochemistry at the C-3 position for the target natural products, beginning with commercially available D-(+)-tryptophan.^{13,24}



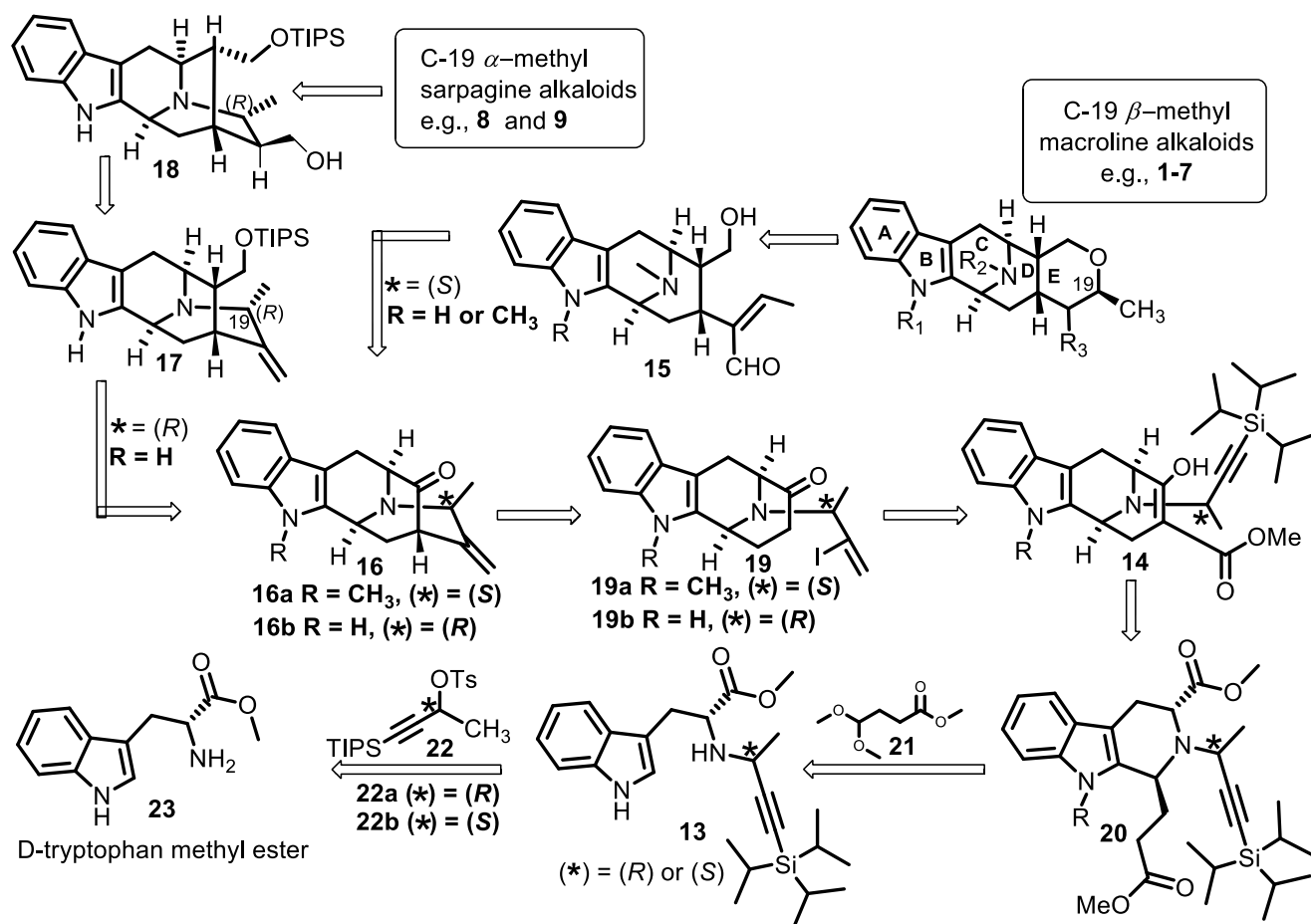
Scheme 1. Stereospecific access to the bicyclo[3.3.1]nonane system **12**

In the present report extension of the asymmetric Pictet-Spengler reaction to other N_b -alkyl systems was explored. The N_b -alkylated compounds (see **12**, Scheme 1) are key intermediates that have been used in the total synthesis of several sarpagine and macroline related indole alkaloids which contain a stereogenic methyl function at the C-19 position of the core structure.²⁶ In the strategy developed by Edwankar et al,²⁶ the N_b -alkyl tethered functionality was introduced after accessing the bicyclo[3.3.1]nonane system in **11**. Despite the robustness of this strategy (Scheme 1a), it was felt useful to reduce the number of steps by avoiding some earlier transformations while retaining compatibility with various conditions necessary for accessing the desired system in high *ee* and *de*. In this respect, the strategy was to avoid the initial benzylation and later debenylation by simply alkylating the N_b -nitrogen atom at the beginning of the synthesis (Scheme 1b). It would be advantageous if this could be done in a stereospecific fashion. This would shorten the synthesis by two steps but still retain the robust nature of the route. In addition, as mentioned, this would expand the use of the asymmetric Pictet-Spengler reaction and the Dieckmann cyclization with the bulky TIPS protected ethynyl N_b -alkyl system. The target system **12** would be accessible simply by decarboxylation of the products (see **14**) from the Dieckmann cyclization.

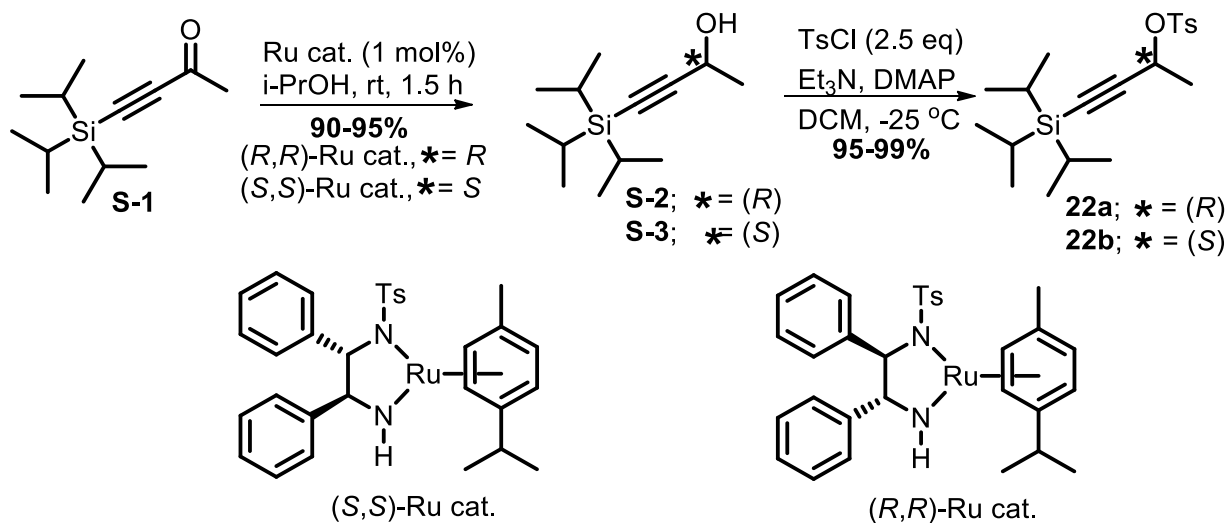
2. Results and Discussion

Retrosynthetically, the E-ring of the macroline system present in e.g., macrocarpines A-C (**1-3**) should originate in a stereocontrolled fashion from the Michael-type ring closure²⁷ of the deprotected alcohol onto the α,β -unsaturated aldehyde (**15**, Scheme 2), which in turn would be available from the pentacyclic ketone intermediates **16** [R = H or CH₃ and (*) = (*S*)], according to the previously reported route.^{26,28} On the other hand, the C-19 α -methylated alkaloids

dihydroperaksine **8** and deoxyperaksine **9** would be available from the TIPS protected diol **18**, which in turn would be, available from **17** by a hydroboration-oxidation. The olefin **17** would be accessed from the ketone **16** [with R = H and (*) = (*R*)] in a few steps. The pentacyclic ketone intermediates (see **16**) would be available *via* a copper-mediated intramolecular cross-coupling of the vinyl iodides **19** with the enolate.²⁸ The vinyl iodides (**19**) would be available from the TIPS-protected terminal alkyne *via* a completely regioselective iodoboration, after the decarboxylation of the β -keto ester **14**. The *trans*-diester would originate as a sole product from the asymmetric Pictet-Spengler reaction of the *N*_b-alkylated tryptophan derivative **13** with the acetal **21** under thermodynamic control. Under these conditions the total synthesis would begin from commercially available D-(+)-tryptophan **23** and the optically pure ethynyl tosylates (see **22**).



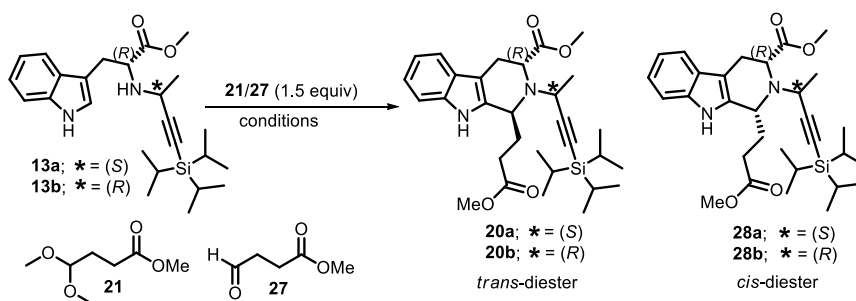
Scheme 2. Retrosynthetic analysis for the total synthesis of the C-19 methyl substituted macroline/sarpagine-related alkaloids via the asymmetric Pictet-Spengler reaction



Scheme 3. Synthesis of the optically pure tosylate units **22a** and **22b** via Noyori asymmetric hydrogenation of ketone **S-1**

The optically pure tosylate units **22a** and **22b** were synthesized²⁹ via Noyori asymmetric hydrogenation³⁰ of the ketone **S-1** with (*S,S*)-Ru and (*R,R*)-Ru catalysts to provide the corresponding chiral alcohol **S-3** and **S-2**, respectively (Scheme 3).

Table 1: Pictet-Spengler reaction of **13a** or **13b** with **21** or **27** under different conditions (see Table)



entry	SM	(*)	21 or 27 (equiv)	conditions	<i>trans</i> : <i>cis</i> ^a 20a: 28a or 20b: 28b	% overall yield ^b
1	13a	(<i>S</i>)	21 (1.5)	CF ₃ COOH, CH ₂ Cl ₂ , rt, 11 d	95: 5	89

2	13a	(<i>S</i>)	21 (1.5)	CH ₃ COOH, CH ₂ Cl ₂ , rt- reflux, up to 72 h	NR	SM
3	13a	(<i>S</i>)	21 (1.5)	CH ₃ COOH, CHCl ₃ , rt- reflux, up to 72 h	NR	SM
4	13a	(<i>S</i>)	21 (1.5)	CH ₃ SO ₃ H, CH ₂ Cl ₂ , 0 °C-rt	decomposition	-
5	13b	(<i>R</i>)	21 (1.5)	CF ₃ COOH, CH ₂ Cl ₂ , rt, 10 d	inseparable	-
6	13b	(<i>R</i>)	21 (1.5)	CH ₃ COOH, CHCl ₃ , reflux, up to 72 h	NR	SM
7	13b	(<i>R</i>)	27 (1.5)	CH ₂ Cl ₂ , rt, 36 h	NR	SM
8	13b	(<i>R</i>)	27 (1.5)	CH ₃ COOH, CH ₂ Cl ₂ , rt, up to 70 h	30: 70	95
9	28a	(<i>S</i>)	-	CF ₃ COOH, CH ₂ Cl ₂ , rt, 8 h	100: 0	84 (20a)
10	28a	(<i>S</i>)	-	CH ₃ COOH, CH ₂ Cl ₂ , rt, 24 h	-	SM (28a)
11	28b	(<i>R</i>)	-	CF ₃ COOH, CH ₂ Cl ₂ , rt, 8 h	100: 0	80 (20b)
12	28b	(<i>R</i>)	-	CH ₃ COOH, CH ₂ Cl ₂ , rt, 24 h	-	SM (28b)

[a] *trans: cis* ratio after chromatographic separation; [b] combined isolated yield

According to the plan, The *N*_b-nitrogen atom was alkylated with the optically pure TIPS protected tosylate units **22a** or **22b**, to introduce the ethynyl functions into indoles **13a** (Scheme 4) and **13b** (Scheme 5), respectively. The tosylate units were synthesized from the corresponding ketone (see the Experimental Section for details) *via* a ruthenium catalyzed Noyori asymmetric hydrogenation,^{29,31} followed by tosylation of the alcohol with TsCl. Reaction of the tosylate units **22a/22b** with the amine **23** in the presence of K₂CO₃ in CH₃CN furnished the S_N2 substituted products **13a** or **13b** (individually) in high yield, respectively. The structures and stereochemistry of **13a** (Figure 2) and **13b** (Figure 3) were confirmed by X-ray analysis (see Appendix A for X-ray data).

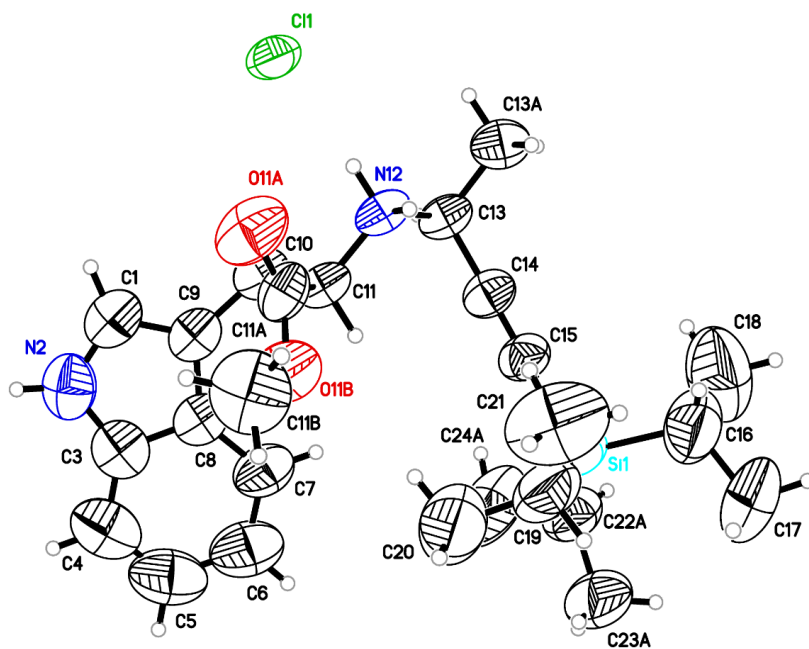


Figure 2: ORTEP representation of **13a·HCl**

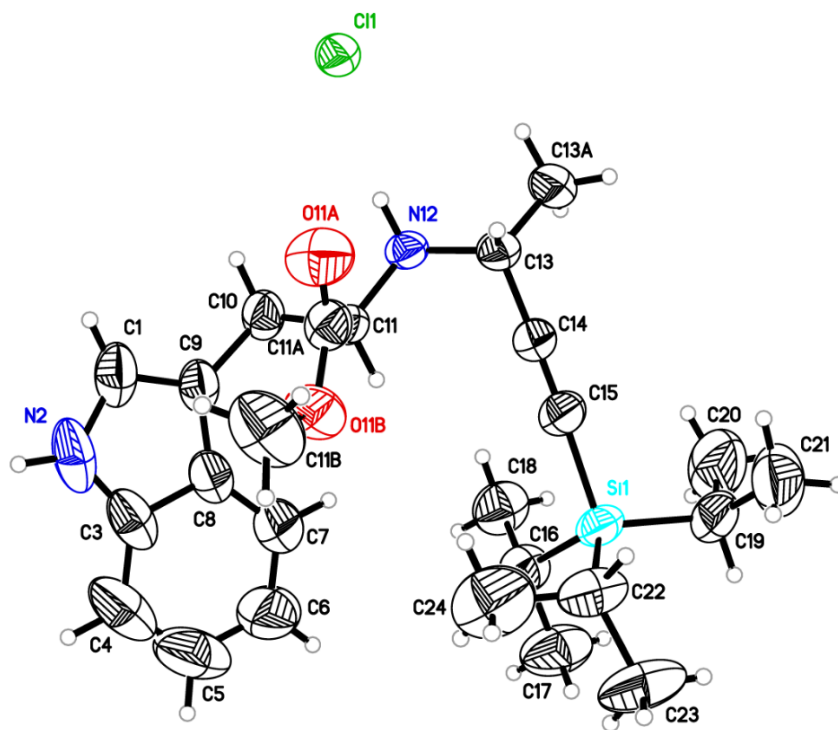
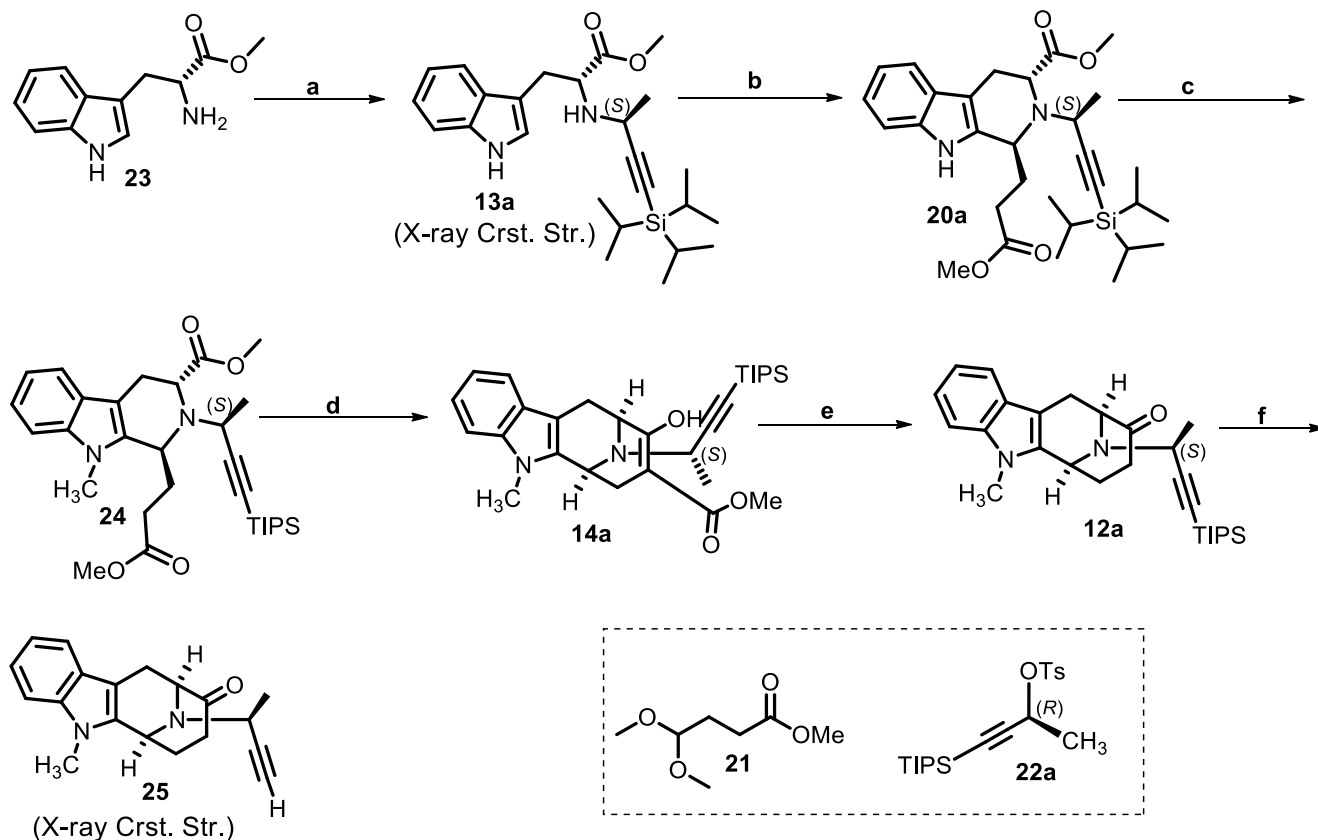


Figure 3: ORTEP representation of **13b·HCl**

When **13a** was reacted with the acetal **21** under the thermodynamic conditions of the Pictet-Spengler reaction developed previously,²⁵ the *trans*-diester was obtained in >95:5 diastereoselectivity (Table 1, entry 1). After initial success of the Pictet-Spengler reaction with the β -methyl [i.e., (*S*)] function **13a**, the same reaction conditions were then applied to the α -methyl [i.e., (*R*)] version **13b**, but this process resulted in incomplete reaction and complex reaction mixtures (Table 1, entry 5). At that point, a modified method was required to reduce the reaction time in the case of the α -methyl compound **13b** in order to obtain conversion before decomposition. The use of a weaker acid (acetic acid) than TFA or a stronger acid (methanesulfonic acid) were not successful (Table 1, entries 2-4, 6). The lack of conversion was, presumably, due to the low acidity of acetic acid and low reactivity of the acetal **21** whereas, MeSO₃H was too acidic. However, when the acetal **21** was replaced by the aldehyde **27**, which was freshly prepared by the hydrolysis of the acetal **21**, and this mixture was stirred with the amine and acetic acid in DCM at room temperature, this gave the *cis*-diester as the major product (*cis*:*trans* = 70:30) and in overall 95% isolated yield (Table 1, entry 8). Both the *cis*- and *trans*-diesters could easily be purified by chromatography and their stereochemistry was confirmed by NOE analysis. Importantly, the isolated *cis*-diester could be converted into the *trans*-diester with 100% diastereoselectivity on treatment with TFA in DCM at room temperature (Table 1, entries 9, 11). If the *cis* compound was stirred in acetic acid, the stereochemistry of these diastereomers (**28a** or **28b**) remained unchanged (table 1, entries 10, 12). Nevertheless, having the *trans*-diester with both α and β -methyl functions in hand, with 100% diastereoselectivity, was key to test the feasibility of this synthetic strategy.



Scheme 4: Reagents and conditions: a) **22a** (1.5 equiv), K₂CO₃ (2.5 equiv), CH₃CN, 65 °C, 12 h, **85%**; b) **21** (1.5 equiv), TFA (2.5 equiv), CH₂Cl₂, 11 d, dr = >95: 5, **89%**; c) NaH (1.1 equiv), CH₃I (1.1 equiv), DMF, -10 °C to 0 °C, 3 h, **96%**; d) NaH (3 equiv), MeOH (6 equiv), toluene, 110 °C, 8 h, **80%**; e) CH₃COOH (glacial), HCl (conc.), H₂O, 110-130 °C, 7 h, **82%**; f) TBAF (1.5 equiv), THF, 0 °C-rt, 3 h, **90%**.

The *N*_b-alkylated intermediate **13a** reacted with the acetal **21** under thermodynamically controlled conditions of the asymmetric Pictet-Spengler condensation to furnish the desired *trans*-diester **20a** in excellent yield (Scheme 4). This *trans*-transfer of chirality set the required (*S*) stereochemistry at C-3 of the macroline-sarpagine related alkaloids. Methylation of the indole nitrogen with iodomethane in the presence of sodium hydride in DMF at 0 °C, yielded the *N*_a-CH₃ intermediate

24 in 96% yield. Dieckmann cyclization of the *trans*-diester was felt to be troublesome due to the steric congestion surrounding the 1,2,3,-trisubstituted tetrahydro- β -carboline system **24**. However, when 3 equivalents of NaOMe (produced *in situ*) was reacted with *trans*-diester **31** in pre-dried toluene at reflux (DST), the Dieckmann cyclization proceeded smoothly to furnish the β -keto ester (**14a**) in 80% yield. The hydrolysis of the ester or deprotection of the TIPS group was not observed during the cyclization. This step was crucial for the success of this synthetic route. Subsequently, decarboxylation of the β -keto ester under acidic conditions furnished the N_b - ethinyl tethered tetracyclic ketone **12a** without deprotection of the TIPS function. This route provided an improved synthesis of this intermediate **12a** by successfully avoiding the initial benzylation/debenzylation steps and effectively shortened the route by at least two steps. The spectral properties of this intermediate **12a** and optical rotation were identical in all respects, to an authentic sample of **12a**, synthesized *via* the previously reported route.²⁶ This was further confirmed by X-ray crystallography after the deprotection of the TIPS function (**25**) with TBAF in THF (90% yield). An ORTEP drawing of ketone **25** is included in Figure 4 (see Appendix A for X-ray crystallographic data).

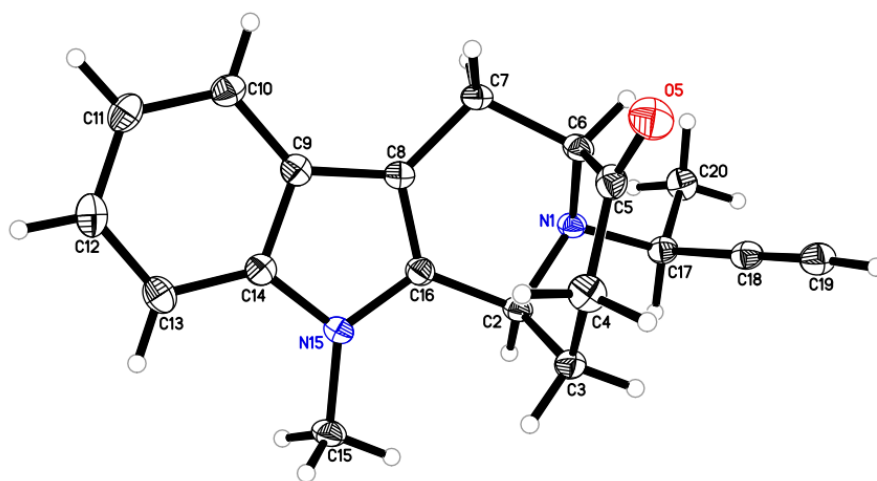
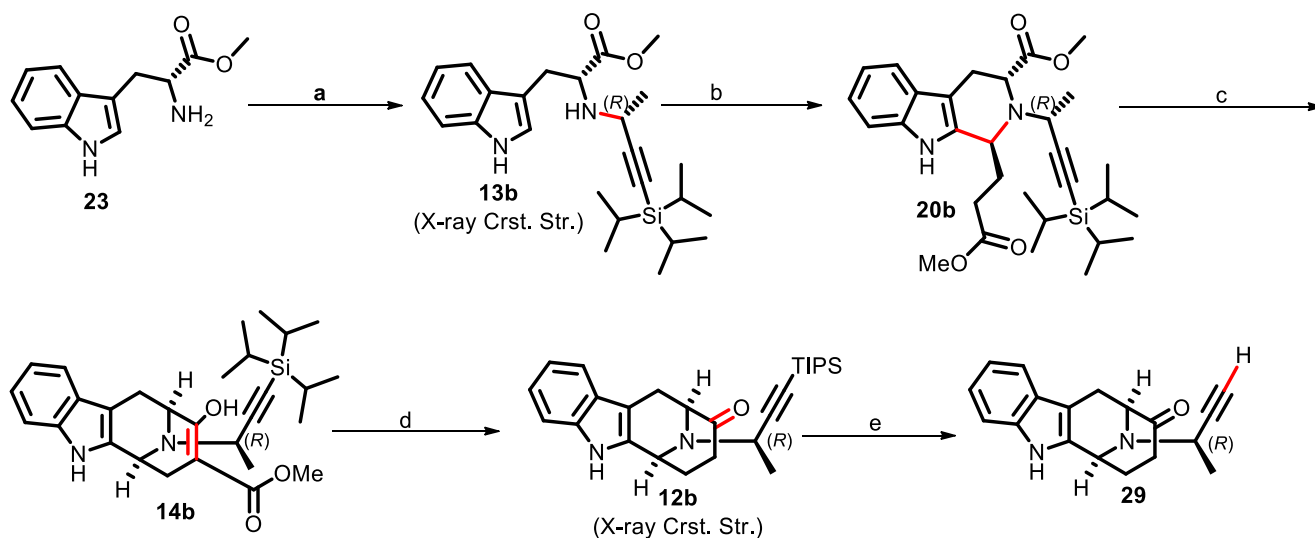


Figure 4: ORTEP representation of **25**



Scheme 5: Reagents and conditions: a) **22b** (1.5 equiv), K_2CO_3 (2.5 equiv), MeCN, 65 °C, 12 h, **92%**; b) $OHC(CH_2)_2CO_2Me$ (**27**, 1.5 equiv), acetic acid (2.5 equiv), rt, 70 h, **95%** overall; c) NaH (9 equiv), MeOH (18 equiv), toluene, 110 °C, 72 h; d) HOAc (glacial), HCl (conc), H_2O , reflux, 36 h, **75%** in 2 steps; e) TBAF (1.5 equiv), THF, 0 °C, **90%**.

The *trans*-diester **20b** was accessed via the process described above (Scheme 5). The Dieckmann cyclization of the *trans*-diester **20b**, which contained the α -methyl [(*R*)] function, in the presence of 9 equivalents of sodium hydride and excess methanol in toluene at reflux furnished the cyclized product; the desired β -keto ester **14b**, which upon subsequent acid mediated decarboxylation provided the ketone intermediate **12b** in excellent yield (Scheme 5). The optical properties of this intermediate were found to be identical with an authentic sample synthesized by the previous approach.²⁸ The structure was further confirmed by X-ray crystallography depicted in Figure 5 (see Appendix A for the X-ray crystallographic data).

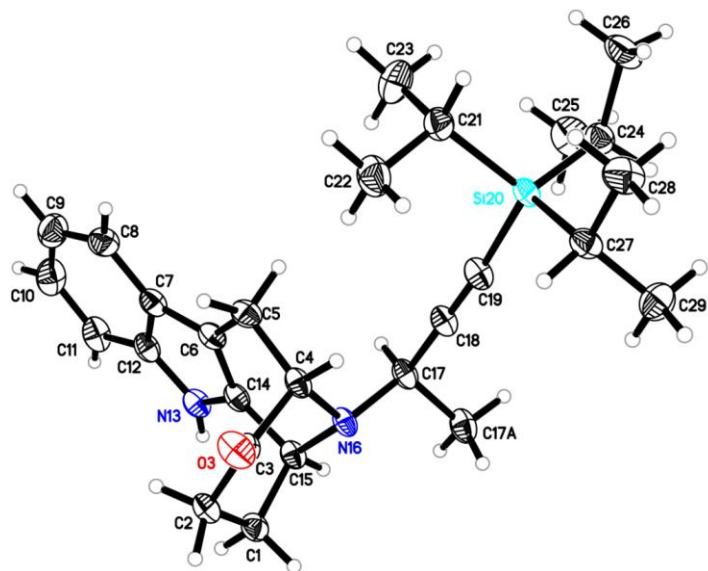
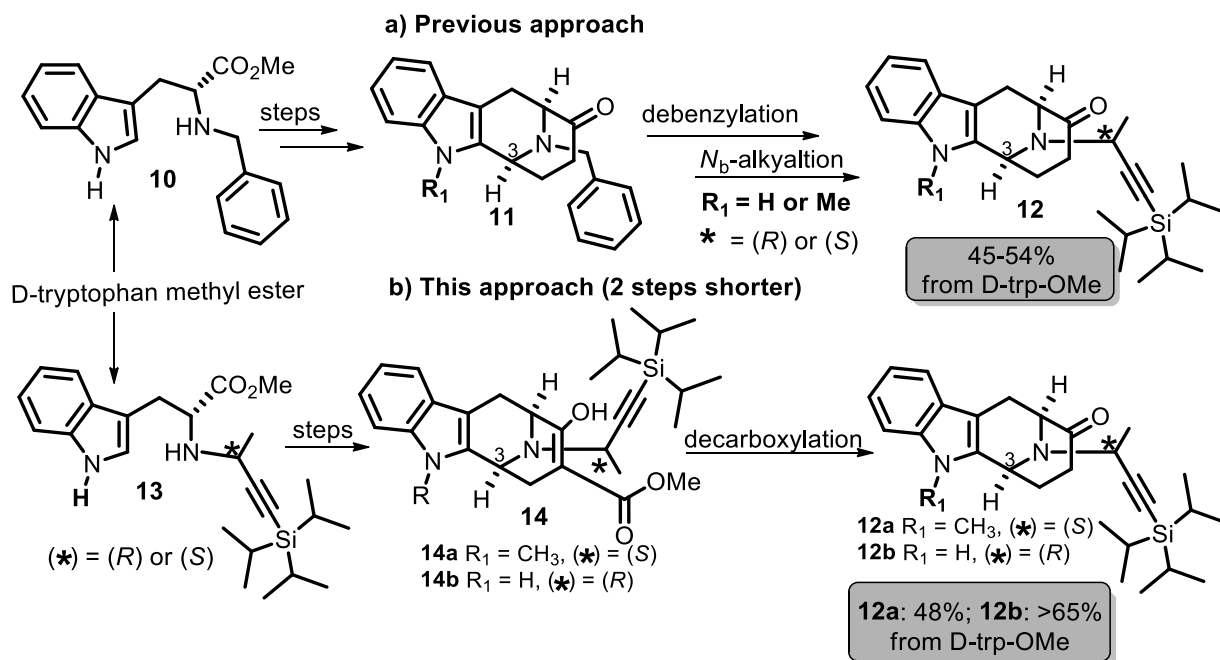


Figure 5: ORTEP representation of **12b**

As depicted in Scheme 6, the current approach (entry b) provided access to the bicyclo[3.3.1] framework **12** in 48% (**12a**) to >65% (**12b**) from D-tryptophan methylester **23**. On the other hand the former approach (entry a) provided the same system in 45-54% yield starting from **23**.



Scheme 6: Comparison between the former and current approach to access the bicyclo[3.3.1] framework **12**

3. Conclusion

This work clearly indicated that a large group other than benzyl on the N_b -nitrogen atom of the D-(+)-tryptophan starting material could still provide 100% *trans*-diastereoselectivity via internal asymmetric induction. It is important to note that use of L-tryptophan would have provided the enantiomers of these alkaloids for biological study. This general strategy will be useful to access any member of C-19 methyl substituted sarpagine/macrolone alkaloids that are potential drug candidates, as indicated by their biological activity reported in the literature and presented in the introduction. Furthermore, the 70% selectivity towards the *cis*-diester in the asymmetric Pictet-Spengler reaction was somewhat unexpected and encouraging. This unusual *cis*-selectivity, if optimized, could enable one to begin the total synthesis with the naturally occurring and cheaper L-tryptophan as the chiral auxiliary. Much of the future efforts here

would be focused on the optimization of the *cis*-selective P-S cyclization to make it completely *cis*-selective, which would be of significance to the synthesis of C-19 methyl substituted indole alkaloids.

4. Experimental Section

General Experimental Considerations

All reactions were carried out under an argon atmosphere with dry solvents using anhydrous conditions unless otherwise stated. Tetrahydrofuran (THF) and diethyl ether were freshly distilled from Na/benzophenone ketyl prior to use. Dichloromethane was distilled from calcium hydride prior to use. Methanol was distilled over magnesium sulfate. Benzene and toluene were distilled over Na. Acetonitrile was distilled over CaH₂ prior to use. Reagents were purchased of the highest commercial quality and used without further purification unless otherwise stated. Thin layer chromatography (TLC) was performed on UV active silica gel plates, 200 μm, aluminum backed and UV active alumina N plates, 200 μm, F-254 aluminum backed plates. Flash and gravity chromatography were performed using silica gel P60A, 40-63 μm, basic alumina (Act I, 50-200 μm) and neutral alumina (Brockman I, ~150 mesh). TLC plates were visualized by exposure to short wavelength UV light (254 nm). Indoles were visualized with a saturated solution of ceric ammonium sulfate in 50% phosphoric acid. The ¹H NMR data are reported as follows: chemical shift, multiplicity (br s = broad singlet, s = singlet, d = doublet, t = triplet, q = quartet, quin = quintet, dd = doublet of doublets, dt = doublet of triplets, ddd = doublet of doublet of doublets, td = triplet of doublets, qd = quartet of doublets, m = multiplet), integration, and coupling constants (Hz). The ¹³C NMR data are reported in parts per million (ppm) on the δ scale. The low resolution mass spectra (LRMS) were obtained either as electron impact (EI, 70eV) or as chemical ionization

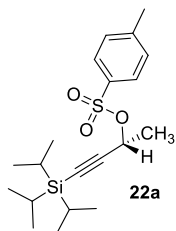
(CI) using a magnetic sector (EBE) analyzer. HRMS were recorded by electrospray ionization (ESI) using a TOF analyzer, electron impact (EI) was recorded using a trisector analyzer and Atmospheric Pressure Chemical Ionization (APCI) using a TOF analyzer. Optical rotations were measured on a JASCO Model DIP-370 digital polarimeter.

Experimental Procedures and Analytical Data

General Procedure for the Synthesis of **22a** or **22b** from Ketone **S-1**

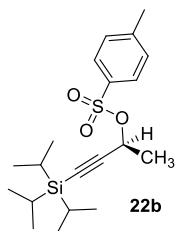
The (*S, S*)-Ru Catalyst and (*R, R*)-Ru catalyst were prepared following the procedure available in the literature.^{29,30} Optically active (*R*) and (*S*)-alcohols, **S-2** (90%) and **S-3** (95%) were synthesized following the literature procedure.^{29,31} A 2 L round bottom flask equipped with a large magnetic stir bar was flame dried under a continuous flow of argon and was then allowed to cool. The flask was then charged with freshly distilled CH₂Cl₂ (284 mL) and (*R*)-alcohol (**S-2**) or (*S*)-alcohol (**S-3**, 10 g, 44.2 mmol), after which the mixture was cooled to -25 °C (outside bath temperature). Triethylamine (17.7 g, 177 mmol) and a catalytic amount of DMAP (0.53 g, 4.4 mmol) were added, and after a few minutes of stirring, tosyl chloride (18.53 g, 97.3 mmol, Acros Organics, 99%) was added in one portion. The reaction mixture was allowed to stir at -25 °C for 45 min and the solution was allowed to slowly warm to rt. After the reaction mixture was stirred for 3 h at rt, analysis by TLC (silica gel) was carried out, after which the reaction mixture was quenched with a large excess of water (1L) and the mixture was allowed to stir vigorously for 45 min. After 45 min, the two layers were separated. The CH₂Cl₂ layer was dried (MgSO₄), filtered and concentrated under reduced pressure to furnish **22a** (15.97 g, 95%) or **22b** (16.64 g, 99%) as a light brown oil, which was used without further purification.

(R)-4-(Triisopropylsilyl)but-3-yn-2-yl 4-methylbenzenesulfonate (22a)



¹H NMR (300 MHz, CDCl₃): δ 7.81 (d, 2H, *J* = 8.1 Hz), 7.30 (d, 2H, *J* = 8.1 Hz), 5.20 (q, 1H, *J* = 6.6 Hz), 2.41 (s, 3H), 1.60 (d, 3H, *J* = 6.6 Hz), 0.96 (m, 21 H). All other spectroscopic data were identical with the published data for **22a**.³² The material was used for the next step without further characterization.

(S)-4-(Triisopropylsilyl)but-3-yn-2-yl 4-methylbenzenesulfonate (22b)



¹H NMR (300 MHz, CDCl₃): δ 7.81 (d, 2H, *J* = 8.2 Hz), 7.30 (d, 2H, *J* = 8.1 Hz), 5.20 (q, 1H, *J* = 6.6 Hz), 2.42 (s, 3H), 1.60 (d, 3H, *J* = 6.7 Hz), 0.97 (m, 21H); **¹³C NMR** (75 MHz, CDCl₃) δ 144.6 (C), 134.1 (C), 129.7 (2x CH), 127.9 (2 x CH), 103.1 (C), 89.1 (C), 68.4 (CH), 23.3 (CH₃), 21.6 (CH₃), 18.4 (6 x CH₃), 10.9 (3 x CH); **HRMS** (ESI) *m/z* (M + Na)⁺ calcd for C₂₀H₃₂O₃SSiNa, 403.1734, found 403.1742; [α]_D²⁵ (c 1.75 CHCl₃): -92.00.

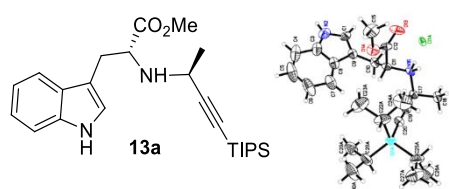
General Procedure for the Synthesis of 13a or 13b from 23

The synthesis of **13a**: D-(+)-tryptophan methyl ester (**23**, 10.0 g, 45.82 mmol) was dissolved in freshly distilled acetonitrile (150 mL) in a 500 mL round bottom flask. The tosylate **22a** (26.16 g, 68.7 mmol) was dissolved in acetonitrile and added into the round bottom flask with a syringe. Anhydrous K₂CO₃ (15.8 g) was added and the mixture, which resulted, was heated to reflux under argon for 12 h. After the completion of the reaction as indicated by disappearance of starting material (TLC, EtOAc/hexane, 1: 3) and LRMS (M+H⁺ = 427.35), the reaction was cooled to rt

and the K_2CO_3 was filtered by passing through a bed of celite. The celite was washed with EtOAc and the solvent was removed under reduced pressure to furnish crude **13a** as brownish oil. The residue was purified by flash column chromatography (silica gel, EtOAc/hexanes) to provide **13a** as light yellowish oil (16.6g, **85%**).

Synthesis of **13b**: By following the same procedure with **23** (2.0 g, 9.16 mmol) and **22b** (5.23 g, 13.74 mmol) under the same conditions, this reaction furnished **13b** (3.6 g, **92%**) yield as light yellowish solid.

(R)-Methyl 3-(1H-indol-3-yl)-2-(((S)-4-(triisopropylsilyl)but-3-yn-2-yl)amino)propanoate(13a)



1H NMR (300 MHz, $CDCl_3$): δ 8.31 (br s, 1H), 7.67 (d, 1H, $J = 7.6$ Hz), 7.32 (d, 1H, $J = 7.8$ Hz), 7.24-7.11 (m, 2H), 7.04 (d, 1H, $J = 1.7$ Hz), 4.02 (t, 1H, $J = 6.1$ Hz), 3.65 (s, 3H),

3.62 (q, 1 H, $J = 6.8$ Hz), 3.22 (d, 2H, $J = 6.1$ Hz), 1.38 (d, 3H, $J = 6.7$ Hz), 1.14-1.06 (m, 21H);

^{13}C NMR (75 MHz, $CDCl_3$): δ 175.1, 136.1, 127.6, 122.9, 121.9, 119.3, 118.8, 111.2, 110.0, 83.1,

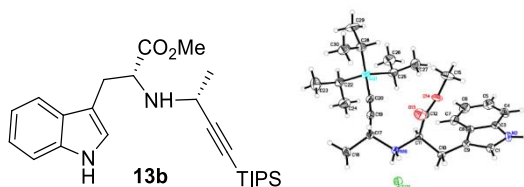
59.5, 51.9, 44.7, 28.9, 22.6, 18.6, 11.2. **HRMS** (ESI) m/z ($M+H$)⁺ calcd for $C_{25}H_{39}N_2O_2Si$,

427.2775, found 427.2776; **$[\alpha]^{25}_D$** (c 0.76 $CHCl_3$): -96.05 ; **R_f**: 0.52 (30% EtOAc in Hexane). The

structure and absolute stereochemistry were confirmed by X-ray crystallographic analysis (see X-ray data in Appendix A).

(R)-Methyl 3-(1H-indol-3-yl)-2-(((R)-4-(triisopropylsilyl)but-3-yn-2-yl)amino)propanoate

(13b)



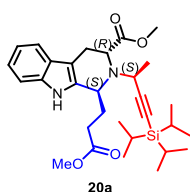
¹H NMR (300 MHz, CDCl₃): δ 8.67 (brs, 1H), 7.67 (d, 1H, *J* = 7.7 Hz), 7.35 (d, 1H, *J* = 7.9 Hz), 7.25-7.10 (m, 2H), 7.06 (d, 1H, *J* = 1.7 Hz), 4.25-4.18 (m, 1H), 3.72 (s, 3H), 3.71-3.64 (m, 1H), 3.33 (dd, 1H, *J* = 14.3, 5.4 Hz), 3.20 (dd, 1H, *J* = 14.3, 7.9 Hz), 1.37 (d, 3H, *J* = 6.7 Hz), 1.12-1.04 (m, 21H); **¹³C NMR** (75 MHz, CDCl₃): δ 175.0, 136.4, 127.5, 123.1, 122.0, 119.4, 118.7, 111.3, 110.6, 109.4, 83.5, 59.6, 51.8, 44.4, 29.7, 22.8, 18.6, 11.2. **HRMS** (ESI) *m/z* (M+H)⁺ calcd for C₂₅H₃₉N₂O₂Si, 427.2775, found 427.2779; [α]_D²⁵ (c 0.91 CHCl₃): +49.45, **m.p.**: 88-89 °C; **R_f**: 0.35 (30% EtOAc in hexane). The structure and absolute stereochemistry were confirmed by X-ray crystallographic analysis (see Appendix A for X-ray data).

Procedure for the Preparation of Diester 20a

The *N*₆-alkylated tryptophan **13a** (1.0 g, 2.34 mmol) was dissolved in dry DCM (15 mL) in a 100 mL round bottom flask equipped with a magnetic stir. To that above solution, the acetal **21** (570 mg, 3.51 mmol) and trifluoroacetic acid (0.45 mL, 5.86 mmol) were added at rt. The solution, which resulted, was stirred at rt for 11 d. The progress of the reaction was monitored by TLC analysis as indicated by the consumption of the SM and the appearance of two non-polar spots (UV and CAN stain). The reaction mixture was diluted with DCM (20 mL) and water (10 mL). The organic layer was separated and washed with water (10 mL) and brine (2 x 20 mL) and dried (Na₂SO₄). The solvent was removed under reduced pressure to give a mixture of **20a** and **28a** in >95:5 (HPLC) ratio as a light yellow oil. The *trans*-diester **20a** (LRMS M+H⁺ = 525.50, **R_f** = 0.35

in 20% EtOAc in hexanes) was purified by column chromatography (silica gel, 10-20% EtOAc in hexanes) along with the *cis*-diester **28a** (LRMS $M+H^+$ = 525.45, R_f = 0.25 in 20% EtOAc in hexanes) to furnish **20a** (1.04 g, 85%) and **28a** (49 mg, 4%).

(1*S*,3*R*)-Methyl 1-(3-methoxy-3-oxopropyl)-2-((*S*)-4-(triisopropylsilyl)but-3-yn-2-yl)-2,3,4,9-tetrahydro-1*H*-pyrido[3,4-*b*]indole-3-carboxylate (20a**)**



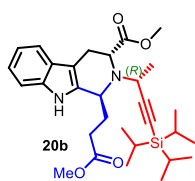
¹H NMR (300 MHz, CDCl₃): δ 7.92 (brs, 1H), 7.45 (d, 1H, J = 7.6 Hz), 7.27 (d, 1H, J = 7.9 Hz), 7.15-7.02 (m, 2H), 4.17 (dd, 1H, J = 9.7 Hz, 3.7 Hz), 4.05 (dd, 1H, J = 10 Hz, 4.3 Hz), 3.82 (q, 1H, J = 7.0 Hz, overlapped), 3.80 (s, 3H), 3.73 (s, 3H), 3.29-3.18 (m, 1H), 3.01 (dd, 1H, J = 15.5 Hz, 4.2 Hz), 2.73-2.50 (m, 2H), 2.23-2.10 (m, 1H), 2.08-1.92 (m, 1H), 1.39 (d, 3H, J = 6.9 Hz), 0.08-0.71 (m, 18H), 0.62-0.48 (m, 3H); **¹³C NMR** (75 MHz, CDCl₃): δ 174.4, 173.3, 136.1, 135.1, 127.1, 121.4, 119.1, 118.2, 110.5, 109.1, 108.7, 83.7, 57.7, 52.5, 52.0, 51.6, 46.1, 30.6, 29.7, 23.1, 21.6, 18.3, 18.3, 10.9; **HRMS** (ESI) m/z ($M+H^+$)⁺ calcd for C₃₀H₄₅N₂O₄Si 525.3143, found 525.3153; **[α]_D²⁵** (*c* 0.80 CHCl₃): – 86.25; **R_f** : 0.35 (20% EtOAc in hexanes/NH₄OH, silica gel).

Procedure for the Preparation of Diester 20b

The *N*₆-alkylated tryptophan **13b** (1.0 g, 2.34 mmol) was dissolved in 15 mL of dry DCM in a 100 mL round bottom flask equipped with a magnetic stir. To that above solution, the aldehyde **27** (408 mg, 3.51 mmol) and acetic acid (335 μL, 5.86 mmol) was added at rt. The solution, which resulted, was stirred at rt for 70 h. The progress of the reaction was monitored by TLC analysis as indicated by the consumption of SM and appearance of two non-polar spots (UV and CAN stain). The

reaction mixture was diluted with DCM (20 mL) and water (10 mL). The organic layer was separated and washed with water (10 mL), brine (2 x 20 mL) and dried (Na₂SO₄). The solvent was removed under reduced pressure to give a mixture of **20b** and **28b** as a light yellow oil. The *trans*-diester **20b** (LRMS M+H⁺ = 525.45, R_f = 0.7 in 30% EtOAc in hexanes) was purified by column chromatography (silica gel, 10-20% EtOAc in hexanes), accompanied by the *cis*-diester **28b** (LRMS M+H⁺ = 525.45, R_f = 0.57 in 30% EtOAc in hexanes) to furnish (1.17 g,) 95% combined yield. The isolated *cis*-diester (**28b**, 861 mg, 1.64 mmol) was dissolved in dry DCM (15 mL) and treated with trifluoroacetic acid (2.46 mmol, 188 μL). The solution, which resulted, was stirred for 5 h at rt. After the workup (same as above), drying and evaporation of the solvent and purification by column chromatography (silica gel) this furnished the stereospecific *trans*-diester (**20b**, 689 mg, 80%) as a colorless oil.

(1S,3R)-Methyl 1-(3-methoxy-3-oxopropyl)-2-((R)-4-(triisopropylsilyl)but-3-yn-2-yl)-2,3,4,9-tetrahydro-1H-pyrido[3,4-b]indole-3-carboxylate (20b)



¹H NMR (500 MHz, CDCl₃): δ 8.03 (br s, 1H), 7.48 (d, 1H, *J* = 7.7 Hz), 7.33 (d, 1H, *J* = 7.9 Hz), 7.19-7.14 (m, 1H), 7.13-7.09 (m, 1H), 4.64 (br t, 1H, *J* = 8.5 Hz), 4.16 (t, 1H, *J* = 5.6 Hz), 4.09 (q, 1H, *J* = 6.8 Hz), 3.65 (s, 3H), 3.64 (s, 3H), 3.14-3.04 (m, 2H), 2.56-2.48 (m, 1H), 2.37-2.22 (m, 2H), 2.14-2.06 (m, 1H), 1.42 (d, 3H, *J* = 6.8 Hz), 1.10-1.08 (m, 21H); ¹³C NMR (125 MHz, CDCl₃): δ 174.8, 173.3, 136.2, 134.9, 127.0, 121.5, 119.3, 118.0, 110.9, 108.2, 107.6, 84.9, 54.7, 53.2, 51.6, 51.4, 46.8, 29.1, 28.4, 24.8, 21.9, 18.6, 11.3; HRMS (ESI) *m/z* (M+H)⁺ calcd for C₃₀H₄₅N₂O₄Si 525.3143, found 525.3142; [α]_D²⁵ (c 1.2 CHCl₃): +5.0; R_f: 0.7 (30% EtOAc in hexane, silica gel).

Procedure for the Conversion of *cis*-Diester **28a** and **28b** into Their Corresponding *trans*-Diester **20a** and **20b**, Respectively

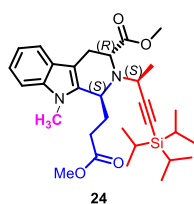
To a solution of the pure *cis*-diester **28a** or **28b** (30 mg, 0.057 mmol) individually in dry DCM (2 mL), TFA (6.6 μ L, 0.086 mmol) was added at 0 °C and the mixture which resulted was stirred at rt until the complete consumption of **28a** (**Rf**: 0.25, 20% EtOAc in hexane, silica gel) or **28b** (**Rf**: 0.6, 30% EtOAc in hexane, silica gel) and the appearance of the *trans*-diester **20a** (**Rf**: 0.35, 20% EtOAc in hexane) or **20b** (**Rf**: 0.7, 30% EtOAc in hexane) as indicated by TLC (UV and CAN stain). After the completion of reaction, the reaction mixture was diluted with DCM and brought to pH 8-9 with 14% aq NH₄OH. The organic layer was separated, washed with brine (2 x 10 mL) and dried (K₂CO₃). The solvent was removed under reduced pressure to furnish **20a** or **20b** as a light yellow oil which was purified by flash column chromatography on silica gel (10-20 % EtOAc in hexane) to provide pure *trans*-diester **20a** (25.2 mg, 84%) or **20b** (24.0 mg, 80%) as yellow oils individually.

Procedure for the Preparation of **24** from **20a**

To a round-bottom flask (25 mL) that was equipped with a reflux condenser were added *N*_a-H *trans*-diester **20a** (512 mg, 0.98 mmol), CH₃I (67 μ L, 1.07 mmol), and dry DMF (3 mL) and then the mixture was cooled to -10 °C with stirring. To this solution was added NaH (60% dispersion in mineral oil, 43 mg, 1.07 mmol) at -10 °C. The slurry, which resulted, was allowed to stir at rt for 2 h until analysis by TLC indicated the disappearance of **20a** and appearance of **24**, LRMS of the *N*_a-Me product, **24**: (M+H)⁺ = 539.55. The reaction solution was quenched by careful addition of CH₃OH (0.5 mL) and was then neutralized with an aq solution of NH₄Cl (5 mL) and extracted

with EtOAc (2 x 10 mL). The combined organic layers were washed with brine (3 x 10 mL) and dried (K₂CO₃). The solvent was removed under reduced pressure and the residue was subjected to a short wash column (silica gel, 20% EtOAc in hexane) to provide the *N*_a-methyl diester **24** (505 mg, 96%) as a light yellow oil.

(1*S*,3*R*)-Methyl 1-(3-methoxy-3-oxopropyl)-9-methyl-2-((*S*)-4-(triisopropylsilyl)but-3-yn-2-yl)-2,3,4,9-tetra-hydro-1*H*-pyrido[3,4-*b*]indole-3-carboxylate (24**)**



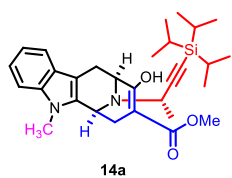
¹H NMR (500 MHz, CDCl₃): δ 7.47 (d, 1H, *J* = 7.7 Hz), 7.24 (d, 1H, *J* = 8.1 Hz), 7.17 (t, 1H, *J* = 7.5 Hz), 7.07 (t, 1H, *J* = 7.3 Hz), 4.17 (brd, 1H, *J* = 10.7 Hz), 4.08 (dd, 1H, *J* = 11.6 Hz, 5.1 Hz), 3.88-3.81 (m, 4H), 3.76 (s, 3H), 3.74 (s, 3H), 3.30-3.22 (m, 1H), 3.04 (dd, 1H, *J* = 15.4 Hz, 3.9 Hz), 2.86-2.77 (m, 1H), 2.65-2.57 (m, 1H), 2.22-2.14 (m, 1H), 1.95-1.86 (m, 1H), 1.41 (d, 3H, *J* = 6.8 Hz), 0.77-0.69 (m, 18H), 0.54-0.46 (m, 3H); **¹³C NMR** (125 MHz, CDCl₃): δ 174.4, 173.2, 137.3, 136.6, 126.6, 121.0, 118.7, 118.2, 108.8, 108.5, 107.9, 83.4, 57.2, 52.0, 51.6, 51.2, 45.7, 30.4, 30.1, 28.5, 23.2, 21.4, 18.3, 18.3, 10.9; **HRMS** (ESI) *m/z* (M+H)⁺ calcd for C₃₁H₄₇N₂O₄Si 539.3300, found 539.3314; **R_f**: 0.5 (20% EtOAc in hexane).

Procedure for the Preparation of 14a from 24

The *trans*-diester **24** (412 mg, 0.76 mmol) was dissolved in toluene (25 mL). This solution was dried by azeotropic removal of H₂O with toluene by use of a DST (refluxed 6 h). To this solution was added sodium hydride (91.8 mg, 2.29 mmol of 60% dispersion in mineral oil) at 0 °C. Anhydrous CH₃OH (186 μL, 4.6 mmol) was then added into the above mixture under Ar at 0 °C. The solution, which resulted, was then stirred at rt for 0.5 h and then held at reflux for an additional

5 h (the flask was covered with aluminum foil on the top to keep the temperature at reflux without carbonizing any compound on the sides of the flask). The reaction mixture was cooled to rt and was quenched with ice. The aq layer was extracted with CH₂Cl₂ (3 x 20 mL). The combined organic extracts were washed with brine (2 x 30 mL) and dried (K₂CO₃). The solvent was removed under reduced pressure to provide the crude product (LRMS M+H⁺ = 507.45) as light brown residue (330 mg, 85%) which could be used for the next transformation without purification. The residue was purified by flash chromatography (silica gel, EtOAc/hexane) to furnish the *N*_a-Me, β-ketoester **14a** (310 mg, 80%).

(6*S*,10*S*)-Methyl 9-hydroxy-5-methyl-12-((*S*)-4-(triisopropylsilyl)but-3-yn-2-yl)-6,7,10,11-tetrahydro-5*H*-6,10-epiminocycloocta[*b*]indole-8-carboxylate (14a**)**

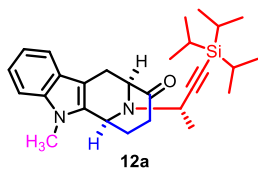


¹H NMR (500 MHz, CDCl₃): δ 12.00 (s, 1H), 7.50 (d, 1H, *J* = 7.7 Hz), 7.32 (d, 1H, *J* = 8.0 Hz), 7.22 (t, 1H, *J* = 15.0 Hz), 7.13 (t, 1H, *J* = 7.3 Hz), 4.95 (d, 1H, *J* = 5.0 Hz), 4.12 (d, 1H, *J* = 4.9 Hz), 3.7 (s, 3H), 3.69 (s, 3H), 3.65-3.59 (m, 1H), 3.10 (dd, 1H, *J* = 16.1 Hz, 5.1 Hz), 2.99-2.91 (m, 2H), 2.4 (d, 1H, *J* = 15.3 Hz), 1.55 (d, 3H, *J* = 6.3 Hz), 1.11-1.06 (m, 21H); **¹³C NMR** (125 MHz, CDCl₃): δ 171.4, 171.5, 137.0, 134.1, 126.5, 121.3, 119.2, 118.2, 108.8, 108.7, 105.6, 94.4, 84.4, 52.1, 51.5, 48.2, 47.2, 29.2, 28.8, 21.2, 20.3, 18.7, 18.6, 11.2; **HRMS** (ESI) *m/z* (M+H)⁺ calcd for C₃₀H₄₃N₂O₃Si 507.3037, found 507.3043; **R_f**: 0.6 (20% EtOAc in hexane, silica gel)

Procedure for the Preparation of **12a** from **14a**

To a round bottom flask (25 mL) which contained the *N*_a-Me, β -ketoester **14a** (233 mg, 0.46 mmol) was added glacial acetic acid (0.7 mL), hydrochloric acid (1.0 mL, conc.) and water (0.3 mL) with stirring (magnetic stir). The solution, which resulted, was heated at reflux for 7 h. After removal of the solvent under reduced pressure, the residue was brought to pH = 9 with a cold aq solution of NaOH (3 *N*). The mixture, which resulted, was extracted with CH₂Cl₂ (3 x 20 mL) and the combined organic extracts were washed with a saturated aq solution of NH₄Cl (10 mL), brine (2 x 20 mL) and dried (K₂CO₃). The removal of the solvent under reduced pressure afforded the ketone **12a** as a brown oil. The residue was purified by column chromatography (silica gel, 20% EtOAc in hexanes) to provide pure **12a** (LRMS M+H⁺ = 449.40) as a colorless oil (169 mg, 82%).

(6*S*,10*S*)-5-Methyl-12-((*S*)-4-(triisopropylsilyl)but-3-yn-2-yl)-7,8,10,11-tetrahydro-5H-6,10-epiminocycloocta[b]indol-9(6H)-one (**12a**)

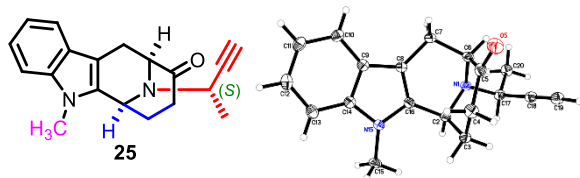


¹H NMR (300 MHz, CDCl₃): δ 7.49 (d, 1H, *J* = 7.7 Hz), 7.33 (d, 1H, *J* = 8.1 Hz), 7.28-7.21 (m, 1H), 7.17-7.10 (m, 1H), 4.96-4.89 (m, 1H), 3.99 (d, 1H, *J* = 6.2 Hz), 3.70 (s, 3H), 3.66 (q, 1H, *J* = 6.5 Hz, overlapped with *N*_a-Me), 3.17 (dd, 1H, *J* = 16.7, 6.6 Hz), 2.72 (d, 1H, *J* = 16.8 Hz), 2.65-2.44 (m, 2H), 2.20-2.01 (m, 2H), 1.49 (d, 3H, *J* = 6.6 Hz), 1.08-1.03 (m, 21H); **HRMS** (ESI) *m/z* (M+H)⁺ Calcd for C₂₈H₄₁N₂OSi 449.2983, found 449.2990. All other spectroscopic data were identical with the published data for **12a** that was synthesized *via* the previous route.²⁶ This material was used for the next step without further characterization.

Procedure for the Preparation of **25** from **12a**

To a solution of **12a** (50 mg, 0.11 mmol) in THF (5 mL), TBAF (167 μ L, 0.167 mmol, 1.0 M solution in THF) was added at 0 $^{\circ}$ C. The solution, which resulted, was stirred at 0 $^{\circ}$ C for 30 min or until the completion of the reaction, as monitored by TLC (silica gel). After this, the reaction mixture was diluted with EtOAc (20 mL) and water (10 mL). The organic layer was separated and the aq layer was extracted with EtOAc (5 mL). The combined organic layers were washed with brine (3 x 20 mL) and dried (Na_2SO_4). The solvent was removed under reduced pressure to provide the alkyne **25** (LRMS $M+\text{H}^+ = 293.20$) as a brown residue (33 mg, 101% crude yield). The residue was purified by silica gel column chromatography (30% EtOAc in hexanes) to provide **25** as a light brown solid (29.3 mg, 90%).

(6*S*,10*S*)-12-((*S*)-But-3-yn-2-yl)-5-methyl-7,8,10,11-tetrahydro-5*H*-6,10-epiminocycloocta- [b]indol-9(6*H*)-one (**25**)



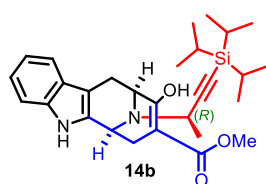
^1H NMR (300 MHz, CDCl_3): δ 7.4 (d, 1H, $J = 7.7$ Hz), 7.31 (d, 1H, $J = 8.1$ Hz), 7.25-7.18 (m, 1H), 7.14-7.07 (m, 1H), 4.77-4.73 (m, 1H), 3.95 (d, 1H, $J = 6.6$ Hz), 3.70 (s, 3H), 3.61 (qd, 1H, $J = 6.7, 2.1$ Hz), 3.13 (dd, 1H, $J = 16.8, 6.7$ Hz), 2.70 (d, 1H, $J = 16.8$ Hz), 2.67-2.54 (m, 1H), 2.52-2.43 (m, 1H), 2.28 (d, 1H, $J = 2.2$ Hz), 2.18-2.09 (m, 1H), 2.07-1.98 (m, 1H), 1.45 (d, 3H, $J = 6.7$ Hz); **HRMS** (ESI) m/z ($M+\text{H}^+$) Calcd for $\text{C}_{19}\text{H}_{21}\text{N}_2\text{O}$ 293.1654, found 293.1656. All other spectroscopic data were identical with the published data for **25**.²⁶ This material was used for the next step without further characterization. The structure of this

compound **25** was further confirmed by X-ray crystallographic analysis (see Appendix A for X-ray data).

Procedure for the Synthesis of **14b** from **20b**

The *trans*-diester **20b** (336 mg, 0.76 mmol) was dissolved in toluene (30 mL). This solution was dried by azeotropic removal of H₂O by toluene with a DST (refluxed 6 h). To this above mixture, sodium hydride (230 mg, 5.76 mmol of 60% dispersion in mineral oil) was added at 0 °C. Anhydrous CH₃OH (466 μL, 11.5 mmol) was then added into the above mixture under Ar at 0 °C. The solution, which resulted, was then stirred at rt for 0.5 h and then held at reflux for an additional 72 h (the flask was covered with aluminum foil on the top to keep the temperature at reflux without carbonizing any compound on the sides of the flask). The reaction was quenched with ice. The aq layer was extracted with CH₂Cl₂ (3 x 30 mL). The combined organic extracts were washed with brine (3 x 30 mL) and dried (K₂CO₃). The solvent was removed under reduced pressure to provide the crude β-keto ester **14b** (LRMS M+H⁺ = 493.40) as a light brown residue (293 mg, 93% crude) which could be used for the next transformation without purification.

(6*S*,10*S*)-Methyl 9-hydroxy-12-((*R*)-4-(triisopropylsilyl)but-3-yn-2-yl)-6,7,10,11-tetrahydro-5*H*-6,10-epimi-nocycloocta[*b*]indole-8-carboxylate (**14b**)



¹H NMR (500 MHz, CDCl₃): δ 11.98 (s, 1H), (7.72 (br s, 1H), 7.51 (d, 1H, *J* = 7.7 Hz), 7.34 (d, 1H, *J* = 8.0 Hz), 7.18 (t, 1H, *J* = 7.1 Hz), 7.13 (t, 1H, *J* = 7.1 Hz), 4.49 (d, 1H, *J* = 5.2 Hz), 4.38 (d, 1H, *J* = 5.7 Hz), 3.69 (s, 3H),

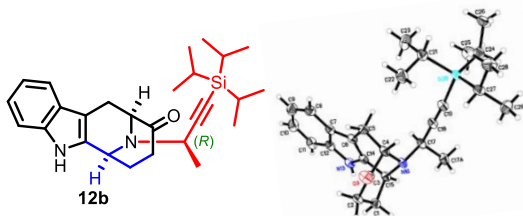
3.64 (q, 1H, *J* = 6.4 Hz), 3.27 (dd, 1H, *J* = 16.1, 5.9 Hz), 2.97 (br d, 1H, *J* = 16.6 Hz), 2.93 (dd, 1H, *J* = 15.7, 5.6 Hz), 2.43 (br d, 1H, *J* = 15.6 Hz), 1.50 (d, 3H, *J* = 6.4 Hz), 1.12-1.08 (m, 21H);

^{13}C NMR (125 MHz, CDCl_3): δ 172.4, 171.4, 135.7, 132.8, 127.0, 121.9, 119.7, 118.3, 110.8, 107.6, 107.3, 94.5, 85.4, 53.7, 51.5, 48.2, 46.7, 29.0, 22.7, 20.9, 18.7, 11.2; **HRMS** (ESI) m/z ($\text{M}+\text{H}$) $^+$ calcd for $\text{C}_{29}\text{H}_{41}\text{N}_2\text{O}_3\text{Si}$ 493.2881, found 493.2890; $[\alpha]_{\text{D}}^{25}$: +28.95 (c 0.76 CHCl_3); **R_f**: 0.52 (30% EtOAc in hexane, silica gel).

Procedure for the Synthesis of **12b** from **14b**

To a round bottom flask (25 mL) which contained the β -keto ester **14b** (290 mg, 0.595 mmol) was added glacial acetic acid (0.7 mL), hydrochloric acid (1.0 mL, conc.) and water (0.3 mL) with stirring (magnetic stir). The solution, which resulted, was held at reflux for 36 h. After removal of the solvent under reduced pressure, the residue was brought to pH = 9 with a cold aq solution of NaOH (3 N). The mixture, which resulted, was extracted with CH_2Cl_2 (3 x 20 mL) and the combined organic extracts were washed with a saturated aq solution of NH_4Cl (10 mL), brine (2 x 20 mL) and dried (K_2CO_3). The removal of the solvent under reduced pressure afforded the ketone **12b** as a brown oil (LRMS $\text{M}+\text{H}^+$ = 435.40). The residue was purified by column chromatography (silica gel, 20% EtOAc in hexanes) to provide pure **12b** (209 mg, 75% in two steps).

(6*S*,10*S*)-12-((*R*)-4-(Triisopropylsilyl)but-3-yn-2-yl)-7,8,10,11-tetrahydro-5*H*-6,10-epimino-cycloocta[*b*]indol-9(6*H*)-one (**12b**)



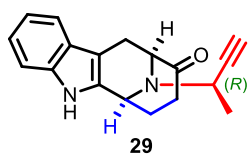
^1H NMR (300 MHz, CDCl_3): δ 7.92 (br s, 1H), 7.49 (d, 1H, J = 7.7 Hz), 7.35 (d, 1H, J = 7.9 Hz), 7.23-7.10 (m, 2H), 4.37 (br d, 2H, J = 5.8 Hz), 3.73 (q, 1H, J = 6.4 Hz), 3.32 (dd, 1H, J = 16.7, 6.8 Hz), 2.72 (br d, 1H, J = 16.8 Hz), 2.58-2.43 (m, 2H),

2.17-2.02 (m, 2H), 1.48 (d, 3H, $J = 6.4$ Hz), 1.10-1.04 (m, 21H); ^{13}C NMR (75 MHz, CDCl_3): δ 210.6, 135.9, 132.0, 126.9, 122.0, 119.7, 118.3, 110.9, 107.9, 107.6, 85.4, 63.4, 48.5, 47.4, 34.6, 30.0, 21.7, 21.1, 18.6, 12.2; HRMS (ESI) m/z ($\text{M}+\text{H}$) $^+$ calcd for $\text{C}_{27}\text{H}_{38}\text{N}_2\text{OSi}$ 435.2826, found 435.2835; Rf: 0.38 (30% EtOAc in hexane, silica gel). This compound was further confirmed by X-ray crystallographic analysis (see Appendix A for X-ray data).

Preparation of **29** from **12b**

To a solution of ketone **12b** (120 mg, 0.28 mmol) in THF (8 mL), TBAF (414 μL , 0.414 mmol, 1.0 M solution in THF) was added at 0 °C. The solution, which resulted, was stirred at 0 °C for 30 min or until the completion of the reaction as monitored by TLC. After that, the reaction was diluted with EtOAc (30 mL) and water (10 mL). The organic layer was separated and the aq layer was extracted with EtOAc (10 mL). The combined organic layers were washed with brine (3 x 30 mL) and dried (Na_2SO_4). The solvent was removed under reduced pressure to provide the alkyne **29** (LRMS $\text{M}+\text{H}^+ = 279.45$) as a brown residue (33 mg, 101% crude yield). The residue was purified by silica gel column chromatography (30% EtOAc in hexanes, silica gel) to provide **29** as a light brown solid (69.2 mg, 90%).

(6*S*,10*S*)-12-((*R*)-But-3-yn-2-yl)-7,8,10,11-Tetrahydro-5*H*-6,10-epiminocycloocta[b]indol-9(6*H*)-one (**29**)



^1H NMR (300 MHz, CDCl_3) δ 7.90 (brs, 1H), 7.48 (dd, 1H, $J = 7.7, 0.5$ Hz), 7.36 (d, 1H, $J = 8.0$ Hz), 7.11-7.23 (m, 2H), 4.37-4.41 (m, 1H), 4.35 (d, 1H, $J = 6.6\text{Hz}$), 3.68 (qd, 1H, $J = 6.5, 2.1$ Hz), 3.30 (dd, 1H, $J = 16.9, 6.7$ Hz),

2.72 (d, 1H, $J = 16.9$ Hz), 2.44 - 2.57 (m, 2H), 2.33-2.34 (m, 1H), 2.05 - 2.21 (m, 2H), 1.47 (d, 3H, $J = 6.5$ Hz); ^{13}C NMR (75 MHz, CDCl_3) δ 210.4 (C), 135.9 (C), 131.6(C), 126.8 (C), 122.2 (CH), 119.8 (CH), 118.3 (CH), 110.9 (CH), 107.8 (C), 83.9 (C), 72.7 (CH), 63.3 (CH), 48.0 (CH), 46.3 (CH), 34.5 (CH_2), 30.1 (CH_2), 21.5 (CH_2), 20.6 (CH_3); **HRMS** (ESI) m/z ($\text{M} + \text{H}$)⁺ calcd for $\text{C}_{18}\text{H}_{19}\text{N}_2\text{O}$, 279.1492, found 279.1498; **Rf**: 0.15 (30% EtOAc in hexanes, silica gel); **m.p.**: 158-61 °C.

5. References

- (1) Schmeller, T.; Wink, W. In *Alkaloids: Biochemistry, Ecology, and Medicinal Applications* (Eds.: M. F. Roberts, M. Wink), Springer US, Boston, MA, **1998**, pp. 435-459.
- (2) Kam, T.-S.; Choo, Y.-M.; Komiyama, K. *Tetrahedron* **2004**, *60*, 3957.
- (3) Keawpradub, N.; Kirby, G.; Steele, J.; Houghton, P. *Planta Med.* **1999**, *65*, 690.
- (4) Naranjo, J.; Pinar, M.; Hesse, M.; Schmid, H. *Helv. Chim. Acta* **1972**, *55*, 752.
- (5) Wong, W.-H.; Lim, P.-B.; Chuah, C.-H. *Phytochemistry* **1996**, *41*, 313.
- (6) Pan, L.; Terrazas, C.; Acuña, U. M.; Ninh, T. N.; Chai, H.; de Blanco, E. J. C.; Soejarto, D. D.; Satoskar, A. R.; Kinghorn, A. D. *Phytochem. Lett.* **2014**, *10*, 54.
- (7) Tan, S.-J.; Lim, J.-L.; Low, Y.-Y.; Sim, K.-S.; Lim, S.-H.; Kam, T.-S. *J. Nat. Prod.* **2014**, *77*, 2068.
- (8) Buckingham, J.; Baggaley, K. H.; Roberts, A. D.; Szabo, L. F. *Dictionary of Alkaloids, with CD-ROM*; CRC press, 2010.
- (9) Iwu, M. *Planta Med.* **1982**, *45*, 105.

- (10) Kiang, A.; Loh, S.; Demanczyk, M.; Gemenden, C.; Papariello, G.; Taylor, W. *Tetrahedron* **1966**, *22*, 3293.
- (11) Nasser, A. M.; Court, W. E. *Phytochemistry* **1983**, *22*, 2297.
- (12) Stöckigt, J.; Antonchick, A. P.; Wu, F.; Waldmann, H. *Angew. Chem. Int. Ed.* **2011**, *50*, 8538.
- (13) Cox, E. D.; Cook, J. M. *Chem. Rev.* **1995**, *95*, 1797.
- (14) Mayer, J. P.; Bankaitis-Davis, D.; Zhang, J.; Beaton, G.; Bjergarde, K.; Andersen, C. M.; Goodman, B. A.; Herrera, C. J. *Tetrahedron Lett.* **1996**, *37*, 5633.
- (15) Weber, L. *Curr. Med. Chem.* **2002**, *9*, 2085.
- (16) Klausen, R. S.; Jacobsen, E. N. *Org. Lett.* **2009**, *11*, 887.
- (17) Bailey, P. D.; Hollinshead, S. P.; McLay, N. R. *Tetrahedron Lett.* **1987**, *28*, 5177.
- (18) Rahman, M. T.; Tiruveedhula, V. V.; Cook, J. M. *Molecules* **2016**, *21*, 1525.
- (19) Tsuji, R.; Nakagawa, M.; Nishida, A. *Tetrahedron: Asymmetry* **2003**, *14*, 177.
- (20) Kawate, T.; Yamanaka, M.; Nakagawa, M. *Heterocycles* **1999**, *2*, 1033.
- (21) Herlé, B.; Wanner, M. J.; van Maarseveen, J. H.; Hiemstra, H. *J. Org. Chem.* **2011**, *76*, 8907.
- (22) Sewgobind, N. V.; Wanner, M. J.; Ingemann, S.; de Gelder, R.; van Maarseveen, J. H.; Hiemstra, H. *J. Org. Chem.* **2008**, *73*, 6405.
- (23) Seayad, J.; Seayad, A. M.; List, B. *J. Am. Chem. Soc.* **2006**, *128*, 1086.
- (24) Czerwinski, K. M.; Cook, J. M. *Stereochemical control of the Pictet-Spengler reaction in the synthesis of natural products*; JAI Press: Greenwich, CT, 1996; Vol. 3.
- (25) Li, J.; Wang, T.; Yu, P.; Peterson, A.; Weber, R.; Soerens, D.; Grubisha, D.; Bennett, D.; Cook, J. *J. Am. Chem. Soc.* **1999**, *121*, 6998.

- (26) Edwankar, R. V.; Edwankar, C. R.; Deschamps, J. R.; Cook, J. M. *J. Org. Chem.* **2014**, *79*, 10030.
- (27) Garnick, R. L.; Le Quesne, P. W. *J. Am. Chem. Soc.* **1978**, *100*, 4213.
- (28) Rahman, M. T.; Deschamps, J. R.; Imler, G. H.; Schwabacher, A. W.; Cook, J. M. *Org. Lett.* **2016**, *18*, 4174.
- (29) Marshall, J. A.; Eidam, P.; Eidam, H. S. *Org. Syn.* **2007**, 120.
- (30) Haack, K. J.; Hashiguchi, S.; Fujii, A.; Ikariya, T.; Noyori, R. *Angew. Chem. Int. Ed.* **1997**, *36*, 285.
- (31) Matsumura, K.; Hashiguchi, S.; Ikariya, T.; Noyori, R. *J. Am. Chem. Soc.* **1997**, *119*, 8738.
- (32) Edwankar, R. V.; Edwankar, C. R.; Deschamps, J.; Cook, J. M. *Org. Lett.* **2011**, *13*, 5216.

Chapter 2

Unprecedented Stereocontrol in the Synthesis of 1,2,3-Trisubstituted Tetrahydro- β -carbolines: The Ambidextrous Pictet-Spengler Reaction

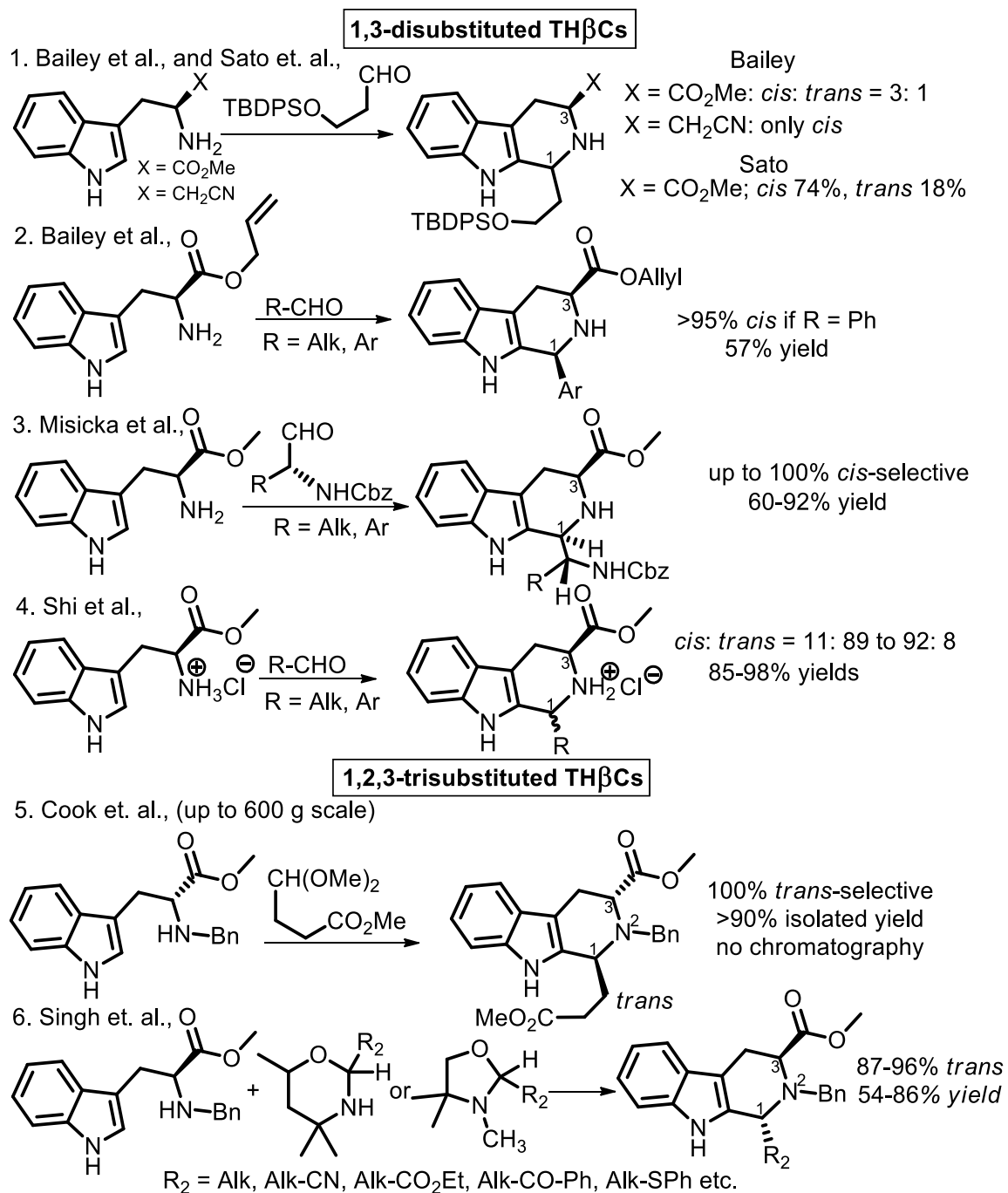
1. Introduction

The asymmetric Pictet-Spengler (P-S) reaction of chiral *N*_b-ethynyl substituted tryptophan methyl ester derivatives (from both D- and L-tryptophan) with a simple aliphatic aldehyde, exhibited unprecedented selectivity towards either of the diastereomeric *cis* or *trans* products. A simple variation of conditions could alter the outcome of the cyclization from either 100% *trans*-selective to 100% *cis*-selective originating entirely from internal asymmetric induction under mild conditions. This resulted in a highly efficient access to both 1,3-*cis*-(1,2,3-trisubstituted tetrahydro- β -carbolines, TH β Cs) and 1,3-*trans*-(1,2,3-trisubstituted TH β Cs). To the best of our knowledge, this type of stereocontrol has never been observed from tryptophan methyl ester derivatives (either D or L) in accessing either 1,3-disubstituted or 1,2,3-trisubstituted TH β Cs. By exploiting this very useful ambidextrous-diastereoselectivity, the crucial C-3 and C-5 stereocenters of C-19 methyl substituted sarpagine-macroline-ajmaline alkaloids has been set beginning with the DNA-encoded and cheaper L-(-)-tryptophan, as well as optionally from commercially available D-(+)-tryptophan.

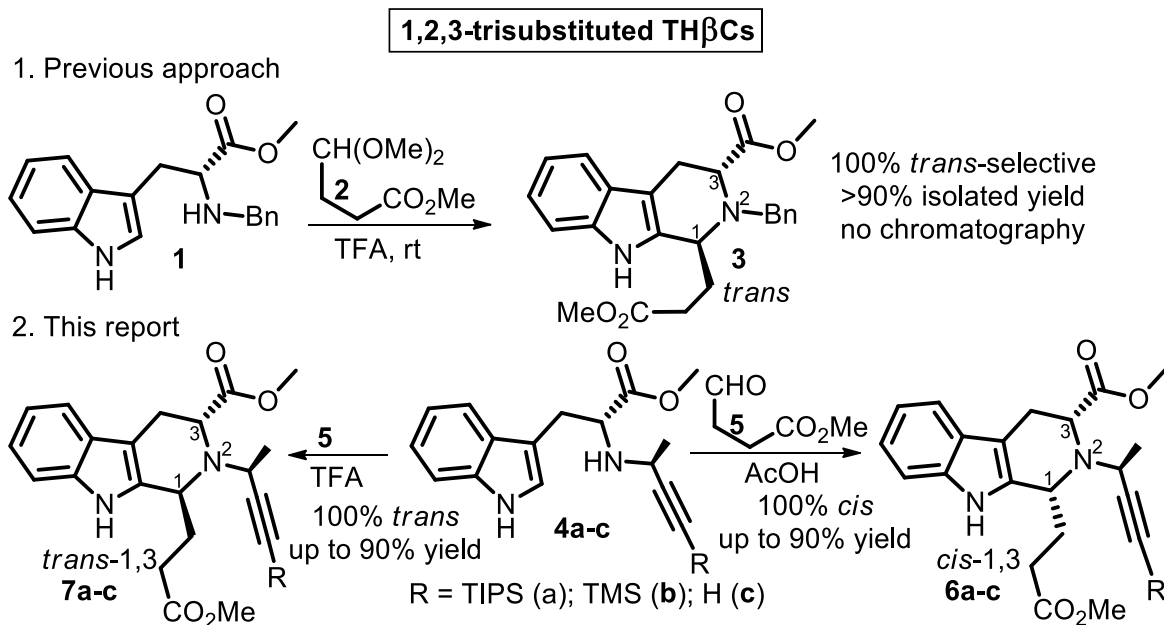
The Pictet-Spengler (P-S) reaction of tryptophan derivatives with an aldehyde other than formaldehyde results in two diastereomeric TH β Cs (at C-1 and C-3 of the TH β C, see Scheme 1). The TH β C moiety deserves special attention in its own right as it is at the core of numerous bioactive alkaloids, as well as medicinally important synthetic analogs. As a consequence, numerous studies accessing this moiety by various strategies have been undertaken.¹⁻⁶ Almost all useful compounds containing the TH β C core (both natural and synthetic) bear a stereocenter at C-1. On the other hand, in the vast majority of the sarpagine/ajmaline-type alkaloids, there is *cis*-1,3-disubstitution in the TH β C core (see *cis*-3,5 of alkaloids in Figure 1). As a result, the diastereoselectivity of the P-S reaction to access the 1,3-*cis*-TH β C core is of special importance. Numerous

attempts have been made to gain control in the selectivity in this process by varying the temperature, solvent, chiral catalysts, chiral reactive partners (including chiral aldehyde equivalents), and different tryptophan alkyl esters, etc.^{1,7-10}

The asymmetric P-S reaction has undergone elegant advances by Jacobsen,¹¹⁻¹³ Nakagawa,^{14,15} Bailey,¹⁶⁻¹⁸ Misicka,^{19,20} Hiemstra,²¹⁻²⁴ Van Maarseveen,²¹⁻²⁴ List,²⁵⁻³⁶ and many others.²⁵⁻³⁶ *Cis*-Selectivity in the asymmetric P-S reaction has been reported in the preparation of 1,3-disubstituted TH β Cs.^{17-19,31,32,37} In the case of 1,3-disubstituted TH β C, Bailey, Sato, Misicka, and Shi have made notable advances in devising a *cis*-selective P-S reaction to gain access to the *cis*-1,3-disubstituted TH β C system (Scheme 1). These strategies are logical in a chemical sense because of their promise to access the C-3 stereochemistry of indole alkaloids, starting from L-tryptophan. The requirement of pi-systems either at C-1 or C-3; however, is not desirable since very often these esters or aldehyde equivalents are surprisingly hard to prepare and require special processes for removing them. Moreover, often the products are not useful toward the synthesis of alkaloids which would require complex transformations. To the best of our knowledge, completely *cis*-selectivity in the P-S reaction with tryptophan methyl esters and aliphatic aldehydes have not been reported yet.



Scheme 1. Comparison between different methods for access to 1,3-disubstituted and 1,2,3-trisubstituted TH β Cs *via* the asymmetric Pictet-Spengler reaction



Scheme 2. Access to 1,3-disubstituted and 1,2,3-trisubstituted TH β Cs via the asymmetric Pictet-Spengler reaction

On the other hand, for 1,2,3-trisubstituted TH β C systems, the P-S reaction of *N*_β-benzylated tryptophan methyl esters (e.g., **1** in Scheme 2) with aldehydes or acetals (e.g., **2**) is well known for complete *trans*-selectivity under thermodynamic conditions yielding 1,3-*trans*-1,2,3-trisubstituted TH β Cs **3** (Scheme 2, entry 1).¹ This robust strategy has been employed on up to a 600 gram scale process and in excellent diastereo (100% *de*) and enantioselectivity (up to 98% *ee*) in excellent yield, while avoiding chromatographic purification. The syntheses of numerous indole and oxindole alkaloids with potent biological activity have utilized this *trans*-specific method.³⁸⁻⁴⁰ Many examples of the preparation of 1,2,3-trisubstituted TH β Cs are present in the literature *via* thermodynamic control to give mostly (if not exclusively), *trans*-1,3-disubstitution.^{29,33,35} To the best of our knowledge, *cis*-specificity in preparing 1,2,3-trisubstituted TH β Cs from tryptophan alkyl esters is absent in the literature. Herein, we report unprecedented stereocontrol in *cis*- and *trans*-selectivity in accessing 1,2,3-trisubstituted TH β Cs from chiral *N*_β-ethynyl substituted

tryptophan derivatives **4** with simple aliphatic aldehydes **5** to furnish either the *cis*-diastereomer **6** completely or the *trans*-isomer **7**, controlled by simple changes in reaction conditions (Scheme 2, entry 2). This strategy will greatly improve the approach towards the total synthesis of either the (+) or (-) enantiomer of a group of more than seventy sarpagine/macroline-/ajmaline indole alkaloids. Depicted in Figure 1 are a few representative examples (**8-13**)⁴¹⁻⁴⁷ from this group of bioactive alkaloids (for more examples see Figure 1A). Furthermore, the complete *cis*-selectivity would permit the synthesis to begin with the natural and cheaper L-tryptophan methyl ester instead of D-tryptophan methyl ester which has been used previously. In this version of the P-S reaction, it is the ability to prepare both the (+) or (-) enantiomer of these indole alkaloids from either D-(+)-tryptophan or L-(-)-tryptophan that is of significance and illustrated here for the first time.

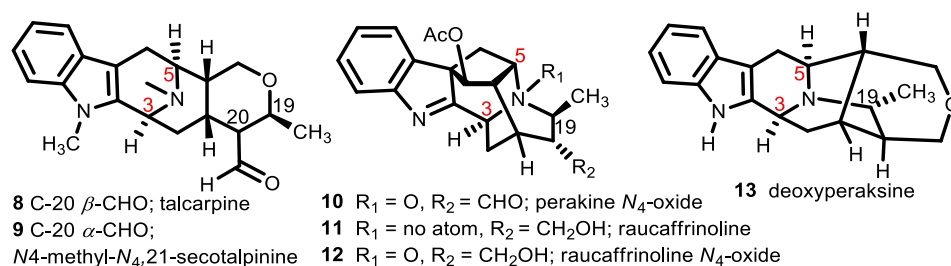


Figure 1. Representative examples of C-19 methyl substituted sarpagine/ajmaline indole alkaloids **8-13** (for more examples, see Figure 1A).

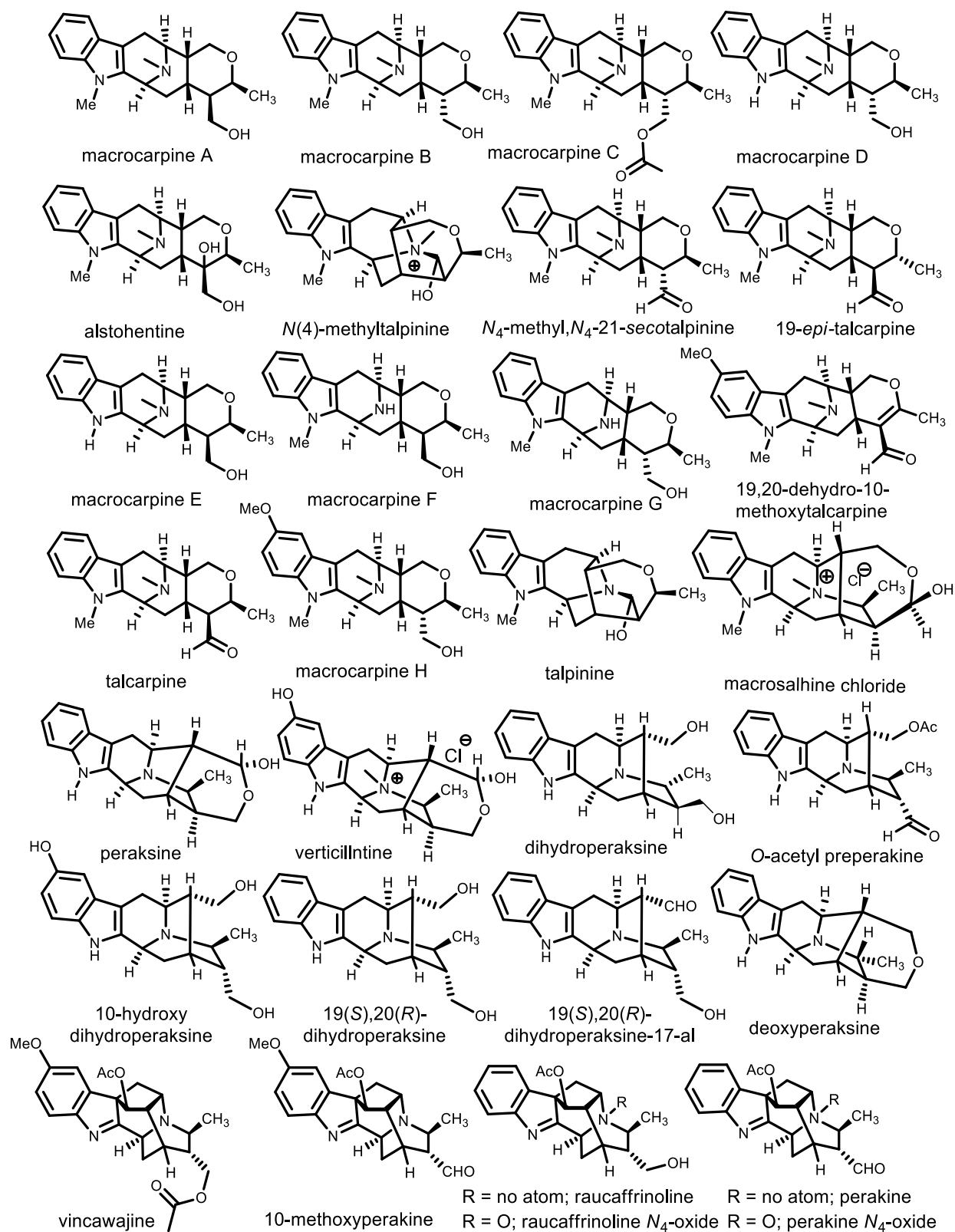
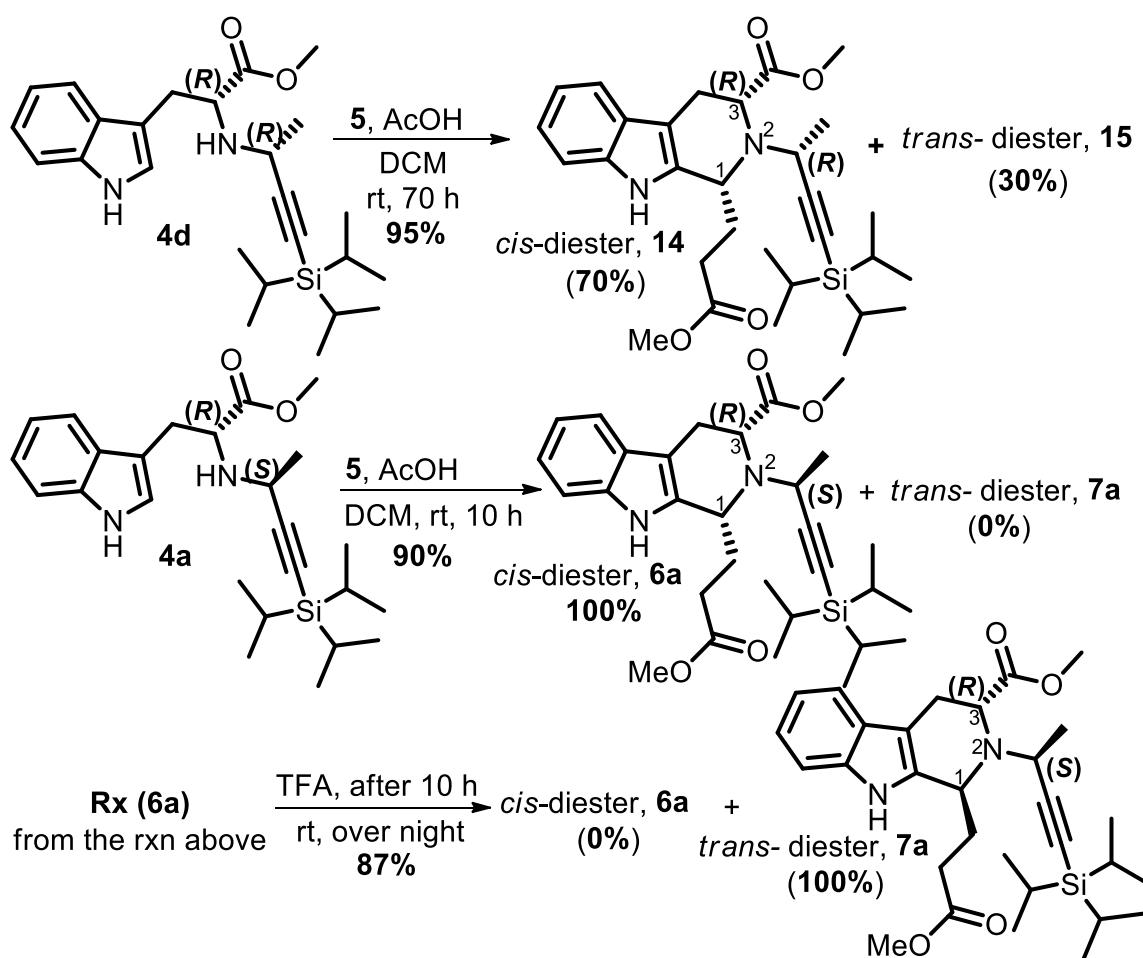


Figure 1A. Representative examples of C-19 methyl substituted macroline, sarganine, and ajmaline-type indole alkaloids^{40,48}

2. Results and Discussion

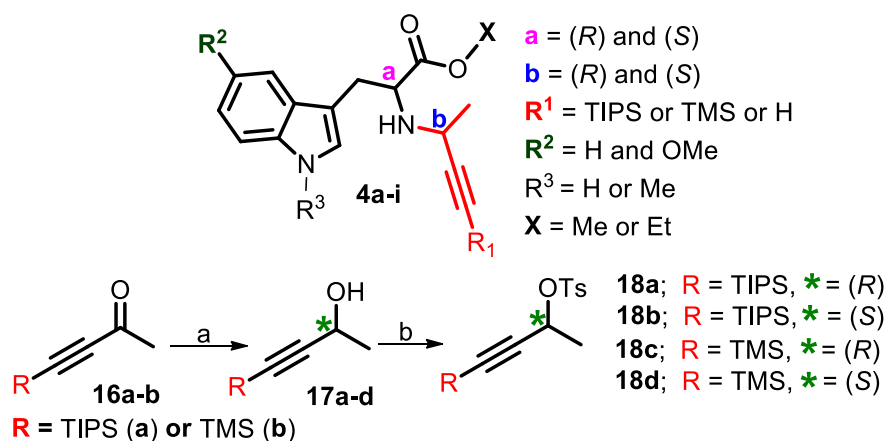
Recently, the total synthesis of a number of sarpagine-related bioactive indole alkaloids was published *via* a better and shorter route for accessing the core-tetracyclic intermediates employing an improved P-S strategy.^{49,50} One of the principal goals of that study was to gain quicker access to the key intermediates, improving the previous strategy, and developing a shorter route to the tetracyclic-core required for an important group of more than seventy^{40,48,62} alkaloids. Several interesting observations were noted in the P-S/Dieckmann protocol.⁴⁹ When the D-tryptophan methyl ester derivative with an *N*_b-ethynyl substituent bearing a methyl group with the (*S*) stereochemistry (**4a**) was reacted with acetal **2** in acidic media (TFA in DCM), excellent diastereoselectivity (>95:5) towards the *trans*-diester (**7a**) was observed (not shown here).⁴⁹ On the other hand, when the reaction of the tryptophan methyl ester derivative with the (*R*)-methyl substituent (**4d**) was stirred under the same conditions, this resulted in a complex reaction mixture. Afterwards, it was discovered milder reaction conditions using the aldehyde **5** and acetic acid instead of the acetal **2** and trifluoroacetic acid altered the chemistry. The asymmetric P-S reaction of the amine **4d** with aldehyde **5** proceeded smoothly under the modified and milder conditions to provide a 70 to 30 mixture of *cis* to *trans*-diastereomers in 95% combined isolated yield (Scheme 3).^{49,50} The excellent overall yield and diastereoselectivity towards the *cis*-diester captured our attention. A further investigation of this reaction, in order to find conditions for better selectivity, became the focus. As a step toward this the same conditions were applied to *N*_b-(*S*)-methyl-ethynyl substituted tryptophan derivative (**4a**). To our surprise, the reaction was complete in 10 hours and provided the *cis*-diester **6a** with 100% *cis*-diastereoselectivity. The addition of 3 equivalents of TFA, after the initial P-S reaction (at 10 hours), converted the *cis*-diester **6a** completely into the corresponding *trans*-diester **7a** (Scheme 3). Furthermore, addition of 4 Å molecular sieves to the

reaction had, as expected, a tremendous effect on the rate. The reactions run in the presence of molecular sieves were complete in several hours instead of several days. It is felt, the amine **4a** reacts with the aldehyde **5** in the presence of AcOH to form the kinetic product (*cis*-diester, **6a**) while acetic acid is not acidic enough to facilitate cleavage of the C(1)-N(2) bond which previously provided (TFA) only the *trans*-diastereomer.⁵¹ Conversely, when the kinetic product (i.e., **6a**) was treated with TFA in DCM, the *cis*-diastereomer rearranged completely to the thermodynamically more stable product (i.e., the *trans*-product **7a**). To the best of our knowledge, this type of selectivity in the formation of completely *cis*- or *trans*-TH β C from a single tryptophan derivative has never been seen in the formation of the 1,2,3-trisubstituted TH β C-system.



Scheme 3. Unprecedented stereocontrol in the asymmetric P-S reaction

Encouraged by the unprecedented outcome of the P-S reaction, it was felt of importance to investigate the underlying reason(s) for this ambidextrous-diastereoselectivity. It was obvious exploitation of complete *cis*-selectivity would permit the synthesis of sarpagine alkaloids with the cheaper and natural L-(-)-tryptophan, instead of D-(+)-tryptophan. The optically pure tosylate units (**18a-d**) required for amines **4a-i** were synthesized, as depicted in Scheme 4 (see the Experimental section for details⁵²⁻⁵⁶).

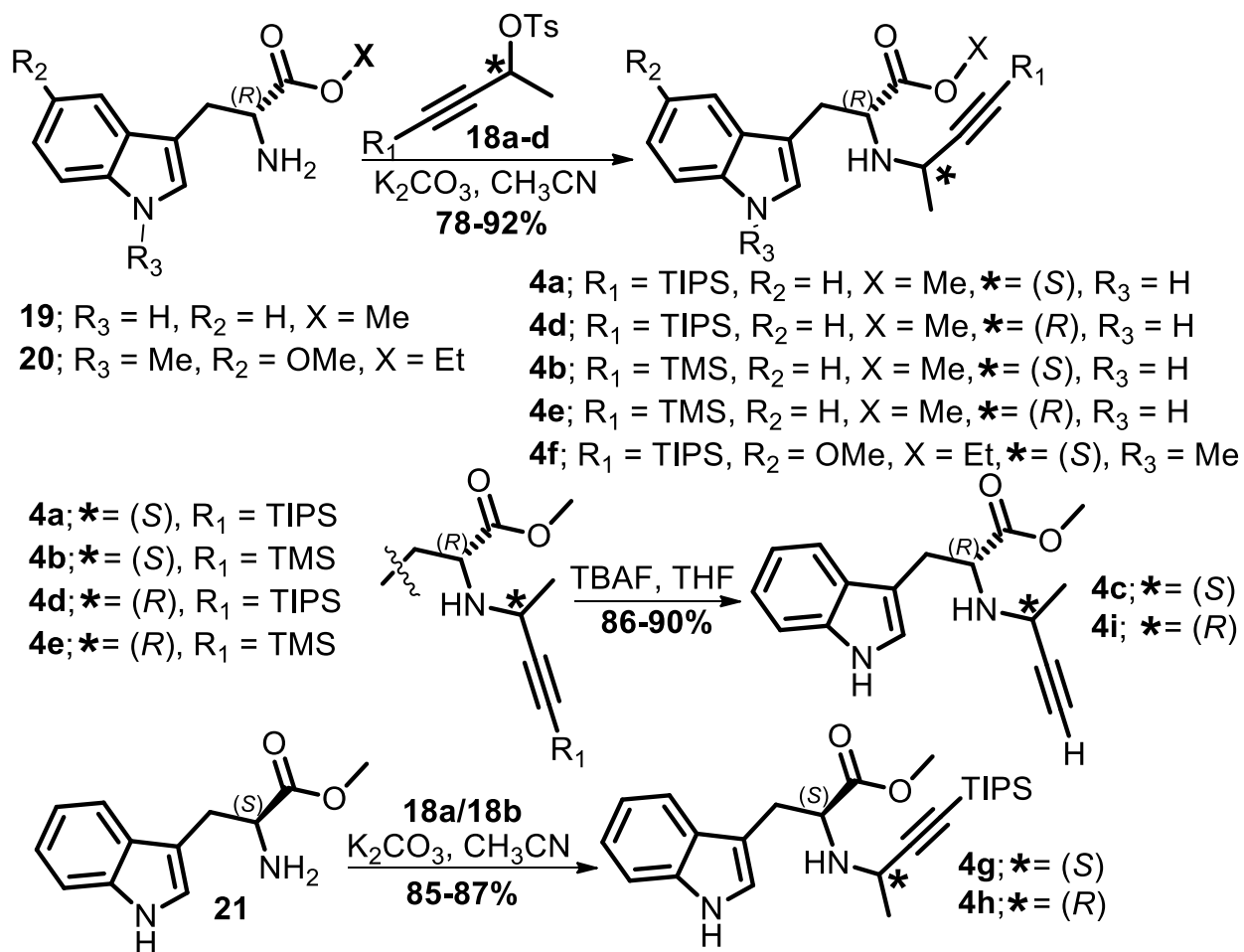


Scheme 4. Different amine-substrates for the P-S reaction and synthesis of tosylate units;

Reagents and conditions: a) (*S,S*)-Ru or (*R,R*)-Ru catalyst (1 mol%), *i*-PrOH, rt, 3 h, **85-90%**; b) TsCl (2.5 equiv), Et₃N (4 equiv), DMAP (10 mol%), CH₂Cl₂, -30 °C to rt, **92-95%**.

The synthesis of the tryptophan amine-substrates (**4a-i**) for the P-S reaction were carried out, as shown in Scheme 5. With all the required substrates in hand, the planned reactions were performed with 1 equivalent of the amines, 1.5 equivalents of the aldehyde **5**, 3 equivalents of acetic acid, 200 mg 4 Å MS (per mmol of amines). The reactions were performed in parallel at 0 °C and at rt. The outcome of these experiments are listed in Table 1. These reaction processes gave excellent overall isolated yields (up to 95%) with selectivity towards *cis*-diesters. All the *cis*- and *trans*-diester products were easily separable by silica gel column chromatography except for entry 6

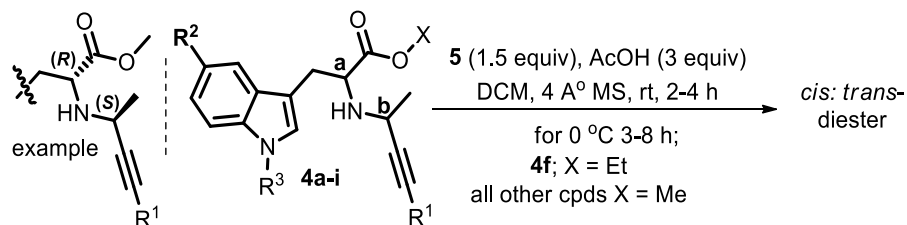
where both *cis* and *trans* diastereomers had the same R_f in several solvent systems. Interestingly, some clear patterns emerged. For example, when the carbon atoms **a** and **b** had the same configurations (*S,S*) or (*R,R*) (Table 1, entries 2, 4, 6, and 8), reactions were up to 82% *cis*-selective. The *cis*-selectivity improved at lower temperature (e.g., Table 1, entries 2, 8) and the bulky TIPS containing amines exhibited better *cis*-selectivity (compare entry 2 and 8 vs 4 and 6 in Table 1) than amines which contained a TMS- or H-substitution. Interestingly, on the other hand, when the configurations of carbon atoms **a** and **b** in the amine substrates were opposite to each other i.e., (*R,S*) or (*S,R*), reactions were 100% *cis*-selective regardless of temperature, and size of the alkyne protecting groups (TIPS, TMS and H), as indicated by entries 1, 3, 5, 7, and 9. As expected, the P-S reaction with an electron rich tryptophan (**4f**, 5-MeO) reacted faster. The C-5 ring-A oxygen function, however, had no effect on the outcome of the diastereoselectivity other than speeding up the rate. Similarly, the same pattern was observed with the L-(-)-tryptophan derivatives (entries 8 and 9). More importantly, all of the diastereomers could easily be separated and the pure, isolated *cis*-diesters could be converted into the corresponding *trans*-diesters (100% *de*), simply by treatment with TFA in DCM for 2-20 hours at room temperature (see the Experimental section for details).



Scheme 5. Synthesis of Pictet-Spengler substrates (**4a-i**)

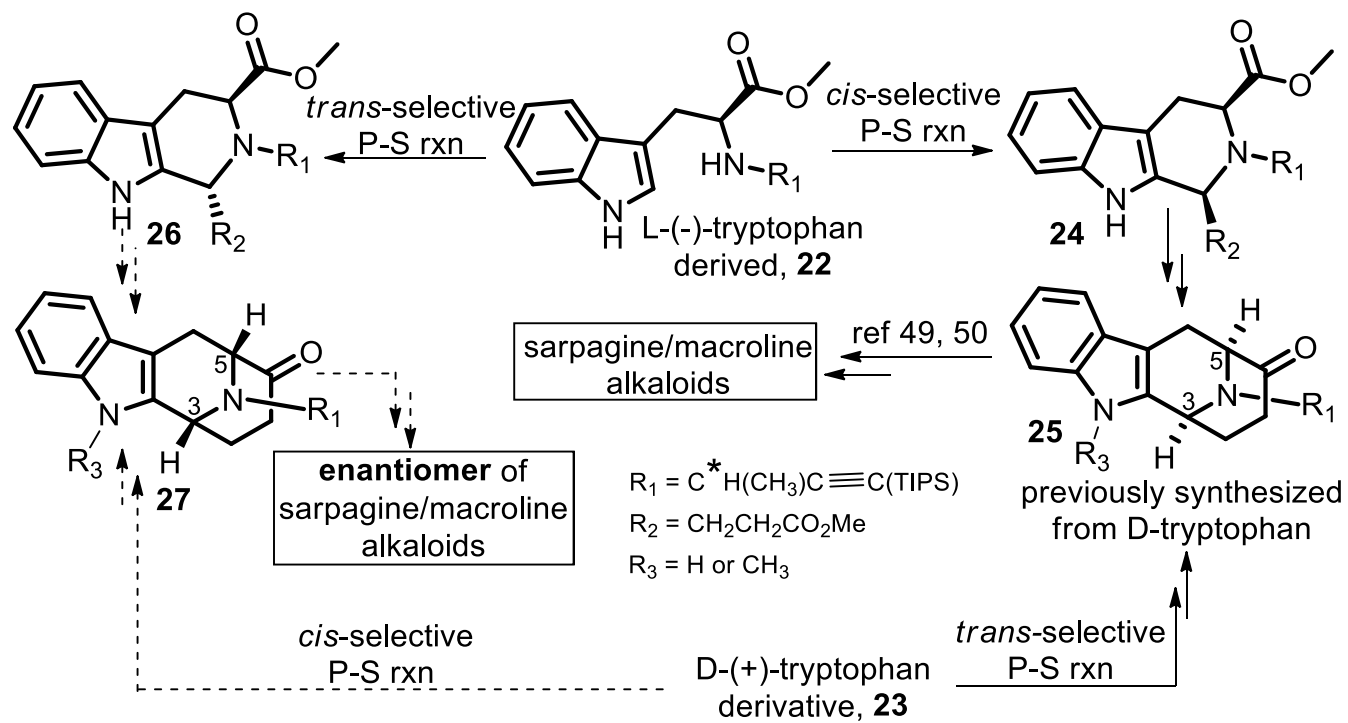
Consequently, conditions were designed for selective generation of either the *trans*- or the *cis*-diesters from either D(+)- or L(-)-tryptophan. It is well known that plants or natural sources generally produce one enantiomer of the chiral natural products. Due to this, it is possible to isolate and screen for bioactivity only one series of the enantiomers. Logically, the unnatural enantiomer might actually be as good as the natural enantiomer or even better in activity, as well as in toxicity profile depending on the rate of metabolism. The development of the life-saving anti-HIV/AIDS drug emtricitabine by Professor Liotta at Emory exemplified the tremendous potential of unnatural enantiomers of bioactive molecules in drug discovery.⁵⁷ As depicted in Scheme 5, the 3,5-*cis*-

disubstitution (biogenetic numbering, **24** and **25**) of the natural enantiomer of the sarpagine/macrorline alkaloids could be furnished from either natural L-tryptophan via a *cis*-selective P-S reaction or alternatively from D-tryptophan via a *trans*-selective P-S reaction. Conversely, the unnatural enantiomer of these alkaloids would also be accessible either from L-tryptophan *via* a *trans*-selective P-S reaction (**26** and **27**) or alternatively from D-tryptophan *via* a *cis*-selective P-S reaction (see Scheme 6 for details). This novel ambidextrous approach to the synthesis of both the natural and unnatural enantiomers of bioactive sarpagine-type alkaloids would permit the rapid screening of the biological activity of both of the enantiomers. To illustrate the usefulness of this method, the synthesis of key intermediates for natural product synthesis,⁴⁹ **28** and **30**, starting from L-tryptophan derivative **21** were undertaken. The β -ketoesters **28**, and **30** are key intermediates for the total synthesis of a group of sarpagine-related indole alkaloids and were employed previously for the total synthesis of natural alkaloids and were synthesized from D-(-)-tryptophan methyl ester.⁴⁹ As shown in Scheme 6, the *cis*-diester **29** was synthesized from L-(+)-tryptophan methyl ester **21** *via* N_b -alkylation (**4h**) and the *cis*-specific P-S reaction (100% *cis*, Table 1, entry 9). The *cis*-diester **29** upon Dieckmann cyclization provided the β -ketoester **28** in excellent yield. The ester **28** was previously synthesized from (-)-**19**.⁴⁹ The indoles from both routes were identical in all respects (R_f , ^1H NMR, and ^{13}C NMR), as well as the optical rotation (see Figure 2). This enabled one to access the same group of indole alkaloids starting from L-tryptophan *via* the unprecedented *cis*-specific P-S reaction reported herein (Scheme 7).

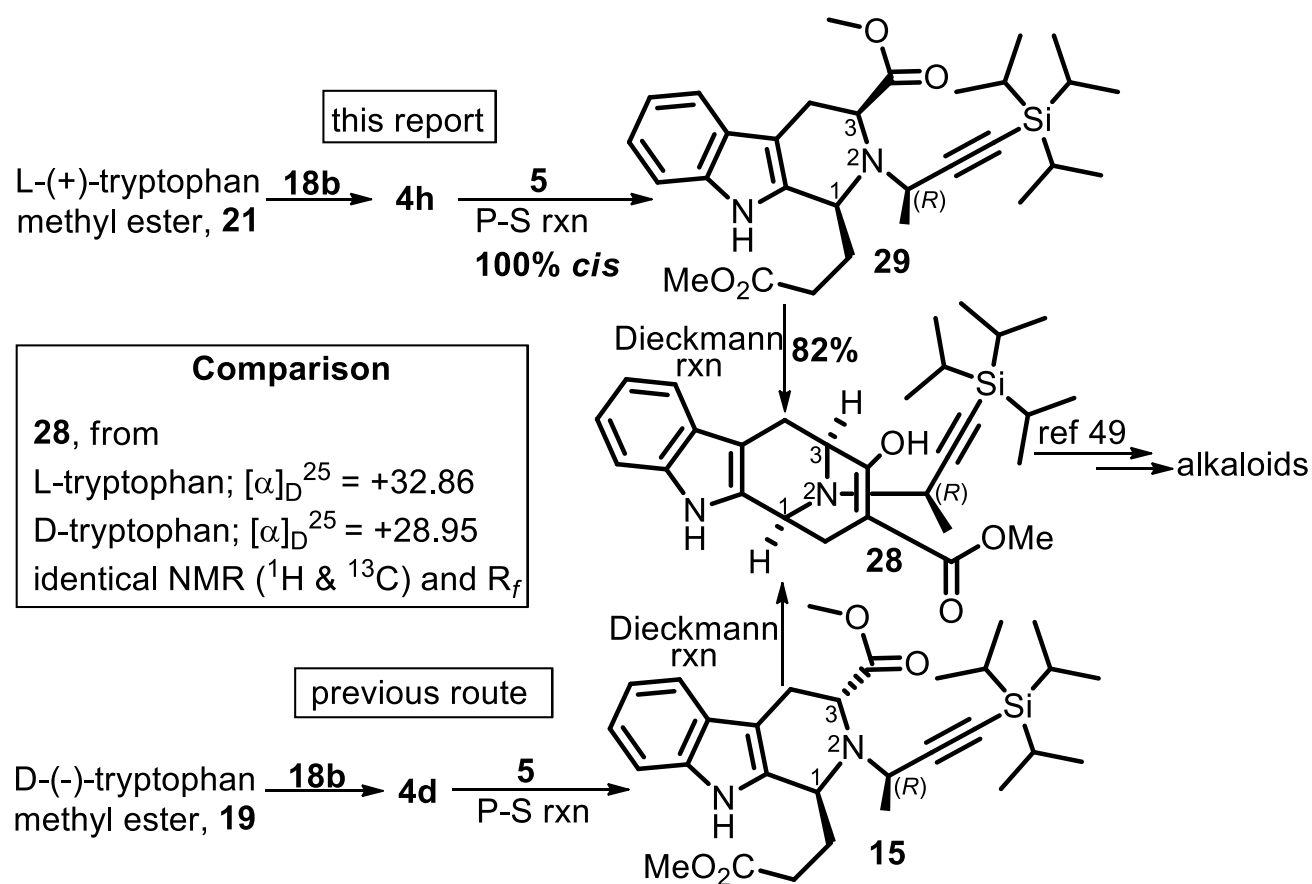
Table 1. P-S reaction of amines **4a-i** with aldehyde **5**

entry	amine-substrate						<i>cis:trans</i> (0 °C) ^d	<i>cis:trans</i> (rt) ^e	yield ^a (%)
	cpd	R ₁	R ₂	R ₃	a	b			
1	4a	TIPS	H	H	R	S	100:0	100:0	90
2	4d	TIPS	H	H	R	R	72:28	65:35	95
3	4b	TMS	H	H	R	S	100:0	100:0	82
4	4e	TMS	H	H	R	R	43:57	50:50	84
5	4c	H	H	H	R	S	100:0	100:0	85
6	4i	H	H	H	R	R	58:42 ^b	_c	78
7	4f	TIPS	OMe	Me	R	S	100:0	100:0	85
8	4g	TIPS	H	H	S	S	82:18	72:28	85
9	4h	TIPS	H	H	S	R	100:0	100:0	88

[a] Isolated yields; [b] both *cis* and *trans* isomers had the same R_f, and were isolated after complete conversion into the *trans*-diester; [c] not done; *cis:trans* at [d] 0 °C; [e] room temp.



Scheme 6. Stereospecific total synthesis of both enantiomers of C-19 methyl substituted macroline/sarpagine indole alkaloids from either L-(-)- or D-(+)-tryptophan



Scheme 7. Synthesis of the key β -ketoester (+)-**28** towards sarpagine-type indole alkaloids from either (+)-**21** or (-)-**19**

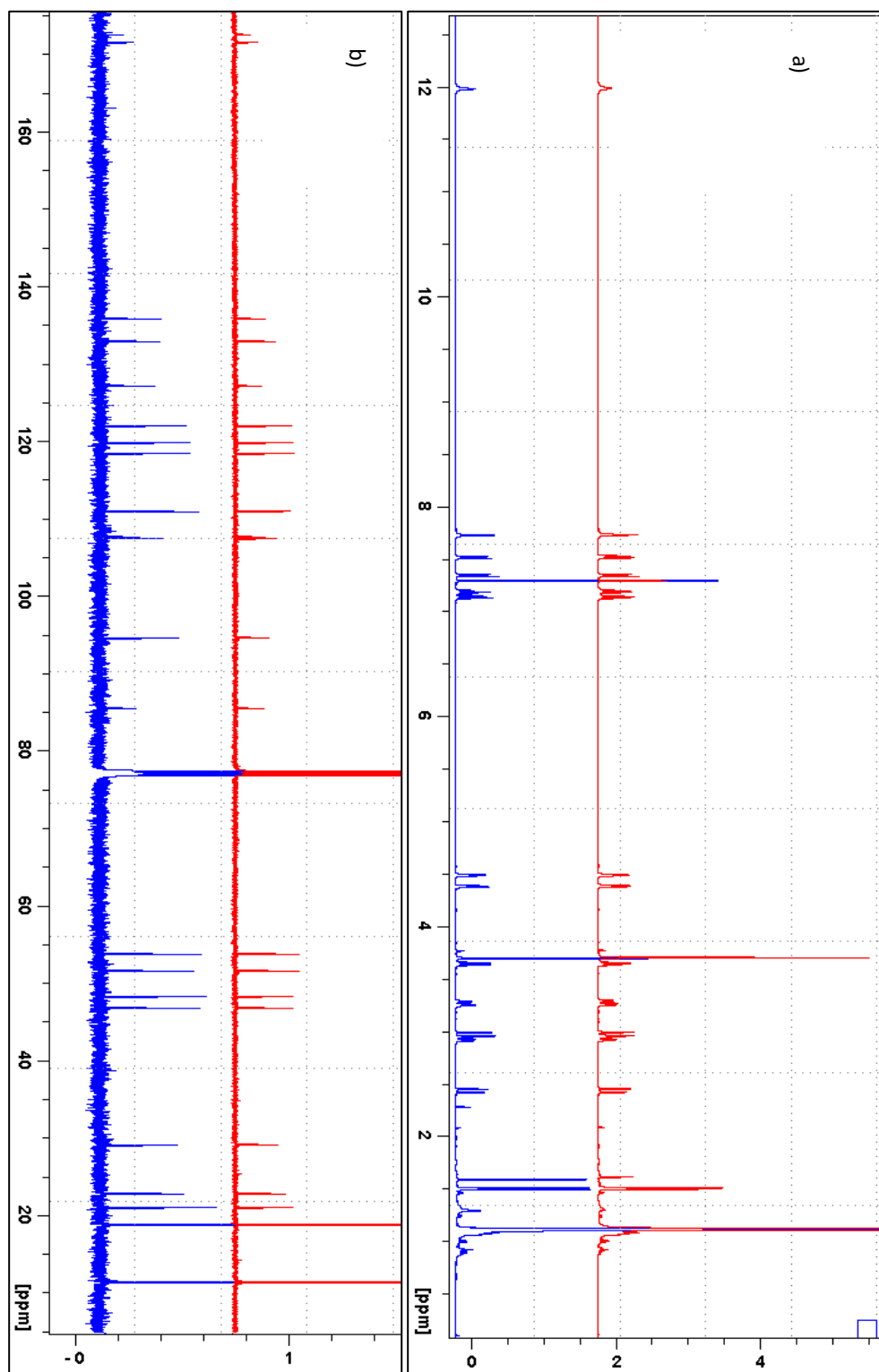
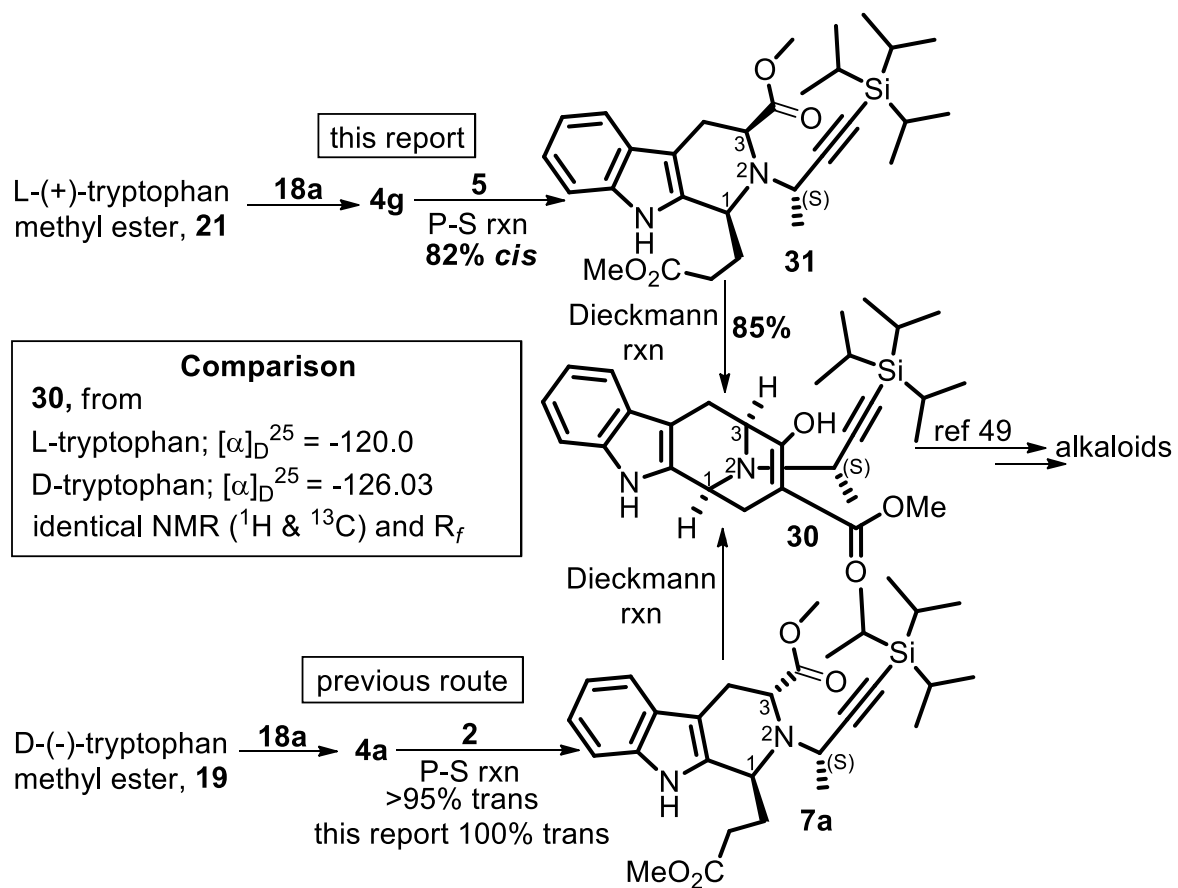


Figure 2. Comparison between the (a) ^1H and (b) ^{13}C NMR spectra of (+)-**28** from L-tryptophan (red) and D-tryptophan (blue) as shown in Scheme 7.



Scheme 8. Synthesis of (-)-**30** from either (+)-**21** or (-)-**19**

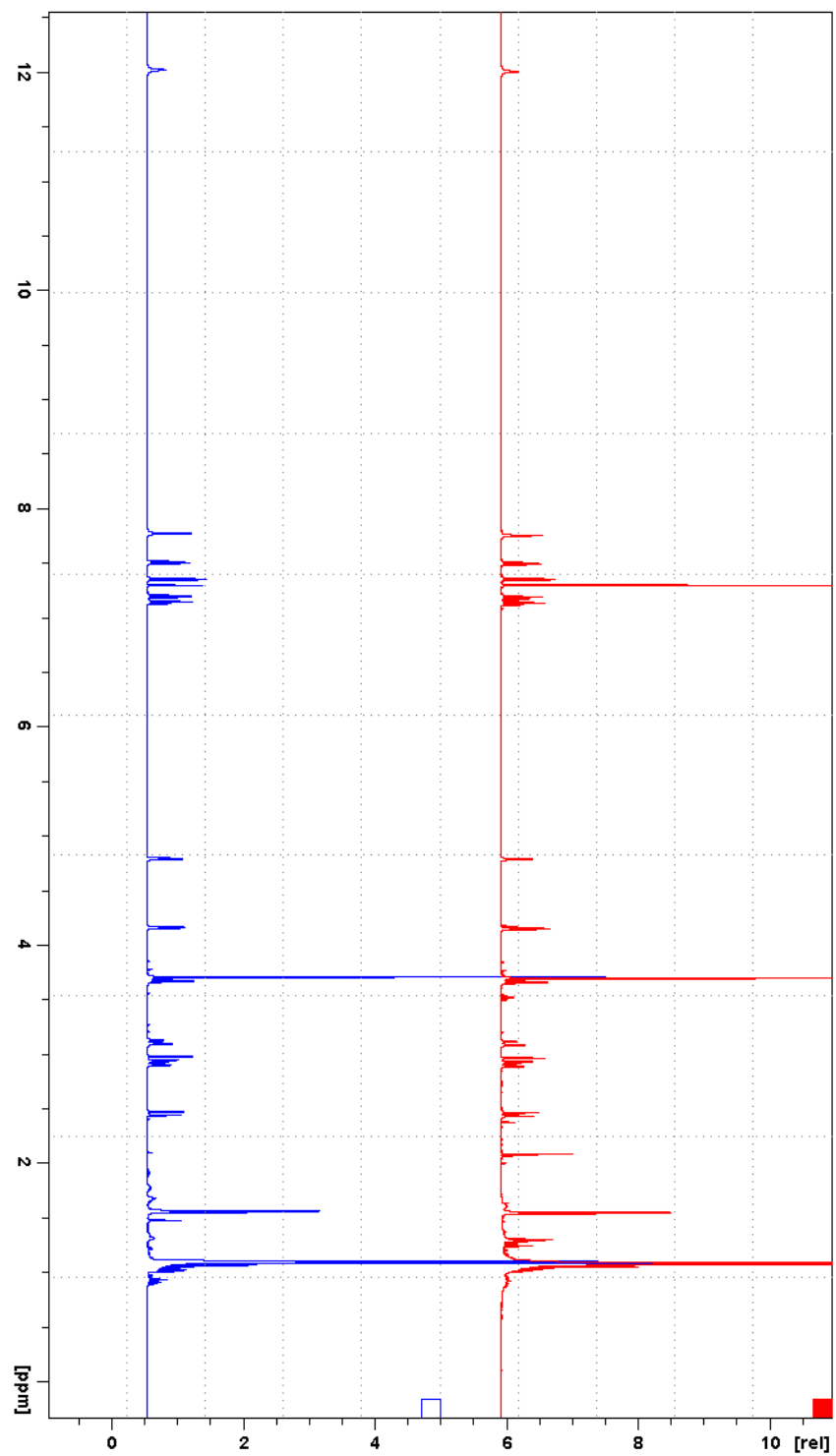


Figure 3a: Comparison between ^1H of (-)-**30** prepared from **L-tryptophan** (red) and **D-tryptophan** (blue)

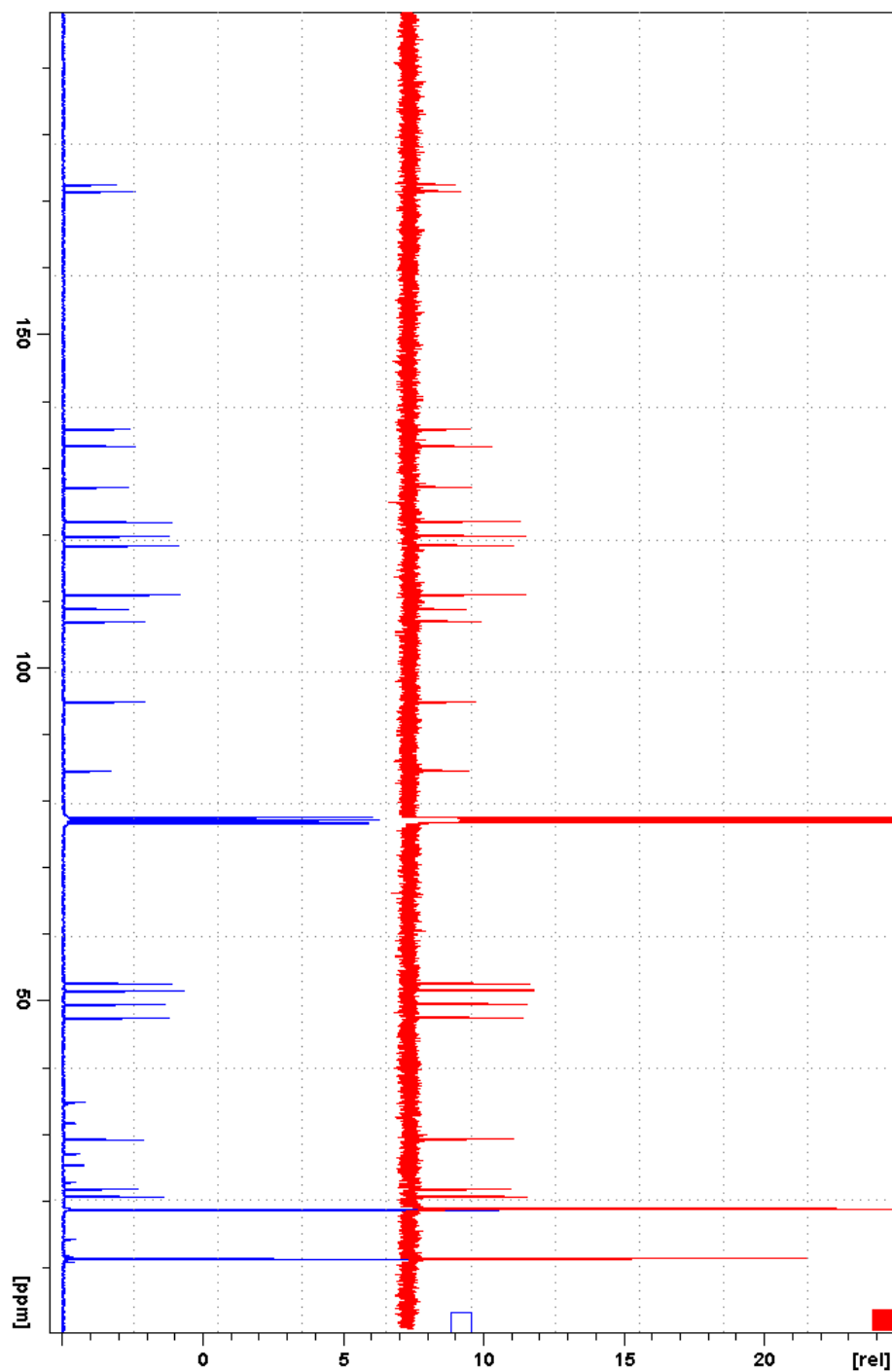


Figure 3b: Comparison between ¹³C of (-)-**30** prepared from **L-tryptophan** (red) and **D-tryptophan** (blue)

Similarly, the β -ketoester **30** could be prepared from D-tryptophan via **7a** (100% *trans*-selective P-S reaction, which was shown to be >95% *dr* previously⁴⁹), as depicted in Scheme 8. Importantly

the same β -ketoester **30** could be synthesized from (+)-**21** via a *cis*-selective (82% *cis*) P-S reaction. The spectral properties of (-)-**30** from both (+)-**21** and (-)-**19** are identical in all respects [see Figures 3a and 3b).

3. Conclusion

In summary, we have developed a novel strategy to gain access to the 1,2,3-trisubstituted TH β Cs with the required C-3/C-5 stereochemistry of a group of sarpagine-related indole alkaloids with unprecedented control of the asymmetric P-S reaction. This report also illustrates the ability to achieve the complete *cis*-selectivity of the PS reaction to form the 1,2,3-trisubstituted TH β C by internal asymmetric induction. Key intermediates [(+)-**28** and (-)-**30**] towards the total synthesis of a group of seventy C-19 methyl substituted alkaloids have been accessed from the natural and cheaper L-(-)-tryptophan now instead of the previously developed route from D-(+)-tryptophan. This permits the synthesis of either enantiomer from the same TH β C branching point. The total synthesis of the unnatural enantiomers of bioactive alkaloids from this group and investigation of the mechanism of this Pictet-Spengler reaction is underway and will be reported in due course.

4. Experimental Section

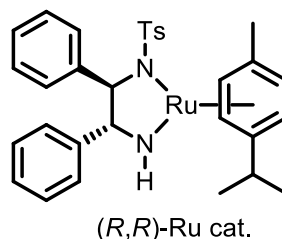
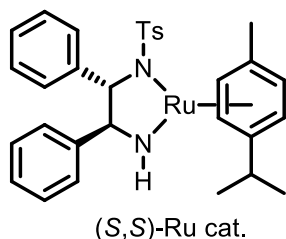
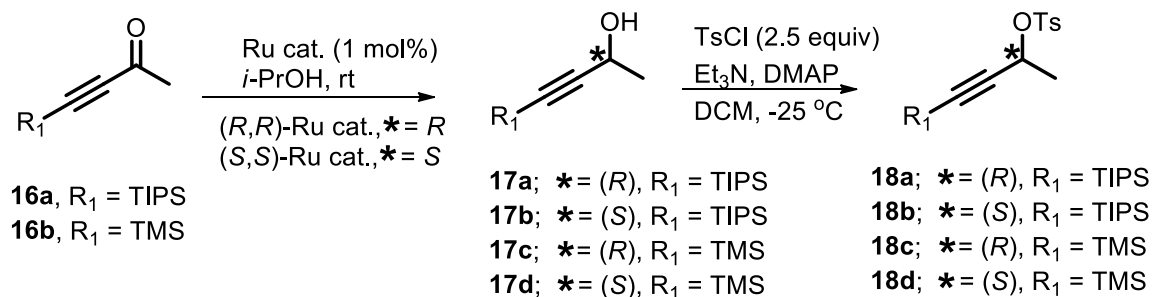
General Experimental Considerations

All reactions were carried out under an argon atmosphere with dry solvents using anhydrous conditions unless otherwise stated. Tetrahydrofuran (THF) and diethyl ether were freshly distilled from Na/benzophenone ketyl prior to use. Dichloromethane was distilled from calcium hydride prior to use. Methanol was distilled over magnesium sulfate. Benzene and toluene were distilled over Na. Acetonitrile was distilled over CaH₂ prior to use. Reagents were purchased of the highest commercial quality and used without further purification unless otherwise stated. Thin layer chromatography (TLC) was performed on UV active silica gel plates, 200 μm, aluminum backed and UV active alumina N plates, 200 μm, F-254 aluminum backed plates. Flash and gravity chromatography were performed using silica gel P60A, 40-63 μm, basic alumina (Act I, 50-200 μm) and neutral alumina (Brockman I, ~150 mesh). TLC plates were visualized by exposure to short wavelength UV light (254 nm). Indoles were visualized with a saturated solution of ceric ammonium nitrate in 50% phosphoric acid. The ¹H NMR data are reported as follows: chemical shift, multiplicity (br s = broad singlet, s = singlet, d = doublet, t = triplet, q = quartet, quin = quintet, dd = doublet of doublets, dt = doublet of triplets, ddd = doublet of doublet of doublets, td = triplet of doublets, qd = quartet of doublets, m = multiplet), integration, and coupling constants (Hz). The ¹³C NMR data are reported in parts per million (ppm) on the δ scale. The low resolution mass spectra (LRMS) were obtained as electron impact (EI, 70eV) and as chemical ionization (CI) using a magnetic sector (EBE) analyzer. HRMS were recorded by electrospray ionization (ESI) using a TOF analyzer, electron impact (EI) using a trisector analyzer and Atmospheric Pressure

Chemical Ionization (APCI) using a TOF analyzer. Optical rotations were measured on a JASCO Model DIP-370 digital polarimeter.

Experimental Procedures and Analytical Data

Procedure for the synthesis of optically active tosylates 21a-d from ketone 19a-b

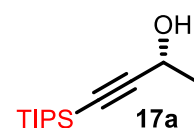


RuCl[(S,S)-NTsCH(C₆H₅)CH(C₆H₅)NH₂(η 6-cymene); (*S*, *S*)-Ru Catalyst and **RuCl[(R, R)-NTsCH(C₆H₅)CH(C₆H₅)NH₂(η 6-cymene)**; (*R*, *R*)-Ru catalyst were prepared following the procedure available in the literature. They were dark purple colored solids and were used for the subsequent reductions without further purification and characterization.^{58,59} The optically active (*R*) or (*S*)-alcohols, **17a** (*R*, 90%) and **17b** (*S*, 95%), **17c** (*R*, 85%), and **17d** (*S*, 90%) were synthesized following the literature procedure.^{53,55,59}

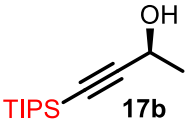
Representative example, (17c): A 250 mL round bottom flask was flame dried and loaded with a magnetic stir bar. The flask was flushed with argon and subsequently charged with dry isopropyl alcohol (125 mL) and 4-trimethylsilyl-3butyn-2-one **16b** (2.5 g, 2.93 mL, 17.8 mmol, TCI America, >97%). The Ru catalyst [(*R, R*)-Ru cat.] (113 mg, 0.18 mmol) was dissolved in a small amount of DCM (2 mL) and added to the above reaction mixture with a syringe, in a single portion. The reaction mixture, which resulted, was stirred at rt for 2 hours. The solvent was removed under reduced pressure and the dark brown residue was purified by a semi-micro distillation kit to furnish the optically active alcohol **17c** (2.12 g) in 85% yield as a colorless liquid.

Similarly, by following the same procedure, **17a** (1.7 g, 85%) was synthesized from **16a** (2.0 g, 8.91 mmol) and (*R, R*)-Ru catalyst (57 mg, 0.09 mmol); **17b** (2.2g, 87%) was synthesized from **16a** (2.5 g, 11.1 mmol) and (*S, S*)-Ru catalyst (71 mg, 0.11 mmol); **17d** (2.25 g, 90%) was synthesized from **16b** (2.5 g, 17.8 mmol) and (*S, S*)-Ru catalyst (113 mg, 0.18 mmol).

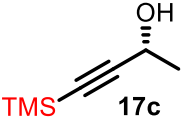
(*R*)-4-(Triisopropylsilyl)but-3-yn-2-ol (**17a**)

 **17a** ¹H NMR (300 MHz, CDCl₃): δ 4.55 (q, 1H, *J* = 6.39 Hz), 2.07 (br s, 1H), 1.48 (d, 3H, *J* = 6.54 Hz), 1.09-1.04 (m, 21H); ¹³C NMR (75 MHz, CDCl₃): δ 109.9, 84.4, 58.8, 24.5, 18.5, 11.1; [α]_D²⁵ = +22.5 (*c* 1.6, CHCl₃); *R*_f: 0.6 (10% EtOAc in hexanes, KMnO₄ stain). The spectral and optical properties were in excellent agreement with the previously reported values. ^[3]

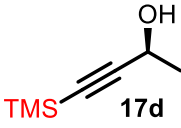
(S)-4-(Triisopropylsilyl)but-3-yn-2-ol (17b)

 **¹H NMR** (500 MHz, CDCl₃): δ 4.55 (q, 1H, *J* = 6.58 Hz), 2.15 (br s, 1H), 1.48 (d, 3H, *J* = 6.60 Hz), 1.10-1.04 (m, 21H); **¹³C NMR** (125 MHz, CDCl₃): δ 109.9, 84.4, 58.8, 24.5, 18.5, 11.10; [α]_D²⁵ = -21.60 (*c* 1.5, CHCl₃); **R_f**: 0.6 (10% EtOAc in hexanes). The spectral and optical properties were in excellent agreement with the previously reported values. [3]

(R)-4-(Trimethylsilyl)but-3-yn-2-ol (17c)

 **¹H NMR** (500 MHz, CDCl₃): 4.56-4.53 (m, 1H), 2.36-2.19 (m, 1H), 1.48-1.45 (m, 3H), 0.19 -0.18 (m, 9H); **¹³C NMR** (125 MHz, CDCl₃): 107.7, 88.4, 58.7, 24.2, 0.13; [α]_D = +28.26 *c* 2.30, CHCl₃; Lit⁵⁶ [α]_D²⁵ = +24.7 (*c* 0.34, CHCl₃), Lit⁵⁴ [α]_D²⁵ = +23.8 (*c* 2.02, CHCl₃); **R_f**: 0.4 (silica gel, 10% EtOAc in hexanes, KMnO₄ stain).

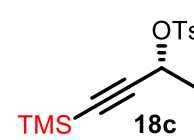
(S)-4-(Trimethylsilyl)but-3-yn-2-ol (17d)

 **¹H NMR** (500 MHz, CDCl₃): 4.55 (m, 1H), 1.78 (d, 1H, *J* = 5.25 Hz), 1.48 (d, 3H, *J* = 6.65 Hz), 0.20 (s, 9H); **¹³C NMR** (125 MHz, CDCl₃): 107.7, 88.4, 58.8, 24.3, -0.12; [α]_D²⁵ = -26.96 (*c* 3.45, CHCl₃), Lit⁵² [α]_D²⁵ = -25.9 (*c* 3.12, CHCl₃); **R_f**: 0.4 (10% EtOAc in hexanes, KMnO₄ stain).

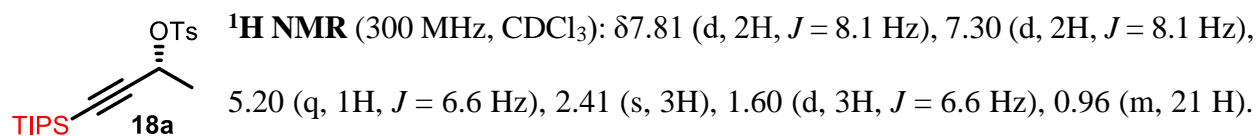
The optically pure tosylate-units **18a** (95%), **18b** (95%), **18c** (95%), and **18d** (92%) were prepared from the corresponding optically pure alcohols **17a-d** by following the procedure available in the literature.^{49,60}

Representative Example, 18c: A 250 mL round bottom flask equipped with a large magnetic stir bar was flame dried under a continuous flow of argon and was then allowed to cool under argon. The flask was then charged with freshly distilled CH₂Cl₂ (50 mL) and (*R*)-alcohol (**17c**, 2.0 g, 14.06 mmol) after which the mixture was cooled to -25 °C (outside bath temperature). Triethylamine (7.84 mL, 56.2 mmol) and a catalytic amount of DMAP (172 mg, 1.4 mmol) were added, and after a few minutes of stirring, tosyl chloride (6.7 g, 35.1 mmol, Acros Organics, 99%) was added in one portion. The reaction mixture was allowed to stir at -25 °C for 45 min and the solution was allowed to slowly warm to rt. After the reaction mixture was stirred for 3 h at rt, analysis by TLC (silica gel) was carried out, after which the reaction mixture was quenched with a large excess of water (200 mL). The mixture was then allowed to stir vigorously for 45 min. After 45 min, the two layers were separated. The CH₂Cl₂ layer was dried (MgSO₄), filtered and concentrated under reduced pressure to furnish **18c** (3.96 g, 95%) as a light brown oil, which was used for the next reaction without further purification.

(*R*)-4-(Trimethylsilyl)but-3-yn-2-yl 4-methylbenzenesulfonate (18c)

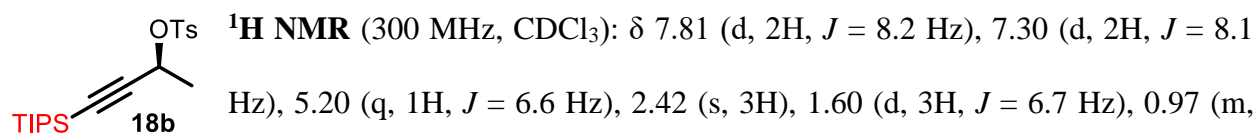
 **¹H NMR** (500 MHz, CDCl₃): 7.84 (d, 2H, *J* = 8.30 Hz), 7.35 (d, 2H, *J* = 8.10 Hz), 5.20 (q, 1H, *J* = 6.68 Hz), 2.46 (s, 3H), 1.58 (d, 3H, *J* = 6.70 Hz), 0.06 (s, 9H); **¹³C NMR** (125 MHz, CDCl₃): 144.6, 134.2, 129.6, 128.1, 100.8, 92.7, 68.5, 22.8, 21.7, -0.5; [α]_D²⁵ = +94.66 (c 2.62, CHCl₃).

(R)-4-(Triisopropylsilyl)but-3-yn-2-yl 4-methylbenzenesulfonate (18a)

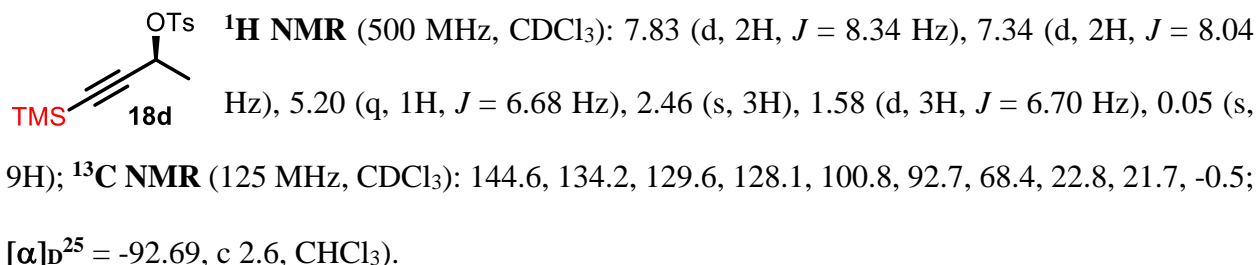


All other spectroscopic data was identical with the published data for **18a**.⁶¹ This material was used for the next step without further characterization.

(S)-4-(Triisopropylsilyl)but-3-yn-2-yl 4-methylbenzenesulfonate (18b)



(S)-4-(Trimethylsilyl)but-3-yn-2-yl 4-methylbenzenesulfonate (18d)



Synthesis of the *N*_b-alkylated tryptophan derivatives (substrates for the P-S reaction)

General procedure for the synthesis of **4a-b, d-h**

Representative example, 4h: L-tryptophan methyl ester hydrochloride (**21·HCl**, 4.0 g, 15.7 mmol) was dissolved in freshly distilled acetonitrile (80 mL) in a 250 mL round bottom flask. The tosylate **18b** (11.36 g, 29.8 mmol) was dissolved in acetonitrile and added into the round bottom flask with a syringe. Anhydrous K₂CO₃ (7.60 g) was added and the mixture, which resulted, was heated to reflux under argon for 12 h. After the completion of the reaction as indicated by the disappearance of the starting material by TLC (silica gel, EtOAc/hexane, 1: 3) and LRMS ($M+H^+ = 427.35$), the reaction was cooled to rt and the K₂CO₃ was filtered off by passing the solution through a bed of celite. The celite was washed with EtOAc and the EtOAc fractions were removed under reduced pressure to furnish crude **4h** as a brownish oil. The residue was purified by flash column chromatography (silica gel, 1-5% EtOAc in hexanes) to provide **4h** as a light yellowish-colored oil (5.83 g, **87%**).

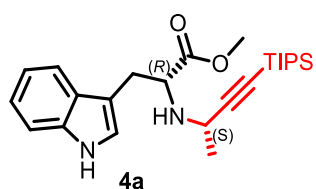
By following the same procedure, **4g** (4.98 g, 85%) was prepared from amine **21·HCl** (3.5 g, 13.7 mmol) and tosylate **18a** (9.94 g, 26.1 mmol); **4a** (16.6 g, 85%) was prepared from amine **19** (10.0 g, 45.8 mmol) and tosylate **18a** (26.2 g, 68.7 mmol); **4d** (5.39 g, 92%) was prepared from amine **19** (3.0 g, 13.7 mmol) and tosylate **18b** (9.94 g, 26.1 mmol); **4b** (2.45 g, 78%) was prepared from amine **19** (2.0 g, 9.2 mmol) and tosylate **18a** (5.16 g, 17.4 mmol); **4e** (1.9 g, 80%) was prepared from amine **19** (1.5 g, 6.9 mmol) and tosylate **18b** (3.87 g, 13.0 mmol); **4f** (772 mg, 88%) was prepared from amine **20** (0.5 g, 1.81 mmol) and tosylate **18a** (1.31 g, 3.44 mmol).

General procedure for the synthesis of **4c** and **4i**

Representative example, 4c: To a solution of **4a** (0.5 g, 1.2 mmol) in THF (10 mL), TBAF (1.76 mL, 1.76 mmol, 1.0 M solution in THF) was added at 0 °C. The solution, which resulted, was stirred at 0 °C for 30 min or until the completion of the reaction, as indicated by TLC. After that, the reaction was diluted with EtOAc (20 mL) and water (10 mL). The organic layer was separated and the aq layer was extracted with EtOAc (5 mL). The combined organic layers were washed with brine (3 x 20 mL) and dried (Na₂SO₄). The solvent was removed under reduced pressure to provide the alkyne **4c** (LRMS M+H⁺ = 271.10) as a brown residue. The residue was purified by silica gel column chromatography (30% EtOAc in hexanes) to provide **4c** as light brown solid (285 mg, 90%).

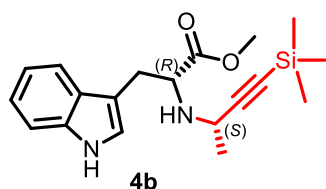
By following the same procedure, **4i** (272 mg, 86%) was prepared from the TIPS-protected alkyne **4d** (500 mg, 1.2 mmol) and TBAF (1.76 mL, 1.76 mmol).

(*R*)-Methyl 3-(1*H*-indol-3-yl)-2-(((*S*)-4-(triisopropylsilyl)but-3-yn-2-yl)amino)propanoate (**4a**)



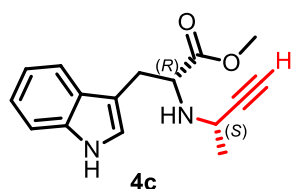
¹H NMR (300 MHz, CDCl₃): δ 8.12 (br s, 1H), 7.65 (d, 1H, *J* = 7.7 Hz), 7.34 (d, 1H, *J* = 7.9 Hz), 7.23-7.06 (m, 3H), 3.97 (t, 1H, *J* = 6.1 Hz), 3.63 (s, 3H), 3.58 (q, 1H, *J* = 6.8 Hz), 3.19 (d, 2H, *J* = 6.1 Hz), 1.98 (br s, 1H), 1.35 (d, 3H, *J* = 6.7 Hz), 1.12-1.06 (m, 21H). All other spectroscopic and optical properties were identical to the published values.⁴⁹

(R)-Methyl 3-(1H-indol-3-yl)-2-(((S)-4-(trimethylsilyl)but-3-yn-2-yl)amino)propanoate (4b)



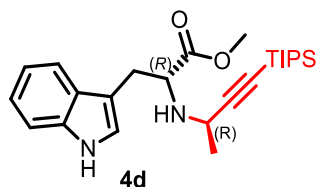
¹H NMR (300 MHz, CDCl₃): 8.39 (br s, 1H), 7.66 (d, 1H, *J* = 7.65 Hz), 7.34 (br d, 1H, *J* = 7.69 Hz), 7.24-7.10 (m, 2H), 7.02 (d, 1H, *J* = 2.19 Hz), 3.89 (t, 1H, *J* = 6.39 Hz), 3.65 (s, 3H), 3.60 (q, 1H, *J* = 6.75 Hz, overlapped with CO₂CH₃ peak), 3.19 (d, 2H, *J* = 6.36 Hz), 1.96 (br s, 1H), 1.34 (d, 3H, *J* = 6.75 Hz), 0.19-0.16 (m, 9H); **¹³C NMR** (75 MHz, CDCl₃): 175.3, 136.2, 127.6, 123.0, 121.9, 119.3, 118.7, 111.2, 111.0, 107.9, 87.3, 59.9, 51.8, 44.7, 29.2, 22.2, 0.07; **HRMS** (ESI) *m/z* (M+H)⁺ Calcd for C₁₉H₂₇N₂O₂Si 343.1836, found 343.1841; [α]_D²⁵ = -77.16 (c 1.27, CHCl₃); **R_f**: 0.33 (silica gel, 20% EtOAc in hexanes).

(R)-Methyl 2-(((S)-but-3-yn-2-ylamino)-3-(1H-indol-3-yl)propanoate (4c)



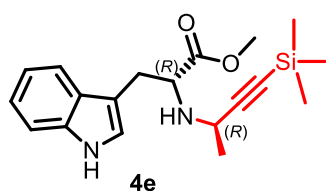
4c, ¹H NMR (500 MHz, CDCl₃): 8.28 (br s, 1H), 7.36 (d, 1H, *J* = 8.09 Hz), 7.24-7.19 (m, 1H), 7.17-7.14 (m, 1H), 7.05 (d, 1H, *J* = 2.10 Hz), 3.87 (t, 1H, *J* = 6.42 Hz), 3.66 (s, 3H), (qd, 1H, *J* = 6.78 Hz, 2.05 Hz), 3.19 (d, 2H, *J* = 6.45 Hz), 2.7 (d, 1H, *J* = 2.05 Hz), 1.95 (br s, 1H), 1.36 (d, 3H, *J* = 6.80 Hz); **¹³C NMR** (125 MHz, CDCl₃): 175.4, 136.2, 127.6, 123.0, 122.0, 119.4, 118.8, 111.2, 111.1, 85.7, 71.1, 60.0, 51.8, 44.0, 29.1, 22.2; **HRMS** (ESI) *m/z* (M+H)⁺ Calcd for C₁₆H₁₉N₂O₂ 271.1441, found 271.1448; [α]_D²⁵ = -66.26 (c 1.66, CHCl₃); **R_f**: 0.30 (silica gel, 40% EtOAc in hexanes).

(R)-methyl 3-(1H-indol-3-yl)-2-(((R)-4-(triisopropylsilyl)but-3-yn-2-yl)amino)propanoate (4d)



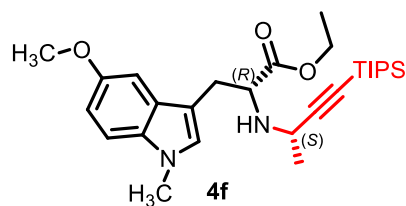
¹H NMR (300 MHz, CDCl₃): 8.13 (br s, 1H), 7.65 (d, 1H, *J* = 7.8 Hz), 7.36 (d, 1H, *J* = 8.0 Hz), 7.24-7.17 (t, 1H, *J* = 7.4 Hz), 7.16-7.09 (m, 2H), 4.17-4.10 (m, 1H), 3.69 (s, 3H), 3.63 (q, 1H, *J* = 6.7 Hz), 3.32-3.23 (m, 1H), 3.20-3.10 (m, 1H), 1.34 (d, 3H, *J* = 6.7 Hz), 1.05-0.99 (m, 21H). All other spectroscopic and optical properties were identical to the published values.⁴⁹

(R)-Methyl 3-(1H-indol-3-yl)-2-(((R)-4-(trimethylsilyl)but-3-yn-2-yl)amino)propanoate (4e)



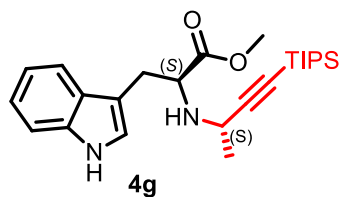
¹H NMR (300 MHz, CDCl₃): 8.45 (br s, 1H), 7.66 (d, 1H, *J* = 7.71 Hz), 7.35 (d, 1H, *J* = 7.92 Hz), 7.24-7.10 (m, 2H), 7.08 (d, 1H, *J* = 1.59 Hz), 4.15-4.08 (m, 1H), 3.70 (s, 3H), 3.59 (q, 1H, *J* = 6.72 Hz), 3.30 (dd, 1H, *J* = 14.40 Hz, 5.46 Hz), 3.16 (dd, 1H, *J* = 14.42 Hz, 8.01 Hz), 1.69 (br s, 1H), 1.31 (d, 3H, *J* = 6.72 Hz), 0.13 (s, 9H); **¹³C NMR** (75 MHz, CDCl₃): 175.0, 136.4, 127.4, 123.0, 122.1, 119.5, 118.8, 111.2, 110.8, 107.7, 87.4, 59.3, 51.9, 44.4, 29.6, 22.4, -0.005; **HRMS** (ESI) *m/z* (M+H)⁺ Calcd for C₁₉H₂₇N₂O₂Si 343.1836, found 343.1832; **[α]_D²⁵** = +42.62 (c 1.22, CHCl₃); **R_f**: 0.2 (silica gel, 20% EtOAc in hexanes).

(R)-Ethyl 3-(5-methoxy-1-methyl-1H-indol-3-yl)-2-(((S)-4-(triisopropylsilyl)but-3-yn-2-yl)amino)propanoate (4f)



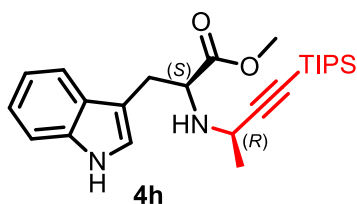
¹H NMR (300 MHz, CDCl₃): 7.16 (d, 1H, *J* = 8.82 Hz), 7.10 (d, 1H, *J* = 2.16 Hz), 6.94 (m, 1H), 6.89 (dd, 1H, *J* = 8.81 Hz, 2.27 Hz), 4.11 (q, 2H, *J* = 7.12 Hz), 3.94-3.89 (m, 1H, overlapped with CO₂Me peak), 3.89 (s, 3H), 3.71 (s, 3H), 3.59 (q, 1H, *J* = 6.75 Hz), 3.14 (d, 2H, *J* = 5.94 Hz), 2.03 (br s, 1H), 1.37 (d, 3H, *J* = 6.75 Hz), 1.16 (t, 3H, *J* = 7.13 Hz), 1.11-1.04 (m, 21H); ¹³C NMR (75 MHz, CDCl₃): 174.6, 153.8, 132.3, 128.6, 128.1, 111.7, 110.2, 109.8, 109.5, 100.9, 82.8, 60.7, 59.5, 55.9, 44.6, 32.8, 28.8, 22.6, 18.6, 14.1, 11.2; HRMS (ESI) *m/z* (M+H)⁺ Calcd for C₂₈H₄₅N₂O₃Si 485.3194, found 481.3203; [α]_D²⁵ = -65.78 (c 1.9, CHCl₃); *R*_f: 0.65 (silica gel, 30% EtOAc in hexanes).

(S)-Methyl 3-(1H-indol-3-yl)-2-(((S)-4-(triisopropylsilyl)but-3-yn-2-yl)amino)propanoate (4g)



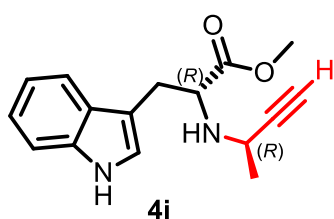
¹H NMR (500 MHz, CDCl₃): 8.21 (br s, 1H), 7.66 (d, 1H, *J* = 7.89 Hz), 7.37 (d, 1H, *J* = 8.04 Hz), 7.21 (t, 1H, *J* = 7.49 Hz), 7.16-7.10 (m, 2H), 4.18-4.13 (m, 1H), 3.70 (s, 3H), 3.64 (q, 1H, *J* = 6.53 Hz), 3.29 (dd, 1H, *J* = 14.41 Hz, 5.27 Hz), 3.16 (dd, 1H, *J* = 14.40 Hz, 8.12 Hz), 1.64 (br s, 1H), 1.35 (d, 3H, *J* = 6.55 Hz), 1.07-1.01 (m, 21H); ¹³C NMR (125 MHz, CDCl₃): 174.9, 136.3, 127.5, 122.8, 122.1, 119.5, 118.8, 111.1, 111.1, 109.5, 83.3, 59.6, 51.8, 44.4, 29.6, 22.8, 18.6, 18.6, 11.1; HRMS (ESI) *m/z* (M+H)⁺ Calcd for C₂₅H₃₉N₂O₂Si 427.2775, found 427.2774; [α]_D²⁵ = -50.64 (c 1.56, CHCl₃); *R*_f: 0.31 (silica gel, 30% EtOAc in hexanes); *m.p.*: 88-89 °C.

(S)-Methyl 3-(1H-indol-3-yl)-2-(((R)-4-(triisopropylsilyl)but-3-yn-2-yl)amino)propanoate (4h)



¹H NMR, (500 MHz, CDCl₃): 8.22 (br s, 1H), 7.67 (d, 1H, *J* = 7.84 Hz), 7.35 (d, 1H, *J* = 8.10 Hz), 7.23-7.18 (m, 1H), 7.16-7.12 (m, 1H), 7.08-7.06 (m, 1H), 4.00 (t, 1H, *J* = 6.15 Hz), 3.65 (s, 3H), 3.61 (q, 1H, *J* = 6.75 Hz), 3.21 (d, 2H, *J* = 6.10 Hz), 2.01 (br s, 1H), 1.37 (d, 3H, *J* = 6.75 Hz), 1.12-1.07 (m, 21H); **¹³C NMR** (125 MHz, CDCl₃): 175.1, 136.1, 127.7, 122.9, 121.9, 119.3, 118.8, 111.3, 111.1, 110.0, 83.1, 59.5, 51.9, 44.7, 28.9, 22.6, 18.6, 11.2; **HRMS** (ESI) *m/z* (M+H)⁺ Calcd for C₂₅H₃₉N₂O₂Si 427.2775, found 427.2776; [α]_D²⁵ = +88.98 (c 1.18, CHCl₃); **R_f**: 0.45 (silica gel, 30% EtOAc in hexanes).

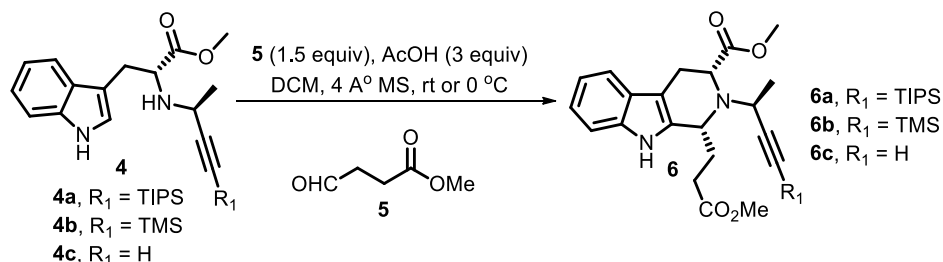
(R)-Methyl 2-(((R)-but-3-yn-2-ylamino)-3-(1H-indol-3-yl)propanoate (4i)



¹H NMR (500 MHz, CDCl₃): 8.32 (br s, 1H), 7.67 (d, 1H, *J* = 7.84 Hz), 7.36 (d, 1H, *J* = 8.09 Hz), 7.24-7.20 (m, 1H), 7.17-7.13 (m, 1H), 7.10 (d, 1H, *J* = 2.10 Hz), 4.14-4.10 (m, 1H), 3.71 (s, 3H), 3.59 (qd, 1H, *J* = 6.71 Hz, 2.05 Hz), 3.30 (dd, 1H, *J* = 14.42 Hz, 5.55 Hz), 3.18 (dd, 1H, *J* = 14.49 Hz, 7.80 Hz), 2.19 (d, 1H, *J* = 2.05 Hz), 1.67 (br s, 1H), 1.34 (d, 3H, *J* = 6.75 Hz); **¹³C NMR** (125 MHz, CDCl₃): 175.0, 136.3, 127.5, 123.0, 122.1, 119.4, 118.9, 111.2, 110.8, 85.4, 59.3, 51.9, 43.7, 29.5, 22.4; **HRMS** (ESI) *m/z* (M+H)⁺ Calcd for C₁₆H₁₉N₂O₂ 271.1441, found 271.1451; [α]_D²⁵ = +51.03 (c 1.45, CHCl₃); **R_f**: 0.42 (silica gel, 50% EtOAc in hexanes).

General procedure for the Pictet-Spengler reactions

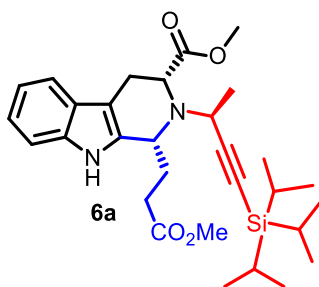
Synthesis of *cis*-diesters **6a-c**



Representative example: Procedure for the synthesis of the *cis*-diester **6a:** The *N*_b-alkylated tryptophan **4a** (100 mg, 0.23 mmol) was dissolved in 10 mL of dry DCM in a 50 mL round bottom flask equipped with a magnetic stir. To that above solution, the aldehyde **5** (41 mg, 0.35 mmol) and acetic acid (42 mg, 0.70 mmol), as well as 4 Å MS (46 mg) were added at rt or at 0 °C. The solution, which resulted, was stirred at rt or 0 °C for 10 h. The progress of the reaction was monitored by TLC (silica gel) analysis, as indicated by the consumption of SM and appearance of a less-polar spot (UV and CAN stain). The reaction mixture was diluted with DCM (20 mL), water (10 mL) and brought to pH 8-9 with cold aq NaOH (1 *N*). The organic layer was separated and washed with water (10 mL), brine (2 x 20 mL) and dried (Na₂SO₄). The solvent was removed under reduced pressure to give **6a** as a light yellow-colored oil. The residue (**LRMS** M+H⁺ = 525, **R_f** = 0.6, silica gel, 30% EtOAc in hexanes) was purified by column chromatography (silica gel, 10-20% EtOAc in hexanes) to furnish pure *cis*-diester **6a** (111 mg, 90%) as a colorless oil.

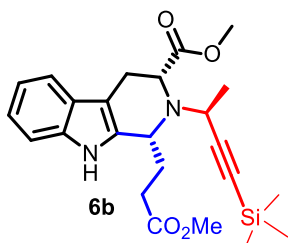
By following the same procedure, the *cis*-diesters **6b** (82%), and **6c** (85%) were synthesized. The *cis*-diester **29** (88%) was synthesized from the *N*_b-alkylated L-tryptophan derivative **4h** using the same procedure described above.

(1*R*,3*R*)-Methyl 1-(3-methoxy-3-oxopropyl)-2-((*S*)-4-(triisopropylsilyl)but-3-yn-2-yl)-2,3,4,9-tetrahydro-1*H*-pyrido[3,4-*b*]indole-3-carboxylate (6a)



¹H NMR (300 MHz, CDCl₃): 7.92 (br s, 1H), 7.49 (d, 1H, *J* = 7.38 Hz), 7.33-7.28 (m, 1H, overlapped with CDCl₃ peak); 7.19-7.04 (m, 2H), 4.30 (t, 1H, *J* = 4.40 Hz), 4.12-4.03 (m, 1H), 3.83 (q, 1H, *J* = 6.81 Hz), 3.71 (s, 3H), 3.65 (s, 3H), 3.24 (d, 2H, *J* = 4.38 Hz), 2.80-2.58 (m, 2H), 2.13-2.00 (m, 1H), 1.98-1.84 (m, 1H), 1.48 (d, 3H, *J* = 6.78 Hz), 0.97-0.86 (m, 21H); ¹H NMR (500 MHz, CDCl₃): 7.92 (br s, 1H), 7.49 (d, 1H, *J* = 7.70 Hz), 7.31 (d, 1H, *J* = 8.0 Hz), 7.15 (t, 1H, *J* = 7.43 Hz), 7.11-7.07 (m, 1H), 4.30 (t, 1H, *J* = 4.22 Hz), 4.10-4.05 (m, 1H), 3.83 (q, 1H, *J* = 6.80 Hz), 3.72 (s, 3H), 3.65 (s, 3H), 3.24 (d, 2H, *J* = 4.30 Hz), 2.78-2.61 (m, 2H), 2.11-2.02 (m, 1H), 1.96-1.86 (m, 1H), 1.48 (d, 3H, *J* = 6.70 Hz), 0.95-0.85 (m, 21H); ¹³C NMR (75 MHz, CDCl₃): 174.8 (2xC), 136.1, 133.6, 127.1, 121.5, 119.2, 118.2, 110.6, 108.5, 107.0, 84.5, 55.6, 54.5, 52.7, 51.8, 51.6, 30.7, 30.4, 21.7, 21.2, 18.4, 18.4, 11.1; HRMS (ESI) *m/z* (M+H)⁺ Calcd for C₃₀H₄₅N₂O₄Si 525.3143, found 525.3147; [α]_D²⁵: -23.52 (c 0.8, CHCl₃); R_f: 0.3 (silica gel, 20% EtOAc in hexane)

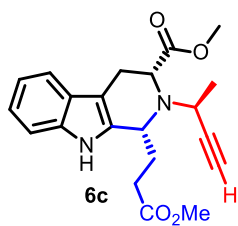
(1*R*,3*R*)-Methyl 1-(3-methoxy-3-oxopropyl)-2-((*S*)-4-(trimethylsilyl)but-3-yn-2-yl)-2,3,4,9-tetrahydro-1*H*-pyrido[3,4-*b*]indole-3-carboxylate (6b)



¹H NMR (500 MHz, CDCl₃): 8.01 (br s, 1H), 7.53 (d, 1H, *J* = 7.64 Hz), 7.33 (d, 1H, *J* = 7.89 Hz), 7.17 (t, 1H, *J* = 7.40 Hz), 7.11 (d, 1H, *J* = 7.20 Hz), 4.22 (d, 1H, *J* = 5.0 Hz), 4.11-4.06 (m, 1H), 3.81 (q, 1H, *J* = 6.40 Hz), 3.73 (s, 3H), 3.66 (s, 3H), 3.29 (br s, 1H, *J* = 15.44 Hz), 3.20 (dd,

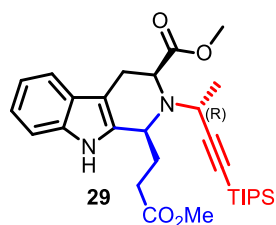
1H, $J = 15.53$ Hz, 6.29 Hz), 2.79-2.62 (m, 2H), 2.11-2.02 (m, 1H), 1.97-1.87 (m, 1H), 1.44 (d, 3H, $J = 6.65$ Hz), -0.1 (s, 9H); $^{13}\text{C NMR}$ (75 MHz, CDCl_3): 174.8, 174.7, 136.0, 133.8, 127.1, 121.5, 119.2, 118.2, 110.7, 107.0, 88.2, 55.4, 54.8, 52.9, 51.9, 51.6, 30.7, 30.4, 21.3, 21.2, -0.3; **HRMS** (ESI) m/z ($\text{M}+\text{H}$)⁺ Calcd for $\text{C}_{24}\text{H}_{33}\text{N}_2\text{O}_4\text{Si}$ 441.2204, found 441.2207; **LRMS** ($\text{M}+\text{H}$)⁺: 441.25; $[\alpha]_{\text{D}}^{25}$: -41.67 (c 0.84, CHCl_3); **R_f**: 0.4 (silica gel, 30% EtOAc in hexanes).

(1*R*,3*R*)-methyl-2-((*S*)-but-3-yn-2-yl)-1-(3-methoxy-3-oxopropyl)-2,3,4,9-tetrahydro-1*H*-pyrido[3,4-*b*]indole-3-carboxylate (6c)



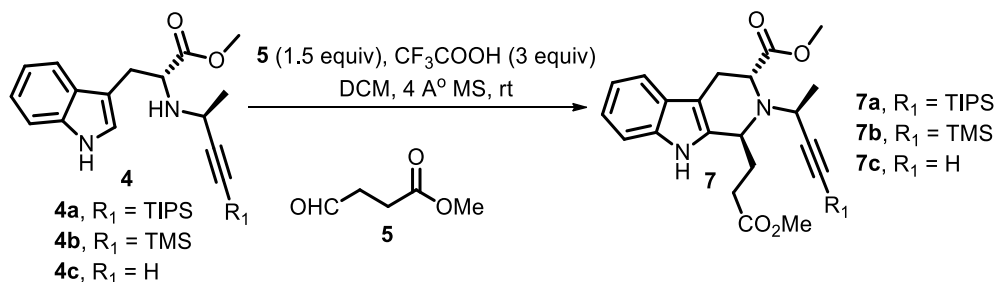
$^1\text{H NMR}$ (500 MHz, CDCl_3): 8.03 (br s, 1H), 7.54 (d, 1H, $J = 7.69$ Hz), 7.34 (d, 1H, $J = 7.99$ Hz), 7.20-7.16 (m, 1H), 7.14-7.10 (m, 1H), 4.22 (dd, 1H, $J = 6.5$ Hz, 2.60 Hz), 4.15-4.11 (m, 1H), 3.84 (qd, 1H, $J = 6.88$ Hz, 2.15 Hz), 3.73 (s, 3H), 3.67 (s, 3H), 3.29 (dd, 1H, $J = 15.58$ Hz, 2.50 Hz), 3.21 (dd, 1H, $J = 6.40$ Hz, 1.20 Hz), 3.18 (dd, 1H, $J = 6.55$ Hz, 1.20 Hz), 2.81-2.73 (m, 1H), 2.67-2.59 (m, 1H), 2.20 (d, 1H, $J = 2.20$ Hz), 2.12-2.04 (m, 1H), 1.94-1.86 (m, 1H), 1.45 (d, 3H, $J = 6.90$ Hz); $^{13}\text{C NMR}$ (125 MHz, CDCl_3): 174.8, 174.6, 136.0, 133.7, 127.0, 121.7, 119.3, 118.3, 110.8, 106.9, 84.8, 71.9, 55.1, 54.6, 52.1, 52.0, 51.7, 30.7, 30.3, 21.3, 21.1; **HRMS** (ESI) m/z ($\text{M}+\text{H}$)⁺ Calcd for $\text{C}_{21}\text{H}_{25}\text{N}_2\text{O}_4$ 369.1809, found 369.1815; $[\alpha]_{\text{D}}^{25} = -41.97$ (c 0.81, CHCl_3); **R_f**: 0.56 (silica gel, 40% EtOAc in hexanes).

(1*S*,3*S*)-methyl 1-(3-methoxy-3-oxopropyl)-2-((*R*)-4-(triisopropylsilyl)but-3-yn-2-yl)-2,3,4,9-tetrahydro-1*H*-pyrido[3,4-*b*]indole-3-carboxylate (29**)**



¹H NMR (500 MHz, CDCl₃): 7.99 (br s, 1H), 7.51 (d, 1H, *J* = 7.51 Hz), 7.31 (d, 1H, *J* = 7.94 Hz), 7.17-7.13 (m, 1H), 7.12-7.07 (m, 1H), 4.32 (t, 1H, *J* = 5.59 Hz), 4.11-4.06 (m, 1H), 3.84 (q, 1H, *J* = 6.90 Hz), 3.73 (s, 3H), 3.66 (s, 3H), 3.25 (d, 1H, *J* = 4.50 Hz), 2.79-2.63 (m, 2H), 2.12-2.04 (m, 1H), 1.96-1.87 (m, 1H), 1.49 (d, 3H, *J* = 6.90 Hz), 0.97-0.91 (m, 21H); **¹³C NMR** (125 MHz, CDCl₃): 174.9, 174.8, 136.1, 133.6, 127.1, 121.5, 119.2, 118.3, 110.7, 108.5, 107.0, 84.5, 55.6, 54.5, 52.7, 51.9, 51.7, 30.7, 30.4, 21.8, 21.2, 18.5, 18.4, 11.1; **HRMS** (ESI) *m/z* (*M*+*H*)⁺ Calcd for C₃₀H₄₅N₂O₄Si 525.3143, found 525.3149; **[α]_D²⁵** = +19.53 (c 1.7, CHCl₃); **R_f**: 0.3 (silica gel, 20% EtOAc in hexanes), 0.5 (silica gel, 30% EtOAc in hexanes).

Synthesis of *trans*-diesters **7a-c**

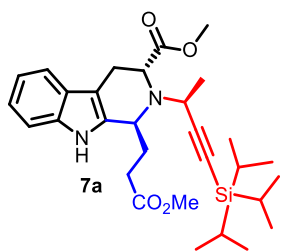


Representative example: Procedure for the synthesis of the *trans*-diester **7a:** The *N_b*-alkylated tryptophan **4a** (200 mg, 0.47 mmol) was dissolved dry DCM (20 mL) in a 50 mL round bottom flask equipped with a magnetic stir. To the above solution, the aldehyde **5** (82 mg, 0.70 mmol) and trifluoroacetic acid (160 mg, 1.41 mmol), as well as 4 Å MS (95 mg) was added at rt. The reaction solution, which resulted, was stirred at rt for 12 h. After complete consumption of the SM as

indicated by TLC on silica gel (UV and CAN stain) and LRMS analysis, the reaction mixture was diluted with DCM (30 mL) and water (10 mL), as well as brought to pH 8-9 with cold aq NaOH (1 N). The organic layer was washed with water (10 mL), brine (2 x 30 mL) and dried (Na₂SO₄). The solvent was removed under reduced pressure to give **7a** as a light yellow oil. The residue (LRMS M+H⁺ = 525, R_f = 0.7, silica gel, 30% EtOAc in hexanes) was purified by column chromatography (silica gel, 10-15% EtOAc in hexanes) to furnish pure *trans*-diester **7a** (214 mg, 87%) as a colorless oil.

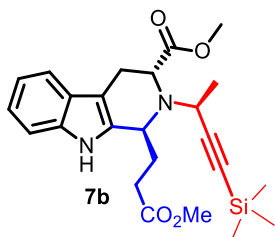
By following the same procedure, *trans*-diesters **7b** (80%) and **7c** (90%) were synthesized.

(1*S*,3*R*)-Methyl-1-(3-methoxy-3-oxopropyl)-2-((*S*)-4-(triisopropylsilyl)but-3-yn-2-yl)-2,3,4,9-tetrahydro-1*H*-pyrido[3,4-*b*]indole-3-carboxylate (7a**)**



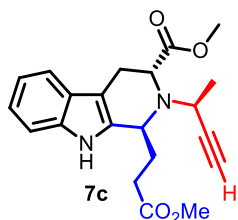
¹H NMR (300 MHz, CDCl₃): δ 7.92 (brs, 1H), 7.45 (d, 1H, *J* = 7.6 Hz), 7.27 (d, 1H, *J* = 7.9 Hz), 7.15-7.02 (m, 2H), 4.17 (dd, 1H, *J* = 9.7 Hz, 3.7 Hz), 4.05 (dd, 1H, *J* = 10.0 Hz, 4.3 Hz), 3.82 (q, 1H, *J* = 7.0 Hz, overlapped), 3.80 (s, 3H), 3.73 (s, 3H), 3.29-3.18 (m, 1H), 3.01 (dd, 1H, *J* = 15.5 Hz, 4.2 Hz), 2.73-2.50 (m, 2H), 2.23-2.10 (m, 1H), 2.08-1.92 (m, 1H), 1.39 (d, 3H, *J* = 6.9 Hz), 0.08-0.71 (m, 18H), 0.62-0.48 (m, 3H). The spectral data were in excellent agreement with the published values.⁴⁹

(1*S*,3*R*)-Methyl 1-(3-methoxy-3-oxopropyl)-2-((*S*)-4-(trimethylsilyl)but-3-yn-2-yl)-2,3,4,9-tetrahydro-1*H*-pyrido[3,4-*b*]indole-3-carboxylate (7b**)**



¹H NMR (500 MHz, CDCl₃): 7.94 (br s, 1H), 7.49 (d, 1H, *J* = 7.69 Hz), 7.32 (d, 1H, *J* = 7.99 Hz), 7.14 (t, 1H, *J* = 7.37 Hz), 7.09 (t, 1H, *J* = 7.35 Hz), 4.13-4.05 (m, 2H), 3.81 (s, 3H), 3.77 (q, 1H, *J* = 6.90 Hz, overlapped with CO₂Me methyl peaks), 3.75 (s, 3H), 3.26-3.18 (m, 1H), 3.02 (dd, 1H, *J* = 15.49 Hz, 3.90 Hz), 2.72-2.64 (m, 1H), 2.62-2.54 (m, 1H), 2.19-2.10 (m, 1H), 2.08-1.98 (m, 1H), 1.35 (d, 3H, *J* = 6.90 Hz), -0.38 (s, 9H); **¹³C NMR** (75 MHz, CDCl₃): 174.4, 173.1, 136.1, 135.4, 126.9, 121.5, 119.3, 118.1, 110.6, 109.1, 106.9, 87.4, 57.5, 52.4, 52.0, 51.7, 45.8, 30.7, 29.6, 22.3, 21.5, -0.8; **HRMS**: (ESI) *m/z* (M+H)⁺ Calcd for C₂₄H₃₃N₂O₄Si 441.2204, found 441.2210; **LRMS** (M+H⁺): 441.30; [α]_D²⁵: -77.61 (c 0.67, CHCl₃); **R_f**: 0.5 (silica gel, 30% EtOAc in hexanes).

(1S,3R)-Methyl 2-((S)-but-3-yn-2-yl)-1-(3-methoxy-3-oxopropyl)-2,3,4,9-tetrahydro-1H-pyrido[3,4-b]indole-3-carboxylate (7c)



¹H NMR (300 MHz, CDCl₃): 7.95 (br s, 1H), 7.51 (d, 1H, *J* = 7.35 Hz), 7.33 (d, 1H, *J* = 7.68 Hz), 7.21-7.10 (m, 2H), 4.27-4.19 (m, 1H), 4.13-4.05 (m, 1H), 3.88-3.80 (m, 1H, overlapped), 3.78 (s, 3H), 3.72 (s, 3H), 3.26-3.13 (m, 1H), 3.08-2.98 (m, 1H), 2.72-2.59 (m, 1H), 2.56-2.44 (m, 1H), 2.25-2.11 (m, 1H), 2.10-1.94 (m, 1H), 1.80 (m, 1H), 1.38 (d, 3H, *J* = 6.81 Hz); **¹³C NMR** (75 MHz, CDCl₃): δ 174.4, 173.3, 136.0, 135.3, 126.8, 121.5, 119.3, 118.1, 110.8, 108.9, 84.7, 71.3, 57.3, 52.6, 52.0, 51.6, 45.3, 30.3, 29.5, 22.3, 21.9; **HRMS**: (ESI) *m/z* (M+H)⁺ Calcd for C₂₁H₂₅N₂O₄ 369.1809, found 369.1815; [α]_D²⁵ = -48.61 (c 0.72, CHCl₃); **R_f**: 0.6 (silica gel, 40% EtOAc in hexanes), 0.5 (silica gel, 30% EtOAc in hexanes).

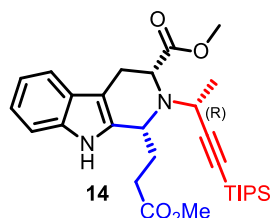
Procedure for the synthesis of *cis*-diesters with (a,b) = (*S,S*) or (*R,R*) configurations (14, 15, and 31)

Representative example: Synthesis of *cis*-diester 31

By following the same procedure for the preparation **6a** (see above) with amine **4g** (215 mg, 0.50 mmol), aldehyde **5** (88 mg, 0.75 mmol), acetic acid (91 mg, 1.51 mmol), and 4 Å MS (100 mg) at 0 °C for 8 h furnished a mixture of *cis*- (major) and *trans*- (minor) diesters as mixture of products. After the workup as described above, the residue was subjected to silica gel column chromatography to provide the *cis*-diester **31** (185 mg, 70%) along with the *trans*-diester (40 mg, 15%) in 85% combined isolated yield.

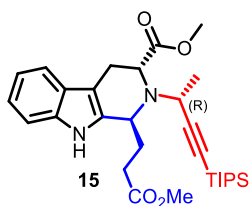
By following the same procedure, the *cis*-diester **14** (443 mg, 72% along with *trans*-diester **15**, 172 mg, 28%) was synthesized from the amine **4d** and aldehyde **5**, respectively.

(1*R*,3*R*)-methyl 1-(3-methoxy-3-oxopropyl)-2-((*R*)-4-(triisopropylsilyl)but-3-yn-2-yl)-2,3,4,9-tetrahydro-1*H*-pyrido[3,4-*b*]indole-3-carboxylate (14**)**



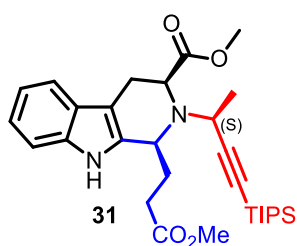
¹H NMR (500 MHz, CDCl₃): 7.99 (br s, 1H), 7.49 (d, 1H, *J* = 7.74 Hz), 7.31-7.27 (m, 1H), 7.17-7.12 (m, 1H), 7.11-7.06 (m, 1H), 4.18-4.14 (m, 1H), 4.04 (t, 1H, *J* = 4.92 Hz), 3.81 (q, 1H, *J* = 6.98 Hz), 3.72 (s, 3H), 3.68 (s, 3H), 3.22 (d, *J* = 4.70 Hz), 2.74-2.66 (m, 1H), 2.65-2.57 (m, 1H), 2.11-2.03 (m, 1H), 1.95-1.87 (m, 1H), 1.46 (d, 3H, *J* = 7.00 Hz), 0.87-0.83 (m, 18H), 0.79-0.71 (m, 3H); **¹³C NMR** (125 MHz, CDCl₃): 174.8, 174.0, 136.0, 134.2, 127.0, 121.4, 119.1, 118.2, 110.6, 108.1, 107.2, 84.3, 60.5, 53.8, 51.9, 51.6, 51.3, 32.1, 30.5, 22.6, 21.7, 18.3, 11.0; **HRMS**: (ESI) *m/z* (M+H)⁺ Calcd for C₃₀H₄₅N₂O₄Si 525.3143, found 525.3142; [α]_D²⁵ = -0.81 (c 1.23, CHCl₃); **R_f**: 0.57 (silica gel, 30% EtOAc in hexanes).

(1*S*,3*R*)-Methyl 1-(3-methoxy-3-oxopropyl)-2-((*R*)-4-(triisopropylsilyl)but-3-yn-2-yl)-2,3,4,9-tetrahydro-1*H*-pyrido[3,4-*b*]indole-3-carboxylate (15)



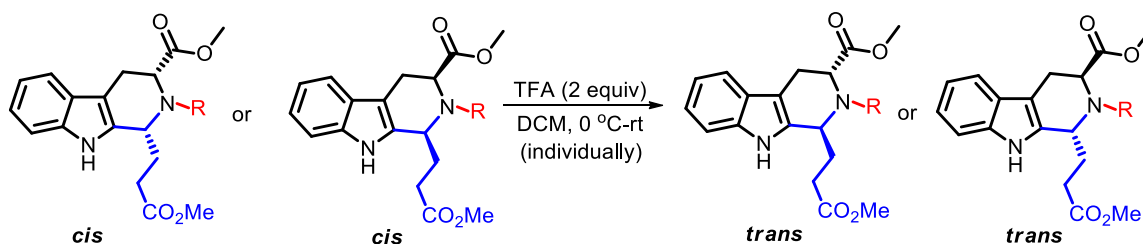
¹H NMR (500 MHz, CDCl₃): 8.03 (br s, 1H), 7.16 (d, 1H, *J* = 7.80 Hz), 7.34 (d, 1H, *J* = 7.94 Hz), 7.19-7.15 (m, 1H), 7.13-7.10 (b, 1H), 4.66-4.62 (m, 1H), 4.16 (t, 1H, *J* = 5.62 Hz), 4.09 (q, 1H, *J* = 6.83 Hz), 3.65 (s, 3H), 3.64 (s, 3H), 3.14-3.03 (m, 2H), 2.56-2.48 (m, 1H), 2.37-2.23 (m, 2H), 2.14-2.10 (m, 1H), 1.42 (d, 3H, *J* = 6.85 Hz), 1.12-1.03 (m, 21H); **¹³C NMR** (125 MHz, CDCl₃): 174.8, 173.3, 136.2, 134.9, 127.0, 121.5, 119.3, 118.0, 110.9, 84.9, 54.7, 53.2, 51.6, 51.4, 46.8, 29.1, 28.4, 24.8, 21.9, 18.6, 18.6, 11.3; **HRMS** (ESI) *m/z* (M+H)⁺ Calcd for C₃₀H₄₅N₂O₄Si 525.3143, found 525.3139; **[α]_D²⁵** = +5.0 (c 1.2, CHCl₃); **R_f**: 0.7 (silica gel, 30% EtOAc in hexanes).

(1*S*,3*S*)-Methyl 1-(3-methoxy-3-oxopropyl)-2-((*S*)-4-(triisopropylsilyl)but-3-yn-2-yl)-2,3,4,9-tetrahydro-1*H*-pyrido[3,4-*b*]indole-3-carboxylate (31)



¹H NMR (500 MHz, CDCl₃): 8.02 (br s, 1H), 7.49 (d, 1H, *J* = 7.64 Hz), 7.30 (d, 1H, *J* = 4.30 Hz), 7.16-7.12 (m, 1H), 7.11-7.06 (m, 1H), 4.18-4.14 (m, 1H), 4.05 (t, 1H, *J* = 4.92 Hz), 3.81 (q, 1H, *J* = 6.91 Hz), 3.72 (s, 3H), 3.68 (s, 3H), 3.23 (d, 1H, *J* = 4.80 Hz), 2.74-2.58 (m, 2H), 2.11-2.03 (m, 1H), 1.96-1.86 (m, 1H), 1.46 (d, 3H, *J* = 6.95 Hz), 0.88-0.82 (m, 18H), 0.80-0.71 (m, 3H); **¹³C NMR** (125 MHz, CDCl₃): 174.8, 174.1, 136.5, 134.2, 127.0, 121.4, 119.1, 118.2, 110.6, 108.1, 107.2, 84.3, 60.5, 53.8, 51.9, 51.6, 51.4, 32.1, 30.5, 22.6, 21.7, 18.3, 18.3, 11.0; **HRMS** (ESI) *m/z* (M+H)⁺ Calcd for C₃₀H₄₅N₂O₄Si 525.3143, found 525.3148; **[α]_D²⁵** = +1.2 (c 0.8, CHCl₃); **R_f**: 0.5 (silica gel, 30% EtOAc in hexanes).

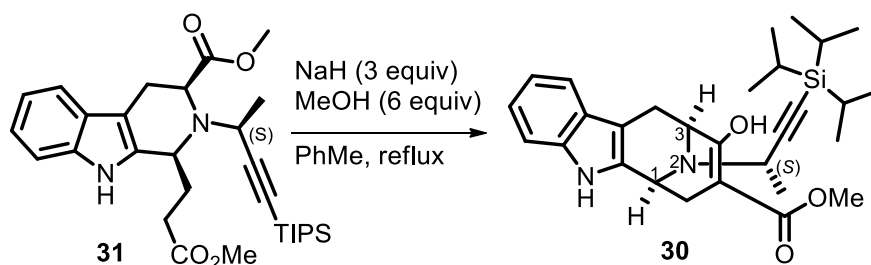
Procedure for the conversion of *cis*-diesters into their corresponding *trans*-diesters



To a solution of pure *cis*-diester (0.1 mmol) in dry DCM (5 mL) and TFA (0.2) was added at 0 °C and the mixture, which resulted, was stirred at rt until the *cis*-diester was completely converted into the corresponding *trans*-diester as indicated by TLC on silica gel (UV and CAN stain). After that, the reaction mixture was diluted with additional DCM and water and then carefully brought to pH 8-9 with cold aq NaOH (1 *N*). The organic layer was separated and washed with water, brine and dried (Na₂SO₄). The solvent was removed under reduced pressure to provide a light yellow residue, which was subjected to silica gel column chromatographic purification to provide the corresponding *trans*-diester as a colorless oil.

The *cis*-diesters with (a,b) = (*S*, *R*) or (*R*, *S*) configurations were completely converted into their corresponding *trans*-diester diastereomers in 2-4 hours whereas, the *cis*-diesters with (a, b) = (*S*, *S*) or (*R*, *R*) configurations took up to 20 hours to be converted into the corresponding *trans*-diastereomers.

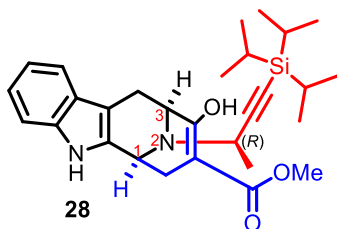
Procedure for the Dieckmann cyclization:



Representative example: Procedure for the synthesis of 30: The *cis*-diester **31** (616 mg, 1.17 mmol) was dissolved in toluene (50 mL). This solution was dried by azeotropic removal of H₂O with toluene by a DST (refluxed 6 h). To this solution was added sodium hydride (141 mg, 3.52 mmol of 60% dispersion in mineral oil) at 0 °C. Anhydrous CH₃OH (285 μ L, 7.0 mmol) was then added into the above mixture under Ar at 0 °C. The solution, which resulted, was then stirred at rt for 0.5 h and then held at reflux for an additional 60 h (the flask was covered with aluminum foil on the top to keep the temperature at reflux without carbonizing any compound on the sides of the flask). The reaction was quenched then with ice. The aq layer was extracted with CH₂Cl₂ (3 x 20 mL). The combined organic extracts were washed with brine and dried (K₂CO₃). The solvent was removed under reduced pressure to provide the crude product (LRMS M+H⁺ = 493.40) as a light brown residue. The residue was purified by flash chromatography (silica gel, EtOAc/hexane) to provide the β -ketoester **30** (491 mg, **85%**) as a colorless oil.

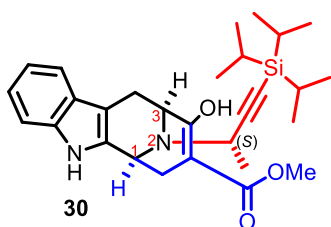
By following the same procedure with the *cis*-diester **29** (300 mg, 0.57 mmol), this furnished the β -ketoester **28** (231 mg, **82%**).

(6*S*,10*S*)-Methyl 9-hydroxy-12-((*R*)-4-(triisopropylsilyl)but-3-yn-2-yl)-6,7,10,11-tetrahydro-5*H*-6,10-epiminocycloocta[*b*]indole-8-carboxylate (28)



¹H NMR, (500 MHz, CDCl₃): 11.98 (s, 1H), 7.73 (br s, 1H), 7.52 (d, 1H, *J* = 7.74 Hz), 7.34 (d, 1H, *J* = 7.80 Hz), 7.21-7.17 (m, 1H), 7.16-7.11 (m, 1H), 4.49 (d, 1H, *J* = 5.20 Hz), 4.39 (d, 1H, *J* = 6.65 Hz), 3.70 (s, 3H), 3.64 (q, 1H, *J* = 6.33 Hz), 3.37 (dd, 1H, *J* = 16.09 Hz, 5.90 Hz), 2.97 (br d, 1H, *J* = 16.79 Hz), 2.95-2.89 (m, 1H), 2.43 (d, 1H, *J* = 15.74 Hz), 1.50 (d, 3H, *J* = 6.35 Hz), 1.13-1.05 (m, 21H); ¹³C NMR (125 MHz, CDCl₃): 172.4, 171.4, 135.7, 132.8, 127.0, 121.9, 119.7, 118.3, 110.8, 107.6, 107.3, 94.5, 85.4, 53.7, 51.5, 48.2, 46.7, 29.0, 22.7, 20.9, 18.7, 11.2; HRMS (ESI) *m/z* (M+H)⁺ Calcd for C₂₉H₄₁N₂O₃Si 493.2881, found 493.2888; [α]_D²⁵ = +32.86 (c 0.7, CHCl₃); *R_f*: 0.52 (silica gel, 30% EtOAc in hexanes).

(6*S*,10*S*)-Methyl 9-hydroxy-12-((*S*)-4-(triisopropylsilyl)but-3-yn-2-yl)-6,7,10,11-tetrahydro-5*H*-6,10-epiminocycloocta[*b*]indole-8-carboxylate (30)



¹H NMR (500 MHz, CDCl₃): 12.00 (s, 1H), 7.75 (br s, 1H), 7.49 (d, 1H, *J* = 7.64 Hz), 7.35 (d, 1H, *J* = 8.04 Hz), 7.20-7.16 (m, 1H), 7.14-7.10 (m, 1H), 4.78 (br d, 1H, *J* = 5.04 Hz), 4.14 (d, 1H, *J* = 5.60 Hz), 3.69 (s, 3H), 3.66 (q, 1H, *J* = 6.58 Hz), 3.09 (dd, 1H, *J* = 16.10 Hz, 5.75 Hz), 2.97-2.87 (m, 2H), 2.44 (dd, 1H, *J* = 15.67 Hz, 1.32 Hz), 1.54 (d, 3H, *J* = 6.65 Hz), 1.09-1.03 (m, 21H); ¹³C NMR (125 MHz, CDCl₃): 172.4, 171.4, 135.7, 133.2, 127.0, 121.8, 119.7, 118.2, 110.8, 108.7, 106.8, 94.7, 84.4, 52.5, 51.5, 49.4, 47.3, 29.2, 21.7, 20.5, 18.6, 11.2; HRMS (ESI) *m/z* (M+H)⁺ Calcd for C₂₉H₄₁N₂O₃Si 493.2881, found 493.2885; [α]_D²⁵ = -120.0 (c 0.5, CHCl₃); *R_f*: 0.6 (silica gel, 30% EtOAc in hexanes).

5. References

- (1) Cox, E. D.; Cook, J. M. *Chem. Rev.* **1995**, *95*, 1797.
- (2) Dalpozzo, R. *Molecules* **2016**, *21*, 699.
- (3) Ingallina, C.; D'Acquarica, I.; Delle Monache, G.; Ghirga, F.; Quaglio, D.; Ghirga, P.; Berardozzi, S.; Markovic, V.; Botta, B. *Curr. Pharm. Des.* **2016**, *22*, 1808.
- (4) Larghi, E. L.; Amongero, M.; Bracca, A. B.; Kaufman, T. S. *ARKIVOC* **2005**, *12*.
- (5) Rao, R. N.; Maiti, B.; Chanda, K. *ACS Comb. Sci.* **2017**, *19*, 199.
- (6) Stöckigt, J.; Antonchick, A. P.; Wu, F.; Waldmann, H. *Angew. Chem. Int. Ed.* **2011**, *50*, 8538.
- (7) Cox, E. D.; Hamaker, L. K.; Li, J.; Yu, P.; Czerwinski, K. M.; Deng, L.; Bennett, D. W.; Cook, J. M.; Watson, W. H.; Krawiec, M. *J. Org. Chem.* **1997**, *62*, 44.
- (8) Deng, L.; Czerwinski, K.; Cook, J. M. *Tetrahedron letters* **1991**, *32*, 175.
- (9) Soerens, D.; Sandrin, J.; Ungemach, F.; Mokry, P.; Wu, G.; Yamanaka, E.; Hutchins, L.; DiPierro, M.; Cook, J. *J. Org. Chem.* **1979**, *44*, 535.
- (10) Ungemach, F.; DiPierro, M.; Weber, R.; Cook, J. *J. Org. Chem.* **1981**, *46*, 164.
- (11) Klausen, R. S.; Jacobsen, E. N. *Org. Lett.* **2009**, *11*, 887.
- (12) Raheem, I. T.; Thiara, P. S.; Peterson, E. A.; Jacobsen, E. N. *J. Am. Chem. Soc.* **2007**, *129*, 13404.
- (13) Taylor, M. S.; Jacobsen, E. N. *J. Am. Chem. Soc.* **2004**, *126*, 10558.
- (14) Kawate, T.; Yamada, H.; Soe, T.; Nakagawa, M. *Tetrahedron: Asymmetry* **1996**, *7*, 1249.
- (15) Soe, T.; Kawate, T.; Fukui, N.; Hino, T.; Nakagawa, M. *Heterocycles* **1996**, *42*, 347.

- (16) Alberch, L.; Bailey, P. D.; Clingan, P. D.; Mills, T. J.; Price, R. A.; Pritchard, R. G. *Eur. J. Org. Chem.* **2004**, 2004, 1887.
- (17) Bailey, P. D.; Beard, M. A.; Phillips, T. R. *Tetrahedron Lett.* **2009**, 50, 3645.
- (18) Bailey, P. D.; Clingan, P. D.; Mills, T. J.; Price, R. A.; Pritchard, R. G. *Chem. Commun.* **2003**, 2800.
- (19) Pulka, K.; Kulis, P.; Tymecka, D.; Frankiewicz, L.; Wilczek, M.; Kozminski, W.; Misicka, A. *Tetrahedron* **2008**, 64, 1506.
- (20) Pulka, K.; Misicka, A. *Tetrahedron* **2011**, 67, 1955.
- (21) Herlé, B.; Wanner, M. J.; van Maarseveen, J. H.; Hiemstra, H. *J. Org. Chem.* **2011**, 76, 8907.
- (22) Kerschgens, I. P.; Claveau, E.; Wanner, M. J.; Ingemann, S.; van Maarseveen, J. H.; Hiemstra, H. *Chem. Commun.* **2012**, 48, 12243.
- (23) Sewgobind, N. V.; Wanner, M. J.; Ingemann, S.; de Gelder, R.; van Maarseveen, J. H.; Hiemstra, H. *J. Org. Chem.* **2008**, 73, 6405.
- (24) Wanner, M. J.; van der Haas, R. N.; de Cuba, K. R.; van Maarseveen, J. H.; Hiemstra, H. *Angew. Chem. Int. Ed.* **2007**, 46, 7485.
- (25) Seayad, J.; Seayad, A. M.; List, B. *J. Am. Chem. Soc.* **2006**, 128, 1086.
- (26) Abe, T.; Yamada, K. *J. Nat. Prod.* **2017**, 80, 241.
- (27) de la Figuera, N.; Rozas, I.; García-López, M. T.; González-Muñiz, R. *J. Chem. Soc., Chem. Commun.* **1994**, 613.
- (28) Gremmen, C.; Willemsse, B.; Wanner, M. J.; Koomen, G.-J. *Org. Lett.* **2000**, 2, 1955.
- (29) Massiot, G.; Mulamba, T. *J. Chem. Soc., Chem. Commun.* **1983**, 1147.

- (30) Meng, T.-Z.; Shi, X.-X.; Qu, H.-Y.; Zhang, Y.; Huang, Z.-S.; Fan, Q.-Q. *RSC Advances* **2017**, *7*, 47753.
- (31) Mizuno, T.; Oonishi, Y.; Takimoto, M.; Sato, Y. *Eur. J. Org. Chem.* **2011**, *2011*, 2606.
- (32) Rashid, N.; Alam, S.; Hasan, M.; Khan, N.; Khan, K. M.; Duddeck, H.; Pescitelli, G.; Kenéz, Á.; Antus, S.; Kurtán, T. *Chirality* **2012**, *24*, 789.
- (33) Saha, B.; Sharma, S.; Sawant, D.; Kundu, B. *Tetrahedron Lett.* **2007**, *48*, 1379.
- (34) Schmidt, G.; Waldmann, H.; Henke, H.; Burkard, M. *Chem. Eur. J.* **1996**, *2*, 1566.
- (35) Singh, K.; Deb, P. K.; Venugopalan, P. *Tetrahedron* **2001**, *57*, 7939.
- (36) Srinivasan, N.; Ganesan, A. *Chem. Commun.* **2003**, 916.
- (37) Bailey, P. D.; Beard, M. A.; Cresswell, M.; Dang, H. P.; Pathak, R. B.; Phillips, T. R.; Price, R. A. *Tetrahedron Lett.* **2013**, *54*, 1726.
- (38) Stephen, M. R.; Rahman, M. T.; Tiruveedhula, V.; Fonseca, G. O.; Deschamps, J. R.; Cook, J. M. *Chem. Eur. J.* **2017**, *23*, 15805.
- (39) Rahman, M. T.; Tiruveedhula, V. V.; Cook, J. M. *Molecules* **2016**, *21*, 1525.
- (40) Namjoshi, O. A.; Cook, J. M. In *The Alkaloids: Chemistry and Biology*; Knölker, H.-J., Ed.; Academic Press: San Diego, CA, 2016; Vol. 76, p 63.
- (41) Ataullah Khan, M.; Siddiqui, S. *Cell. Mol. Life Sci.* **1972**, *28*, 127.
- (42) Buckingham, J.; Baggaley, K. H.; Roberts, A. D.; Szabo, L. F. *Dictionary of Alkaloids, with CD-ROM*; CRC press, 2010.
- (43) Cao, P.; Liang, Y.; Gao, X.; Li, X.-M.; Song, Z.-Q.; Liang, G. *Molecules* **2012**, *17*, 13631.

- (44) Keawpradub, N.; Kirby, G.; Steele, J.; Houghton, P. *Planta Med.* **1999**, *65*, 690.
- (45) Naranjo, J.; Pinar, M.; Hesse, M.; Schmid, H. *Helv. Chim. Acta* **1972**, *55*, 752.
- (46) Pan, L.; Terrazas, C.; Acuña, U. M.; Ninh, T. N.; Chai, H.; de Blanco, E. J. C.; Soejarto, D. D.; Satoskar, A. R.; Kinghorn, A. D. *Phytochem. Lett.* **2014**, *10*, 54.
- (47) Wong, W.-H.; Lim, P.-B.; Chuah, C.-H. *Phytochemistry* **1996**, *41*, 313.
- (48) Lounasmaa, M.; Hanhinen, P.; Westersund, M. In *The Alkaloids: Chemistry and Biology*; Cordell, G. A., Ed.; Academic Press: San Diego, CA, 1999; Vol. 52, p 103.
- (49) Rahman, M. T.; Deschamps, J. R.; Imler, G. H.; Cook, J. M. *Chem. Eur. J.* **2018**, *24*, 2354.
- (50) Rahman, M. T.; Deschamps, J. R.; Imler, G. H.; Schwabacher, A. W.; Cook, J. M. *Org. Lett.* **2016**, *18*, 4174.
- (51) Czerwinski, K. M.; Cook, J. M. In *Advances in Heterocyclic Natural Products Synthesis*; Pearson, W., Ed.; JAI Press: Greenwich, CT, 1996; Vol. 3, pp 217-277.
- (52) Burgess, K.; Jennings, L. D. *J. Am. Chem. Soc.* **1991**, *113*, 6129.
- (53) Edwankar, R. V.; Edwankar, C. R.; Deschamps, J. R.; Cook, J. M. *J. Org. Chem.* **2014**, *79*, 10030.
- (54) Marshall, J. A.; Chobanian, H. R.; Yanik, M. M. *Org. Lett.* **2001**, *3*, 3369.
- (55) Matsumura, K.; Hashiguchi, S.; Ikariya, T.; Noyori, R. *J. Am. Chem. Soc.* **1997**, *119*, 8738.
- (56) Nakamura, S.; Kusuda, S.; Kawamura, K.; Toru, T. *J. Org. Chem.* **2002**, *67*, 640.
- (57) Liotta, D. C.; Painter, G. R. *Acc. Chem. Res.* **2016**, *49*, 2091.
- (58) Haack, K. J.; Hashiguchi, S.; Fujii, A.; Ikariya, T.; Noyori, R. *Angew. Chem. Int. Ed.* **1997**, *36*, 285.

- (59) Marshall, J. A.; Eidam, P.; Eidam, H. S. *Org. Syn.* **2007**, 120.
- (60) Edwankar, R. V.; Edwankar, C. R.; Deschamps, J. R.; Cook, J. M. *J. Org. Chem.* **2014**, 79, 10030.
- (61) Edwankar, R. V.; Edwankar, C. R.; Deschamps, J.; Cook, J. M. *Org. Lett.* **2011**, 13, 5216.
- (62) Rahman, M. T.; Cook, J. M. In *Studies in Natural Products Chemistry*; Atta-ur-Rahman, Ed.; Elsevier Publications: Amsterdam, Netherlands (In Press)

Chapter 3

Access to the (+)- or (-)-Enantiomers of the Bioactive C-19 Methyl Substituted Sarpagine/Macroline/Ajmaline Alkaloids from Either D- or L-Tryptophan via the Ambidextrous Pictet-Spengler Reaction

1. Introduction

An important and useful application of the ambidextrous Pictet-Spengler cyclization would be accessing the key bicyclo[3.3.1] framework of the sarpagine/ajmaline-related indole alkaloids in a convergent fashion from either of the starting chiral auxiliaries D- or L-tryptophan. Depicted in the following work is the proof of concept, which is important to illustrate the full potential of the ambidextrous Pictet-Spengler (P-S) reaction. Previously, both D-tryptophan and L-tryptophan were employed to synthesize the key intermediates toward the natural enantiomers of alkaloids. Now the enantiomeric series of the same key intermediates could also be synthesized from both D- and L-tryptophan in high yield and optical purity via this P-S/Dieckmann protocol. One can either make the natural or unnatural alkaloids from the either of the starting amino acid ester, stereo and enantiospecifically.

Natural products have been an important source of useful drug candidates and as a result natural products, as well as compounds derived from or inspired by natural products, play an important role in modern drug discovery.¹⁻⁵ Many compounds with direct natural origin (e.g., reserpine, paclitaxel, vinblastine, vincristine, morphine, quinine, and vancomycin) or derived from natural products (synthetic analogs) have successfully entered clinical practice and have saved millions of lives.^{6,7} Generally, from a medicinal chemistry point of view, synthetic analogs which are inspired by natural scaffolds, exhibit potential, clinically, because many natural products (especially alkaloids) possess drug-like properties.^{8,9} More importantly, their enantiomers, if active will normally have a longer duration of action. For example, the life saving anti HIV drug emtricitabine was derived from the unnatural L-nucleoside, which was about 100 times more potent than its natural D-nucleoside counterpart.¹⁰ Furthermore, rationally designed synthetic analogs of natural

products have resulted in drug-candidates with superior properties than the native compounds (e.g., bryostatin and vinblastine analogs).^{11,12} In this regard, the unnatural enantiomers of natural alkaloids may have important biological properties or even better properties depending on the rate of metabolism.

The C-19 methyl substituted sarpagine/macroline/ajmaline alkaloids are an emerging group of structurally and biosynthetically related alkaloids as pointed out in an earlier chapter.¹³⁻¹⁵ To date, there are more than seventy alkaloids that belong to this group.¹⁶ About two dozen of these alkaloids have been shown to possess important biological activity including antileishmanial, anti-hypertensive, anti-inflammatory, antimicrobial, and anticancer activity (see General Introduction).¹⁶ Some selected examples (**1-12**) of bioactive C-19 methyl substituted alkaloids of this group are depicted in Figure 1. All of the alkaloids in this group contain the *cis*-fused (*S, S*) stereochemistry at C-3 and C-5 of the core-structure (C-1 and C-3 of the tetrahydro- β -carboline, TH β C moiety). Bioactive alkaloids from this group belong to the sarpagine-type, macroline-type and ajmaline-type natural products. The structural complexity and important biological activity engender this group of alkaloids as an attractive target for synthetic and medicinal chemistry studies. A general strategy for accessing most of the alkaloids (if not all) via a few common precursors would be a practical approach to gain entry into these natural products. In addition, biological screening of the unnatural enantiomers of the natural alkaloids, which may have useful and important bioactivity, is feasible only if a practical and robust synthetic strategy is developed.

Furthermore, providing both the natural and unnatural enantiomers of these alkaloids via the same route and from the same chiral pool is undoubtedly a better strategy.

The Asymmetric Pictet-Spengler cyclization has been one of the most effective processes to gain access to many natural products containing the TH β C and tetrahydroisoquinoline moieties.¹⁷⁻²⁵ In the continued effort to develop a practical, enantiospecific, and general strategy for accessing the C-19 methyl substituted alkaloids, more than a dozen of these alkaloids have been successfully synthesized enantiospecifically (the natural enantiomer) from this subgroup. Some of these exhibit important bioactivity as stated earlier (see General Introduction). The asymmetric Pictet-Spengler reaction has been employed as one of the key transformations in the total synthesis of these alkaloids.²⁶⁻³⁰ Recently, a shorter and better route to the key tetracyclic-core, which contains the azabicyclo[3.3.1]nonane moiety (**18-23**), has improved the access to a number of alkaloids from this group (Figure 2, entry 1).²⁷ Afterwards, the discovery of the unprecedented ambidextrous diastereoselectivity in the key asymmetric transformation of the Pictet-Spengler cyclization (P-S), permitted access to the crucial and common intermediates (**15-17**), stereospecifically, from D- as well as from L-tryptophan, at will (Figure 2, entry 1).²⁶ The intermediates **15-23** served as the common branching point for the synthesis of the majority of the alkaloids in this group.^{26,27,29,30} Gratifyingly, the useful *cis*-specificity (or selectivity) also has enabled one to access the enantiomers of the important intermediates from the same starting material, D-tryptophan, as well as L-tryptophan, when desired (Figure 2, entry 2). Herein is reported the synthesis of the

enantiomers (**24-32**) of the key-intermediates **15-23** from both L- or D-tryptophan. This provides a practical and scalable strategy for accessing the unnatural enantiomers of the bioactive alkaloids from this group for biological studies beginning with either of the chiral auxiliaries (L- or D-tryptophan), which were employed earlier for the natural enantiomers.

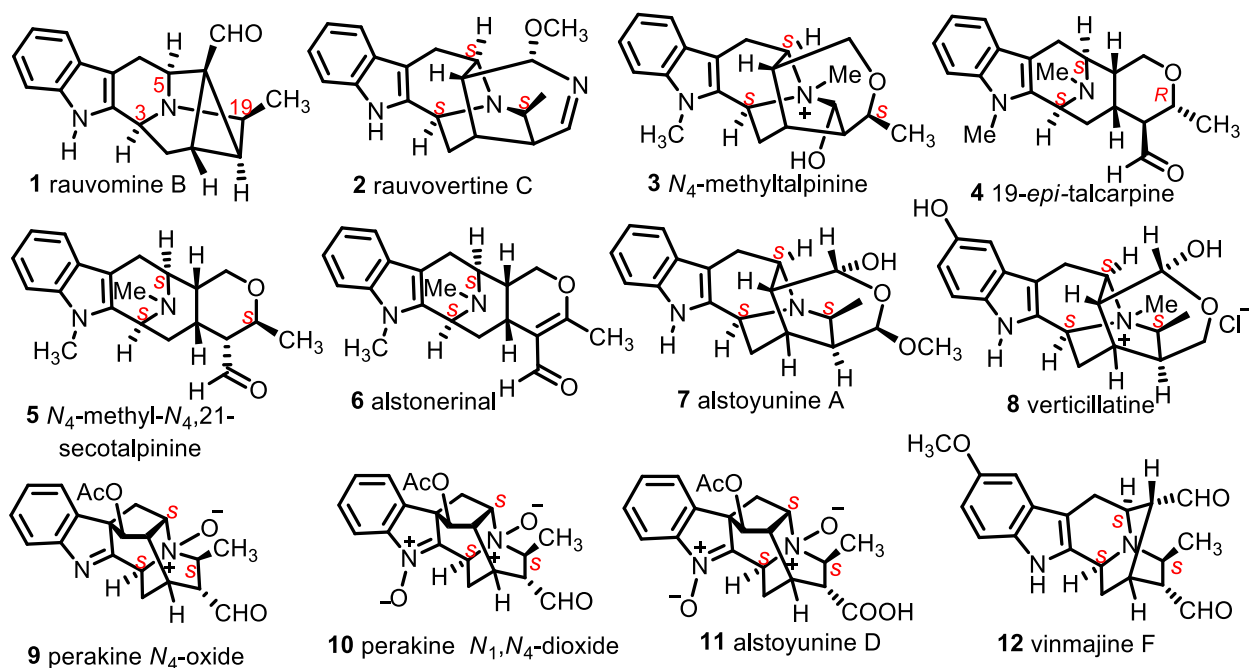


Figure 1. Representative examples of bioactive C-19 methyl substituted sarpagine/macroline-/ajmaline alkaloids.^{13,15,16,31-40}

2. Results and Discussion

As depicted in Scheme 1, the (*R, R, S*) intermediates **26**, **31**, and **32** were synthesized starting from the *N*_b-ethynyl substituted D-tryptophan derivative **33**. A *cis*-specific P-S reaction, according to the previous report,²⁶ provided the *cis*-diester **35** with 100% diastereoselectivity and 83% isolated yield on a 1.7 g scale. This *cis*-specific P-S cyclization secured the desired unnatural stereocenters

(*R, R*) within the tetrahydro- β -carboline (TH β C) framework. The (*R, R, S*)-TH β C intermediate **35** was subjected to the Dieckmann cyclization conditions in a DST-dried solution of toluene and in the presence of sodium methoxide to furnish the β -ketoester **26** in 81% isolated yield. Importantly, the β -ketoester **26** could also be accessed easily from the L-tryptophan derivative **39** via the *trans*-specific P-S reaction to provide the (*R, S, S*)-TH β C intermediate **40** as the sole product. The reaction mixture from the initial acetic acid mediated P-S reaction was subjected to a rapid wash column and treated with trifluoroacetic acid in methylene chloride to give the thermodynamically more stable *trans* (at C-1) product **40** (see Scheme 1 for details). The subsequent Dieckmann cyclization of the TH β C **40** furnished the β -ketoester in excellent yield. This provided the desired β -ketoester from both the L-tryptophan and D-tryptophan derivatives **39** and **33**, respectively. An acid mediated decarboxylation of the β -ketoester **26** provided the ketone **31** in 78% yield. The subsequent removal of the TIPS function with TBAF in THF provided the terminal alkyne **32** in excellent yield. This series of intermediates **26**, **31**, and **32** are the enantiomers of the intermediates **17**, **22**, and **23**, respectively, which were previously synthesized from the same starting material **33** (see Appendix G for NMR comparisons of the enantiomeric pairs).^{26,27} These intermediates are the key bicyclo[3.3.1] systems required for the total synthesis of the unnatural enantiomers of the sarpgaine/macroline/ajmaline alkaloids of Figure 1 with the *N*_a-H, C-3(*R*), C-5(*R*), and C-19(*S*) stereochemical configurations.

On the other hand, the (*R, R, R*) intermediates in either the *N*_a-H or *N*_a-CH₃ series (**24-25**, **27-30**) were synthesized from the corresponding *N*_b-ethynyl substituted D-tryptophan derivative **36**,^{26,27} as shown in Scheme 2. The Pictet-Spengler reaction, *N*_a-methylation, Dieckmann cyclization, decarboxylation, and TIPS deprotection went smoothly to furnish the desired intermediates in good

to excellent yields (Scheme 2). In this case as well, the β -ketoester **24** could be easily prepared via the *trans*-

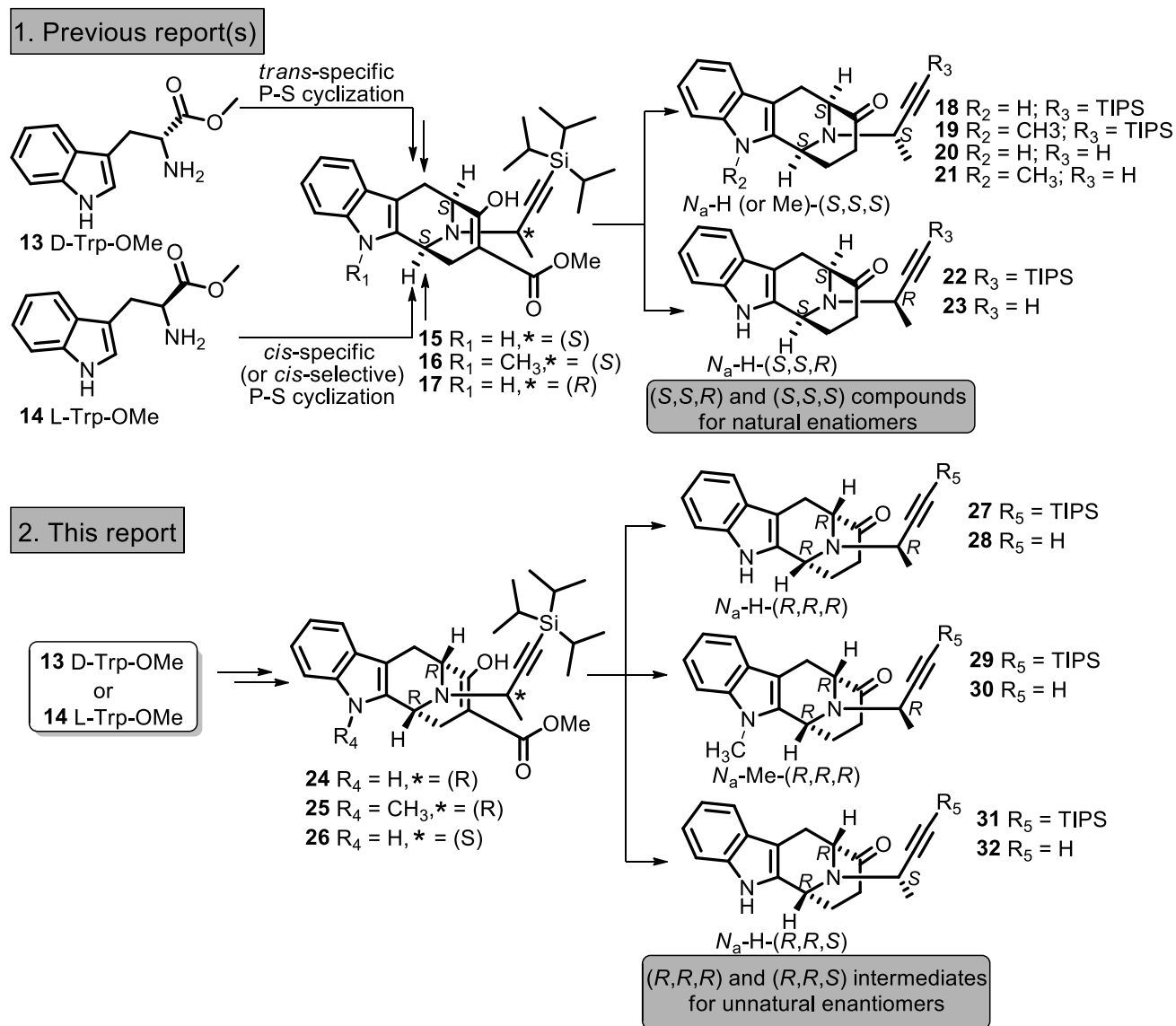
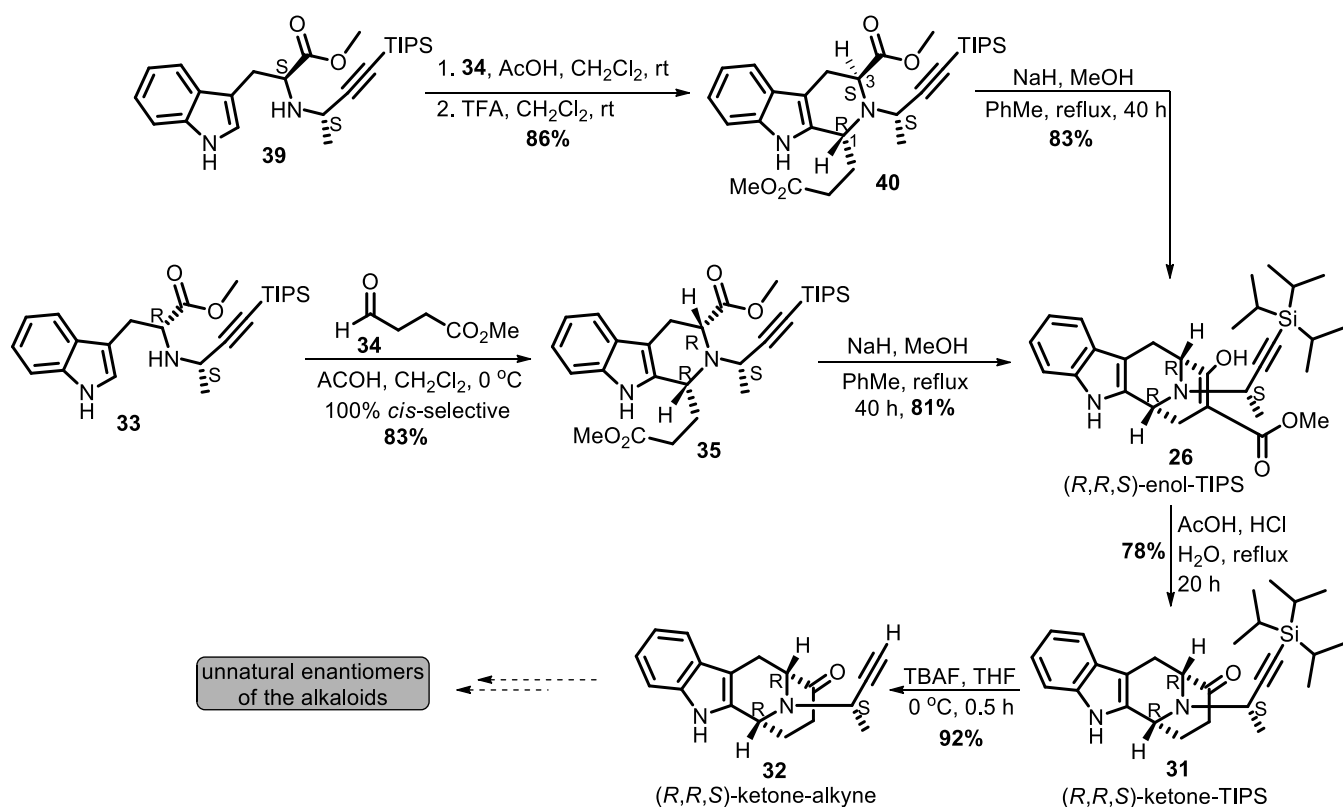


Figure 2. Access to both the natural and unnatural series of intermediates from D- and L-tryptophan

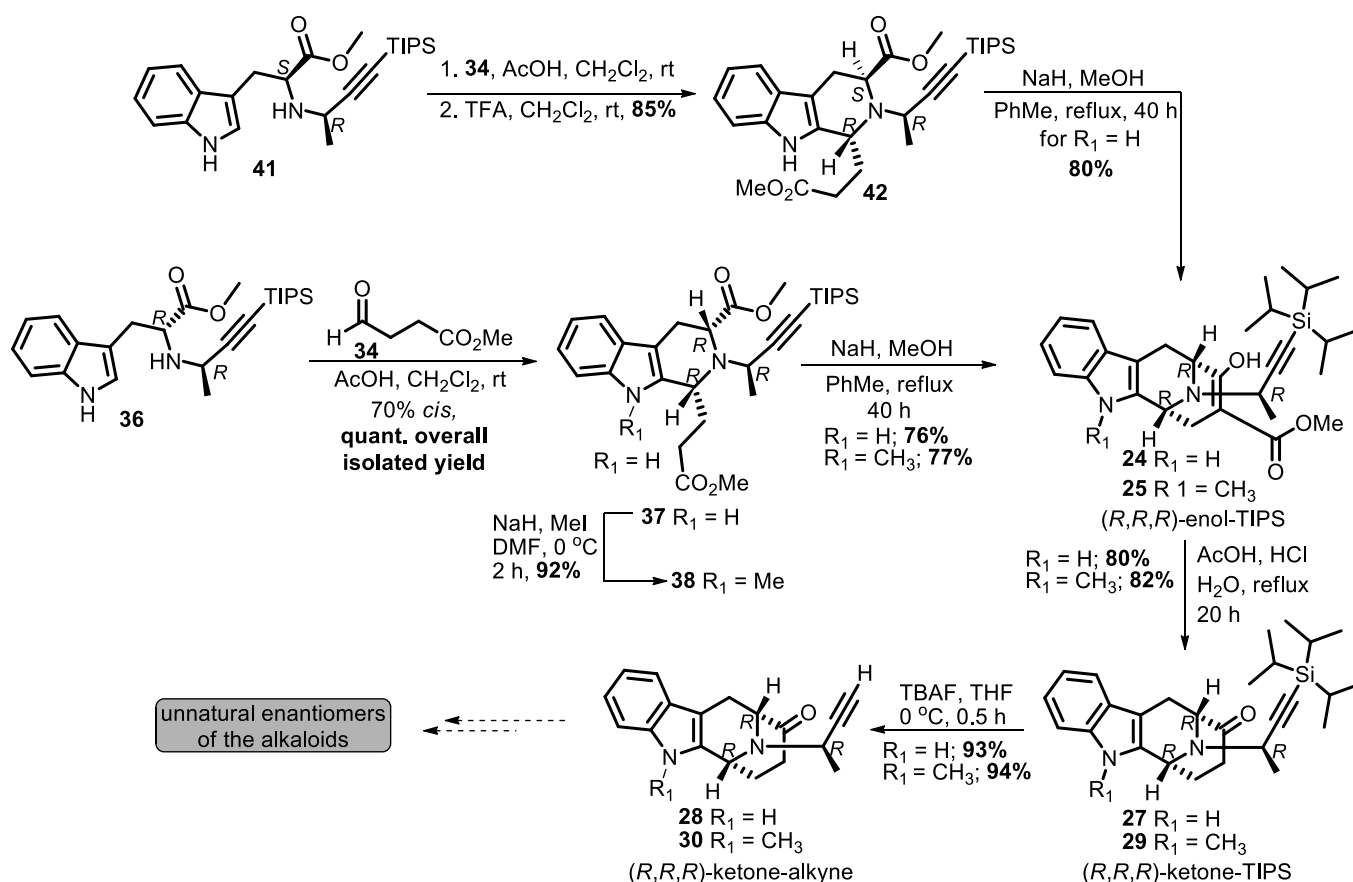
specific P-S reaction of the L-tryptophan derivative **41** to furnish the (*R*, *S*, *R*)-TH β C **42** as the sole product (85% isolated yield), following the procedure described above. The TH β C intermediate **42**,

upon Dieckmann cyclization, furnished the N_a -H (R, R, R) β -ketoester **24** in 80% isolated yield. This convergent approach provided access to the (R, R, R) β -ketoesters (**24** and **25**) from both L-tryptophan or D-tryptophan derivatives **41** and **36**, respectively. The N_a -H or N_a -CH₃ intermediates with the (R, R, R) configurations **24**, **25**, **27**, **28**, **29**, and **30** are the enantiomers of **15**, **16**, **18**, **20**, **19**, and **21**, respectively, which were previously synthesized from the D-tryptophan derivative **36**.^{26,27} These intermediates (**24-25**, **27-30**) are the key precursors for the total synthesis of the unnatural enantiomers of the sarpagine/macroline/ajmaline alkaloids with N_a -H (or CH₃), C-3(R), C-5(R), and C-19(R) stereochemical centers.



Scheme 1. Access to the (R, R, S) intermediates **26**, **31**, and **32** toward the unnatural enantiomers of C-19 (S)-methyl substituted sarpagine/macroline/ajmaline alkaloids.

At this point, an extensive comparison between the enantiomeric pairs (**24** vs **15**), (**25** vs **16**), (**26** vs **17**), (**27** vs **18**), (**29** vs **19**), (**28** vs **20**), (**30** vs **21**), (**31** vs **22**), and (**32** vs **23**) was performed (see Table 1 for details) as proof of concept. As expected, the MS, *R_f* and NMR (both ¹H and ¹³C) were identical for all enantiomeric pairs (see Appendix G for the NMR comparisons). The specific optical rotations for all enantiomeric pairs were also found to exhibit the opposite values, as expected and in good agreement within experimental error (JASCO polarimeter).



Scheme 2. Access to the (*R, R, R*) intermediates (**24**, **25**, **27**, **28**, **29**, and **30**) toward the unnatural enantiomers of C-19 (*R*)-methyl substituted sarpagine/macroline/ajmaline alkaloids

Table 1. Comparison of optical rotations between the natural and unnatural enantiomers of the key intermediates towards C-19 methyl substituted sarpagine/macroline/ajmaline alkaloids

enantiomeric pairs	compound	comparison among properties		
		$[\alpha]_D^{25}$	R_f co-elution TLC	^1H and ^{13}C NMR comparison ^d
natural	15 ; [N_a -H (<i>S,S,S</i>)-enol-TIPS]	-120.00	0.8 ^a	Identical NMR 15 vs 24
unnatural	24 ; [N_a -H (<i>R,R,R</i>)-enol-TIPS]	+118.80		
natural	16 ; [N_a -Me (<i>S,S,S</i>)-enol-TIPS]	-149.90	0.8 ^a	Identical NMR 16 vs 25
unnatural	25 ; [N_a -Me (<i>R,R,R</i>)-enol-TIPS]	+143.20		
natural	17 ; [N_a -H (<i>S,S,R</i>)-enol-TIPS]	+32.86	0.7 ^a	Identical NMR 17 vs 26
unnatural	26 ; [N_a -H (<i>R,R,S</i>)-enol-TIPS]	-32.31		
natural	18 ; [N_a -H (<i>S,S,S</i>)-ketone-TIPS]	-166.67	0.7 ^a	Identical NMR 18 vs 27
unnatural	27 ; [N_a -H (<i>R,R,R</i>)-ketone-TIPS]	+161.67		
natural	19 ; [N_a -Me (<i>S,S,S</i>)-ketone-TIPS]	-166.83	0.6 ^b	Identical NMR 19 vs 29
unnatural	29 ; [N_a -Me (<i>R,R,R</i>)-ketone-TIPS]	+170.59		
natural	20 ; [N_a -H (<i>S,S,S</i>)-ketone-alkyne]	-149.00	0.4 ^c	Identical NMR 20 vs 28
unnatural	28 ; [N_a -H (<i>R,R,R</i>)-ketone-alkyne]	+154.78		
natural	21 ; [N_a -Me (<i>S,S,S</i>)-ketone-alkyne]	-191.30	0.5 ^c	Identical NMR 21 vs 30
unnatural	30 ; [N_a -Me (<i>R,R,R</i>)-ketone-alkyne]	+188.89		
natural	22 ; [N_a -H (<i>S,S,R</i>)-ketone-TIPS]	-2.38	0.5 ^a	Identical NMR 22 vs 31
unnatural	31 ; [N_a -H (<i>R,R,S</i>)-ketone-TIPS]	+3.99		
natural	23 ; [N_a -H (<i>S,S,R</i>)-ketone-alkyne]	-48.25	0.2 ^c	Identical NMR 23 vs 32
unnatural	32 ; [N_a -H (<i>R,R,S</i>)-ketone-alkyne]	+50.85		

[a] = 30% EtOAc in hexanes; [b] = 15% EtOAc in hexanes; [c] = 30% EtOAc in hexanes+NH₄OH; [d] = see Appendix G for comparison between ^1H and ^{13}C NMR spectra for all enantiomeric pairs

3. Conclusion

In summary, a series of crucial precursors with the unnatural (*R, R, R*) and (*R, R, S*) configurations with either the N_a -H or N_a -CH₃ patterns of substitution were accessed enantiospecifically from both L- or D-tryptophan which also served as the chiral auxiliary and starting material for the natural (*S, S, R*) and (*S, S, S*) series. This work confirms the proof of concept for the synthesis of the (+) or (-) enantiomers of these alkaloids from either the chiral auxiliary (L- or D-tryptophan)

via internal asymmetric induction. Furthermore, this unambiguously illustrates the capability of the strategy developed here for accessing both the natural and the unnatural enantiomers of the C-19 methyl substituted sarpagine/macroline/ajmaline alkaloids from the same precursor(s). The completion of the total synthesis of the unnatural enantiomers is in progress and will be reported in due course.

4. Experimental Section

General Experimental Considerations

All reactions were carried out under an argon atmosphere with dry solvents using anhydrous conditions unless mentioned otherwise. The solvents (THF, DMF, toluene, DCM, MeCN, and MeOH) were dried using an Innovative Technology Solvent Purification System, Pure Solv™. Occasionally, tetrahydrofuran was freshly distilled from Na/benzophenone ketyl prior to use. Dichloromethane was distilled from calcium hydride prior to use. Methanol was distilled over magnesium sulfate. Benzene was distilled over CaH₂. Reagents were purchased of the highest commercial quality and used without further purification unless otherwise stated. Thin layer chromatography (TLC) was performed on UV active silica gel plates, 200 μm, aluminum backed and UV active alumina N plates, 200 μm, F-254 aluminum backed plates. Flash and gravity chromatography were performed using silica gel P60A, 40-63 μm, basic alumina (Act I, 50-200 μm) and neutral alumina (Brockman I, ~150 mesh). TLC plates were visualized by exposure to short wavelength UV light (254 nm). Indoles were visualized with a saturated solution of ceric

ammonium nitrate (CAN) in 50% phosphoric acid. The ^1H NMR data are reported as follows: chemical shift, multiplicity (br s = broad singlet, s = singlet, d = doublet, t = triplet, q = quartet, quin = quintet, dd = doublet of doublets, dt = doublet of triplets, ddd = doublet of doublet of doublets, td = triplet of doublets, qd = quartet of doublets, m = multiplet), integration, and coupling constants (Hz). The ^{13}C NMR data are reported in parts per million (ppm) on the δ scale. The low-resolution mass spectra (LRMS) were obtained as electron impact (EI, 70eV) and as chemical ionization (CI) using a magnetic sector (EBE) analyzer. HRMS were recorded by electrospray ionization (ESI) using a TOF analyzer, electron impact (EI) using a trisector analyzer and Atmospheric Pressure Chemical Ionization (APCI) using a TOF analyzer. Optical rotations were measured on a JASCO Model DIP-370 polarimeter.

Procedures

Procedure for the Pictet-Spengler (P-S) Cyclization

Compounds **35** and **37** were prepared from **33** and **36**, respectively following the previously reported procedures.^{26,27}

Representative example, 35: The N_b -alkylated tryptophan **33** (1.5 g, 3.51 mmol) was dissolved in dry DCM (50 mL) in a 100 mL round bottom flask equipped with a magnetic stir. To that above solution, the aldehyde⁴¹ **34** (612 mg, 5.27 mmol) and acetic acid (633 mg, 10.55 mmol, 603 μL), as well as 4 Å MS (0.7 g) were added at rt. The solution, which resulted, was stirred at rt for 10 h. The progress of the reaction was monitored by TLC analysis, as indicated by the consumption of **33** and appearance of a non-polar spot (UV and CAN stain). The reaction mixture was diluted with

DCM (50 mL) and water (50 mL) and then brought to pH 8-9 with cold aq NaOH (1 N). The organic layer was separated and washed with water (2 x 50 mL), brine (3 x 100 mL) and dried (Na₂SO₄). The solvent was removed under reduced pressure to give **35** as a light yellow-colored oil. The residue [LRMS (M+H)⁺ = 525, R_f = silica gel, 0.3 in 20% EtOAc in hexanes+NH₄OH] was purified by column chromatography (silica gel, 10-20% EtOAc in hexanes) to furnish the pure *cis*-diester **35** (1.52 g, **83%**) as a colorless oil as the sole product.

By following the same procedure, the *cis*-diesters **37** [LRMS (M+H)⁺ = 525; R_f = silica gel, 0.6, 30% EtOAc in hexanes] (1.72 g, 70% along with 0.73 g 30% of the corresponding *trans*-diester [R_f = 0.7 in 30% EtOAc in hexanes], which resulted in a quantitative overall isolated yield) was prepared from **36**^{26,27} (2.0 g, 4.69 mmol). Both **35** and **37** were used for the next transformation without further characterization.

Procedure for the *trans*-Specific Pictet-Spengler Cyclization

Indoles **40** and **42** were prepared from **39** and **41**, respectively according to the previously published procedure.^{26,27}

Representative example, 42: The *N*_b-alkylated tryptophan **41** (1.0 g, 2.34 mmol) was dissolved in dry DCM (40 mL) in a 100 mL round bottom flask equipped with a magnetic stir. To that above solution, the aldehyde **34** (408 mg, 3.51 mmol) and acetic acid (422 mg, 7.03 mmol, 402 μL), as well as 4 Å MS (0.5 g) were added at rt. The solution, which resulted, was stirred at rt for 10 h. The progress of the reaction was monitored by TLC analysis (silica gel), as indicated by the consumption of **41** and appearance of a non-polar spot (UV and CAN stain). The reaction mixture

was diluted with DCM (50 mL) and water (50 mL) and then brought to pH 8-9 with cold aq NaOH (1 N). The organic layer was separated and washed with water (2 x 50 mL), brine (3 x 100 mL) and dried (Na₂SO₄). The solvent was removed under reduced pressure to give a light yellow oil. The residue was subjected to a short wash column (silica gel) to remove any baseline material. The solvent was removed under reduced pressure and the residue, which resulted, was dissolved in dry DCM (30 mL). To that above solution, trifluoroacetic acid was added (267 mg, 2.34 mmol, 180 μL) at rt and the reaction, which resulted, was stirred at rt until complete conversion. After the reaction was complete, the reaction was brought to pH 8-9 with cold aq NaOH (1 N). The organic layer was separated and the aq layer was extracted with additional DCM (2 x 10 mL). The combined organic layers were washed with brine (3 x 100 mL) and dried (Na₂SO₄). The solvent was removed under reduced pressure to give a light yellow oil which was purified by column chromatography (silica gel, 0-20% EtOAc in hexanes) to furnish pure *trans*-diester **42** (1.05 g, 85%) as a colorless oil as the sole product [LRMS (M+H)⁺ = 525].

By following the same procedure with the **39** (1.0 g, 2.34 mmol), this process furnished the *trans*-diester **40**, [LRMS (M+H)⁺ = 525] (1.06 g, 86%) as the sole product.

Procedure for the *N*_α-Methylation

Procedure for the preparation of **38 from **37****

To a round-bottom flask (50 mL), which was equipped with a reflux condenser, the *N*_α-H *cis*-diester **37** (727 mg, 1.38 mmol), CH₃I (95 μL, 1.52 mmol), and dry DMF (10 mL) were added and then the mixture was cooled to -10 °C. To this solution was added NaH (60% dispersion in mineral oil, 61 mg, 1.52 mmol) at -10 °C. The slurry, which resulted, was allowed to stir at rt for 2 h until

analysis by TLC indicated the disappearance of **37** and appearance of **38** [LRMS (M+H)⁺ = 540]. The reaction solution was quenched by careful addition of CH₃OH (0.5 mL) and then was neutralized with an aq solution of NH₄Cl (20 mL) and extracted with EtOAc (3 x 30 mL). The combined organic layers were washed with brine (3 x 100 mL) and dried (K₂CO₃). The solvent was removed under reduced pressure and the residue was subjected to a short wash column (silica gel, 20% EtOAc in hexane) to provide the *N*_a-CH₃-(*R, R, R*)-diester **38** (688 mg, 92%) as a colorless oil.

Procedure for the Dieckmann cyclization

Representative example, 26: The *cis*-diester **35** (1.5 g, 2.86 mmol) was dissolved in toluene (150 mL). This solution was dried by azeotropic removal of H₂O by toluene with a DST (refluxed 6 h). To this mixture sodium hydride (687 mg, 17.1 mmol of 60% dispersion in mineral oil) at 0 °C was added. Anhydrous CH₃OH (2.1 mL, 51.4 mmol) was then added into the above mixture under Ar at 0 °C. The solution, which resulted, was then stirred at rt for 0.5 h and then held at reflux for an additional 30 h (the flask was covered with aluminum foil on the top to keep the temperature at reflux without carbonizing any compound on the sides of the flask). The reaction mixture was cooled to rt and quenched with ice (~50 g). The aq layer was extracted with CH₂Cl₂ (3 x 50 mL). The combined organic extracts were washed with brine and dried (K₂CO₃). The solvent was removed under reduced pressure to provide the crude product [LRMS (M+H)⁺ = 494] as a light brown residue. The residue was purified by flash chromatography (silica gel, EtOAc/hexane) to provide the β-ketoester **26** (1.14 g, 81%) as a colorless oil.

By following the same procedure with the *cis*-diester **37** (1.0 g, 1.90 mmol), this process furnished the β -ketoester **24**, [LRMS (M+H)⁺ = 494] (713 mg, 76%). The same process with the *cis*-diester **38** (300 mg, 0.56 mmol) furnished the β -ketoester **25**, [LRMS (M+H)⁺ = 508] (217 mg, 77%). When this process was carried out with the *trans*-diester **40** (400 mg, 0.76 mmol), this furnished the β -ketoester **26**, [LRMS (M+H)⁺ = 493] (312 mg, 83%); with *trans*-diester **42** (500 mg, 0.95 mmol), this reaction furnished the β -ketoester **24** [LRMS (M+H)⁺ = 493] (375 mg, 80%).

Procedure for the acid mediated decarboxylation reaction

Representative example, 31: To a round bottom flask (100 mL), which contained the *N*_a-H (*R, R, S*)- β -ketoester **26** (675 mg, 1.37 mmol), was added glacial acetic acid (2.6 mL), aq HCl (3.8 mL, conc.) and water (1 mL) with stirring (magnetic stir). The solution, which resulted, was heated at reflux for 20 h. After removal of the solvent under reduced pressure, the residue was brought to pH = 9 with a cold aq solution of NaOH (3 *N*). The mixture, which resulted, was extracted with CH₂Cl₂ (3 x 50 mL) and the combined organic extracts were washed with a saturated aq solution of NH₄Cl (50 mL), brine (3 x 50 mL) and dried (K₂CO₃). The removal of the solvent under reduced pressure afforded the ketone **31** as a brown oil. The residue was purified by column chromatography (silica gel, 20% EtOAc in hexanes) to provide pure **31** [LRMS (M+H)⁺ = 435] as a colorless oil (465 mg, 78%).

By following the same procedure with the β -ketoester **24** (386 mg, 0.78 mmol), this procedure furnished the ketone **27** [LRMS (M+H)⁺ = 435; 273 mg, 80%] and with the β -ketoester **25** (96 mg, 0.19 mmol), this process furnished the ketone **29** [LRMS (M+H)⁺ = 450; 70 mg, 82%].

Procedure for the de-silylation

Representative example, 32: To a solution of **31** (50 mg, 0.11 mmol) in THF (5 mL), TBAF (167 μ L, 0.167 mmol, 1.0 M solution in THF) was added at 0 °C. The solution, which resulted, was stirred at 0 °C for 30 min or until the completion of the reaction as monitored by TLC (silica gel). After that, the reaction mixture was diluted with EtOAc (20 mL) and water (10 mL). The organic layer was separated and the aq layer was extracted with EtOAc (5 mL). The combined organic layers were washed with brine (3 x 20 mL) and dried (Na_2SO_4). The solvent was removed under reduced pressure to provide the N_a -H (*R, R, S*)-alkyne **32** (LRMS 279) as a brown residue. The residue was purified by silica gel column chromatography (30% EtOAc in hexanes) to provide **32** as a colorless oil (29.5 mg, 92%).

By following the same procedure with the ketone **27** (72 mg, 0.17 mmol), this process furnished the alkyne **28** (LRMS ($M+H$)⁺ = 279, 43 mg, 93%) and with the ketone **29** (31 mg, 0.69 mmol), this reaction furnished the alkyne **30** (LRMS 293, 19 mg, 94%).

Analytical Data

Compound 24 [N_a -H-(*R, R, R*)-enol-TIPS]:

¹H NMR (500 MHz, CDCl_3): δ 12.00 (br s, 1H), 7.74 (br s, 1H), 7.49 (d, 1H, $J = 7.7$ Hz), 7.34 (d, 1H, $J = 8.0$ Hz), 7.20-7.16 (m, 1H), 7.14-7.10 (m, 1H), 4.77 (d, 1H, $J = 5.1$ Hz), 4.14 (d, 1H, $J = 5.4$ Hz), 3.69 (s, 3H), 3.66 (q, 1H, $J = 6.6$ Hz), 3.09 (dd, 1H, $J = 16.1$ Hz, 5.7 Hz), 2.94 (br d, 1H, $J = 16.2$ Hz), 2.90 (dd, 1H, $J = 15.7$ Hz, 5.6 Hz), 2.44 (dd, 1H, $J = 15.6$ Hz, 1.1 Hz), 1.54 (d, 3H, $J = 6.6$ Hz), 1.10-1.00 (m, 21H); **¹³C NMR** (125 MHz, CDCl_3): δ 172.4, 171.4, 135.7, 133.2, 127.0,

121.8, 119.7, 118.2, 110.8, 108.7, 106.8, 94.8, 84.4, 52.5, 51.4, 49.4, 47.3, 29.1, 21.7, 20.5, 18.6, 11.2; **Rf**: 0.8 (silica gel, 30% EtOAc in hexanes); $[\alpha]_D^{25} = +118.80$ (*c* 1.41, CHCl₃); **HRMS**: (ESI) *m/z* (M+H)⁺ calcd for C₂₉H₄₁N₂O₃Si, 493.2881, found 493.2850.

Compound 25 [N_a-Me-(R, R, R)-enol-TIPS]:

¹H NMR (500 MHz, CDCl₃): δ 11.99 (br s, 1H), 7.50 (d, 1H, *J* = 7.8 Hz), 7.31 (d, 1H, *J* = 8.2 Hz), 7.22 (t, 1H, *J* = 7.2 Hz), 7.13 (t, 1H, *J* = 7.2 Hz), 4.94 (d, 1H, *J* = 5.4 Hz), 4.11 (br d, 1H, *J* = 5.5 Hz), 3.70 (s, 3H), 3.68 (s, 3H), 3.61 (q, 1H, *J* = 6.5 Hz), 3.09 (dd, 1H, *J* = 16.2 Hz, 5.8 Hz), 2.97-2.91 (m, 1H), 2.39 (br d, 1H, *J* = 15.5 Hz), 1.54 (d, 3H, *J* = 6.6 Hz), 1.10-1.02 (m, 21H); **¹³C NMR** (125 MHz, CDCl₃): δ 172.4, 171.5, 137.0, 134.1, 126.5, 121.3, 119.2, 118.2, 108.8, 108.7, 105.6, 94.4, 84.4, 52.1, 51.4, 48.2, 47.2, 29.2, 28.8, 21.2, 20.3, 18.6, 11.2; **Rf**: 0.85 (silica gel, 30% EtOAc in hexanes); $[\alpha]_D^{25} = +143.20$ (*c* 1.69, CHCl₃); **HRMS**: (ESI) *m/z* (M+H)⁺ calcd for C₃₀H₄₃N₂O₃Si, 507.3037, found 507.3013.

Compound 26, [N_a-H-(R, R, S)-enol-TIPS]:

¹H NMR (500 MHz, CDCl₃): δ 11.97 (br s, 1H), 7.77 (br s, 1H), 7.51 (d, 1H, *J* = 7.7 Hz), 7.33 (d, 1H, *J* = 7.9 Hz), 7.20-7.16 (m, 1H), 7.14-7.10 (m, 1H), 4.48 (d, 1H, *J* = 5.2 Hz), 4.37 (d, 1H, *J* = 5.6 Hz), 3.69 (s, 3H), 3.64 (q, 1H, *J* = 6.3 Hz), 3.26 (dd, 1H, *J* = 16.1 Hz, 5.9 Hz), 2.96 (br d, 1H, *J* = 16.4 Hz), 2.92 (dd, 1H, *J* = 14.9 Hz, 5.6 Hz), 2.42 (dd, 1H, *J* = 15.7 Hz, 1.0 Hz), 1.49 (d, 3H, *J* = 6.3 Hz), 1.13-1.04 (m, 21H); **¹³C NMR** (125 MHz, CDCl₃): δ 172.4, 171.4, 135.7, 132.8, 127.0, 121.9, 119.7, 118.3, 110.8, 107.6, 107.3, 94.5, 85.4, 53.7, 51.4, 48.2, 46.7, 29.0, 22.7, 20.9,

18.6, 11.2; **Rf**: 0.65 (silica gel, 30% EtOAc in hexanes); $[\alpha]_D^{25} = -32.31$ (*c* 0.65, CHCl₃); **HRMS**: (ESI) *m/z* (M+H)⁺ calcd for C₂₉H₄₁N₂O₃Si, 493.2881, found 439.2854.

Compound 27 [N_a-H-(R, R, R)-ketone-TIPS]:

¹H NMR (500 MHz, CDCl₃): δ 8.01 (br s, 1H), 7.48 (d, 1H, *J* = 7.7 Hz), 7.34 (d, 1H, *J* = 8.0 Hz), 7.22-7.18 (m, 1H), 7.15-7.11 (m, 1H), 4.75-4.72 (m, 1H), 3.99 (d, 1H, *J* = 6.2 Hz), 3.72 (q, 1H, *J* = 6.7 Hz), 3.18 (dd, 1H, *J* = 16.5 Hz, 6.4 Hz), 2.74 (br d, 1H, *J* = 16.4 Hz), 2.62-2.48 (m, 2H), 2.17-2.05 (m, 2H), 1.50 (d, 3H, *J* = 6.7 Hz), 1.08-0.96 (m, 21H); **¹³C NMR** (125 MHz, CDCl₃): δ 210.8, 136.0, 132.7, 126.9, 121.9, 119.6, 118.2, 110.9, 108.9, 107.5, 84.7, 62.2, 50.1, 48.0, 34.8, 29.7, 21.7, 21.0, 18.6, 11.2; **Rf**: 0.7 (silica gel, 30% EtOAc in hexanes); $[\alpha]_D^{25} = +161.67$ (*c* 1.2, CHCl₃);

HRMS: (ESI) *m/z* (M+H)⁺ calcd for C₂₇H₃₉N₂O₃Si, 435.2826, found 435.2821.

Compound 28 [N_a-H-(R, R, R)-ketone-alkyne]:

¹H NMR (500 MHz, CDCl₃): δ 7.96 (br s, 1H), 7.48 (d, 1H, *J* = 7.8 Hz), 7.36 (d, 1H, *J* = 8.0 Hz), 7.23-7.18 (m, 1H), 7.16-7.12 (m, 1H), 4.70-4.66 (m, 1H), 3.97 (d, 1H, *J* = 6.4 Hz), 3.66 (qd, 1H, *J* = 6.7 Hz, 2.1 Hz), 3.15 (dd, 1H, *J* = 16.6 Hz, 6.5 Hz), 2.73 (br d, 1H, *J* = 16.6 Hz), 2.64-2.56 (m, 1H), 2.54-2.48 (m, 1H), 2.28 (d, 1H, *J* = 2.2 Hz), 2.18-2.05 (m, 2H), 1.48 (d, 3H, *J* = 6.7 Hz); **¹³C NMR** (125 MHz, CDCl₃): δ 210.7, 135.9, 132.5, 126.8, 122.1, 119.8, 118.2, 111.0, 107.4, 84.9, 72.4, 61.6, 50.5, 47.2, 34.7, 29.6, 21.7, 20.5; **Rf**: 0.4 (silica gel, 30% EtOAc in hexanes/NH₄OH); $[\alpha]_D^{25} = +154.78$ (*c* 1.15, CHCl₃), **HRMS** (ESI) *m/z* (M+H)⁺ calcd for C₁₈H₁₉N₂O, 279.1492, found 279.1468.

Compound 29 [N_a-Me-(R, R, R)-ketone-TIPS]:

¹H NMR (500 MHz, CDCl₃): δ 7.48 (d, 1H, *J* = 7.8 Hz), 7.33 (d, 1H, *J* = 8.2 Hz), 7.26-7.22 (m, 1H), 7.15-7.11 (m, 1H), 4.94-4.91 (m, 1H), 3.98 (d, 1H, *J* = 6.5 Hz), 3.69 (s, 3H), 3.66 (q, 1H, *J* = 6.7 Hz), 3.16 (dd, 1H, *J* = 16.7 Hz, 6.6 Hz), 2.71 (br d, 1H, *J* = 16.7 Hz), 2.63-2.56 (m, 1H), 2.54-2.47 (m, 1H), 2.18-2.02 (m, 2H), 1.48 (d, 3H, *J* = 6.6 Hz), 1.08-1.01 (m, 21H); **¹³C NMR** (125 MHz, CDCl₃): δ 210.0, 137.2, 133.6, 126.4, 121.5, 119.2, 118.2, 108.8, 106.2, 84.7, 61.6, 48.8, 47.7, 34.4, 29.3, 29.2, 21.0, 20.5, 18.6, 18.6, 11.6; **R_f**: 0.55 (silica gel, 15% EtOAc in hexanes); **[α]_D²⁵** = +170.59 (*c* 0.34, CHCl₃); **HRMS**: (ESI) *m/z* (M+H)⁺ calcd for C₂₈H₄₁N₂OSi, 449.2983, found 449.2987.

Compound 30 [N_a-Me-(R, R, R)-ketone-alkyne]:

¹H NMR (500 MHz, CDCl₃): δ 7.49 (d, 1H, *J* = 7.8 Hz), 7.34 (d, 1H, *J* = 8.2 Hz), 7.25 (t, 1H, *J* = 7.6 Hz), 7.13 (t, 1H, *J* = 7.4 Hz), 4.79-4.76 (m, 1H), 3.97 (d, 1H, *J* = 6.6 Hz), 3.72 (s, 3H), 6.64 (qd, 1H, *J* = 6.7 Hz, 2.1 Hz), 3.16 (dd, 1H, *J* = 16.7 Hz, 6.7 Hz), 2.73 (br d, 1H, *J* = 16.6 Hz), 2.68-2.60 (m, 1H), 2.50 (dd, 1H, *J* = 16.9 Hz, 6.2 Hz), 2.30 (d, 1H, *J* = 2.1 Hz), 2.19-2.10 (m, 1H), 2.09-2.03 (m, 1H), 1.48 (d, 3H, *J* = 6.7 Hz); **¹³C NMR** (125 MHz, CDCl₃): δ 210.2, 137.2, 133.6, 126.3, 121.6, 119.3, 118.2, 108.9, 106.2, 84.8, 72.5, 61.3, 49.3, 47.2, 34.5, 29.4, 29.0, 21.5, 20.5; **R_f**: 0.5 (silica gel, 50% EtOAc in hexanes + NH₄OH); **[α]_D²⁵** = +188.89 (*c* 1.35, CHCl₃); **HRMS** (ESI) *m/z* (M+H)⁺ calcd for C₁₉H₂₁N₂O, 293.1648, found 293.1624.

Compound 31 [Na-H-(R, R, S)-ketone-TIPS]:

¹H NMR (500 MHz, CDCl₃): δ 7.88 (br s, 1H), 7.49 (d, 1H, *J* = 7.8 Hz), 7.35 (d, 1H, *J* = 8.0 Hz), 7.22-7.18 (m, 1H), 7.15-7.11 (m, 1H), 4.40-4.37 (m, 1H), 4.36 (d, 1H, *J* = 6.6 Hz), 3.74 (q, 1H, *J* = 6.4 Hz), 3.31 (dd, 1H, *J* = 16.7 Hz, 6.6 Hz), 2.72 (br d, 1H, *J* = 16.7 Hz), 2.58-2.45 (m, 2H), 2.17-2.04 (m, 2H), 1.48 (d, 3H, *J* = 6.5 Hz), 1.10-1.01 (m, 21H); **¹³C NMR** (125 MHz, CDCl₃): δ 210.5, 135.9, 132.0, 126.9, 122.1, 119.7, 118.3, 110.9, 108.0, 107.6, 85.4, 63.4, 48.5, 47.4, 34.6, 30.0, 21.7, 21.1, 18.6, 11.2; **R_f**: 0.5 (silica gel, 30% EtOAc in hexanes); **[α]_D²⁵** = +3.99 (*c* 2.0, CHCl₃); **HRMS**: (ESI) *m/z* (M+H)⁺ calcd for C₂₇H₃₉N₂OSi, 435.2826 found 435.2811.

Compound 32 [Na-H-(R, R, S)-ketone-alkyne]:

¹H NMR (500 MHz, CDCl₃): δ 7.86 (br s, 1H), 7.49 (d, 1H, *J* = 7.8 Hz), 7.36 (d, 1H, *J* = 8.1 Hz), 7.21 (t, 1H, *J* = 7.5 Hz), 7.14 (t, 1H, *J* = 7.7 Hz), 4.41-4.37 (m, 1H), 4.35 (d, 1H, *J* = 6.6 Hz), 3.68 (qd, 1H, *J* = 6.5 Hz, 2.2 Hz), 3.30 (dd, 1H, *J* = 16.8 Hz, 6.7 Hz), 2.72 (br d, 1H, *J* = 16.8 Hz), 2.58-2.46 (m, 2H), 2.33 (d, 1H, *J* = 2.2 Hz), 2.20-2.06 (m, 2H), 1.47 (d, 3H, *J* = 6.5 Hz); **¹³C NMR** (125 MHz, CDCl₃): 210.4, 135.9, 131.7, 126.8, 122.2, 119.8, 118.3, 110.9, 107.9, 83.9, 72.6, 63.3, 48.0, 46.3, 34.5, 30.1, 21.5, 20.6; **R_f**: 0.2 (silica gel, 30% EtOAc in hexanes+NH₄OH); **[α]_D²⁵** = +50.85 (*c* 0.59, CHCl₃); **HRMS**: (ESI) *m/z* (M+H)⁺ calcd for C₁₈H₁₉N₂O, 279.1492, found 279.1467.

Compound 38 [Na-Me-(R, R, R)-THβC]:

¹H NMR (500 MHz, CDCl₃): δ 7.49 (d, 1H, *J* = 7.8 Hz), 7.25 (d, 1H, *J* = 8.1 Hz), 7.20-7.16 (m, 1H), 7.10-7.06 (m, 1H), 4.31-4.26 (m, 1H), 3.96 (t, 1H, *J* = 5.7 Hz), 3.84-3.78 (m, 1H), 3.72 (s, 3H), 3.70 (s, 3H), 3.65 (s, 3H), 3.26-3.16 (m, 2H), 2.84-2.77 (m, 1H), 2.53-2.45 (m, 1H), 2.11-

2.03 (m, 1H), 1.72-1.63 (m, 1H), 1.48 (d, 3H, $J = 7.0$ Hz), 0.85-0.79 (m, 18H), 0.76-0.68 (m, 3H); $^{13}\text{C NMR}$ (125 MHz, CDCl_3): δ 174.6, 174.4, 137.4, 135.7, 126.4, 121.0, 118.8, 118.1, 108.6, 107.9, 106.2, 84.0, 60.5, 53.7, 52.0, 51.5, 49.9, 31.1, 29.8, 29.6, 22.4, 21.7, 18.3, 10.9; **Rf**: 0.8 (silica gel, 30% EtOAc in hexanes); $[\alpha]_{\text{D}}^{25} = +17.0$ (c 2.0, CHCl_3); **HRMS**: (ESI) m/z ($\text{M}+\text{H}$) $^+$ calcd for $\text{C}_{31}\text{H}_{47}\text{N}_2\text{O}_4\text{Si}$, 539.3300, found 539.3292.

Compound 40 [N_a-H-(R, S, S)-TH β C]:

$^1\text{H NMR}$ (500 MHz, CDCl_3): δ 8.06 (br s, 1H), 7.48 (d, 1H, $J = 7.7$ Hz), 7.32 (d, 1H, $J = 7.9$ Hz), 7.18-7.14 (m, 1H), 7.12-7.08 (m, 1H), 4.64 (t, 1H, $J = 4.5$ Hz), 4.15 (t, 1H, $J = 5.6$ Hz), 4.09 (q, 1H, $J = 6.8$ Hz), 3.64 (s, 3H), 3.64 (s, 3H), 3.09 (m, 2H), 2.55-2.48 (m, 1H), 2.36-2.22 (m, 2H), 2.13-2.05 (m, 1H), 1.41 (d, 3H, $J = 6.8$ Hz), 1.11-1.05 (m, 21H); $^{13}\text{C NMR}$ (125 MHz, CDCl_3): δ 174.8, 173.3, 136.2, 134.9, 127.0, 121.5, 119.3, 118.0, 110.9, 108.2, 107.6, 84.9, 54.7, 53.2, 51.6, 51.4, 46.8, 29.1, 28.4, 24.8, 21.9, 18.6, 11.3; **Rf**: 0.6 (silica gel, 20% EtOAc in hexanes); $[\alpha]_{\text{D}}^{25} = +3.01$ (c 1.33, CHCl_3); **HRMS**: (ESI) m/z ($\text{M}-\text{H}$) $^-$ calcd for $\text{C}_{30}\text{H}_{43}\text{N}_2\text{O}_4\text{Si}$, 525.2998 found 525.2971.

Compound 42 [N_a-H-(R, S, R)-TH β C]:

$^1\text{H NMR}$ (500 MHz, CDCl_3): δ 7.95 (br s, 1H), 7.45 (d, 1H, $J = 7.4$ Hz), 7.27 (d, 1H, $J = 8.0$ Hz), 7.12 (t, 1H, $J = 7.1$ Hz), 7.08-7.04 (m, 1H), 4.20-4.15 (m, 1H), 4.08-4.03 (m, 1H), 3.83 (q, 1H, $J = 6.9$ Hz), 3.80 (s, 3H), 3.73 (s, 3H), 3.24 (dd, 1H, $J = 15.3, 10.9$ Hz), 3.02 (dd, 1H, $J = 15.4, 4.1$ Hz), 2.71-2.63 (m, 1H), 2.61-2.53 (m, 1H), 2.20-2.12 (m, 1H), 2.05-1.94 (m, 1H), 1.39 (d, 3H, $J = 6.9$ Hz), 0.79-0.73 (m, 18H), 0.59-0.51 (m, 3H); $^{13}\text{C NMR}$ (125 MHz, CDCl_3): δ 174.5, 173.3,

136.1, 135.1, 127.0, 121.4, 119.1, 118.2, 110.5, 109.0, 108.7, 83.7, 57.7, 52.5, 52.0, 51.7, 46.1, 30.7, 29.7, 23.1, 21.6, 18.3, 10.9; **R_f**: 0.55 (silica gel, 20% EtOAc in hexanes); [**α**]_D²⁵ = +88.14 (c 0.59, CHCl₃); **HRMS**: (ESI) *m/z* (M-H)⁻ calcd for C₃₀H₄₃N₂O₄Si, 525.2998 found 525.2963.

5. References

- (1) Dias, D. A.; Urban, S.; Roessner, U. *Metabolites* **2012**, *2*, 303.
- (2) Newman, D. J.; Cragg, G. M.; Snader, K. M. *Nat. Prod. Rep.* **2000**, *17*, 215.
- (3) Koehn, F. E.; Carter, G. T. *Nat. Rev. Drug Discov.* **2005**, *4*, 206.
- (4) Paterson, I.; Anderson, E. A. *Science* **2005**, *310*, 451.
- (5) Butler, M. S. *Nat. Prod. Rep.* **2008**, *25*, 475.
- (6) Newman, D. J.; Cragg, G. M. *J. Nat. Prod.* **2016**, *79*, 629.
- (7) Cragg, G. M.; Newman, D. J. *Biochim. Biophys. Acta Gen. Subj.* **2013**, *1830*, 3670.
- (8) O'Neil, M.J. *The Merck Index: An Encyclopedia of Chemicals, Drugs, and Biologicals*; RSC Publishing: London, UK, 2013.
- (9) Feher, M.; Schmidt, J. M. *J. Chem. Inf. Comp. Sci.* **2003**, *43*, 218.
- (10) Liotta, D. C.; Painter, G. R. *Acc. Chem. Res.* **2016**, *49*, 2091.
- (11) Wender, P. A.; DeChristopher, B. A.; Schrier, A. J. *J. Am. Chem. Soc.* **2008**, *130*, 6658.
- (12) Carney, D. W.; Lukesh, J. C.; Brody, D. M.; Brüttsch, M. M.; Boger, D. L. *Proc. Natl. Acad. Sci. U.S.A.* **2016**, *113*, 9691.

- (13) Lounasmaa, M.; Hanhinen, P. In *The Alkaloids: Chemistry and Biology*; Cordell, G. A., Ed.; Academic Press: San Diego, 2001; Vol. 55, pp 1-90.
- (14) Lounasmaa, M.; Hanhinen, P.; Westersund, M.; Halonen, N. In *The Alkaloids: Chemistry and Biology*; Cordell, G. A., Ed.; Academic Press: San Diego, CA: 1999; Vol. 52, p 103.
- (15) Namjoshi, O. A.; Cook, J. M. In *The Alkaloids: Chemistry and Biology*; Knölker, H.-J., Ed.; Academic Press: San Diego, CA: 2016; Vol. 76, p 63.
- (16) Rahman, M. T.; Cook, J. M. In *Studies in Natural Products Chemistry*; Atta-ur-Rahman, Ed.; Elsevier Publications: Amsterdam, Netherlands (In Press).
- (17) Stöckigt, J.; Antonchick, A. P.; Wu, F.; Waldmann, H. *Angew. Chem., Int. Ed.* **2011**, *50*, 8538.
- (18) Klausen, R. S.; Jacobsen, E. N. *Org. Lett.* **2009**, *11*, 887.
- (19) Raheem, I. T.; Thiara, P. S.; Peterson, E. A.; Jacobsen, E. N. *J. Am. Chem. Soc.* **2007**, *129*, 13404.
- (20) Taylor, M. S.; Jacobsen, E. N. *J. Am. Chem. Soc.* **2004**, *126*, 10558.
- (21) Cox, E. D.; Cook, J. M. *Chem. Rev.* **1995**, *95*, 1797.
- (22) Herlé, B.; Wanner, M. J.; van Maarseveen, J. H.; Hiemstra, H. *J. Org. Chem.* **2011**, *76*, 8907.
- (23) Ruiz-Olalla, A.; Würdemann, M. A.; Wanner, M. J.; Ingemann, S.; van Maarseveen, J. H.; Hiemstra, H. *J. Org. Chem.* **2015**, *80*, 5125.

- (24) Kayhan, J.; Wanner, M. J.; Ingemann, S.; van Maarseveen, J. H.; Hiemstra, H. *Eur. J. Org. Chem.* **2016**, 2016, 3705.
- (25) Rahman, M.T.; Tiruveedhula, V. V.; Cook, J. M. *Molecules* **2016**, 21, 1525
- (26) Rahman, M. T.; Cook, J. M. *Eur. J. Org. Chem.* **2018**, 3224.
- (27) Rahman, M. T.; Deschamps, J. R.; Imler, G. H.; Cook, J. M. *Chem. Eur. J.* **2018**, 24, 2354.
- (28) Rahman, M. T.; Deschamps, J. R.; Imler, G. H.; Schwabacher, A. W.; Cook, J. M. *Org. Lett.* **2016**, 18, 4174.
- (29) Edwankar, R. V.; Edwankar, C. R.; Deschamps, J.; Cook, J. M. *Org. Lett.* **2011**, 13, 5216.
- (30) Edwankar, R. V.; Edwankar, C. R.; Deschamps, J. R.; Cook, J. M. *J. Org. Chem.* **2014**, 79, 10030.
- (31) Koskinen, A.; Lounasmaa, M. In *Progress in the Chemistry of Organic Natural Products*; Ingham, J. L., Ed.; Springer-Verlag/Wien: 1983; Vol. 43, p 267.
- (32) Lounasmaa, M.; Hanhinen, P.; Westersund, M. *ChemInform* **1999**, 30.
- (33) Zeng, J.; Zhang, D.-B.; Zhou, P.-P.; Zhang, Q.-L.; Zhao, L.; Chen, J.-J.; Gao, K. *Org. Lett.* **2017**, 19, 3998.
- (34) Gao, Y.; Yu, A.-L.; Li, G.-T.; Hai, P.; Li, Y.; Liu, J.-K.; Wang, F. *Fitoterapia* **2015**, 107, 44.
- (35) Pan, L.; Terrazas, C.; Acuña, U. M.; Ninh, T. N.; Chai, H.; De Blanco, E. J. C.; Soejarto, D. D.; Satoskar, A. R.; Kinghorn, A. D. *Phytochem. Lett.* **2014**, 10, 54.

- (36) Tan, S.-J.; Lim, J.-L.; Low, Y.-Y.; Sim, K.-S.; Lim, S.-H.; Kam, T.-S. *J. Nat. Prod.* **2014**, *77*, 2068.
- (37) Gui-yun, Z.; Bao-hong, T.; Rong, Z.; Li-fen, D.; Chao, X. *Acta Pharmacol. Sinica* **1991**, *12*, 471.
- (38) Cao, P.; Liang, Y.; Gao, X.; Li, X.-M.; Song, Z.-Q.; Liang, G. *Molecules* **2012**, *17*, 13631.
- (39) Zhang, L.; Hua, Z.; Song, Y.; Feng, C. *Fitoterapia* **2014**, *97*, 142.
- (40) Cheng, G.-G.; Zhao, Y.-L.; Zhang, Y.; Lunga, P.-K.; Hu, D.-B.; Li, Y.; Gu, J.; Song, C.-W.; Sun, W.-B.; Liu, Y.-P. *Tetrahedron* **2014**, *70*, 8723.
- (41) Drinan, M. A.; Lash, T. D. *J. Heterocyclic Chem.* **1994**, *31*, 255

PART II. THE TOTAL SYNTHESIS OF A NUMBER OF BIOACTIVE C-19 METHYL SUBSTITUTED MACROLINE-SARPAGINE INDOLE ALKALOIDS INCLUDING MACROCARPINES A-G, TALCARPINE, *N*(4)-METHYL-*N*(4),21-SECOTALPININE, DEOXYPERAKSINE, DIHYDROPERAKSINE, TALPININE, *O*-ACETYLTALPININE, AS WELL AS *N*(4)-METHYLTALPININE

Chapter 4

The Total Synthesis of Macroparpines D and E via an Efficient Copper-Mediated Cross-Coupling Process

1. Introduction

After gaining access to the bicyclo[3.3.1] system via the ambidextrous Pictet-Spengler reaction, the focus turned to the completion of the total synthesis of a number of C-19 methyl substituted sarpagine/macroline/ajmaline alkaloids. As a step towards that, alkaloids with N_a -H and N_b -CH₃ substituents were focused upon. An enolate driven copper-mediated cross-coupling process enabled cheaper and greener access to the key pentacyclic intermediates required for the enantiospecific total synthesis of a number of C-19 methyl substituted sarpagine/macroline indole alkaloids. The replacement of palladium (**60-68%**) with copper iodide (**82-89%**) resulted in much higher yields. The formation of an unusual seven-membered cross-coupling product was completely inhibited by using TEMPO as a radical scavenger. Further functionalization led to the first enantiospecific total synthesis of macrocarpines D and E.

The medicinal plants of the *Alstonia* (Apocynaceae) genus have been used in traditional medicine in many countries of the world from antiquity.¹ Their traditional uses include treatment of ulcers, dysentery, malaria, anthelmintics, diabetes, rheumatism, snake bites, etc.¹ Indole alkaloid secondary metabolites of these plants are the most probable source of their medicinal activity.² According to a review by Cordell et al., among the 60 plant-derived alkaloids of medicinal significance, 39 were directly related to their traditional uses.³ Macroline/sarpagine type indole alkaloids are one of the major classes of alkaloids isolated from these species to date by Le-Quesne, Elderfield, Schmid, Kam, and others.⁴⁻⁷ Macrocarpines A-C (**1-3**) were isolated from the bark extract of *Alstonia macrophylla* in 2004.⁸ Several other alkaloids of the same series, macrocarpine D (**4**) and macrocarpines E-H (**5-8**), were isolated in 2014 from the stem-bark and leaf extracts of *A. macrophylla* and *A. angustifolia* respectively by Kam et al.^{9,10} All of these macroline-type indole

alkaloids, macrocarpines A-H (**1-8**) share the common feature of a β -methyl substituent at the C-19 position. This is a distinct difference from earlier *Alstonia* alkaloids isolated by LeQuesne and Schmid.^{5,7} To date, around seventy alkaloids of the sarpagine/macroline/ajmaline family (see General Introduction), which bear a diastereomeric methyl function at C-19 have been isolated.^{4,11} Macroline related alkaloids *N*(4)-methyl-*N*(4),21-secotalpinine (**9**)^{8,12}, *N*(4)-methyltalpinine (**10**)¹², and 19-epitalcarpine (**11**),¹⁰ as well as the sarpagine-related alkaloids macrosalpine chloride (**12**)¹³, and deoxyperaksine (**13**)¹⁴ also possess the C-19 methyl substitution. Among these, **11** and **13** contain a diastereomeric α -methyl group at C-19. The synthesis of these alkaloids (**1-13**, Figure 1) has not been reported yet. Moreover, *N*(4)-methyltalpinine (**10**) and *N*(4)-methyl-*N*(4),21-secotalpinine (**9**) have been reported recently to have potent anticancer (NF- κ B inhibitor, ED₅₀ 1.2 μ M) activity and profound leishmanicidal¹² activity, respectively. The unique structural features and potential medicinal properties prompted attempts at the first total synthesis of this class of alkaloids *via* a general strategy for the entire series. This is the basis of the approach toward chemical economy described herein.

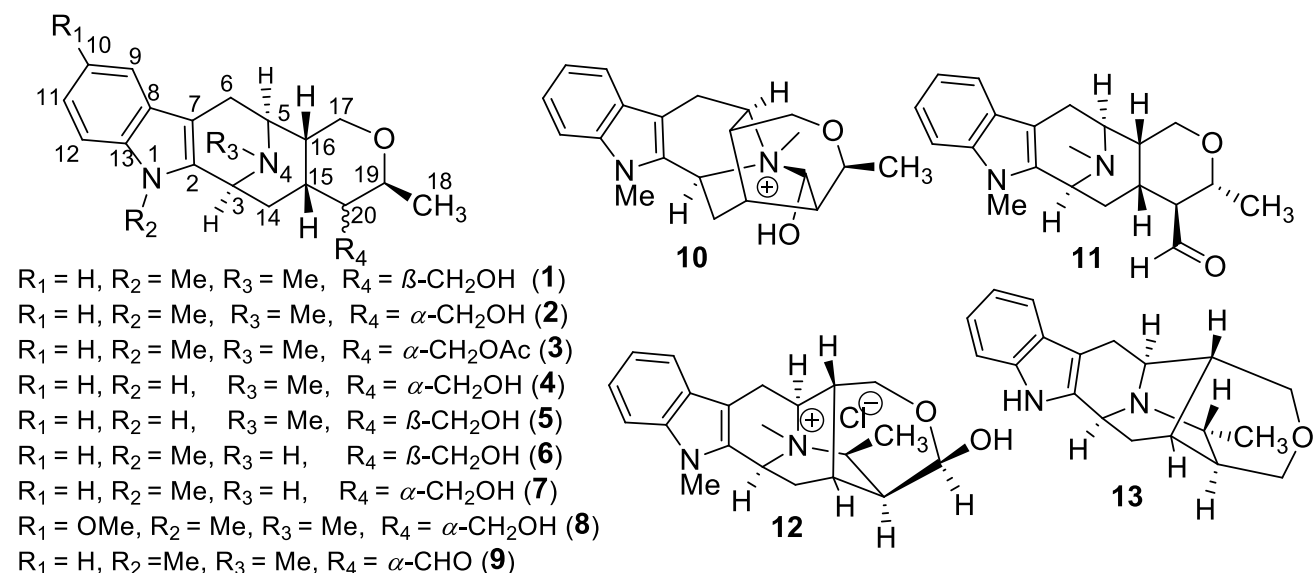


Figure 1: Examples of some C-19 methyl substituted sarpagine/macroline indole alkaloids

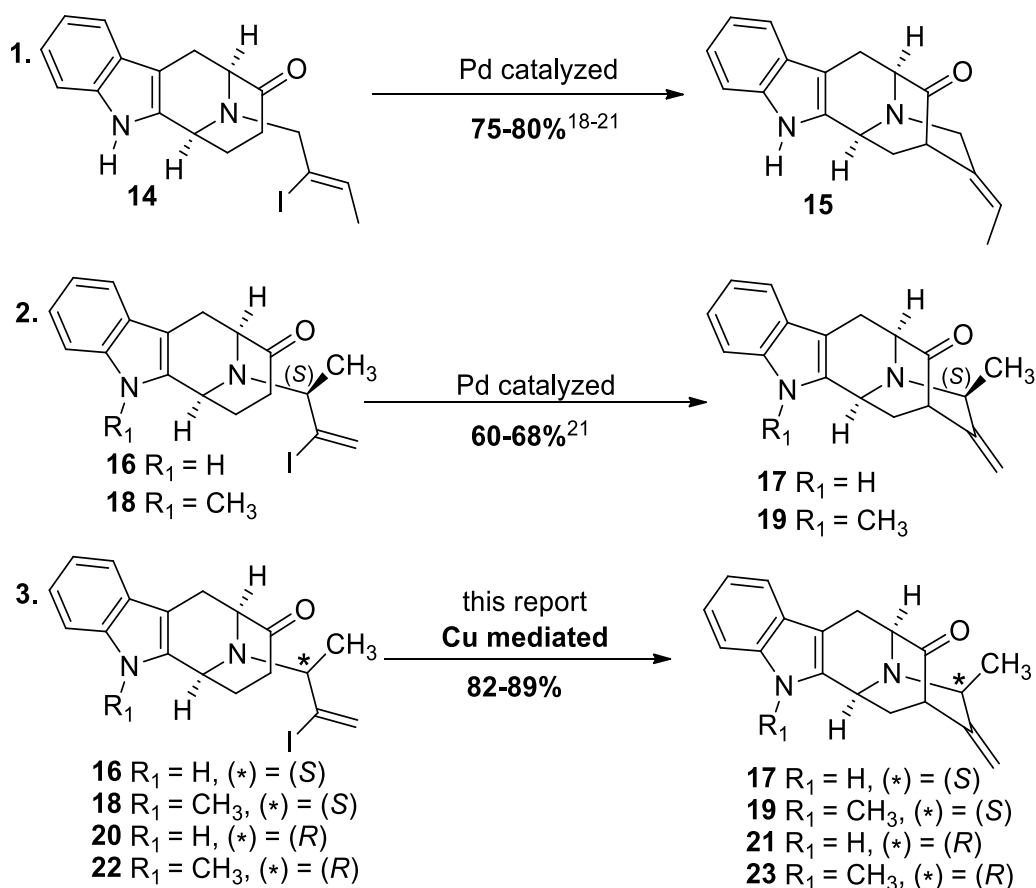
The copper-mediated carbon-carbon bond formation is more than a century old.¹⁵ Although palladium-catalyzed cross-coupling reactions have been the dominant method in the field of total synthesis of complex natural products, copper has proven itself to be an essential alternative, as indicated by the increase in copper-mediated cross-coupling processes over the last decade.¹⁶ As a result, it was decided to investigate a copper catalyzed, or mediated coupling process to offer a less expensive and less toxic alternative to catalytic palladium, while avoiding phosphine based ligands for easier purification. Moreover, potential improvements in yields, as well as workup and purification would be important.¹⁷

Wang et al.¹⁸ in Milwaukee developed an enolate driven palladium catalyzed α -vinylation of a ketone in 2000 (Scheme 1, entry 1). This process has been employed in the total synthesis of several sarpagine/macroline/ajmaline indole alkaloids.¹⁹⁻²¹ Although this palladium catalyzed process was effective in accessing the key intermediate **15** from vinyl iodide **14**, it provided only 60-68% yield in the case of vinyl iodides **16** or **18** (Scheme 1, entry 2), wherein there was a diastereomeric methyl function along with a terminal olefin in place of the ethylidene function in **14** (internal olefin, Wang, 2000). These features in **16** and **18** make them structurally and chemically different than **14**. Since the diastereomeric methyl function was essential for the synthesis of C-19 methyl substituted alkaloids, further improvement was required for better access to the key intermediates **17**, **19**, **21**, and **23**. More importantly, replacement of palladium with the cheaper and less toxic copper, would greatly facilitate use of this enolate-mediated process by others, and formed much of the driving force in this research.

2. Results and Discussion

The copper-catalyzed conditions²² that had been used for the α -vinylation of **14** gave lower yields along with an unusual, undesired product in the case of **22** (Scheme 3). Numerous attempts were made to optimize the desired yield of the olefin **23**, eliminate the unusual side product **23'** and understand the mechanism of multiple competing reactions. The implementation, improvement and extension of the scope of this process to access the C-19 methyl substituted sarpagine/macroline/ajmaline alkaloids with either an (*R*) or (*S*) C-19 methyl substituent in the N_a -H as well as N_a -CH₃ series (Scheme 1, entry 3) form the basis of this discussion.

Scheme 1: Regiospecific access to the pentacyclic core system via a palladium and copper-catalyzed cross-coupling process



All of the vinyl iodide intermediates (**16**, **18**, **20**, and **22**) were prepared according to the previously reported procedures²¹ (Scheme 2) beginning from the tetracyclic ketones **24/25** which had been prepared in the standard two pot process on 300 gram scale.²³ As depicted in Scheme 2, the *N*_b alkylation *via* S_N2 substitution of the chiral tosylates (**26/27**) in CH₃CN with K₂CO₃ and subsequent deprotection of the TIPS protecting group with wet TBAF in THF furnished the *N*_b-alkylated terminal alkynes (**28-31**) in excellent yields. Haloboration²¹ of the terminal alkynes with I-B(Cy)₂ in DCM followed by protodeboronation with HOAc, resulted in the vinyl iodides (**16**, **18**, **20**, and **22**) in 74-79% yield with complete regioselectivity. The structure and absolute configuration of **22** was confirmed by X-ray crystallography. An ORTEP representation of the crystal structure of **22** is shown in Figure 2 (see Appendix B for X-ray crystallographic data).

Initial experiments with vinyl iodide (**22**) and CuI under the reported conditions²² resulted in the desired product (**23**) in lower yields (~42%) along with an unusual/unexpected cyclization product (**23'**), a seven-membered ring with an internal alkene (Scheme 3).

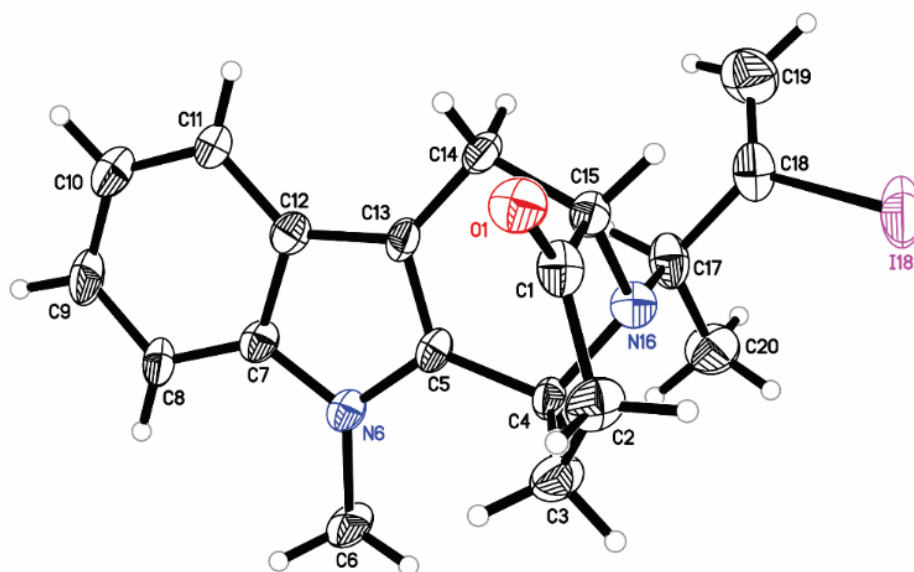


Figure 2. ORTEP representation of **22**

The structures of both the desired (**23**, Figure 3) and unexpected seven-membered ring (**23'**, Figure 4) cross-coupling products have been confirmed by MS, 1D and 2D NMR, and X-ray crystallographic analysis (see Appendix B for X-ray data). In the absence of CuI, the same conditions yielded the seven-membered product to a greater extent. Increasing the equivalents of CuI and ligand to 1.0 equivalent and the base to 4.0 equivalents (entry 3 of Table 1) resulted in a higher overall yield of the desired material (67%), while the unexpected product was still present (~21%).

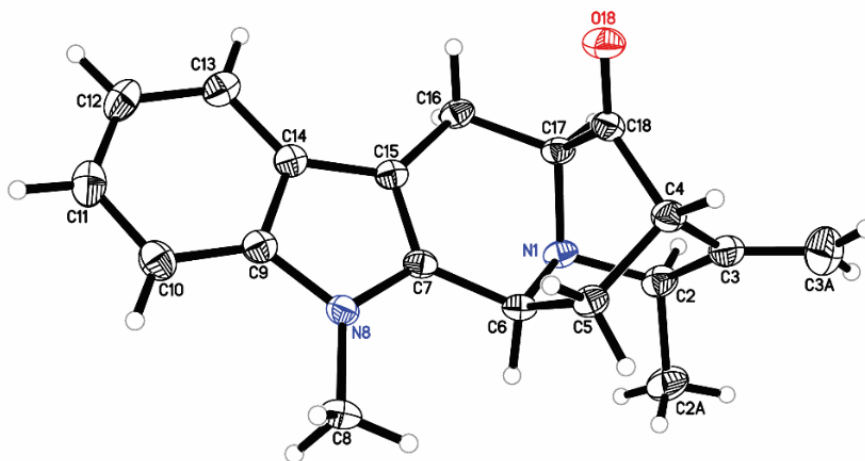


Figure 3. ORTEP representation of **23**

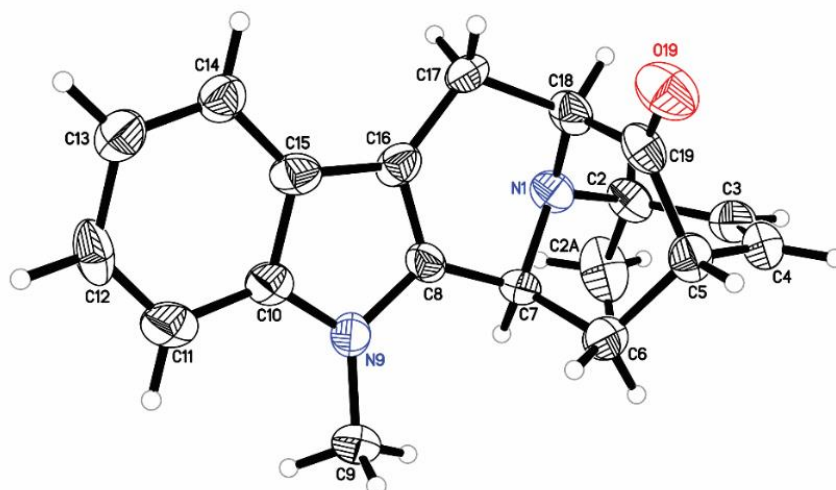
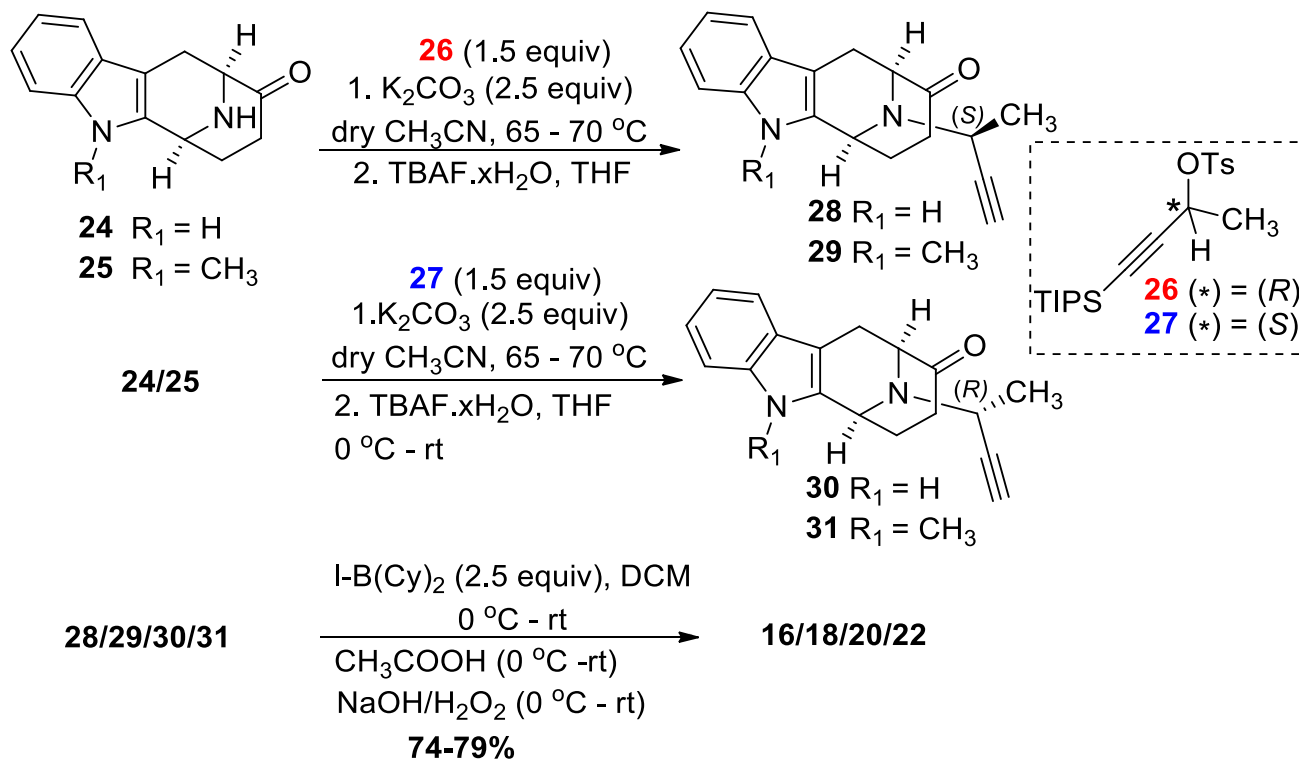
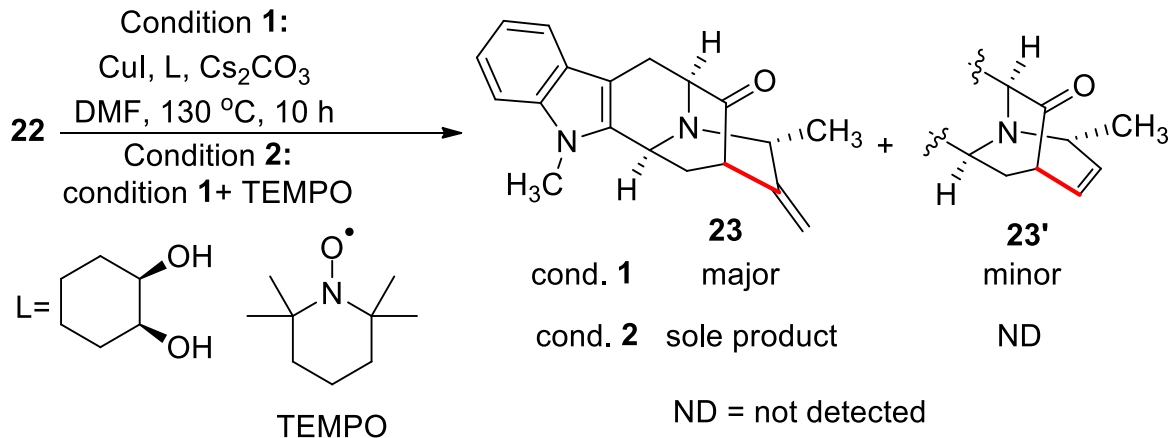


Figure 4. ORTEP representation of **23'**

Scheme 2: Completely Regioselective access to the vinyl iodides 16, 18, 20, and 22



Scheme 3: Enolate driven copper mediated cross-coupling of the vinyl iodide (**22**)



It was not surprising that this series of vinyl iodides (**16**, **18**, **20**, and **22**) would have different reactivities with copper iodide than vinyl iodides reported earlier.¹⁸ Differences in the substituents included the presence of a methyldiene (a terminal alkene) instead of the ethylidene in **14** (an internal alkene), as well as the presence of the chiral methyl function at C-19 instead of an achiral methylene. In order to rationalize this unprecedented seven-membered ring cyclization, it was felt that a radical mechanism may have been involved in its formation. To test this hypothesis, it was decided to use 2,2,6,6-tetramethylpiperidinyl-1-oxyl (TEMPO), the well-known radical scavenger²⁴, to inhibit any radical step or species that may have diverted the mechanism. In support of this hypothesis, an experiment with 2.5 equivalents of TEMPO (entry 5 of Table 1) resulted in almost complete inhibition of the formation of the undesired 7-membered internal alkene (~3% by NMR spectroscopy) with 45% overall yield of **23**. Increasing the amount of TEMPO to 3.0 equivalents completely eliminated the undesired cyclization (see the Experimental Section) and provided the desired cross-coupling product **23** in 66% yield. After many experiments were executed by changing reaction parameters and screening different copper sources (entries 8-15 of Table 1), the optimized condition was found to be 1.0 equiv of CuI, 1.0 equiv of ligand, 4.0 equiv

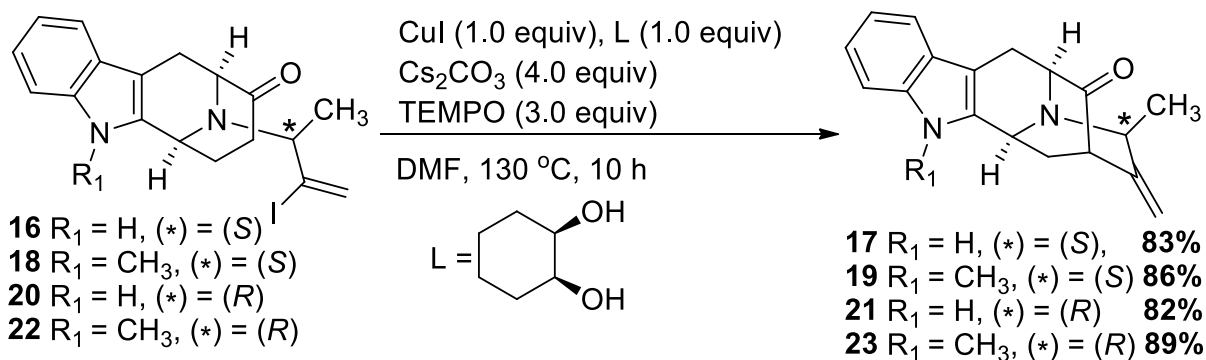
of Cs₂CO₃, and 3.0 equiv of TEMPO. This combination furnished 89% yield of the desired cross-coupled product to the exclusion of the 7-membered byproduct, as compared to (60-68%) with a palladium catalyst.^{21,25} This modified reaction condition was effective for both stereoisomers of the C-19 methyl substitution pattern and in both the *N*_a-H and *N*_a-CH₃ series (**16**, **18**, **20** and, **22**) as well. This permitted the application of this Cu-mediated cross-coupling process to access the key intermediates (**17**, **19**, **21**, and **23**) in gram-quantities toward all of the macroline/sarpagine alkaloids discussed above (Scheme 4). The structure and absolute stereochemistry of **19** was confirmed with X-ray crystallographic analysis (see Figures 5, see Appendix B for X-ray data). While TEMPO was initially chosen as a radical probe, the reason for its useful effect is still under investigation.

Table 1: Optimization of reaction conditions for the Cu-mediated cross-coupling reaction of 22

entry	CuI or cat.	L	Cs ₂ CO ₃	scv.	23:23' (by NMR) ^a	overall yield (%) ^b
1	0.5	0.5	2.0	-	89:11	47
2	-	0.5	2.0	-	63:37	45
3	1.0	1.0	4.0	-	79:21	67
4	-	-	2.0	-	64:36	35
5	0.5	0.5	2.0	2.5	97:3	45
6	0.5	0.5	2.0	3.0	100:0	66
7	1.0	1.0	4.0	3.0	100:0	89
8	0.1	0.1	4.0	3.0	100:0	25
9	0.5	0.5	4.0	3.0	100:0	40
10	1.0	-	4.0	3.0	100:0	11
11	1.0	1.0	-	3.0	-	ND ^c
12	-	1.0	4.0	3.0	-	ND
13	cat.-2 (1.0)	1.0	4.0	3.0	100:0	51
14	cat.-3 (1.0)	1.0	4.0	3.0	100:0	24
15	cat.-4 (1.0)	1.0	4.0	3.0	100:0	28

The unit for all reagent amounts is equivalent (equiv); scv. = TEMPO scavenger; [a] Ratio determined by ¹H NMR spectroscopy; [b] Overall isolated yield after flash chromatography on neutral alumina; [c] Starting material was recovered; ND = not detected; L= *cis*-1-2-cyclo-hexanediol; cat.-2 = Cu(CH₃CN)₄ClO₄; cat.-3 = Cu(CH₃CN)₄PF₆; cat.-4 = Cu(CH₃CN)₄OTf (see the Experimental Section for detailed procedures)

Scheme 4: Access to the key pentacyclic ketone intermediates 17, 19, 21, and 23 via the optimized conditions



Surprisingly, it was observed that the base Cs₂CO₃ alone in DMF (entry 2 of Table 1) yielded both of the products in an approximately 2 to 1 ratio but in poor yield. This observation indicated the possibility of another competing mechanism wherein the vinyl iodide (**22**) or intermediate underwent an E-2 like elimination or radical process to produce a terminal alkyne (**31**, *in situ*). This alkyne subsequently could undergo a 6-(*enolendo*)-*exo-dig* (process A in Scheme 5) which would produce the six-membered external alkene (**23**) as the major product and a 7-(*enolendo*)-*endo-dig* cyclization (process B in Scheme 5) to produce the seven-membered internal alkene (**23'**) as the minor product (Scheme 5). Both of these processes are allowed by Baldwin's rules for ring closure.^{26,27} This hypothesis has been confirmed by stopping the reaction (at 3 hours) before completion. The alkyne **31** was detected along with traces of the cross-coupling products **23** and **23'**.

The investigation of the competing mechanisms is now ongoing. However, gratifying, excellent yields (82-89%) of only the desired six-membered ring were obtained in a stereospecific fashion with copper iodide (Scheme 4).

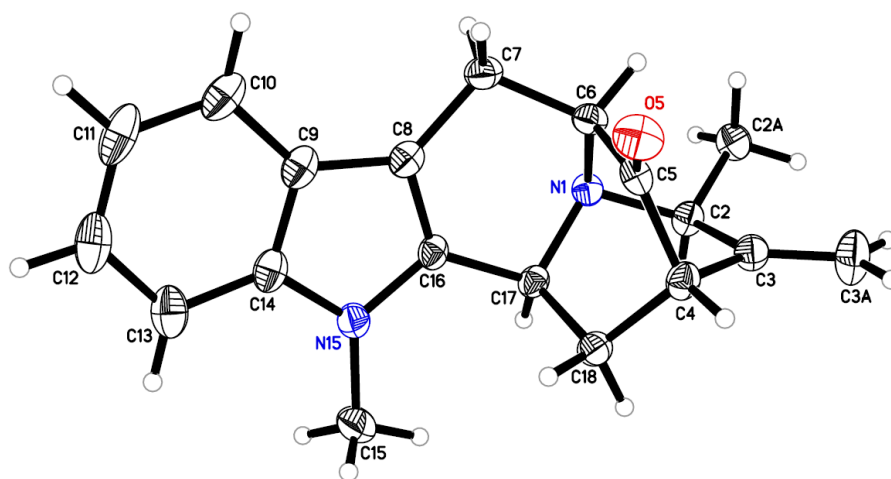
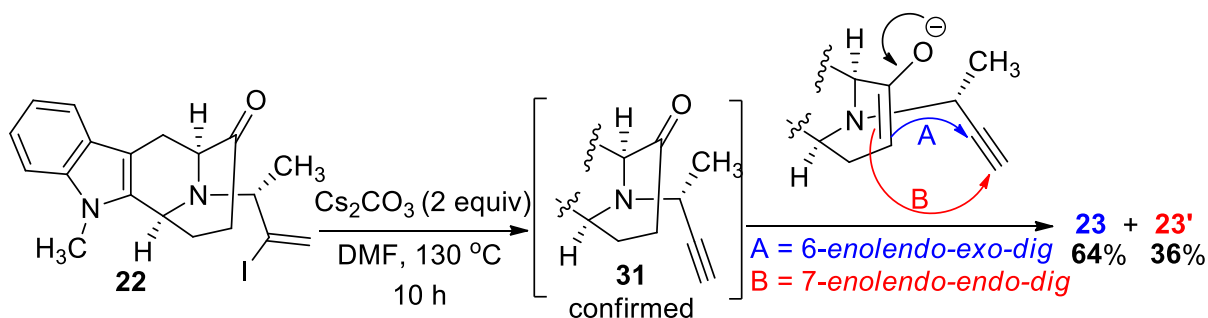
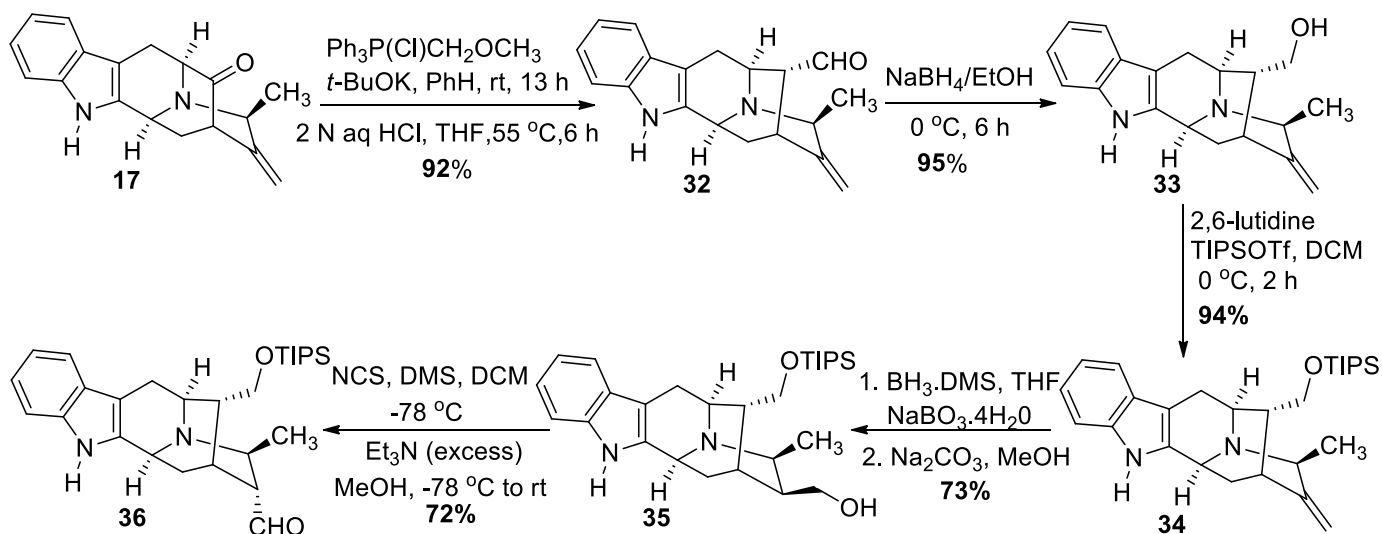


Figure 5. ORTEP representation of pentacyclic intermediate **19**

Scheme 5: Possible mechanism for the observed base mediated cyclization (Table 1, entries 2 and 4)



Scheme 6: Toward macrocarpines D (4) and E (5) from the key intermediate 17

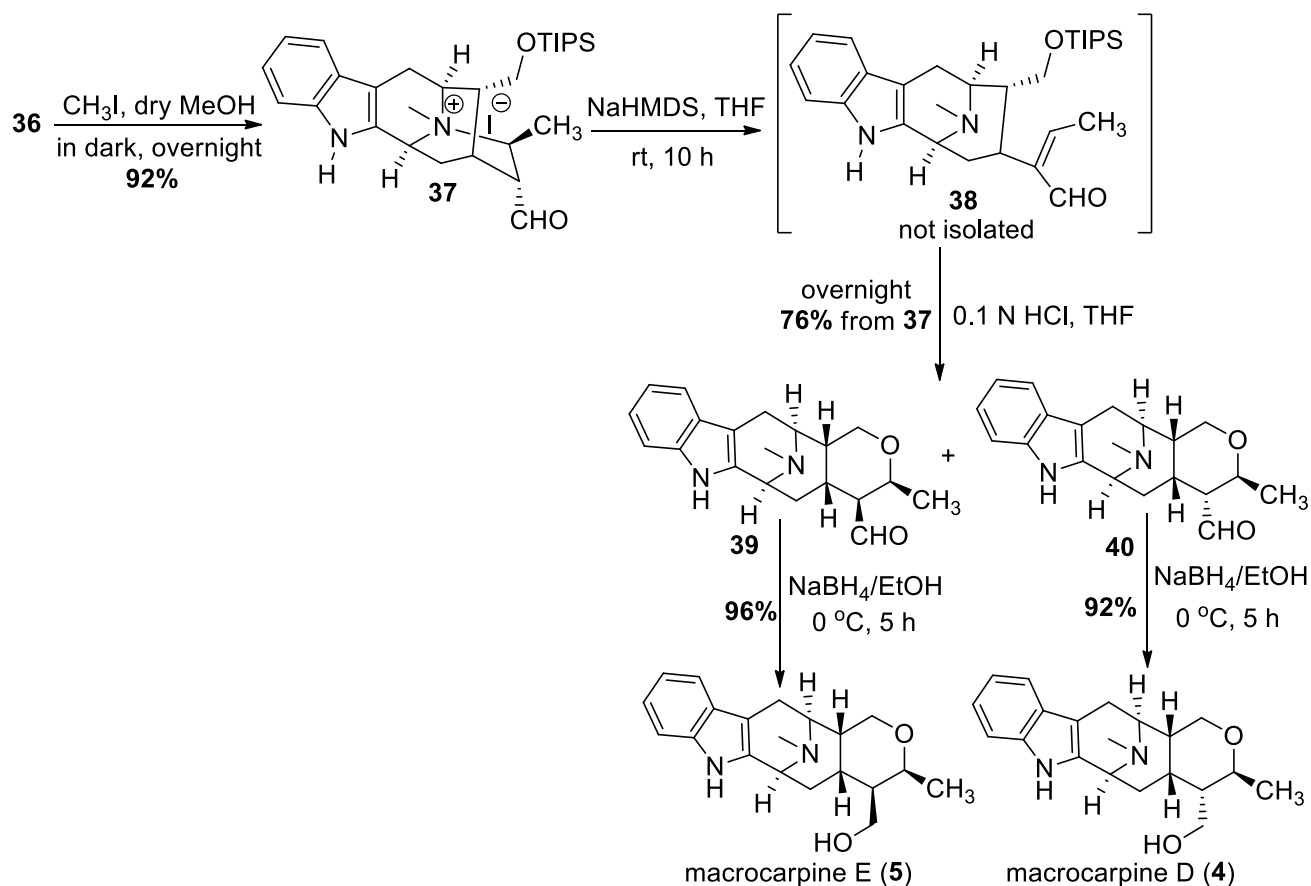


With the pentacyclic ketones in hand in excellent yields, the total synthesis of a series of C-19 methyl substituted sarpagine macroline indole alkaloids was undertaken. This included the potent anticancer alkaloid, *N*(4)-methyltalpinine (**10**), as well as the leishmanicidal base (**9**), macrocarpines A-G (**1-7**), and deoxyperaksine (**13**). Herein is reported the first total synthesis of the $N_a\text{-H}$ bearing macroline indole alkaloids macrocarpine D (**4**) and E (**5**) (Schemes 6 and 7).

The pentacyclic ketone (**17**) was subjected to a one-carbon homologation *via* a Wittig olefination process using methoxymethyl triphenylphosphonium chloride and potassium *tert*-butoxide in

benzene to furnish the enol ether, which was hydrolyzed without purification to aldehyde (**32**) under acidic conditions (Scheme 6). The aldehyde was isolated in the more stable α position even in the presence of the C-19 β -methyl group. The aldehyde (**32**) was reduced to alcohol (**33**) with sodium borohydride in ethanol and subsequently protected with a TIPS group to give the silyl ether (**34**). The alkene (**34**) was subjected to hydroboration (borane dimethyl sulfide) and Kabalka oxidation (NaBO_3) to provide the primary alcohol (**35**) in 73% yield. The oxidation of the primary alcohol under Corey-Kim conditions at -78°C produced a mixture of α and β -aldehydes with the α isomer as the major

Scheme 7: Total synthesis of macrocarpines D (4) and E (5)



product. This mixture was epimerized entirely to the α -aldehyde (**36**) with Et₃N in methanol added to the mixture.

Quaternization of the N_b-group with iodomethane in methanol gave the iodide salt (**37**, Scheme 7). The quaternary ammonium salt underwent a *retro*-Michael ring opening in the presence of NaHMDS in THF to produce the α,β -unsaturated aldehyde (**38**) in 78% yield similar to the work first reported by LeQuesne.⁵

The TIPS group was removed by heating **38** under mildly acidic conditions in THF. The so formed alcohol added in a Michael fashion to the α,β -unsaturated aldehyde to produce (**39**) and (**40**) as an epimeric mixture of aldehydes with the β -methyl group formed stereospecifically. Each of these could be isolated by silica gel flash chromatography. The desired aldehydes (**39**) and (**40**) upon reduction (individually) with sodium borohydride in ethanol gave macrocarpine E (**5**) and macrocarpine D (**4**) in 96% and 92% yield, respectively. The spectroscopic data and optical rotations of the synthetic products are in complete agreement with natural macrocarpine D & E. The total synthesis of other alkaloids of interest in the series will be presented in the next chapters.

3. Conclusion

In summary, the first total synthesis of macrocarpines D (**4**) and E (**5**) have been accomplished *via* a key copper-mediated cross-coupling process toward the important key intermediates. This general strategy will enable one to access all of the indole alkaloids of the same class with stereospecific incorporation of the important β (or α)-methyl function at C-19. Replacement of the palladium catalyst with CuI provides a much more useful and cheaper method since the copper catalyst, even at stoichiometric amounts, is much cheaper than catalytic palladium. More

importantly, accessing **17** in 83% yield with copper iodide compared to 60% with catalytic palladium serves as an example of replacement of palladium in this enolate-mediated process which makes it much more useful for others, especially in the pharmaceutical industry.

4. Experimental Section

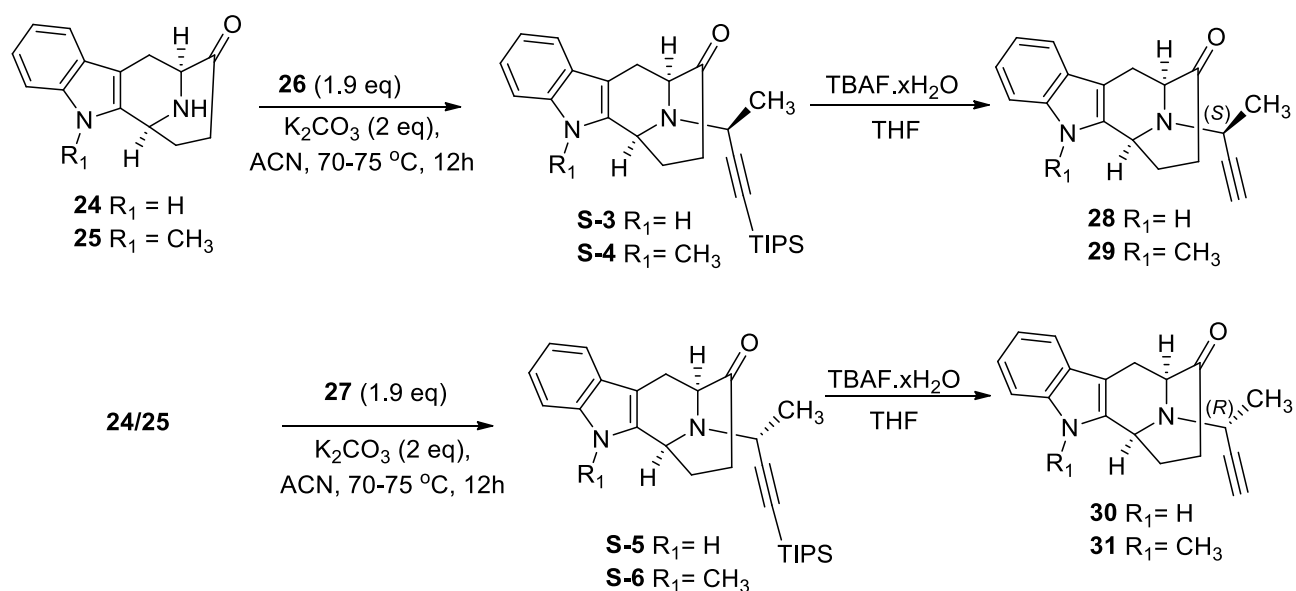
General Information

All reactions were carried out under an argon atmosphere with dry solvents using anhydrous conditions unless otherwise stated. Tetrahydrofuran (THF) and diethyl ether were freshly distilled from Na/benzophenone ketyl prior to use. Dichloromethane was distilled from calcium hydride prior to use. Methanol was distilled over magnesium sulfate. Benzene and toluene were distilled over Na. Acetonitrile was distilled over CaH₂ prior to use. Reagents were purchased of the highest commercial quality and used without further purification unless otherwise stated. Thin layer chromatography (TLC) was performed on UV active silica gel, 200 μm, or aluminum backed and UV active alumina N, 200 μm, or F-254 aluminum backed. Flash and gravity chromatography were performed using silica gel P60A, 40-63 μm, or basic alumina (Act I, 50-200 μm) or neutral alumina (Brockman I, ~150 mesh). The TLC plates were visualized by exposure to short wavelength UV light (254 nm). Indoles were visualized with a 1% solution of ceric ammonium nitrate in 50% phosphoric acid. The ¹H NMR data are reported as follows: chemical shift, multiplicity (brs = broad singlet, s = singlet, d = doublet, t = triplet, q = quartet, quin = quintet, dd = doublet of doublet, dt = doublet of triplet, ddd = doublet of doublet of doublets, td = triplet of doublets, qd = quartet of doublets, m = multiplet), integration, and coupling constants (Hz). The

^{13}C NMR data are reported in parts per million (ppm) on the δ scale. The low resolution mass spectra (LRMS) were obtained as electron impact (EI, 70eV) and as chemical ionization (CI) using a magnetic sector (EBE) analyzer. The HRMS were recorded by electrospray ionization (ESI) using a TOF analyzer, electron impact (EI) using a trisector analyzer and Atmospheric Pressure Chemical Ionization (APCI) using a TOF analyzer.

Experimental Procedures and Analytical Data

General Procedure for Preparation of 28-31²



An oven dried 1 L flask cooled under argon was charged with optically active Na-H , $N_b\text{-H}$ tetracyclic ketone **24** or Na-CH_3 , $N_b\text{-H}$ tetracyclic ketone **25** (15.0 g, 0.062 mol). The solid **24/25** was dissolved (individually) in freshly distilled acetonitrile (1000 mL), after which a solution of (*R*)-4-triisopropylsilyl-3-butyn-2-ol tosylate **26** (47.57 g, 0.116 mol) in dry acetonitrile (50 mL) was added. Anhydrous potassium carbonate (17.27 g, 0.125 mol) was added and the mixture, which resulted, was allowed to heat and stirred at 75 °C (outside oil bath temperature) for 12 h

under argon. Analysis by TLC (silica gel, CHCl₃/EtOH, 9 : 1) indicated the absence of tetracyclic ketone **24/25**, respectively, after 12 h. The reaction mixture was cooled to rt and the K₂CO₃ was filtered off by passing the solution through a bed of celite using EtOAc as the eluent. After removal of the solvent under reduced pressure, the crude product was purified by flash chromatography (silica gel, EtOAc/hexanes) to provide the (*S*)-*Na*-H, TIPS protected acetylenic tetracyclic ketone **S-3/** (*S*)-*Na*-CH₃, or the TIPS protected acetylenic tetracyclic ketone **S-4** as a light yellow colored solid. The compound was purified by silica gel flash column chromatography using 10-20% EtOAc in hexane. By following the same procedure with **24/25** (individually) and (*S*)-4-triisopropylsilyl-3-butyn-2-ol tosylate **27**, this process resulted in (*R*)-*Na*-H, TIPS protected acetylenic tetracyclic ketone **S-5/** (*R*)-*Na*-CH₃, or the TIPS protected acetylenic tetracyclic ketone **S-6**, respectively. Trace amounts of the other diastereomers were detected in both cases, which was due to the ~95% ee of the tosylates **26** and **27**.

A solution of **S-3/S-4/S-5/S-6** in THF (1 mmol) was cooled (individually) to 0 °C and TBAF·xH₂O (1.5 mmol, 1M soln in THF) was added dropwise to the above solution. The solution, which resulted, was stirred at 0 °C for 30 min. After that the ice bath was removed and the solution was allowed to stir at rt for 2h-3h. At that time analysis by TLC (silica gel) indicated the disappearance of the starting material. The reaction solution was then quenched with H₂O (30 mL) at rt, followed by dilution with EtOAc (80 mL). The two layers were separated. The organic layer was washed with water, brine and dried (Na₂SO₄). The EtOAc was removed under reduced pressure and the residue was passed through a small pad of silica gel to give **28/29/30/31**, respectively, as off white/yellowish solids.

(6S,10S)-12-((S)-But-3-yn-2-yl)-7,8,10,11-tetrahydro-5H-6,10-epiminocycloocta[b]indol-9(6H)-one (28)

¹H NMR (300 MHz, CDCl₃) δ 8.00 (brs, 1H), 7.48 (d, 1H, *J* = 7.6 Hz), 7.35 (d, 1H, *J* = 7.8 Hz), 7.11-7.23 (m, 2H), 4.67 (d, 1H, *J* = 3.2 Hz), 3.97 (d, 1H, *J* = 6.4 Hz), 3.66 (qd, 1H, *J* = 6.7 Hz, 2.1 Hz), 3.15 (dd, 1H, *J* = 16.7, 6.5 Hz), 2.73 (d, 1H, *J* = 16.6 Hz), 2.45-2.63 (m, 2H), 2.28 (d, 1H, *J* = 2.1 Hz), 2.04-2.18 (m, 2H), 1.47 (d, 3H, *J* = 6.7 Hz). All other spectroscopic data were identical to the published data for **28**.³ The material was used for the next step without further characterization.

(6S,10S)-12-((S)-But-3-yn-2-yl)-5-methyl-7,8,10,11-tetrahydro-5H-6,10-epiminocycloocta[b]indol-9(6H)-one (29)

¹H NMR (300 MHz, CDCl₃) δ 7.46 (d, 1H, *J* = 7.7 Hz), 7.31 (d, 1H, *J* = 8.1 Hz), 7.19-7.25 (m, 1H), 7.08-7.13 (m, 1H), 4.75 (d, 1H, *J* = 3.1 Hz), 3.95 (d, 1H, *J* = 6.6 Hz), 3.70 (s, 3H), 3.61 (qd, 1H, *J* = 6.6 Hz, 2.1 Hz), 3.13 (dd, 1H, *J* = 16.8, 6.7 Hz), 2.70 (d, 1H, *J* = 16.8 Hz), 2.56-2.65 (m, 1H), 2.44-2.52 (m, 1H), 2.28 (d, 1H, *J* = 2.2 Hz), 2.10-2.18 (m, 1H), 1.99-2.07 (m, 1H), 1.45 (d, 3H, *J* = 6.7 Hz). All other spectroscopic data were identical to the published data for **29**.² The material was used for the next step without further characterization.

(6S,10S)-12-((R)-But-3-yn-2-yl)-7,8,10,11-tetrahydro-5H-6,10-epiminocycloocta[b]indol-9(6H)-one (30)

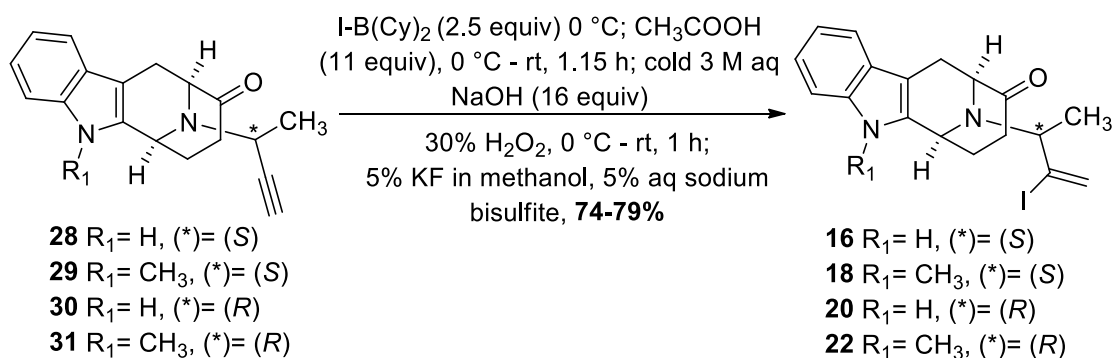
¹H NMR (300 MHz, CDCl₃) δ 7.90 (brs, 1H), 7.48 (dd, 1H, *J* = 7.7, 0.5 Hz), 7.36 (d, 1H, *J* = 8.0 Hz), 7.11-7.23 (m, 2H), 4.37-4.41 (m, 1H), 4.35 (d, 1H, *J* = 6.6 Hz), 3.68 (qd, 1H, *J* = 6.5, 2.1 Hz), 3.30 (dd, 1H, *J* = 16.9, 6.7 Hz), 2.72 (d, 1H, *J* = 16.9 Hz), 2.44 - 2.57 (m, 2H), 2.33-2.34 (m, 1H), 2.05 - 2.21 (m,

2H), 1.47 (d, 3H, $J = 6.5$ Hz); ^{13}C NMR (75 MHz, CDCl_3) δ 210.4 (C), 135.9 (C), 131.6(C), 126.8 (C), 122.2 (CH), 119.8 (CH), 118.3 (CH), 110.9 (CH), 107.8 (C), 83.9 (C), 72.7 (CH), 63.3 (CH), 48.0 (CH), 46.3 (CH), 34.5 (CH_2), 30.1 (CH_2), 21.5 (CH_2), 20.6 (CH_3); HRMS (ESI) m/z ($\text{M} + \text{H}$) $^+$ calcd for $\text{C}_{18}\text{H}_{19}\text{N}_2\text{O}$, 279.1492, found 279.1498.

(6S,10S)-12-((R)-But-3-yn-2-yl)-5-methyl-7,8,10,11-tetrahydro-5H-6,10-epiminocycloocta[b]indol-9(6H)-one (31)

^1H NMR (300 MHz, CDCl_3) δ 7.54 (d, 1H, $J = 7.7$ Hz), 7.37 (d, 1H, $J = 8.1$ Hz), 7.28 (t, 1H, $J = 7.5$ Hz), 7.17 (t, 1H, $J = 7.3$ Hz), 4.49 (brs, 1H), 4.41 (d, 1H, $J = 6.6$ Hz), 3.74 (s, 3H), 3.65-3.71 (m, 1H), 3.35 (dd, 1H, $J = 16.9, 6.8$ Hz), 2.76 (d, 1H, $J = 16.9$ Hz), 2.48 - 2.65 (m, 2H), 2.40 (d, 1H, $J = 1.9$ Hz), 2.05 - 2.22 (m, 2H), 1.52 (d, 3H, $J = 6.5$ Hz); ^{13}C NMR (75 MHz, CDCl_3) δ 210.1 (C), 137.3 (C), 132.8(C), 126.4 (C), 121.7 (CH), 119.4 (CH), 118.3 (CH), 109.0 (CH), 106.7 (C), 84.0 (C), 72.8 (CH), 63.3 (CH), 46.7 (CH), 46.3 (CH), 34.4 (CH_2), 29.5 (CH_2), 29.4 (CH_3), 21.5 (CH_2), 20.7 (CH_3); HRMS (ESI) m/z ($\text{M} + \text{H}$) $^+$ calcd for $\text{C}_{19}\text{H}_{21}\text{N}_2\text{O}$, 293.1492, found 293.1498.

General procedure for the preparation of 16, 18, 20, 22 (individually) via regioselective haloboration^{2,3}



An oven dried flask was fitted with an addition funnel and was cooled under argon. The flask was charged either with **28/29/30/31** (2.10 g, 7.55 mmol) dissolved (individually) in freshly distilled

CH₂Cl₂ (52.5 mL) and hexanes (7.0 mL). The flask was cooled to 0 °C with ice and I-B(Cy)₂ (30.2 mL, 15.1 mmol, 0.5 M solution in hexanes) was added dropwise every 0.5 h in three portions, over a total period of 1.5 h. After the last addition the reaction mixture was allowed to stir at 0 °C for another 0.5 h, after which the ice bath was removed and the mixture was stirred at rt for 2.0 h. After stirring at rt for 2.0 h, another 0.5 eq of I-B(Cy)₂ (7.6 mL, 3.78 mmol) was added dropwise at rt and the mixture was allowed to stir for another 2.0 h. After this 2.0 h, the mixture was treated with glacial acetic acid (4.8 mL, 83.1 mmol) at 0 °C and stirred at rt for 1.15 h. At this point the flask was again cooled to 0 °C and a solution of cold aq 3 M NaOH (40.3 mL, 121 mmol) and 30% H₂O₂ (2.6 mL, 23 mmol) were added and the stirring was maintained for 1.0 h at rt. The biphasic solution, which resulted, was transferred to a bigger flask, diluted with CH₂Cl₂ (400 mL) and water (50 mL), after which the two layers were separated. The original reaction flask still had some residual solid attached to the bottom of the flask. The solid was dissolved in acetone (50 mL). The acetone was evaporated under reduced pressure to 75% of the original volume and the mixture was diluted with CH₂Cl₂ (50 mL). Again, the two layers were separated and the combined CH₂Cl₂ layers were treated with solutions of 5% KF in methanol (160 mL) and 5% aq sodium bisulfite (160 mL) under vigorous stirring for 5 min. The aq layer was separated, extracted with CH₂Cl₂ (2 x 80 mL), after which the combined organic layers were washed with brine, dried (Na₂SO₄), filtered and concentrated under reduced pressure. Purification by chromatography on silica gel (ethyl acetate/hexanes, 1 : 4) afforded vinyl iodides **16** (74%) or **18** (77%) or **20** (76%) or **22** (79%), respectively, as white solids.

(6S,10S)-12-((S)-3-Iodobut-3-en-2-yl)-7,8,10,11-tetrahydro-5H-6,10-epiminocycloocta-[b]indol-9(6H)-one (16)

¹H NMR (300 MHz, CDCl₃): δ 7.83 (brs), 7.50 (d, 1H, *J* = 7.6 Hz), 7.36 (d, 1H, *J* = 7.8 Hz), 7.12-7.24 (m, 2H), 6.26 (s, 1H), 5.87 (s, 1H), 4.21 (brs, 1H), 4.02 (d, 1H, *J* = 6.2 Hz), 3.12 (dd, 1H, *J* = 16.8, 6.2 Hz), 2.79 (d, 1H, *J* = 16.8 Hz), 2.66-2.72 (m, 1H), 2.50-2.61 (m, 2H), 2.01-2.20 (m, 2H), 1.21 (d, 3H, *J* = 6.2Hz), All other spectroscopic data were identical with the published data for **16**.³ This material was used for the next step without further characterization.

(6S,10S)-12-((S)-3-Iodobut-3-en-2-yl)-5-methyl-7,8,10,11-tetrahydro-5H-6,10-epiminocycloocta[b]indol-9(6H)-one (18)

¹³C NMR (75 MHz, CDCl₃): δ 210.2, 137.1, 133.0, 126.4, 125.8, 122.6, 121.6, 119.3, 118.2, 108.9, 106.6, 62.3, 60.7, 47.6, 34.4, 29.7, 29.3, 21.2, 19.7. All other spectroscopic data were identical with the published data for **18**.² This material was used for the next step without further characterization.

(6S,10S)-12-((R)-3-Iodobut-3-en-2-yl)-7,8,10,11-tetrahydro-5H-6,10-epiminocycloocta[b]indol-9(6H)-one (20)

¹H NMR (300 MHz, CDCl₃) δ 7.98 (brs, 1H), 7.50 (d, 1H, *J* = 7.6 Hz), 7.37 (d, 1H, *J* = 7.9 Hz), 7.13-7.28 (m, 2H), 6.39 (s, 1H) 5.91 (s, 1H), 4.36-4.40 (m, 1H), 3.86 (d, 1H, *J* = 6.5 Hz), 3.17 (dd, 1H, *J* = 17.0, 6.6 Hz), 2.65-2.71 (m, 2H), 2.50-2.60 (m, 2H), 2.04-2.20 (m, 2H), 1.17 (d, 3H, *J* = 6.1 Hz); **¹³C NMR** (75 MHz, CDCl₃) δ 210.4 (C), 135.8 (C), 132.8 (C), 126.9 (C), 126.2 (CH₂), 122.2 (C), 121.1 (CH), 119.8 (CH), 118.2 (CH), 111.0 (CH), 107.6 (C), 62.3 (CH), 61.7 (CH), 46.5 (CH), 34.5 (CH₂), 30.8 (CH₂), 20.7 (CH₂), 19.8 (CH₃); **HRMS** (ESI) *m/z* (M + H)⁺ calcd for C₁₈H₂₀IN₂O 407.0615, found 407.0617

(6S,10S)-12-((R)-3-Iodobut-3-en-2-yl)-5-methyl-7,8,10,11-tetrahydro-5H-6,10-epiminocycloocta[b]indol-9(6H)-one (22)

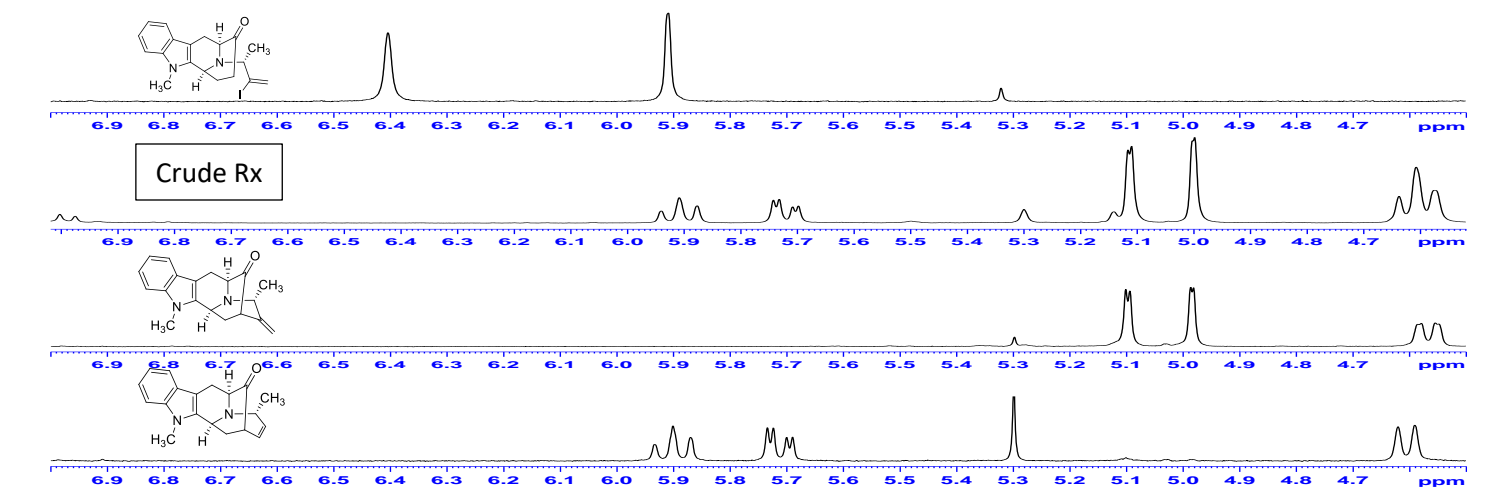
¹H NMR (300 MHz, CDCl₃) δ 7.51 (d, 1H, *J* = 7.7 Hz), 7.35 (d, 1H, *J* = 8.0 Hz), 7.25 (d, 1H, *J* = 8.0 Hz) 7.12-7.17 (m, 1H), 6.40 (s, 1H), 5.91 (s, 1H), 4.43-4.47 (m, 1H), 3.86 (d, 1H, *J* = 6.7 Hz), 3.71 (s, 3H), 3.18 (dd, 1H, *J* = 17.1, 6.8 Hz), 2.52-2.71 (m, 4H), 2.01 – 2.22 (m, 2H), 1.17 (d, 3H, *J* = 6.1 Hz); **¹³C NMR** (75 MHz, CDCl₃) δ 209.9 (C), 137.1 (C), 133.8 (C), 126.4 (C), 126.1 (CH₂), 121.7 (C), 121.0 (CH), 119.4 (CH), 118.2 (CH), 108.9 (CH), 106.6 (C), 62.1 (CH), 61.6 (CH), 45.2 (CH), 34.3 (CH₂), 30.2 (CH₂), 29.3 (CH₃), 20.7 (CH₂), 19.8 (CH₃); **EIMS HRMS** (ESI) *m/z* (M + H)⁺ calcd for C₁₉H₂₂IN₂O, 421.0777, found 421.0789.

General procedure for copper-mediated cross-coupling reaction (preparation of 17/19/21/23, individually)

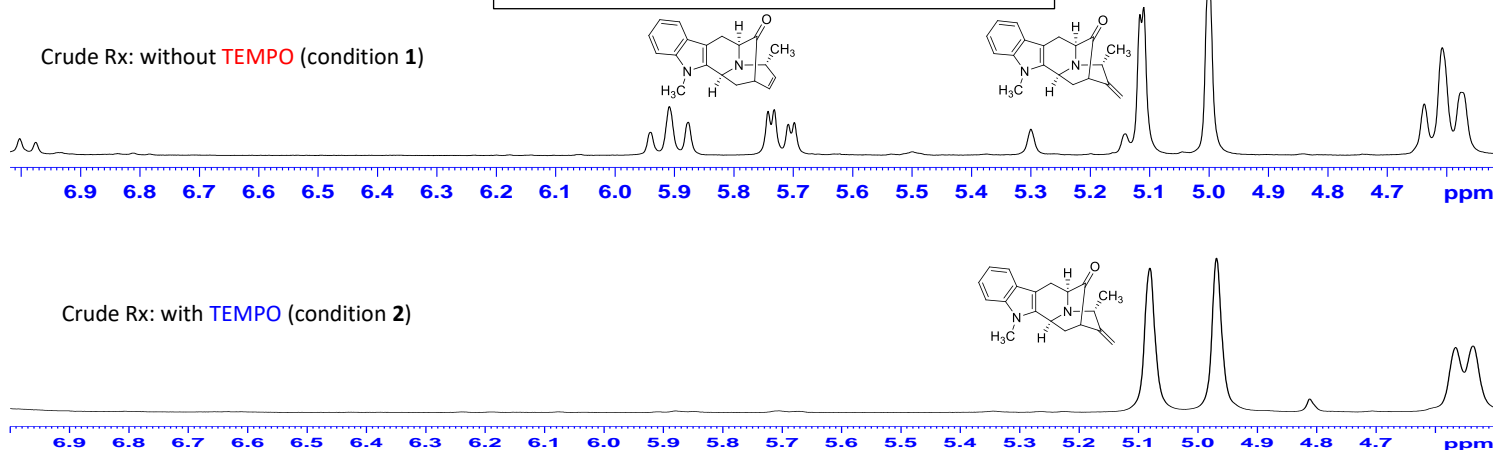
Condition 1 (Table 1, entries 1-4): In a sealed tube with a magnetic stir bar, a mixture of vinyl iodide **22** (1.0 mmol), CuI (0.5 -1.0 equiv), *cis*-1,2- cyclohexanediol (0.5 – 1.0 equiv), and Cs₂CO₃ (2.0 - 4.0 mmol) was added dry DMF (2.0 mL). The mixture was degassed under reduced pressure at rt and refilled with argon (3-4 times). The reaction mixture was then placed on a pre-heated oil bath (130 °C) and heated under argon for 10 h. At this point TLC (silica gel, EtOAc/hexane = 1:3) indicated the absence of starting material **22**. The mixture was cooled to rt and diluted with EtOAc (10 mL) and water. The aqueous layer was separated and extracted with EtOAc (2 x 10 mL). The combined organic layers were washed with water (2 x 50 mL) and brine (3 x 50 mL) and dried (Na₂SO₄). The solvent was removed under reduced pressure and the residue was purified by chromatography on neutral alumina (EtOAc/hexane = 1:3) to provide the cross-coupling products **23** (22-53%) and **23'** (5-17%). Pentacyclic ketones **22**, **23**, and **23'** (individually) gave colorless crystals from DCM, EtOAc and CHCl₃, respectively, and they were used for X-ray analysis (for X-ray data see Appendix B).

Condition 2: In a sealed tube with a magnetic stir bar, a mixture of vinyl iodide **16/18/20/22** (individually, 1.0 mmol), CuI or catalyst (0.1 – 1.0 equiv), *cis*-1,2- cyclohexanediol (0.1 – 1.0 equiv), and Cs₂CO₃ (0 - 4.0 equiv) and TEMPO (2.5- 3.0 equiv) was added dry DMF (2.0 mL). The mixture was degassed under reduced pressure at rt and refilled with argon (3-4 times). The reaction mixtures (individually) were then placed on a pre-heated oil bath (130 °C) and heated under argon for 10 h. At this point TLC (silica gel, EtOAc/hexane = 1:3) indicated the absence of starting material **16/18/20/22**. The mixture was cooled to rt and diluted with EtOAc (10 mL) and water. The aq layer was separated and extracted with EtOAc (2 x 10 mL). The combined organic layers were washed with water (2 x 50 mL), brine (3 x 50 mL) and dried (Na₂SO₄). The solvent was removed under reduced pressure and the residue was purified by chromatography on neutral alumina (EtOAc/hexane = 1:3) to provide the cross-coupling products **17** (83%) /**19** (86%) /**21** (82%) /**23** (24-89%), individually. Compound **19** gave colorless crystals from EtOAc and was used for X-ray analysis (for X-ray data see Appendix B).

Cross-coupling of **22** under condition 1: $^1\text{H NMR } \delta 4.5\text{--}7.0 \text{ ppm}$



Comparison between conditions 1 and 2



(6*S*,8*S*,11*aS*)-8-Methyl-9-methylene-6,8,9,10,11*a*,12-hexahydro-6,10-methanoindolo[3,2-*b*]quinolizin-11(5*H*)-one (17)

$^1\text{H NMR}$ (300 MHz, CDCl_3): δ 7.76 (brs, 1H), 7.50 (d, 1H, $J = 7.5 \text{ Hz}$), 7.27-7.29 (m, 1H), 7.10-7.19 (m, 2H), 5.12 (d, 1H, $J = 2.5 \text{ Hz}$), 5.01 (d, 1H, $J = 2.5 \text{ Hz}$), 4.31-4.35 (m, 1H), 3.81-3.90 (m, 1H), 3.74 (d, 1H, $J = 5.6 \text{ Hz}$), 3.34 (dd, 1H, $J = 15.6, 1.2 \text{ Hz}$), 3.06-3.10 (dd, 1H, $J = 3.6, 1.9 \text{ Hz}$), 2.93 (dd, 1H, $J = 15.6, 6.1 \text{ Hz}$), (2.51-2.60 (m, 1H), 2.16-2.23 (m, 1H), 1.50 (d, 3H, $J = 6.8 \text{ Hz}$)).

All other spectroscopic data were identical with the published data for **17**.²⁵ This material was used for the next step without further characterization.

(6*S*,8*S*,11*aS*)-5,8-Dimethyl-9-methylene-6,8,9,10,11*a*,12-hexahydro-6,10-methanoindolo[3,2-*b*]quinolizin-11(5*H*)-one (19)

¹H NMR (300 MHz, CDCl₃): δ 7.50 (d, 1H, *J* = 7.4 Hz), 7.24-7.26 (m, 1H), 7.18 (td, 1H, *J* = 7.5, 0.9 Hz), 7.05-7.10 (m, 1H), 5.1 (d, 1H, *J* = 2.5 Hz), 5.01 (d, 1H, *J* = 2.5 Hz), 4.41 (dd, 1H, *J* = 9.5, 2.1 Hz), 3.87-3.95 (m, 1H), 3.72 (d, 1H, *J* = 5.6 Hz), 3.6 (s, 3H), 3.34 (dd, 1H, *J* = 15.6, 1.3 Hz), 3.05-3.07 (m, 1H), 2.92 (dd, 1H, *J* = 15.6, 6.1 Hz), 2.57-2.65 (m, 1H), 2.10-2.17 (m, 1H), 1.49 (d, 3H, *J* = 6.7 Hz). All other spectroscopic data were identical with the published data for **19**.²¹ This material was used for the next step without further characterization.

(6*S*,8*S*,11*aS*)-8-Methyl-9-methylene-6,8,9,10,11*a*,12-hexahydro-6,10-methanoindolo[3,2-*b*]quinolizin-11(5*H*)-one (21)

¹H NMR (300 MHz, MeOD): δ 7.42 (d, 1H, *J* = 7.7 Hz), 7.29 (d, 1H, *J* = 8.0 Hz), 7.06-7.11 (m, 1H), 6.98-7.03 (m, 1H), 5.14 (d, 1H, *J* = 2.2 Hz), 5.06 (d, 1H, *J* = 1.6 Hz), 4.57-4.61 (m, 1H), 3.99-4.06 (m, 1H), 3.71 (d, 1H, *J* = 6.0 Hz), 3.25-3.34 (m, 1H, merged with solvent), 2.98-3.05 (m, 2H), 2.56-2.64 (m, 1H), 2.09-2.16 (m, 1H), 1.66 (d, 3H, *J* = 7.1 Hz); **¹³C NMR** (75 MHz, CH₃OD): δ 216.7 (C), 147.6 (C), 136.9 (C), 136.0 (C), 126.6 (C), 121.2 (CH), 118.6 (CH), 117.4 (CH), 110.7 (CH), 110.1(CH₂), 104.0 (C), 66.4 (CH), 58.8 (CH), 51.8 (CH), 44.3 (CH), 36.7 (CH₂), 21.9 (CH₂), 19.2 (CH₃); **HRMS** (ESI) *m/z* (M + H)⁺ calcd for C₁₈H₁₉N₂O, 279.1492, found 279.1491.

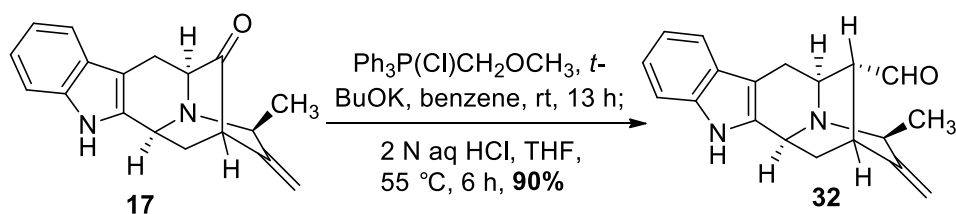
(6*S*,8*R*,11*aS*)-5,8-Dimethyl-9-methylene-6,8,9,10,11*a*,12-hexahydro-6,10-methanoindolo[3,2-*b*]quinolizin-11(5*H*)-one (23)

¹H NMR (300 MHz, CDCl₃) δ 7.48 (d, 1H, *J* = 7.7 Hz), 7.24-7.26 (m, 1H), 7.16-7.21 (m, 1H), 7.06-7.11 (m, 1H), 5.10 (d, 1H, *J* = 1.8 Hz), 4.98 (d, 1H, *J* = 1.8 Hz), 4.57 (dd, 1H, *J* = 9.3, 1.9 Hz), 3.92-4.00 (m, 1H), 3.61 (s, 3H) 3.56 (d, 1H, *J* = 6.1 Hz), 3.29-3.36 (m, 1H), 3.00-3.08 (m, 2H), 2.51-2.59 (m, 1H), 2.11 (dt, 1H, *J* = 12.6, 3.2 Hz), 1.67 (d, 3H, *J* = 7.1 Hz); **¹³C NMR** (75 MHz, CDCl₃) : δ 217.3 (C), 148.0 (C), 137.6 (C), 137.4 (C), 126.6 (C), 121.4 (CH), 119.2 (CH), 118.5 (CH), 110.9 (CH₂), 108.7 (CH), 105.0 (C), 66.9 (CH), 59.1 (CH), 51.7 (CH), 43.2 (CH), 36.5 (CH₂), 29.3 (CH₃), 22.6 (CH₂), 20.7 (CH₃); **HRMS** (ESI) *m/z* (M + H)⁺ calcd for C₁₉H₂₁N₂O, 293.1654, found 293.1678.

(6*S*,8*R*,12*aS*)-5,8-Dimethyl-8,11,12*a*,13-tetrahydro-5*H*-6,11-methanoazepino [1',2':1,6]pyrido [3,4-*b*]indol-12(6*H*)-one (23')

¹H NMR (300 MHz, CDCl₃): δ 7.46 (d, 1H, *J* = 7.7 Hz), 7.23-7.26 (m, 1H), 7.17 (t, 1H, *J* = 7.4 Hz), 7.07 (t, 1H, *J* = 7.3 Hz), 5.9 (t, 1H, *J* = 9.6 Hz), 5.71 (dd, 1H, *J* = 10.2, 3.2 Hz), 4.6 (d, 1H, *J* = 8.9 Hz), 4.04-4.13 (m, 1H), 3.89 (d, 1H, *J* = 5.7 Hz), 3.61 (s, 3H), 3.27 (dd, 1H, *J* = 15.1, 1.3 Hz), 2.99 (dd, 1H, *J* = 15.1, 6.0 Hz), 2.82-2.89 (m, 2H), 2.33 (dd, 1H, *J* = 13.0, 7.2 Hz), 1.56 (d, 3H, *J* = 7.1 Hz); **¹³C NMR** (75 MHz, CDCl₃): δ 213.4 (C), 138.5 (C), 137.4 (C), 135.7 (CH), 126.9 (CH), 126.7(CH), 121.4 (CH), 119.1 (CH), 118.5 (CH), 108.7 (CH), 106.2 (C), 64.2 (CH), 62.4 (CH), 45.9 (CH), 44.3 (CH), 43.0 (CH₂), 29.4 (CH₃), 25.2 (CH₂), 18.9 (CH₃). **HRMS** (ESI): *m/z* (M + H)⁺ calcd for C₁₉H₂₁N₂O, 293.1654, found 293.1661.

Procedure for synthesis of **32** from **17**²¹

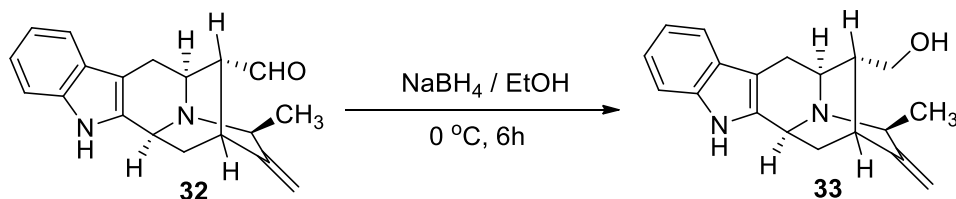


A mixture of anhydrous potassium *tert*-butoxide (3.18 g, 28.36 mmol) and methoxy-methyltriphenylphosphonium chloride (8.98 g, 26.21 mmol) in dry benzene (70 mL) was allowed to stir at rt for 1 h. The solution turned orange-red. The pentacyclic ketone **17** (1.0 g, 3.59 mmol) in THF (20 mL) was then added to the above solution dropwise at 0 °C. The reaction mixture, which resulted, was stirred at rt for 12 h. After 12 h at rt analysis of the mixture by TLC indicated the absence of starting material **17**. The mixture was then diluted with EtOAc (100 mL) and the reaction was quenched with water (50 mL). The aq layer was extracted with EtOAc (2 x 15 mL), and the combined organic layers were washed with brine (2 x 30 mL) and dried (Na_2SO_4). The solvent was removed under reduced pressure to afford the enol ethers as a brownish red oil. The baseline materials (silica gel, TLC) were removed by percolation through a wash column. The solvent was removed under reduced pressure and the residue was dissolved (without further purification) in a solution of THF/ H_2O (1:1, 24 mL). To the above mixture a solution of aq 12 N conc HCl (4 mL) was added and the mixture which resulted was stirred at 55 °C (oil bath temperature) for 6 h. The reaction mixture was then cooled to 0 °C and extracted with hexanes (4 x 100 mL) to remove the phosphorous byproducts, after which the aq layer was then brought to pH 8 with an ice-cold solution of 14% aq NH_4OH . The aq layer was extracted with EtOAc (3 x 15 mL), and the combined organic layers were washed with brine (2 x 30 mL) and dried (Na_2SO_4). The solvent was removed under reduced pressure to afford **32** as a waxy solid (945 mg, 90%).

(6S,8S,11R,11aS)-8-methyl-9-methylene-5,6,8,9,10,11,11a,12-octahydro-6,10-methanoindolo[3,2-b]quinolizine-11-carbaldehyde (32**)**

¹H NMR (300 MHz, CDCl₃): δ 9.61 (s, 1H), 8.12 (brs, 1H), 7.46 (d, 1H, *J* = 7.5 Hz), 7.28-7.32 (m, 1H), 7.08-7.18 (m, 2H), 4.91 (d, 1H, *J* = 2.4 Hz), 4.86 (d, 1H, *J* = 2.0 Hz), 4.23 (d, 1H, *J* = 9.0 Hz), 3.82-3.86 (m, 1H), 3.53-3.60 (m, 1H), 3.10 (dd, 1H, *J* = 15.7, 4.8 Hz), 2.81-2.85 (m, 1H), 2.61 (d, 1H, *J* = 15.7 Hz), 2.43 (d, 1H, *J* = 7.3 Hz), 2.12-2.19 (m, 1H), 1.74-1.82 (m, 1H), 1.42 (d, 3H, *J* = 6.8 Hz); All other spectroscopic data was identical with the published data for **32**.²¹ The material was used for the next step without further characterization.

Procedure for the preparation of **33 from **32****

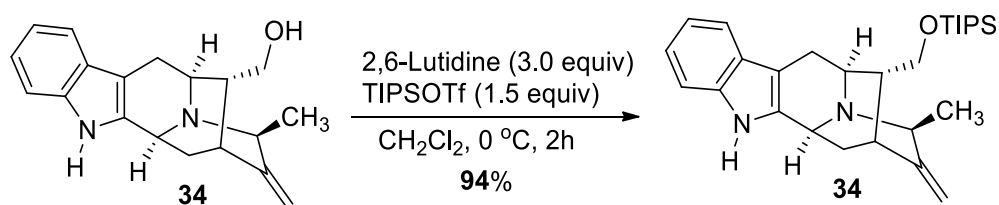


The aldehyde **32** (450 mg, 1.53 mmol) was dissolved in EtOH (8 mL). The NaBH₄ (87 mg, 2.29 mmol) was added to the above solution in one portion at 0 °C. The mixture was then stirred at 0 °C for 6 h. The reaction mixture was diluted with CH₂Cl₂ (50 mL) and poured into ice cold water (30 mL). The aq layer was extracted with additional CH₂Cl₂ (3 × 30 mL), and the combined organic layers were washed with brine (2 × 50 mL) and dried (Na₂SO₄). The solvent was removed under reduced pressure to afford the crude product, which was purified by chromatography on silica gel (CH₂Cl₂/CH₃OH = 10:1) to provide **33** (430 mg, 95%) as a waxy solid. **R_f**: 0.2 (silica gel, 5% MeOH in DCM).

((6S,8S,11R,11aS)-8-Methyl-9-methylene-5,6,8,9,10,11,11a,12-octahydro-6,10-methanoindolo[3,2-b]quinolizin-11-yl)methanol (33)

¹H NMR (300 MHz, CDCl₃) δ 8.0 (s, 1H), 7.38 (d, 1H, *J* = 7.4 Hz), 7.27 (d, 1H, *J* = 8.8 Hz), 7.05-7.16 (m, 2H), 4.84-4.88 (m, 2H), 4.02 (d, 1H, *J* = 9.0 Hz), 3.48-3.53 (m, 1H), 3.43 (d, 1H, *J* = 6.9 Hz), 2.86-2.97 (m, 2H), 2.55 (d, 1H, *J* = 14.3 Hz), 2.39 (bs, 1H), 2.27 (s, 1H), 1.92-2.00 (m, 1H), 1.59 (q, 1H, *J* = 6.7 Hz) 1.50 (dt, 1H, *J* = 12.7, 3.0 Hz), 1.34 (d, 3H, *J* = 6.8 Hz); **¹³C NMR** (75 MHz, CDCl₃) δ 152.3 (C), 138.0 (C), 136.3 (C), 127.7 (C), 121.3 (CH), 119.3 (CH), 118.1 (CH), 110.9 (CH), 107.8 (CH₂), 104.9 (C), 64.7 (CH₂), 57.9 (CH), 51.9 (CH), 48.2 (CH), 44.5 (CH), 36.1 (CH), 33.7 (CH₂), 27.0 (CH₂), 16.6 (CH₃); **HRMS** (ESI) *m/z* (M + H)⁺ calcd for C₁₉H₂₃N₂O, 295.1805, found 295.1802.

Procedure for the preparation of 34 from 33



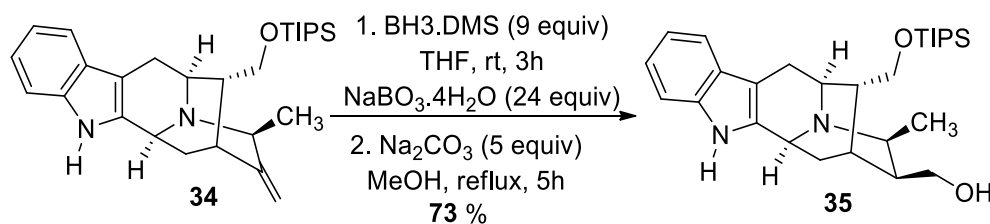
A solution of the alcohol **33** (400 mg, 1.36 mmol) in dry CH₂Cl₂ (20 mL) was cooled to 0 °C, after which 2, 6-lutidine (0.474 mL, 4.08 mmol) was added, and this was followed by addition of TIPSOTf (0.547 mL, 2.04 mmol) to the stirred solution. The mixture was then allowed to stir for an additional 2 hours at 0 °C, after which cold water (5 mL) was added to quench the reaction. The reaction mixture was diluted with CH₂Cl₂ (50 mL) and poured into cold water (20 mL). The aq layer was extracted with additional CH₂Cl₂ (2 x 30 mL), and the combined organic layers were washed with brine (3 x 30 mL) and dried (Na₂SO₄). The solvent was removed under reduced pressure and the residue was purified by chromatography on silica gel using 2-5% MeOH in DCM

to provide the *O*-TIPS ether **34** as a white colored solid (576 mg, 94%). **R_f**: 0.35 (silica gel, 5% MeOH in DCM);

(6S,8S,11R,11aS)-8-Methyl-9-methylene-11-(((triisopropylsilyl)oxy)methyl)-5,6,8,9,10,-11,11a,12-octahydro-6,10-methanoindolo[3,2-b]quinolizine (34)

¹H NMR (300MHz, CDCl₃): δ 8.35 (brs, 1H), 7.48 (d, 1H, *J* = 7.4 Hz), 7.35 (d, 1H, *J* = 7.8 Hz), 7.08-7.18 (m, 2H), 4.88 (dd, 2H, *J* = 8.2, 2.3 Hz), 4.23 (d, 1H, *J* = 9.6 Hz), 3.60 (dd, 2H, *J* = 7.5, 2.3 Hz), 3.47-3.56 (m, 1H), 3.00-3.12 (m, 2H), 2.78 (d, 1H, *J* = 15.1 Hz), 2.42 (bs, 1H), 2.12 (t, 1H, *J* = 11.3 Hz), 1.86 (q, 1H, *J* = 7.4 Hz), 1.76 (d, 1H, *J* = 12.5 Hz), 1.39 (d, 3H, *J* = 6.8 Hz), 1.06-1.07 (m, 21H); **¹³C NMR** (75 MHz, CDCl₃): δ 150.7 (C), 137.2 (C), 136.4 (C), 127.6 (C), 121.5 (CH), 119.3 (CH), 118.1 (CH), 111.1 (CH), 108.2 (CH₂), 104.8 (C), 65.5 (CH₂), 58.3 (CH), 52.3 (CH), 49.3 (CH), 44.1 (CH), 35.6 (CH), 33.6 (CH₂), 27.0 (CH₂), 18.1 (6 x CH₃), 16.5 (CH₃), 11.9 (3 x CH); **HRMS** (ESI) *m/z* (M + H)⁺ calcd for C₂₈H₄₃N₂OSi, 451.3139, found 451.3122.

Procedure for the preparation of 35 from 34



To a solution of the TIPS ether **34** (150 mg, 0.332 mmol) in dry THF (5 mL) was added BH₃·DMS (2.0 M solution in THF, 1.49 mL, 2.99 mmol) at rt. The mixture which resulted was stirred at rt for 3 h. The reaction mixture was then quenched by careful addition of ice cold water (4 mL) at 0

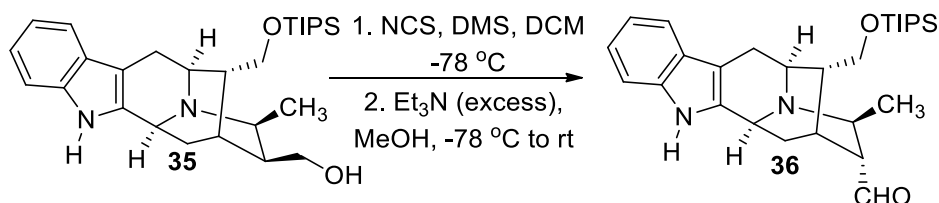
°C (initial addition of water resulted in a large amount of effervescence). At this point $\text{NaBO}_3 \cdot 4\text{H}_2\text{O}$ (1.22 g, 7.97 mmol) was added to the mixture in one portion at 0 °C. The mixture which resulted was allowed to stir at rt for 2 h after which EtOAc (50 mL) and H_2O (15 mL) were added. The organic layer was separated, washed with water (3 x 10 mL), brine (2 x 20 mL) and dried (Na_2SO_4). The EtOAc was then removed under reduced pressure to provide the $N_b\text{-BH}_3$ complex. The residue was dissolved in freshly distilled MeOH (20 mL) and Na_2CO_3 (176 mg, 1.66 mmol) was added. The mixture was then warmed to 60 °C (oil bath) for 5 h under vigorous stirring. The reaction mixture which resulted was cooled to rt and this was followed by filtration through a bed of celite to remove the solids. The filtrate was concentrated under reduced pressure to provide a turbid oil which was redissolved in CH_2Cl_2 . The CH_2Cl_2 layer was washed with H_2O (1 x 10 mL), brine (4 x 10 mL) and dried (Na_2SO_4). The solvent was removed under reduced pressure to afford a crude solid, which was purified by flash chromatography (silica gel, 5-8% MeOH in DCM) and furnished the primary alcohol **35** (113 mg, 73 %). R_f : 0.2 (silica gel, 10 % MeOH in DCM).

((6S,8S,9S,11R,11aS)-8-Methyl-11-(((triisopropylsilyl)oxy)methyl)-5,6,8,9,10,11,11a,12-octahydro-6,10-methanoindolo[3,2-b]quinolizin-9-yl)methanol (35)

$^1\text{H NMR}$ (300MHz, CDCl_3): δ 8.26 (brs, 1H), 7.46 (d, 1H, $J = 7.5$ Hz), 7.35 (d, 1H, $J = 7.8$ Hz), 7.07-7.18 (m, 2H), 4.12-4.18 (m, 1H), 3.86-3.94 (m, 1H), 3.69-3.81 (m, 3H), 3.19-3.32 (m, 2H), 2.99 (dd, 1H, $J = 15.4, 4.8$ Hz), 2.69 (d, 1H, $J = 15.4$ Hz), 2.23 (brs, 1H), 1.83-2.07 (m, 3H), 1.62-1.66 (m, 1H), 1.31 (d, 3H, $J = 7.3$ Hz), 1.03-1.05 (m, 21H); $^{13}\text{C NMR}$ (75 MHz, CDCl_3): δ 137.7 (C), 136.3 (C), 127.8 (C), 121.3 (CH), 119.2 (CH), 118.1 (CH), 111.0 (CH), 104.9 (C), 66.9 (CH_2), 63.1 (CH_2), 54.2 (CH), 52.5 (CH), 49.0 (CH), 41.2 (CH), 40.0 (CH), 36.9 (CH_2), 27.5 (CH_2), 25.0

(CH), 18.0 (6 x CH₃), 13.1 (CH₃), 11.9 (3 x CH); **HRMS** (ESI) m/z (M + H)⁺ calcd for C₂₈H₄₅N₂OSi, 469.3245, found 469.3227.

Procedure for the preparation of 36 from 35



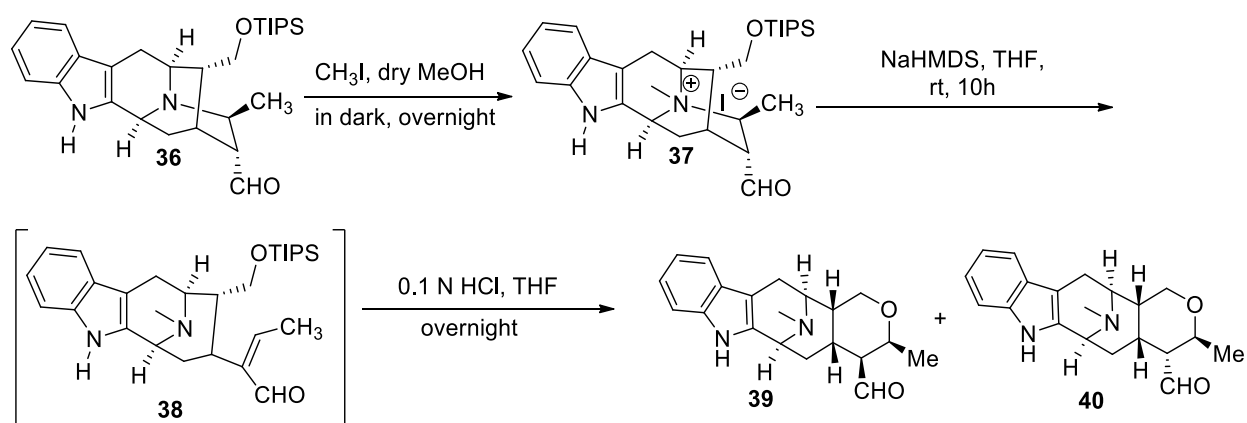
To a stirred solution of *N*-chlorosuccinimide (89.7 mg, 0.672 mmol) in dry CH₂Cl₂ (2.5 mL) was added dimethyl sulfide (99 μL, 1.34 mmol) at -5 to -15 °C (outside bath temperature) under argon. A white precipitate appeared immediately after addition of the sulfide, which was stirred for an additional 0.5 h at the above mentioned temperature range. After 0.5 h, the temperature of the reaction mixture was lowered to -78 °C (acetone-dry ice bath). The alcohol **35** (90 mg, 0.192 mmol) in dry CH₂Cl₂ (3.0 mL) was also cooled at -78 °C and then added to the white complex, and the stirring was continued for 2 h at -78 °C. A solution of distilled triethylamine (105 μL, 0.77 mmol) was then added to the above mixture dropwise (neat) and the stirring was continued for an additional 1 h at -78 °C. Upon completion of the reaction, the reaction mixture was quenched at -78 °C by addition of excess CH₂Cl₂ and H₂O. The organic layer was separated, washed with brine and dried (Na₂SO₄). The solvent was removed under reduced pressure to provide the mixture of crude aldehydes. Analysis of the ¹H NMR spectrum of the residue indicated the formation of the mixture of epimeric aldehydes, which contained the α-aldehyde as major product. The epimeric mixture of aldehydes was dissolved in a solution of MeOH (10 mL) with triethylamine (1.2 mL) and the mixture was stirred overnight at rt to effect the epimerization. The methanol was then

removed under high vacuum to give aldehyde **36** as an oil (65 mg, 72 %). The complete epimerization from the mixture of α and β aldehydes into only the α -aldehyde in high yield was confirmed by ^1H NMR spectroscopy. This compound was not subjected to chromatographic purification and was used for the next step directly.

(6S,8S,9R,11R,11aS)-8-Methyl-11-(((triisopropylsilyl)oxy)methyl)-5,6,8,9,10,11,11a,12-octahydro-6,10-methanoindolo[3,2-b]quinolizine-9-carbaldehyde (36**)**

R_f = 0.3 (silica gel, 10 % MeOH in DCM); ^{13}C NMR (300 MHz, CDCl_3): δ 203.7 (CH), 138.1 (C), 136.4 (C), 127.6 (C), 121.1 (CH), 119.1 (CH), 117.9 (CH), 111.1 (CH), 104.9 (C), 64.4 (CH_2), 52.0 (CH), 51.8 (CH), 51.4 (CH), 47.7 (CH), 42.14 (CH), 30.1 (CH_2), 26.9 (CH_2), 26.8 (CH), 19.1 (CH_3), 18.1 (6 x CH_3), 11.9 (3 x CH); **HRMS** (ESI) m/z ($M + H$) $^+$ calcd for $\text{C}_{28}\text{H}_{43}\text{N}_2\text{O}_2\text{Si}$, 467.3088, found 467.3073.

One-pot conversion of **36 into indolebases **39** and **40** with stereospecific formation of the β -methyl function**



To a solution of the aldehyde **36** (55 mg, 0.12 mmol) in MeOH was added an excess of MeI (0.4 mL) at $0\text{ }^\circ\text{C}$, after which the mixture was allowed to stir in the dark at $0\text{ }^\circ\text{C}$ overnight. Upon

completion of the reaction, the solvent was removed under high vacuum to provide the *N*₄-methyl salt **37** (50.5 mg, 89%): *R_f* 0.3 (basic alumina, DCM/MeOH, 4.9 : 0.1); **LRMS** (ESI) *m/z* (M)⁺ calcd for C₂₉H₄₅N₂O₂Si, 481.32, found 481.35; **HRMS** (ESI) *m/z* (M+CH₃OH)⁺ calcd for C₃₀H₄₉N₂O₃Si, 513.3507, found 513.3497. This material was used for the next reaction without purification.

To a solution of **37** (50 mg, 0.104 mmol) in THF (3 mL), NaHMDS (38.1 mg, 0.21 mmol) was added at rt. The mixture was allowed to stir at rt overnight. After that time examination of a LCMS spectrum indicated the disappearance of **37**, **LRMS** (M+H)⁺ predicted for C₂₉H₄₅N₂O₂Si, 481.33, found 481.45. The THF was removed under reduced pressure to provide **38** as brownish oil (47.5 mg, 95% crude yield). **HRMS** (ESI) *m/z* (M + H)⁺ calcd for C₂₉H₄₅N₂O₂Si, 481.3245, found 481.3229. This material was used directly for the next step.

A solution of **38** (30 mg, 0.06 mmol) in 10 mL of aq 0.1 N HCl (THF: H₂O = 1: 1) was heated overnight at 60 °C. After that time, the solution was cooled to rt and brought to pH 8 with cold aq NH₄OH. The solution was extracted with DCM (3 x 10 mL). The combined organic layers were washed with brine and dried over Na₂SO₄ to provide a mixture of aldehydes **39** and **40** yellowish oil (16.3 mg, 80 % crude yield). This mixture was purified by flash chromatography on silica-gel (1-3% MeOH in DCM) to provide pure **39** (7.5 mg) and **40** (7 mg) with 72% combined isolated yield.

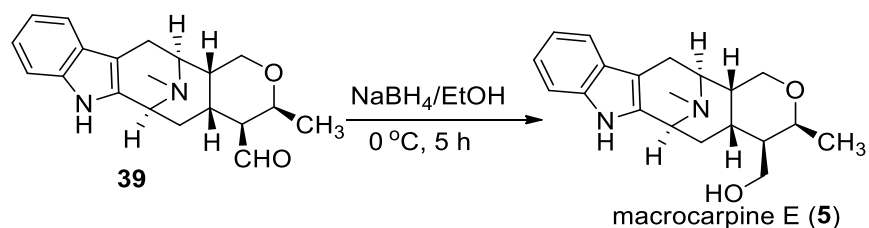
(3S,4S,4aR,6S,13S,13aR)-3,14-Dimethyl-1,3,4,4a,5,6,7,12,13,13a-decahydro-6,13-epiminopy-rano[3',4':5,6]cycloocta[1,2-b]indole-4-carbaldehyde (39)

¹H NMR (300 MHz, CDCl₃): δ 9.97 (d, 1H, *J* = 2.8 Hz), 7.80 (brs, 1H), 7.51 (d, 1H, *J* = 7.4 Hz), 7.35 (d, 1H, *J* = 7.5 Hz), 7.11-7.21 (m, 2H), 4.17 (t, 1H, *J* = 11.6 Hz), 3.88-4.01 (m, 3H), 3.29 (dd, 1H, *J* = 16.5, 7.0 Hz), 2.94 (d, 1H, *J* = 6.4 Hz), 2.46-2.55 (m, 2H), 2.37 (s, 3H), 2.21-2.26 (m, 1H), 2.07-2.11 (m, 1H), 1.81 (brs, 1H), 1.51-1.55 (m, 1H), 1.33 (d, 3H, *J* = 6.7 Hz); **¹³C NMR** (75 MHz, CDCl₃): δ 204.6 (CH), 135.7 (C), 131.3 (C), 126.9 (C), 121.6 (CH), 119.5 (CH), 118.2 (CH), 110.8 (CH), 107.5 (C), 69.5 (CH), 68.8 (CH₂), 54.9 (CH), 54.6 (CH), 54.5 (CH), 41.6 (CH₃), 39.4 (CH), 30.5 (CH₂), 27.0 (CH), 22.4 (CH₂), 19.2 (CH₃); **R_f**: 0.5 (10% MeOH in DCM); **HRMS** (ESI) *m/z* (M + H)⁺ calcd for C₂₀H₂₅N₂O₂, 325.1911, found 325.1916.

(3S,4R,4aR,6S,13S,13aR)-3,14-Dimethyl-1,3,4,4a,5,6,7,12,13,13a-decahydro-6,13-epiminopyrano[3',4':5,6]cycloocta[1,2-b]indole-4-carbaldehyde (40)

¹³C NMR (75 MHz, CDCl₃): δ 203.1 (CH), 135.7 (C), 131.6 (C), 126.9 (C), 121.6 (CH), 119.5 (CH), 118.0 (CH), 111.0 (CH), 107.7 (C), 67.8 (CH), 67.2 (CH₂), 57.8 (CH), 55.0 (CH), 54.5 (CH), 42.6 (CH), 41.6 (CH₃), 27.4 (CH₂), 26.4 (CH), 22.4 (CH₂), 20.3 (CH₃); **R_f**: 0.3 (10% MeOH in DCM, silica gel); **HRMS** (ESI) *m/z* (M + H)⁺ calcd for C₂₀H₂₅N₂O₂, 325.1911, found 325.1917.

Macrocarpine E (5)

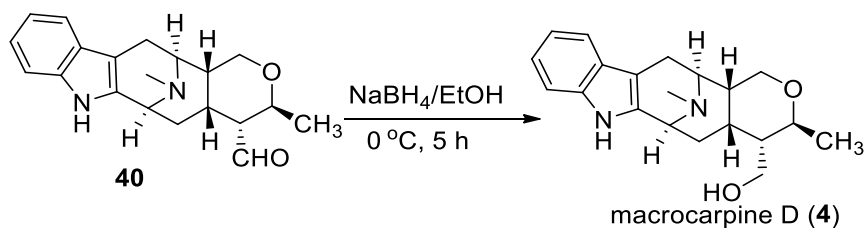


The aldehyde **39** (5.3 mg, 0.016 mmol) was dissolved in EtOH (1 mL) and cooled to 0 °C. Then NaBH₄ (0.93mg, 0.024 mmol) was added to the above solution in one portion. The mixture, which resulted, was stirred at 0 °C for 5 h. After 5 h, examination of TLC and LCMS indicated the

disappearance of the aldehyde. The reaction mixture was diluted with DCM (5 mL) and poured into ice cold water. The organic layer was separated and the aq layer was extracted with additional DCM (2 x 5 mL). The combined organic layers were washed with brine (2 x 10 mL) and dried (Na_2SO_4). The solvent was removed under reduced pressure and the residue was purified by chromatography on silica gel from a Pasteur pipette (2-4 % MeOH in DCM) to give 5.1 mg (96%) of macrocarpine E (**5**) as a white color waxy solid.

^1H NMR (300 MHz, CDCl_3): δ 7.74 (brs, 1H), 7.49 (d, 1H, $J = 7.4$ Hz), 7.33 (d, 1H, $J = 7.4$ Hz), 7.09-7.18 (m, 2H), 4.08 (t, 1H, $J = 11.7$ Hz), 3.94-3.99 (m, 1H), 3.86-3.92 (m, 1H), 3.76-3.84 (m, 2H), 3.64-3.72 (m, 1H), 3.25 (dd, 1H, $J = 16.6, 6.7$ Hz), 2.86 (d, 1H, $J = 6.7$ Hz), 2.47 (d, 1H, $J = 16.6$ Hz), 2.47 (m, 1H, merged), 2.33 (s, 3H), 2.16 (dd, 1H, $J = 11.3, 5.2$ Hz), 1.99-2.05 (m, 1H), 1.44-1.48 (m, 1H), 1.24 (d, 3H, $J = 6.6$ Hz), 1.06 (brs, 1H); **^{13}C NMR** (75 MHz, CDCl_3): δ 135.7 (C), 132.0 (C), 127.0 (C), 121.4 (CH), 119.4 (CH), 118.1 (CH), 110.8 (CH), 107.6 (C), 71.3, 68.9 (CH_2), 63.3, 55.0 (CH), 54.6 (CH), 43.5 (CH), 41.6 (CH_3), 39.4 (CH), 31.4 (CH_2), 28.9 (CH), 22.5 (CH_2), 18.8 (CH_3); **R_f** : 0.4 (10% MeOH in DCM); **HRMS** (ESI) m/z ($M + H$)⁺ calcd for $\text{C}_{20}\text{H}_{27}\text{N}_2\text{O}_2$, 327.2067, found 327.2072; **$[\alpha]_D^{25}$** (c 0.45, CHCl_3): -13.33 lit. **$[\alpha]_D^{25}$** (c 0.8, CHCl_3): -12. The spectroscopic data and optical rotation were in excellent agreement with those of natural macrocarpine E.¹⁰

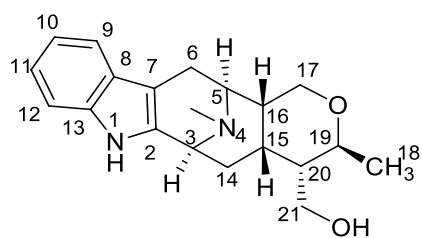
Macrocarpine D (**4**)



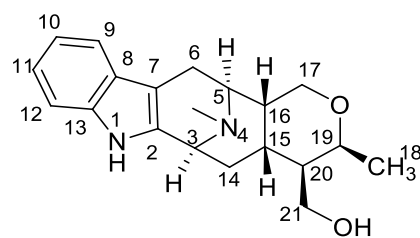
The aldehyde **40** (4.2 mg, 0.013 mmol) was dissolved in EtOH (1mL) and the mixture was cooled to 0 °C. Then NaBH₄ (0.74 mg, 0.02 mmol) was added to the above solution in one portion. The mixture, which resulted, was stirred at 0 °C for 5 h. After 5 h, examination of TLC and LCMS indicated the disappearance of the aldehyde. The reaction mixture was diluted with DCM (5 mL) and poured into ice-cold water. The organic layer was separated and the aq layer was extracted with additional DCM (2 x 5 mL). The combined organic layers were washed with brine and dried (Na₂SO₄). The solvent was removed under reduced pressure and the residue was purified by chromatography on silica gel from a Pasteur pipette (1-3 % MeOH in DCM) to give 3.9 mg (92%) of macrocarpine D (**4**) as a white-color waxy solid.

¹H NMR (500 MHz, CDCl₃): δ 7.71 (brs, 1H), 7.49 (d, 1H, *J* = 7.5 Hz), 7.32 (d, 1H, *J* = 7.7 Hz), 7.15 (t, 1H, *J* = 7.1 Hz), 7.14 (t, 1H, *J* = 7.1 Hz), 4.06 (t, 1H, *J* = 11.6 Hz), 3.89-3.91 (m, 1H), 3.74 (dd, 1H, *J* = 11.4, 4.5 Hz), 3.48-3.53 (m, 2H), 3.35 (dd, 1H, *J* = 10.7, 8.3 Hz), 3.26 (dd, 1H, *J* = 16.5, 6.8 Hz), 2.91 (d, 1H, *J* = 6.8 Hz), 2.43 (d, 1H, *J* = 16.5 Hz), 2.32 (s, 3H), 2.26 (td, 1H, *J* = 12.8, 4.0 Hz), 1.98-2.02 (m, 1H), 1.85-1.89 (m, 1H), 1.58 (dt, 1H, *J* = 12.6, 3.8 Hz), 1.47-1.52 (m, 1H), 1.16 (d, 3H, *J* = 6.1 Hz); **¹³C NMR** (75 MHz, CDCl₃): δ 135.7 (C), 132.2 (C), 127.1 (C), 121.3 (CH), 119.4 (CH), 117.9 (CH), 110.9 (CH), 107.7 (C), 70.5 (CH), 67.7 (CH₂), 61.7 (CH₂), 55.1 (CH), 54.9 (CH), 46.9 (CH), 43.6 (CH), 41.6 (CH₃), 27.1 (CH), 26.1 (CH₂), 22.5 (CH₂), 20.3 (CH₃); **R_f**: 0.33 (10% MeOD in DCM); **HRMS** (ESI) *m/z* (M + H)⁺ calcd for C₂₀H₂₇N₂O₂, 327.2067, found 327.2060. **[α]_D²⁵** (c 0.85, CHCl₃): -44.71 lit. **[α]_D²⁵** (c 0.89, CHCl₃): -43. The spectroscopic data and optical rotation were in excellent agreement with that of the natural macrocarpine D.⁹

4.1 BIOGENETIC NUMBERING FOR MACROCARPINE D (4) AND MACROCARPINE E (5)^{9,10}



macrocarpine D (4)



macrocarpine E (5)

4.2. COMPARISON TABLES 1 & 2 FOR NATURAL AND SYNTHETIC MACROCARPINE D (4)

Macrocarpine D (4)

Specific rotation:

Natural⁹: $[\alpha]_D^{25} = -43$ (c 0.89, CHCl₃); Synthetic: $[\alpha]_D^{25} = -44.7$ (c 0.85, CHCl₃)

Table 2. Comparison of the ¹H NMR Spectral Data for Natural and Synthetic Macrocarpine D (4) in CDCl₃

H	¹ H Natural ⁹ (400 MHz)	¹ H Synthetic (500 MHz)
3	3.95 m	3.89-3.91 m
5	2.94 d (7)	2.91 d (6.8)
6b	2.46 d (16)	2.43 d (16.5)
6a	3.27 dd (16, 7)	3.26 dd (16.5, 6.8)
9	7.49 d (7.5)	7.49 d (7.5)
10	7.11 t (7.5)	7.14t (7.1)
11	7.15 t (7.5)	7.15 t (7.1 Hz)
12	7.32 d (7.5)	7.32 d (7.7)
14b	1.62 dt (13, 4)	1.58 dt (12.6, 3.8)
14a	2.28 td (13, 4)	2.26 td (12.8, 4.0)
15	2.01 m	1.98-2.02 m
16	1.89 dt (12, 4)	1.85-1.89 m
17b	3.74 dd (12, 5)	3.74 dd (11.4, 4.5)
17a	4.08 t (12)	4.06 t (11.6)
18	1.16 d (6)	1.16 d (6.1)
19	3.50 m	3.48-3.53 m (19 and 21b merged together)
20	1.50 m	1.47-1.52 m
21a	3.34 dd (11, 8)	3.35 dd (10.7, 8.3)
21b	3.50 dd (11, 5)	3.48-3.53 m

<i>N</i> _a -H	7.89 br s	7.71 br s
<i>N</i> ₄ -Me	2.34 s	2.32 s

Table 3. Comparison of the ¹³C NMR Spectral Data for Natural and Synthetic Macropine D (4) in CDCl₃

C#	¹³ C Natural ⁹ (100 MHz)	¹³ C Synthetic (75 MHz)
2	132.2	132.2
3	55.0	54.9
5	55.1	55.1
6	22.5	22.5
7	107.7	107.7
8	127.1	127.1
9	118.0	117.9
10	119.4	119.4
11	121.3	121.3
12	110.9	110.9
13	135.5	135.7
14	26.1	26.1
15	27.1	27.1
16	43.6	43.6
17	67.7	67.7
18	20.3	20.3
19	70.5	70.5
20	46.9	46.9
21	61.7	61.7
<i>N</i> ₄ -Me	41.6	41.6

4.3. COMPARISON TABLES 4 & 5 FOR NATURAL AND SYNTHETIC MACROCARPINE E (5)

Macrocarpine E (5)

Specific rotation:

Natural¹⁰: $[\alpha]_{\text{D}}^{25} = -12$ (c 0.8, CHCl₃); Synthetic: $[\alpha]_{\text{D}}^{25} = -13.3$ (c 0.45, CHCl₃)

Table 4. Comparison of the ¹H NMR Spectral Data for Natural and Synthetic macrocarpine E (5) in CDCl₃

H	¹ H Natural ¹⁰ (400 MHz)	¹ H Synthetic (300 MHz)
3	3.85 br t (3)	3.86-3.92 m
5	2.82 d (7)	2.86 d (6.7)
6b	2.43 d (17)	2.47 d (16.6)
6a	3.23 dd (17, 7)	3.25 dd (16.6, 6.7)
9	7.48 dd (7, 1)	7.49 d (7.4)
10	7.10 td (7, 1)	7.09-7.18 m
11	7.14 td (7, 1)	7.09-7.18 m
12	7.31 dd (7, 1)	7.33 d (7.4)
14b	1.44 ddd (13, 5, 3)	1.44-1.48 m
14a	2.43 td (13, 4)	Merged with 6b
15	1.98 dt (13, 5)	1.99-2.05 m
16	2.08 dd (12, 5)	2.16 dd (11.3, 5.2)
17b	3.76 dd (12, 5)	3.76-3.84 m
17a	4.04 t (12)	4.08 t (11.7)
18	1.21 d (6.7)	1.24 d (6.6)
19	3.93 (6.7, 2.6)	3.94-3.99 m
20	1.06 m	1.06 brs

21a	3.64 dd (11, 4)	3.64-3.72 m
21b	3.71 dd (11, 6)	3.76-3.84 m
<i>N</i> ₁ -H	8.14 br s	7.74 br s
<i>N</i> ₄ -Me	2.30 s	2.33 s

Table 5. Comparison of the ¹³C NMR Spectral Data for Natural and Synthetic macrocarpine E (5) in CDCl₃

C#	¹³C Natural¹⁰ (100 MHz)	¹³C Synthetic (75 MHz)
2	132.1	132.0
3	54.9	55.0
5	54.5	54.6
6	22.5	22.5
7	107.4	107.6
8	126.9	127.0
9	118.0	118.1
10	119.3	119.4
11	121.2	121.4
12	110.8	110.8
13	135.7	135.7
14	31.3	31.4
15	28.6	28.9
16	39.2	39.4
17	68.9	68.9
18	18.7	18.8
19	71.1	71.3
20	43.5	43.5
21	62.8	63.3
<i>N</i>₄-Me	41.5	41.6

5. Spectra and X-ray data: See Appendix B for X-ray data for compounds **22**, **23**, **23'**, and **19**. See Appendix C for the spectra of the synthetic macrocarpines D (**4**) and E (**5**).

6. References:

- (1) Khyade, M. S.; Kasote, D. M.; Vaikos, N. P. *J. Ethnopharmacol.* **2014**, *153*, 1.
- (2) Ziegler, J.; Facchini, P. *J. Annu. Rev. Plant Biol.* **2008**, *59*, 735.
- (3) Cordell, G. A.; Quinn-Beattie, M. L.; Farnsworth, N. R. *Phytother. Res.* **2001**, *15*, 183.
- (4) Namjoshi, O. A.; Cook, J. M. In *The Alkaloids: Chemistry and Biology*; Knölker, H.-J., Ed.; Academic Press: San Diego, CA, 2016; Vol. 76, p 63.
- (5) Garnick, R. L.; Le Quesne, P. W. *J. Am. Chem. Soc.* **1978**, *100*, 4213.
- (6) Elderfield, R. C.; Gilman, R. E. *Phytochemistry* **1972**, *11*, 339.
- (7) Kishi, T.; Hesse, M.; Gemenden, C.; Taylor, W.; Schmid, H. *Helv. Chim. Acta* **1965**, *48*, 1349.
- (8) Kam, T.-S.; Choo, Y.-M.; Komiyama, K. *Tetrahedron* **2004**, *60*, 3957.
- (9) Lim, S.-H.; Low, Y.-Y.; Sinniah, S. K.; Yong, K.-T.; Sim, K.-S.; Kam, T.-S. *Phytochemistry* **2014**, *98*, 204.
- (10) Tan, S.-J.; Lim, J.-L.; Low, Y.-Y.; Sim, K.-S.; Lim, S.-H.; Kam, T.-S. *J. Nat. Prod.* **2014**, *77*, 2068.
- (11) Lounasmaa, M.; Hanhinen, P.; Westersund, M. In *The Alkaloids: Chemistry and Biology*; Cordell, G. A., Ed.; Academic Press: San Diego, CA, 1999; Vol. 52, p 103.

- (12) Pan, L.; Terrazas, C.; Acuña, U. M.; Ninh, T. N.; Chai, H.; de Blanco, E. J. C.; Soejarto, D. D.; Satoskar, A. R.; Kinghorn, A. D. *Phytochem. Lett.* **2014**, *10*, liv.
- (13) Khan, Z. M.; Hesse, M.; Schmid, H. *Helv. Chim. Acta* **1967**, *50*, 1002.
- (14) Iwu, M. *Planta Med.* **1982**, *45*, 105.
- (15) Ullmann, F.; Bielecki, J. *Ber. Dtsch. Chem. Ges.* **1901**, *34*, 2174.
- (16) Evano, G.; Blanchard, N.; Toumi, M. *Chem. Rev.* **2008**, *108*, 3054.
- (17) Beletskaya, I. P.; Cheprakov, A. V. *Coord. Chem. Rev.* **2004**, *248*, 2337.
- (18) Wang, T.; Cook, J. M. *Org. Lett.* **2000**, *2*, 2057.
- (19) Zhao, S.; Liao, X.; Wang, T.; Flippen-Anderson, J.; Cook, J. M. *J. Org. Chem.* **2003**, *68*, 6279.
- (20) Edwankar, C. R.; Edwankar, R. V.; Deschamps, J. R.; Cook, J. M. *Angew. Chem., Int. Ed.* **2012**, *51*, 11762.
- (21) Edwankar, R. V.; Edwankar, C. R.; Deschamps, J. R.; Cook, J. M. *J. Org. Chem.* **2014**, *79*, 10030.
- (22) Yin, W.; Kabir, M. S.; Wang, Z.; Rallapalli, S. K.; Ma, J.; Cook, J. M. *J. Org. Chem.* **2010**, *75*, 3339.
- (23) Yu, P.; Wang, T.; Li, J.; Cook, J. M. *J. Org. Chem.* **2000**, *65*, 3173.
- (24) Wright, P. J.; English, A. M. *J. Am. Chem. Soc.* **2003**, *125*, 8655.
- (25) Edwankar, R. V.; Edwankar, C. R.; Deschamps, J.; Cook, J. M. *Org. Lett.* **2011**, *13*, 5216.
- (26) Baldwin, J. E.; Lusch, M. J. *Tetrahedron* **1982**, *38*, 2939.
- (27) Baldwin, J. *Chem. Soc., Chem. Commun.* **1976**, 734.

Chapter 5

The Total Synthesis of Talcarpine, *N*₄-Methyl-*N*_{4,21}-Secotalpinine, Dihydroperaksine, Deoxyperaksine, and Macroparpines A-C

1. Introduction

After the successful completion of the total synthesis of several of the N_a -H, N_b -CH₃ substituted alkaloids, focus turned to the total synthesis of a number of alkaloids bearing the N_a -CH₃, N_b -CH₃ pattern of substitution. In addition, a pair of sarpagine alkaloids, termed dihydroperaksine and deoxyperaksine bear the C-19 (*S*)-methyl substituent in the opposite configuration to many of the alkaloids of this group. Accessing these two alkaloids was envisaged to illustrate the ability of the strategy developed here to access alkaloids with either the C-19 (*S*)- or (*R*)-methyl substitution.

The C-19 methyl substituted macroline/sarpagine and ajmaline alkaloids, as mentioned are an emerging group of biosynthetically related indole alkaloids, some of which have historical significance,¹ and have been primarily isolated from various medicinal plants of the *Apocynaceae* family. Currently, about seventy alkaloids belong to this group (see General Introduction). Some of them are depicted in Figure 1. Most of these alkaloids have not been tested for their biological activity, presumably, due to the paucity of isolated material. Yet, some of these alkaloids have been shown to possess important biological activity ranging from anti-hypertensive to anticancer properties. Macrocarpines A-C (**1-3**) have been isolated from the stem bark of *Alstonia macrophylla* by Kam.² Talcarpine (**4**), which was isolated from *Alstonia macrophylla* and *Pleiocarpa talbotii*, exhibited antimalarial activity.³⁻⁵ The *N*(4)-methyl-*N*(4),21-secotalpinine **5**, isolated from *Pleiocarpa talbotii*, and *Alstonia angustifolia*, demonstrated promising anti-leishmanial activity.^{2,4,6} Talpinine **6**, another related alkaloid, exhibited moderate activity in reversing multidrug resistance in a vincristine-resistant KB/VJ300 cell line in the presence of 0.12 μ M vincristine.^{4,7} The *N*(4)-methyltalpinine **7**, which contains a quaternary N_b -nitrogen atom, is the N_b -methylated version of talpinine **6**, and has shown potent and important NF κ B inhibition.⁶

While the majority of these alkaloids have the β methyl configuration at C-19, a few contain the α C-19 methyl function (e.g., dihydroperaksine **8**, also known as dihydrovomifoline and deoxyperaksine **9**) as mentioned above.⁸⁻¹¹ All of these alkaloids bear either an N_a -methyl or N_a -hydrogen atom substituted indole nitrogen atom. Similarly, the N_b -nitrogen atom also varies in the pattern of substitution. Moreover, all of these alkaloids contain 6 or 7 quaternary centers with various substitution patterns and configurations, which render the synthesis of these alkaloids of interest. The challenge to access the complex architecture of these alkaloids and their promising biological activity stimulated interest in the total synthesis of these natural products *via* a general strategy. To illustrate the feasibility of this strategy to access either the α or β C-19 methyl substituted alkaloids, stereospecifically, herein we report the total synthesis of (-)-macrocarpine A-C (**1-3**), (-)-talcarpine (**4**), (+)- $N(4)$ -methyl- $N(4),21$ -secotalpinine (**5**), (+)-dihydroperaksine (**8**) and (-)-deoxyperaksine (**9**) is reported with complete stereocontrol of the methyl function at C-19.

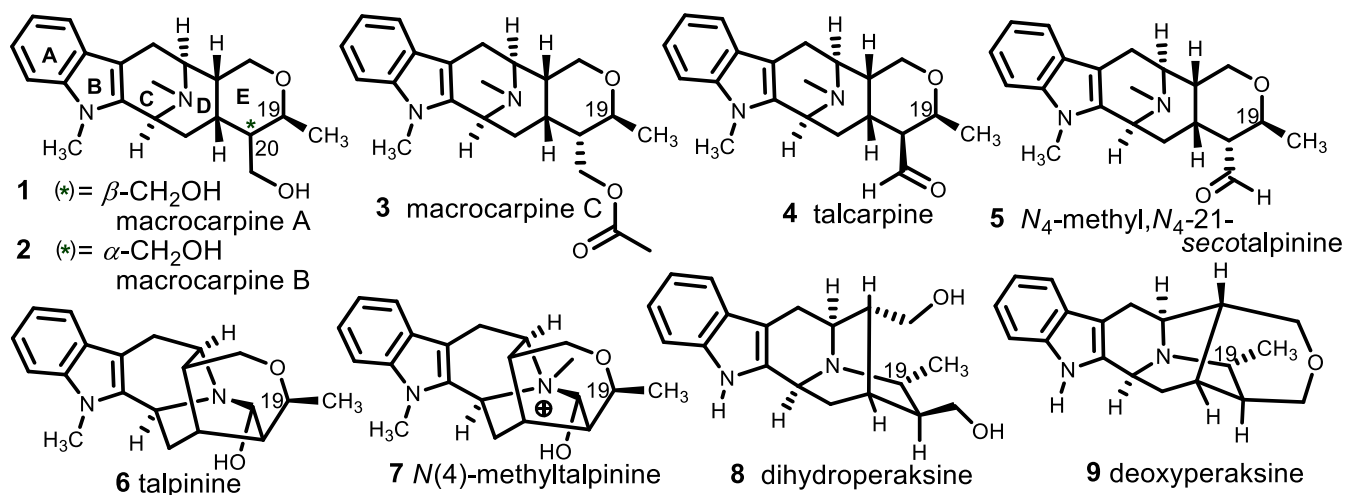
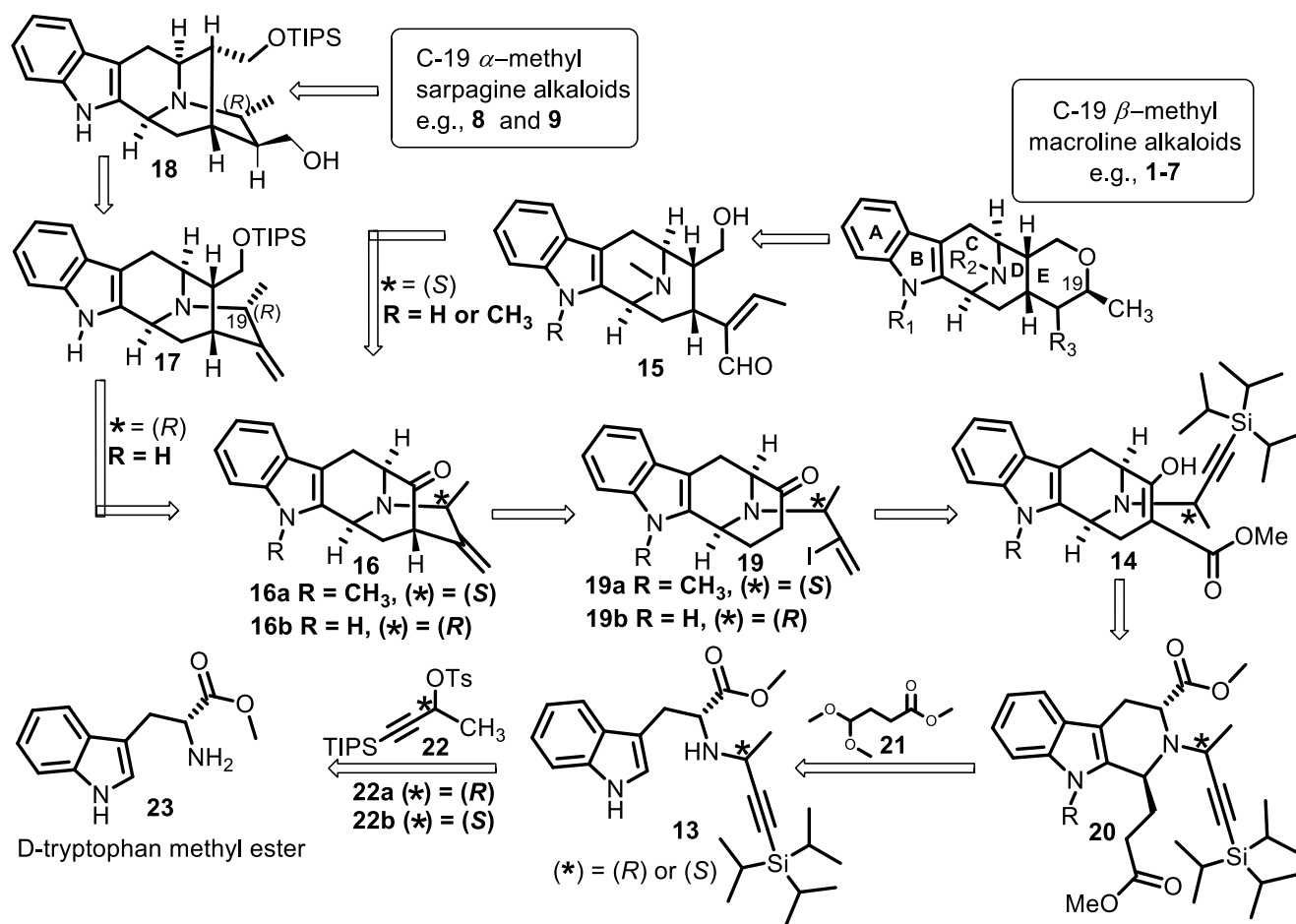


Figure 1. Representative examples of chiral C-19 methyl substituted macroline/sarpagine alkaloids



Scheme 1. Retrosynthetic analysis for the total synthesis of the C-19 methyl substituted sarpagine/macroline alkaloids via the Pictet-Spengler/Dieckmann protocol

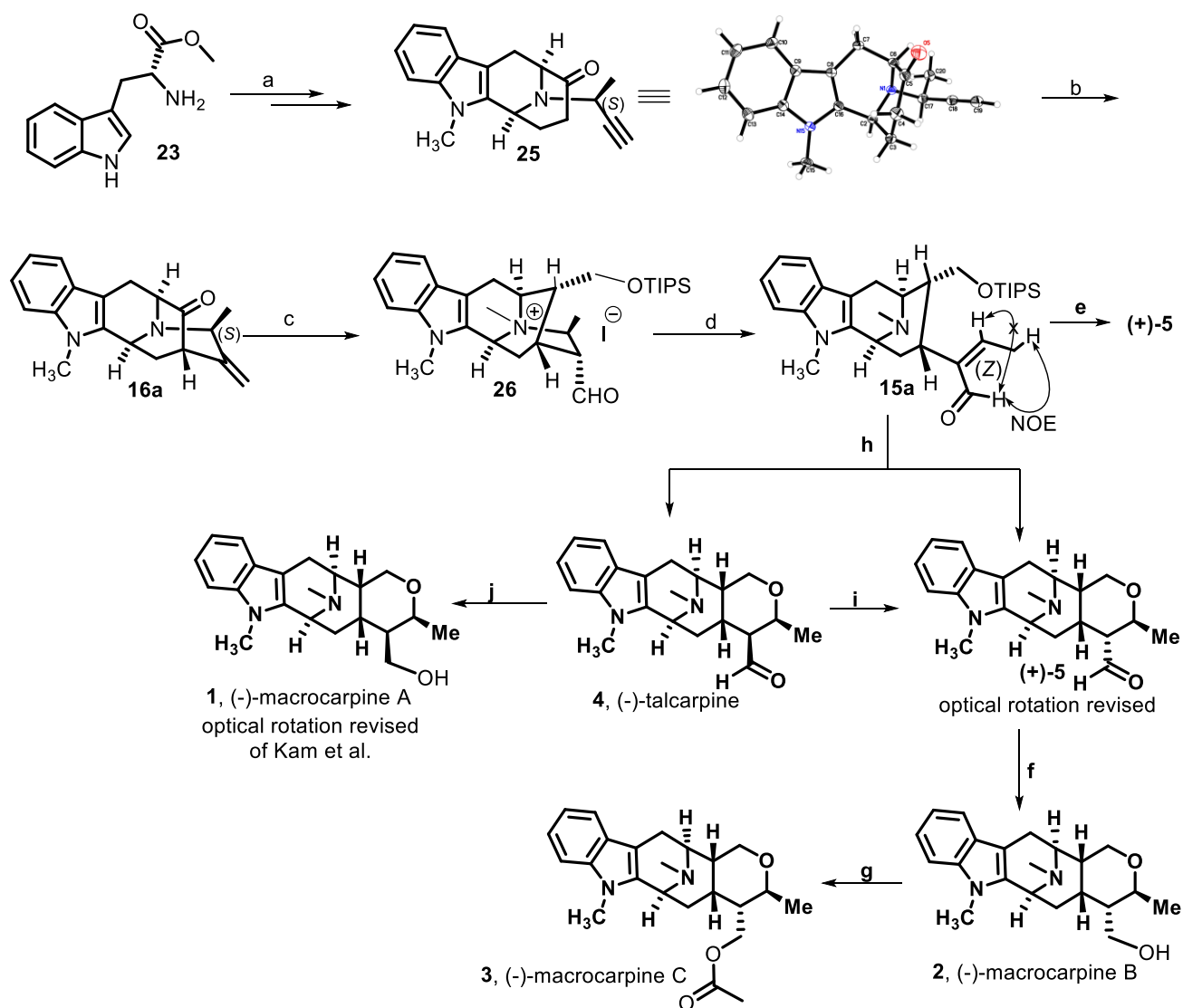
Retrosynthetically, the E-ring of the macroline system present in e.g., macrocarpines A-C (**1-3**) should originate in a stereocontrolled fashion from a Michael-type ring closure¹² of the deprotected alcohol onto the α,β -unsaturated aldehyde (**15**, Scheme 1), which in turn would be available from the pentacyclic ketone intermediates **16** [R = H or CH₃ and (*) = (S)], according to the previously reported route.^{13,14} On the other hand, the C-19 α -methylated alkaloids dihydroperaksine **8** and deoxyperaksine **9** would be available from the TIPS protected diol **18**, which in turn would be available from **17** by a hydroboration-oxidation. The olefin **17** would be accessed from the ketone **16** [with R = H and (*) = (R)] in a few steps. The pentacyclic ketone intermediates **16** would be

available *via* a copper-mediated intramolecular cross-coupling of the vinyl iodides **19** with the enolate.¹³ The vinyl iodides (**19**) would be available from the TIPS-protected terminal alkyne *via* a completely regioselective iodoboration, after the decarboxylation of the β -keto ester **14**. The *trans*-diester would originate as a sole product from the asymmetric Pictet-Spengler reaction of the *N*_b-alkylated tryptophan derivative **13** with the acetal **21** under thermodynamic control. Under these conditions the total synthesis would begin from commercially available D-(+)-tryptophan **23** and the optically pure ethynyl tosylates (see **22**).

2. Results and Discussion

After the successful access to ketone **25** *via* the new route,^{15,16} the key pentacyclic ketone intermediate **16a** was prepared from the terminal alkyne **25** by conversion into the vinyl iodide [see Scheme 1; **19a**, R = CH₃, (*) = (*S*)], and this was followed by a copper-mediated enolate-driven cross-coupling process similar to that reported earlier.¹³ The advanced intermediate, quaternary ammonium salt **26**, which was required for accessing the macroline system, was synthesized by the same procedure reported previously by Edwankar.¹⁴ A *retro*-Michael ring opening of the quaternary salt **26** by treatment with sodium hexamethyldisilazane in THF produced, stereospecifically, the α , β -unsaturated aldehyde **15a** similar to the earlier work of Le Quesne et al.¹² In the previous report, the geometry of the olefin was not determined. We have confirmed the geometry of the olefin to be (*Z*) by the NOE observed upon irradiation of the aldehyde hydrogen atom with the β -methyl group and *vice versa*, as shown in Scheme 2. Deprotection of the TIPS function under mildly acidic conditions and subsequent Michael reaction of the so formed alcohol onto the α , β -unsaturated aldehyde, formed the E-ring of the macroline

type alkaloids in excellent yield. The stereochemistry of the C-19 methyl group was found to be exclusively the β -stereochemistry by NMR experiments, which gave (+)-*N*(4)-methyl-*N*(4),21-*secotalpinine* **5** (major) and (-)-*talcarpine* **4** (minor). Upon aqueous workup after deprotection of the TIPS group under mildly acidic conditions (0.1 *N* aq HCl), and subsequent treatment with *t*-BuOK in THF, the desired (+)-*N*(4)-methyl-*N*(4),21-*secotalpinine* (**5**) was isolated as the exclusive product. This indicated the aldehyde at C-20 was in the thermodynamically more stable position in the α -configuration.

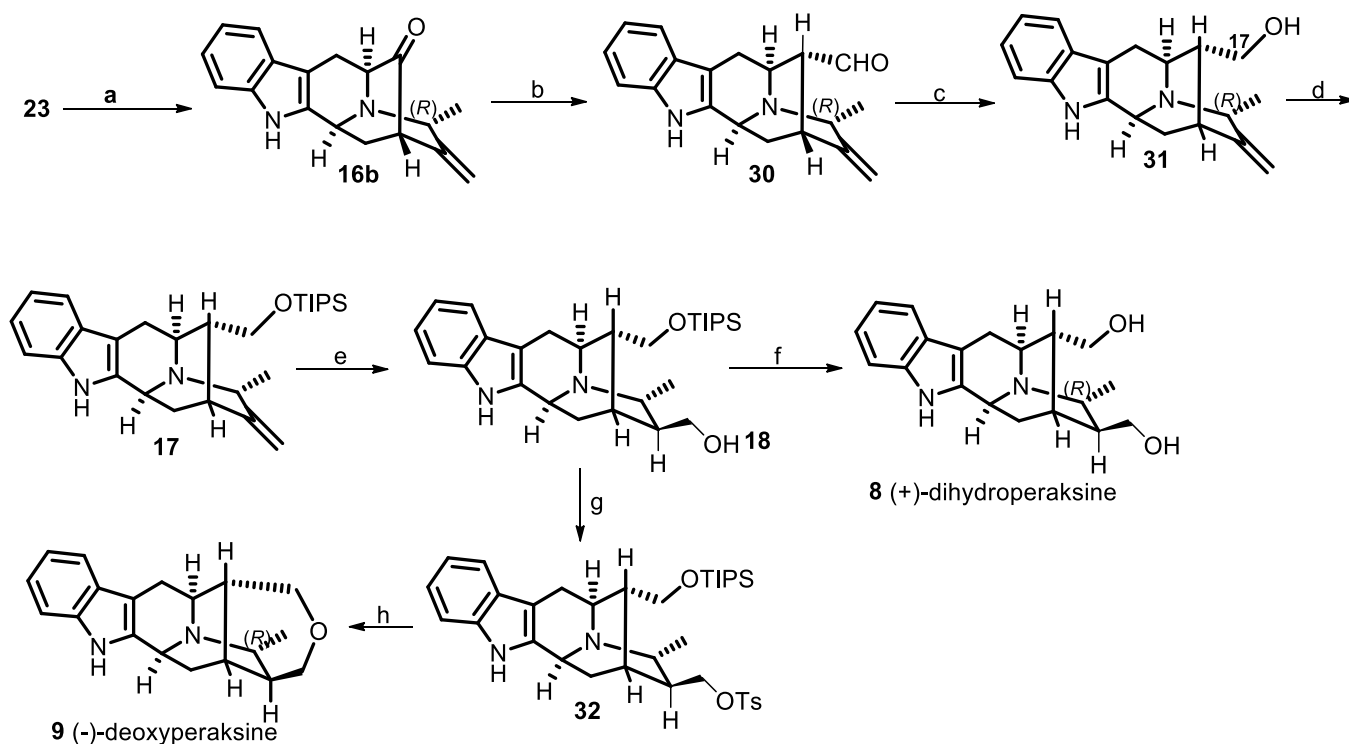


Scheme 2. Reagents and conditions: a) see ref^{15,16}; b) see ref¹³; c) see ref¹⁴; d) NaHMDS (2 equiv), THF, rt, 12 h, **81%**; e) i. 0.1 N HCl, THF, reflux, 3 h; ii. KO*t*-Bu (2 equiv), THF, rt, 10 h, **84%**; f) NaBH₄ (1.5 equiv), EtOH, 0 °C, 5 h, **99%**; g) Ac₂O (1.5 equiv), Py (3 equiv), CH₂Cl₂, rt, 6 h, **92%**; h) 0.1 N HCl, THF, reflux, 3 h, **85%**; i) KO*t*-Bu (2 equiv), THF, rt, 10 h, **82%**; j) NaBH₄ (1.5 equiv), EtOH, 0 °C, 5 h, **99%**;

Both (-)-**4** and (+)-**5** could easily be separated by silica gel chromatography with 1-5% methanol in CH₂Cl₂ (saturated with NH₄OH). (-)-Talcarpine **4** could also be converted completely into (+)-**5** upon treatment with base (Et₃N or K₂CO₃ in MeOH or *tert*-BuOK in THF). The spectral properties of (-)-talcarpine **4** and (+)-*N*(4)-methyl-*N*(4),21-*secotalpinine* **5** were in excellent agreement with the corresponding natural products.² The optical rotation of (+)-**5** has been revised by a personal communication with Professor Toh-Seok Kam [original value, *Tetrahedron*, 2004, $[\alpha]_D^{25} = +19$ (CHCl₃, *c* 0.45); revised value: 2017 $[\alpha]_D^{25} = +36$ (CHCl₃, *c* 0.33); synthetic sample in this report: $[\alpha]_D^{25} = +34.4$ (CHCl₃, *c* 0.61)].¹⁷ The properties of synthetic sample (-)-**4** in this report are in excellent agreement with the ¹H and ¹³C NMR spectra of natural (-)-**4**. The optical rotation was found to be in agreement with the optical rotation reported by Kam et al² (see later for details).

After obtaining the pure aldehydes (-)-**4** and (+)-**5**, completion of the total synthesis of (-)-macrocarpines A-C (**1-3**) was undertaken. Aldehyde (-)-**4** was reduced with sodium borohydride in ethanol to produce (-)-macrocarpine A **1** in 99% isolated yield (Scheme 2). The ¹H, ¹³C, 2D NMR, UV and MS spectra of synthetic (-)-**1** were in excellent agreement with the reported material **1**, except for the optical rotation ($[\alpha]_D^{25} = +117$ (CHCl₃, *c* 0.11)].² The original optical rotation of

(-)-**1** has been revised by a personal communication with Professor Toh-Seok Kam and was in complete accord with a recent natural sample of (-)-**1** [natural: Lim, 2014, unpublished, $[\alpha]_D^{25} = -28$ (CHCl₃, *c* 0.25);¹⁸ synthetic, this report: $[\alpha]_D^{25} = -28$ (CHCl₃, *c* 0.25)] and hence, the optical rotation of the synthetic (-)-macrocarpine A (**1**) and the natural product are in excellent agreement. The reduction of (+)-**5** with sodium borohydride in ethanol furnished the natural product (-)-macrocarpine B (**2**), the spectral properties and optical rotation of which were again in agreement with that of the natural product.² Acetylation of alcohol (-)-**2** with acetic anhydride and pyridine in DCM, produced (-)-macrocarpine C (**3**), whose properties were also in excellent agreement with those of the natural alkaloid (-)-**3**.²



Scheme 3: Reagents and conditions: a) see ref^{13,15,16}; b) Ph₃P(Cl)CH₂OCH₃, *t*-BuOK, benzene, rt, 13 h; 2 *N* aq HCl, THF, 55 °C, 6 h, **80%** in 2 steps; c) NaBH₄, EtOH, 0 °C, 3 h, **90%**; d) 2,6-lutidine, TIPS-OTf, 0 °C to rt, 2 h, **92%**; e) i. BH₃·DMS, THF, rt 2 h; NaBO₃·4H₂O, 2 h; ii.

Na₂CO₃, MeOH, reflux, 5 h, **76%** over 2 steps; f) HF (aq), CH₃CN, 0 °C, 40 min, **89%**; g) TsCl, Et₃N, DMAP, DCM, 2 h, **85%**; h) TBAF, THF, -30 °C to rt, 1 h, **82%**;

After the completion of the total synthesis of the C-19 β -methyl substituted macroline related alkaloids; **1-5**, the focus changed to the synthesis of C-19 α -methyl substituted sarpagine alkaloids (+)-dihydroperaksine **8**, and (-)-deoxyperaksine **9** as mentioned before.

The pentacyclic key intermediate **16b** was accessed from alkyne **29** via the vinyl iodide **19b** (see Scheme 1) by the previously reported copper-mediated enolate-driven cross-coupling process¹³ and its structure was also confirmed by X-ray analysis (see Appendix D for X-ray data).

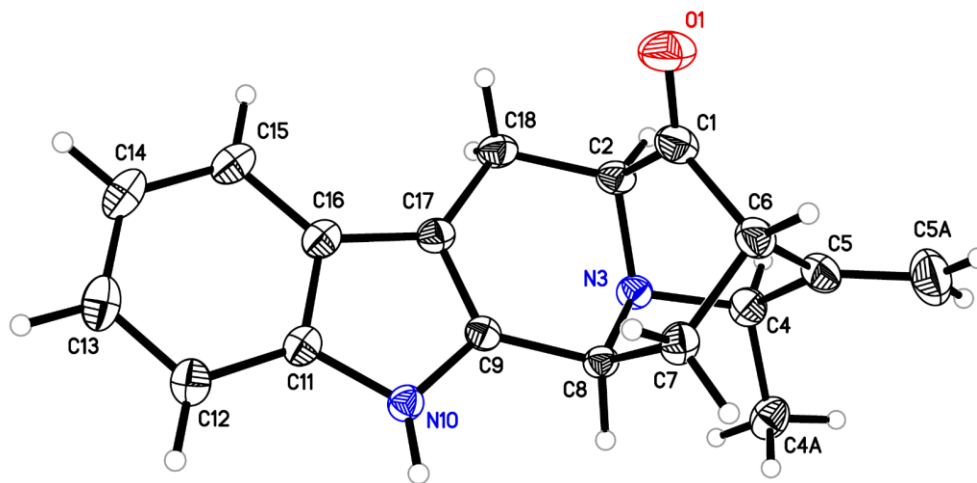


Figure 2. ORTEP representation of **16b**

With the ketone **16b** in hand, a one-carbon homologation of the ketone function was carried out *via* the Wittig-olefination process with (Ph)₃P⁺(Cl⁻)CH₂OCH₃ and potassium *tert*-butoxide in benzene-THF. This furnished a mixture of enol ethers (structures not shown). The mixture of enol

ethers, upon acid mediated hydrolysis (2 N aq HCl in THF), furnished the thermodynamically more stable α -aldehyde **30** as the sole product. The reduction of the aldehyde **30** was performed with sodium borohydride in ethanol, to produce the primary alcohol **31** in 90% yield. The desired product from the Wittig-olefination and hydrolysis could be carried onto the reduction step without purification and the alcohol **31** was isolated in this one-pot process. The protection of the hydroxyl function at C-17 with a TIPS function (**17**) was effected with TIPS-trifluoromethane sulfonate in DCM with 2, 6-lutidine in 92% yield. The hydroboration with $\text{BH}_3\cdot\text{DMS}$, followed by Kabalka oxidation with sodium perborate, was performed to access the primary alcohol from the olefin **17** and this produced the primary alcohol **18** in 76% yield as the exclusive product. The corresponding tertiary alcohol was not observed. Formation of the tertiary alcohol, observed in systems with a C-19 β -methyl function, presumably, was retarded in olefin **17** because of the C-19 α -methyl group. (+)-Dihydroperaksine **8** was prepared simply by removing the TIPS function from **18** with a source of fluoride anion. The TIPS deprotection with TBAF proceeded smoothly and completely but the tetrabutylammonium salt could not be readily removed from the product. The aqueous extraction was avoided due to the very polar nature of the alkaloid, which would have resulted in the partial loss of material. Consequently, it was decided to use an alternative fluoride source of Corey et al., aqueous hydrogen fluoride,¹⁹ in order to remove the solvents and TIPS-F together effectively, *in vacuo*. Accordingly, deprotection of the TIPS function in **18** with aqueous HF in CH_3CN was completed smoothly in 40 minutes at 0 °C and pure synthetic (+)-**8** could be isolated after chromatography in 89% yield (Scheme 3). The optical rotation and spectral data for this synthetic (+)-**8** were in complete agreement with the values reported in the literature for (+)-**8**.¹⁰

To access the ether linkage present in (-)-deoxyperaksine **9**, the primary alcohol in **18** which remained, was activated by tosylation in **32** (Scheme 3). The tosylation was effected in excellent yield with tosyl chloride and DMAP in DCM in 2 hours. Upon TIPS deprotection with TBAF in THF at -30 °C in 1 hour, the so formed primary alcohol reacted with the tosyl group *in situ* to furnish the ether ring present in (-)-deoxyperaksine **9**. The ¹H and ¹³C spectral data of (-)-**9** were not found in the literature.²⁰ This report represents the first report of the ¹H, ¹³C, 2D NMRs, IR and MS characterization of (-)-deoxyperaksine **9**.

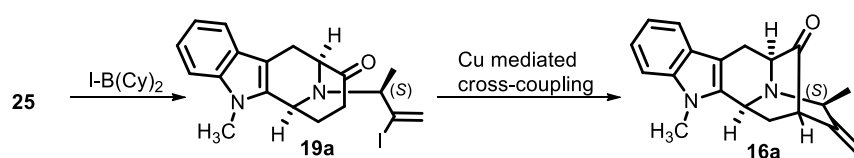
3. Conclusion

In summary, the first total synthesis of member of the C-19 methyl substituted sarpagine/macroline-related alkaloids have been completed *via* the shorter and expanded Pictet-Spengler reaction. The strategy reported here has been illustrated to efficiently access alkaloids with both the α and β C-19 methyl function with 100% diastereoselectivity. Examination of this report also corrects the optical rotation values of (-)-macrocarpine A (**1**) and (+)-*N*(4)-methy, *N*(4), 21-*secotalpinine* (**5**) reported by others.² The optical rotation of (-)-talcarpine **4** was found to be in agreement with (Kam et al., *Tetrahedron*, 2004), one of the two different optical rotations present in literature.^{2,5} Examination of this work clearly indicated that a large group other than benzyl on the *N*_b-nitrogen atom of the D-(+)-tryptophan starting material can still provide 100% diastereoselectivity via internal asymmetric induction. It is important to note that the use of L-tryptophan would have provided the enantiomers of these alkaloids for biological study. In addition, the syntheses described herein have extended the use of the CuI mediated enolate-driven cross-coupling reaction to a completely new system. This general strategy will be useful to access any member of the C-19 methyl substituted sarpagine/macroline alkaloids that are potential drug

candidates, as indicated by their biological activity reported in the literature and presented in the Introduction (see General Introduction).

4. Experimental Section

Preparation of 16a from 25^{13,14}

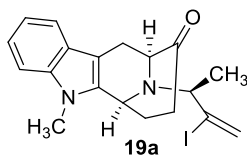


An oven dried flask fitted with an addition funnel was cooled under argon and charged with the alkyne **25** (2.10 g, 7.55 mmol) and it was dissolved in freshly distilled CH₂Cl₂ (50 mL) and hexanes (7.0 mL). The flask was cooled to 0 °C with ice and I-B(Cy)₂ (30.2 mL, 15.1 mmol, 0.5 M solution in hexanes) was added dropwise every 0.5 h in three portions, over a total period of 1.5 h. After the last addition, the reaction mixture was allowed to stir at 0 °C for another 0.5 h, after which the ice bath was removed and the mixture was stirred at rt for 2 h. After stirring at rt for 2 h, another 0.5 eq of I-B(Cy)₂ (7.6 mL, 3.78 mmol) was added dropwise at rt and the mixture was allowed to stir for another 2 h. After this 2 h period, the mixture was treated with glacial acetic acid (4.8 ml, 83.1 mmol) at 0 °C and stirred at rt for 1.15 h. At this point the flask was again cooled to 0 °C and a solution of cold aq 3 M NaOH (40.3 mL, 121 mmol) and 30% H₂O₂ (2.6 mL, 23 mmol) was added and the stirring was maintained for 1 h at rt. The biphasic solution which resulted was transferred to a larger flask and diluted with CH₂Cl₂ (200 mL) and water (50 mL), after which the two layers were separated. The aq layer was extracted with another 200 mL of CH₂Cl₂. The

combined CH₂Cl₂ layers were treated sequentially with solutions of 5% KF in methanol (160 mL) and 5% aq sodium bisulfite (160 mL) under vigorous stirring for 5 min. The aq layer was separated, extracted with CH₂Cl₂ (2 x 80 mL), after which the combined organic layers were washed with brine, dried (Na₂SO₄), filtered and concentrated under reduced pressure. Purification by chromatography on silica gel (EtOAc/hexane, 1: 4) afforded vinyl iodide **19a** (2.32 g, 77%) as a white solid.

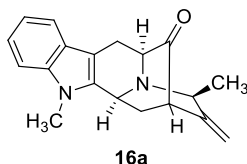
In a sealed tube with a magnetic stir bar, a mixture of vinyl iodide **19a** (420 mg, 1.0 mmol), CuI (190 mg, 1.0 mmol), *cis*-1,2- cyclohexanediol (116 mg, 1.0 mmol), Cs₂CO₃ (1.30 g, 4.0 mmol) and TEMPO (468 mg, 3.0 mmol) was added dry DMF (2.0 mL). The mixture was degassed under reduced pressure at rt and refilled with argon (3-4 times). The reaction mixture was then placed on a pre-heated oil bath (130 °C) and heated under argon for 10 h. At this point, TLC (silica gel, EtOAc/hexane = 1: 3) indicated the absence of starting material **19a**. The mixture was cooled to rt and diluted with EtOAc (10 mL) and water. The aq layer was separated and extracted with EtOAc (2 x 10 mL). The combined organic layer was washed with water (2 x 50 mL), brine (3 x 50 mL) and dried (Na₂SO₄). The solvent was removed under reduced pressure and the residue was purified by chromatography on neutral alumina (EtOAc/hexane = 1: 3) to provide the cross-coupling product **16a** (251 mg) in 86% isolated yield.

(6*S*,10*S*)-12-((*S*)-3-Iodobut-3-en-2-yl)-5-methyl-7,8,10,11-tetrahydro-5*H*-6,10-epiminocycloocta[*b*]indol-9(6*H*)-one (19a)



^{13}C NMR (75 MHz, CDCl_3): δ 210.2, 137.1, 133.0, 126.4, 125.8, 122.6, 121.6, 119.3, 118.2, 108.9, 106.6, 62.3, 60.7, 47.6, 34.4, 29.7, 29.3, 21.2, 19.7. All other spectroscopic data were identical with the published data for **19a**.¹⁴ This material was used for the next step without further characterization.

(6*S*,8*S*,11*aS*)-5,8-Dimethyl-9-methylene-6,8,9,10,11*a*,12-hexahydro-6,10-methanoindolo[3,2-*b*]quinolizin-11(5*H*)-one (16a)



^1H NMR (300 MHz, CDCl_3): δ 7.50 (d, 1H, $J = 7.4$ Hz), 7.24-7.26 (m, 1H), 7.18 (td, 1H, $J = 7.5$, 0.9 Hz), 7.05-7.10 (m, 1H), 5.1 (d, 1H, $J = 2.5$ Hz), 5.01 (d, 1H, $J = 2.5$ Hz), 4.41 (dd, 1H, $J = 9.5$, 2.1 Hz), 3.87-3.95 (m, 1H), 3.72 (d, 1H, $J = 5.6$ Hz), 3.6 (s, 3H), 3.34 (dd, 1H, $J = 15.6$, 1.3 Hz), 3.05-3.07 (m, 1H), 2.92 (dd, 1H, $J = 15.6$, 6.1 Hz), 2.57-2.65 (m, 1H), 2.10-2.17 (m, 1H), 1.49 (d, 3H, $J = 6.7$ Hz). All other spectroscopic data were identical with the published data for **16a**.¹⁴ This material was used for the next step without further characterization.

Procedure for the Preparation of **26 from **16a****¹⁴

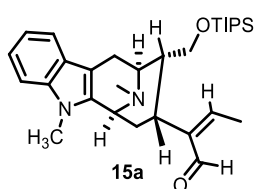
The methiodide salt **26** was prepared from the ketone **16a**, according to the previously reported method.¹⁴

Procedure for the Preparation of **15a from **26****

To a solution of the methiodide salt **26** (50 mg, 0.10 mmol) in dry THF (5 mL), NaHMDS (37 mg, 0.2 mmol) was added at 0 °C, after which the mixture was allowed to stir for 12 h at rt. At that time, analysis by TLC and LCMS indicated the disappearance of **26**. The THF was removed under reduced pressure and the residue was purified by flash chromatography (silica gel, 2-5 % MeOH

in DCM) to provide the olefin **15a** (40.4 mg) in 81% yield as a colorless oil (LRMS $M+H^+ = 495.50$).

(Z)-2-((6S,8R,9R,10S)-5,12-Dimethyl-9-(((triisopropylsilyl)oxy)methyl)-6,7,8,9,10,11-hexahydro-5H-6,10-epiminocycloocta[b]indol-8-yl)but-2-enal (15a**)**



¹H NMR (500 MHz, $CDCl_3$): δ 10.08 (s, 1H), 7.6 (d, 1H, $J = 7.7$ Hz), 7.31-7.28 (m, 1H, overlapped with chloroform peak), 7.20 (t, 1H, $J = 7.5$ Hz), 7.13 (t, 1H, $J = 7.3$ Hz), 6.37 (q, 1H, $J = 7.3$ Hz), 4.04 (br s, 1H), 3.94 (t, 1H, $J = 8.7$ Hz), 3.62 (s, 3H), 3.50-3.43 (m, 1H), 3.33 (dd, 1H, $J = 16.6$ Hz, 7.4 Hz), 2.94 (d, 1H, $J = 12.8$ Hz), 2.65 (d, 1H, $J = 16.7$ Hz), 2.34 (s, 3H), 2.23-2.15 (m, 1H), 2.10 (d, 3H, $J = 7.2$ Hz), 1.38-1.31 (m, 1H), 1.07 (s, 21H). **HRMS** (ESI) m/z ($M+H^+$)⁺ Calcd for $C_{30}H_{47}N_2O_2Si$ 495.3401, found 495.3404. **Rf**: 0.27 (5% MeOH in DCM); $[\alpha]^{25}_D$ (c 0.2 $CHCl_3$): +20.0. The characterization data for this compound were in complete agreement with that in the earlier report.¹⁴ The geometry of the olefin was determined to be (Z) by NMR NOE spectroscopic analysis (see Appendix E for NOE spectra).

Procedure for the preparation of (-)-talcarpine (4**) and (+)-N(4)-methyl-N(4), 21-secotalpinine (**5**) from (+)-**15a****

The α , β -unsaturated aldehyde **15a** (50 mg, 0.1 mmol) was placed in a round bottom flask equipped with a magnetic stir and a reflux condenser. The THF (18 mL) and 2 N aq HCl (2 mL) was added to the round bottom flask. The mixture, which resulted, was held at reflux for 5 h. After that, the

solvent was removed under reduced pressure and ice cold water was added to the flask. The pH of the solution was brought to 8-9 with cold NH_4OH . The solution was extracted with DCM (4 x 20 mL) and the organic layer was washed with brine and dried (Na_2SO_4). The solvent was removed under reduced pressure to provide a mixture of aldehydes as a colorless oil. The residue was purified by silica gel column chromatography (1-5% MeOH in DCM sat with aq NH_4OH) to provide (-)-**4** (LRMS $\text{M}+\text{H}^+ = 339.30$, 8.6 mg, 25%) and (+)-**5** (LRMS $\text{M}+\text{H}^+ = 339.30$, 20.5 mg, 60%) as colorless oils.

Procedure for the preparation of (+)-5** from (+)-**15a****

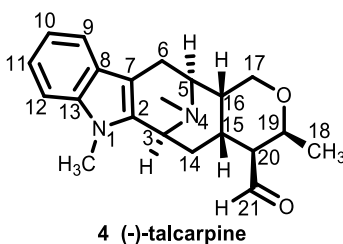
The α, β -unsaturated aldehyde **15a** (50 mg, 0.1 mmol) was placed in a round bottom flask equipped with a magnetic stir and a reflux condenser. The THF (18 mL) and 2 N aq HCl (2 mL) was added to the round bottom flask. The mixture, which resulted, was held at reflux for 5 h. After that, the solvent was removed under reduced pressure and ice cold water was added to the flask. The pH of the solution was brought to 8-9 with cold aq NH_4OH . The solution was extracted with DCM (4 x 20 mL) and the organic layer was washed with brine and dried (Na_2SO_4). The solvent was removed under reduced pressure to provide a mixture of aldehydes as a colorless oil (31 mg, 90% crude). The residue was dried under high vacuum for 5 h before dissolving in 5 mL of dry THF. Potassium *tert*-butoxide (22.7 mg, 0.2 mmol) was added to the above solution and it was left stirring at rt for 12 h. After that, the solvent was removed under reduced pressure and the residue was dissolved in DCM (10 mL) and ice cold water (5 mL). The organic layer was separated and the aq layer was extracted with another 5 mL of DCM. The combined organic layers were washed with brine and dried (Na_2SO_4) to provide 32.8 mg (96%) of crude **5** which was purified by silica gel column

chromatography (1-5% MeOH in DCM sat. with aq NH₄OH) to provide the aldehyde (+)-**5** (28.7 mg, 84%) as a white waxy solid.

Procedure for the conversion of (-)-**4** into (+)-**5**

To a solution of (-)-talcarpine **4** (5 mg, 0.01 mmol) in THF (2 mL), potassium *tert*-butoxide (2.3 mg, 0.02 mmol) was added and the solution, which resulted, was stirred at rt for 5 h. After that, the THF was removed under reduced pressure and the residue was dissolved in DCM (5 mL) and to this ice cold water (5 mL) was added. The organic layer was separated and the aq layer was extracted with another 3 mL of DCM. The combined DCM layers were washed with brine (3 x 20 mL) and dried (Na₂SO₄). The solvent was evaporated under reduced pressure to provide a light yellow residue which was purified by silica gel column chromatography (1-5% MeOH in DCM sat. with aq NH₄OH) to provide (+)-**5** (2.8 mg, 82%) as a white waxy solid.

(-)-Talcarpine (**4**)



¹H NMR (500 MHz, CDCl₃): see Table 1; **¹³C NMR** (75 MHz, CDCl₃): see Table 2; **HRMS** (ESI) *m/z* (M+H)⁺ Calcd for C₂₁H₂₇N₂O₂ 339.2067, found 339.2075; **R_f**: 0.42 (silica gel, 5 % MeOH in DCM);

Note: To the best of our knowledge there are at least two different values for the optical rotation of the minor diastereomer, (-)-talcarpine **4**, present in the literature. In the first report of **4** by

Schmid et al, there was no optical rotation reported.⁴ Wong et al. reported the optical rotation to be $[\alpha]_{\text{D}}^{25} = -49$ (CHCl_3 , c 0.077)⁵ and Kam et al. reported the rotation as $[\alpha]_{\text{D}}^{25} = -26$ (CHCl_3 , c 0.12).²

Optical rotation: Synthetic sample, this report $[\alpha]_{\text{D}}^{25}$ (c 0.1 CHCl_3): -30.0; natural sample, reported by Kam et al, 2004² $[\alpha]_{\text{D}}^{25}$ (c 0.12 CHCl_3): -26; natural sample, reported by Wong et al, 1996⁵ $[\alpha]_{\text{D}}^{25}$ (c 0.077 CHCl_3): -49. The characterization data of the synthetic talcarpine were in complete agreement with that of natural (-)-talcarpine 4, reported by Kam et al.²

Comparison between Natural and Synthetic (-)-Talcarpine (4)

Table 1: ¹H NMR Spectral Data for Natural and Synthetic (-)-Talcarpine (4) in CDCl₃

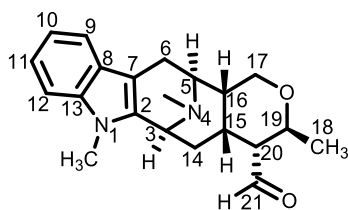
H#	¹ H Natural ² by Kam et al (400 MHz)	¹ H Natural ⁵ by Wong et al (270 MHz) ^a	¹ H Synthetic (this report) (500 MHz)
3	3.98 (1H, m)	4.05-3.92 (1H, m)	4.00-3.95 (1H, m)
5	2.90 (1H, d, <i>J</i> = 7 Hz)	2.89 (1H, d, <i>J</i> = 7 Hz)	2.90 (1H, d, <i>J</i> = 6.8 Hz)
6	2.45 (1H, d, <i>J</i> = 16 Hz) 3.27 (1H, dd, <i>J</i> = 16, 7 Hz)	-a 3.24 (1H, dd, <i>J</i> = 16, 7 Hz)	2.45 (1H, d, <i>J</i> = 16.7 Hz) 3.27 (1H, dd, <i>J</i> = 16.4, 6.8 Hz)
9	7.49 (1H, br d, <i>J</i> = 8 Hz)	7.48 (1H, br d, <i>J</i> = 7 Hz)	7.48 (1H, br d, <i>J</i> = 7.8 Hz)
10	7.10 (1H, td, <i>J</i> = 8, 1 Hz)	7.09 (1H, br t, <i>J</i> = 7 Hz)	7.12-7.07 (1H, m)
11	7.19 (1H, td, <i>J</i> = 8, 1 Hz)	7.19 (br t, <i>J</i> = 7 Hz)	7.21-7.17 (1H, m)
12	7.29 (1H, br d, <i>J</i> = 8 Hz)	7.28 (1H, br d, <i>J</i> = 7 Hz)	7.29 (1H, br d, <i>J</i> = 8.2 Hz)
14	1.45 (1H, ddd, <i>J</i> = 12, 4, 3 Hz) 2.50 (1H, td, <i>J</i> = 12, 4 Hz)	1.48-1.40 (1H, m) 2.55-2.41 (1H, m)	1.47-1.42 (1H, m) 2.50 (1H, td, <i>J</i> = 12.9, 3.9 Hz)
15	2.20 (1H, m)	2.24-2.15 (1H, m)	2.22-2.16 (1H, m)
16	2.06 (1H, dt, <i>J</i> = 11, 5 Hz)	2.09-2.00 (1H, m)	2.08-2.02 (1H, m)
17	3.89 (1H, dd, <i>J</i> = 12, 5 Hz) 4.14 (1H, t, <i>J</i> = 12 Hz)	3.89 (1H, dd, <i>J</i> = 11, 5 Hz) 4.13 (1H, t, <i>J</i> = 11 Hz)	3.89 (1H, dd, <i>J</i> = 11.4, 4.9 Hz) 4.13 (1H, t, <i>J</i> = 11.7 Hz)
19	3.98 (1H, m)	4.05-3.92 (1H, m) ^a	4.00-3.95 (1H, m)
20	1.79 (1H, br s,)	1.78 (1H, br s)	1.79 (1H, br s)
21	9.95 (1H, d, <i>J</i> = 3 Hz)	9.94 (1H, d, <i>J</i> = 3 Hz)	9.95 (1H, d, <i>J</i> = 3.2 Hz)
18-Me	1.30 (3H, d, <i>J</i> = 7 Hz)	1.30 (3 H, <i>J</i> = 6.8 Hz)	1.30 (3H, d, <i>J</i> = 6.7 Hz)
<i>N</i> (1)-Me	3.62 (3H, s)	3.62 (3H, s)	3.62 (3H, s)
<i>N</i> (4)-Me	2.32 (3H, s)	2.32 (3H, s)	2.32 (3H, s)

^aThere are typos and missing proton signals in the ¹H NMR reported by Wong et al.⁵

Table 2: Comparison of the ^{13}C NMR Spectral Data for Natural and Synthetic (-)-Talcarpine (4) in CDCl_3

C#	^{13}C Natural ² (100 MHz) Kam et al.	^{13}C Natural ⁵ (67.8 MHz) Wong et al.	^{13}C Synthetic (this report) (75 MHz)
2	132.8	132.6	132.6
3	53.5	53.5	53.5
5	54.5	54.4	54.5
6	22.5	22.4	22.5
7	106.6	106.6	106.6
8	126.2	126.3	126.4
9	118.1	118.1	118.1
10	118.9	118.9	118.9
11	121.0	120.9	121.0
12	108.7	108.7	108.8
13	137.2	136.9	137.0
14	30.1	30.0	30.0
15	27.0	27.0	27.0
16	39.4	39.4	39.4
17	68.8	68.8	68.8
18	19.2	19.2	19.2
19	69.4	69.4	69.5
20	54.6	54.5	54.6
21	204.7	204.7	204.7
N(4)-Me	41.8	41.7	41.8
N(1)-Me	29.1	28.9	29.0

(+)-N(4)-Methyl-N(4), 21-secotalpinine (5)



5 (+)-N(4)-methyl-N(4), 21-secotalpinine

¹H NMR (500 MHz, CDCl₃): see Table 3; **¹³C NMR** (125 MHz, CDCl₃): see Table 4; **HRMS** (ESI) *m/z* (M+H)⁺ Calcd for C₂₁H₂₇N₂O₂ 339.2067, found 339.2073; **R_f**: 0.24 (5 % MeOH in DCM); The characterization data of the synthetic (+)-**5** were in complete agreement with that of natural (+)-**5**.²

Optical rotation: Synthetic sample, this report [α]_D²⁵ (*c* 0.61 CHCl₃): +34.43; Natural sample, original report (2004) [α]_D²⁵ (*c* 0.45 CHCl₃): +19; Natural sample, revised (2017) [α]_D²⁵ (*c* 0.33 CHCl₃): +36. The optical rotation value of (+)-**5** was revised *via* a personal communication with Professor Toh-Seok Kam and it is excellent agreement with the synthetic (+)-**5**.

Comparison between Natural and Synthetic (+)-5

Table 3: ¹H NMR Spectral Data for Natural and Synthetic (+)-*N*(4)-Methyl-*N*(4), 21-secotalpinine (5) in CDCl₃

H#	¹ H Natural ² (400 MHz)	¹ H Synthetic (this report) (500 MHz)
3	3.93 (1H, m)	4.00-3.92 (1H, m)
5	2.96 (1H, d, J = 7 Hz)	3.0 (1H, d, J = 6.2 Hz)
6	2.49 (1H, d, J = 16 Hz) 3.30 (1H, dd, J = 16, 7 Hz)	2.52 (1H, d, J = 16.5 Hz) 3.34 (1H, dd, J = 16.5, 7 Hz)
9	7.52 (1H, br d, J = 8 Hz)	7.55 (1H, br d, J = 7.8 Hz)
10	7.13 (1H, td, J = 8 Hz)	7.18-7.14 (1H, m)
11	7.21 (1H, td, J = 8, 1 Hz)	7.27-7.23 (1H, m)
12	7.31 (1H, br d, J = 8 Hz)	7.34 (1H, br d, J = 8.1 Hz)
14	1.28 (1H, m) 2.37 (1H, m)	1.30 (1H, br d, J = 8.8 Hz)) 2.44-2.38 (1H, m)
15	2.37 (1H, m)	2.44-2.38 (1H, m)
16	1.93 (1H, m)	1.98-1.93 (1H, m)
17	3.75 (1H, dd, J = 12, 5 Hz) 4.06 (1H, t, J = 12 Hz)	3.79 (1H, dd, J = 11.7, 4.5 Hz) 4.10 (1H, t, J = 11.7 Hz)
19	3.93 (1H, m)	4.00-3.92 (1H, m)
20	2.37 (1H, m)	2.44-2.38 (1H, m)
21	9.41 (1H, br s)	9.95 (1H, br s)
18-Me	1.20 (3H, d, J = 7 Hz)	1.23 (3H, d, J = 6.0 Hz)
<i>N</i> (1)-Me	3.58 (3H, s)	3.62 (3H, s)
<i>N</i> (4)-Me	2.31 (3H, s)	2.35 (3H, s)

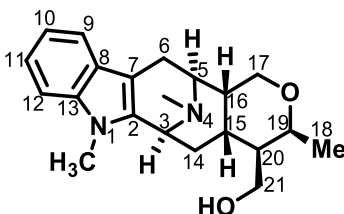
Table 4: Comparison of the ^{13}C NMR Spectral Data for Natural and Synthetic (+)-*N*(4)-Methyl-*N*(4), 21-secotalpinine (5) in CDCl_3

C#	^{13}C Natural ² (100 MHz)	^{13}C Synthetic (this report) (125 MHz)
2	132.8	132.9
3	53.1	53.2
5	54.9	55.0
6	22.4	22.5
7	106.6	106.7
8	126.2	126.3
9	117.9	118.0
10	118.9	119.0
11	121.0	121.1
12	108.9	109.0
13	137.0	137.0
14	26.7	26.8
15	26.1	26.2
16	42.5	42.6
17	67.1	67.2
18	20.2	20.3
19	67.8	67.9
20	57.7	57.9
21	203.0	203.3
<i>N</i> (4)-Me	41.6	41.7
<i>N</i> (1)-Me	29.0	29.1

Procedure for the Synthesis of (-)-Macrocarpine A (1) from (-)-Talcarpine (4)

A solution of the aldehyde (-)-4 (12 mg, 0.035 mmol) in dry ethanol (2 mL) was cooled to 0 °C and stirred for 5 min. To that above solution, NaBH₄ (1.5 mg, 0.039 mmol) was added at 0 °C and the mixture, which resulted, was stirred at 0 °C for 5 h. After completion of the reaction, as indicated by TLC (silica gel) and LRMS, the reaction mixture was diluted with DCM (10 mL) and water (5 mL). The organic layer was separated and the aq layer was extracted with another portion of DCM (10 mL). The combined organic layers were washed with brine and dried (Na₂SO₄). The solvent was removed under reduced pressure to provide a colorless oil. This material was purified by column chromatography (silica gel, 1-5% MeOH in DCM sat. aq NH₄OH) to provide (-)-1 (LRMS M+H⁺ = 341.15) as waxy white solid (12 mg, 99%).

(-)-Macrocarpine A (1)



¹H NMR: see Table 5; **¹³C NMR:** see Table 6; **HRMS (ESI) *m/z* (M+H)⁺** Calcd for C₂₁H₂₉N₂O₂ 341.2224, found 341.2228; **R_f:** 0.14 (5 % MeOH in DCM), 0.6 (5% MeOH in EtOAc, sat. aq NH₄OH);

Optical rotation: The synthetic sample, this report [α]²⁵_D (*c* 0.25 CHCl₃): -28.0; The natural sample, original report (2004)² [α]²⁵_D (*c* 0.11 CHCl₃): +117; The natural sample, revised (2016) [α]²⁵_D (*c* 0.25 CHCl₃): -28.0. The optical rotation value was revised *via* a personal communication

with professor Toh-Seok Kam and the synthetic (-)-macrocarpine A (**1**) was in excellent agreement with natural (-)-macrocarpine A (**1**).²

Comparison between Natural and Synthetic (-)-Macrocarpine A (**1**)

Table 5: Comparison of the ¹H NMR Spectral Data for Natural and Synthetic (-)-Macrocarpine A (1**) in CDCl₃**

H#	¹ H Natural ² (400 MHz)	¹ H Synthetic (this report) (500 MHz)
3	3.96 (1H, m)	4.0-3.91 (1H, m)
5	2.87 (1H, d, <i>J</i> = 7 Hz)	2.85 (1H, d, <i>J</i> = 6.9 Hz)
6	2.47 (1H, d, <i>J</i> = 17 Hz) 3.25 (1H, dd, <i>J</i> = 17, 7 Hz)	2.47 (1H, d, <i>J</i> = 16.5 Hz) 3.25 (1H, dd, <i>J</i> = 17, 7 Hz)
9	7.49 (1H, br d, <i>J</i> = 8 Hz)	7.50 (1H, br d, <i>J</i> = 7.7 Hz)
10	7.10 (1H, td, <i>J</i> = 8, 1 Hz)	7.13-7.07 (1H,m)
11	7.19 (1H, td, <i>J</i> = 8, 1 Hz)	7.22-7.16 (1H, m)
12	7.29 (1H, br d, <i>J</i> = 8 Hz)	7.29 (1H, br d, <i>J</i> = 8 Hz)
14	1.42 (1H, ddd, <i>J</i> = 13, 5, 2 Hz) 2.50 (1H, td, <i>J</i> = 13, 4 Hz)	1.42 (1H, ddd, <i>J</i> = 12.7, 4.4, 1.8 Hz) 2.50 (1H, td, <i>J</i> = 12.9, 4.1 Hz)
15	2.06 (1H, dt, <i>J</i> = 13, 5 Hz))	2.07-1.97 (1H, m)
16	2.15 (1H, dt, <i>J</i> = 11, 5 Hz)	2.20-2.10 (1H, m)
17	3.79 (1H, dd, <i>J</i> = 11, 5 Hz) 4.07 (1H, t, <i>J</i> = 11 Hz)	3.81-3.75 (1H, m) 4.07 (1H, t, <i>J</i> = 11.7 Hz)
19	3.96 (1H, m)	4.0-3.91 (1H, m)
20	1.07 (1H, m)	1.07 (1H, m)
21	3.69 (1H, dd, <i>J</i> = 11, 4 Hz) 3.81 (1H, dd, <i>J</i> = 11, 6 Hz)	3.69 (1H, dd, <i>J</i> = 11.2, 3.7 Hz) 3.81-3.75 (1H, m)
18-Me	1.24 (3H, d, <i>J</i> = 7 Hz)	1.24 (3H, d, <i>J</i> = 6.6 Hz)

<i>N</i> (1)-Me	3.62 (3H, s)	3.63 (3H, s)
<i>N</i> (4)-Me	2.31 (3H, s)	2.31 (3H, s)

Table 6: Comparison of the ^{13}C NMR Spectral Data for Natural and Synthetic (-)-Macropine A (1) in CDCl_3

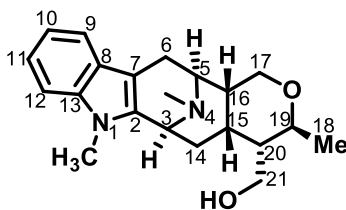
C#	^{13}C Natural ² (100 MHz)	^{13}C Synthetic (this report) (75 MHz)
2	133.2	133.2
3	53.7	53.6
5	54.6	54.5
6	22.6	22.5
7	106.6	106.6
8	126.4	126.4
9	118.1	118.1
10	118.8	118.8
11	120.8	120.8
12	108.7	108.7
13	136.9	136.9
14	30.7	30.8
15	28.6	28.7
16	39.3	39.3
17	68.9	96.0
18	18.8	18.8

19	71.2	71.2
20	43.6	43.5
21	63.1	63.2
<i>N</i> (4)-Me	41.7	41.7
<i>N</i> (1)-Me	29.0	29.0

Procedure for Synthesis of (-)-Macroparpine B (2) from (+)-*N*(4)-Methyl-*N*(4), 21-secotalpinine (5)

A solution of the aldehyde (+)-**5** (20 mg, 0.06 mmol) in dry ethanol (3 mL) was cooled to 0 °C and stirred for 5 min. To that above solution, NaBH₄ (2.4 mg, 0.065 mmol) was added at 0 °C and the reaction, which resulted, was stirred at 0 °C for 5 h. After completion of the reaction as indicated by TLC and LRMS, the reaction was diluted with DCM (10 mL) and water (5 mL). The organic layer was separated and the aq layer was extracted with another portion of DCM (10 mL). The combined organic layers were washed with brine and dried (Na₂SO₄). The solvent was removed under reduced pressure to provide a colorless oil. This material was purified by column chromatography (silica gel, 1-5% MeOH in DCM sat. aq NH₄OH) to provide (-)-**2** (LRMS M+H⁺ = 341.15) as waxy white solid (19.9 mg, 99%).

(-)-Macroparpine B (2)



¹H NMR: see Table 7; **¹³C NMR:** see Table 8; **HRMS (ESI) *m/z* (M+H)⁺** Calcd for C₂₁H₂₉N₂O₂ 341.2224, found 341.2223; **R_f:** 0.4 (silica gel, 10 % MeOH in DCM), 0.1 (silica gel, 5% MeOH in DCM);

Optical rotation: The synthetic sample, this report [α]_D²⁵ (*c* 1.0 CHCl₃): -49.0; The natural sample [α]_D²⁵ (*c* 0.34 CHCl₃): -51; The characterization data of the synthetic (-)-**2** were in complete agreement with that of natural (-)-**2**.²

Comparison between Natural and Synthetic (-)-Macrocarpine B (2)

Table 7: Comparison of the ¹H NMR Spectral Data for Natural and Synthetic (-)-Macroparpine B (2) in CDCl₃

H#	¹ H Natural ² (400 MHz)	¹ H Synthetic (this report) (300 MHz)
3	3.98 (1H, t, J = 3 Hz)	3.98 (1H, br t, J = 3.1 Hz)
5	2.91 (1H, d, J = 7 Hz)	2.91 (1H, d, J = 6.9 Hz)
6	2.43 (1H, d, J = 17 Hz) 3.26 (1H, dd, J = 17, 7 Hz)	2.43 (1H, d, J = 16.5 Hz) 3.36-3.21 (1H, m)
9	7.49 (1H, br d, J = 8 Hz)	7.50 (1H, br d, J = 7.6 Hz)
10	7.10 (1H, td, J = 8, 1 Hz)	7.14-7.07 (1H, m)
11	7.18 (1H, td, J = 8, 1 Hz)	7.19 (1H, br t, J = 7.1 Hz)
12	7.29 (1H, br d, J = 8 Hz)	7.29 (1H, br d, J = 8.0 Hz)
14	1.54 (1H, ddd, J = 12, 4, 3 Hz) 2.29 (1H, m)	1.58-1.49 (1H, m) 2.29-2.22 (1H, m)
15	1.97 (1H, dt, J = 13, 4 Hz)	2.02-1.92 (1H, m)
16	1.86 (1H, dt, J = 11, 4 Hz)	1.90-1.81 (1H, m)
17	3.73 (1H, dd, J = 11, 4 Hz) 4.06 (1H, t, J = 11 Hz)	3.73 (1H, dd, J = 11.4, 4.6 Hz) 4.07 (1H, t, J = 11.6 Hz)
19	3.49 (1H, m)	3.54-3.44 (1H, m)
20	1.46 (1H, m)	1.49-1.40 (1H, m)
21	3.31 (1H, dd, J = 11, 8 Hz)	3.36-3.21 (1H, m)

	3.49 (1H, m)	3.54-3.44 (1H, m)
18-Me	1.15 (3H, d, J = 6 Hz)	1.16 (3H, d, J = 6.1 Hz)
N(1)-Me	3.62 (3H, s)	3.62 (3H, s)
N(4)-Me	2.30 (3H, s)	2.31 (3H, s)

Table 8: Comparison of the ¹H NMR Spectral Data for Natural and Synthetic (-)-Macroparpine B (2) in CDCl₃

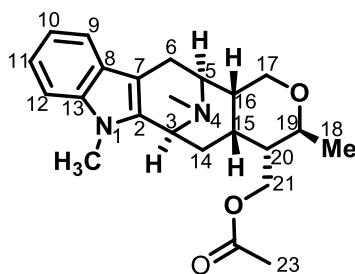
C#	¹³ C Natural ² (100 MHz)	¹³ C Synthetic (this report) (75 MHz)
2	133.2	133.3
3	53.6	53.6
5	55.1	55.0
6	22.5	22.5
7	106.7	106.7
8	126.4	126.4
9	117.9	117.9
10	118.8	118.8
11	120.7	120.7
12	108.8	108.8
13	137.0	137.0
14	25.3	25.4

15	26.7	27.0
16	43.7	43.5
17	67.6	67.6
18	20.2	20.3
19	70.5	70.5
20	46.8	46.8
21	61.6	61.7
<i>N</i> (4)-Me	41.7	41.7
<i>N</i> (1)-Me	29.0	29.0

Preparation of (-)-Macropine C (3) from (-)-Macropine B (2)

In a round bottom flask, the alcohol (-)-2 (10 mg, 0.03 mmol) was dissolved in DCM (2 mL). To that above solution, acetic anhydride (5 μ L, 0.044 mmol) and pyridine (7 μ L, 0.088 mmol) were added and the solution, which resulted, was stirred at rt for 6 h, until the disappearance of the SM as indicated by TLC (silica gel) and LRMS. The reaction mixture was diluted with DCM (10 mL) and water (5 mL). The organic layer was separated and the aq layer was extracted with another portion of DCM (5 mL). The combined organic layers were washed with brine and dried (Na_2SO_4). The solvent was removed under reduced pressure to provide a brownish residue which was purified by column chromatography (silica gel, 1-3% MeOH in DCM sat aq NH_4OH) to provide (-)-macropine C 3 (LRMS $\text{M}+\text{H}^+ = 383.30$) as a colorless oil (10.3 mg, 92%).

Macrocarpine C (3)



¹H NMR: see Table 9; **¹³C NMR:** see Table 10; **HRMS (ESI) m/z (M+H)⁺** Calcd for C₂₃H₃₁N₂O₃ 383.2329, found 383.2327; **R_f:** 0.6 (silica gel, 10 % MeOH in DCM);

Optical rotation: Synthetic material, this report [α]_D²⁵ (*c* 1.0 CHCl₃): -39; Natural sample [α]_D²⁵ (*c* 1.55 CHCl₃): -35; The characterization data of the synthetic (-)-**3** were in complete agreement with that of natural (-)-**3**.²

Comparison between Natural and Synthetic (-)-Macropine C (3)

Table 9: Comparison of the ¹H NMR Spectral Data for Natural and Synthetic Macropine C (3) in CDCl₃

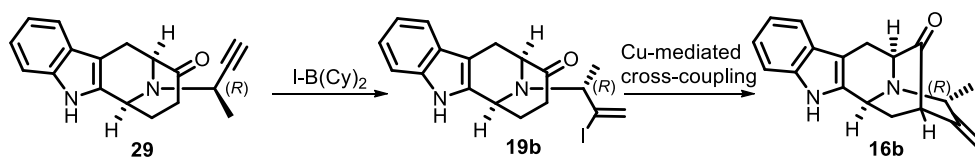
H#	¹ H Natural ² (400 MHz)	¹ H Synthetic (this report) (300 MHz)
3	3.97 (1H, t, <i>J</i> = 4 Hz)	4.03-3.98 (1H, m)
5	2.91 (1H, d, <i>J</i> = 7 Hz)	2.94 (1H, d, <i>J</i> = 6.7 Hz)
6	2.45 (1H, d, <i>J</i> = 17 Hz) 3.27 (1H, dd, <i>J</i> = 17, 7 Hz)	2.48 (1H, d, <i>J</i> = 16.5 Hz) 3.28 (1H, dd, <i>J</i> = 16.5, 6.9 Hz)
9	7.49 (1H, dd, <i>J</i> = 8, 1 Hz)	7.50 (1H, d, <i>J</i> = 7.6 Hz)
10	7.09 (1H, td, <i>J</i> = 8, 1 Hz)	7.13-7.07 (1H, m)
11	7.17 (1H, td, <i>J</i> = 8, 1 Hz)	7.18 (1H, br t, <i>J</i> = 7.3 Hz)
12	7.27 (1H, dd, <i>J</i> = 8, 1 Hz)	7.28 (1H, br d, <i>J</i> = 8.1 Hz)
14	1.39 (1H, dt, <i>J</i> = 13, 4 Hz) 2.26 (1H, td, <i>J</i> = 13, 4 Hz)	1.45-1.37 (1H, m) 2.32-2.24 (1H, m)
15	1.86 (1H, m)	1.93-1.79 (1H, m)
16	1.86 (1H, m)	1.93-1.79 (1H, m)
17	3.74 (1H, dd, <i>J</i> = 11, 4 Hz) 4.07 (1H, t, <i>J</i> = 11 Hz)	3.74 (1H, dd, <i>J</i> = 11.4, 4.5 Hz) 4.10 (1H, t, <i>J</i> = 11.5 Hz)
19	3.51 (1H, dq, <i>J</i> = 10, 6 Hz)	3.57-3.48 (1H, m)
20	1.69 (1H, m)	1.75-1.69 (1H, m)
21	3.83 (1H, d, <i>J</i> = 7 Hz) 3.83 (1H, d, <i>J</i> = 7 Hz)	3.83 (2H, d, <i>J</i> = 7.1 Hz)
23	1.68 (3H, s)	1.68 (3H, s)
18-Me	1.13 (3H, d, <i>J</i> = 6 Hz)	1.14 (3H, d, <i>J</i> = 6.1 Hz)
N(1)-Me	3.60 (3H, s)	3.61 (3H, s)
N(4)-Me	2.34 (3H, s)	2.37 (3H, s)

Table 10: Comparison of the ^{13}C NMR Spectral Data for Natural and Synthetic Macrocarpine C (3) in CDCl_3

C#	^{13}C Natural ² (100 MHz)	^{13}C Synthetic (this report) (75 MHz)
2	133.0	132.7
3	53.5	53.7
5	54.9	55.0
6	22.4	22.5
7	106.7	106.8
8	126.3	126.2
9	117.9	117.9
10	118.8	118.9
11	120.8	120.9
12	108.5	108.6
13	136.9	137.0
14	25.0	25.0
15	27.1	27.1
16	43.4	43.4
17	67.5	67.5
18	20.1	20.1
19	70.3	70.4
20	43.2	43.2
21	62.9	62.9
22	170.8	170.7
23	20.3	20.4

<i>N</i>(4)-Me	41.6	41.6
<i>N</i>(1)-Me	28.9	29.0

Preparation of ketone **16b** from alkyne **29**^{13,14}

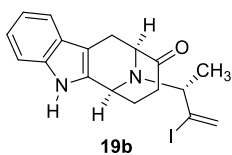


An oven dried flask fitted with an addition funnel was cooled under argon and charged with the alkyne **29** (2.10 g, 7.55 mmol) and freshly distilled CH_2Cl_2 (50 mL) and hexanes (7.0 mL) were added to dissolve **29**. The flask was cooled to 0 °C with ice and I-B(Cy)_2 (30.2 mL, 15.1 mmol, 0.5 M solution in hexanes) was added dropwise every 0.5 h in three portions, over a total period of 1.5 h. After the last addition, the reaction mixture was allowed to stir at 0 °C for another 0.5 h, after which the ice bath was removed and the mixture was stirred at rt for 2 h. After stirring at rt for 2 h, another 0.5 eq of I-B(Cy)_2 (7.6 mL, 3.78 mmol) was added dropwise at rt and the mixture was allowed to stir for another 2 h. After this 2 h, the mixture was treated with glacial acetic acid (4.8 mL, 83.1 mmol) at 0 °C and stirred at rt for 1.25 h. At this point the flask was again cooled to 0 °C and a solution of cold aq 3 M NaOH (40.3 mL, 121 mmol) and 30% H_2O_2 (2.6 mL, 23 mmol) was added and the stirring was maintained for 1 h at rt. The biphasic solution, which resulted, was transferred to a bigger flask, diluted with CH_2Cl_2 (200 mL) and water (50 mL), after which the two layers were separated. The aq layer was extracted with another 200 mL of CH_2Cl_2 . The combined CH_2Cl_2 layers were treated sequentially with solutions of 5% KF in methanol (160 mL) and 5% aq sodium bisulfite (160 mL) under vigorous stirring for 5 min. The aq layer was separated,

extracted with CH₂Cl₂ (2 x 80 mL), after which the combined organic layers were washed with brine, dried (Na₂SO₄), filtered and concentrated under reduced pressure. The purification by chromatography on silica gel (EtOAc/hexanes, 1: 4) afforded the vinyl iodide **19b** (2.94 g, 76%) as a white solid.

In a sealed tube with a magnetic stir bar, a mixture of vinyl iodide **19b** (420 mg, 1.0 mmol), CuI (190 mg, 1.0 mmol), *cis*-1,2- cyclohexanediol (116 mg, 1.0 mmol), Cs₂CO₃ (1.30 g, 4.0 mmol) and TEMPO (468 mg, 3.0 mmol) was dissolved in dry DMF (2.0 mL). The mixture was degassed under reduced pressure at rt and refilled with argon (3-4 times). The reaction mixture was then placed in a pre-heated oil bath (130 °C) and heated under argon for 10 h. At this point, TLC (silica gel, EtOAc/hexane = 1: 3 indicated the absence of starting material **19b**). The mixture was cooled to rt and diluted with EtOAc (10 mL) and water. The aq layer was separated and extracted with EtOAc (2 x 10 mL). The combined organic layer was washed with water (2 x 50 mL), brine (3 x 50 mL) and dried (Na₂SO₄). The solvent was removed under reduced pressure and the residue was purified by chromatography on neutral alumina (EtOAc/hexane = 1:3) to provide the cross-coupling product **16b** (240 mg, 82%). The indole **16b** gave colorless crystals from EtOAc which were used for X-ray analysis (see X-ray data in Appendix D).

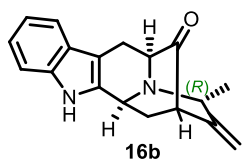
**(6*S*,10*S*)-12-((*R*)-3-Iodobut-3-en-2-yl)-7,8,10,11-tetrahydro-5*H*-6,10-epiminocycloocta-
[b]indol-9(6*H*)-one (19b)**



¹H NMR (300 MHz, CDCl₃) δ 7.98 (brs, 1H), 7.50 (d, 1H, *J* = 7.6 Hz), 7.37 (d, 1H, *J* = 7.9 Hz), 7.13-7.28 (m, 2H), 6.39 (s, 1H) 5.91 (s, 1H), 4.36-4.40 (m, 1H), 3.86 (d, 1H, *J* = 6.5 Hz), 3.17 (dd, 1H, *J* = 17.0, 6.6 Hz), 2.65-2.71 (m, 2H), 2.50-2.60 (m, 2H), 2.04-2.20 (m, 2H), 1.17 (d, 3H, *J* = 6.1 Hz); **¹³C NMR** (75 MHz,

CDCl₃) δ 210.4 (C), 135.8 (C), 132.8 (C), 126.9 (C), 126.2 (CH₂), 122.2 (C), 121.1 (CH), 119.8 (CH), 118.2 (CH), 111.0 (CH), 107.6 (C), 62.3 (CH), 61.7 (CH), 46.5 (CH), 34.5 (CH₂), 30.8 (CH₂), 20.7 (CH₂), 19.8 (CH₃); **HRMS** (ESI) m/z (M + H)⁺ calcd for C₁₈H₂₀IN₂O 407.0615, found 407.0617

(6*S*,8*S*,11*aS*)-8-Methyl-9-methylene-6,8,9,10,11*a*,12-hexahydro-6,10-methanoindolo[3,2-*b*]quinolizin-11(5*H*)-one (16*b*)



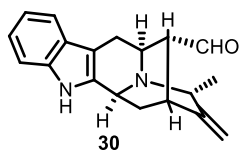
¹H NMR (300 MHz, CD₃OD): δ 7.42 (d, 1H, $J = 7.7$ Hz), 7.29 (d, 1H, $J = 8.0$ Hz), 7.06-7.11 (m, 1H), 6.98-7.03 (m, 1H), 5.14 (d, 1H, $J = 2.2$ Hz), 5.06 (d, 1H, $J = 1.6$ Hz), 4.57-4.61 (m, 1H), 3.99-4.06 (m, 1H), 3.71 (d, 1H, $J = 6.0$ Hz), 3.25-3.34 (m, 1H, merged with solvent), 2.98-3.05 (m, 2H), 2.56-2.64 (m, 1H), 2.09-2.16 (m, 1H), 1.66 (d, 3H, $J = 7.1$ Hz). The structure of this compound was further confirmed by X-ray crystallographic analysis (see X-ray in Appendix D).

Preparation of aldehyde 30 from ketone 16*b*

A mixture of anhydrous potassium *tert*-butoxide (4.73 g, 42.6 mmol) and methoxy-methyltriphenylphosphonium chloride (13.49 g, 39.34 mmol) in dry benzene (100 mL) was allowed to stir at rt for 1 h. The pentacyclic ketone **16*b*** (1.5 g, 5.39 mmol) in THF (20 mL) was then added to the above red colored solution dropwise at 0 °C. The mixture, which resulted, was stirred at rt for 12 h. After 12 h at rt, analysis of the mixture by TLC (silica gel) indicated the absence of starting material **16*b***. The mixture was then diluted with EtOAc (100 mL) and the

reaction was quenched with water (50 mL). The aq layer was extracted with EtOAc (2 x 30 mL), and the combined organic layers were washed with brine (2 x 30 mL) and dried (Na₂SO₄). The solvent was removed under reduced pressure to afford the enol ethers as a brownish red oil. The baseline materials (silica gel, TLC) were removed by percolation through a wash column of silica gel. The solvent was removed under reduced pressure and the residue was dissolved (without further purification) in a solution of THF/H₂O (1:1, 28 mL). To the above mixture, a solution of conc HCl (12 N) was added and the mixture, which resulted, was stirred at 55 °C (oil bath temperature) for 6 h. The reaction mixture was then cooled to 0 °C and extracted with ethyl ether (4 x 30 mL) to remove the phosphorous byproducts, after which the aq layer was brought to pH 8 with an ice-cold solution of 14% aq NH₄OH. The aq layer was extracted with EtOAc (3 x 25 mL), and the combined organic layers were washed with brine (2 x 50 mL) and dried (Na₂SO₄). The solvent was removed under reduced pressure to afford the α -aldehyde **30** as a brownish oil (1.42 g crude). This material was purified by silica gel column chromatography (5% MeOH in DCM) to provide pure **30** (LRMS M+H⁺ = 293.20) as a colorless oil (1.26 g, 80% in two steps). This material could be used for the next transformation without purification.

(6*S*,8*R*,11*R*,11*aS*)-8-Methyl-9-methylene-5,6,8,9,10,11,11*a*,12-octahydro-6,10-methanoindolo[3,2-*b*]quinolizine-11-carbaldehyde (30**)**



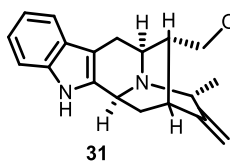
¹H NMR (300 MHz, CDCl₃): δ 9.64 (s, 1H), 8.00 (br s, 1H), 7.47 (br d, 1H, $J = 7.5$ Hz), 7.32 (br d d, 1H, $J = 7.7$ Hz), 7.21-7.07 (m, 2H), 4.93 (d, 1H, $J = 2.0$ Hz), 4.85 (d, 1H, $J = 1.3$ Hz), 4.39 (br d, 1H, $J = 9.0$ Hz), 3.71 (q, 1H, $J = 7.1$ Hz), 3.66-3.59 (m, 1H), 3.22 (dd, 1H, $J = 15.7, 5.1$ Hz), 2.86-2.81 (m, 1H), 2.64 (br d, 1H, $J =$

15.7 Hz), 2.48 (d, 1H, $J = 7.5$ Hz), 2.17-2.07 (m, 1H), 1.82-1.73 (m, 1H), 1.45 (d, 3H, $J = 7.1$ Hz); **Rf**: 0.25 (silica gel, 10% MeOH in DCM); **HRMS** (ESI) m/z ($M + H$)⁺ calcd for C₁₉H₂₁N₂O, 293.1648, found 293.1647. This material was used for the next step without further characterization.

Preparation of alcohol **31** from aldehyde **30**

The aldehyde **30** (600 mg, 2.05 mmol) was dissolved in EtOH (10 mL). Then NaBH₄ (116 mg, 3.08 mmol) was added to the above solution in one portion at 0 °C. The mixture, which resulted, was then stirred at 0 °C for 3 h. The reaction mixture was diluted with CH₂Cl₂ (100 mL) and poured into ice-cold water (50 mL). The aq layer was extracted with additional CH₂Cl₂ (3 × 20 mL), and the combined organic layers were washed with brine (3 x 50 mL) and dried (K₂CO₃). The solvent was removed under reduced pressure to afford the crude product, which was purified by chromatography on silica gel (10% MeOH in DCM) to provide alcohol **31** (LRMS $M+H^+$ = 295.25) as a colorless oil (571 mg, 90%).

((6*S*,8*R*,11*R*,11*aS*)-8-Methyl-9-methylene-5,6,8,9,10,11,11*a*,12-octahydro-6,10-methanoindolo[3,2-*b*]quinolizin-11-yl)methanol (**31**)



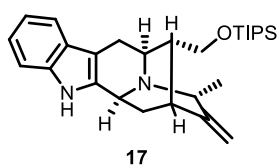
¹H NMR (300 MHz, CD₃OD): δ 7.43 (d, 1H, $J = 7.7$ Hz), 7.32 (d, 1H, $J = 8.0$ Hz), 7.13-7.06 (m, 1H), 7.05-6.98 (m, 1H), 5.04-4.97 (m, 2H), 4.54 (br d, 1H, $J = 9.3$ Hz), 3.80 (q, 1H, $J = 6.9$ Hz), 3.52 (br d, 2H, $J = 7.3$ Hz), 3.17 (dd, 1H, $J = 15.7, 5.2$ Hz), 2.97-2.89 (m, 1H), 2.81 (br d, 1H, $J = 15.8$ Hz), 2.54-2.49 (m, 1H), 2.27-2.16 (m, 1H), 1.93-1.73 (m, 2H), 1.5345 (d, 3H, $J = 7.1$ Hz); **¹³C NMR** (75 MHz, CD₃OD): δ 148.8, 137.0, 136.3, 127.1, 121.0, 118.6, 117.3, 110.7, 108.0, 103.0, 63.8, 59.5, 57.9, 44.6, 42.6,

35.2, 33.3, 26.2, 18.4; **HRMS** (ESI) m/z ($M + H$)⁺ calcd for C₁₉H₂₃N₂O, 295.1805, found 295.1807; $[\alpha]_D^{25}$ (*c* 0.3 CHCl₃): +46.67; **Rf**: 0.15 (silica gel, 10% MeOH in DCM);

Preparation of *O*-TIPS ether **17** from alcohol **31**

A solution of the alcohol **31** (100 mg, 0.34 mmol) in dry CH₂Cl₂ (10 mL) was cooled to 0 °C, after which 2, 6-lutidine (119 μL, 1.02 mmol) was added, and this was followed by the addition of TIPSOTf (137 μL, 0.51 mmol) to the stirred solution. The mixture was then allowed to stir for an additional 2 h at 0 °C, after which cold water (2 mL) was added to quench the reaction. The reaction mixture was diluted with CH₂Cl₂ (50 mL) and poured into cold water (20 mL). The aq layer was extracted with additional CH₂Cl₂ (2 × 50 mL), and the combined organic layers were washed with brine (3 x 20 mL) and dried (Na₂SO₄). The solvent was removed under reduced pressure to afford the crude product, which was dried in *vacuo* to remove the extra 2,6-lutidine before the solid was purified by chromatography on silica gel (5-10% MeOH in DCM) to provide the *O*-TIPS ether **17** (LRMS $M+H^+$ = 451.40) as a white solid (141 mg, 92%).

(6*S*,8*R*,11*R*,11*aS*)-8-Methyl-9-methylene-11-(((triisopropylsilyl)oxy)methyl)-5,6,8,9,10,11,11*a*,12-octahydro-6,10-methanoindolo[3,2-*b*]quinolizine (**17**)



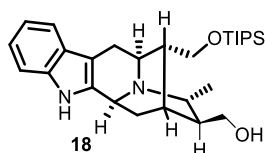
¹H NMR (300 MHz, CDCl₃): δ 8.42 (br s, 1H), 7.47 (br d, 1H, $J = 7.5$ Hz), 7.35 (br d, 1H, $J = 7.7$ Hz), 7.20-7.06 (m, 2H), 4.87 (br d, 2H, $J = 15.0$ Hz), 4.41 (br d, 1H, $J = 9.6$ Hz), 3.71-3.53 (m, 3H), 3.19 (dd, 1H, $J = 15.5$, 4.7 Hz), 2.92-2.82 (m, 1H), 2.76 (br d, 1H, $J = 15.5$ Hz), 2.45 (br s, 1H), 2.16-2.04 (m, 1H), 1.94-1.83 (m, 1H), 1.79-1.69 (m, 1H), 1.34-1.21 (m, 3H), 1.10-0.98 (m, 21H); **¹³C NMR** (75 MHz, CDCl₃): δ 137.3, 136.5, 127.7, 121.5, 119.3, 118.1, 111.0, 107.8, 104.9, 66.0, 59.5, 57.9, 44.6,

42.9, 35.6, 34.1, 27.0, 19.7, 18.0, 11.9; **HRMS** (ESI) m/z ($M + H$)⁺ calcd for C₂₈H₄₃N₂OSi, 451.3139, found 451.3135; $[\alpha]_D^{25}$ (*c* 0.6 CHCl₃): +68.33; **Rf**: 0.48 (silica gel, 10% MeOH in DCM).

Preparation of monol 18 from methine 17

To a solution of the alkenic *O*-TIPS ether **17** (100 mg, 0.222 mmol) in dry THF (10 mL) was added BH₃·DMS (189 μL, 2.0 mmol) at rt. The mixture, which resulted, was stirred at rt for 2 h. The reaction mixture was then quenched by careful addition of ice cold water (8 mL) at 0 °C (initial addition of water resulted in a large amount of effervescence). At this point NaBO₃·4H₂O (819 mg, 5.3 mmol) was added to the mixture in one portion at 0 °C. The mixture, which resulted, was allowed to stir at rt for 2 h after which EtOAc (100 mL) and H₂O (25 mL) were added. The organic layer was separated, washed with water (2 x 20 mL), brine (2 x 20 mL) and dried (Na₂SO₄). The EtOAc was then removed under reduced pressure to provide the *N*_b-BH₃ complex as a mixture of isomers. The above mixture of isomers was dissolved in freshly distilled MeOH (20 mL) and Na₂CO₃ (118 mg, 1.11 mmol) was added. The mixture was heated at 60 °C (oil bath) for 5 h under vigorous stirring. The reaction mixture, which resulted, was cooled to rt, followed by filtration through a bed of celite to remove the solids. The filtrate was concentrated under reduced pressure to provide a turbid oil which was redissolved in CH₂Cl₂. The CH₂Cl₂ layer was washed with H₂O (10 mL), brine (4 x 10 mL) and dried (Na₂SO₄). The solvent was removed under reduced pressure to afford a crude solid, which was purified by flash chromatography (silica gel, 5-10% MeOH in DCM) to furnish the primary alcohol **18** (79 mg, 76%) as a colorless oil (LRMS $[M+H]^+ = 469.45$).

((6*S*,8*R*,9*S*,11*R*,11*aS*)-8-Methyl-11-(((triisopropylsilyl)oxy)methyl)-5,6,8,9,10,11,11*a*,12-octahydro-6,10-methanoindolo[3,2-*b*]quinolizin-9-yl)methanol (18)



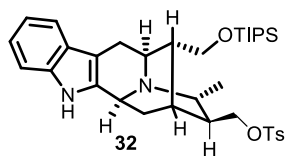
¹H NMR (500 MHz, CD₃OD): δ 7.32 (d, 1H, *J* = 7.7 Hz), 7.28 (d, 1H, *J* = 8.1 Hz), 7.05 (t, 1H, *J* = 7.5 Hz), 6.98-6.94 (m, 1H), 4.57 (d, 1H, *J* = 9.8 Hz), 3.88 (t, 1H, *J* = 9.4 Hz), 3.74-3.69 (m, 1H), 3.66-3.61 (m, 1H), 3.59-3.53 (m, 1H), 3.39-3.33 (m, 1H), 3.17-3.09 (m, 2H), 2.99 (br d, 1H, *J* = 15.5 Hz), 2.10-2.02 (m, 2H), 1.96-1.88 (m, 1H), 1.74-1.67 (m, 1H), 1.64-1.57 (m, 1H), 1.44 (d, 3H, *J* = 6.8 Hz), 1.04-0.98 (m, 21H); **¹³C NMR** (75 MHz, CDCl₃): δ 137.0, 135.1, 127.0, 121.3, 121.3, 118.8, 117.4, 110.9, 102.9, 66.8, 65.4, 60.3, 59.6, 46.2, 45.3, 41.6, 36.7, 27.3, 26.5, 19.3, 17.2, 11.7; **HRMS** (ESI) *m/z* (M + H)⁺ calcd for C₂₈H₄₅N₂O₂Si, 469.3245, found 469.3234; **[α]_D²⁵** (*c* 0.47 CHCl₃): +51.1; **R_f**: 0.2 (silica gel, 10% MeOH in DCM).

Preparation of tosylate 32 from alcohol 18

A flame dried round bottom flask was charged with freshly distilled CH₂Cl₂ (10 mL) and primary alcohol **18** (50 mg, 0.11 mmol), after which the mixture was cooled to -10 (outside bath temperature). Triethylamine (74 μL, 0.53 mmol) and DMAP (1.3 mg, 0.011 mmol) were added, and after a few minutes of stirring, tosyl chloride (51 mg, 0.27 mmol) was added in one portion. The reaction mixture was allowed to stir at -10 °C for 45 min and the solution was allowed to slowly warm to rt. After the reaction mixture was stirred for 3 h at rt, analysis by TLC (silica gel) was carried out, after which the reaction mixture was quenched with a large excess of water (100 mL). Then the mixture was allowed to stir vigorously for 45 min. After 45 min the two layers were separated. The CH₂Cl₂ layer was dried over MgSO₄, filtered and concentrated under reduced

pressure to furnish **32** (62 mg crude) as a waxy white solid, which was purified by silica gel chromatography (5-10% MeOH in DCM) to provide pure **32** as white waxy solid (56.5 mg, 85%).

((6*S*,8*R*,9*S*,11*R*,11*aS*)-8-Methyl-11-(((triisopropylsilyl)oxy)methyl)-5,6,8,9,10,11,11*a*,12-octahydro-6,10-methanoindolo[3,2-*b*]quinolizin-9-yl)methyl 4-methylbenzenesulfonate (32**)**



¹H NMR (500 MHz, CDCl₃): δ 7.89 (br s, 1H), 7.83 (br d, 2H, *J* = 8.2 Hz), 7.45 (d, 1H, *J* = 7.7 Hz), 7.39 (d, 2H, *J* = 8.0 Hz), 7.31 (d, 1H, *J* = 7.9 Hz), 7.17-7.13 (m, 1H), 7.11-7.07 (m, 1H), 4.25-4.20 (m, 1H), 4.18-4.08 (m, 2H), 3.73 (dd, 1H, *J* = 9.9, 8.0 Hz), 3.54 (dd, 1H, *J* = 10.0, 7.4 Hz), 3.08 (dd, 1H, *J* = 15.3, 5.3 Hz), 2.93-2.88 (m, 1H), 2.80-2.70 (m, 2H), 2.50 (s, 3H), 2.02-1.98 (m, 1H), 1.80 (t, 1H, *J* = 10.5 Hz), 1.73 (q, 1H, *J* = 7.8 Hz), 1.63-1.57 (m, 1H), 1.55 (dt, 1H, *J* = 12.2, 3.3 Hz), 1.35 (d, 3H, *J* = 6.8 Hz), 1.05-1.01 (m, 21H); **¹³C NMR** (75 MHz, CDCl₃): δ 144.9, 138.1, 136.3, 133.0, 129.9, 128.0, 127.8, 121.3, 119.3, 118.1, 110.8, 105.0, 74.6, 67.0, 59.0, 58.9, 44.1, 43.4, 41.0, 38.4, 27.8, 27.7, 21.7, 21.3, 18.0, 11.8; **HRMS** (ESI) *m/z* (M + H)⁺ calcd for C₃₅H₅₁N₂O₄SiS, 623.3333, found 623.3332; **[α]_D²⁵** (c 0.1 CHCl₃): -30.0; **R_f**: 0.55 (silica gel, 10% MeOH in DCM).

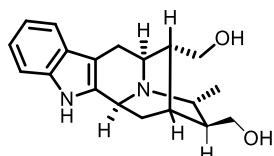
Synthesis of (+)-dihydroperaksine (8**) from (+)-**18****

The removal of the TIPS protecting group using the common fluoride source TBAF furnished the desired product in good yield and a clean reaction but it was not possible to remove the TBAF from the compound. As a consequence large peaks from the TBAF were observed in the ¹H NMR (and MS) that hindered the characterization of the desired compound. Consequently, it was decided

to use aq HF as the fluoride source where up the fluoride can be removed as TIPS fluoride under reduced pressure (Corey et al.).

To a solution of the *O*-TIPS ether (+)-**18** (16 mg, 0.034 mmol) in acetonitrile (4 mL), 0.4 mL of 48% aq HF was added at 0 °C. The solution, which resulted, was stirred at 0 °C for 40 min (**caution: glassware should not be used with HF, Teflon or plasticware should be used**). At that time, TLC (silica gel, UV and CAN stain) and LRMS indicated the disappearance of starting material. The solvent was removed under reduced pressure and the residue was dried *in vacuo*. The residue was further purified by silica gel column chromatography (5-10% MeOH in DCM) to furnish the diol **8** (LRMS $M+H^+ = 313.20$) as a white solid 9.5 mg, 89%).

(+)-Dihydroperaksine (**8**)



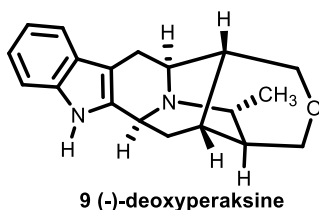
8, (+)-dihydroperaksine

¹H NMR (500 MHz, CD₃OD): δ 7.45 (d, 1H, *J* = 7.8 Hz), 7.34 (d, 1H, *J* = 8.1 Hz), 7.12 (t, 1H, *J* = 7.2 Hz), 7.03 (t, 1H, *J* = 7.2 Hz), 4.64 (br d, 1H, *J* = 8.9 Hz), 3.80-3.71 (m, 2H), 3.70-3.63 (m, 2H), 3.39-3.35 (m, 1H), 3.22 (dd, 1H, *J* = 15.7, 5.2 Hz), 3.17 (t, 1H, *J* = 6.2 Hz), 2.94 (br d, 1H, *J* = 15.8 Hz), 2.22-2.17 (m, 1H), 2.14 (t, 1H, *J* = 11.3 Hz), 1.95-1.88 (m, 1H), 1.79-1.74 (m, 1H), 1.71-1.66 (m, 1H), 1.52 (d, 3H, *J* = 6.9 Hz); **¹³C NMR** (75 MHz, CD₃OD): δ 137.0 (C), 135.4 (C), 127.0 (C), 121.2 (CH), 118.7 (CH), 117.4 (CH), 110.8 (CH), 102.8 (C), 65.3 (CH₂), 64.6 (CH₂), 59.6 (2 x CH), 59.5 (CH), 46.4 (CH), 45.2 (CH), 41.5 (CH), 36.8 (CH₂), 26.9 (CH), 26.2 (CH₂), 19.2 (CH₃); **HRMS** (ESI) *m/z* ($M + H^+$)⁺ calcd for C₁₉H₂₅N₂O₂, 313.1911, found 313.1913; **[α]_D²⁵**: **Synthetic**, this report = +40.0 (*c* 0.1 MeOH), **Natural alkaloid**¹⁰ = +40.0 (*c* 1.0, Py); **R_f**: 0.1 (silica gel, 10% MeOH in DCM).

Synthesis of (-)-Deoxyperaksine (**9**) from (-)-**32**

To a solution of the tosylate (-)-**32** (10 mg, 0.016 mmol) in THF (5 mL), TBAF (24 μ L, 0.024 mmol, 1.0 M solution in THF) was added at -30 °C. The solution, which resulted, was stirred at -30 °C to rt for 1 h, until the complete consumption of **32**, as indicated by TLC (silica gel) and LRMS. The reaction mixture was diluted with 30 mL of EtOAc and 5 mL of water. The aq layer was separated and extracted with another 5 mL of EtOAc. The combined EtOAc layers were washed with brine (2 x 20 mL) and dried (Na₂SO₄) to furnish the ether (-)-**9** as a colorless oil which was purified by column chromatography (silica gel, 2-5% MeOH in DCM) to furnish pure (-)-**9** (LRMS M+H⁺ = 295.15) as a white solid (3.9 mg, 82%).

(-)-Deoxyperksine



¹H NMR (500 MHz, CDCl₃): δ 7.73 (br s, 1H), 7.49 (d, 1H, J = 7.6 Hz), 7.33 (d, 1H, J = 7.9 Hz), 7.18-7.14 (m, 1H), 7.13-7.09 (m, 1H), 4.23 (br d, 1H, J = 9.5 Hz), 3.78-3.73 (m, 2H), 3.52-3.46 (m, 2H), 3.40 (br d, 1H, J = 10.9 Hz), 3.22 (dd, 1H, J = 15.6, 5.9 Hz), 3.19-3.13 (m, 1H), 2.61 (br d, 1H, J = 15.7 Hz), 1.82 (br t, 1H, J = 11.6 Hz), 1.67-1.63 (m, 1H), 1.55-1.49 (m, 1H), 1.40 (d, 3H, J = 7.0 Hz), 1.37-1.32 (m, 1H), 1.23-1.18 (m, 1H);

¹H NMR (500 MHz, CD₃OD): δ 7.42 (d, 1H, J = 7.8 Hz), 7.30 (d, 1H, J = 8.0 Hz), 7.07 (t, 1H, J = 7.1 Hz), 7.02-6.98 (m, 1H), 4.30-4.25 (m, 1H), 3.77-3.70 (m, 2H), 3.52 (dd, 1H, J = 11.2, 1.7 Hz), 3.45-3.40 (m, 2H), 3.19 (dd, 1H, J = 15.7, 5.8 Hz), 3.10-3.05 (m, 1H), 2.67 (br d, 1H, J = 15.5 Hz), 1.99-1.93 (m, 1H), 1.74-1.70 (m, 1H), 1.58-1.53 (m, 1H), 1.42 (d, 3H, J = 7.1 Hz), 1.40-1.37 (m, 1H), 1.33-1.28 (m, 1H);

¹³C NMR (75 MHz, CD₃OD): δ 139.3 (C), 138.3 (C), 128.7 (C), 122.0 (CH), 119.7 (CH), 118.6 (CH), 111.9 (CH), 103.7 (C), 71.5 (CH₂), 71.5 (CH₂), 58.9 (CH), 56.6 (CH), 43.7 (CH), 40.5 (CH), 37.2 (CH), 34.5 (CH₂), 30.5 (CH), 27.8 (CH₂), 20.3 (CH₃); HRMS (ESI) *m/z* (M + H)⁺ calcd for C₁₉H₂₃N₂O, 295.1805, found 295.1801; [α]_D²⁵ = -17.14 (*c* 0.17 CHCl₃); R_f: 0.4 (silica gel, 10% MeOH in DCM, NH₄OH).

5. Spectra and X-ray Data: See Appendix D for X-ray data for compound **16b**. See Appendix E for the NMR spectra for the synthetic alkaloids **1-5**, **8**, and **9**.

6. References

- (1) Schmeller, T.; Wink, M. In *Alkaloids: Biochemistry, Ecology, and Medicinal Applications*, Roberts, M. F., Wink, M., Eds.; Plenum Press: New York, 1998.
- (2) Kam, T.-S.; Choo, Y.-M.; Komiyama, K. *Tetrahedron* **2004**, *60*, 3957.
- (3) Keawpradub, N.; Kirby, G.; Steele, J.; Houghton, P. *Planta Med.* **1999**, *65*, 690.
- (4) Naranjo, J.; Pinar, M.; Hesse, M.; Schmid, H. *Helv. Chim. Acta* **1972**, *55*, 752.
- (5) Wong, W.-H.; Lim, P.-B.; Chuah, C.-H. *Phytochemistry* **1996**, *41*, 313.
- (6) Pan, L.; Terrazas, C.; Acuña, U. M.; Ninh, T. N.; Chai, H.; de Blanco, E. J. C.; Soejarto, D. D.; Satoskar, A. R.; Kinghorn, A. D. *Phytochem. Lett.* **2014**, *10*, 54.
- (7) Tan, S.-J.; Lim, J.-L.; Low, Y.-Y.; Sim, K.-S.; Lim, S.-H.; Kam, T.-S. *J. Nat. Prod.* **2014**, *77*, 2068.

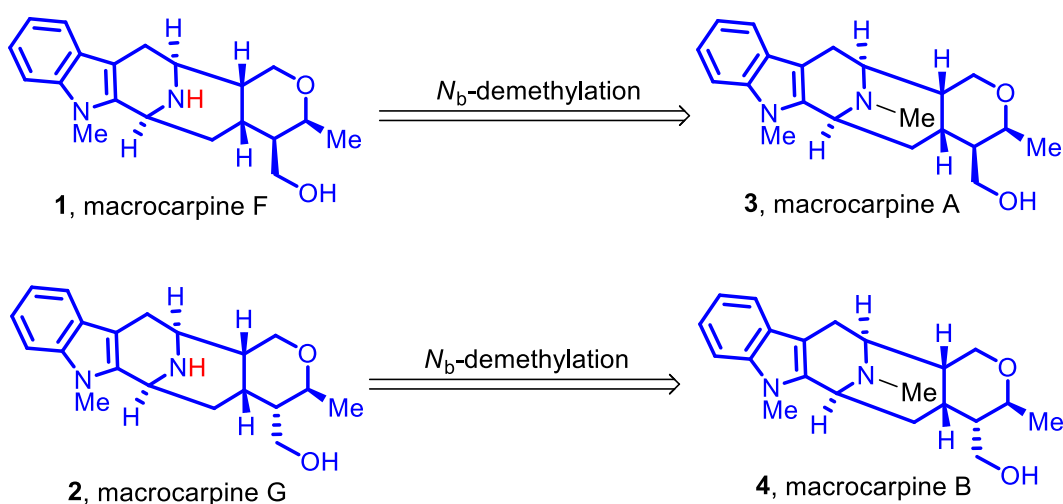
- (8) Buckingham, J.; Baggaley, K. H.; Roberts, A. D.; Szabo, L. F. *Dictionary of Alkaloids, with CD-ROM*; CRC press, 2010.
- (9) Iwu, M. *Planta Med.* **1982**, *45*, 105.
- (10) Kiang, A.; Loh, S.; Demanczyk, M.; Gemenden, C.; Papariello, G.; Taylor, W. I. *Tetrahedron* **1966**, *22*, 3293.
- (11) Nasser, A. M.; Court, W. E. *Phytochemistry* **1983**, *22*, 2297.
- (12) Garnick, R. L.; Le Quesne, P. W. *J. Am. Chem. Soc.* **1978**, *100*, 4213.
- (13) Rahman, M. T.; Deschamps, J. R.; Imler, G. H.; Schwabacher, A. W.; Cook, J. M. *Org. Lett.* **2016**, *18*, 4174.
- (14) Edwankar, R. V.; Edwankar, C. R.; Deschamps, J. R.; Cook, J. M. *J. Org. Chem.* **2014**, *79*, 10030.
- (15) Rahman, M. T.; Cook, J. M. *Eur. J. Org. Chem.* **2018**, 3224.
- (16) Rahman, M. T.; Deschamps, J. R.; Imler, G. H.; Cook, J. M. *Chem. Eur. J.* **2018**, *24*, 2354.
- (17) T. S. Kam, personal communication, July 12, 2017. Revised optical rotation of N(4)-methyl-N(4),21-secotalpinine is: $[\alpha]_D = +36$ (CHCl₃, c 0.33)
- (18) T.S. Kam, Personal Communication. April 09, 2016. Updated values for macrocarpine A: Choo, *Tetrahedron*, 2004, $[\alpha]_D = -22$ (c 0.36, CHCl₃); Lim, 2014, unpublished, $[\alpha]_D = -28$ (c 0.25 CHCl₃)
- (19) Corey, E. J.; Wu, Y. J. *J. Am. Chem. Soc.* **1993**, *115*, 8871.
- (20) Lounasmaa, M.; Hanhinen, P.; Westersund, M. In *The Alkaloids: Chemistry and Biology*; Cordell, G. A., Ed.; Academic Press: San Diego, CA, 1999; Vol. 52, p 103.

Chapter 6

The Total Synthesis of Macroparpines F and G, Talpinine, *O*-Acetyltalpinine, as well as *N*₄-Methyltalpinine

1. Introduction

Macrocarpine F (**1**)¹ and macrocarpine G (**2**)¹ are two macroline alkaloids bearing N_a -CH₃ and N_b -H substituents. After the synthesis of N_a -CH₃, N_b -CH₃ alkaloids macrocarpines A-C (**3**, **4**, and **7**),² it was felt that the N_b -H substitution in macrocarpines F **1** and G **2** would be accessible via an N_b -demethylation process from macrocarpine A (**3**)³ and B (**4**),³ respectively (Scheme 1).

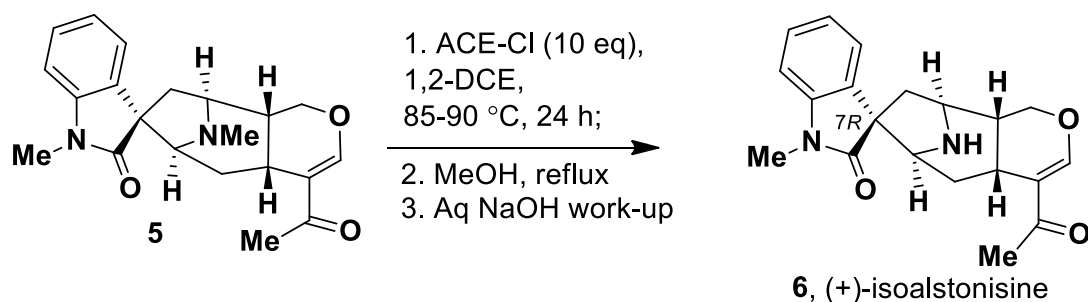


Scheme 1. Retrosynthetic analysis for the synthesis of macrocarpines F **1** and G **2** from macrocarpines A **3** and B **4**, respectively.

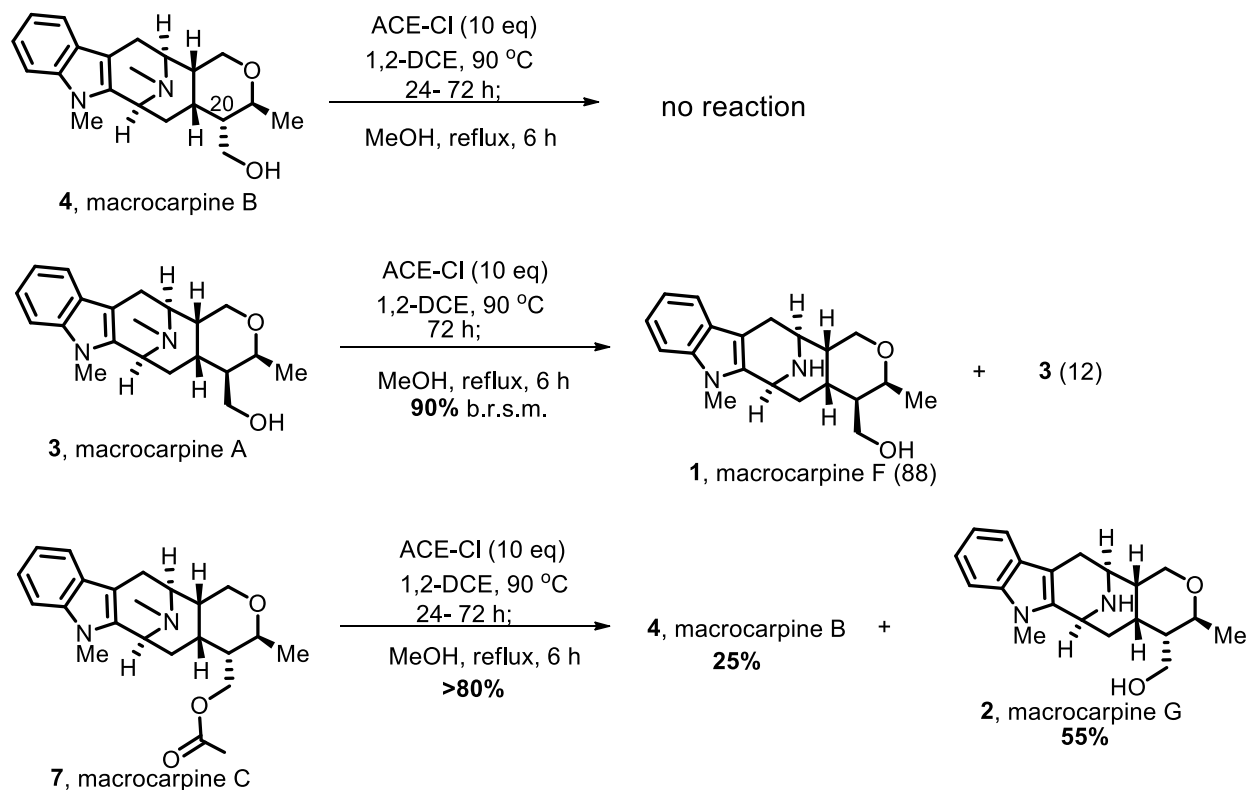
2. Results and Discussion

The N_b -methyl function is inert to many chemical transformations and aggressive reagents consequently, it is considered as a persistent protecting group for amines.⁴ In addition, it is an additional challenge to remove a methyl group on amines in functionally rich and sterically hindered systems such as macrocarpines A **1** and B **2**. In order to remove the N_b -methyl group regioselectively, it was decided to attempt a number of available methods present in the literature. The use of cyanogen bromide (Von Braun reaction)⁵ and carbonochloridates⁶ (chloroformates) are

well-known for regioselective dealkylation of alkylamines. It was also reported that the chloroformates are one of the best methods for this purpose due to better selectivity, as well as cleaner, and milder reaction conditions. In addition, one looked for inspiration from similar transformations in related systems. Inspired by the methods in the total synthesis of isoalstonisine by Fonseca⁷ (Scheme 2) wherein the chloroformate was successfully used to *N*-dealkylate the *N*_b-methyl group at the final stage of the synthesis, it was decided to employ the well-known *N*-dealkylation process developed by Olofson⁸ et al. This process employs an excess of ACE-Cl in 1,2-DCE at reflux. The so formed quaternary ammonium carbamate upon refluxing in methanol, followed by a basic work-up would provide the desired *N*_b-demethylated products **1** and **2**.



Scheme 2. Synthesis of (+)-isoalstonisine by *N*-dealkylation by Fonseca⁹



Scheme 3. Synthesis of macrocarpines F (**1**) and G (**2**) by N_6 -demethylation process using ACE-Cl

2.1 Synthesis of Macrocarpines F (**1**) and Macrocarpine G (**2**)

As planned, macrocarpine A (**3**) and B (**4**) (individually) were reacted with 10 equivalents of ACE-Cl in refluxing 1,2-dichloroethane. After that, the reaction mixture was dissolved in dry methanol and heated at reflux and this was followed by basic work-up with cold aq 1 *N* NaOH. It was observed that the C-20 α hydroxymethyl compound **4** (macrocarpine B) remained unchanged (LRMS: $M+H^+ = 341$) even after prolonged heating at reflux (up to 72 h) ligand **4** did not form the quaternary ammonium carbamate salt and the subsequent decarboxylation did not proceed. On the other hand, the C-20 β hydroxymethyl compound, macrocarpine A **3**, furnished the N_6 -demethylated secondary amine, macrocarpine F (**1**, LRMS: $M+H^+ = 327$), along with unreacted starting material **3**, which resulted in a 90% yield (based on recovered starting material). An LC-MS analysis of the reaction mixture indicated that the desired product **1** and the starting material

3 were present in a ratio of 88 to 12 (see Figure 1). Consequently, the *O*-acetyl variant of macrocarpine B (**4**), macrocarpine C (**7**, MW = 382.5) was subjected to the same conditions used for macrocarpine B **4**. It was observed that the desired *N*_b-demethylated secondary amine **2** formed (LRMS: M+H⁺ = 327), and this was accompanied by the deacetylated compound macrocarpine B **4** (LRMS: M+H⁺ = 341).

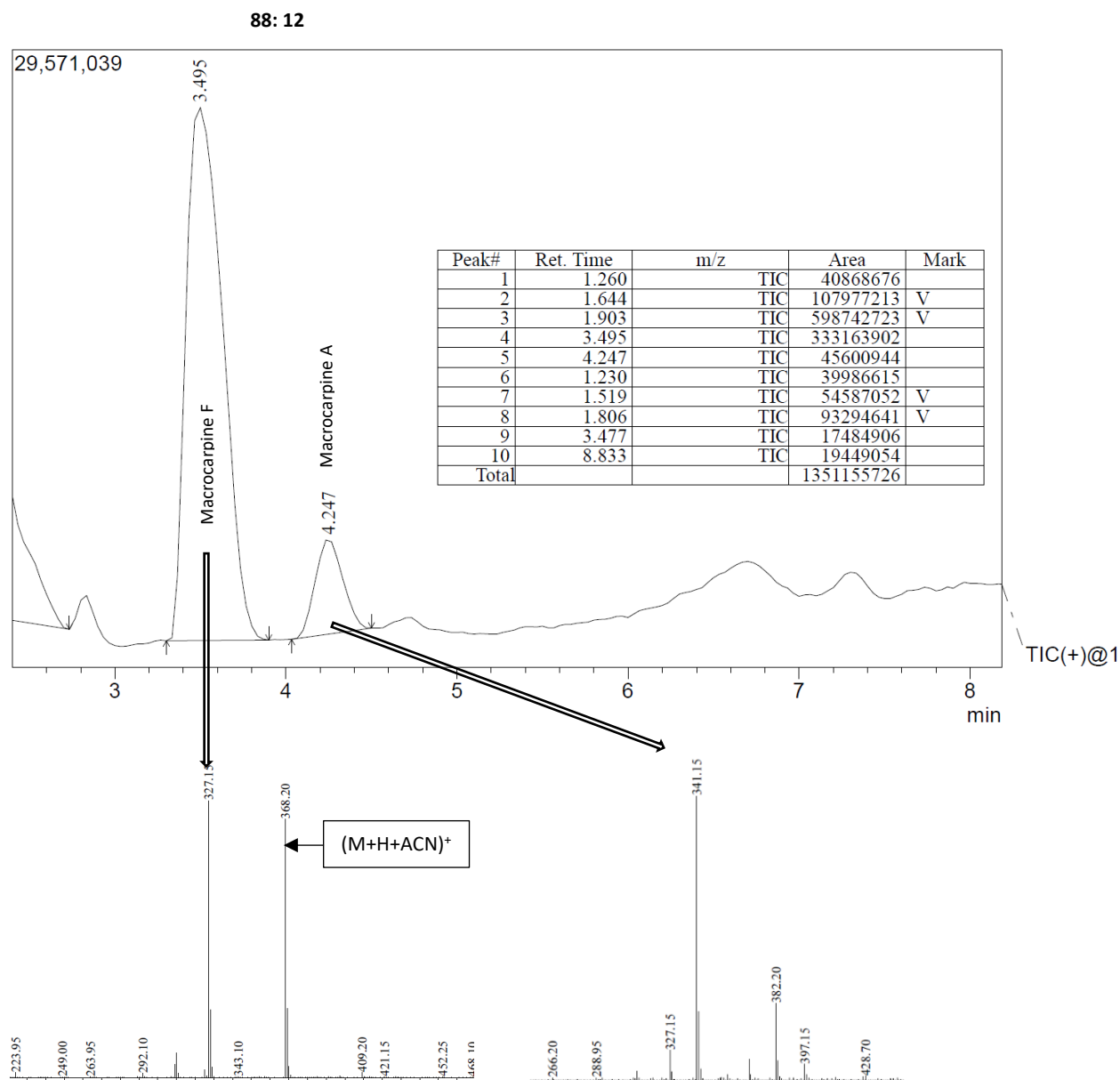
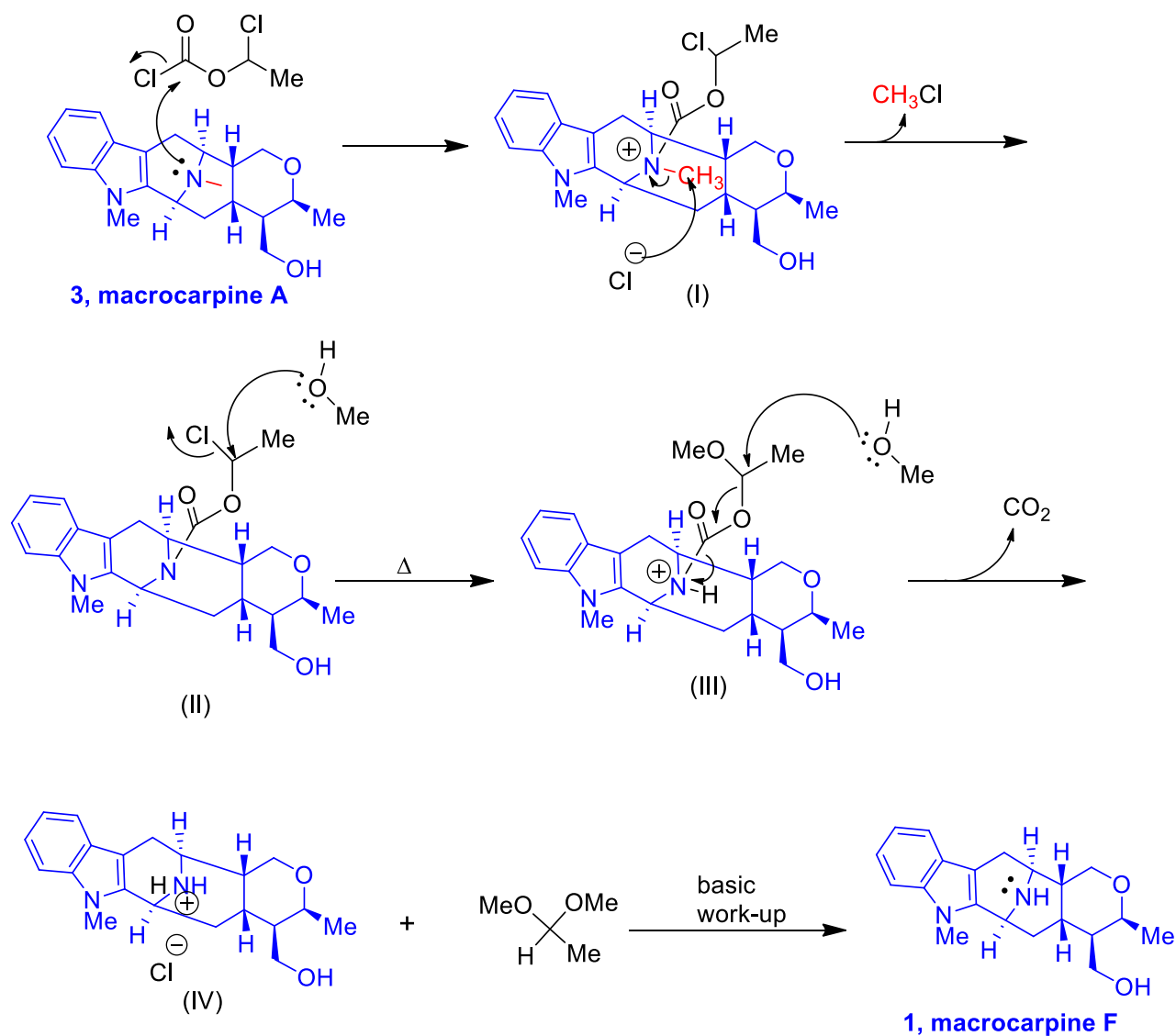


Figure 1. LC-MS analysis of the ACE-Cl mediated *N*_b-demethylation of macrocarpine A (**1**)

From these observations, it was concluded that in the C-20 α hydroxymethyl group in tertiary amine **4**, was too close to the amine function which created some steric congestion, which probably hindered the amine function from reacting with the chloroformate. More importantly, from molecular models it is clear a hydrogen bond between the tertiary amine function in **4** with the primary alcohol would also retard the amine from reacting with the chloroformate. This was evident from the fact that both macrocarpine A **3** and the *O*-acetyl version of macrocarpine B (macrocarpine C, **7**) did react to form the desired *N*_b-demethylated products **1** and **2**, respectively.

A proposed mechanism of the *N*_b-demethylation of Olofson^{8,9} employed here for macrocarpine A (**3**) is shown in Scheme 4.



Scheme 4. The proposed mechanism of the ACE-Cl mediated N_6 -demethylation of macrocarpine A **3** to provide macrocarpine F **1**.

2.1.1 Macrocarpine F (1)

^1H NMR: see Table 1; **^{13}C NMR:** see Table 2; [note: complete structural assignment was done based on ^1H , ^{13}C , DEPT-135, COSY, and HSQC NMRs, see Appendix F for NMR spectra)

HRMS: (ESI) m/z ($\text{M}+\text{H}$) $^+$ calcd for $\text{C}_{20}\text{H}_{27}\text{N}_2\text{O}_2$ 327.2067, found 327.2060; **R_f:** 0.1 (silica gel, 5% MeOH in DCM/ NH_4OH); [Note: The optical rotation was not measured due to the loss of material during re-purification]

Table 1. Comparison between the ^1H NMR of natural¹ and synthetic macrocarpine F (**1**)

H#	^1H Natural ¹ (400 MHz)	^1H Synthetic (300 MHz)
3	4.27 (m)	4.37 (br s)
5	3.21 (m)	3.23-3.15 (m)
6 β 6 α	2.63 (d, $J = 15$ Hz) 3.17 (m)	2.68 (br d, $J = 14.7$ Hz) 3.30-3.23 (m)
9	7.46 (br d, $J = 8$ Hz)	7.49 (d, $J = 7.6$ Hz)
10	7.07 (br t, $J = 8$ Hz)	7.14-7.06 (m)
11	7.18 (br t, $J = 8$ Hz)	7.23-7.16 (m)
12	7.75 (br d, $J = 8$ Hz)*	7.32-7.23 (d, $J = 8.1$ Hz)#
14 β 14 α	1.35 (m) 2.45 (td, $J = 12, 4$ Hz)	1.31-1.25 (m) ^{\$} 1.46-1.35 (m)
15	2.10 (m)	2.19-2.11 (m) ^{\$}
16	2.08 (m)	2.28-2.12 (m) ^{\$}
17 β 17 α	3.78 (dd, $J = 11, 5$ Hz) 4.07 (t, $J = 11$ Hz)	3.88-3.79 (m) 4.19-4.08 (t, $J = 11.6$ Hz)
19	3.94 (qd, $J = 6.8, 2$ Hz)	4.02-3.90 (m)
20	1.04 (m)	1.13-1.01 (m)
21	3.65 (dd, $J = 11, 4$ Hz)	3.75-3.65 (m)
21'	3.72 (dd, $J = 11, 6$ Hz)	3.88-3.79 (m) ^{\$}
18-Me	1.21 (d, $J = 6.8$ Hz)	1.29-1.19 (m) ^{\$}
N(1)- Me	3.52 (s)	3.61 (s)

[*] There is a typographical error in the natural¹ macrocarpine F at H-12; [#] merged with chloroform peak. Confirmed from COSY and HSQC NMRs; [\$] overlapped peaks

Table 2. Comparison between the ^{13}C NMR of natural¹ and synthetic macrocarpine F (**1**)

C#	^{13}C Natural ¹ (100 MHz)	^{13}C and DEPT-135 Synthetic (75 MHz)
2	136.4	136.3
3	46.5	46.5
5	48.2	48.2
6	28.5	28.4
7	107.7	107.9
8	126.6	126.2
9	118.1	118.1
10	119.1	119.0
11	121.2	121.1
12	108.9	108.8
13	136.8	-#
14	29.8	29.7
15	29.0	29.5
16	38.1	38.3
17	68.6	68.6
18	18.9	18.8
19	71.3	71.4
20	44.1	43.9
21	62.5	63.1
N(1)-Me	29.0	29.0

[#] quaternary carbon (C-13) was not visible in ^{13}C NMR spectrum at this concentration

2.1.2 Macrocarpine G (2)

¹H NMR: see Table 3; **R_f**: 0.1 (silica gel, 5% MEOH in DCM/NH₄OH); **[α]_D²⁵**: Synthetic = +12.0 (c 0.5, CHCl₃); Natural¹: = +7 (c 1.1, CHCl₃); **HRMS**: (ESI) *m/z* (M+H)⁺ calcd for C₂₀H₂₆N₂O₂ 327.2067, found 327.2074. [Note: ¹³C NMR measurement was attempted but due to very small amount of sample available, it was not successful even after a longer experiment time. The full structural assignment was done based on ¹H, COSY, NOESY (see Figure 2 for important NOE confirmation) and comparison with the spectra of the natural alkaloid¹].

Table 3. Comparison between the ^1H NMR of natural¹ and synthetic macrocarpine G (2)

H#	^1H Natural ¹ (400 MHz)	^1H Synthetic (500 MHz)
3	4.27 (br t, $J = 3$ Hz)	4.35 (br s)
5	3.25 (m)	3.31 (d, $J = 7.3$ Hz)
6 β 6 α	2.58 (d, $J = 16$ Hz) 3.18 (dd, $J = 16, 7$ Hz)	2.65 (br d, $J = 16.2$ Hz) 3.25-3.19 (m)
9	7.46 (br d, $J = 7.5$ Hz)	7.49 (d, $J = 7.9$ Hz)
10	7.08 (td, $J = 7.5, 1$ Hz)	7.10 (t, $J = 7.5$ Hz)
11	7.17 (td, $J = 7.5, 1$ Hz)	7.19 (t, $J = 7.5$ Hz)
12	7.24 (br d, $J = 7.5$ Hz)	7.29 (d, $J = 8.1$ Hz)
14 β 14 α	1.49 (dt, $J = 12, 2$ Hz) 2.18 (td, $J = 12, 4$ Hz)	1.58-1.53 (m)* 2.28 (td, $J = 12.6, 3.8$ Hz)
15	2.02 (m)	2.15-2.08 (m)
16	1.81 (dt, $J = 12, 5$ Hz)	1.91-1.86 (m)*
17 β 17 α	3.72 (dd, $J = 12, 4$ Hz) 4.03 (t, $J = 12$ Hz)	3.78 (dd, $J = 11.4, 4.4$ Hz) 4.10 (br t, $J = 12.2$ Hz)
19	3.46 (m)	3.58-3.54 (m)*
20	1.37 (m)	1.52-1.45 (m)*
21	3.22 (m)	3.39-3.34 (m)
21'	3.40 (dd, $J = 11, 5$ Hz)	3.51 (dd, $J = 11.0, 5.3$ Hz)*
18-Me	1.11 (d, $J = 6$ Hz)	1.17 (d, 6.1 Hz)
N(1)-Me	3.52 (s)	3.63 (s)

* overlapped peaks

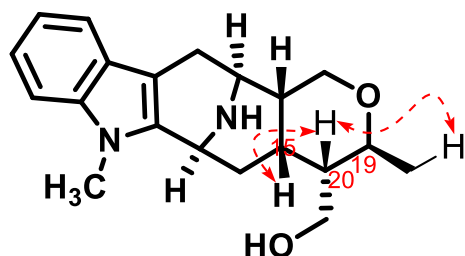
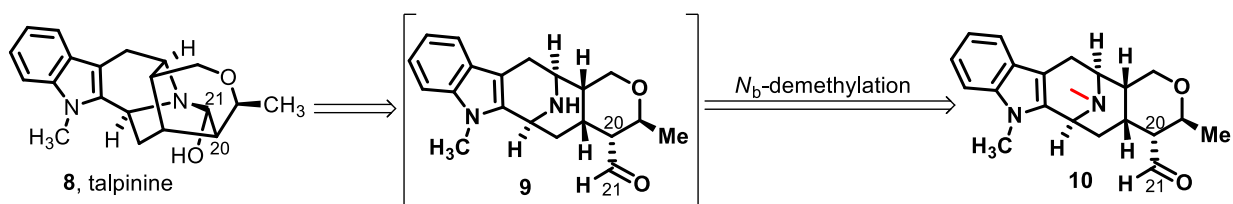


Figure 2: Selected NOE that confirms C-20 stereochemistry of macrocarpine G

2.3 Synthesis of Talpinine (8)

Talpinine¹⁰ is a sarpagine-macroline alkaloid containing a hemiaminal (carbinolamine) function at C-21. Retrosynthetically, the hemiaminal function at C-21 would originate from an intramolecular cyclization between the secondary N_b -nitrogen atom (as in **9**) with the C-20 α formyl function (Scheme 5). The secondary amine **9** would be available from the tertiary amine **10** (termed, N_4 -methyl- $N_4,21$ -secotalpinine). The same N_b -demethylation reaction employed for the synthesis of macrocarpines F (**1**) and G (**2**) should also be useful in this case.



Scheme 5. Retrosynthetic analysis for the synthesis of talpinine **8** by N_a -demethylation of tertiary amine **10**.

As planned, the C-20 α aldehyde **10** was subjected to the Olofson⁸ N_b -demethylation conditions which furnished the demethylated secondary amine **9** *in situ* and it subsequently cyclized in an

intramolecular fashion to form the desired hemiaminal present in talpinine **8**. During the initial trials it was observed that the starting tertiary amine **10** was somewhat unreactive with the chloroformate (ACE-Cl) and the conversion was very slow. It was felt that using a bulky and non-nucleophilic base such as pempidine (1,2,2,6,6-pentamethylpiperidine) would facilitate the carbamate formation at the initial stage of the demethylation process by scavenging any residual protons present in the reaction solution. By using a stoichiometric amount of pempidine and an excess of ACE-Cl in DCE at reflux (for 18 h), it was observed that the corresponding carbamates (**11**, LRMS: $M^+ = 445$; **12**, LRMS: $(M+H)^+ = 431$) formed but the starting tertiary amine (**10**, LRMS: $(M+H)^+ = 339$) still remained (Figure 3). This indicated that the first intermediate **11**, which formed by the reaction between the tertiary amine nitrogen with the ACE-Cl carbonyl function, was present as the major product in the reaction mixture (after 18 h), while the N_b -demethylated carbamate **12** was present as the minor product. Gratifyingly, this observation indicated that the reaction was progressing, albeit slowly. Accordingly, the reaction mixture was subjected to prolonged heat (up to 42 h) which completed the conversion, as indicated by the absence of the starting material **10** on analysis by LC-MS. After the subsequent decarboxylation reaction in refluxing methanol was followed by an alkaline workup, this process furnished the secondary amine **9**. The amine N_b -nitrogen atom reacted with the C-21 formyl function ultimately to form the hemiaminal present in talpinine **8**. Examination of the ^1H NMR spectrum confirmed the absence of the formyl function (at δ 9.44 ppm) and the presence of the H-21 (at carbinolamine carbon, C-21) at δ 4.71 ppm.

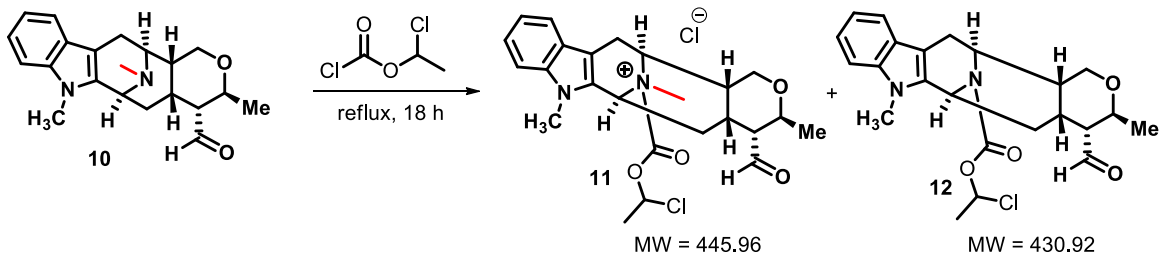
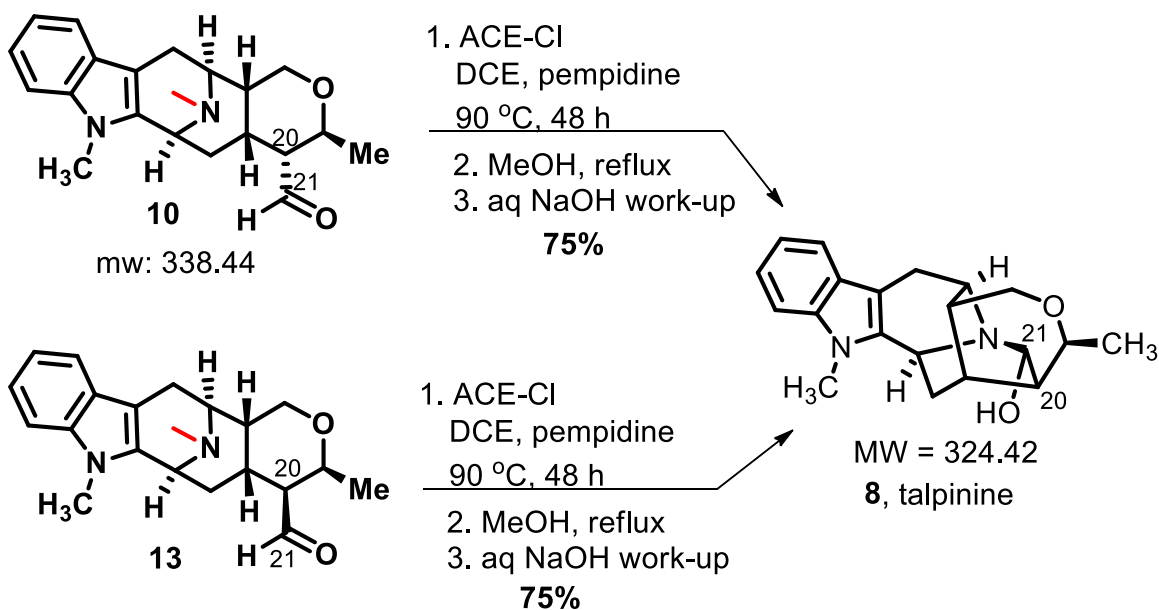


Figure 3. N_b -demethylation of **10** using ACE-Cl

The C-20 β aldehyde function containing indole base **13**, was also subjected to the same conditions to check whether the stereochemistry at the C-20 function played a significant role in the initial carbamate formation. It was found that talcapine **13** also underwent demethylation and furnished the same product, talpinine **8**. This indicated that the C-20 aldehyde undergoes epimerization under these conditions to the α -stereochemistry and then cyclizes.



Scheme 6. Synthesis of talpinine **8**

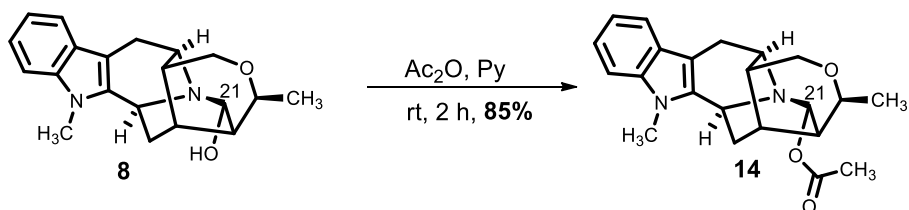
The spectral and optical properties of synthetic talpinine were in excellent agreement with the literature^{10,11} values for natural product (-)-**8**.

Talpinine **8**

¹H NMR (300 MHz, CDCl₃) 1.38-1.20 (6H, m), 1.87-1.79 (1H, m), 1.93-1.86 (1H, m), 2.65 (1H, d, *J* = 15.6 Hz), , 3.21 (1H, dd, *J* = 15.6, 6.0 Hz), 3.52-3.41(2H, m), 3.59 (3H, s), 3.72-3.62 (1H, m), 4.10-3.99 (1H, m), 4.43(1H, d, *J* = 7.9 Hz), 4.71 (1H, m), 7.12-7.05 (1H, m), 7.19 (1H, t, *J* = 7.7 Hz), 7.31-7.27 (1H, m, merged with chloroform peak), 7.47 (1H, d, *J* = 7.5 Hz); **¹³C NMR** (75 MHz, CDCl₃) δ 15.7, 23.3, 26.3, 29.2, 31.9, 35.2, 40.2, 43.6, 49.8, 64.0, 72.6, 87.9, 103.3, 108.7, 118.3, 118.9, 120.9, 127.3, 137.5, 139.1; [α]_D²⁵ = -30.0 (c 0.2, CHCl₃), Natural¹⁰: [α]_D²⁵ = -30 (c 0.302, CHCl₃); **HRMS**: (ESI) *m/z* (M+H)⁺ calcd for C₂₀H₂₅N₂O₂ 325.1911, found 325.1919; **R_f**: 0.1 (silica gel, 5% MeOH in DCM/NH₄OH)

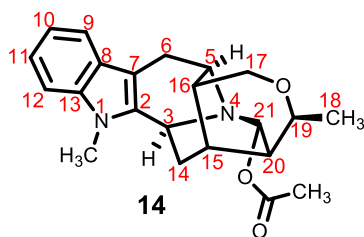
2.4 Synthesis of *O*-Acetyltalpinine (**14**)

O-Acetyltalpinine (**14**)¹ contains an acetyl function at the C-21 hydroxyl function of talpinine **8**. A simple acetylation of talpinine **8** with acetic anhydride in the presence of excess pyridine furnished *O*-acetyltalpinine **14** in 85% yield. The spectra and optical properties of the synthetic alkaloid were in agreement with the literature values for the natural product. There was an unidentified minor impurity in the synthetic, sample as indicated by examination of the ¹H NMR spectrum but the compound appeared as single spot on TLC (silica gel). In addition, only the desired compound's (**14**) peak (LRMS M+H⁺ = 367) was observed in the LCMS spectrum. The minor impurity could not be removed after several chromatographic purifications. Further attempts for the synthesis or purification of this impurity could not be undertaken due to the lack of material. In spite of the presence of the impurity, the synthetic *O*-acetyltalpinine **14** was fully characterized and the structural assignment could be done to confirm the synthesis unambiguously, by high resolution NMR spectroscopy.



Scheme 7. Synthesis of *O*-acetyltalpinine **14** from talpinine **8**

O-Acetyltalpinine **14**



¹H NMR: see Table 4; **¹³C NMR:** see Table 5; **R_f:** 0.3 (silica gel, 5% MeOH in DCM/NH₄OH);

Synthetic: [α]_D²⁵ = -9.1 (c 0.12, CHCl₃)*; **Natural¹:** [α]_D²⁵ = -8 (c 0.2, CHCl₃); **HRMS:** (ESI)

m/z (M+H)⁺ calcd for C₂₂H₂₇N₂O₃ 367.2016, found 367.1995.

(*Note: The full structural assignment was based on ¹H, ¹³C, and HSQC NMR correlations, as well as by comparison with spectra of the natural alkaloid. The synthetic sample contained an unidentified minor impurity that was seen in the ¹H and HSQC NMR spectra. The impurity persisted even after multiple purification cycles. Further attempts could not be made to determine its structure due to the lack of material.)

O-Acetyltalpinine 14

Table 4. Comparison between the ¹H NMR spectra of natural¹ and synthetic *O*-acetyltalpinine **14**

H#	¹ H Natural (400 MHz)	¹ H Synthetic (500 MHz)
3	4.48 (br dd, <i>J</i> = 10, 2 Hz)	4.46 (br d, <i>J</i> = 9.3 Hz)
5	3.52 (br t, <i>J</i> = 5.5 Hz)	3.56 (br t, <i>J</i> = 5.5 Hz)
6 β 6 α	2.66 (d, <i>J</i> = 15.6 Hz) 3.20 (dd, <i>J</i> = 15.6, 5.5 Hz)	2.62 (br d, <i>J</i> = 15.8 Hz) 3.18 (dd, <i>J</i> = 15.2, 5.9 Hz)
9	7.47 (br d, <i>J</i> = 7.5 Hz)	7.47 (d, <i>J</i> = 7.7 Hz)
10	7.09 (br td, <i>J</i> = 7.5 Hz)	7.09 (t, <i>J</i> = 7.4 Hz)
11	7.19 (td, <i>J</i> = 7.5, 1 Hz)	7.18 (t, <i>J</i> = 7.6 Hz)
12	7.29 (br d, <i>J</i> = 7.5 Hz)	7.29 (d, <i>J</i> = 8.2 Hz)
14 β 14 α	1.52 (ddd, <i>J</i> = 12, 4, 2.8 Hz) 1.89 (ddd, <i>J</i> = 12, 10, 1.6 Hz)	1.53-1.47 (m) 1.91-1.83 (m)*
15	2.00 (m)	2.03-1.97 (m)
16	1.30 (m)	1.30 (m)*
17 β 17 α	3.47 (dd, <i>J</i> = 11, 2 Hz) 3.71 (dd, <i>J</i> = 11, 1 Hz)	3.47 (dd, <i>J</i> = 11.4, 1.9 Hz) 3.71 (dd, <i>J</i> = 11.4, 1.1 Hz)
19	4.34 (q, <i>J</i> = 7 Hz)	4.34 (q, <i>J</i> = 7.0 Hz)
20	1.34 (m)	1.34-1.31 (m)*
21	5.63 (br d, <i>J</i> = 2 Hz)	5.61 (m)
18-Me	1.30 (d, <i>J</i> = 7 Hz)	1.30 (d, 6.8 Hz)
<i>N</i> (1)- Me	3.66 (s)	3.66 (s)

[*] = merged peaks

Table 5. Comparison between the ^{13}C NMR spectrum of natural¹ and synthetic *O*-acetylalpinine
14

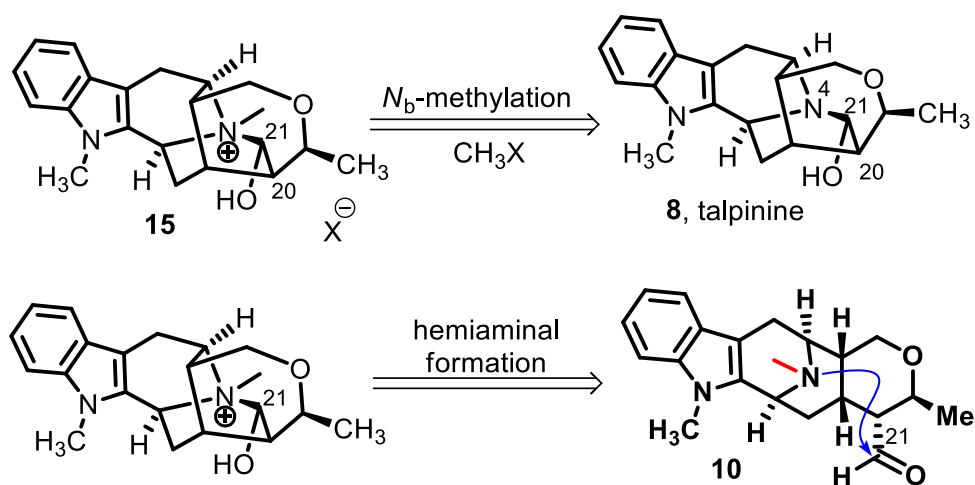
C#	^{13}C Natural ¹ (100 MHz)	^{13}C Synthetic (125 MHz)
2	138.9	-*
3	41.7	41.7
5	50.3	50.3
6	26.6	26.6
7	103.1	130.1
8	127.2	127.2
9	118.1	118.1
10	120.9	120.9
11	118.8	118.9
12	108.7	108.7
13	137.4	137.4
14	32.3	32.3
15	23.2	23.2
16	35.2	35.2
17	63.8	63.8
18	15.6	15.7

19	71.6	71.6
20	43.6	43.6
21	88.9	88.9
<i>N</i> (1)-Me	29.3	29.3
21-OAc	21.2	21.3
21-OAc	169.6	169.6

* The peak for C-2 did not show up in the ^{13}C NMR spectrum at this concentration

2.5 Synthesis of *N*₄-Methyltalpinine (15)

The *N*₄-methyltalpinine¹² is a quaternary ammonium alkaloid containing a methyl function at the *N*_b-nitrogen atom of talpinine. From a retrosynthetic point of view, the most obvious precursor for *N*₄-methyltalpinine would be talpinine itself, which would be accessible by an *N*_b-methylation process with a methyl halide (Scheme 8). Although, the counter anion for the quaternary ammonium ion in the natural sample was not known,¹² the synthetic *N*₄-methyltalpinine would have the counter anion corresponding to the methyl halide used. Another possible way to accessing *N*₄-methyltalpinine would be the intramolecular reaction between the tertiary *N*_b-amine nitrogen atom with the C-21 carbonyl function of *N*₄-methyl-*N*_{4,21}-secotalpinine **10**. However, potential steric hindrance and conformational restriction of the tertiary *N*_b-nitrogen atom could deter it from reacting with the aldehyde function to furnish the hemiaminal (carbinolamine) function present in the desired *N*₄-methyltalpinine. The carbonyl function in **10** could be further activated towards the nucleophilic addition by means of a Lewis or Brønsted acid catalyst.



Scheme 8. Retrosynthetic analysis for the synthesis of *N*₄-methyltalpinine **15** from talpinine **8**

As planned, talpinine **8** was treated with iodomethane in methanol at rt in the dark for 16 h. A ^1H NMR spectrum of the reaction mixture in deuterated methanol indicated the disappearance of the aldehydic proton (at δ 9.44 ppm), whereas, a broad multiplet at δ 5.0-4.9 ppm appeared, which was expected for the hemiaminal proton (H-21 on the carbinolamine carbon, C-21). This result was encouraging. However, the NMR spectra of the crude reaction mixture was not clean enough for full characterization and for comparison with the natural alkaloid.¹² Consequently, silica gel chromatography (5% MeOH in DCM/sat NH_4OH) was attempted in order to obtain a pure sample of synthetic N_4 -methyltalpinine. Unfortunately, the compound that was isolated by chromatography lacked the hemiaminal proton peak at $\sim\delta$ 5 ppm, as well as the aldehydic proton peak at δ 9.44 ppm. Intrigued by this result, attempts were taken to identify this product. The product was found to be identical to N_4 -methyl- $N_{4,21}$ -secotalpinine **10** in deuterated methanol (Scheme 9). One important observation was made. In deuterated methanol the aldehyde peak of **10** was not well defined in comparison to the ^1H NMR spectrum of **10** in CDCl_3 (see Figure 4).

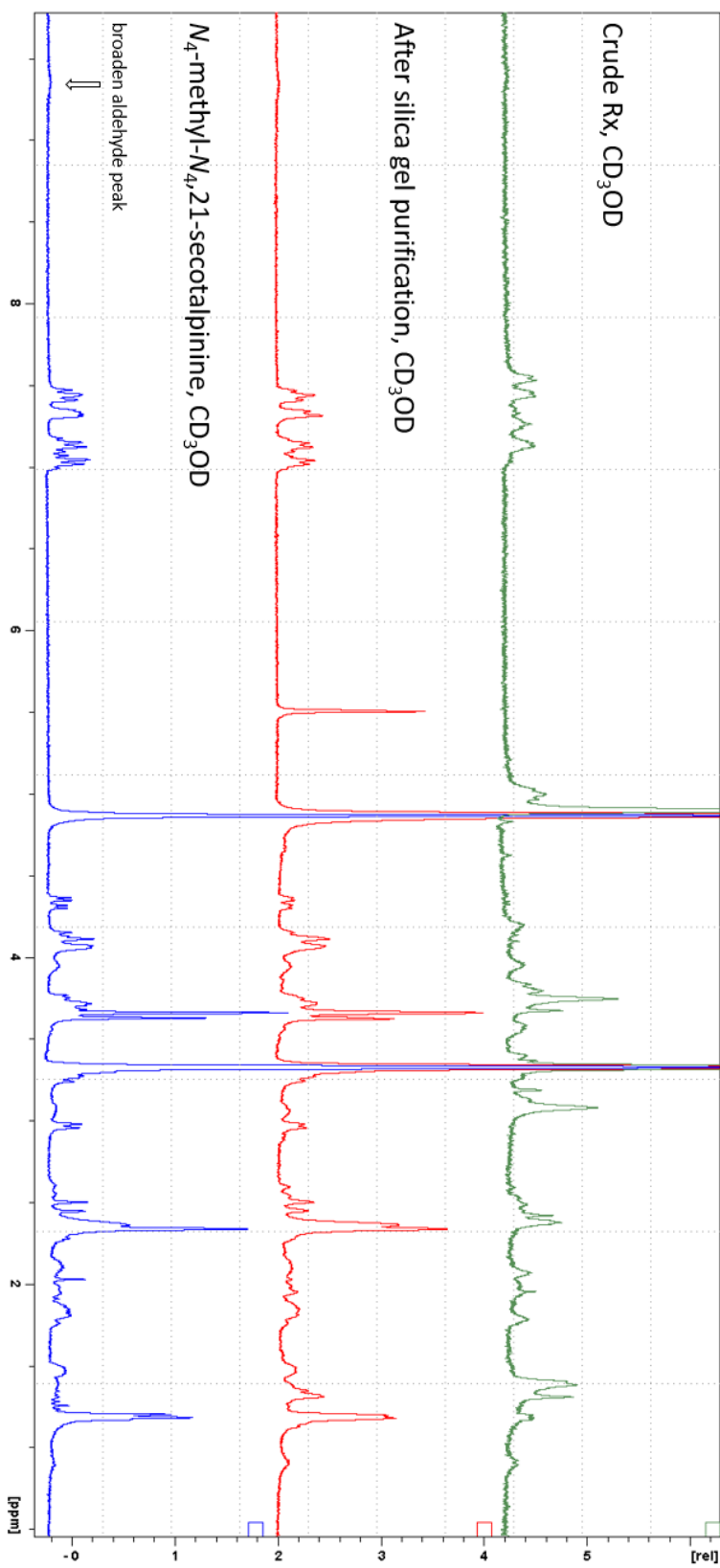
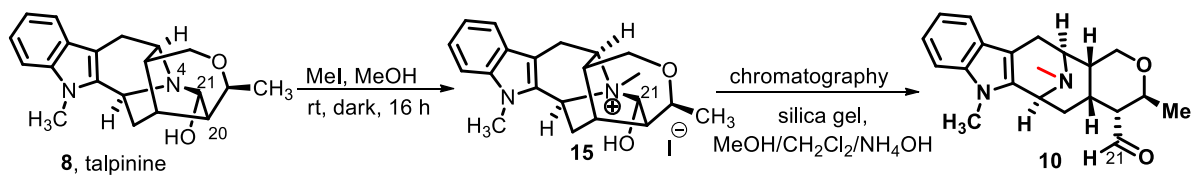


Figure 4. ¹H NMR spectra of the crude reaction mixture and alkaloid **10** in CD₃OD



Scheme 9. Attempted synthesis of N_4 -methyltalpinine

Upon further investigation of this result it was found that while the $C-20\beta$ aldehyde of alkaloid talcarpine **13** exhibited a well define aldehyde peak (δ 9.9 ppm) in deuterated methanol; the $C-20\alpha$ aldehyde of the alkaloid N_4 -methyl- $N_{4,21}$ -secotalpinine **10** exhibited a broaden aldehyde peak ($\sim\delta$ 9.3 ppm) in deuterated methanol. On the other hand, both talcarpine and secotalpinine showed well-defined sharp singlets for the aldehyde protons in $CDCl_3$ at δ 9.9 ppm and δ 9.4 ppm, respectively (Figure 5).

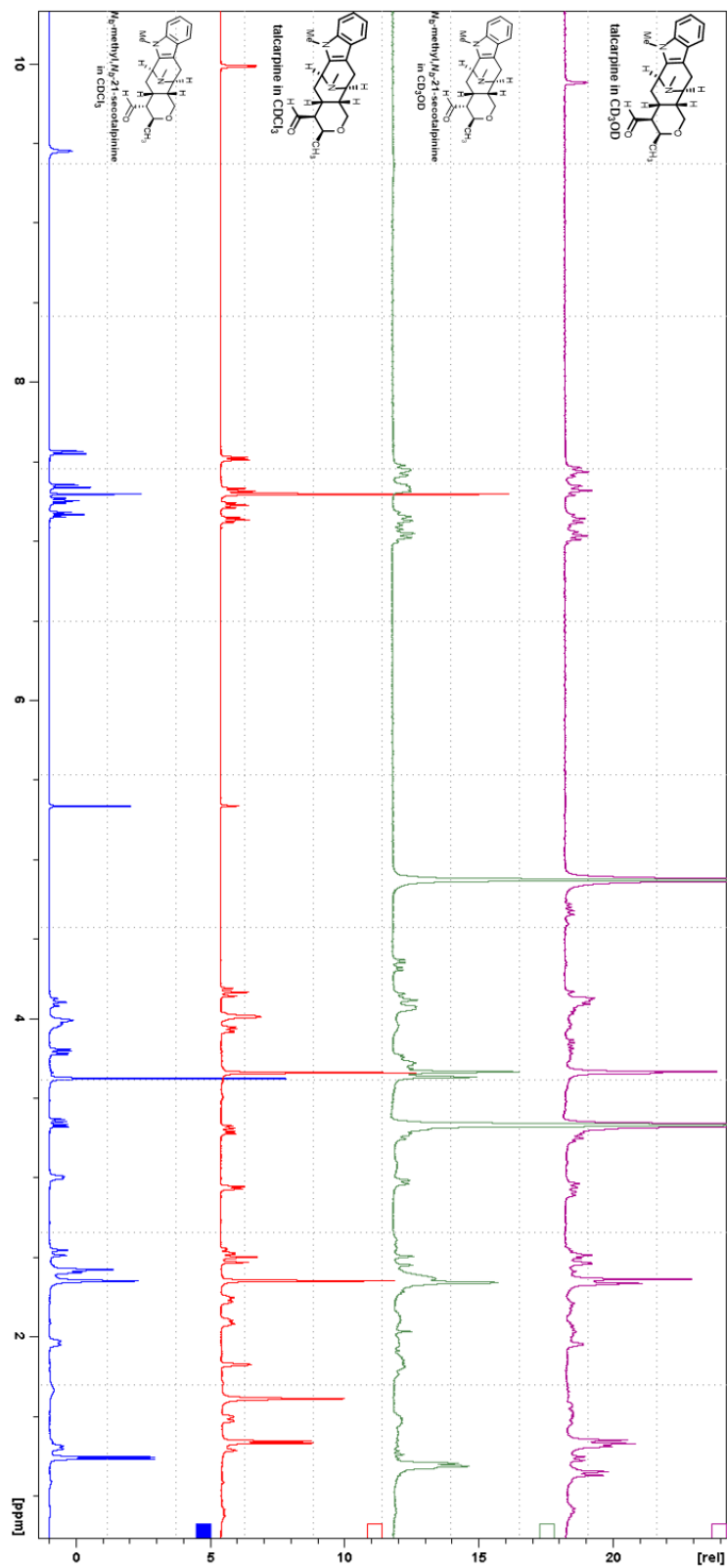


Figure 5. Comparison between the ¹H NMR spectra of talcarpine **13** and *N*₄-methyl-*N*_{4,21}-secotalpinine in CD₃OD and CDCl₃

This result indicated that while the C-20 β aldehyde in talcarpine **13** remained as an aldehyde moiety in methanol, there was an equilibrium mixture in case of *N*₄-methyl-*N*_{4,21}-secotalpinine **10**. Furthermore, it was observed that the aldehyde peak broadened or sharpened in a temperature dependent manner. At higher temperature, the aldehyde peak was found to be broader than the aldehyde peak at lower temperatures (see Figure 6).

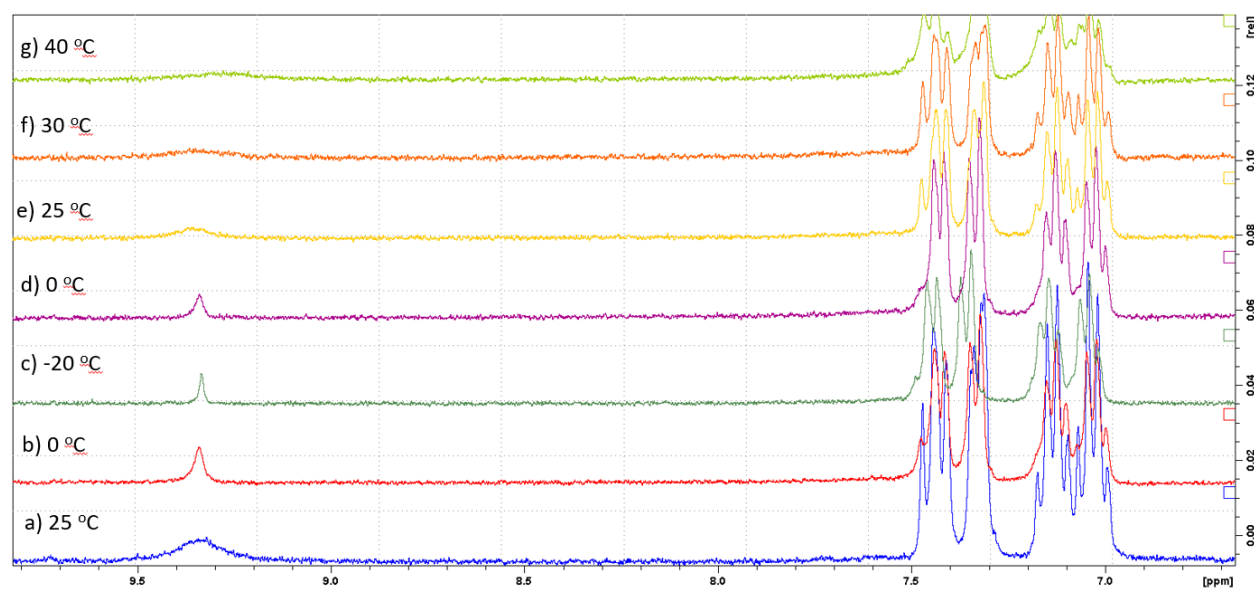


Figure 6. Temperature dependence of the broadness of the aldehydic peak of **10**.

Furthermore, it was determined the aldehyde peak broadened after the epimerization of talcarpine **13** into secotalpinine **10**. Talcarpine **13** was treated with triethylamine in methanol at rt. It was observed that the aldehyde peak of talcarpine **10** (at δ 9.9 ppm) gradually diminished and a broad peak corresponding to the C-20 α aldehyde appeared at δ ~9.3 ppm. This experiment indicated that the β -aldehyde function in talcarpine **13** epimerized in the presence of a base and gradually formed the corresponding α -aldehyde **10**, which is the thermodynamically more stable epimer. As soon as the α -aldehyde **10** was formed, it reacted with the tertiary amine, which was in the vicinity and

formed an equilibrium favoring the cyclized form. As a result this altered the sharp peak for the aldehyde to a broader peak (Figure 8).

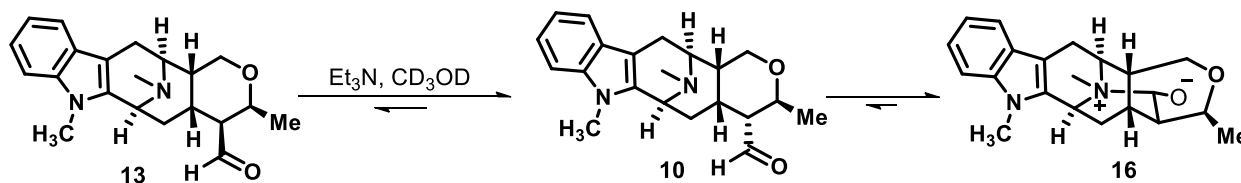


Figure 7. Epimerization of talcarpine **13** into *N*₄-methyl-*N*_{4,21}-secotalpinine **10** under basic conditions

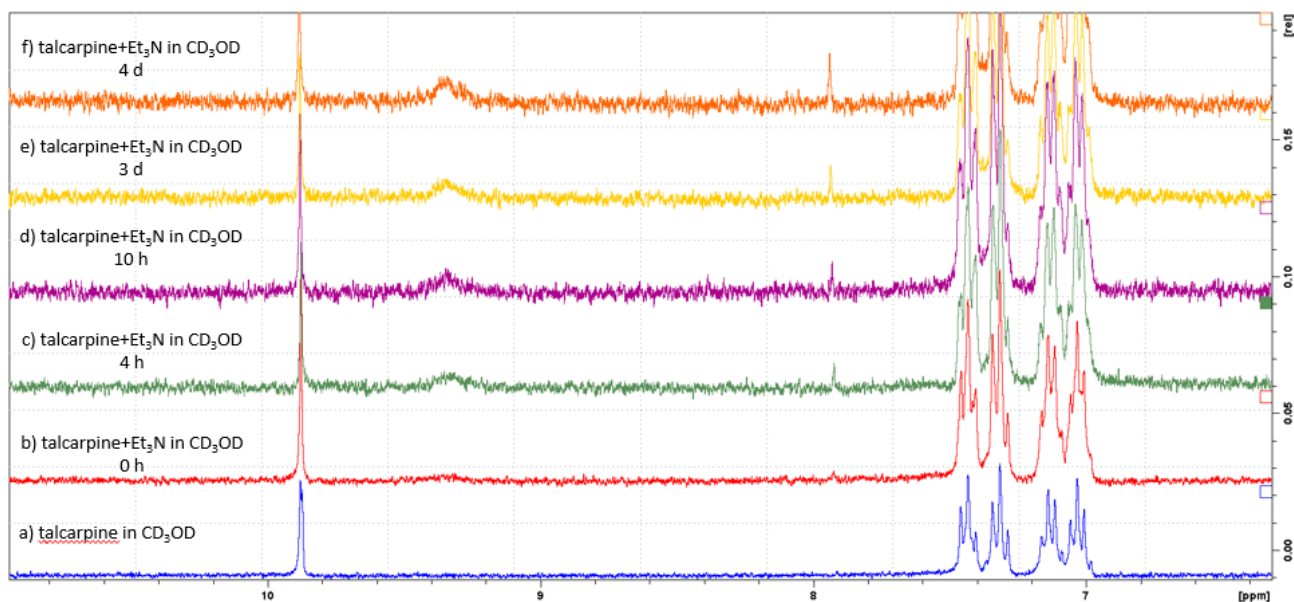
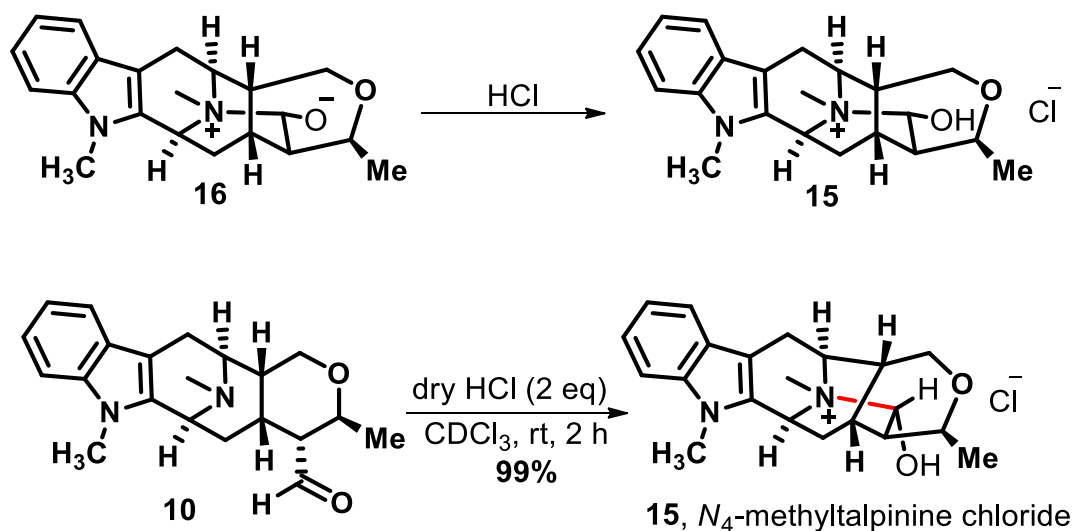


Figure 8. Epimerization of **13** in the presence of triethylamine to form **16** via **10**

From the experiments described above it was felt that the indole base **10** would stay in an Zwitterionic form with **16** in methanol (Figure 8). In the presence of dry HCl in solution the oxygen atom would be protonated and the chloride ion would act as the counter anion for the quaternary ammonium nitrogen atom. This would lead to the desired stable *N*₄-methyltalpinine as a chloride salt (Scheme 10) if silica gel chromatography was avoided. Consequently, the *N*₄-methyl-*N*_{4,21}-secotalpinine was stirred with dry HCl (4.0 M solution in dioxane) at rt. The deuterated chloroform

was used as the solvent instead of CD₃OD to avoid any peak overlap with the peak at δ 4.87 ppm (residual moisture) with the desired H-21 peaks at δ 5.00-4.95 ppm. After adding a catalytic amount of dry HCl, a small broad peak at δ 5.0 ppm appeared, which indicated the conversion began, albeit in very small amount (entry b, Figure 9). After adding 2 additional equivalents of HCl it was observed that the multiplet at δ 5 ppm increased in intensity, while the aldehydic peak at δ 9.44 ppm began to diminish in intensity (entry c, Figure 9). After standing at rt for an additional 2 h, examination of the ¹H NMR spectrum indicated that the aldehydic peak was completely gone and the spectrum appeared much cleaner (entry d, Figure 9). After that, the solvent was removed under reduced pressure and the alkaloid was dissolved in deuterated methanol for comparison with the literature values (see Figure 10 in Appendix F). A ¹H NMR spectrum of the residue in CD₃OD was found to be identical to that of the literature values.¹² All other spectroscopic and optical rotation values were in excellent agreement with the literature values¹² for the desired alkaloid *N*₄-methyltalpinine **15**.¹ **Caution:** In Zwitterionic molecules such as **15/16**, it is best to avoid silica gel chromatography.



Scheme 10. Synthesis of *N*₄-methyltalpinine **15** from the indole base **10**

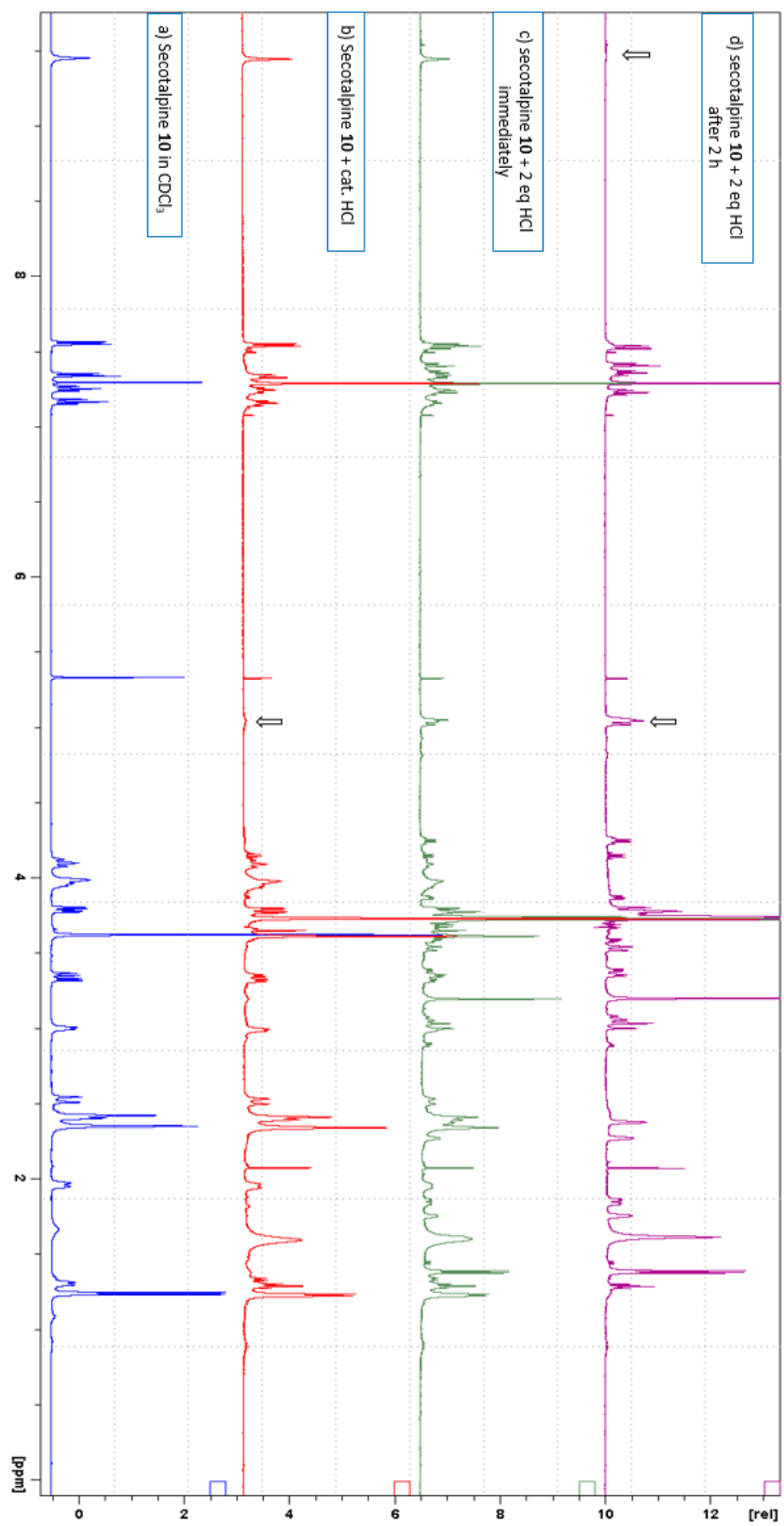


Figure 9. Progress of the reaction of dry HCl with indole base **10** (^1H NMR spectra)

***N*₄-methyltalpinine 15**

¹H NMR: see Table 6; ¹³C NMR: see Table 7; [α]_D²⁵: Synthetic = -9.1 (c 0.11, EtOH); Natural¹²: = -10 (c 0.1, MeOH); **HRMS**: (ESI) *m/z* M⁺ calculated for C₂₁H₂₇N₂O₂ 339.2067, found 339.2036

Table 6. Comparison between the ¹H NMR spectra of natural and synthetic *N*₄-methyltalpinine **15** in CD₃OD

H#	¹ H Natural ¹² (400 MHz)	¹ H Synthetic (500 MHz)
3	4.99 (1H, d, <i>J</i> = 10.7 Hz)	4.99 (1H, d, <i>J</i> = 10.4 Hz)
5	3.91 (1H, t, <i>J</i> = 5.4 Hz)	3.92 (1H, t, <i>J</i> = 5.5 Hz)
6β 6α	3.09 (1H, d, <i>J</i> = 16.6 Hz) 3.36 (1H, dd, <i>J</i> = 17.4, 5.3 Hz)	3.09 (1H, d, <i>J</i> = 17.4 Hz) 3.36 (1H, dd, <i>J</i> = 17.2, 5.4 Hz)
9	7.53 (1H, d, <i>J</i> = 7.9 Hz)	7.53 (1H, d, <i>J</i> = 7.9 Hz)
10	7.12 (1H, t, <i>J</i> = 7.8 Hz)	7.12 (1H, t, <i>J</i> = 7.6 Hz)
11	7.25 (1H, t, <i>J</i> = 7.7 Hz)	7.25 (1H, t, <i>J</i> = 7.7 Hz)
12	7.43 (1H, d, <i>J</i> = 8.2 Hz)	7.43 (1H, d, <i>J</i> = 8.3 Hz)
14β 14α	1.98 (1H, ddd, <i>J</i> = 13.2, 5.0, 1.8 Hz) 2.47 (1H, br t, <i>J</i> = 12.2 Hz)	1.96 (1H, ddd, <i>J</i> = 13.3, 5.0, 1.8 Hz) 2.47 (1H, m)
15	2.36 (1H, br s)	2.36 (1H, m)
16	1.77 (1H, br s)	1.77 (1H, br s)
17β 17α	3.80 (1H, d, <i>J</i> = 11.7 Hz) 3.54 (1H, dd, <i>J</i> = 11.9, 2.1 Hz)	3.80 (1H, d, <i>J</i> = 11.7 Hz) 3.54 (1H, dd, <i>J</i> = 11.9, 2.2 Hz)
19	4.15 (1H, q, <i>J</i> = 6.8 Hz)	4.15 (1H, q, <i>J</i> = 6.9 Hz)
20	2.04 (1H, br s)	2.04 (1H, br s)
21	4.95 (1H, d, <i>J</i> = 1.9 Hz)	4.95 (1H, d, <i>J</i> = 1.7 Hz)
18-Me	1.38 (3H, d, <i>J</i> = 6.8 Hz)	1.38 (3H, d, <i>J</i> = 6.8 Hz)
<i>N</i> (1)-Me	3.73 (3H, s)	3.73 (3H, s)
<i>N</i> (4)-Me	3.07 (3H, s)	3.07 (3H, s)

Table 7. Comparison between the ^{13}C NMR spectra of synthetic and natural¹² *N*₄-metyltalpinine in CD₃OD

C#	^{13}C Natural ¹² (100 MHz)	^{13}C Synthetic (125 MHz)
2	134.2	134.2
3	53.1	53.1
5	61.3	61.3
6	24.7	24.7
7	101.2	101.6
8	127.3	127.3
9	119.5	119.5
10	121.0	121.0
11	123.7	123.7
12	110.6	110.6
13	139.7	139.7
14	32.4	32.3
15	22.7	22.6
16	38.2	38.2
17	63.1	63.1
18	15.7	15.7
19	72.7	72.7
20	48.2	48.2
21	98.4	98.4
<i>N</i> (4)-Me	43.5	43.5
<i>N</i> (1)-Me	29.9	29.9

3. Conclusion

The first total synthesis of several bioactive indole alkaloids has been successfully completed in stereospecific fashion. Macrocarpines F and G, and bioactive alkaloid *O*-acetyltalpinine, as well as the potent NFκB inhibitor *N*₄-methyltalpinine have been synthesized for the first time. The other bioactive alkaloid talpinine has been previously synthesized by Yu et al.¹¹ (see General Introduction), but the strategy developed here is shorter and in higher yield.

4. Experimental Section

Macrocarpine F 1

The indole **3** (3 mg, 0.009 mmol) was dissolved in dry 1,2-dichloroethane (2 mL) in a thick walled vessel that can be sealed with a screw cap. The ACE-Cl (1-chloroethyl chloroformate, 12.6 mg, 0.09 mmol) was added to the above solution at 0 °C under argon. The reaction vessel was sealed and heated at 90 °C (oil bath) for 72 h. The reaction was then cooled to rt and the solvent was removed under reduced pressure. Then distilled methanol (5 mL) was added to the residue and the solution, which resulted, was heated at reflux under argon for 6 h with stirring. After that, the solvent was removed under reduced pressure and the residue was dissolved in EtOAc (5 mL) and brought to pH 8 with cold aq 1 *N* NaOH. The organic layer was separated and the aq layer was extracted with additional EtOAc (2 x 5 mL). The combined organic layers were washed with brine and dried (K₂CO₃). The solvent was removed under reduced pressure to give a brown residue. The residue was purified by column chromatography (silica gel) with 0-5% MeOH in CH₂Cl₂/sat NH₄OH to provide macrocarpine F **1** as a colorless residue (2.3 mg, **80%**). The spectroscopic data of the synthetic alkaloid were in excellent agreement with that of the natural product.¹

Macrocarpine G 2

The indole **7** (4 mg, 0.01 mmol) was dissolved in dry 1,2-dichloroethane (3 mL) in a thick walled vessel that can be sealed with a screw cap cap. The ACE-Cl (1-chloroethyl chloroformate, 14.9 mg, 0.10 mmol) was added to the above solution at 0 °C under argon. The reaction vessel was sealed and heated at 90 °C (oil bath) for 72 h. The reaction mixture was then cooled to rt and the solvent was removed under reduced pressure. Then distilled methanol (5 mL) was added to the residue and the solution, which resulted, was heated at reflux under argon for 6 h with stirring. After that, the solvent was removed under reduced pressure and the residue was dissolved in EtOAc (5 mL) and brought to pH 8 with cold aq 1 N NaOH. The organic layer was separated and the aq layer was extracted with additional EtOAc (2 x 5 mL). The combined organic layers were washed with brine and dried (K₂CO₃). The solvent was removed under reduced pressure to give a brown residue. The residue was purified by column chromatography (silica gel) with 0-5% MeOH in CH₂Cl₂/sat NH₄OH to provide macrocarpine G **2** as a colorless residue (1.9 mg, **55%**) accompanied by macrocarpine B **4** (0.9 mg, **25%**). The optical rotation and spectroscopic data were in agreement with that of the natural product.¹

Talpinine 8

The indole **10** or **13** (6 mg, 0.018 mmol) was dissolved in dry 1,2-dichloroethane (4 mL) in a thick walled vessel that can be sealed with a screw cap. The ACE-Cl (1-chloroethyl chloroformate, 25.3 mg, 0.18 mmol) and pempidine (2.7 mg, 0.018 mmol) were added to the above solution at 0 °C under argon. The reaction vessel was sealed and heated at 90 °C (oil bath) for 42 h. The reaction was then cooled to rt and the solvent was removed under reduced pressure. Then distilled methanol

(5 mL) was added to the residue and the solution, which resulted, was heated at reflux under argon for 6 h with stirring. After that, the solvent was removed under reduced pressure and the residue was dissolved in EtOAc (5 mL) and brought to pH 8 with cold aq 1 N NaOH. The organic layer was separated and the aq layer was extracted with additional EtOAc (2 x 5 mL). The combined organic layers were washed with brine and dried (K₂CO₃). The solvent was removed under reduced pressure to give a brown residue. The residue was purified by chromatography (silica gel) with 0-5% MeOH in CH₂Cl₂/sat NH₄OH to provide talpinine **8** as a colorless oil (4.3 mg, **75%**). The spectral data were in excellent agreement with that of the natural product.^{10,11}

O*-Acetyltalpinine **14*

To a mixture of Ac₂O and pyridine (1:1, 0.5 mL), talpinine **8** (1 mg, 0.003 mmol) was added at rt under argon. The solution, which resulted, was stirred at rt for 2 h. After that, a cold solution of saturated aq Na₂CO₃ (2 mL) was added to the above reaction. The solution was extracted with CH₂Cl₂ (3 x 3 mL). The combined organic layers were washed with brine. The solvent was removed under reduced pressure and the residue was purified by column chromatography (silica gel) in a Pasteur pipette with 0-3% MeOH in CH₂Cl₂ to afford *O*-acetyltalpinine **14** (0.96 mg, **85%**) as a colorless waxy residue. The spectral data for **14** were identical to that of the natural product.¹

N*₄-Methyltalpinine **15*

[**Preparation of the HCl solution for NMR titration:** Anhydrous HCl (0.3 mL, 4.0 M solution in dioxane) was dissolved in 5.0 mL of CDCl₃. The solution, which resulted, was gradually added via a micropipette into the reaction vessel.]

The indole **10** (1.0 mg, 0.003 mmol) was dissolved in dry CDCl₃ (1.0 mL) in an oven dried NMR tube (5 mm OD). The above HCl solution (25 μL in total) was added to the NMR tube via a micropipette. The reaction, which resulted, was kept at rt for 2 h. After that, examination of the ¹H NMR spectrum indicated complete conversion of the aldehyde into the desired product. The solvent was removed under reduced pressure to afford the *N*₄-methyltalpinine **15** as chloride salt (1.1 mg, **99%**) as a colorless residue. This residue was used for characterization without any purification. The optical rotation and spectroscopic data for the synthetic *N*₄-methyltalpinine **15** were in excellent agreement with the values reported in the literature for the natural product¹² by Kinghorn et al.

5. Spectra Section: See Appendix F for the NMR spectra of synthetic alkaloids **1**, **2**, **8**, **14**, and **15**

6. References

- (1) Tan, S.-J.; Lim, J.-L.; Low, Y.-Y.; Sim, K.-S.; Lim, S.-H.; Kam, T.-S. *J. Nat. Prod.* **2014**, *77*, 2068.
- (2) Rahman, M. T.; Deschamps, J. R.; Imler, G. H.; Cook, J. M. *Chem. Eur. J.* **2018**, *24*, 2354.

- (3) Kam, T.-S.; Choo, Y.-M.; Komiyama, K. *Tetrahedron* **2004**, *60*, 3957.
- (4) Wuts, P. G.; Greene, T. W. *Greene's Protective Groups in Organic Synthesis*; John Wiley & Sons, 2006.
- (5) v. Braun, J. *Ber. Dtsch. Chem. Ges.* **1900**, *33*, 1438.
- (6) Cooley, J.; Evain, E. *Synthesis* **1989**, *1989*, 1.
- (7) Stephen, M. R.; Rahman, M. T.; Tiruveedhula, V. P. B.; Fonseca, G. O.; Deschamps, J. R.; Cook, J. M. *Chem. Eur. J.* **2017**, *23*, 15805.
- (8) Olofson, R.; Martz, J. T.; Senet, J. P.; Piteau, M.; Malfroot, T. *J. Org. Chem.* **1984**, *49*, 2081.
- (9) Fonseca Cabrera, G. O. Ph.D. Thesis, University of Wisconsin-Milwaukee, **2015**.
- (10) Naranjo, J.; Pinar, M.; Hesse, M.; Schmid, H. *Helv. Chim. Acta* **1972**, *55*, 752.
- (11) Yu, P.; Wang, T.; Li, J.; Cook, J. M. *J. Org. Chem.* **2000**, *65*, 3173.
- (12) Pan, L.; Terrazas, C.; Acuña, U. M.; Ninh, T. N.; Chai, H.; De Blanco, E. J. C.; Soejarto, D. D.; Satoskar, A. R.; Kinghorn, A. D. *Phytochem. Lett.* **2014**, *10*, 54.

General Conclusion and Future Direction

In the Part I of this dissertation an improved and shorter access to the important azabicyclo[3.3.1] framework of the sarpagine/macroline-related indole alkaloids has been described. By employing a bulky alkyl substituent on the *N*_b-nitrogen atom of D-tryptophan derivatives, this provided a more direct access toward the important key intermediates. The crucial intermediates toward a number of alkaloids from this group could be synthesized in a two-step shorter process and in higher yields (see Chapter 1). More importantly, on further investigation of the improved process, an unprecedented stereoselectivity in the Pictet-Spengler reaction was realized and enabled access to the key intermediates from either of the starting amino acid ester chiral auxiliaries (see Chapter 2). Furthermore, the ambidextrous nature of the recently developed Pictet-Spengler reaction permitted the synthesis of a series of important intermediates enantiomeric to the intermediates toward the natural alkaloids. This route would eventually provide entry into the unnatural enantiomers of the alkaloids in enantiospecific fashion (see Chapter 3) for biological screening.

Described in Part II of this dissertation is the completion of the total synthesis of fourteen C-19 methyl substituted sarpagine/macroline alkaloids. A more efficient method for the enolate-driven metal-mediated cross-coupling process greatly improved (82-89% with CuI as the catalyst) the intramolecular α -vinylation of the ketone by replacing catalytic palladium (60-68% yield with Pd catalyst) with CuI. This enabled an much better entry into the pentacyclic framework with all the substituents and stereocenters required for most of the alkaloids in this group in place. To illustrate the effectiveness of this method the first total synthesis of macrocarpines D and E have been completed (see Chapter 4). In addition, application of the improved entry into the azabicyclo[3.3.1] moiety via the modified P-S/Dieckmann protocol, accompanied by the copper mediated cross-

coupling process, provided the total synthesis of talcarpine, *N*₄-methyl-*N*_{4,21}-secotalpinine, and macrocarpines A-C. The examination of the optical rotations and spectral data resulted in the correction of optical rotation values for macrocarpine A and *N*₄-methyl-*N*_{4,21}-secotalpinine, which were reported incorrectly earlier by others. Furthermore, to illustrate the versatility of the synthetic method described herein, the synthesis of two sarpagine alkaloids with the C-19 α methyl substitution pattern, termed dihydroperaksine and deoxyperaksine, have also been completed (see Chapter 5). This is the first stereospecific synthesis of alkaloids in this series, which contained either an α -methyl or β -methyl substituent at C-19.

Finally, a late stage demethylation of the *N*₆-methyl function furnished the total synthesis of macrocarpines F and G from macrocarpine A and macrocarpine C, respectively. A similar transformation also furnished talpinine from both *N*₄-methyl-*N*_{4,21}-secotalpinine and talcarpine. *O*-Acetyltalpinine has been accessed from talpinine by acetylation. Furthermore, a facile acid mediated hemiaminal formation process furnished the unusual quaternary hemiaminal containing alkaloid *N*₄-methyltalpinine from *N*₄-methyl-*N*_{4,21}-secotalpinine in excellent yield (see Chapter 6).

In summary, a total of fourteen alkaloids, which comprise macrocarpines A-G, talcarpine, *N*₄-methyl-*N*_{4,21}-secotalpinine, talpinine, *O*-acetyltalpinine, as well as *N*₄-methyltalpinine has been completed. Several of these alkaloids exhibited potential and important biological activity. In addition, the unnatural enantiomers of the bioactive alkaloids would also be accessible from the enantiomeric series of intermediates that have been synthesized from both D- and L-tryptophan in stereospecific fashion. Furthermore, the other bioactive alkaloids, which form this subgroup of bases (see General Introduction) would also be accessible by employing the synthetic strategy described herein.

Further investigation to extend the synthetic strategy, as well as to fully understand some of the transformations which could not be investigated to the full extent due to the lack of time and required material, will be of interest. It would be important to fully understand and rationalize the outcomes of the ambidextrous Pictet-Spengler reaction with the help of Density Field Theory (DFT) calculations and other computational methods. Further investigation would also be fruitful in understanding the copper-mediated cross-coupling process and the actual role of TEMPO in the complete formation of the desired α -vinaltion product. Elucidation of the complete mechanism of several competing reaction pathways would also be of interest in this process. In addition, the total synthesis of several alkaloids (e.g., rauvomines A and B, rauvovertine C) with important bioactivity and unusual structures would be easily accessible from the key intermediates prepared here in either enantiomeric form.

APPENDICES

III Appendix A (Chapter 1)

Single Crystal X-ray Analysis

The X-ray crystallographic work was supported by NIDA through Interagency Agreement #Y1-DA1101 with the Naval Research Laboratory (NRL).

The single-crystal X-ray diffraction data on compounds **12b** and **25** were collected using Mo K α radiation and a Bruker APEX II area detector. The single-crystal X-ray diffraction data on compounds **13a**, and **13b** were collected using Cu K α radiation and a Bruker Bruker Photon 100 CMOS area detector. All crystals were prepared for data collection by coating with high viscosity microscope oil and mounted on a micro-mesh mount (MiteGen, Inc.). The data for **25** were collected at 150 K, data for compounds **12b**, **13a**, and **13b** data were collected at 293 K. Corrections were applied for Lorentz, polarization, and absorption effects. The structures were solved by direct methods and refined by full-matrix least squares on F² values using the programs found in the SHELXL suite (Bruker, SHELXL v2014.7, 2014, Bruker AXS Inc., Madison, WI). The parameters refined included atomic coordinates and anisotropic thermal parameters for all non-hydrogen atoms. The H atoms were included using a riding model. The complete information on data collection and refinement is available in the corresponding sections.

The 0.660 x 0.456 x 0.236 mm³ crystal of **12b** was orthorhombic in space group P2₁2₁2₁, with unit cell dimensions a = 8.2529(2) Å, b = 13.1314(4) Å, c = 22.8333(6) Å, $\alpha = 90^\circ$, $\beta = 90^\circ$, and $\gamma = 90^\circ$. Data was 99.9% complete to 25° θ (~0.83 Å) with an average redundancy of 7.93. The final anisotropic full matrix least-squares refinement on F² with 281 variables converged at R₁ = 3.53%, for the observed data and wR₂ = 8.88% for all data.

The 0.220 x 0.167 x 0.082 mm³ crystal of **13a** was monoclinic in space group P2₁, with unit cell dimensions a = 9.4596(5) Å, b = 8.0074(3) Å, c = 18.4232(7) Å, $\alpha = 90^\circ$, $\beta = 98.023(3)^\circ$, and $\gamma = 90^\circ$. Data was 92.7% complete to 67.7° θ (~0.83 Å) with an average redundancy of 3.49. The final anisotropic full matrix least-squares refinement on F² with 326 variables converged at R₁ = 4.94%, for the observed data and wR2 = 13.85% for all data.

The 0.226 x 0.212 x 0.061 mm³ crystal of **13b** was triclinic in space group P1, with unit cell dimensions a = 7.5923(2) Å, b = 10.1456(3) Å, c = 18.6690(6) Å, $\alpha = 78.6760(10)^\circ$, $\beta = 89.2370(10)^\circ$, and $\gamma = 87.1770(10)^\circ$. Data was 86.0% complete to 67.7° θ (~0.83 Å) with an average redundancy of 2.57. The final anisotropic full matrix least-squares refinement on F² with 576 variables converged at R₁ = 3.39%, for the observed data and wR2 = 8.63% for all data.

The 0.733 x 0.708 x 0.586 mm³ crystal of **25** was monoclinic in space group P2₁, with unit cell dimensions a = 8.6453(9) Å, b = 8.3913(8) Å, c = 10.2653(11) Å, $\alpha = 90^\circ$, $\beta = 93.327(3)^\circ$, and $\gamma = 90^\circ$. Data was 100% complete to 25° θ (~0.83 Å) with an average redundancy of 4.5. The final anisotropic full matrix least-squares refinement on F² with 205 variables converged at R₁ = 3.35%, for the observed data and wR2 = 8.48% for all data.

X-ray Crystal Data for 12b

Table A1. Crystal data and structure refinement for **12b**.

Empirical formula	C ₂₇ H ₃₈ N ₂ OSi	
Formula weight	434.68	
Temperature	296(2) K	
Wavelength	0.71073 Å	
Crystal system	Orthorhombic	
Space group	P2 ₁ 2 ₁ 2 ₁	
Unit cell dimensions	a = 8.2529(2) Å	α = 90°.
	b = 13.1314(4) Å	β = 90°.
	c = 22.8333(6) Å	γ = 90°.
Volume	2474.49(12) Å ³	
Z	4	
Density (20 °C)	1.167 Mg/m ³	
Absorption coefficient	0.116 mm ⁻¹	
F(000)	944	
Crystal size	0.660 x 0.456 x 0.236 mm ³	
θ range for data collection	2.915 to 29.135°.	
Index ranges	-11 ≤ h ≤ 11, -17 ≤ k ≤ 17, -30 ≤ l ≤ 30	
Reflections collected	27470	
Independent reflections	6639 [R(int) = 0.0374]	
Completeness to θ = 25.000°	99.8 %	
Absorption correction	Semi-empirical from equivalents	
Max. and min. transmission	0.7458 and 0.6641	
Refinement method	Full-matrix least-squares on F ²	
Data / restraints / parameters	6639 / 0 / 281	
Goodness-of-fit on F ²	1.017	
Final R indices [I > 2σ(I)]	R1 = 0.0353, wR2 = 0.0836	
R indices (all data)	R1 = 0.0465, wR2 = 0.0888	
Absolute structure parameter	0.02(4)	
Largest diff. peak and hole	0.310 and -0.149 e.Å ⁻³	

Table A2. Atomic coordinates (x 10⁴) and equivalent isotropic displacement parameters (Å²x 10³)

for **12b**. U(eq) is defined as one third of the trace of the orthogonalized U^{ij} tensor.

	x	y	z	U(eq)
C(1)	5326(2)	3037(2)	5793(1)	25(1)
C(2)	6697(2)	2508(2)	5459(1)	25(1)
O(3)	9381(2)	1989(1)	5695(1)	31(1)
C(3)	7970(2)	2039(2)	5848(1)	22(1)
C(4)	7448(2)	1582(2)	6430(1)	22(1)

C(5)	6799(2)	488(2)	6350(1)	25(1)
C(6)	5062(2)	512(1)	6150(1)	23(1)
C(7)	4051(2)	-269(2)	5904(1)	25(1)
C(8)	4272(3)	-1290(2)	5746(1)	31(1)
C(9)	3017(3)	-1808(2)	5482(1)	38(1)
C(10)	1533(3)	-1329(2)	5367(1)	39(1)
C(11)	1268(3)	-324(2)	5515(1)	33(1)
C(12)	2538(2)	199(2)	5782(1)	25(1)
N(13)	2643(2)	1209(1)	5946(1)	24(1)
C(14)	4180(2)	1389(2)	6170(1)	23(1)
C(15)	4833(2)	2414(1)	6333(1)	22(1)
N(16)	6304(2)	2305(1)	6702(1)	21(1)
C(17)	5884(2)	2091(2)	7322(1)	23(1)
C(17A)	5293(2)	3072(2)	7614(1)	30(1)
C(18)	7297(2)	1683(2)	7645(1)	24(1)
C(19)	8409(2)	1337(2)	7924(1)	26(1)
Si(20)	10069(1)	705(1)	8326(1)	21(1)
C(21)	10584(2)	-486(2)	7902(1)	28(1)
C(22)	11067(3)	-221(2)	7269(1)	37(1)
C(23)	9213(3)	-1271(2)	7903(1)	43(1)
C(24)	9353(2)	467(2)	9099(1)	27(1)
C(25)	7548(3)	230(2)	9151(1)	43(1)
C(26)	10360(3)	-354(2)	9405(1)	40(1)
C(27)	11870(2)	1593(2)	8323(1)	25(1)
C(28)	13417(3)	1089(2)	8560(1)	35(1)
C(29)	11509(3)	2586(2)	8647(1)	34(1)
<hr/>				
C(1)-C(2)	1.531(3)		C(1)-C(15)	1.534(3)
C(1)-H(1A)	0.9700		C(1)-H(1B)	0.9700
C(2)-C(3)	1.506(3)		C(2)-H(2A)	0.9700
C(2)-H(2B)	0.9700		O(3)-C(3)	1.217(2)
C(3)-C(4)	1.522(3)		C(4)-N(16)	1.476(2)
C(4)-C(5)	1.545(3)		C(4)-H(4A)	0.9800
C(5)-C(6)	1.505(3)		C(5)-H(5A)	0.9700
C(5)-H(5B)	0.9700		C(6)-C(14)	1.363(3)
C(6)-C(7)	1.437(3)		C(7)-C(8)	1.399(3)
C(7)-C(12)	1.419(3)		C(8)-C(9)	1.379(3)
C(8)-H(8A)	0.9300		C(9)-C(10)	1.402(4)
C(9)-H(9A)	0.9300		C(10)-C(11)	1.379(3)
C(10)-H(10A)	0.9300		C(11)-C(12)	1.394(3)
C(11)-H(11A)	0.9300		C(12)-N(13)	1.380(3)
N(13)-C(14)	1.388(2)		N(13)-H(13A)	0.8600
C(14)-C(15)	1.498(3)		C(15)-N(16)	1.484(2)
C(15)-H(15A)	0.9800		N(16)-C(17)	1.484(2)
C(17)-C(18)	1.480(3)		C(17)-C(17A)	1.531(3)
C(17)-H(17A)	0.9800		C(17A)-H(17B)	0.9600
C(17A)-H(17C)	0.9600		C(17A)-H(17D)	0.9600

C(18)-C(19)	1.206(3)	C(19)-Si(20)	1.846(2)
Si(20)-C(21)	1.887(2)	Si(20)-C(24)	1.888(2)
Si(20)-C(27)	1.8885(19)	C(21)-C(23)	1.530(3)
C(21)-C(22)	1.541(3)	C(21)-H(21A)	0.9800
C(22)-H(22A)	0.9600	C(22)-H(22B)	0.9600
C(22)-H(22C)	0.9600	C(23)-H(23A)	0.9600
C(23)-H(23B)	0.9600	C(23)-H(23C)	0.9600
C(24)-C(25)	1.527(3)	C(24)-C(26)	1.531(3)
C(24)-H(24A)	0.9800	C(25)-H(25A)	0.9600
C(25)-H(25B)	0.9600	C(25)-H(25C)	0.9600
C(26)-H(26A)	0.9600	C(26)-H(26B)	0.9600
C(26)-H(26C)	0.9600	C(27)-C(29)	1.529(3)
C(27)-C(28)	1.537(3)	C(27)-H(27A)	0.9800
C(28)-H(28A)	0.9600	C(28)-H(28B)	0.9600
C(28)-H(28C)	0.9600	C(29)-H(29A)	0.9600
C(29)-H(29B)	0.9600	C(29)-H(29C)	0.9600
C(2)-C(1)-C(15)	110.76(16)	C(2)-C(1)-H(1A)	109.5
C(15)-C(1)-H(1A)	109.5	C(2)-C(1)-H(1B)	109.5
C(15)-C(1)-H(1B)	109.5	H(1A)-C(1)-H(1B)	108.1
C(3)-C(2)-C(1)	114.07(15)	C(3)-C(2)-H(2A)	108.7
C(1)-C(2)-H(2A)	108.7	C(3)-C(2)-H(2B)	108.7
C(1)-C(2)-H(2B)	108.7	H(2A)-C(2)-H(2B)	107.6
O(3)-C(3)-C(2)	121.36(18)	O(3)-C(3)-C(4)	120.00(17)
C(2)-C(3)-C(4)	118.59(15)	N(16)-C(4)-C(3)	107.17(15)
N(16)-C(4)-C(5)	115.24(15)	C(3)-C(4)-C(5)	111.18(15)
N(16)-C(4)-H(4A)	107.7	C(3)-C(4)-H(4A)	107.7
C(5)-C(4)-H(4A)	107.7	C(6)-C(5)-C(4)	110.26(15)
C(6)-C(5)-H(5A)	109.6	C(4)-C(5)-H(5A)	109.6
C(6)-C(5)-H(5B)	109.6	C(4)-C(5)-H(5B)	109.6
H(5A)-C(5)-H(5B)	108.1	C(14)-C(6)-C(7)	107.84(17)
C(14)-C(6)-C(5)	121.13(17)	C(7)-C(6)-C(5)	131.02(17)
C(8)-C(7)-C(12)	118.65(19)	C(8)-C(7)-C(6)	135.12(19)
C(12)-C(7)-C(6)	106.13(18)	C(9)-C(8)-C(7)	119.2(2)
C(9)-C(8)-H(8A)	120.4	C(7)-C(8)-H(8A)	120.4
C(8)-C(9)-C(10)	121.1(2)	C(8)-C(9)-H(9A)	119.5
C(10)-C(9)-H(9A)	119.5	C(11)-C(10)-C(9)	121.5(2)
C(11)-C(10)-H(10A)	119.3	C(9)-C(10)-H(10A)	119.3
C(10)-C(11)-C(12)	117.3(2)	C(10)-C(11)-H(11A)	121.3
C(12)-C(11)-H(11A)	121.3	N(13)-C(12)-C(11)	129.73(19)
N(13)-C(12)-C(7)	107.96(17)	C(11)-C(12)-C(7)	122.2(2)
C(12)-N(13)-C(14)	108.68(16)	C(12)-N(13)-H(13A)	125.7
C(14)-N(13)-H(13A)	125.7	C(6)-C(14)-N(13)	109.40(18)
C(6)-C(14)-C(15)	125.12(17)	N(13)-C(14)-C(15)	125.03(17)
N(16)-C(15)-C(14)	110.43(15)	N(16)-C(15)-C(1)	106.92(14)
C(14)-C(15)-C(1)	111.94(15)	N(16)-C(15)-H(15A)	109.2
C(14)-C(15)-H(15A)	109.2	C(1)-C(15)-H(15A)	109.2

C(4)-N(16)-C(15)	110.28(14)	C(4)-N(16)-C(17)	115.38(14)
C(15)-N(16)-C(17)	111.65(13)	C(18)-C(17)-N(16)	111.08(15)
C(18)-C(17)-C(17A)	109.84(16)	N(16)-C(17)-C(17A)	109.27(16)
C(18)-C(17)-H(17A)	108.9	N(16)-C(17)-H(17A)	108.9
C(17A)-C(17)-H(17A)	108.9	C(17)-C(17A)-H(17B)	109.5
C(17)-C(17A)-H(17C)	109.5	H(17B)-C(17A)-	
H(17C)	109.5	H(17B)-C(17A)-	
C(17)-C(17A)-H(17D)	109.5		
H(17D)	109.5		
H(17C)-C(17A)-H(17D)	109.5	C(19)-C(18)-C(17)	177.5(2)
C(18)-C(19)-Si(20)	175.3(2)	C(19)-Si(20)-C(21)	106.56(9)
C(19)-Si(20)-C(24)	107.84(9)	C(21)-Si(20)-C(24)	114.35(9)
C(19)-Si(20)-C(27)	107.77(9)	C(21)-Si(20)-C(27)	109.45(9)
C(24)-Si(20)-C(27)	110.59(9)	C(23)-C(21)-C(22)	110.21(18)
C(23)-C(21)-Si(20)	113.01(15)	C(22)-C(21)-Si(20)	110.57(15)
C(23)-C(21)-H(21A)	107.6	C(22)-C(21)-H(21A)	107.6
Si(20)-C(21)-H(21A)	107.6	C(21)-C(22)-H(22A)	109.5
C(21)-C(22)-H(22B)	109.5	H(22A)-C(22)-H(22B)	109.5
C(21)-C(22)-H(22C)	109.5	H(22A)-C(22)-H(22C)	109.5
H(22B)-C(22)-H(22C)	109.5	C(21)-C(23)-H(23A)	109.5
C(21)-C(23)-H(23B)	109.5	H(23A)-C(23)-H(23B)	109.5
C(21)-C(23)-H(23C)	109.5	H(23A)-C(23)-H(23C)	109.5
H(23B)-C(23)-H(23C)	109.5	C(25)-C(24)-C(26)	110.51(19)
C(25)-C(24)-Si(20)	114.32(15)	C(26)-C(24)-Si(20)	111.97(15)
C(25)-C(24)-H(24A)	106.5	C(26)-C(24)-H(24A)	106.5
Si(20)-C(24)-H(24A)	106.5	C(24)-C(25)-H(25A)	109.5
C(24)-C(25)-H(25B)	109.5	H(25A)-C(25)-H(25B)	109.5
C(24)-C(25)-H(25C)	109.5	H(25A)-C(25)-H(25C)	109.5
H(25B)-C(25)-H(25C)	109.5	C(24)-C(26)-H(26A)	109.5
C(24)-C(26)-H(26B)	109.5	H(26A)-C(26)-H(26B)	109.5
C(24)-C(26)-H(26C)	109.5	H(26A)-C(26)-H(26C)	109.5
H(26B)-C(26)-H(26C)	109.5	C(29)-C(27)-C(28)	110.98(18)
C(29)-C(27)-Si(20)	111.83(14)	C(28)-C(27)-Si(20)	112.73(14)
C(29)-C(27)-H(27A)	107.0	C(28)-C(27)-H(27A)	107.0
Si(20)-C(27)-H(27A)	107.0	C(27)-C(28)-H(28A)	109.5
C(27)-C(28)-H(28B)	109.5	H(28A)-C(28)-H(28B)	109.5
C(27)-C(28)-H(28C)	109.5	H(28A)-C(28)-H(28C)	109.5
H(28B)-C(28)-H(28C)	109.5	C(27)-C(29)-H(29A)	109.5
C(27)-C(29)-H(29B)	109.5	H(29A)-C(29)-H(29B)	109.5
C(27)-C(29)-H(29C)	109.5	H(29A)-C(29)-H(29C)	109.5
H(29B)-C(29)-H(29C)	109.5		

Table A3. Anisotropic displacement parameters ($\text{\AA}^2 \times 10^3$) for **12b**. The anisotropic displacement factor exponent takes the form: $-2\pi^2[h^2a^{*2}U^{11} + \dots + 2hk a^* b^* U^{12}]$

	U11	U22	U33	U23	U13	U12
C(1)	24(1)	27(1)	23(1)	1(1)	-6(1)	4(1)
C(2)	25(1)	31(1)	19(1)	4(1)	-3(1)	0(1)
O(3)	22(1)	44(1)	28(1)	6(1)	4(1)	6(1)
C(3)	21(1)	24(1)	21(1)	-3(1)	0(1)	2(1)
C(4)	16(1)	31(1)	18(1)	1(1)	-2(1)	5(1)
C(5)	20(1)	29(1)	25(1)	5(1)	-2(1)	5(1)
C(6)	20(1)	28(1)	20(1)	4(1)	-1(1)	1(1)
C(7)	25(1)	31(1)	19(1)	5(1)	1(1)	-2(1)
C(8)	35(1)	30(1)	29(1)	5(1)	2(1)	-1(1)
C(9)	46(1)	34(1)	35(1)	-3(1)	4(1)	-9(1)
C(10)	36(1)	45(1)	35(1)	-5(1)	2(1)	-16(1)
C(11)	24(1)	48(1)	28(1)	-1(1)	0(1)	-7(1)
C(12)	22(1)	35(1)	19(1)	3(1)	2(1)	-3(1)
N(13)	16(1)	33(1)	24(1)	3(1)	-3(1)	3(1)
C(14)	17(1)	32(1)	18(1)	3(1)	-2(1)	2(1)
C(15)	16(1)	29(1)	20(1)	1(1)	-3(1)	6(1)
N(16)	17(1)	30(1)	16(1)	1(1)	-2(1)	4(1)
C(17)	17(1)	33(1)	19(1)	1(1)	-2(1)	0(1)
C(17A)	27(1)	41(1)	22(1)	-4(1)	-1(1)	7(1)
C(18)	23(1)	32(1)	18(1)	1(1)	0(1)	-1(1)
C(19)	23(1)	34(1)	20(1)	2(1)	0(1)	1(1)
Si(20)	18(1)	26(1)	18(1)	2(1)	-2(1)	-1(1)
C(21)	27(1)	30(1)	26(1)	-2(1)	-5(1)	1(1)
C(22)	39(1)	46(1)	27(1)	-5(1)	1(1)	7(1)
C(23)	43(1)	39(1)	47(1)	-12(1)	-2(1)	-10(1)
C(24)	28(1)	30(1)	23(1)	2(1)	0(1)	-5(1)
C(25)	31(1)	57(2)	41(1)	8(1)	9(1)	-6(1)
C(26)	46(1)	44(1)	28(1)	14(1)	-6(1)	-2(1)
C(27)	21(1)	28(1)	25(1)	6(1)	-2(1)	-1(1)
C(28)	22(1)	37(1)	45(1)	8(1)	-6(1)	-3(1)
C(29)	30(1)	33(1)	39(1)	-3(1)	-1(1)	-5(1)

Table A4. Hydrogen coordinates ($\times 10^4$) and isotropic displacement parameters ($\text{\AA}^2 \times 10^3$) for **12b**.

	x	y	z	U(eq)
H(1A)	4397	3118	5537	30
H(1B)	5679	3709	5915	30
H(2A)	6234	1979	5214	30
H(2B)	7212	3001	5204	30
H(4A)	8409	1545	6682	26
H(5A)	7454	132	6062	30
H(5B)	6875	122	6718	30
H(8A)	5254	-1614	5819	38
H(9A)	3158	-2487	5378	46
H(10A)	708	-1697	5188	46
H(11A)	280	-9	5440	40
H(13A)	1882	1653	5914	29
H(15A)	4006	2789	6553	26
H(17A)	5010	1586	7333	28
H(17B)	5164	2960	8027	45
H(17C)	4272	3269	7447	45
H(17D)	6073	3604	7551	45
H(21A)	11526	-801	8091	33
H(22A)	11927	272	7273	56
H(22B)	11427	-825	7071	56
H(22C)	10148	57	7066	56
H(23A)	8922	-1430	8300	64
H(23B)	8289	-995	7703	64
H(23C)	9568	-1878	7708	64
H(24A)	9535	1101	9316	32
H(25A)	6934	751	8957	65
H(25B)	7326	-416	8971	65
H(25C)	7248	206	9557	65
H(26A)	11490	-194	9369	59
H(26B)	10071	-381	9812	59
H(26C)	10149	-1003	9227	59
H(27A)	12081	1772	7913	30
H(28A)	13618	468	8350	52
H(28B)	14318	1543	8509	52
H(28C)	13281	940	8969	52
H(29A)	10540	2886	8492	51
H(29B)	11363	2446	9056	51
H(29C)	12399	3049	8597	51

Table A5. Torsion angles [°] for **12b**.

C(15)-C(1)-C(2)-C(3)	-40.4(2)	C(1)-C(2)-C(3)-O(3)	-148.12(19)
C(1)-C(2)-C(3)-C(4)	34.5(2)	O(3)-C(3)-C(4)-N(16)	138.52(18)
C(2)-C(3)-C(4)-N(16)	-44.1(2)	O(3)-C(3)-C(4)-C(5)	-94.7(2)
C(2)-C(3)-C(4)-C(5)	82.7(2)	N(16)-C(4)-C(5)-C(6)	40.7(2)
C(3)-C(4)-C(5)-C(6)	-81.46(19)	C(4)-C(5)-C(6)-C(14)	-12.7(2)
C(4)-C(5)-C(6)-C(7)	165.45(18)	C(14)-C(6)-C(7)-C(8)	176.1(2)
C(5)-C(6)-C(7)-C(8)	-2.2(4)	C(14)-C(6)-C(7)-C(12)	0.1(2)
C(5)-C(6)-C(7)-C(12)	-178.25(18)	C(12)-C(7)-C(8)-C(9)	-0.3(3)
C(6)-C(7)-C(8)-C(9)	-176.1(2)	C(7)-C(8)-C(9)-C(10)	0.2(3)
C(8)-C(9)-C(10)-C(11)	-0.2(4)	C(9)-C(10)-C(11)-C(12)	0.2(3)
C(10)-C(11)-C(12)-N(13)	176.1(2)	C(10)-C(11)-C(12)-C(7)	-0.4(3)
C(8)-C(7)-C(12)-N(13)	-176.73(17)	C(6)-C(7)-C(12)-N(13)	0.1(2)
C(8)-C(7)-C(12)-C(11)	0.4(3)	C(6)-C(7)-C(12)-C(11)	177.28(18)
C(11)-C(12)-N(13)-C(14)	-177.1(2)	C(7)-C(12)-N(13)-C(14)	-0.3(2)
C(7)-C(6)-C(14)-N(13)	-0.2(2)	C(5)-C(6)-C(14)-N(13)	178.29(15)
C(7)-C(6)-C(14)-C(15)	-172.80(17)	C(5)-C(6)-C(14)-C(15)	5.7(3)
C(12)-N(13)-C(14)-C(6)	0.3(2)	C(12)-N(13)-C(14)-C(15)	172.88(17)
C(6)-C(14)-C(15)-N(16)	-24.0(2)	N(13)-C(14)-C(15)-N(16)	164.56(16)
C(6)-C(14)-C(15)-C(1)	95.0(2)	N(13)-C(14)-C(15)-C(1)	-76.4(2)
C(2)-C(1)-C(15)-N(16)	58.40(19)	C(2)-C(1)-C(15)-C(14)	-62.7(2)
C(3)-C(4)-N(16)-C(15)	63.12(18)	C(5)-C(4)-N(16)-C(15)	-61.2(2)
C(3)-C(4)-N(16)-C(17)	-169.25(15)	C(5)-C(4)-N(16)-C(17)	66.4(2)
C(14)-C(15)-N(16)-C(4)	49.26(19)	C(1)-C(15)-N(16)-C(4)	-72.76(18)
C(14)-C(15)-N(16)-C(17)	-80.41(19)	C(1)-C(15)-N(16)-C(17)	157.57(16)
C(4)-N(16)-C(17)-C(18)	36.0(2)	C(15)-N(16)-C(17)-C(18)	162.96(16)
C(4)-N(16)-C(17)-C(17A)	157.36(15)	C(15)-N(16)-C(17)-C(17A)	-75.70(18)
C(19)-Si(20)-C(21)-C(23)	-66.11(18)	C(24)-Si(20)-C(21)-C(23)	52.92(18)
C(27)-Si(20)-C(21)-C(23)	177.62(16)	C(19)-Si(20)-C(21)-C(22)	57.96(16)
C(24)-Si(20)-C(21)-C(22)	177.00(14)	C(27)-Si(20)-C(21)-C(22)	-58.30(17)
C(19)-Si(20)-C(24)-C(25)	33.8(2)	C(21)-Si(20)-C(24)-C(25)	-84.49(19)
C(27)-Si(20)-C(24)-C(25)	151.42(17)	C(19)-Si(20)-C(24)-C(26)	160.48(15)
C(21)-Si(20)-C(24)-C(26)	42.17(18)	C(27)-Si(20)-C(24)-C(26)	-81.92(17)
C(19)-Si(20)-C(27)-C(29)	63.07(17)	C(21)-Si(20)-C(27)-C(29)	178.58(14)
C(24)-Si(20)-C(27)-C(29)	-54.57(17)	C(19)-Si(20)-C(27)-C(28)	-171.05(16)
C(21)-Si(20)-C(27)-C(28)	-55.55(18)	C(24)-Si(20)-C(27)-C(28)	71.30(18)

Table A6. Hydrogen bonds for **12b** [\AA and $^\circ$].

D-H...A	d(D-H)	d(H...A)	d(D...A)	$\angle(\text{DHA})$
N(13)-H(13A)...O(3)#1	0.86	2.17	2.937(2)	148.4

Symmetry transformations used to generate equivalent atoms:

#1 $x-1, y, z$ **X-ray Crystal Data for 13a****Table A7.** Crystal data and structure refinement for **13a**.

Empirical formula	$\text{C}_{25}\text{H}_{39}\text{ClN}_2\text{O}_2\text{Si}$	
Formula weight	463.12	
Temperature	293(2) K	
Wavelength	1.54178 \AA	
Crystal system	Monoclinic	
Space group	$P2_1$	
Unit cell dimensions	$a = 9.4596(5) \text{\AA}$ $b = 8.0074(3) \text{\AA}$ $c = 18.4232(7) \text{\AA}$	$\alpha = 90^\circ$ $\beta = 98.023(3)^\circ$ $\gamma = 90^\circ$
Volume	$1381.84(10) \text{\AA}^3$	
Z	2	
Density (20 $^\circ\text{C}$)	1.113 Mg/m^3	
Absorption coefficient	1.800 mm^{-1}	
F(000)	500	
Crystal size	$0.220 \times 0.167 \times 0.082 \text{ mm}^3$	
θ range for data collection	5.602 to 68.758° .	
Index ranges	$-11 \leq h \leq 9$, $-9 \leq k \leq 9$, $-20 \leq l \leq 21$	
Reflections collected	8129	
Independent reflections	4166 [R(int) = 0.0462]	
Completeness to $\theta = 67.679^\circ$	92.7 %	
Absorption correction	Semi-empirical from equivalents	
Max. and min. transmission	0.7531 and 0.6026	
Refinement method	Full-matrix least-squares on F^2	
Data / restraints / parameters	4166 / 259 / 326	
Goodness-of-fit on F^2	1.043	
Final R indices [$I > 2\sigma(I)$]	$R1 = 0.0494$, $wR2 = 0.1158$	
R indices (all data)	$R1 = 0.0857$, $wR2 = 0.1385$	
Absolute structure parameter	0.068(14)	
Largest diff. peak and hole	0.213 and $-0.192 \text{ e.\AA}^{-3}$	

Table A8. Atomic coordinates ($\times 10^4$) and equivalent isotropic displacement parameters ($\text{\AA}^2 \times 10^3$)

for **13a**. $U(\text{eq})$ is defined as one third of the trace of the orthogonalized U_{ij} tensor.

	x	y	z	U(eq)
Cl(1)	5836(13)	4263(17)	5814(7)	75(2)
Cl(1B)	5395(13)	4080(14)	5834(7)	86(3)
C(1)	9457(8)	2054(8)	4290(4)	87(2)
N(2)	10488(6)	1550(6)	3898(4)	96(2)
C(3)	9956(7)	1596(7)	3175(4)	83(2)
C(4)	10574(9)	1200(9)	2563(5)	112(2)
C(5)	9783(13)	1301(11)	1899(5)	132(3)
C(6)	8357(12)	1818(11)	1825(4)	126(3)
C(7)	7710(8)	2229(8)	2428(3)	93(2)
C(8)	8521(6)	2136(6)	3114(3)	72(1)
C(9)	8223(6)	2446(6)	3843(3)	71(1)
C(10)	6848(7)	2965(7)	4091(3)	76(1)
O(11B)	7926(5)	6467(5)	3380(2)	91(1)
O(11A)	7808(5)	6575(6)	4575(3)	110(2)
C(11A)	7433(6)	6025(7)	3973(3)	71(1)
C(11)	6313(5)	4680(6)	3817(3)	64(1)
C(11B)	8976(9)	7793(9)	3443(5)	129(3)
N(12)	5050(4)	5194(5)	4179(2)	64(1)
C(13)	3657(5)	4380(6)	3864(2)	65(1)
C(13A)	2493(7)	5077(7)	4259(3)	81(2)
C(14)	3406(6)	4719(6)	3072(3)	68(1)
C(15)	3239(6)	5061(7)	2430(3)	73(1)
Si(1)	3049(2)	5846(2)	1484(1)	82(1)
C(16)	1286(10)	6979(14)	1307(5)	138(3)
C(17)	1027(12)	7830(18)	558(6)	196(6)
C(18)	55(11)	6001(18)	1509(9)	204(6)
C(19)	4484(9)	7463(11)	1492(4)	121(2)
C(20)	5996(10)	6670(20)	1555(7)	217(7)
C(21)	4434(15)	8768(15)	2083(6)	195(5)
C(22A)	2810(20)	4007(18)	840(8)	106(6)
C(23A)	3040(40)	4520(60)	77(11)	144(10)
C(24A)	3870(40)	2690(30)	1143(13)	207(17)
C(22B)	3670(30)	4210(20)	866(12)	136(9)
C(24B)	3070(40)	2470(30)	887(12)	192(15)
C(23B)	3880(50)	4770(70)	105(15)	230(30)

Table A9. Bond lengths [Å] and angles [°] for **13a**.

C(1)-N(2)	1.353(9)	C(1)-C(9)	1.368(8)
C(1)-H(1)	0.9300	N(2)-C(3)	1.356(9)
N(2)-H(2)	0.8600	C(3)-C(4)	1.377(10)
C(3)-C(8)	1.414(9)	C(4)-C(5)	1.344(12)
C(4)-H(4)	0.9300	C(5)-C(6)	1.400(13)
C(5)-H(5)	0.9300	C(6)-C(7)	1.382(10)
C(6)-H(6)	0.9300	C(7)-C(8)	1.385(8)
C(7)-H(7)	0.9300	C(8)-C(9)	1.431(8)
C(9)-C(10)	1.496(8)	C(10)-C(11)	1.525(7)
C(10)-H(10A)	0.9700	C(10)-H(10B)	0.9700
O(11B)-C(11A)	1.296(7)	O(11B)-C(11B)	1.448(7)
O(11A)-C(11A)	1.199(7)	C(11A)-C(11)	1.509(7)
C(11)-N(12)	1.505(7)	C(11)-H(11)	0.9800
C(11B)-H(11A)	0.9600	C(11B)-H(11B)	0.9600
C(11B)-H(11C)	0.9600	N(12)-C(13)	1.511(6)
N(12)-H(12A)	0.8900	N(12)-H(12B)	0.8900
C(13)-C(14)	1.471(7)	C(13)-C(13A)	1.508(8)
C(13)-H(13)	0.9800	C(13A)-H(13A)	0.9600
C(13A)-H(13B)	0.9600	C(13A)-H(13C)	0.9600
C(14)-C(15)	1.203(7)	C(15)-Si(1)	1.839(6)
Si(1)-C(19)	1.874(9)	Si(1)-C(22B)	1.883(11)
Si(1)-C(22A)	1.885(11)	Si(1)-C(16)	1.886(9)
C(16)-C(18)	1.493(15)	C(16)-C(17)	1.528(13)
C(16)-H(16)	0.9800	C(17)-H(17A)	0.9600
C(17)-H(17B)	0.9600	C(17)-H(17C)	0.9600
C(18)-H(18A)	0.9600	C(18)-H(18B)	0.9600
C(18)-H(18C)	0.9600	C(19)-C(21)	1.515(14)
C(19)-C(20)	1.555(13)	C(19)-H(19)	0.9800
C(20)-H(20A)	0.9600	C(20)-H(20B)	0.9600
C(20)-H(20C)	0.9600	C(21)-H(21A)	0.9600
C(21)-H(21B)	0.9600	C(21)-H(21C)	0.9600
C(22A)-C(23A)	1.510(12)	C(22A)-C(24A)	1.510(13)
C(22A)-H(22A)	0.9800	C(23A)-H(23A)	0.9600
C(23A)-H(23B)	0.9600	C(23A)-H(23C)	0.9600
C(24A)-H(24A)	0.9600	C(24A)-H(24B)	0.9600
C(24A)-H(24C)	0.9600	C(22B)-C(24B)	1.508(13)
C(22B)-C(23B)	1.511(12)	C(22B)-H(22B)	0.9800
C(24B)-H(24D)	0.9600	C(24B)-H(24E)	0.9600
C(24B)-H(24F)	0.9600	C(23B)-H(23D)	0.9600
C(23B)-H(23E)	0.9600	C(23B)-H(23F)	0.9600
N(2)-C(1)-C(9)	111.4(6)	N(2)-C(1)-H(1)	124.3
C(9)-C(1)-H(1)	124.3	C(1)-N(2)-C(3)	108.6(6)
C(1)-N(2)-H(2)	125.7	C(3)-N(2)-H(2)	125.7
N(2)-C(3)-C(4)	130.9(7)	N(2)-C(3)-C(8)	107.9(6)

C(4)-C(3)-C(8)	121.2(7)	C(5)-C(4)-C(3)	119.0(8)
C(5)-C(4)-H(4)	120.5	C(3)-C(4)-H(4)	120.5
C(4)-C(5)-C(6)	120.9(8)	C(4)-C(5)-H(5)	119.5
C(6)-C(5)-H(5)	119.5	C(7)-C(6)-C(5)	121.4(8)
C(7)-C(6)-H(6)	119.3	C(5)-C(6)-H(6)	119.3
C(6)-C(7)-C(8)	118.0(7)	C(6)-C(7)-H(7)	121.0
C(8)-C(7)-H(7)	121.0	C(7)-C(8)-C(3)	119.5(6)
C(7)-C(8)-C(9)	133.6(6)	C(3)-C(8)-C(9)	106.9(5)
C(1)-C(9)-C(8)	105.1(6)	C(1)-C(9)-C(10)	125.8(6)
C(8)-C(9)-C(10)	128.9(5)	C(9)-C(10)-C(11)	114.3(4)
C(9)-C(10)-H(10A)	108.7	C(11)-C(10)-H(10A)	108.7
C(9)-C(10)-H(10B)	108.7	C(11)-C(10)-H(10B)	108.7
H(10A)-C(10)-H(10B)	107.6	C(11A)-O(11B)-C(11B)	117.1(5)
O(11A)-C(11A)-O(11B)	125.8(5)	O(11A)-C(11A)-C(11)	123.1(5)
O(11B)-C(11A)-C(11)	111.1(4)	N(12)-C(11)-C(11A)	107.5(4)
N(12)-C(11)-C(10)	110.3(4)	C(11A)-C(11)-C(10)	112.9(4)
N(12)-C(11)-H(11)	108.7	C(11A)-C(11)-H(11)	108.7
C(10)-C(11)-H(11)	108.7	O(11B)-C(11B)-H(11A)	109.5
O(11B)-C(11B)-H(11B)	109.5	H(11A)-C(11B)-H(11B)	109.5
O(11B)-C(11B)-H(11C)	109.5	H(11A)-C(11B)-H(11C)	109.5
H(11B)-C(11B)-H(11C)	109.5	C(11)-N(12)-C(13)	114.6(4)
C(11)-N(12)-H(12A)	108.6	C(13)-N(12)-H(12A)	108.6
C(11)-N(12)-H(12B)	108.6	C(13)-N(12)-H(12B)	108.6
H(12A)-N(12)-H(12B)	107.6	C(14)-C(13)-C(13A)	112.5(4)
C(14)-C(13)-N(12)	108.2(4)	C(13A)-C(13)-N(12)	108.1(4)
C(14)-C(13)-H(13)	109.3	C(13A)-C(13)-H(13)	109.3
N(12)-C(13)-H(13)	109.3	C(13)-C(13A)-H(13A)	109.5
C(13)-C(13A)-H(13B)	109.5	H(13A)-C(13A)-H(13B)	109.5
C(13)-C(13A)-H(13C)	109.5	H(13A)-C(13A)-H(13C)	109.5
H(13B)-C(13A)-H(13C)	109.5	C(15)-C(14)-C(13)	177.0(5)
C(14)-C(15)-Si(1)	172.9(5)	C(15)-Si(1)-C(19)	104.7(3)
C(15)-Si(1)-C(22B)	109.7(7)	C(19)-Si(1)-C(22B)	101.4(8)
C(15)-Si(1)-C(22A)	108.4(6)	C(19)-Si(1)-C(22A)	124.7(7)
C(15)-Si(1)-C(16)	107.2(4)	C(19)-Si(1)-C(16)	106.9(4)
C(22B)-Si(1)-C(16)	125.0(10)	C(22A)-Si(1)-C(16)	103.9(6)
C(18)-C(16)-C(17)	115.3(9)	C(18)-C(16)-Si(1)	114.0(8)
C(17)-C(16)-Si(1)	113.4(8)	C(18)-C(16)-H(16)	104.2
C(17)-C(16)-H(16)	104.2	Si(1)-C(16)-H(16)	104.2
C(16)-C(17)-H(17A)	109.5	C(16)-C(17)-H(17B)	109.5
H(17A)-C(17)-H(17B)	109.5	C(16)-C(17)-H(17C)	109.5
H(17A)-C(17)-H(17C)	109.5	H(17B)-C(17)-H(17C)	109.5
C(16)-C(18)-H(18A)	109.5	C(16)-C(18)-H(18B)	109.5
H(18A)-C(18)-H(18B)	109.5	C(16)-C(18)-H(18C)	109.5
H(18A)-C(18)-H(18C)	109.5	H(18B)-C(18)-H(18C)	109.5
C(21)-C(19)-C(20)	110.4(10)	C(21)-C(19)-Si(1)	112.8(7)
C(20)-C(19)-Si(1)	112.1(8)	C(21)-C(19)-H(19)	107.1

C(20)-C(19)-H(19)	107.1	Si(1)-C(19)-H(19)	107.1
C(19)-C(20)-H(20A)	109.5	C(19)-C(20)-H(20B)	109.5
H(20A)-C(20)-H(20B)	109.5	C(19)-C(20)-H(20C)	109.5
H(20A)-C(20)-H(20C)	109.5	H(20B)-C(20)-H(20C)	109.5
C(19)-C(21)-H(21A)	109.5	C(19)-C(21)-H(21B)	109.5
H(21A)-C(21)-H(21B)	109.5	C(19)-C(21)-H(21C)	109.5
H(21A)-C(21)-H(21C)	109.5	H(21B)-C(21)-H(21C)	109.5
C(23A)-C(22A)-C(24A)	111(2)	C(23A)-C(22A)-Si(1)	110.5(19)
C(24A)-C(22A)-Si(1)	107.3(12)	C(23A)-C(22A)-H(22A)	109.3
C(24A)-C(22A)-H(22A)	109.3	Si(1)-C(22A)-H(22A)	109.3
C(22A)-C(23A)-H(23A)	109.5	C(22A)-C(23A)-H(23B)	109.5
H(23A)-C(23A)-H(23B)	109.5	C(22A)-C(23A)-H(23C)	109.5
H(23A)-C(23A)-H(23C)	109.5	H(23B)-C(23A)-H(23C)	109.5
C(22A)-C(24A)-H(24A)	109.5	C(22A)-C(24A)-H(24B)	109.5
H(24A)-C(24A)-H(24B)	109.5	C(22A)-C(24A)-H(24C)	109.5
H(24A)-C(24A)-H(24C)	109.5	H(24B)-C(24A)-H(24C)	109.5
C(24B)-C(22B)-C(23B)	113(3)	C(24B)-C(22B)-Si(1)	118.5(18)
C(23B)-C(22B)-Si(1)	116(2)	C(24B)-C(22B)-H(22B)	101.5
C(23B)-C(22B)-H(22B)	101.5	Si(1)-C(22B)-H(22B)	101.5
C(22B)-C(24B)-H(24D)	109.5	C(22B)-C(24B)-H(24E)	109.5
H(24D)-C(24B)-H(24E)	109.5	C(22B)-C(24B)-H(24F)	109.5
H(24D)-C(24B)-H(24F)	109.5	H(24E)-C(24B)-H(24F)	109.5
C(22B)-C(23B)-H(23D)	109.5	C(22B)-C(23B)-H(23E)	109.5
H(23D)-C(23B)-H(23E)	109.5	C(22B)-C(23B)-H(23F)	109.5
H(23D)-C(23B)-H(23F)	109.5	H(23E)-C(23B)-H(23F)	109.5

Table A10. Anisotropic displacement parameters ($\text{\AA}^2 \times 10^3$) for **13a**. The anisotropic displacement factor exponent takes the form: $-2 \square^2 [h^2 a^* 2U^{11} + \dots + 2 h k a^* b^* U^{12}]$

	U11	U22	U33	U23	U13	U12
Cl(1)	95(5)	84(4)	45(3)	-2(2)	6(3)	10(3)
Cl(1B)	141(9)	60(3)	59(3)	10(2)	26(5)	28(5)
C(1)	100(5)	78(4)	80(4)	7(3)	-4(3)	-22(3)
N(2)	80(4)	83(3)	120(4)	10(3)	-2(3)	-14(3)
C(3)	92(4)	53(3)	106(4)	1(3)	18(3)	-14(3)
C(4)	123(6)	74(4)	149(6)	-1(4)	58(5)	-9(4)
C(5)	186(8)	104(6)	119(6)	-16(5)	71(6)	-2(6)
C(6)	178(8)	118(6)	82(5)	-17(4)	22(5)	-7(6)
C(7)	123(5)	81(4)	72(4)	-8(3)	6(3)	-2(4)
C(8)	89(4)	53(3)	71(3)	2(2)	6(3)	-10(2)
C(9)	85(4)	54(3)	72(3)	5(2)	2(3)	-14(2)
C(10)	94(4)	62(3)	71(3)	4(2)	9(3)	-10(3)
O(11B)	112(3)	68(2)	93(3)	13(2)	15(2)	-33(2)

O(11A)	121(4)	113(3)	89(3)	-14(2)	-15(2)	-48(3)
C(11A)	78(3)	60(3)	69(3)	3(3)	-11(2)	-8(2)
C(11)	83(3)	63(3)	45(3)	1(2)	2(2)	-13(2)
C(11B)	128(7)	88(5)	170(8)	14(5)	20(5)	-52(4)
N(12)	90(3)	56(2)	43(2)	0(2)	-1(2)	-13(2)
C(13)	84(3)	60(3)	49(3)	-2(2)	4(2)	-14(2)
C(13A)	100(4)	72(3)	71(4)	0(3)	19(3)	-12(3)
C(14)	75(3)	68(3)	57(3)	-8(2)	-1(2)	-15(2)
C(15)	72(3)	90(4)	54(3)	-7(3)	-1(2)	-12(3)
Si(1)	99(1)	94(1)	50(1)	4(1)	1(1)	7(1)
C(16)	121(6)	155(8)	127(6)	12(6)	-22(5)	22(5)
C(17)	184(10)	250(15)	137(8)	42(8)	-44(7)	80(10)
C(18)	98(7)	191(12)	320(18)	19(11)	18(8)	5(7)
C(19)	136(6)	135(6)	91(5)	43(4)	15(4)	-3(5)
C(20)	101(7)	352(19)	196(11)	136(12)	12(6)	13(8)
C(21)	284(15)	150(9)	147(9)	-10(7)	17(8)	-98(9)
C(22A)	140(16)	115(13)	63(7)	-6(8)	13(9)	19(10)
C(23A)	190(20)	190(30)	59(10)	-22(11)	13(11)	30(20)
C(24A)	330(40)	147(19)	111(16)	-71(13)	-71(19)	130(20)
C(22B)	220(30)	107(11)	92(11)	-3(9)	63(16)	16(14)
C(24B)	370(40)	123(14)	85(16)	-18(13)	40(20)	-50(20)
C(23B)	420(80)	190(20)	120(20)	-6(19)	150(40)	20(40)

Table A11. Hydrogen coordinates ($\times 10^4$) and isotropic displacement parameters ($\text{\AA}^2 \times 10^3$) for **13a**.

	x	y	z	U(eq)
H(1)	9573	2124	4798	105
H(2)	11339	1251	4077	115
H(4)	11524	868	2609	134
H(5)	10189	1023	1484	158
H(6)	7833	1886	1359	151
H(7)	6758	2558	2376	111
H(10A)	6973	2967	4622	91
H(10B)	6123	2142	3924	91
H(11)	6016	4620	3287	77
H(11A)	8605	8753	3665	194
H(11B)	9188	8085	2964	194
H(11C)	9832	7422	3741	194
H(12A)	4949	6297	4141	77
H(12B)	5231	4948	4654	77
H(13)	3727	3171	3945	78
H(13A)	2410	6257	4173	121

H(13B)	2725	4872	4775	121
H(13C)	1604	4544	4079	121
H(16)	1392	7907	1657	165
H(17A)	900	6997	180	294
H(17B)	1833	8518	496	294
H(17C)	185	8510	528	294
H(18A)	-795	6669	1425	306
H(18B)	241	5697	2018	306
H(18C)	-73	5010	1214	306
H(19)	4317	8045	1020	145
H(20A)	6691	7528	1517	325
H(20B)	6021	5873	1167	325
H(20C)	6211	6116	2020	325
H(21A)	4339	8227	2539	292
H(21B)	3633	9494	1948	292
H(21C)	5300	9411	2138	292
H(22A)	1838	3564	826	128
H(23A)	2293	5278	-121	216
H(23B)	3018	3553	-230	216
H(23C)	3945	5069	97	216
H(24A)	3648	2309	1608	311
H(24B)	4816	3157	1206	311
H(24C)	3829	1766	808	311
H(22B)	4661	4039	1093	163
H(24D)	2832	2057	396	288
H(24E)	2231	2491	1125	288
H(24F)	3772	1750	1155	288
H(23D)	4399	3939	-120	347
H(23E)	4400	5805	136	347
H(23F)	2962	4938	-184	347

Table A12. Torsion angles [°] for **13a**.

C(9)-C(1)-N(2)-C(3)	0.0(7)	C(1)-N(2)-C(3)-C(4)	-179.7(6)
C(1)-N(2)-C(3)-C(8)	-0.7(6)	N(2)-C(3)-C(4)-C(5)	177.6(7)
C(8)-C(3)-C(4)-C(5)	-1.3(10)	C(3)-C(4)-C(5)-C(6)	0.8(12)
C(4)-C(5)-C(6)-C(7)	-0.5(13)	C(5)-C(6)-C(7)-C(8)	0.8(11)
C(6)-C(7)-C(8)-C(3)	-1.3(9)	C(6)-C(7)-C(8)-C(9)	-179.5(6)
N(2)-C(3)-C(8)-C(7)	-177.5(5)	C(4)-C(3)-C(8)-C(7)	1.6(8)
N(2)-C(3)-C(8)-C(9)	1.1(6)	C(4)-C(3)-C(8)-C(9)	-179.8(5)
N(2)-C(1)-C(9)-C(8)	0.7(6)	N(2)-C(1)-C(9)-C(10)	176.8(5)
C(7)-C(8)-C(9)-C(1)	177.2(6)	C(3)-C(8)-C(9)-C(1)	-1.1(6)
C(7)-C(8)-C(9)-C(10)	1.3(9)	C(3)-C(8)-C(9)-C(10)	-177.0(5)
C(1)-C(9)-C(10)-C(11)	121.0(6)	C(8)-C(9)-C(10)-C(11)	-63.8(7)
C(11B)-O(11B)-C(11A)-O(11A)	-3.0(9)	C(11B)-O(11B)-C(11A)-C(11)	
	177.9(5)		
O(11A)-C(11A)-C(11)-N(12)	49.1(7)	O(11B)-C(11A)-C(11)-N(12)	-131.7(5)
O(11A)-C(11A)-C(11)-C(10)	-72.7(7)	O(11B)-C(11A)-C(11)-C(10)	106.4(5)
C(9)-C(10)-C(11)-N(12)	-172.0(4)	C(9)-C(10)-C(11)-C(11A)	-51.7(6)
C(11A)-C(11)-N(12)-C(13)	158.4(4)	C(10)-C(11)-N(12)-C(13)	-78.2(5)
C(11)-N(12)-C(13)-C(14)	-55.4(5)	C(11)-N(12)-C(13)-C(13A)	-177.5(4)
C(15)-Si(1)-C(16)-C(18)	-50.1(10)	C(19)-Si(1)-C(16)-C(18)	-161.9(9)
C(22B)-Si(1)-C(16)-C(18)	80.3(12)	C(22A)-Si(1)-C(16)-C(18)	64.6(11)
C(15)-Si(1)-C(16)-C(17)	175.3(8)	C(19)-Si(1)-C(16)-C(17)	63.5(9)
C(22B)-Si(1)-C(16)-C(17)	-54.3(13)	C(22A)-Si(1)-C(16)-C(17)	-70.0(11)
C(15)-Si(1)-C(19)-C(21)	-53.1(8)	C(22B)-Si(1)-C(19)-C(21)	-167.2(11)
C(22A)-Si(1)-C(19)-C(21)	-178.5(9)	C(16)-Si(1)-C(19)-C(21)	60.4(8)
C(15)-Si(1)-C(19)-C(20)	72.2(7)	C(22B)-Si(1)-C(19)-C(20)	-41.9(11)
C(22A)-Si(1)-C(19)-C(20)	-53.2(10)	C(16)-Si(1)-C(19)-C(20)	-174.3(7)
C(15)-Si(1)-C(22A)-C(23A)	-165.0(16)	C(19)-Si(1)-C(22A)-C(23A)	-41.2(19)
C(16)-Si(1)-C(22A)-C(23A)	81.2(18)	C(15)-Si(1)-C(22A)-C(24A)	-44(2)
C(19)-Si(1)-C(22A)-C(24A)	80(2)	C(16)-Si(1)-C(22A)-C(24A)	-157(2)
C(15)-Si(1)-C(22B)-C(24B)	52(3)	C(19)-Si(1)-C(22B)-C(24B)	162(2)
C(16)-Si(1)-C(22B)-C(24B)	-78(3)	C(15)-Si(1)-C(22B)-C(23B)	-168(2)
C(19)-Si(1)-C(22B)-C(23B)	-57(3)	C(16)-Si(1)-C(22B)-C(23B)	63(3)

Table A13. Hydrogen bonds for **13a** [Å and °].

D-H...A	d(D-H)	d(H...A)	d(D...A)	<(DHA)
N(12)-H(12A)...Cl(1B)#3	0.89	2.25	3.139(12)	173.6
N(12)-H(12B)...Cl(1)	0.89	2.20	3.091(12)	175.7
N(12)-H(12B)...Cl(1B)	0.89	2.27	3.150(13)	171.4

Symmetry transformations used to generate equivalent atoms:
 #1 -x+2,y-1/2,-z+1 #2 -x+1,y-1/2,-z+1 #3 -x+1,y+1/2,-z+1
 #4 x-1,y,z

X-ray Crystal Data for 13b

Table A14. Crystal data and structure refinement for **13b**.

Empirical formula	C ₂₅ H ₃₉ ClN ₂ O ₂ Si	
Formula weight	463.12	
Temperature	293(2) K	
Wavelength	1.54178 Å	
Crystal system	Triclinic	
Space group	P1	
Unit cell dimensions	a = 7.5923(2) Å	α = 78.6760(10)°.
	b = 10.1456(3) Å	β = 89.2370(10)°.
	c = 18.6690(6) Å	γ = 87.1770(10)°.
Volume	1408.33(7) Å ³	
Z	2	
Density (20 °C)	1.092 Mg/m ³	
Absorption coefficient	1.766 mm ⁻¹	
F(000)	500	
Crystal size	0.226 x 0.212 x 0.061 mm ³	
θ range for data collection	2.414 to 74.515°.	
Index ranges	-9<=h<=7, -10<=k<=12, -20<=l<=22	
Reflections collected	10787	
Independent reflections	6840 [R(int) = 0.0265]	
Completeness to θ = 67.500°	86.0 %	
Absorption correction	Semi-empirical from equivalents	
Max. and min. transmission	0.7538 and 0.6249	
Refinement method	Full-matrix least-squares on F ²	
Data / restraints / parameters	6840 / 3 / 576	
Goodness-of-fit on F ²	1.065	
Final R indices [I>2σ(I)]	R1 = 0.0339, wR2 = 0.0848	
R indices (all data)	R1 = 0.0356, wR2 = 0.0863	
Absolute structure parameter	0.057(8)	
Extinction coefficient	0.0303(10)	
Largest diff. peak and hole	0.205 and -0.191 e.Å ⁻³	

Table A15. Atomic coordinates ($\times 10^4$) and equivalent isotropic displacement parameters ($\text{\AA}^2 \times 10^3$)

for **13b**. $U(\text{eq})$ is defined as one third of the trace of the orthogonalized U^{ij} tensor.

	x	y	z	U(eq)
Cl(1')	2054(1)	253(1)	5760(1)	51(1)
Cl(1)	6972(1)	9563(1)	4207(1)	49(1)
C(1)	10756(6)	4538(4)	5588(2)	74(1)
N(2)	11327(5)	3338(3)	6009(2)	88(1)
C(3)	11822(5)	3546(3)	6678(3)	73(1)
C(4)	12470(7)	2669(5)	7285(4)	104(2)
C(5)	12777(8)	3166(7)	7884(4)	120(2)
C(6)	12546(9)	4527(7)	7898(3)	115(2)
C(7)	11947(6)	5417(5)	7293(3)	85(1)
C(8)	11566(5)	4941(3)	6667(2)	61(1)
C(9)	10886(5)	5539(3)	5965(2)	56(1)
C(10)	10343(5)	6991(3)	5687(2)	56(1)
C(11)	8865(4)	7491(3)	6153(2)	45(1)
C(11A)	7298(5)	6630(3)	6168(2)	53(1)
O(11A)	6168(4)	6798(3)	5718(2)	80(1)
O(11B)	7449(4)	5611(2)	6736(2)	69(1)
C(11B)	6368(7)	4486(4)	6729(3)	104(2)
N(12)	8358(3)	8927(2)	5829(1)	42(1)
C(13)	6970(4)	9603(3)	6242(2)	46(1)
C(13A)	6963(6)	11119(3)	5951(2)	66(1)
C(14)	7330(4)	9257(3)	7025(2)	49(1)
C(15)	7675(5)	8966(4)	7663(2)	55(1)
C(16)	10702(5)	7892(4)	8645(2)	64(1)
Si(1)	8312(1)	8494(1)	8630(1)	54(1)
C(17)	11500(6)	7696(7)	9408(3)	102(2)
C(18)	11886(6)	8704(5)	8080(3)	80(1)
C(19)	7876(6)	10030(5)	9042(2)	76(1)
C(20)	8977(12)	11191(6)	8685(4)	132(3)
C(21)	5898(8)	10430(7)	9014(3)	121(2)
C(22)	6867(6)	7086(5)	9050(2)	79(1)
C(23)	6894(9)	6754(7)	9890(3)	117(2)
C(24)	7182(10)	5823(7)	8727(4)	124(2)
C(1')	5326(5)	5265(3)	4434(2)	57(1)
N(2')	5792(4)	6496(3)	4055(2)	66(1)
C(3')	5976(4)	6433(3)	3331(2)	54(1)
C(4')	6410(6)	7423(4)	2739(3)	74(1)
C(5')	6493(7)	7079(5)	2073(3)	89(2)
C(6')	6178(7)	5771(5)	1979(3)	87(1)
C(7')	5748(5)	4789(4)	2567(2)	68(1)
C(8')	5626(4)	5114(3)	3260(2)	50(1)

C(9')	5220(4)	4390(3)	3973(2)	46(1)
C(10')	4841(4)	2929(3)	4211(2)	50(1)
C(11')	3407(4)	2435(3)	3780(2)	43(1)
C(11C)	1688(5)	3242(3)	3802(2)	52(1)
O(11C)	586(4)	2975(3)	4264(2)	74(1)
O(11D)	1644(3)	4292(2)	3261(2)	69(1)
C(11D)	189(7)	5274(5)	3256(4)	106(2)
N(12')	3148(3)	984(2)	4104(1)	41(1)
C(13')	1736(4)	304(3)	3755(2)	44(1)
C(13B)	2126(6)	-1201(3)	3919(2)	62(1)
C(14')	1612(4)	836(3)	2972(2)	49(1)
C(15')	1415(5)	1231(4)	2329(2)	56(1)
Si(1')	832(1)	1728(1)	1355(1)	57(1)
C(16')	1364(6)	214(5)	940(2)	75(1)
C(17')	3323(8)	-166(7)	973(4)	114(2)
C(18')	298(11)	-983(6)	1269(4)	128(2)
C(19')	-1583(5)	2284(5)	1338(3)	77(1)
C(20')	-2711(6)	1444(6)	1906(3)	94(2)
C(21')	-2352(7)	2480(8)	573(3)	114(2)
C(22')	2242(6)	3165(5)	943(2)	80(1)
C(23')	1771(10)	4437(5)	1252(4)	110(2)
C(24')	2259(8)	3475(7)	103(3)	113(2)

Table A16. Bond lengths [\AA] and angles [$^\circ$] for **13b**.

C(1)-C(9)	1.352(4)	C(1)-N(2)	1.368(6)
C(1)-H(1)	0.9300	N(2)-C(3)	1.367(6)
N(2)-H(2)	0.8600	C(3)-C(4)	1.376(8)
C(3)-C(8)	1.416(5)	C(4)-C(5)	1.342(9)
C(4)-H(4)	0.9300	C(5)-C(6)	1.389(9)
C(5)-H(5)	0.9300	C(6)-C(7)	1.367(7)
C(6)-H(6)	0.9300	C(7)-C(8)	1.388(6)
C(7)-H(7)	0.9300	C(8)-C(9)	1.424(5)
C(9)-C(10)	1.502(4)	C(10)-C(11)	1.537(4)
C(10)-H(10A)	0.9700	C(10)-H(10B)	0.9700
C(11)-N(12)	1.497(3)	C(11)-C(11A)	1.507(5)
C(11)-H(11)	0.9800	C(11A)-O(11A)	1.191(5)
C(11A)-O(11B)	1.329(4)	O(11B)-C(11B)	1.440(5)
C(11B)-H(11A)	0.9600	C(11B)-H(11B)	0.9600
C(11B)-H(11C)	0.9600	N(12)-C(13)	1.514(4)
N(12)-H(12A)	0.8900	N(12)-H(12B)	0.8900
C(13)-C(14)	1.462(5)	C(13)-C(13A)	1.526(4)
C(13)-H(13)	0.9800	C(13A)-H(13A)	0.9600
C(13A)-H(13B)	0.9600	C(13A)-H(13C)	0.9600
C(14)-C(15)	1.197(5)	C(15)-Si(1)	1.841(4)
C(16)-C(18)	1.519(6)	C(16)-C(17)	1.529(6)
C(16)-Si(1)	1.885(4)	C(16)-H(16)	0.9800
Si(1)-C(19)	1.881(4)	Si(1)-C(22)	1.884(4)
C(17)-H(17A)	0.9600	C(17)-H(17B)	0.9600
C(17)-H(17C)	0.9600	C(18)-H(18A)	0.9600
C(18)-H(18B)	0.9600	C(18)-H(18C)	0.9600
C(19)-C(20)	1.518(8)	C(19)-C(21)	1.534(7)
C(19)-H(19)	0.9800	C(20)-H(20A)	0.9600
C(20)-H(20B)	0.9600	C(20)-H(20C)	0.9600
C(21)-H(21A)	0.9600	C(21)-H(21B)	0.9600
C(21)-H(21C)	0.9600	C(22)-C(24)	1.527(9)
C(22)-C(23)	1.539(7)	C(22)-H(22)	0.9800
C(23)-H(23A)	0.9600	C(23)-H(23B)	0.9600
C(23)-H(23C)	0.9600	C(24)-H(24A)	0.9600
C(24)-H(24B)	0.9600	C(24)-H(24C)	0.9600
C(1')-C(9')	1.358(4)	C(1')-N(2')	1.370(4)
C(1')-H(1')	0.9300	N(2')-C(3')	1.371(5)
N(2')-H(2')	0.8600	C(3')-C(4')	1.387(5)
C(3')-C(8')	1.409(4)	C(4')-C(5')	1.357(7)
C(4')-H(4')	0.9300	C(5')-C(6')	1.404(7)
C(5')-H(5')	0.9300	C(6')-C(7')	1.377(6)
C(6')-H(6')	0.9300	C(7')-C(8')	1.397(5)
C(7')-H(7')	0.9300	C(8')-C(9')	1.427(5)
C(9')-C(10')	1.502(4)	C(10')-C(11')	1.524(4)

C(10')-H(10C)	0.9700	C(10')-H(10D)	0.9700
C(11')-N(12')	1.499(3)	C(11')-C(11C)	1.511(4)
C(11')-H(11')	0.9800	C(11C)-O(11C)	1.195(4)
C(11C)-O(11D)	1.316(4)	O(11D)-C(11D)	1.450(5)
C(11D)-H(11D)	0.9600	C(11D)-H(11E)	0.9600
C(11D)-H(11F)	0.9600	N(12')-C(13')	1.522(4)
N(12')-H(12C)	0.8900	N(12')-H(12D)	0.8900
C(13')-C(14')	1.459(5)	C(13')-C(13B)	1.513(4)
C(13')-H(13')	0.9800	C(13B)-H(13D)	0.9600
C(13B)-H(13E)	0.9600	C(13B)-H(13F)	0.9600
C(14')-C(15')	1.197(5)	C(15')-Si(1')	1.843(4)
Si(1')-C(16')	1.875(5)	Si(1')-C(22')	1.886(4)
Si(1')-C(19')	1.890(4)	C(16')-C(18')	1.516(7)
C(16')-C(17')	1.517(8)	C(16')-H(16')	0.9800
C(17')-H(17D)	0.9600	C(17')-H(17E)	0.9600
C(17')-H(17F)	0.9600	C(18')-H(18D)	0.9600
C(18')-H(18E)	0.9600	C(18')-H(18F)	0.9600
C(19')-C(20')	1.509(6)	C(19')-C(21')	1.522(7)
C(19')-H(19')	0.9800	C(20')-H(20D)	0.9600
C(20')-H(20E)	0.9600	C(20')-H(20F)	0.9600
C(21')-H(21D)	0.9600	C(21')-H(21E)	0.9600
C(21')-H(21F)	0.9600	C(22')-C(24')	1.537(7)
C(22')-C(23')	1.539(8)	C(22')-H(22')	0.9800
C(23')-H(23D)	0.9600	C(23')-H(23E)	0.9600
C(23')-H(23F)	0.9600	C(24')-H(24D)	0.9600
C(24')-H(24E)	0.9600	C(24')-H(24F)	0.9600
C(9)-C(1)-N(2)	109.9(4)	C(9)-C(1)-H(1)	125.0
N(2)-C(1)-H(1)	125.0	C(3)-N(2)-C(1)	109.2(3)
C(3)-N(2)-H(2)	125.4	C(1)-N(2)-H(2)	125.4
N(2)-C(3)-C(4)	131.4(4)	N(2)-C(3)-C(8)	107.1(4)
C(4)-C(3)-C(8)	121.5(5)	C(5)-C(4)-C(3)	117.9(5)
C(5)-C(4)-H(4)	121.1	C(3)-C(4)-H(4)	121.1
C(4)-C(5)-C(6)	122.4(5)	(4)-C(5)-H(5)	118.8
C(6)-C(5)-H(5)	118.8	C(7)-C(6)-C(5)	120.4(6)
C(7)-C(6)-H(6)	119.8	C(5)-C(6)-H(6)	119.8
C(6)-C(7)-C(8)	119.1(5)	C(6)-C(7)-H(7)	120.4
C(8)-C(7)-H(7)	120.4	C(7)-C(8)-C(3)	118.6(4)
C(7)-C(8)-C(9)	134.7(3)	C(3)-C(8)-C(9)	106.7(3)
C(1)-C(9)-C(8)	107.1(3)	C(1)-C(9)-C(10)	125.2(4)
C(8)-C(9)-C(10)	127.7(3)	C(9)-C(10)-C(11)	112.1(3)
C(9)-C(10)-H(10A)	109.2	C(11)-C(10)-H(10A)	109.2
C(9)-C(10)-H(10B)	109.2	C(11)-C(10)-H(10B)	109.2
H(10A)-C(10)-H(10B)	107.9	N(12)-C(11)-C(11A)	110.2(3)
N(12)-C(11)-C(10)	109.0(2)	C(11A)-C(11)-C(10)	109.5(2)
N(12)-C(11)-H(11)	109.4	C(11A)-C(11)-H(11)	109.4
C(10)-C(11)-H(11)	109.4	O(11A)-C(11A)-O(11B)	125.8(3)

O(11A)-C(11A)-C(11)	125.2(3)	O(11B)-C(11A)-C(11)	108.9(3)
C(11A)-O(11B)-C(11B)	116.8(4)	O(11B)-C(11B)-H(11A)	109.5
O(11B)-C(11B)-H(11B)	109.5	H(11A)-C(11B)-H(11B)	109.5
O(11B)-C(11B)-H(11C)	109.5	H(11A)-C(11B)-H(11C)	109.5
H(11B)-C(11B)-H(11C)	109.5	C(11)-N(12)-C(13)	116.0(2)
C(11)-N(12)-H(12A)	108.3	C(13)-N(12)-H(12A)	108.3
C(11)-N(12)-H(12B)	108.3	C(13)-N(12)-H(12B)	108.3
H(12A)-N(12)-H(12B)	107.4	C(14)-C(13)-N(12)	109.9(2)
C(14)-C(13)-C(13A)	112.1(3)	N(12)-C(13)-C(13A)	108.4(3)
C(14)-C(13)-H(13)	108.8	N(12)-C(13)-H(13)	108.8
C(13A)-C(13)-H(13)	108.8	C(13)-C(13A)-H(13A)	109.5
C(13)-C(13A)-H(13B)	109.5	H(13A)-C(13A)-H(13B)	109.5
C(13)-C(13A)-H(13C)	109.5	H(13A)-C(13A)-H(13C)	109.5
H(13B)-C(13A)-H(13C)	109.5	C(15)-C(14)-C(13)	178.1(3)
C(14)-C(15)-Si(1)	177.3(3)	C(18)-C(16)-C(17)	110.9(4)
C(18)-C(16)-Si(1)	115.9(3)	C(17)-C(16)-Si(1)	112.2(3)
C(18)-C(16)-H(16)	105.7	C(17)-C(16)-H(16)	105.7
Si(1)-C(16)-H(16)	105.7	C(15)-Si(1)-C(19)	106.87(18)
C(15)-Si(1)-C(22)	106.04(18)	C(19)-Si(1)-C(22)	111.7(2)
C(15)-Si(1)-C(16)	106.53(17)	C(19)-Si(1)-C(16)	114.1(2)
C(22)-Si(1)-C(16)	111.0(2)	C(16)-C(17)-H(17A)	109.5
C(16)-C(17)-H(17B)	109.5	H(17A)-C(17)-H(17B)	109.5
C(16)-C(17)-H(17C)	109.5	H(17A)-C(17)-H(17C)	109.5
H(17B)-C(17)-H(17C)	109.5	C(16)-C(18)-H(18A)	109.5
C(16)-C(18)-H(18B)	109.5	H(18A)-C(18)-H(18B)	109.5
C(16)-C(18)-H(18C)	109.5	H(18A)-C(18)-H(18C)	109.5
H(18B)-C(18)-H(18C)	109.5	C(20)-C(19)-C(21)	111.8(5)
C(20)-C(19)-Si(1)	112.1(3)	C(21)-C(19)-Si(1)	110.3(4)
C(20)-C(19)-H(19)	107.5	C(21)-C(19)-H(19)	107.5
Si(1)-C(19)-H(19)	107.5	C(19)-C(20)-H(20A)	109.5
C(19)-C(20)-H(20B)	109.5	H(20A)-C(20)-H(20B)	109.5
C(19)-C(20)-H(20C)	109.5	H(20A)-C(20)-H(20C)	109.5
H(20B)-C(20)-H(20C)	109.5	C(19)-C(21)-H(21A)	109.5
C(19)-C(21)-H(21B)	109.5	H(21A)-C(21)-H(21B)	109.5
C(19)-C(21)-H(21C)	109.5	H(21A)-C(21)-H(21C)	109.5
H(21B)-C(21)-H(21C)	109.5	C(24)-C(22)-C(23)	111.6(5)
C(24)-C(22)-Si(1)	113.2(4)	C(23)-C(22)-Si(1)	114.2(4)
C(24)-C(22)-H(22)	105.6	C(23)-C(22)-H(22)	105.6
Si(1)-C(22)-H(22)	105.6	C(22)-C(23)-H(23A)	109.5
C(22)-C(23)-H(23B)	109.5	H(23A)-C(23)-H(23B)	109.5
C(22)-C(23)-H(23C)	109.5	H(23A)-C(23)-H(23C)	109.5
H(23B)-C(23)-H(23C)	109.5	C(22)-C(24)-H(24A)	109.5
C(22)-C(24)-H(24B)	109.5	H(24A)-C(24)-H(24B)	109.5
C(22)-C(24)-H(24C)	109.5	H(24A)-C(24)-H(24C)	109.5
H(24B)-C(24)-H(24C)	109.5	C(9')-C(1')-N(2')	110.1(3)
C(9')-C(1')-H(1')	124.9	N(2')-C(1')-H(1')	124.9

C(1')-N(2')-C(3')	108.7(3)	C(1')-N(2')-H(2')	125.6
C(3')-N(2')-H(2')	125.6	N(2')-C(3')-C(4')	129.9(3)
N(2')-C(3')-C(8')	107.5(3)	C(4')-C(3')-C(8')	122.6(4)
C(5')-C(4')-C(3')	117.4(4)	C(5')-C(4')-H(4')	121.3
C(3')-C(4')-H(4')	121.3	C(4')-C(5')-C(6')	121.8(4)
C(4')-C(5')-H(5')	119.1	C(6')-C(5')-H(5')	119.1
C(7')-C(6')-C(5')	120.7(5)	C(7')-C(6')-H(6')	119.6
C(5')-C(6')-H(6')	119.6	C(6')-C(7')-C(8')	118.9(4)
C(6')-C(7')-H(7')	120.5	C(8')-C(7')-H(7')	120.5
C(7')-C(8')-C(3')	118.5(3)	C(7')-C(8')-C(9')	134.6(3)
C(3')-C(8')-C(9')	106.9(3)	C(1')-C(9')-C(8')	106.8(3)
C(1')-C(9')-C(10')	124.4(3)	C(8')-C(9')-C(10')	128.8(3)
C(9')-C(10')-C(11')	115.1(2)	C(9')-C(10')-H(10C)	108.5
C(11')-C(10')-H(10C)	108.5	C(9')-C(10')-H(10D)	108.5
C(11')-C(10')-H(10D)	108.5	H(10C)-C(10')-H(10D)	107.5
N(12')-C(11')-C(11C)	109.6(2)	N(12')-C(11')-C(10')	108.2(2)
C(11C)-C(11')-C(10')	111.6(2)	N(12')-C(11')-H(11')	109.1
C(11C)-C(11')-H(11')	109.1	C(10')-C(11')-H(11')	109.1
O(11C)-C(11C)-O(11D)	126.2(3)	O(11C)-C(11C)-C(11')	124.1(3)
O(11D)-C(11C)-C(11')	109.6(3)	C(11C)-O(11D)-C(11D)	116.9(4)
O(11D)-C(11D)-H(11D)	109.5	O(11D)-C(11D)-H(11E)	109.5
H(11D)-C(11D)-H(11E)	109.5	O(11D)-C(11D)-H(11F)	109.5
H(11D)-C(11D)-H(11F)	109.5	H(11E)-C(11D)-H(11F)	109.5
C(11')-N(12')-C(13')	116.4(2)	C(11')-N(12')-H(12C)	108.2
C(13')-N(12')-H(12C)	108.2	C(11')-N(12')-H(12D)	108.2
C(13')-N(12')-H(12D)	108.2	H(12C)-N(12')-H(12D)	107.3
C(14')-C(13')-C(13B)	111.8(3)	C(14')-C(13')-N(12')	111.3(2)
C(13B)-C(13')-N(12')	109.1(3)	C(14')-C(13')-H(13')	108.2
C(13B)-C(13')-H(13')	108.2	N(12')-C(13')-H(13')	108.2
C(13')-C(13B)-H(13D)	109.5	C(13')-C(13B)-H(13E)	109.5
H(13D)-C(13B)-H(13E)	109.5	C(13')-C(13B)-H(13F)	109.5
H(13D)-C(13B)-H(13F)	109.5	H(13E)-C(13B)-H(13F)	109.5
C(15')-C(14')-C(13')	175.9(3)	C(14')-C(15')-Si(1')	172.4(3)
C(15')-Si(1')-C(16')	106.22(19)	C(15')-Si(1')-C(22')	107.33(18)
C(16')-Si(1')-C(22')	111.0(2)	C(15')-Si(1')-C(19')	105.58(18)
C(16')-Si(1')-C(19')	114.9(2)	C(22')-Si(1')-C(19')	111.3(2)
C(18')-C(16')-C(17')	110.9(5)	C(18')-C(16')-Si(1')	113.0(3)
C(17')-C(16')-Si(1')	111.7(3)	C(18')-C(16')-H(16')	107.0
C(17')-C(16')-H(16')	107.0	Si(1')-C(16')-H(16')	107.0
C(16')-C(17')-H(17D)	109.5	C(16')-C(17')-H(17E)	109.5
H(17D)-C(17')-H(17E)	109.5	C(16')-C(17')-H(17F)	109.5
H(17D)-C(17')-H(17F)	109.5	H(17E)-C(17')-H(17F)	109.5
C(16')-C(18')-H(18D)	109.5	C(16')-C(18')-H(18E)	109.5
H(18D)-C(18')-H(18E)	109.5	C(16')-C(18')-H(18F)	109.5
H(18D)-C(18')-H(18F)	109.5	H(18E)-C(18')-H(18F)	109.5
C(20')-C(19')-C(21')	112.5(4)	C(20')-C(19')-Si(1')	115.0(3)

C(21')-C(19')-Si(1')	111.8(4)	C(20')-C(19')-H(19')	105.5
C(21')-C(19')-H(19')	105.5	Si(1')-C(19')-H(19')	105.5
C(19')-C(20')-H(20D)	109.5	C(19')-C(20')-H(20E)	109.5
H(20D)-C(20')-H(20E)	109.5	C(19')-C(20')-H(20F)	109.5
H(20D)-C(20')-H(20F)	109.5	H(20E)-C(20')-H(20F)	109.5
C(19')-C(21')-H(21D)	109.5	C(19')-C(21')-H(21E)	109.5
H(21D)-C(21')-H(21E)	109.5	C(19')-C(21')-H(21F)	109.5
H(21D)-C(21')-H(21F)	109.5	H(21E)-C(21')-H(21F)	109.5
C(24')-C(22')-C(23')	111.4(5)	C(24')-C(22')-Si(1')	113.9(4)
C(23')-C(22')-Si(1')	111.8(4)	C(24')-C(22')-H(22')	106.4
C(23')-C(22')-H(22')	106.4	Si(1')-C(22')-H(22')	106.4
C(22')-C(23')-H(23D)	109.5	C(22')-C(23')-H(23E)	109.5
H(23D)-C(23')-H(23E)	109.5	C(22')-C(23')-H(23F)	109.5
H(23D)-C(23')-H(23F)	109.5	H(23E)-C(23')-H(23F)	109.5
C(22')-C(24')-H(24D)	109.5	C(22')-C(24')-H(24E)	109.5
H(24D)-C(24')-H(24E)	109.5	C(22')-C(24')-H(24F)	109.5
H(24D)-C(24')-H(24F)	109.5	H(24E)-C(24')-H(24F)	109.5

Table A17. Anisotropic displacement parameters ($\text{\AA}^2 \times 10^3$) for **13b**. The anisotropic displacement factor exponent takes the form: $-2h^2a^2U^{11} + \dots + 2hkab^*U^{12}$

	U11	U22	U33	U23	U13	U12
Cl(1')	63(1)	42(1)	50(1)	-10(1)	2(1)	-9(1)
Cl(1)	56(1)	45(1)	48(1)	-10(1)	-7(1)	0(1)
C(1)	90(3)	55(2)	83(3)	-33(2)	20(2)	-12(2)
N(2)	97(3)	46(2)	128(3)	-38(2)	27(2)	-11(2)
C(3)	69(2)	42(2)	104(3)	-6(2)	27(2)	0(2)
C(4)	90(3)	57(2)	145(6)	20(3)	32(4)	12(2)
C(5)	101(4)	120(5)	110(5)	36(4)	12(3)	42(4)
C(6)	121(4)	131(5)	81(4)	-8(3)	-14(3)	50(4)
C(7)	98(3)	78(3)	80(3)	-22(2)	-10(2)	24(2)
C(8)	62(2)	47(2)	73(2)	-13(2)	11(2)	2(2)
C(9)	65(2)	42(1)	62(2)	-17(1)	15(2)	-6(1)
C(10)	72(2)	43(1)	54(2)	-11(1)	15(2)	-7(2)
C(11)	62(2)	38(1)	37(2)	-6(1)	0(1)	-5(1)
C(11A)	65(2)	44(2)	52(2)	-12(2)	4(2)	-13(2)
O(11A)	89(2)	72(2)	80(2)	-12(1)	-22(2)	-30(2)
O(11B)	71(2)	54(1)	76(2)	7(1)	11(1)	-15(1)
C(11B)	105(3)	59(2)	141(5)	2(3)	17(3)	-32(2)
N(12)	53(1)	39(1)	36(1)	-6(1)	-7(1)	-6(1)
C(13)	50(2)	47(2)	41(2)	-10(1)	-11(1)	2(1)
C(13A)	90(3)	48(2)	58(2)	-8(2)	-13(2)	11(2)
C(14)	51(2)	51(2)	43(2)	-11(1)	-4(1)	3(1)
C(15)	58(2)	65(2)	43(2)	-12(2)	-2(2)	2(2)
C(16)	55(2)	74(2)	60(2)	-10(2)	-2(2)	-1(2)
Si(1)	52(1)	73(1)	35(1)	-8(1)	-3(1)	4(1)
C(17)	65(3)	159(5)	69(3)	6(3)	-10(2)	2(3)
C(18)	65(2)	101(3)	74(3)	-13(2)	7(2)	-7(2)
C(19)	85(3)	94(3)	51(2)	-27(2)	-6(2)	14(2)
C(20)	205(8)	81(3)	116(5)	-35(3)	35(5)	-17(4)
C(21)	109(4)	151(5)	113(4)	-63(4)	-21(3)	55(4)
C(22)	64(2)	108(3)	55(3)	7(2)	-4(2)	-12(2)
C(23)	123(4)	154(5)	58(3)	25(3)	10(3)	-38(4)
C(24)	157(6)	108(4)	108(5)	-14(3)	4(4)	-62(4)
C(1')	66(2)	50(2)	59(2)	-16(1)	-12(2)	-3(2)
N(2')	78(2)	42(1)	82(2)	-24(1)	-11(2)	-6(1)
C(3')	51(2)	40(1)	71(2)	-6(1)	-10(1)	-2(1)
C(4')	72(2)	48(2)	96(4)	3(2)	-8(2)	-10(2)
C(5')	87(3)	78(3)	88(4)	22(2)	-2(3)	-23(2)
C(6')	101(3)	99(3)	59(3)	-4(2)	3(2)	-31(3)
C(7')	78(2)	65(2)	62(2)	-15(2)	1(2)	-18(2)
C(8')	50(2)	41(1)	58(2)	-9(1)	-8(1)	-2(1)
C(9')	50(2)	40(1)	49(2)	-9(1)	-13(1)	-2(1)

C(10')	57(2)	41(1)	51(2)	-5(1)	-19(1)	1(1)
C(11')	52(2)	34(1)	41(2)	-5(1)	-8(1)	-1(1)
C(11C)	57(2)	45(2)	56(2)	-15(2)	-16(2)	2(2)
O(11C)	79(2)	74(2)	69(2)	-17(1)	11(1)	16(1)
O(11D)	60(1)	50(1)	89(2)	9(1)	-21(1)	7(1)
C(11D)	93(3)	73(3)	144(5)	-4(3)	-39(3)	31(3)
N(12')	46(1)	38(1)	37(1)	-6(1)	-3(1)	-1(1)
C(13')	45(1)	47(1)	41(2)	-10(1)	1(1)	-9(1)
C(13B)	81(2)	44(2)	57(2)	-1(1)	-4(2)	-13(2)
C(14')	54(2)	48(2)	48(2)	-11(1)	-7(1)	-11(1)
C(15')	59(2)	59(2)	49(2)	-9(2)	-10(2)	-11(2)
Si(1')	53(1)	74(1)	43(1)	-4(1)	-9(1)	-11(1)
C(16')	80(3)	94(3)	54(3)	-20(2)	-3(2)	-13(2)
C(17')	108(4)	120(4)	119(5)	-43(4)	1(3)	15(4)
C(18')	171(6)	99(4)	131(5)	-54(4)	43(5)	-48(4)
C(19')	61(2)	92(3)	75(3)	-11(2)	-9(2)	-1(2)
C(20')	63(2)	133(4)	85(4)	-16(3)	6(2)	-5(3)
C(21')	64(3)	176(6)	89(4)	7(4)	-25(3)	4(3)
C(22')	67(2)	93(3)	67(3)	18(2)	-13(2)	-20(2)
C(23')	138(5)	82(3)	107(4)	-4(3)	-13(4)	-39(3)
C(24')	117(4)	141(5)	68(4)	19(3)	6(3)	-38(4)

Table A18. Hydrogen coordinates ($\times 10^4$) and isotropic displacement parameters ($\text{\AA}^2 \times 10^3$) for **13b**.

	x	y	z	U(eq)
H(1)	10340	4650	5112	88
H(2)	11368	2573	5874	105
H(4)	12688	1760	7280	124
H(5)	13158	2577	8306	144
H(6)	12800	4835	8321	137
H(7)	11797	6329	7301	102
H(10A)	9942	7104	5187	67
H(10B)	11358	7536	5689	67
H(11)	9291	7431	6652	55
H(11A)	5155	4798	6670	156
H(11B)	6507	3852	7182	156
H(11C)	6723	4059	6331	156
H(12A)	7969	8965	5377	51
H(12B)	9324	9400	5794	51
H(13)	5813	9281	6151	55
H(13A)	5955	11548	6140	99
H(13B)	6911	11294	5427	99
H(13C)	8020	11467	6102	99
H(16)	10711	6992	8527	76
H(17A)	12636	7236	9412	152
H(17B)	10739	7171	9755	152
H(17C)	11625	8557	9537	152
H(18A)	12052	9563	8206	121
H(18B)	11346	8835	7608	121
H(18C)	13007	8228	8070	121
H(19)	8214	9789	9557	91
H(20A)	8865	11325	8164	198
H(20B)	10191	10987	8818	198
H(20C)	8570	11994	8847	198
H(21A)	5667	11122	9292	182
H(21B)	5241	9659	9217	182
H(21C)	5550	10759	8517	182
H(22)	5657	7415	8916	94
H(23A)	6011	6122	10065	175
H(23B)	6653	7563	10076	175
H(23C)	8034	6370	10055	175
H(24A)	8338	5432	8858	185
H(24B)	7090	6057	8204	185
H(24C)	6314	5186	8915	185
H(1')	5114	5058	4935	69

H(2')	5943	7194	4241	79
H(4')	6637	8288	2797	89
H(5')	6765	7728	1666	107
H(6')	6262	5566	1516	105
H(7')	5541	3923	2504	81
H(10C)	4499	2770	4722	60
H(10D)	5921	2395	4172	60
H(11')	3790	2513	3270	52
H(11D)	-900	4822	3325	159
H(11E)	165	5895	2796	159
H(11F)	338	5756	3644	159
H(12C)	2882	921	4575	49
H(12D)	4170	526	4079	49
H(13')	598	489	3979	53
H(13D)	1138	-1646	3778	92
H(13E)	2334	-1499	4433	92
H(13F)	3154	-1414	3651	92
H(16')	1048	464	422	90
H(17D)	3702	-355	1473	171
H(17E)	3961	567	704	171
H(17F)	3546	-950	763	171
H(18D)	657	-1737	1053	193
H(18E)	-933	-760	1177	193
H(18F)	494	-1209	1787	193
H(19')	-1624	3181	1460	92
H(20D)	-3876	1859	1899	142
H(20E)	-2201	1380	2380	142
H(20F)	-2773	559	1800	142
H(21D)	-2475	1619	444	171
H(21E)	-1580	3002	231	171
H(21F)	-3488	2944	563	171
H(22')	3456	2883	1095	95
H(23D)	2641	5090	1098	165
H(23E)	1743	4209	1776	165
H(23F)	634	4806	1075	165
H(24D)	1131	3867	-73	169
H(24E)	2496	2656	-73	169
H(24F)	3159	4094	-68	169

Table A19. Torsion angles [°] for **13b**.

C(9)-C(1)-N(2)-C(3)	0.7(5)	C(1)-N(2)-C(3)-C(4)	179.6(4)
C(1)-N(2)-C(3)-C(8)	-0.7(4)	N(2)-C(3)-C(4)-C(5)	-177.3(5)
C(8)-C(3)-C(4)-C(5)	3.1(7)	C(3)-C(4)-C(5)-C(6)	-3.2(9)
C(4)-C(5)-C(6)-C(7)	1.5(10)	C(5)-C(6)-C(7)-C(8)	0.3(9)
C(6)-C(7)-C(8)-C(3)	-0.3(7)	C(6)-C(7)-C(8)-C(9)	177.6(5)
N(2)-C(3)-C(8)-C(7)	178.9(4)	C(4)-C(3)-C(8)-C(7)	-1.4(6)
N(2)-C(3)-C(8)-C(9)	0.4(4)	C(4)-C(3)-C(8)-C(9)	-179.9(4)
N(2)-C(1)-C(9)-C(8)	-0.4(4)	N(2)-C(1)-C(9)-C(10)	-178.5(3)
C(7)-C(8)-C(9)-C(1)	-178.1(4)	C(3)-C(8)-C(9)-C(1)	0.0(4)
C(7)-C(8)-C(9)-C(10)	-0.1(7)	C(3)-C(8)-C(9)-C(10)	178.0(3)
C(1)-C(9)-C(10)-C(11)	118.3(4)	C(8)-C(9)-C(10)-C(11)	-59.4(5)
C(9)-C(10)-C(11)-N(12)	-178.2(3)	C(9)-C(10)-C(11)-C(11A)	-57.6(4)
N(12)-C(11)-C(11A)-O(11A)	34.6(4)	C(10)-C(11)-C(11A)-O(11A)	-85.3(4)
N(12)-C(11)-C(11A)-O(11B)	-149.5(3)	C(10)-C(11)-C(11A)-O(11B)	90.7(3)
O(11A)-C(11A)-O(11B)-C(11B)	12.8(5)	C(11)-C(11A)-O(11B)-C(11B)	-
163.1(3)			
C(11A)-C(11)-N(12)-C(13)	62.6(3)	C(10)-C(11)-N(12)-C(13)	-177.2(3)
C(11)-N(12)-C(13)-C(14)	43.1(3)	C(11)-N(12)-C(13)-C(13A)	165.8(3)
C(18)-C(16)-Si(1)-C(15)	41.4(4)	C(17)-C(16)-Si(1)-C(15)	170.1(3)
C(18)-C(16)-Si(1)-C(19)	-76.3(4)	C(17)-C(16)-Si(1)-C(19)	52.4(4)
C(18)-C(16)-Si(1)-C(22)	156.4(3)	C(17)-C(16)-Si(1)-C(22)	-74.9(4)
C(15)-Si(1)-C(19)-C(20)	-62.0(5)	C(22)-Si(1)-C(19)-C(20)	-177.6(4)
C(16)-Si(1)-C(19)-C(20)	55.5(5)	C(15)-Si(1)-C(19)-C(21)	63.3(4)
C(22)-Si(1)-C(19)-C(21)	-52.3(4)	C(16)-Si(1)-C(19)-C(21)	-179.2(4)
C(15)-Si(1)-C(22)-C(24)	63.7(4)	C(19)-Si(1)-C(22)-C(24)	179.8(4)
C(16)-Si(1)-C(22)-C(24)	-51.6(5)	C(15)-Si(1)-C(22)-C(23)	-167.1(4)
C(19)-Si(1)-C(22)-C(23)	-51.0(5)	C(16)-Si(1)-C(22)-C(23)	77.6(5)
C(9')-C(1')-N(2')-C(3')	0.7(4)	C(1')-N(2')-C(3')-C(4')	179.2(4)
C(1')-N(2')-C(3')-C(8')	-0.5(4)	N(2')-C(3')-C(4')-C(5')	-179.7(4)
C(8')-C(3')-C(4')-C(5')	0.0(6)	C(3')-C(4')-C(5')-C(6')	-0.9(7)
C(4')-C(5')-C(6')-C(7')	0.9(8)	C(5')-C(6')-C(7')-C(8')	0.0(7)
C(6')-C(7')-C(8')-C(3')	-0.9(6)	C(6')-C(7')-C(8')-C(9')	179.8(4)
N(2')-C(3')-C(8')-C(7')	-179.3(3)	C(4')-C(3')-C(8')-C(7')	0.9(5)
N(2')-C(3')-C(8')-C(9')	0.2(4)	C(4')-C(3')-C(8')-C(9')	-179.6(3)
N(2')-C(1')-C(9')-C(8')	-0.5(4)	N(2')-C(1')-C(9')-C(10')	176.4(3)
C(7')-C(8')-C(9')-C(1')	179.6(4)	C(3')-C(8')-C(9')-C(1')	0.2(3)
C(7')-C(8')-C(9')-C(10')	2.9(6)	C(3')-C(8')-C(9')-C(10')	-176.5(3)
C(1')-C(9')-C(10')-C(11')	131.2(3)	C(8')-C(9')-C(10')-C(11')	-52.6(4)
C(9')-C(10')-C(11')-N(12')	-177.8(2)	C(9')-C(10')-C(11')-C(11C)	-57.1(4)
N(12')-C(11')-C(11C)-O(11C)	31.2(4)	C(10')-C(11')-C(11C)-O(11C)	-88.7(4)
N(12')-C(11')-C(11C)-O(11D)	-151.5(3)	C(10')-C(11')-C(11C)-O(11D)	88.6(3)
O(11C)-C(11C)-O(11D)-C(11D)	5.1(6)	C(11')-C(11C)-O(11D)-C(11D)	-
172.1(3)			
C(11C)-C(11')-N(12')-C(13')	57.1(3)	C(10')-C(11')-N(12')-C(13')	179.0(2)

C(11')-N(12')-C(13')-C(14')	33.4(3)	C(11')-N(12')-C(13')-C(13B)	157.3(3)
C(15')-Si(1')-C(16')-C(18')	62.0(5)	C(22')-Si(1')-C(16')-C(18')	178.4(4)
C(19')-Si(1')-C(16')-C(18')	-54.3(5)	C(15')-Si(1')-C(16')-C(17')	-63.8(4)
C(22')-Si(1')-C(16')-C(17')	52.5(4)	C(19')-Si(1')-C(16')-C(17')	179.9(4)
C(15')-Si(1')-C(19')-C(20')	-39.5(4)	C(16')-Si(1')-C(19')-C(20')	77.2(4)
C(22')-Si(1')-C(19')-C(20')	-155.6(4)	C(15')-Si(1')-C(19')-C(21')	-169.4(4)
C(16')-Si(1')-C(19')-C(21')	-52.8(5)	C(22')-Si(1')-C(19')-C(21')	74.4(4)
C(15')-Si(1')-C(22')-C(24')	165.8(4)	C(16')-Si(1')-C(22')-C(24')	50.1(5)
C(19')-Si(1')-C(22')-C(24')	-79.1(5)	C(15')-Si(1')-C(22')-C(23')	-66.8(4)
C(16')-Si(1')-C(22')-C(23')	177.5(4)	C(19')-Si(1')-C(22')-C(23')	48.3(4)

Table A20. Hydrogen bonds for **13b** [\AA and $^\circ$].

D-H...A	d(D-H)	d(H...A)	d(D...A)	$\angle(\text{DHA})$
N(12)-H(12A)...Cl(1)	0.89	2.28	3.154(2)	167.3
N(12)-H(12B)...Cl(1')#2	0.89	2.28	3.161(2)	170.0
N(12')-H(12C)...Cl(1')	0.89	2.27	3.146(2)	166.4
N(12')-H(12D)...Cl(1)#3	0.89	2.29	3.169(2)	168.0

Symmetry transformations used to generate equivalent atoms:

#1 $x+1, y, z$ #2 $x+1, y+1, z$ #3 $x, y-1, z$ #4 $x-1, y-1, z$ **X-ray Crystal Data for 25****Table A21.** Crystal data and structure refinement for **25**.

Empirical formula	$\text{C}_{19}\text{H}_{20}\text{N}_2\text{O}$	
Formula weight	292.37	
Temperature	150(2) K	
Wavelength	0.71073 \AA	
Crystal system	Monoclinic	
Space group	$P2_1$	
Unit cell dimensions	$a = 8.6453(9) \text{\AA}$ $b = 8.3913(8) \text{\AA}$ $c = 10.2653(11) \text{\AA}$	$\alpha = 90^\circ$ $\beta = 93.327(3)^\circ$ $\gamma = 90^\circ$
Volume	$743.44(13) \text{\AA}^3$	
Z	2	
Density (-123 $^\circ\text{C}$)	1.306 Mg/m^3	
Absorption coefficient	0.081 mm^{-1}	
F(000)	312	
Crystal size	$0.733 \times 0.708 \times 0.586 \text{ mm}^3$	
θ range for data collection	1.987 to 29.204°	
Index ranges	$-11 \leq h \leq 11, -11 \leq k \leq 11, -13 \leq l \leq 14$	
Reflections collected	16701	
Independent reflections	16701 [$R_{\text{int}} = 0.0263$]	
Completeness to $\theta = 25.000^\circ$	100.0 %	
Refinement method	Full-matrix least-squares on F^2	
Data / restraints / parameters	16701 / 1 / 205	
Goodness-of-fit on F^2	1.021	
Final R indices [$I > 2\sigma(I)$]	$R1 = 0.0335, wR2 = 0.0832$	
R indices (all data)	$R1 = 0.0353, wR2 = 0.0848$	
Absolute structure parameter	0.0(4)	
Largest diff. peak and hole	0.253 and $-0.206 \text{ e.\AA}^{-3}$	

Table A22. Atomic coordinates ($\times 10^4$) and equivalent isotropic displacement parameters ($\text{\AA}^2 \times 10^3$)for **25**. $U(\text{eq})$ is defined as one third of the trace of the orthogonalized U_{ij} tensor.

	x	y	z	U(eq)
N(1)	9940(2)	6522(2)	2310(2)	16(1)
C(2)	8984(2)	7863(2)	2738(2)	16(1)
C(3)	7738(2)	8334(2)	1687(2)	19(1)
C(4)	6678(2)	6914(2)	1353(2)	23(1)
C(5)	7454(2)	5297(2)	1348(2)	19(1)
O(5)	6815(2)	4164(2)	821(1)	30(1)
C(6)	8999(2)	5065(2)	2138(2)	17(1)
C(7)	8673(2)	4404(2)	3500(2)	18(1)
C(8)	8122(2)	5748(2)	4314(2)	17(1)
C(9)	7259(2)	5734(2)	5464(2)	18(1)
C(10)	6801(2)	4539(2)	6317(2)	21(1)
C(11)	5960(2)	4969(2)	7368(2)	23(1)
C(12)	5526(2)	6559(2)	7569(2)	23(1)
C(13)	5971(2)	7766(2)	6752(2)	22(1)
C(14)	6873(2)	7341(2)	5719(2)	18(1)
N(15)	7495(2)	8293(2)	4784(2)	18(1)
C(15)	7470(2)	10025(2)	4794(2)	22(1)
C(16)	8259(2)	7304(2)	3950(2)	17(1)
C(17)	10858(2)	6910(2)	1180(2)	17(1)
C(18)	10025(2)	6640(2)	-105(2)	18(1)
C(19)	9345(2)	6410(2)	-1121(2)	22(1)
C(20)	12377(2)	5976(2)	1266(2)	21(1)

Table A23. Bond lengths [\AA] and angles [$^\circ$] for **25**.

N(1)-C(6)	1.474(2)	N(1)-C(2)	1.478(2)
N(1)-C(17)	1.479(2)	C(2)-C(16)	1.501(3)
C(2)-C(3)	1.531(2)	C(2)-H(2A)	1.0000
C(3)-C(4)	1.529(3)	C(3)-H(3A)	0.9900
C(3)-H(3B)	0.9900	C(4)-C(5)	1.514(3)
C(4)-H(4A)	0.9900	C(4)-H(4B)	0.9900
C(5)-O(5)	1.211(2)	C(5)-C(6)	1.534(3)
C(6)-C(7)	1.544(3)	C(6)-H(6A)	1.0000
C(7)-C(8)	1.498(2)	C(7)-H(7A)	0.9900
C(7)-H(7B)	0.9900	C(8)-C(16)	1.365(2)
C(8)-C(9)	1.432(3)	C(9)-C(10)	1.403(2)
C(9)-C(14)	1.417(2)	C(10)-C(11)	1.383(3)
C(10)-H(10A)	0.9500	C(11)-C(12)	1.404(3)

C(11)-H(11A)	0.9500	C(12)-C(13)	1.383(3)
C(12)-H(12A)	0.9500	C(13)-C(14)	1.398(3)
C(13)-H(13A)	0.9500	C(14)-N(15)	1.381(2)
N(15)-C(16)	1.387(2)	N(15)-C(15)	1.454(2)
C(15)-H(15A)	0.9800	C(15)-H(15B)	0.9800
C(15)-H(15C)	0.9800	C(17)-C(18)	1.483(3)
C(17)-C(20)	1.527(2)	C(17)-H(17A)	1.0000
C(18)-C(19)	1.183(3)	C(19)-H(19)	0.91(3)
C(20)-H(20A)	0.9800	C(20)-H(20B)	0.9800
C(20)-H(20C)	0.9800		
C(6)-N(1)-C(2)	110.65(12)	C(6)-N(1)-C(17)	113.96(14)
C(2)-N(1)-C(17)	113.57(13)	N(1)-C(2)-C(16)	105.99(14)
N(1)-C(2)-C(3)	111.71(14)	C(16)-C(2)-C(3)	110.77(14)
N(1)-C(2)-H(2A)	109.4	C(16)-C(2)-H(2A)	109.4
C(3)-C(2)-H(2A)	109.4	C(4)-C(3)-C(2)	110.18(15)
C(4)-C(3)-H(3A)	109.6	C(2)-C(3)-H(3A)	109.6
C(4)-C(3)-H(3B)	109.6	C(2)-C(3)-H(3B)	109.6
H(3A)-C(3)-H(3B)	108.1	C(5)-C(4)-C(3)	116.04(14)
C(5)-C(4)-H(4A)	108.3	C(3)-C(4)-H(4A)	108.3
C(5)-C(4)-H(4B)	108.3	C(3)-C(4)-H(4B)	108.3
H(4A)-C(4)-H(4B)	107.40(5)	O(5)-C(5)-C(4)	120.93(16)
O(5)-C(5)-C(6)	119.83(17))C(4)-C(5)-C(6)	118.97(15)
N(1)-C(6)-C(5)	114.56(14)	N(1)-C(6)-C(7)	108.55(14)
C(5)-C(6)-C(7)	108.99(14)	N(1)-C(6)-H(6A)	108.2
C(5)-C(6)-H(6A)	108.2	C(7)-C(6)-H(6A)	108.2
C(8)-C(7)-C(6)	108.34(14)	C(8)-C(7)-H(7A)	110.0
C(6)-C(7)-H(7A)	110.0	C(8)-C(7)-H(7B)	110.0
C(6)-C(7)-H(7B)	110.0	H(7A)-C(7)-H(7B)	108.4
C(16)-C(8)-C(9)	106.93(16)	C(16)-C(8)-C(7)	122.13(16)
C(9)-C(8)-C(7)	130.64(15)	C(10)-C(9)-C(14)	119.11(16)
C(10)-C(9)-C(8)	134.38(17)	C(14)-C(9)-C(8)	106.50(15)
C(11)-C(10)-C(9)	118.72(17)	C(11)-C(10)-H(10A)	120.6
C(9)-C(10)-H(10A)	120.6	C(10)-C(11)-C(12)	121.27(18)
C(10)-C(11)-H(11A)	119.4	C(12)-C(11)-H(11A)	119.4
C(13)-C(12)-C(11)	121.34(17)	C(13)-C(12)-H(12A)	119.3
C(11)-C(12)-H(12A)	119.3	C(12)-C(13)-C(14)	117.41(18)
C(12)-C(13)-H(13A)	121.3	C(14)-C(13)-H(13A)	121.3
N(15)-C(14)-C(13)	129.52(17)	N(15)-C(14)-C(9)	108.44(15)
C(13)-C(14)-C(9)	122.03(17)	C(14)-N(15)-C(16)	107.57(14)
C(14)-N(15)-C(15)	124.54(16)	C(16)-N(15)-C(15)	127.58(16)
N(15)-C(15)-H(15A)	109.5	N(15)-C(15)-H(15B)	109.5
H(15A)-C(15)-H(15B)	109.5	N(15)-C(15)-H(15C)	109.5
H(15A)-C(15)-H(15C)	109.5	H(15B)-C(15)-H(15C)	109.5
C(8)-C(16)-N(15)	110.53(16)	C(8)-C(16)-C(2)	124.98(16)
N(15)-C(16)-C(2)	124.18(15)	N(1)-C(17)-C(18)	114.15(14)
N(1)-C(17)-C(20)	109.87(14)	C(18)-C(17)-C(20)	110.17(15)

N(1)-C(17)-H(17A)	107.5	C(18)-C(17)-H(17A)	107.5
C(20)-C(17)-H(17A)	107.5	C(19)-C(18)-C(17)	179.0(2)
C(18)-C(19)-H(19)	175.5(16)	C(17)-C(20)-H(20A)	109.5
C(17)-C(20)-H(20B)	109.5	H(20A)-C(20)-H(20B)	109.5
C(17)-C(20)-H(20C)	109.5	H(20A)-C(20)-H(20C)	109.5
H(20B)-C(20)-H(20C)	109.5		

Table A24. Anisotropic displacement parameters ($\text{\AA}^2 \times 10^3$) for **25**. The anisotropic displacement factor exponent takes the form: $-2 \sum h^2 a^* U^{11} + \dots + 2 h k a^* b^* U^{12}$

	U ¹¹	U ²²	U ³³	U ²³	U ¹³	U ¹²
N(1)	16(1)	12(1)	19(1)	0(1)	3(1)	-1(1)
C(2)	18(1)	12(1)	19(1)	-1(1)	1(1)	0(1)
C(3)	20(1)	17(1)	19(1)	2(1)	2(1)	3(1)
C(4)	18(1)	25(1)	25(1)	-1(1)	-2(1)	1(1)
C(5)	19(1)	21(1)	18(1)	-1(1)	4(1)	-4(1)
O(5)	30(1)	26(1)	33(1)	-5(1)	-1(1)	-10(1)
C(6)	18(1)	13(1)	20(1)	-2(1)	2(1)	-2(1)
C(7)	22(1)	12(1)	21(1)	1(1)	3(1)	0(1)
C(8)	19(1)	14(1)	19(1)	0(1)	1(1)	0(1)
C(9)	16(1)	19(1)	18(1)	-1(1)	-1(1)	0(1)
C(10)	21(1)	19(1)	21(1)	2(1)	0(1)	-3(1)
C(11)	20(1)	27(1)	22(1)	4(1)	0(1)	-5(1)
C(12)	18(1)	33(1)	18(1)	-3(1)	1(1)	-3(1)
C(13)	20(1)	24(1)	21(1)	-5(1)	0(1)	0(1)
C(14)	17(1)	18(1)	17(1)	-1(1)	-1(1)	-2(1)
N(15)	22(1)	14(1)	18(1)	-2(1)	2(1)	1(1)
C(15)	28(1)	13(1)	23(1)	-3(1)	0(1)	2(1)
C(16)	18(1)	16(1)	16(1)	-1(1)	0(1)	1(1)
C(17)	16(1)	16(1)	20(1)	1(1)	2(1)	-2(1)
C(18)	16(1)	16(1)	23(1)	2(1)	4(1)	0(1)
C(19)	22(1)	19(1)	25(1)	1(1)	-1(1)	-1(1)
C(20)	16(1)	24(1)	23(1)	-1(1)	0(1)	2(1)

Table A25. Hydrogen coordinates ($\times 10^4$) and isotropic displacement parameters ($\text{\AA}^2 \times 10^3$) for **25**.

	x	y	z	U(eq)
H(2A)	9664	8802	2951	19
H(3A)	7117	9229	2005	22
H(3B)	8236	8692	893	22
H(4A)	5860	6885	1988	27
H(4B)	6163	7099	479	27
H(6A)	9620	4255	1680	20
H(7A)	7873	3560	3417	22
H(7B)	9630	3936	3917	22
H(10A)	7063	3456	6175	25
H(11A)	5670	4174	7965	27
H(12A)	4914	6812	8280	28
H(13A)	5676	8841	6887	26
H(15A)	8018	10430	4053	32
H(15B)	7982	10415	5609	32
H(15C)	6394	10398	4726	32
H(17A)	11125	8068	1237	21
H(19)	8840(30)	6310(30)	-1920(30)	33
H(20A)	12984	6247	520	32
H(20B)	12152	4831	1256	32
H(20C)	12968	6251	2078	32

Table A26. Torsion angles [°] for **25**.

C(6)-N(1)-C(2)-C(16)	55.34(18)	C(17)-N(1)-C(2)-C(16)	-175.02(14)
C(6)-N(1)-C(2)-C(3)	-65.39(18)	C(17)-N(1)-C(2)-C(3)	64.24(18)
N(1)-C(2)-C(3)-C(4)	59.02(18)	C(16)-C(2)-C(3)-C(4)	-58.89(19)
C(2)-C(3)-C(4)-C(5)	-37.0(2)	C(3)-C(4)-C(5)-O(5)	-163.13(18)
C(3)-C(4)-C(5)-C(6)	22.9(2)	C(2)-N(1)-C(6)-C(5)	47.9(2)
C(17)-N(1)-C(6)-C(5)	-81.57(18)	C(2)-N(1)-C(6)-C(7)	-74.20(17)
C(17)-N(1)-C(6)-C(7)	156.37(14)	O(5)-C(5)-C(6)-N(1)	158.15(16)
C(4)-C(5)-C(6)-N(1)	-27.8(2)	O(5)-C(5)-C(6)-C(7)	-80.0(2)
C(4)-C(5)-C(6)-C(7)	93.98(18)	N(1)-C(6)-C(7)-C(8)	48.18(17)
C(5)-C(6)-C(7)-C(8)	-77.22(17)	C(6)-C(7)-C(8)-C(16)	-13.4(2)
C(6)-C(7)-C(8)-C(9)	159.48(18)	C(16)-C(8)-C(9)-C(10)	-176.85(19)
C(7)-C(8)-C(9)-C(10)	9.5(3)	C(16)-C(8)-C(9)-C(14)	1.66(19)
C(7)-C(8)-C(9)-C(14)	-172.03(18)	C(14)-C(9)-C(10)-C(11)	1.2(3)
C(8)-C(9)-C(10)-C(11)	179.52(19)	C(9)-C(10)-C(11)-C(12)	1.8(3)
C(10)-C(11)-C(12)-C(13)	-2.4(3)	C(11)-C(12)-C(13)-C(14)	-0.1(3)
C(12)-C(13)-C(14)-N(15)	-178.56(18)	C(12)-C(13)-C(14)-C(9)	3.2(3)
C(10)-C(9)-C(14)-N(15)	177.66(15)	C(8)-C(9)-C(14)-N(15)	-1.12(19)
C(10)-C(9)-C(14)-C(13)	-3.8(3)	C(8)-C(9)-C(14)-C(13)	177.46(17)
C(13)-C(14)-N(15)-C(16)	-178.28(18)	C(9)-C(14)-N(15)-C(16)	0.2(2)
C(13)-C(14)-N(15)-C(15)	7.7(3)	C(9)-C(14)-N(15)-C(15)	-173.84(17)
C(9)-C(8)-C(16)-N(15)	-1.6(2)	C(7)-C(8)-C(16)-N(15)	172.72(16)
C(9)-C(8)-C(16)-C(2)	-175.46(16)	C(7)-C(8)-C(16)-C(2)	-1.1(3)
C(14)-N(15)-C(16)-C(8)	0.9(2)	C(15)-N(15)-C(16)-C(8)	174.70(17)
C(14)-N(15)-C(16)-C(2)	174.83(16)	C(15)-N(15)-C(16)-C(2)	-11.4(3)
N(1)-C(2)-C(16)-C(8)	-18.8(2)	C(3)-C(2)-C(16)-C(8)	102.6(2)
N(1)-C(2)-C(16)-N(15)	168.22(16)	C(3)-C(2)-C(16)-N(15)	-70.4(2)
C(6)-N(1)-C(17)-C(18)	40.3(2)	C(2)-N(1)-C(17)-C(18)	-87.64(18)
C(6)-N(1)-C(17)-C(20)	-84.01(17)	C(2)-N(1)-C(17)-C(20)	148.04(15)

IV Appendix B (Chapter 4)

Single Crystal X-ray Diffraction Analysis of compounds 22, 23, 23', and 19

Table B1. Crystal data and structure refinement for 22.

Empirical formula	C ₁₉ H ₂₁ IN ₂ O	
Formula weight	420.28	
Temperature	150(2) K	
Wavelength	1.54178 Å	
Crystal system	Monoclinic	
Space group	P2 ₁	
Unit cell dimensions	a = 7.2720(10) Å	α = 90°
	b = 9.1963(12) Å	β = 101.735(5)°
	c = 13.4788(18) Å	γ = 90°
Volume	882.6(2) Å ³	
Z	2	
Density (calculated)	1.582 Mg/m ³	
Absorption coefficient	14.293 mm ⁻¹	
F(000)	420	
Crystal size	0.439 x 0.062 x 0.036 mm ³	
Theta range for data collection	3.349 to 68.197°	
Index ranges	-8<=h<=8, -10<=k<=10, -16<=l<=13	
Reflections collected	3852	
Independent reflections	2307 [R(int) = 0.0513]	
Completeness to theta = 67.679°	92.7 %	
Absorption correction	Semi-empirical from equivalents	
Max. and min. transmission	0.7531 and 0.3189	
Refinement method	Full-matrix least-squares on F ²	
Data / restraints / parameters	2307 / 1 / 211	
Goodness-of-fit on F ²	1.127	
Final R indices [I>2sigma(I)]	R1 = 0.0648, wR2 = 0.1865	
R indices (all data)	R1 = 0.0650, wR2 = 0.1873	
Absolute structure parameter	0.278(13)	
Extinction coefficient	0.0038(12)	
Largest diff. peak and hole	1.681 and -1.225 e.Å ⁻³	

Table B2. Atomic coordinates ($\times 10^4$) and equivalent isotropic displacement parameters ($\text{\AA}^2 \times 10^3$) for **22**. $U(\text{eq})$ is defined as one third of the trace of the orthogonalized U_{ij} tensor.

x	y	z	U(eq)	
O(1)	1045(8)	6867(8)	7940(6)	33(2)
C(1)	808(12)	5584(11)	7903(8)	28(2)
C(2)	-1111(11)	4867(13)	7708(9)	36(2)
C(3)	-1344(11)	3575(13)	6979(8)	36(2)
C(4)	572(10)	2835(9)	6997(6)	24(2)
C(5)	1583(10)	3428(10)	6213(7)	24(2)
N(6)	1074(9)	3167(8)	5187(6)	23(2)
C(6)	-425(12)	2184(10)	4690(8)	34(2)
C(7)	2305(11)	3874(10)	4708(9)	24(2)
C(8)	2396(12)	3920(10)	3689(8)	28(2)
C(9)	3779(14)	4779(14)	3419(9)	38(2)
C(10)	5029(13)	5572(12)	4155(9)	36(2)
C(11)	4997(12)	5502(12)	5165(8)	30(2)
C(12)	3614(10)	4631(10)	5461(8)	25(2)
C(13)	3107(10)	4353(10)	6415(8)	24(2)
C(14)	3875(10)	4882(11)	7451(7)	27(2)
C(15)	2473(12)	4515(11)	8135(9)	25(2)
N(16)	1738(9)	3040(9)	8030(6)	26(2)
C(17)	3213(14)	1940(12)	8333(8)	34(2)
C(18)	4247(13)	2251(15)	9397(8)	41(3)
I(18)	2558(1)	2479(2)	10483(1)	54(1)
C(19)	6118(14)	2291(18)	9690(10)	51(3)
C(20)	2422(17)	371(14)	8244(12)	44(3)

Table B3. Bond lengths [\AA] and angles [$^\circ$] for **22**.

O(1)-C(1)	1.192(13)	C(1)-C(2)	1.518(12)
C(1)-C(15)	1.541(12)	C(2)-C(3)	1.529(16)
C(2)-H(2A)	0.9900	C(2)-H(2B)	0.9900
C(3)-C(4)	1.546(11)	C(3)-H(3A)	0.9900
C(3)-H(3B)	0.9900	C(4)-N(16)	1.488(11)
C(4)-C(5)	1.506(11)	C(4)-H(4A)	1.0000
C(5)-N(6)	1.378(12)	C(5)-C(13)	1.380(12)
N(6)-C(7)	1.370(13)	N(6)-C(6)	1.469(11)
C(6)-H(6A)	0.9800	C(6)-H(6B)	0.9800
C(6)-H(6C)	0.9800	C(7)-C(8)	1.390(14)
C(7)-C(12)	1.424(13)	C(8)-C(9)	1.384(14)
C(8)-H(8A)	0.9500	C(9)-C(10)	1.406(17)
C(9)-H(9A)	0.9500	C(10)-C(11)	1.367(16)

C(10)-H(10A)	0.9500	C(11)-C(12)	1.405(13)
C(11)-H(11A)	0.9500	C(12)-C(13)	1.432(14)
C(13)-C(14)	1.476(14)	C(14)-C(15)	1.545(13)
C(14)-H(14A)	0.9900	C(14)-H(14B)	0.9900
C(15)-N(16)	1.455(12)	C(15)-H(15A)	1.0000
N(16)-C(17)	1.471(12)	C(17)-C(18)	1.504(15)
C(17)-C(20)	1.548(15)	C(17)-H(17A)	1.0000
C(18)-C(19)	1.338(14)	C(18)-I(18)	2.105(11)
C(19)-H(19A)	0.9500	C(19)-H(19B)	0.9500
C(20)-H(20A)	0.9800	C(20)-H(20B)	0.9800
C(20)-H(20C)	0.9800	O(1)-C(1)-C(2)	123.9(9)
O(1)-C(1)-C(15)	121.4(9)	C(2)-C(1)-C(15)	114.5(9)
C(1)-C(2)-C(3)	115.2(7)	C(1)-C(2)-H(2A)	108.5
C(3)-C(2)-H(2A)	108.5	C(1)-C(2)-H(2B)	108.5
C(3)-C(2)-H(2B)	108.5	H(2A)-C(2)-H(2B)	107.5
C(2)-C(3)-C(4)	110.5(7)	C(2)-C(3)-H(3A)	109.5
C(4)-C(3)-H(3A)	109.5	C(2)-C(3)-H(3B)	109.5
C(4)-C(3)-H(3B)	109.5	H(3A)-C(3)-H(3B)	108.1
N(16)-C(4)-C(5)	110.1(7)	N(16)-C(4)-C(3)	107.4(7)
C(5)-C(4)-C(3)	113.3(8)	N(16)-C(4)-H(4A)	108.6
C(5)-C(4)-H(4A)	108.6	C(3)-C(4)-H(4A)	108.6
N(6)-C(5)-C(13)	110.3(8)	N(6)-C(5)-C(4)	124.8(7)
C(13)-C(5)-C(4)	124.9(8)	C(7)-N(6)-C(5)	108.8(7)
C(7)-N(6)-C(6)	124.9(8)	C(5)-N(6)-C(6)	126.0(8)
N(6)-C(6)-H(6A)	109.5	N(6)-C(6)-H(6B)	109.5
H(6A)-C(6)-H(6B)	109.5	N(6)-C(6)-H(6C)	109.5
H(6A)-C(6)-H(6C)	109.5	H(6B)-C(6)-H(6C)	109.5
N(6)-C(7)-C(8)	130.4(8)	N(6)-C(7)-C(12)	107.6(9)
C(8)-C(7)-C(12)	122.0(9)	C(9)-C(8)-C(7)	117.4(9)
C(9)-C(8)-H(8A)	121.3	C(7)-C(8)-H(8A)	121.3
C(8)-C(9)-C(10)	120.7(11)	C(8)-C(9)-H(9A)	119.6
C(10)-C(9)-H(9A)	119.6	C(11)-C(10)-C(9)	122.6(10)
C(11)-C(10)-H(10A)	118.7	C(9)-C(10)-H(10A)	118.7
C(10)-C(11)-C(12)	117.9(9)	C(10)-C(11)-H(11A)	121.1
C(12)-C(11)-H(11A)	121.1	C(11)-C(12)-C(7)	119.3(10)
C(11)-C(12)-C(13)	133.4(9)	C(7)-C(12)-C(13)	107.2(8)
C(5)-C(13)-C(12)	106.0(8)	C(5)-C(13)-C(14)	121.6(9)
C(12)-C(13)-C(14)	132.3(8)	C(13)-C(14)-C(15)	108.9(7)
C(13)-C(14)-H(14A)	109.9	C(15)-C(14)-H(14A)	109.9
C(13)-C(14)-H(14B)	109.9	C(15)-C(14)-H(14B)	109.9
H(14A)-C(14)-H(14B)	108.3	N(16)-C(15)-C(1)	108.5(7)
N(16)-C(15)-C(14)	114.8(9)	C(1)-C(15)-C(14)	109.0(8)
N(16)-C(15)-H(15A)	108.1	C(1)-C(15)-H(15A)	108.1
C(14)-C(15)-H(15A)	108.1	C(15)-N(16)-C(17)	112.5(7)
C(15)-N(16)-C(4)	109.7(8)	C(17)-N(16)-C(4)	114.7(8)
N(16)-C(17)-C(18)	109.2(9)	N(16)-C(17)-C(20)	112.4(8)

C(18)-C(17)-C(20)	110.9(10)	N(16)-C(17)-H(17A)	108.1
C(18)-C(17)-H(17A)	108.1	C(20)-C(17)-H(17A)	108.1
C(19)-C(18)-C(17)	124.6(11)	C(19)-C(18)-I(18)	119.6(9)
C(17)-C(18)-I(18)	115.7(7)	C(18)-C(19)-H(19A)	120.0
C(18)-C(19)-H(19B)	120.0	H(19A)-C(19)-H(19B)	120.0
C(17)-C(20)-H(20A)	109.5	C(17)-C(20)-H(20B)	109.5
H(20A)-C(20)-H(20B)	109.5	C(17)-C(20)-H(20C)	109.5
H(20A)-C(20)-H(20C)	109.5	H(20B)-C(20)-H(20C)	109.5

Table B4. Anisotropic displacement parameters ($\text{\AA}^2 \times 10^3$) for **22**. The anisotropic displacement factor exponent takes the form: $-2\pi^2 [h^2 a^{*2} U^{11} + \dots + 2 h k a^* b^* U^{12}]$

	U11	U22	U33	U23	U13	U12
O(1)	37(3)	22(3)	40(5)	-1(3)	5(2)	2(2)
C(1)	38(4)	22(5)	26(5)	-4(4)	13(3)	7(3)
C(2)	27(3)	41(6)	44(6)	-7(5)	16(3)	4(4)
C(3)	29(4)	43(5)	40(6)	-5(5)	13(3)	-6(4)
C(4)	32(3)	24(5)	18(4)	-1(3)	9(3)	-6(3)
C(5)	26(3)	24(5)	25(5)	1(4)	13(3)	0(3)
N(6)	30(3)	14(3)	27(4)	-1(3)	9(3)	-1(3)
C(6)	46(4)	22(6)	37(5)	-7(4)	13(3)	-18(4)
C(7)	32(4)	15(5)	27(5)	-2(4)	10(3)	-3(3)
C(8)	42(4)	21(5)	22(5)	4(4)	11(3)	-1(3)
C(9)	51(5)	42(6)	26(6)	8(5)	20(4)	-3(4)
C(10)	41(4)	34(5)	39(6)	5(5)	19(4)	-6(4)
C(11)	32(3)	30(4)	29(6)	7(4)	8(3)	-7(4)
C(12)	24(3)	24(4)	28(5)	1(4)	10(3)	2(3)
C(13)	25(3)	23(5)	25(5)	8(4)	8(3)	0(3)
C(14)	25(3)	26(5)	30(5)	7(4)	9(3)	-6(3)
C(15)	33(4)	21(5)	23(5)	-2(4)	9(3)	-2(4)
N(16)	33(3)	15(3)	30(4)	-4(3)	8(3)	3(3)
C(17)	50(5)	27(5)	26(6)	0(4)	12(4)	5(4)
C(18)	48(4)	44(7)	31(5)	7(6)	13(4)	7(5)
I(18)	81(1)	54(1)	32(1)	8(1)	22(1)	-5(1)
C(19)	46(4)	51(8)	51(7)	9(7)	-2(4)	5(5)
C(20)	52(6)	28(6)	51(8)	-1(6)	7(5)	-7(5)

Table B5. Hydrogen coordinates ($\times 10^4$) and isotropic displacement parameters ($\text{\AA}^2 \times 10^3$) for **22**.

	x	y	z	U(eq)
H(2A)	-2067	5607	7433	43
H(2B)	-1372	4532	8364	43
H(3A)	-1881	3915	6283	43
H(3B)	-2225	2863	7176	43
H(4A)	358	1770	6873	28
H(6A)	-1355	2071	5119	52
H(6B)	113	1233	4586	52
H(6C)	-1034	2593	4034	52
H(8A)	1544	3382	3196	33
H(9A)	3883	4834	2729	46
H(10A)	5932	6181	3943	44
H(11A)	5881	6024	5651	36
H(14A)	4074	5947	7440	32
H(14B)	5100	4412	7719	32
H(15A)	3126	4660	8856	30
H(17A)	4126	2028	7873	40
H(19A)	6890	2117	9212	61
H(19B)	6675	2495	10377	61
H(20A)	3426	-314	8525	66
H(20B)	1932	140	7530	66
H(20C)	1408	295	8622	66

Table B6. Torsion angles [°] for **22**.

O(1)-C(1)-C(2)-C(3)	137.6(12)	C(15)-C(1)-C(2)-C(3)	-46.9(13)
C(1)-C(2)-C(3)-C(4)	27.0(13)	C(2)-C(3)-C(4)-N(16)	30.2(11)
C(2)-C(3)-C(4)-C(5)	-91.7(10)	N(16)-C(4)-C(5)-N(6)	166.8(8)
C(3)-C(4)-C(5)-N(6)	-72.8(11)	N(16)-C(4)-C(5)-C(13)	-15.7(11)
C(3)-C(4)-C(5)-C(13)	104.6(10)	C(13)-C(5)-N(6)-C(7)	2.3(10)
C(4)-C(5)-N(6)-C(7)	-180.0(8)	C(13)-C(5)-N(6)-C(6)	177.0(8)
C(4)-C(5)-N(6)-C(6)	-5.3(14)	C(5)-N(6)-C(7)-C(8)	178.7(9)
C(6)-N(6)-C(7)-C(8)	3.9(15)	C(5)-N(6)-C(7)-C(12)	-1.1(10)
C(6)-N(6)-C(7)-C(12)	-175.9(8)	N(6)-C(7)-C(8)-C(9)	177.8(10)
C(12)-C(7)-C(8)-C(9)	-2.4(14)	C(7)-C(8)-C(9)-C(10)	-0.1(16)
C(8)-C(9)-C(10)-C(11)	2.3(17)	C(9)-C(10)-C(11)-C(12)	-1.9(16)
C(10)-C(11)-C(12)-C(7)	-0.5(15)	C(10)-C(11)-C(12)-C(13)	-176.7(10)
N(6)-C(7)-C(12)-C(11)	-177.4(9)	C(8)-C(7)-C(12)-C(11)	2.7(14)
N(6)-C(7)-C(12)-C(13)	-0.3(10)	C(8)-C(7)-C(12)-C(13)	179.8(8)
N(6)-C(5)-C(13)-C(12)	-2.4(10)	C(4)-C(5)-C(13)-C(12)	179.8(8)
N(6)-C(5)-C(13)-C(14)	176.4(8)	C(4)-C(5)-C(13)-C(14)	-1.4(13)
C(11)-C(12)-C(13)-C(5)	178.2(10)	C(7)-C(12)-C(13)-C(5)	1.7(9)
C(11)-C(12)-C(13)-C(14)	-0.4(18)	C(7)-C(12)-C(13)-C(14)	-177.0(9)
C(5)-C(13)-C(14)-C(15)	-12.2(12)	C(12)-C(13)-C(14)-C(15)	166.3(9)
O(1)-C(1)-C(15)-N(16)	179.9(11)	C(2)-C(1)-C(15)-N(16)	4.2(13)
O(1)-C(1)-C(15)-C(14)	-54.4(13)	C(2)-C(1)-C(15)-C(14)	129.9(9)
C(13)-C(14)-C(15)-N(16)	46.0(10)	C(13)-C(14)-C(15)-C(1)	-75.9(10)
C(1)-C(15)-N(16)-C(17)	-174.5(9)	C(14)-C(15)-N(16)-C(17)	63.3(11)
C(1)-C(15)-N(16)-C(4)	56.6(10)	C(14)-C(15)-N(16)-C(4)	-65.6(9)
C(5)-C(4)-N(16)-C(15)	46.6(9)	C(3)-C(4)-N(16)-C(15)	-77.2(9)
C(5)-C(4)-N(16)-C(17)	-81.1(10)	C(3)-C(4)-N(16)-C(17)	155.1(8)
C(15)-N(16)-C(17)-C(18)	55.2(11)	C(4)-N(16)-C(17)-C(18)	-178.5(8)
C(15)-N(16)-C(17)-C(20)	178.7(9)	C(4)-N(16)-C(17)-C(20)	-55.0(12)
N(16)-C(17)-C(18)-C(19)	-131.6(14)	C(20)-C(17)-C(18)-C(19)	104.0(15)
N(16)-C(17)-C(18)-I(18)	52.9(11)	C(20)-C(17)-C(18)-I(18)	-71.5(11)

Table B7. Crystal data and structure refinement for **23**.

Empirical formula	C ₁₉ H ₂₀ N ₂ O	
Formula weight	292.37	
Temperature	150(2) K	
Wavelength	0.71073 Å	
Crystal system	Orthorhombic	
Space group	P2 ₁ 2 ₁ 2 ₁	
Unit cell dimensions	a = 6.8328(5) Å	α = 90°
	b = 11.6515(6) Å	β = 90°
	c = 19.2975(7) Å	γ = 90°
Volume	1536.32(15) Å ³	
Z	4	
Density (calculated)	1.264 Mg/m ³	
Absorption coefficient	0.079 mm ⁻¹	
F(000)	624	
Crystal size	0.551 x 0.241 x 0.109 mm ³	
Theta range for data collection	2.042 to 29.147°.	
Index ranges	-9<=h<=9, -15<=k<=15, -26<=l<=26	
Reflections collected	12917	
Independent reflections	4097 [R(int) = 0.0291]	
Completeness to theta = 25.000°	99.9 %	
Absorption correction	None	
Refinement method	Full-matrix least-squares on F ²	
Data / restraints / parameters	4097 / 0 / 201	
Goodness-of-fit on F ²	1.116	
Final R indices [I>2sigma(I)]	R1 = 0.0351, wR2 = 0.0861	
R indices (all data)	R1 = 0.0425, wR2 = 0.1031	
Absolute structure parameter	-0.8(5)	
Extinction coefficient	n/a	
Largest diff. peak and hole	0.293 and -0.359 e.Å ⁻³	

Table B8. Atomic coordinates ($\times 10^4$) and equivalent isotropic displacement parameters ($\text{\AA}^2 \times 10^3$) for **23**. $U(\text{eq})$ is defined as one third of the trace of the orthogonalized U^{ij} tensor.

	x	y	z	$U(\text{eq})$
N(1)	5237(2)	2088(1)	2412(1)	19(1)
C(2)	5643(3)	1860(2)	1666(1)	24(1)
C(2A)	7805(3)	1597(2)	1542(1)	33(1)
C(3)	4866(3)	2851(2)	1227(1)	25(1)
C(3A)	4704(3)	2840(2)	544(1)	39(1)
C(4)	4259(2)	3859(2)	1672(1)	21(1)
C(5)	6001(3)	4157(2)	2153(1)	20(1)
C(6)	6327(2)	3124(2)	2654(1)	18(1)
C(7)	5611(2)	3390(2)	3370(1)	18(1)
N(8)	6589(2)	4089(1)	3838(1)	19(1)
C(8)	8499(2)	4618(2)	3752(1)	24(1)
C(9)	5491(2)	4141(2)	4440(1)	20(1)
C(10)	5887(3)	4693(2)	5066(1)	25(1)
C(11)	4548(3)	4549(2)	5597(1)	29(1)
C(12)	2868(3)	3868(2)	5514(1)	28(1)
C(13)	2451(3)	3337(2)	4889(1)	24(1)
C(14)	3777(3)	3468(2)	4339(1)	19(1)
C(15)	3884(2)	3017(2)	3649(1)	18(1)
C(16)	2504(3)	2274(2)	3251(1)	21(1)
C(17)	3108(2)	2308(2)	2489(1)	19(1)
O(18)	1048(2)	3941(1)	2209(1)	30(1)
C(18)	2597(3)	3445(2)	2135(1)	20(1)

Table B9. Bond lengths [\AA] and angles [$^\circ$] for **23**.

N(1)-C(17)	1.484(2)	N(1)-C(2)	1.489(2)
N(1)-C(6)	1.493(2)	C(2)-C(3)	1.527(3)
C(2)-C(2A)	1.528(3)	C(2)-H(2A)	0.9800
C(2A)-H(2AA)	0.9600	C(2A)-H(2AB)	0.9600
C(2A)-H(2AC)	0.9600	C(3)-C(3A)	1.321(3)
C(3)-C(4)	1.513(3)	C(3A)-H(3AA)	0.9300
C(3A)-H(3AB)	0.9300	C(4)-C(18)	1.524(2)
C(4)-C(5)	1.548(2)	C(4)-H(4A)	0.9800
C(5)-C(6)	1.560(2)	C(5)-H(5A)	0.9700
C(5)-H(5B)	0.9700	C(6)-C(7)	1.497(2)
C(6)-H(6A)	0.9800	C(7)-C(15)	1.368(2)

C(7)-N(8)	1.387(2)	N(8)-C(9)	1.385(2)
N(8)-C(8)	1.453(2)	C(8)-H(8A)	0.9600
C(8)-H(8B)	0.9600	C(8)-H(8C)	0.9600
C(9)-C(10)	1.395(3)	C(9)-C(14)	1.424(2)
C(10)-C(11)	1.384(3)	C(10)-H(10A)	0.9300
C(11)-C(12)	1.405(3)	C(11)-H(11A)	0.9300
C(12)-C(13)	1.385(3)	C(12)-H(12A)	0.9300
C(13)-C(14)	1.404(3)	C(13)-H(13A)	0.9300
C(14)-C(15)	1.433(2)	C(15)-C(16)	1.493(2)
C(16)-C(17)	1.527(2)	C(16)-H(16A)	0.9700
C(16)-H(16B)	0.9700	C(17)-C(18)	1.530(3)
C(17)-H(17A)	0.9800	O(18)-C(18)	1.214(2)
C(17)-N(1)-C(2)	108.06(14)	C(17)-N(1)-C(6)	108.54(13)
C(2)-N(1)-C(6)	110.72(14)	N(1)-C(2)-C(3)	109.72(15)
N(1)-C(2)-C(2A)	111.60(16)	C(3)-C(2)-C(2A)	113.56(17)
N(1)-C(2)-H(2A)	107.2	C(3)-C(2)-H(2A)	107.2
C(2A)-C(2)-H(2A)	107.2	C(2)-C(2A)-H(2AA)	109.5
C(2)-C(2A)-H(2AB)	109.5	H(2AA)-C(2A)-H(2AB)	109.5
C(2)-C(2A)-H(2AC)	109.5	H(2AA)-C(2A)-H(2AC)	109.5
H(2AB)-C(2A)-H(2AC)	109.5	C(3A)-C(3)-C(4)	123.39(19)
C(3A)-C(3)-C(2)	125.14(19)	C(4)-C(3)-C(2)	111.46(16)
C(3)-C(3A)-H(3AA)	120.0	C(3)-C(3A)-H(3AB)	120.0
H(3AA)-C(3A)-H(3AB)	120.0	C(3)-C(4)-C(18)	106.96(15)
C(3)-C(4)-C(5)	107.69(15)	C(18)-C(4)-C(5)	107.01(14)
C(3)-C(4)-H(4A)	111.6	C(18)-C(4)-H(4A)	111.6
C(5)-C(4)-H(4A)	111.6	C(4)-C(5)-C(6)	107.95(14)
C(4)-C(5)-H(5A)	110.1	C(6)-C(5)-H(5A)	110.1
C(4)-C(5)-H(5B)	110.1	C(6)-C(5)-H(5B)	110.1
H(5A)-C(5)-H(5B)	108.4	N(1)-C(6)-C(7)	107.05(14)
N(1)-C(6)-C(5)	110.99(14)	C(7)-C(6)-C(5)	111.45(14)
N(1)-C(6)-H(6A)	109.1	C(7)-C(6)-H(6A)	109.1
C(5)-C(6)-H(6A)	109.1	C(15)-C(7)-N(8)	110.23(15)
C(15)-C(7)-C(6)	125.36(16)	N(8)-C(7)-C(6)	124.38(15)
C(9)-N(8)-C(7)	108.16(14)	C(9)-N(8)-C(8)	124.23(15)
C(7)-N(8)-C(8)	127.45(15)	N(8)-C(8)-H(8A)	109.5
N(8)-C(8)-H(8B)	109.5	H(8A)-C(8)-H(8B)	109.5
N(8)-C(8)-H(8C)	109.5	H(8A)-C(8)-H(8C)	109.5
H(8B)-C(8)-H(8C)	109.5	N(8)-C(9)-C(10)	129.97(17)
N(8)-C(9)-C(14)	107.81(15)	C(10)-C(9)-C(14)	122.19(16)
C(11)-C(10)-C(9)	117.19(18)	C(11)-C(10)-H(10A)	121.4
C(9)-C(10)-H(10A)	121.4	C(10)-C(11)-C(12)	121.63(19)
C(10)-C(11)-H(11A)	119.2	C(12)-C(11)-H(11A)	119.2
C(13)-C(12)-C(11)	121.31(18)	C(13)-C(12)-H(12A)	119.3
C(11)-C(12)-H(12A)	119.3	C(12)-C(13)-C(14)	118.53(18)
C(12)-C(13)-H(13A)	120.7	C(14)-C(13)-H(13A)	120.7
C(13)-C(14)-C(9)	119.11(17)	C(13)-C(14)-C(15)	134.10(17)

C(9)-C(14)-C(15)	106.73(15)	C(7)-C(15)-C(14)	107.04(16)
C(7)-C(15)-C(16)	121.79(15)	C(14)-C(15)-C(16)	131.16(16)
C(15)-C(16)-C(17)	108.02(14)	C(15)-C(16)-H(16A)	110.1
C(17)-C(16)-H(16A)	110.1	C(15)-C(16)-H(16B)	110.1
C(17)-C(16)-H(16B)	110.1	H(16A)-C(16)-H(16B)	108.4
N(1)-C(17)-C(16)	110.94(15)	N(1)-C(17)-C(18)	109.16(14)
C(16)-C(17)-C(18)	112.95(15)	N(1)-C(17)-H(17A)	107.9
C(16)-C(17)-H(17A)	107.9	C(18)-C(17)-H(17A)	107.9
O(18)-C(18)-C(4)	124.58(17)	O(18)-C(18)-C(17)	123.98(17)
C(4)-C(18)-C(17)	111.43(15)		

Table B10. Anisotropic displacement parameters ($\text{\AA}^2 \times 10^3$) for **23**. The anisotropic displacement factor exponent takes the form: $-2\pi^2 [h^2 a^{*2} U^{11} + \dots + 2 h k a^* b^* U^{12}]$

	U11	U22	U33	U23	U13	U12
N(1)	16(1)	16(1)	25(1)	-1(1)	4(1)	0(1)
C(2)	22(1)	22(1)	27(1)	-6(1)	4(1)	0(1)
C(2A)	26(1)	36(1)	37(1)	-5(1)	9(1)	8(1)
C(3)	19(1)	30(1)	26(1)	-2(1)	2(1)	-2(1)
C(3A)	47(1)	43(1)	28(1)	-5(1)	1(1)	0(1)
C(4)	18(1)	22(1)	23(1)	3(1)	0(1)	1(1)
C(5)	19(1)	18(1)	23(1)	0(1)	3(1)	-2(1)
C(6)	13(1)	17(1)	24(1)	1(1)	1(1)	1(1)
C(7)	15(1)	16(1)	22(1)	2(1)	-1(1)	1(1)
N(8)	17(1)	22(1)	20(1)	1(1)	-1(1)	-2(1)
C(8)	15(1)	27(1)	31(1)	1(1)	-2(1)	-3(1)
C(9)	20(1)	19(1)	22(1)	5(1)	-1(1)	3(1)
C(10)	27(1)	22(1)	26(1)	0(1)	-5(1)	1(1)
C(11)	38(1)	27(1)	22(1)	-1(1)	-2(1)	7(1)
C(12)	35(1)	26(1)	22(1)	3(1)	8(1)	6(1)
C(13)	24(1)	21(1)	25(1)	5(1)	4(1)	2(1)
C(14)	20(1)	16(1)	20(1)	5(1)	0(1)	2(1)
C(15)	17(1)	16(1)	21(1)	2(1)	1(1)	1(1)
C(16)	18(1)	19(1)	25(1)	-1(1)	4(1)	-4(1)
C(17)	15(1)	19(1)	24(1)	-3(1)	1(1)	-3(1)
O(18)	18(1)	37(1)	33(1)	3(1)	1(1)	7(1)
C(18)	16(1)	24(1)	21(1)	-3(1)	-2(1)	-1(1)

Table B11. Hydrogen coordinates ($\times 10^4$) and isotropic displacement parameters ($\text{\AA}^2 \times 10^3$) for **23**.

	x	y	z	U(eq)
H(2A)	4901	1173	1537	28
H(2AA)	8248	1044	1875	49
H(2AB)	8556	2289	1588	49
H(2AC)	7971	1294	1083	49
H(3AA)	4196	3475	314	47
H(3AB)	5099	2198	295	47
H(4A)	3864	4518	1390	25
H(5A)	5714	4847	2415	24
H(5B)	7170	4291	1880	24
H(6A)	7727	2945	2674	22
H(8A)	8398	5428	3839	37
H(8B)	8955	4494	3288	37
H(8C)	9405	4283	4074	37
H(10A)	7004	5139	5124	30
H(11A)	4767	4912	6019	35
H(12A)	2018	3773	5886	34
H(13A)	1319	2904	4835	28
H(16A)	1175	2554	3302	25
H(16B)	2557	1493	3423	25
H(17A)	2405	1694	2247	23

Table B12. Torsion angles [°] for **23**.

C(17)-N(1)-C(2)-C(3)	54.52(19)	C(6)-N(1)-C(2)-C(3)	-64.21(18)
C(17)-N(1)-C(2)-C(2A)	-178.70(16)	C(6)-N(1)-C(2)-C(2A)	62.6(2)
N(1)-C(2)-C(3)-C(3A)	-168.63(18)	C(2A)-C(2)-C(3)-C(3A)	65.7(3)
N(1)-C(2)-C(3)-C(4)	10.4(2)	C(2A)-C(2)-C(3)-C(4)	-115.27(18)
C(3A)-C(3)-C(4)-C(18)	116.7(2)	C(2)-C(3)-C(4)-C(18)	-62.37(18)
C(3A)-C(3)-C(4)-C(5)	-128.6(2)	C(2)-C(3)-C(4)-C(5)	52.36(19)
C(3)-C(4)-C(5)-C(6)	-65.27(18)	C(18)-C(4)-C(5)-C(6)	49.43(18)
C(17)-N(1)-C(6)-C(7)	53.33(17)	C(2)-N(1)-C(6)-C(7)	171.78(13)
C(17)-N(1)-C(6)-C(5)	-68.50(18)	C(2)-N(1)-C(6)-C(5)	49.95(18)
C(4)-C(5)-C(6)-N(1)	13.80(19)	C(4)-C(5)-C(6)-C(7)	-105.42(16)
N(1)-C(6)-C(7)-C(15)	-19.8(2)	C(5)-C(6)-C(7)-C(15)	101.8(2)
N(1)-C(6)-C(7)-N(8)	162.52(15)	C(5)-C(6)-C(7)-N(8)	-75.9(2)
C(15)-C(7)-N(8)-C(9)	1.7(2)	C(6)-C(7)-N(8)-C(9)	179.69(15)
C(15)-C(7)-N(8)-C(8)	177.33(16)	C(6)-C(7)-N(8)-C(8)	-4.7(3)
C(7)-N(8)-C(9)-C(10)	177.30(18)	C(8)-N(8)-C(9)-C(10)	1.5(3)
C(7)-N(8)-C(9)-C(14)	-0.75(19)	C(8)-N(8)-C(9)-C(14)	-176.57(15)
N(8)-C(9)-C(10)-C(11)	-176.89(18)	C(14)-C(9)-C(10)-C(11)	0.9(3)
C(9)-C(10)-C(11)-C(12)	0.5(3)	C(10)-C(11)-C(12)-C(13)	-1.8(3)
C(11)-C(12)-C(13)-C(14)	1.6(3)	C(12)-C(13)-C(14)-C(9)	-0.2(3)
C(12)-C(13)-C(14)-C(15)	176.52(19)	N(8)-C(9)-C(14)-C(13)	177.14(16)
C(10)-C(9)-C(14)-C(13)	-1.1(3)	N(8)-C(9)-C(14)-C(15)	-0.39(19)
C(10)-C(9)-C(14)-C(15)	-178.62(16)	N(8)-C(7)-C(15)-C(14)	-1.90(19)
C(6)-C(7)-C(15)-C(14)	-179.88(15)	N(8)-C(7)-C(15)-C(16)	178.33(16)
C(6)-C(7)-C(15)-C(16)	0.3(3)	C(13)-C(14)-C(15)-C(7)	-175.60(19)
C(9)-C(14)-C(15)-C(7)	1.39(19)	C(13)-C(14)-C(15)-C(16)	4.1(3)
C(9)-C(14)-C(15)-C(16)	-178.87(18)	C(7)-C(15)-C(16)-C(17)	-14.3(2)
C(14)-C(15)-C(16)-C(17)	166.02(18)	C(2)-N(1)-C(17)-C(16)	166.88(14)
C(6)-N(1)-C(17)-C(16)	-73.00(18)	C(2)-N(1)-C(17)-C(18)	-68.02(18)
C(6)-N(1)-C(17)-C(18)	52.10(18)	C(15)-C(16)-C(17)-N(1)	49.4(2)
C(15)-C(16)-C(17)-C(18)	-73.55(18)	C(3)-C(4)-C(18)-O(18)	-130.30(19)
C(5)-C(4)-C(18)-O(18)	114.5(2)	C(3)-C(4)-C(18)-C(17)	48.73(19)
C(5)-C(4)-C(18)-C(17)	-66.45(18)	N(1)-C(17)-C(18)-O(18)	-167.38(17)
C(16)-C(17)-C(18)-O(18)	-43.5(2)	N(1)-C(17)-C(18)-C(4)	13.6(2)
C(16)-C(17)-C(18)-C(4)	137.49(15)		

Table B13. Crystal data and structure refinement for **23'**.

Empirical formula	$C_{57}H_{60}N_6O_{5.04}$	
Formula weight	909.69	
Temperature	150(2) K	
Wavelength	0.71073 Å	
Crystal system	Trigonal	
Space group	R3	
Unit cell dimensions	$a = 24.3565(13)$ Å	$\alpha = 90^\circ$
	$b = 24.3565(13)$ Å	$\beta = 90^\circ$
	$c = 7.2166(5)$ Å	$\gamma = 120^\circ$
Volume	$3707.6(5)$ Å ³	
Z	3	
Density (calculated)	1.222 Mg/m ³	
Absorption coefficient	0.079 mm ⁻¹	
F(000)	1453	
Crystal size	0.400 x 0.135 x 0.122 mm ³	
Theta range for data collection	1.672 to 29.147°.	
Index ranges	-33 ≤ h ≤ 24, -33 ≤ k ≤ 30, -9 ≤ l ≤ 5	
Reflections collected	6956	
Independent reflections	3408 [R(int) = 0.1067]	
Completeness to theta = 25.000°	99.9 %	
Absorption correction	None	
Refinement method	Full-matrix least-squares on F ²	
Data / restraints / parameters	3408 / 1 / 212	
Goodness-of-fit on F ²	1.316	
Final R indices [I > 2σ(I)]	R1 = 0.1273, wR2 = 0.3285	
R indices (all data)	R1 = 0.1425, wR2 = 0.3465	
Absolute structure parameter	1.4(10)	
Extinction coefficient	0.005(3)	
Largest diff. peak and hole	1.758 and -0.404 e.Å ⁻³	

Table B14. Atomic coordinates ($\times 10^4$) and equivalent isotropic displacement parameters ($\text{\AA}^2 \times 10^3$) for **23'**. $U(\text{eq})$ is defined as one third of the trace of the orthogonalized U_{ij} tensor.

	x	y	z	U(eq)
N(1)	4694(3)	8469(3)	3446(9)	35(1)
C(2)	4445(3)	8858(4)	2661(11)	37(2)
C(2A)	4296(6)	8736(6)	592(14)	63(3)
C(3)	4824(4)	9566(4)	2991(11)	42(2)
C(4)	5404(4)	9865(4)	3726(11)	40(2)
C(5)	5776(3)	9550(3)	4354(11)	38(2)
C(6)	5867(3)	9196(3)	2754(11)	36(2)
C(7)	5262(3)	8518(3)	2527(10)	30(1)
C(8)	5368(3)	8024(3)	3400(10)	31(1)
N(9)	5726(3)	7790(3)	2598(9)	32(1)
C(9)	6069(4)	7996(4)	895(13)	47(2)
C(10)	5723(3)	7357(3)	3800(10)	32(1)
C(11)	6013(3)	6987(3)	3627(12)	40(2)
C(12)	5940(3)	6583(3)	5051(14)	43(2)
C(13)	5568(4)	6528(4)	6602(12)	42(2)
C(14)	5277(4)	6892(3)	6782(11)	38(2)
C(15)	5355(3)	7306(3)	5354(11)	36(2)
C(16)	5136(3)	7752(3)	5059(10)	35(2)
C(17)	4731(4)	7922(4)	6197(12)	41(2)
C(18)	4788(3)	8535(3)	5443(11)	35(2)
C(19)	5424(3)	9120(3)	5971(10)	33(1)
O(19)	5610(3)	9232(3)	7558(8)	54(2)
O(1S)	2982(8)	7106(8)	400(20)	52(6)
O(2S)	3636(7)	7264(7)	2620(20)	23(6)

Table B15. Bond lengths [\AA] and angles [$^\circ$] for **23'**.

N(1)-C(18)	1.455(10)	N(1)-C(2)	1.470(9)
N(1)-C(7)	1.484(8)	C(2)-C(3)	1.513(11)
C(2)-C(2A)	1.530(12)	C(2)-H(2A)	1.0000
C(2A)-H(2AA)	0.9800	C(2A)-H(2AB)	0.9800
C(2A)-H(2AC)	0.9800	C(3)-C(4)	1.335(12)
C(3)-H(3A)	0.9500	C(4)-C(5)	1.518(10)
C(4)-H(4A)	0.9500	C(5)-C(19)	1.516(11)
C(5)-C(6)	1.523(11)	C(5)-H(5A)	1.0000
C(6)-C(7)	1.578(10)	C(6)-H(6A)	0.9900
C(6)-H(6B)	0.9900	C(7)-C(8)	1.491(9)
C(7)-H(7A)	1.0000	C(8)-C(16)	1.348(10)
C(8)-N(9)	1.386(8)	N(9)-C(10)	1.363(9)
N(9)-C(9)	1.428(10)	C(9)-H(9A)	0.9800
C(9)-H(9B)	0.9800	C(9)-H(9C)	0.9800
C(10)-C(11)	1.400(10)	C(10)-C(15)	1.403(10)
C(11)-C(12)	1.372(13)	C(11)-H(11A)	0.9500
C(12)-C(13)	1.404(13)	C(12)-H(12A)	0.9500
C(13)-C(14)	1.390(11)	C(13)-H(13A)	0.9500
C(14)-C(15)	1.388(11)	C(14)-H(14A)	0.9500
C(15)-C(16)	1.443(10)	C(16)-C(17)	1.493(10)
C(17)-C(18)	1.530(10)	C(17)-H(17A)	0.9900
C(17)-H(17B)	0.9900	C(18)-C(19)	1.539(10)
C(18)-H(18A)	1.0000	C(19)-O(19)	1.212(9)
C(18)-N(1)-C(2)	113.7(5)	C(18)-N(1)-C(7)	110.2(5)
C(2)-N(1)-C(7)	116.4(6)	N(1)-C(2)-C(3)	117.5(6)
N(1)-C(2)-C(2A)	112.6(6)	C(3)-C(2)-C(2A)	109.0(7)
N(1)-C(2)-H(2A)	105.6	C(3)-C(2)-H(2A)	105.6
C(2A)-C(2)-H(2A)	105.6	C(2)-C(2A)-H(2AA)	109.5
C(2)-C(2A)-H(2AB)	109.5	H(2AA)-C(2A)-H(2AB)	109.5
C(2)-C(2A)-H(2AC)	109.5	H(2AA)-C(2A)-H(2AC)	109.5
H(2AB)-C(2A)-H(2AC)	109.5	C(4)-C(3)-C(2)	124.1(7)
C(4)-C(3)-H(3A)	118.0	C(2)-C(3)-H(3A)	118.0
C(3)-C(4)-C(5)	125.4(7)	C(3)-C(4)-H(4A)	117.3
C(5)-C(4)-H(4A)	117.3	C(19)-C(5)-C(4)	107.7(6)
C(19)-C(5)-C(6)	112.6(6)	C(4)-C(5)-C(6)	110.6(6)
C(19)-C(5)-H(5A)	108.6	C(4)-C(5)-H(5A)	108.6
C(6)-C(5)-H(5A)	108.6	C(5)-C(6)-C(7)	110.3(5)
C(5)-C(6)-H(6A)	109.6	C(7)-C(6)-H(6A)	109.6
C(5)-C(6)-H(6B)	109.6	C(7)-C(6)-H(6B)	109.6
H(6A)-C(6)-H(6B)	108.1	N(1)-C(7)-C(8)	106.1(5)
N(1)-C(7)-C(6)	112.6(5)	C(8)-C(7)-C(6)	110.7(5)
N(1)-C(7)-H(7A)	109.2	C(8)-C(7)-H(7A)	109.2
C(6)-C(7)-H(7A)	109.2	C(16)-C(8)-N(9)	111.3(6)
C(16)-C(8)-C(7)	125.0(6)	N(9)-C(8)-C(7)	123.7(6)

C(10)-N(9)-C(8)	107.0(6)	C(10)-N(9)-C(9)	126.6(6)
C(8)-N(9)-C(9)	126.3(6)	N(9)-C(9)-H(9A)	109.5
N(9)-C(9)-H(9B)	109.5	H(9A)-C(9)-H(9B)	109.5
N(9)-C(9)-H(9C)	109.5	H(9A)-C(9)-H(9C)	109.5
H(9B)-C(9)-H(9C)	109.5	N(9)-C(10)-C(11)	129.2(7)
C(11)-C(12)-H(12A)	119.6	C(13)-C(12)-H(12A)	119.6
N(9)-C(10)-C(15)	109.4(6)	C(11)-C(10)-C(15)	121.5(7)
C(12)-C(11)-C(10)	117.9(7)	C(12)-C(11)-H(11A)	121.0
C(10)-C(11)-H(11A)	121.0	C(11)-C(12)-C(13)	120.7(7)
C(14)-C(13)-C(12)	121.7(7)	C(14)-C(13)-H(13A)	119.1
C(12)-C(13)-H(13A)	119.1	C(15)-C(14)-C(13)	117.8(7)
C(15)-C(14)-H(14A)	121.1	C(13)-C(14)-H(14A)	121.1
C(14)-C(15)-C(10)	120.4(7)	C(14)-C(15)-C(16)	133.5(7)
C(10)-C(15)-C(16)	106.1(6)	C(8)-C(16)-C(15)	106.2(6)
C(8)-C(16)-C(17)	121.6(6)	C(15)-C(16)-C(17)	132.2(6)
C(16)-C(17)-C(18)	109.1(6)	C(16)-C(17)-H(17A)	109.9
C(18)-C(17)-H(17A)	109.9	C(16)-C(17)-H(17B)	109.9
C(18)-C(17)-H(17B)	109.9	H(17A)-C(17)-H(17B)	108.3
N(1)-C(18)-C(17)	108.1(6)	N(1)-C(18)-C(19)	112.1(6)
C(17)-C(18)-C(19)	111.9(6)	N(1)-C(18)-H(18A)	108.2
C(17)-C(18)-H(18A)	108.2	C(19)-C(18)-H(18A)	108.2
O(19)-C(19)-C(5)	123.6(7)	O(19)-C(19)-C(18)	122.2(7)
C(5)-C(19)-C(18)	114.1(6)		

Table B16. Anisotropic displacement parameters ($\text{\AA}^2 \times 10^3$) for **23'**. The anisotropic displacement factor exponent takes the form: $-2\pi^2[h^2 a^{*2}U^{11} + \dots + 2 h k a^* b^* U^{12}]$

	U11	U22	U33	U23	U13	U12
N(1)	28(3)	37(3)	45(4)	0(2)	5(2)	20(2)
C(2)	34(3)	45(4)	40(4)	-9(3)	-12(3)	25(3)
C(2A)	80(7)	76(7)	56(6)	-17(5)	-32(5)	57(6)
C(3)	48(4)	46(4)	43(4)	12(3)	10(3)	31(4)
C(4)	47(4)	34(3)	42(4)	-2(3)	4(3)	23(3)
C(5)	30(3)	33(3)	48(4)	-7(3)	-4(3)	14(3)
C(6)	34(3)	35(3)	40(4)	5(3)	7(3)	18(3)
C(7)	28(3)	30(3)	33(3)	-1(3)	3(3)	15(2)
C(8)	31(3)	29(3)	34(3)	-2(3)	7(3)	17(3)
N(9)	30(3)	28(2)	40(3)	1(2)	5(2)	14(2)
C(9)	52(4)	44(4)	51(5)	7(4)	21(4)	28(4)
C(10)	20(2)	28(3)	38(4)	-1(3)	4(2)	6(2)
C(11)	23(3)	30(3)	57(5)	-8(3)	5(3)	5(2)

C(12)	26(3)	29(3)	75(6)	-7(3)	-3(3)	15(3)
C(13)	42(4)	38(4)	47(4)	4(3)	-2(3)	22(3)
C(14)	37(3)	31(3)	40(4)	2(3)	2(3)	13(3)
C(15)	21(3)	34(3)	48(4)	4(3)	6(3)	11(2)
C(16)	29(3)	34(3)	41(4)	11(3)	7(3)	16(3)
C(17)	40(4)	37(4)	48(4)	14(3)	19(3)	20(3)
C(18)	33(3)	41(3)	39(4)	2(3)	3(3)	25(3)
C(19)	37(3)	40(3)	35(3)	-6(3)	-3(3)	29(3)
O(19)	60(4)	71(4)	42(3)	-6(3)	-6(3)	41(3)

Table b17. Hydrogen coordinates ($\times 10^4$) and isotropic displacement parameters ($\text{\AA}^2 \times 10^3$) for **23'**.

	x	y	z	U(eq)
114375				
H(2A)	4028	8711	3284	45
H(2AA)	4073	8278	357	94
H(2AB)	4692	8941	-118	94
H(2AC)	4027	8909	213	94
H(3A)	4636	9812	2654	50
H(4A)	5601	10312	3869	48
H(5A)	6203	9887	4794	45
H(6A)	6244	9152	2992	44
H(6B)	5941	9440	1593	44
H(7A)	5171	8421	1178	36
H(9A)	5981	7627	140	71
H(9B)	6524	8244	1157	71
H(9C)	5937	8260	221	71
H(11A)	6253	7015	2556	48
H(12A)	6143	6337	4986	52
H(13A)	5514	6236	7553	50
H(14A)	5032	6857	7847	45
H(17A)	4870	7982	7506	49
H(17B)	4284	7576	6141	49
H(18A)	4439	8586	5993	42

Table B18. Torsion angles [°] for **23'**.

C(18)-N(1)-C(2)-C(3)	57.2(9)	C(7)-N(1)-C(2)-C(3)	-72.5(8)
C(18)-N(1)-C(2)-C(2A)	-174.9(8)	C(7)-N(1)-C(2)-C(2A)	55.4(9)
N(1)-C(2)-C(3)-C(4)	9.3(12)	C(2A)-C(2)-C(3)-C(4)	-120.3(9)
C(2)-C(3)-C(4)-C(5)	-0.3(13)	C(3)-C(4)-C(5)-C(19)	-65.1(10)
C(3)-C(4)-C(5)-C(6)	58.3(10)	C(19)-C(5)-C(6)-C(7)	37.6(8)
C(4)-C(5)-C(6)-C(7)	-83.1(7)	C(18)-N(1)-C(7)-C(8)	55.9(7)
C(2)-N(1)-C(7)-C(8)	-172.7(6)	C(18)-N(1)-C(7)-C(6)	-65.2(7)
C(2)-N(1)-C(7)-C(6)	66.2(8)	C(5)-C(6)-C(7)-N(1)	18.8(8)
C(5)-C(6)-C(7)-C(8)	-99.7(7)	N(1)-C(7)-C(8)-C(16)	-20.0(9)
C(6)-C(7)-C(8)-C(16)	102.3(8)	N(1)-C(7)-C(8)-N(9)	160.4(6)
C(6)-C(7)-C(8)-N(9)	-77.2(8)	C(16)-C(8)-N(9)-C(10)	-0.4(8)
C(7)-C(8)-N(9)-C(10)	179.2(6)	C(16)-C(8)-N(9)-C(9)	-176.4(7)
C(7)-C(8)-N(9)-C(9)	3.1(11)	C(8)-N(9)-C(10)-C(11)	179.7(7)
C(9)-N(9)-C(10)-C(11)	-4.3(12)	C(8)-N(9)-C(10)-C(15)	1.0(7)
C(9)-N(9)-C(10)-C(15)	177.0(7)	N(9)-C(10)-C(11)-C(12)	179.8(7)
C(15)-C(10)-C(11)-C(12)	-1.7(10)	C(10)-C(11)-C(12)-C(13)	2.1(10)
C(11)-C(12)-C(13)-C(14)	-1.9(12)	C(12)-C(13)-C(14)-C(15)	1.2(11)
C(13)-C(14)-C(15)-C(10)	-0.7(11)	C(13)-C(14)-C(15)-C(16)	-179.4(7)
N(9)-C(10)-C(15)-C(14)	179.8(7)	C(11)-C(10)-C(15)-C(14)	1.0(10)
N(9)-C(10)-C(15)-C(16)	-1.2(8)	C(11)-C(10)-C(15)-C(16)	180.0(6)
N(9)-C(8)-C(16)-C(15)	-0.3(8)	C(7)-C(8)-C(16)-C(15)	-179.9(6)
N(9)-C(8)-C(16)-C(17)	-179.7(7)	C(7)-C(8)-C(16)-C(17)	0.8(12)
C(14)-C(15)-C(16)-C(8)	179.7(8)	C(10)-C(15)-C(16)-C(8)	0.9(8)
C(14)-C(15)-C(16)-C(17)	-1.1(15)	C(10)-C(15)-C(16)-C(17)	-179.8(8)
C(8)-C(16)-C(17)-C(18)	-14.7(10)	C(15)-C(16)-C(17)-C(18)	166.1(7)
C(2)-N(1)-C(18)-C(17)	153.2(6)	C(7)-N(1)-C(18)-C(17)	-74.1(7)
C(2)-N(1)-C(18)-C(19)	-83.0(7)	C(7)-N(1)-C(18)-C(19)	49.7(7)
C(16)-C(17)-C(18)-N(1)	49.0(8)	C(16)-C(17)-C(18)-C(19)	-74.9(8)
C(4)-C(5)-C(19)-O(19)	-108.4(7)	C(6)-C(5)-C(19)-O(19)	129.3(7)
C(4)-C(5)-C(19)-C(18)	69.0(7)	C(6)-C(5)-C(19)-C(18)	-53.2(7)
N(1)-C(18)-C(19)-O(19)	-174.5(6)	C(17)-C(18)-C(19)-O(19)	-52.9(9)
N(1)-C(18)-C(19)-C(5)	8.0(7)	C(17)-C(18)-C(19)-C(5)	129.7(6)

Table B19. Crystal data and structure refinement for **19**.

Empirical formula	C ₁₉ H ₂₀ N ₂ O	
Formula weight	292.37	
Temperature	150(2) K	
Wavelength	1.54178 Å	
Crystal system	Monoclinic	
Space group	P2 ₁	
Unit cell dimensions	a = 10.3077(3) Å	α = 90°
	b = 7.8255(2) Å	β = 117.8590(10)°
	c = 10.6948(3) Å	γ = 90°
Volume	762.69(4) Å ³	
Z	2	
Density (calculated)	1.274 Mg/m ³	
Absorption coefficient	0.622 mm ⁻¹	
F(000)	312	
Crystal size	0.997 x 0.516 x 0.334 mm ³	
Theta range for data collection	4.68 to 68.20°.	
Index ranges	-12 ≤ h ≤ 12, -8 ≤ k ≤ 9, -11 ≤ l ≤ 12	
Reflections collected	4369	
Independent reflections	2288 [R(int) = 0.0369]	
Completeness to theta = 68.20°	97.4 %	
Absorption correction	Semi-empirical from equivalents	
Max. and min. transmission	0.7530 and 0.6194	
Refinement method	Full-matrix least-squares on F ²	
Data / restraints / parameters	2288 / 1 / 202	
Goodness-of-fit on F ²	1.111	
Final R indices [I > 2σ(I)]	R1 = 0.0430, wR2 = 0.1160	
R indices (all data)	R1 = 0.0430, wR2 = 0.1160	
Absolute structure parameter	-0.1(3)	
Extinction coefficient	0.078(4)	
Largest diff. peak and hole	0.278 and -0.267 e.Å ⁻³	

Table B20. Atomic coordinates ($\times 10^4$) and equivalent isotropic displacement parameters ($\text{\AA}^2 \times 10^3$) for **19**. $U(\text{eq})$ is defined as one third of the trace of the orthogonalized U^{ij} tensor.

	x	y	z	$U(\text{eq})$
N(1)	10925(2)	7985(2)	3995(2)	19(1)
C(2)	12109(2)	9290(3)	4420(2)	21(1)
C(2A)	13621(2)	8477(3)	5104(2)	25(1)
C(3)	11810(2)	10447(3)	3167(2)	23(1)
C(3A)	12774(2)	11404(4)	3009(3)	37(1)
C(4)	10210(2)	10320(3)	2049(2)	22(1)
C(5)	10049(2)	8533(3)	1454(2)	20(1)
O(5)	9561(2)	8198(2)	213(2)	30(1)
C(6)	10632(2)	7171(3)	2629(2)	20(1)
C(7)	9594(2)	5644(3)	2283(2)	23(1)
C(8)	8294(2)	6183(3)	2470(2)	22(1)
C(9)	6840(2)	5490(3)	1945(2)	24(1)
C(10)	6098(3)	4055(3)	1129(2)	32(1)
C(11)	4639(3)	3826(3)	773(2)	38(1)
C(12)	3882(2)	4984(4)	1196(2)	36(1)
C(13)	4569(2)	6411(3)	1994(2)	31(1)
C(14)	6055(2)	6621(3)	2361(2)	24(1)
N(15)	6984(2)	7941(2)	3130(2)	23(1)
C(15)	6580(2)	9415(3)	3681(3)	34(1)
C(16)	8330(2)	7643(2)	3170(2)	19(1)
C(17)	9570(2)	8889(3)	3792(2)	19(1)
C(18)	9252(2)	10475(3)	2800(2)	22(1)

Table B20. Bond lengths [\AA] and angles [$^\circ$] for **19**.

N(1)-C(17)	1.488(3)	N(1)-C(6)	1.489(2)
N(1)-C(2)	1.491(3)	C(2)-C(2A)	1.517(3)
C(2)-C(3)	1.524(3)	C(2)-H(2A)	1.0000
C(2A)-H(2AA)	0.9800	C(2A)-H(2AB)	0.9800
C(2A)-H(2AC)	0.9800	C(3)-C(3A)	1.317(3)
C(3)-C(4)	1.522(2)	C(3A)-H(3AA)	0.9500
C(3A)-H(3AB)	0.9500	C(4)-C(5)	1.513(3)
C(4)-C(18)	1.541(3)	C(4)-H(4A)	1.0000
C(5)-O(5)	1.208(2)	C(5)-C(6)	1.539(3)
C(6)-C(7)	1.529(3)	C(6)-H(6A)	1.0000
C(7)-C(8)	1.504(3)	C(7)-H(7A)	0.9900
C(7)-H(7B)	0.9900	C(8)-C(16)	1.357(3)
C(8)-C(9)	1.439(3)	C(9)-C(14)	1.404(3)
C(9)-C(10)	1.409(3)	C(10)-C(11)	1.380(3)
C(10)-H(10A)	0.9500	C(11)-C(12)	1.401(4)
C(11)-H(11A)	0.9500	C(12)-C(13)	1.383(4)
C(12)-H(12A)	0.9500	C(13)-C(14)	1.402(3)
C(13)-H(13A)	0.9500	C(14)-N(15)	1.387(3)
N(15)-C(16)	1.388(3)	N(15)-C(15)	1.443(3)
C(15)-H(15A)	0.9800	C(15)-H(15B)	0.9800
C(15)-H(15C)	0.9800	C(16)-C(17)	1.494(3)
C(17)-C(18)	1.565(3)	C(17)-H(17A)	1.0000
C(18)-H(18A)	0.9900	C(18)-H(18B)	0.9900
C(17)-N(1)-C(6)	108.31(14)	C(17)-N(1)-C(2)	107.30(16)
C(6)-N(1)-C(2)	110.73(15)	N(1)-C(2)-C(2A)	111.69(17)
N(1)-C(2)-C(3)	109.77(15)	C(2A)-C(2)-C(3)	114.42(17)
N(1)-C(2)-H(2A)	106.8	C(2A)-C(2)-H(2A)	106.8
C(3)-C(2)-H(2A)	106.8	C(2)-C(2A)-H(2AA)	109.5
C(2)-C(2A)-H(2AB)	109.5	H(2AA)-C(2A)-H(2AB)	109.5
C(2)-C(2A)-H(2AC)	109.5	H(2AA)-C(2A)-H(2AC)	109.5
H(2AB)-C(2A)-H(2AC)	109.5	C(3A)-C(3)-C(4)	122.8(2)
C(3A)-C(3)-C(2)	126.56(18)	C(4)-C(3)-C(2)	110.61(16)
C(3)-C(3A)-H(3AA)	120.0	C(3)-C(3A)-H(3AB)	120.0
H(3AA)-C(3A)-H(3AB)	120.0	C(5)-C(4)-C(3)	104.85(17)
C(5)-C(4)-C(18)	108.69(16)	C(3)-C(4)-C(18)	107.95(16)
C(5)-C(4)-H(4A)	111.7	C(3)-C(4)-H(4A)	111.7
C(18)-C(4)-H(4A)	111.7	O(5)-C(5)-C(4)	124.74(19)
O(5)-C(5)-C(6)	123.39(19)	C(4)-C(5)-C(6)	111.84(16)
N(1)-C(6)-C(7)	111.71(16)	N(1)-C(6)-C(5)	109.14(16)
C(7)-C(6)-C(5)	112.38(15)	N(1)-C(6)-H(6A)	107.8
C(7)-C(6)-H(6A)	107.8	C(5)-C(6)-H(6A)	107.8
C(8)-C(7)-C(6)	108.32(17)	C(8)-C(7)-H(7A)	110.0
C(6)-C(7)-H(7A)	110.0	C(8)-C(7)-H(7B)	110.0
C(6)-C(7)-H(7B)	110.0	H(7A)-C(7)-H(7B)	108.4

C(16)-C(8)-C(9)	106.68(18)	C(16)-C(8)-C(7)	120.87(18)
C(9)-C(8)-C(7)	132.30(19)	C(14)-C(9)-C(10)	118.2(2)
C(14)-C(9)-C(8)	106.78(18)	C(10)-C(9)-C(8)	135.0(2)
C(11)-C(10)-C(9)	118.7(2)	C(11)-C(10)-H(10A)	120.7
C(9)-C(10)-H(10A)	120.7	C(10)-C(11)-C(12)	121.8(2)
C(10)-C(11)-H(11A)	119.1	C(12)-C(11)-H(11A)	119.1
C(13)-C(12)-C(11)	121.3(2)	C(13)-C(12)-H(12A)	119.4
C(11)-C(12)-H(12A)	119.4	C(12)-C(13)-C(14)	116.4(2)
C(12)-C(13)-H(13A)	121.8	C(14)-C(13)-H(13A)	121.8
N(15)-C(14)-C(13)	127.9(2)	N(15)-C(14)-C(9)	108.48(17)
C(13)-C(14)-C(9)	123.6(2)	C(14)-N(15)-C(16)	107.23(17)
C(14)-N(15)-C(15)	125.93(17)	C(16)-N(15)-C(15)	126.67(17)
N(15)-C(15)-H(15A)	109.5	N(15)-C(15)-H(15B)	109.5
H(15A)-C(15)-H(15B)	109.5	N(15)-C(15)-H(15C)	109.5
H(15A)-C(15)-H(15C)	109.5	H(15B)-C(15)-H(15C)	109.5
C(8)-C(16)-N(15)	110.82(18)	C(8)-C(16)-C(17)	126.31(18)
N(15)-C(16)-C(17)	122.62(17)	N(1)-C(17)-C(16)	107.67(16)
N(1)-C(17)-C(18)	111.15(16)	C(16)-C(17)-C(18)	110.56(16)
N(1)-C(17)-H(17A)	109.1	C(16)-C(17)-H(17A)	109.1
C(18)-C(17)-H(17A)	109.1	C(4)-C(18)-C(17)	107.99(16)
C(4)-C(18)-H(18A)	110.1	C(17)-C(18)-H(18A)	110.1
C(4)-C(18)-H(18B)	110.1	C(17)-C(18)-H(18B)	110.1
H(18A)-C(18)-H(18B)	108.4		

Table B22. Anisotropic displacement parameters ($\text{\AA}^2 \times 10^3$) for **19**. The anisotropic displacement factor exponent takes the form: $-2\pi^2 [h^2 a^{*2} U^{11} + \dots + 2 h k a^* b^* U^{12}]$

	U11	U22	U33	U23	U13	U12
N(1)	19(1)	21(1)	18(1)	-1(1)	9(1)	-1(1)
C(2)	20(1)	21(1)	20(1)	2(1)	7(1)	-1(1)
C(2A)	20(1)	29(1)	23(1)	1(1)	7(1)	1(1)
C(3)	21(1)	23(1)	23(1)	3(1)	10(1)	1(1)
C(3A)	25(1)	42(1)	37(1)	13(1)	10(1)	-7(1)
C(4)	22(1)	21(1)	21(1)	5(1)	9(1)	0(1)
C(5)	16(1)	27(1)	19(1)	1(1)	9(1)	0(1)
O(5)	35(1)	37(1)	18(1)	-1(1)	12(1)	3(1)
C(6)	23(1)	20(1)	21(1)	0(1)	12(1)	3(1)
C(7)	30(1)	20(1)	24(1)	0(1)	15(1)	1(1)
C(8)	27(1)	20(1)	18(1)	0(1)	11(1)	-2(1)
C(9)	31(1)	24(1)	17(1)	2(1)	11(1)	-6(1)
C(10)	44(1)	25(1)	24(1)	-4(1)	13(1)	-10(1)

C(11)	42(1)	38(1)	23(1)	-4(1)	6(1)	-22(1)
C(12)	30(1)	46(2)	25(1)	3(1)	7(1)	-15(1)
C(13)	26(1)	41(1)	25(1)	4(1)	10(1)	-7(1)
C(14)	27(1)	26(1)	19(1)	2(1)	11(1)	-6(1)
N(15)	23(1)	23(1)	26(1)	-4(1)	14(1)	-3(1)
C(15)	29(1)	32(1)	48(2)	-10(1)	23(1)	-1(1)
C(16)	23(1)	19(1)	18(1)	1(1)	12(1)	-3(1)
C(17)	23(1)	18(1)	19(1)	-3(1)	11(1)	-3(1)
C(18)	22(1)	20(1)	24(1)	0(1)	10(1)	0(1)

Table B23. Hydrogen coordinates ($\times 10^4$) and isotropic displacement parameters ($\text{\AA}^2 \times 10^3$) for **19**.

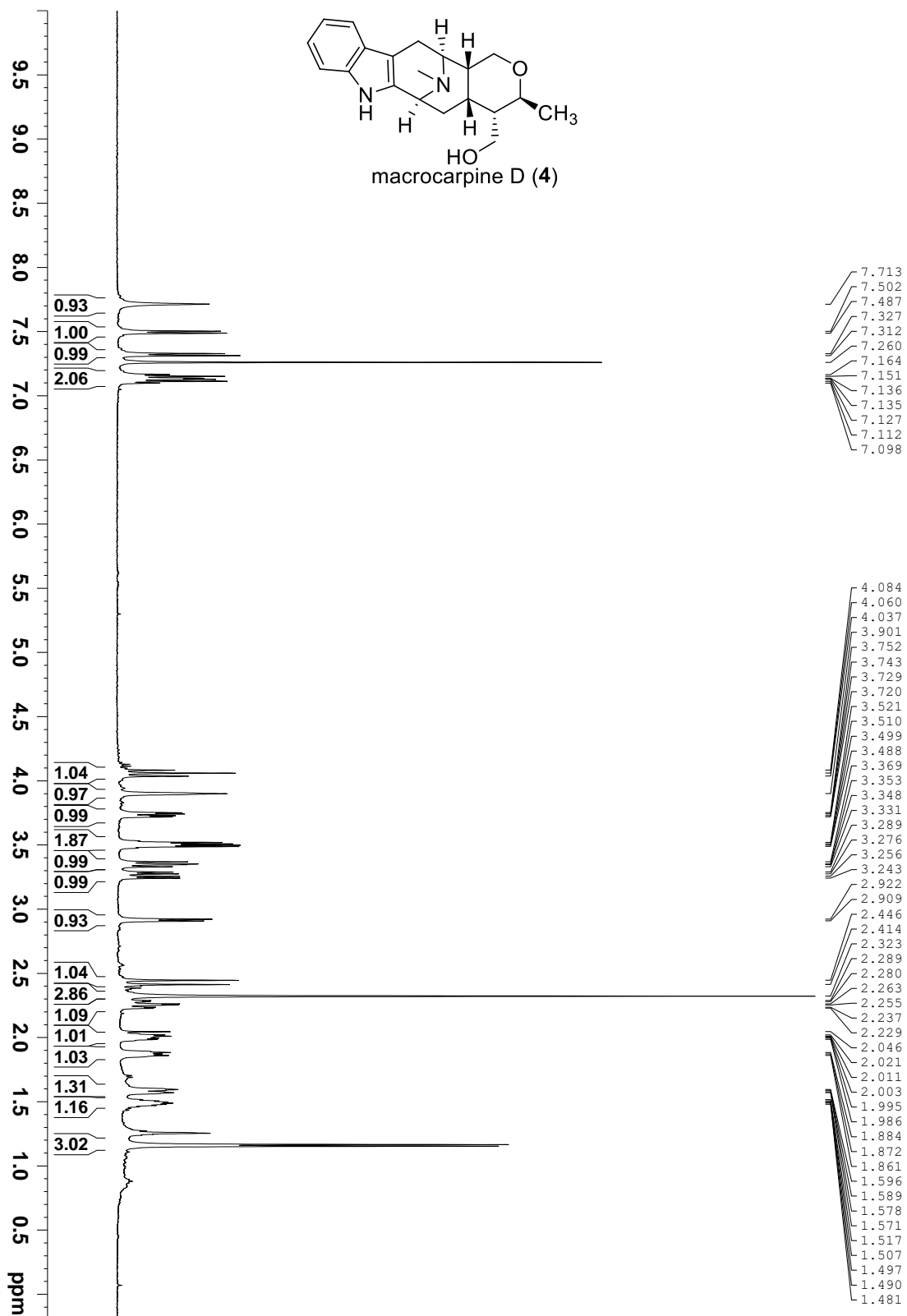
	x	y	z	U(eq)
H(2A)	12048	10024	5156	25
H(2AA)	13783	7898	5978	38
H(2AB)	14368	9363	5324	38
H(2AC)	13687	7644	4452	38
H(3AA)	12482	12053	2170	44
H(3AB)	13763	11445	3735	44
H(4A)	9952	11209	1298	26
H(6A)	11587	6741	2724	24
H(7A)	9266	5269	1296	28
H(7B)	10106	4678	2922	28
H(10A)	6592	3260	829	38
H(11A)	4133	2858	227	46
H(12A)	2877	4784	930	43
H(13A)	4062	7206	2279	38
H(15A)	6171	9040	4299	52
H(15B)	5844	10085	2896	52
H(15C)	7450	10121	4224	52
H(17A)	9695	9279	4732	23
H(18A)	8201	10504	2094	27
H(18B)	9491	11542	3361	27

Table B24. Torsion angles [°] for **19**.

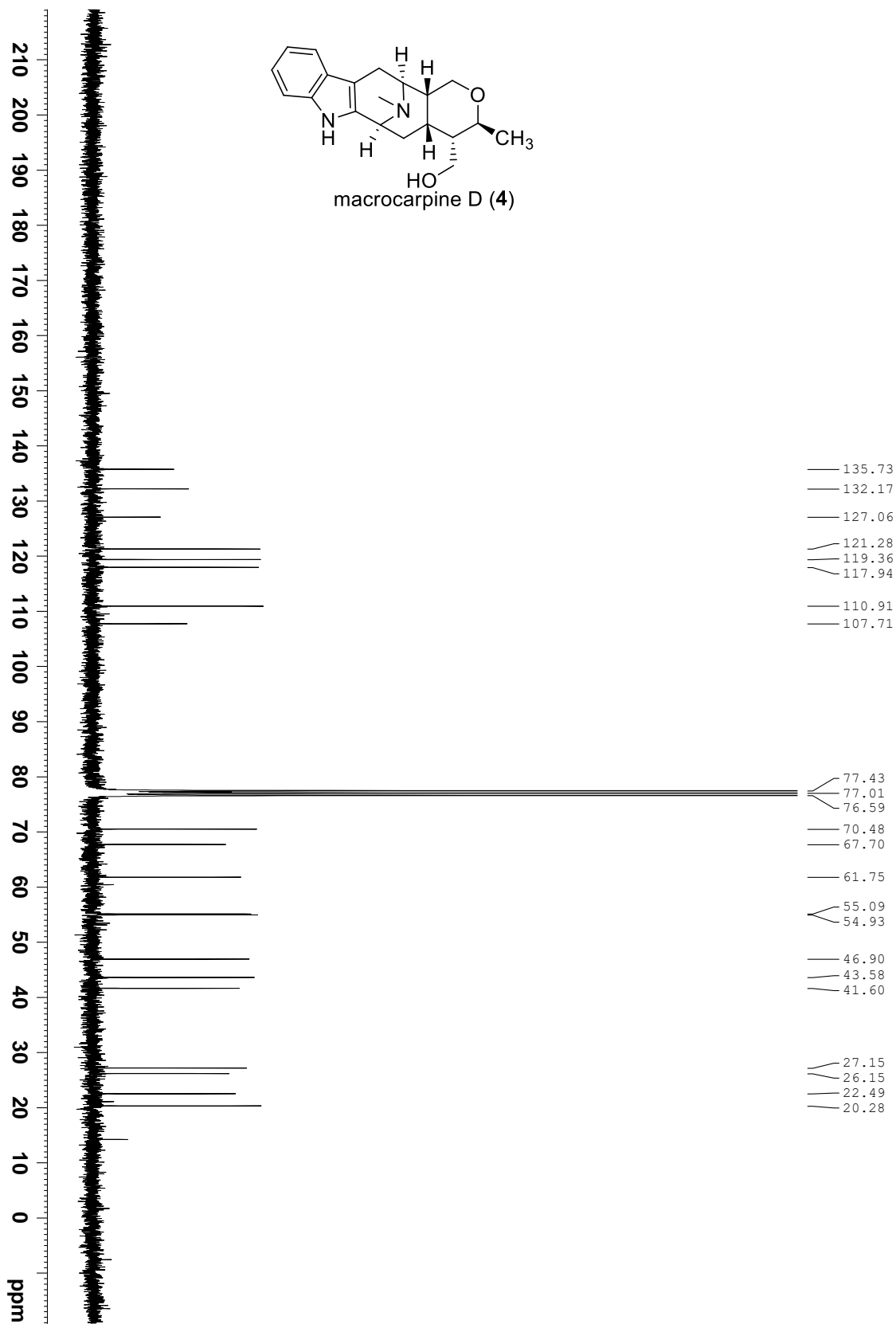
C(17)-N(1)-C(2)-C(2A)	161.60(17)	C(6)-N(1)-C(2)-C(2A)	-80.4(2)
C(17)-N(1)-C(2)-C(3)	-70.39(19)	C(6)-N(1)-C(2)-C(3)	47.6(2)
N(1)-C(2)-C(3)-C(3A)	-159.7(2)	C(2A)-C(2)-C(3)-C(3A)	-33.2(3)
N(1)-C(2)-C(3)-C(4)	18.4(2)	C(2A)-C(2)-C(3)-C(4)	144.92(18)
C(3A)-C(3)-C(4)-C(5)	109.7(3)	C(2)-C(3)-C(4)-C(5)	-68.5(2)
C(3A)-C(3)-C(4)-C(18)	-134.5(2)	C(2)-C(3)-C(4)-C(18)	47.3(2)
C(3)-C(4)-C(5)-O(5)	-126.6(2)	C(18)-C(4)-C(5)-O(5)	118.2(2)
C(3)-C(4)-C(5)-C(6)	51.5(2)	C(18)-C(4)-C(5)-C(6)	-63.71(19)
C(17)-N(1)-C(6)-C(7)	-71.3(2)	C(2)-N(1)-C(6)-C(7)	171.26(15)
C(17)-N(1)-C(6)-C(5)	53.6(2)	C(2)-N(1)-C(6)-C(5)	-63.84(19)
O(5)-C(5)-C(6)-N(1)	-171.14(17)	C(4)-C(5)-C(6)-N(1)	10.7(2)
O(5)-C(5)-C(6)-C(7)	-46.6(3)	C(4)-C(5)-C(6)-C(7)	135.23(18)
N(1)-C(6)-C(7)-C(8)	48.7(2)	C(5)-C(6)-C(7)-C(8)	-74.3(2)
C(6)-C(7)-C(8)-C(16)	-14.7(3)	C(6)-C(7)-C(8)-C(9)	160.2(2)
C(16)-C(8)-C(9)-C(14)	0.7(2)	C(7)-C(8)-C(9)-C(14)	-174.7(2)
C(16)-C(8)-C(9)-C(10)	178.4(2)	C(7)-C(8)-C(9)-C(10)	3.0(4)
C(14)-C(9)-C(10)-C(11)	0.1(3)	C(8)-C(9)-C(10)-C(11)	-177.4(2)
C(9)-C(10)-C(11)-C(12)	0.3(3)	C(10)-C(11)-C(12)-C(13)	-0.1(4)
C(11)-C(12)-C(13)-C(14)	-0.5(3)	C(12)-C(13)-C(14)-N(15)	179.0(2)
C(12)-C(13)-C(14)-C(9)	0.9(3)	C(10)-C(9)-C(14)-N(15)	-179.15(18)
C(8)-C(9)-C(14)-N(15)	-1.0(2)	C(10)-C(9)-C(14)-C(13)	-0.8(3)
C(8)-C(9)-C(14)-C(13)	177.4(2)	C(13)-C(14)-N(15)-C(16)	-177.4(2)
C(9)-C(14)-N(15)-C(16)	0.9(2)	C(13)-C(14)-N(15)-C(15)	-1.9(4)
C(9)-C(14)-N(15)-C(15)	176.4(2)	C(9)-C(8)-C(16)-N(15)	-0.1(2)
C(7)-C(8)-C(16)-N(15)	175.94(18)	C(9)-C(8)-C(16)-C(17)	-174.37(19)
C(7)-C(8)-C(16)-C(17)	1.7(3)	C(14)-N(15)-C(16)-C(8)	-0.5(2)
C(15)-N(15)-C(16)-C(8)	-175.9(2)	C(14)-N(15)-C(16)-C(17)	174.01(17)
C(15)-N(15)-C(16)-C(17)	-1.4(3)	C(6)-N(1)-C(17)-C(16)	52.5(2)
C(2)-N(1)-C(17)-C(16)	172.12(15)	C(6)-N(1)-C(17)-C(18)	-68.7(2)
C(2)-N(1)-C(17)-C(18)	50.90(19)	C(8)-C(16)-C(17)-N(1)	-20.7(3)
N(15)-C(16)-C(17)-N(1)	165.63(17)	C(8)-C(16)-C(17)-C(18)	100.8(2)
N(15)-C(16)-C(17)-C(18)	-72.8(2)	C(5)-C(4)-C(18)-C(17)	48.27(19)
C(3)-C(4)-C(18)-C(17)	-64.9(2)	N(1)-C(17)-C(18)-C(4)	14.5(2)
C(16)-C(17)-C(18)-C(4)	-105.05(18)		

V Appendix C (Chapter 4)

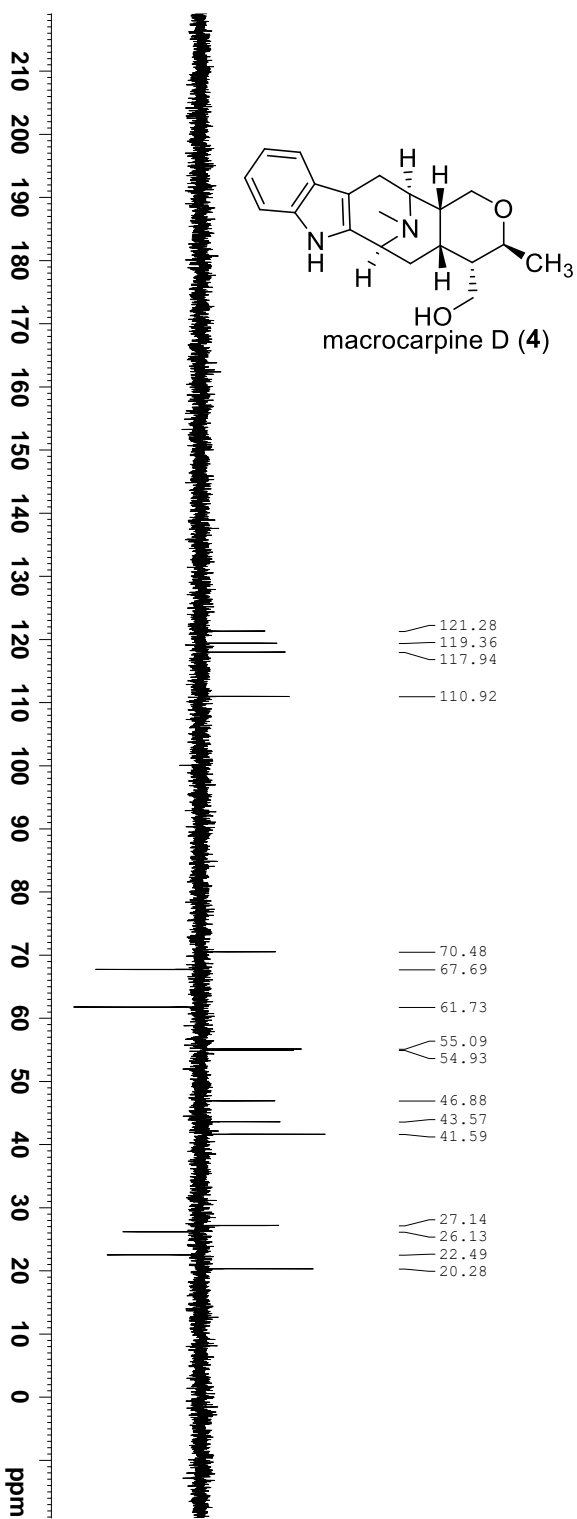
NMR and Mass Spectra of the Synthetic Macrocarpines D (4) and E (5)



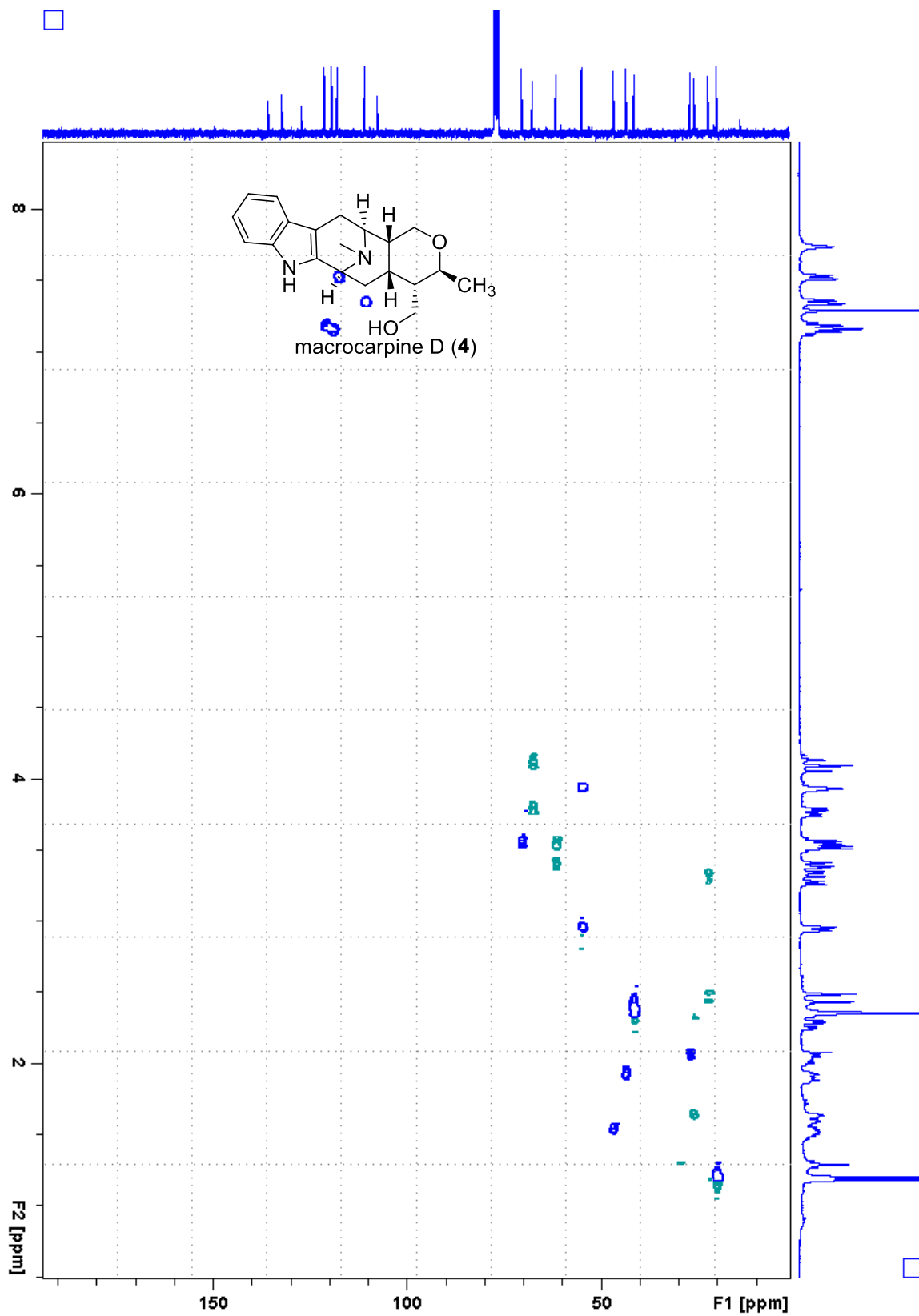
¹H NMR spectrum of macrocarpine D (4) (500 MHz, CDCl₃)



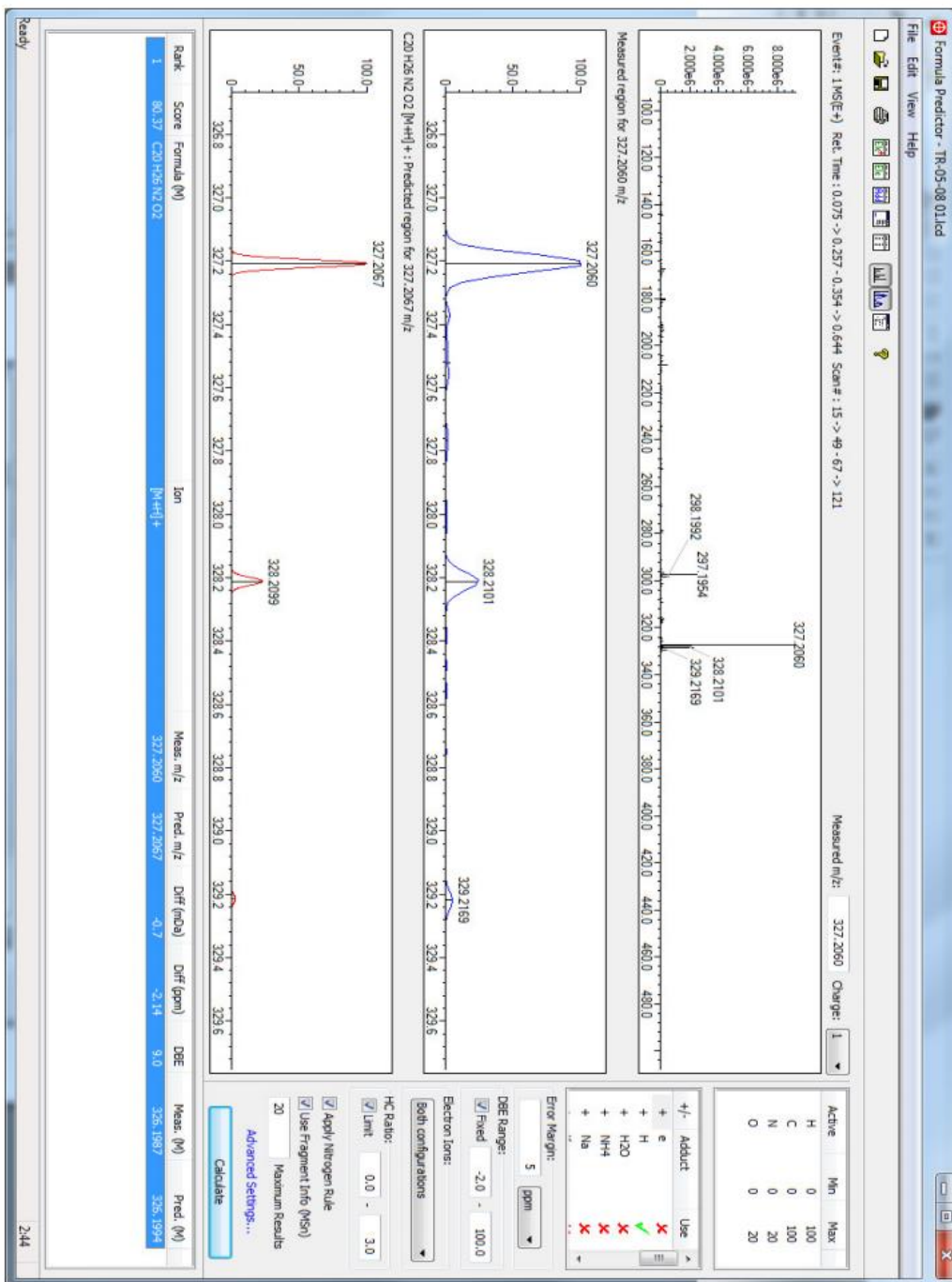
¹³C NMR spectrum of macrocarpine D (4) (75 MHz, CDCl₃)



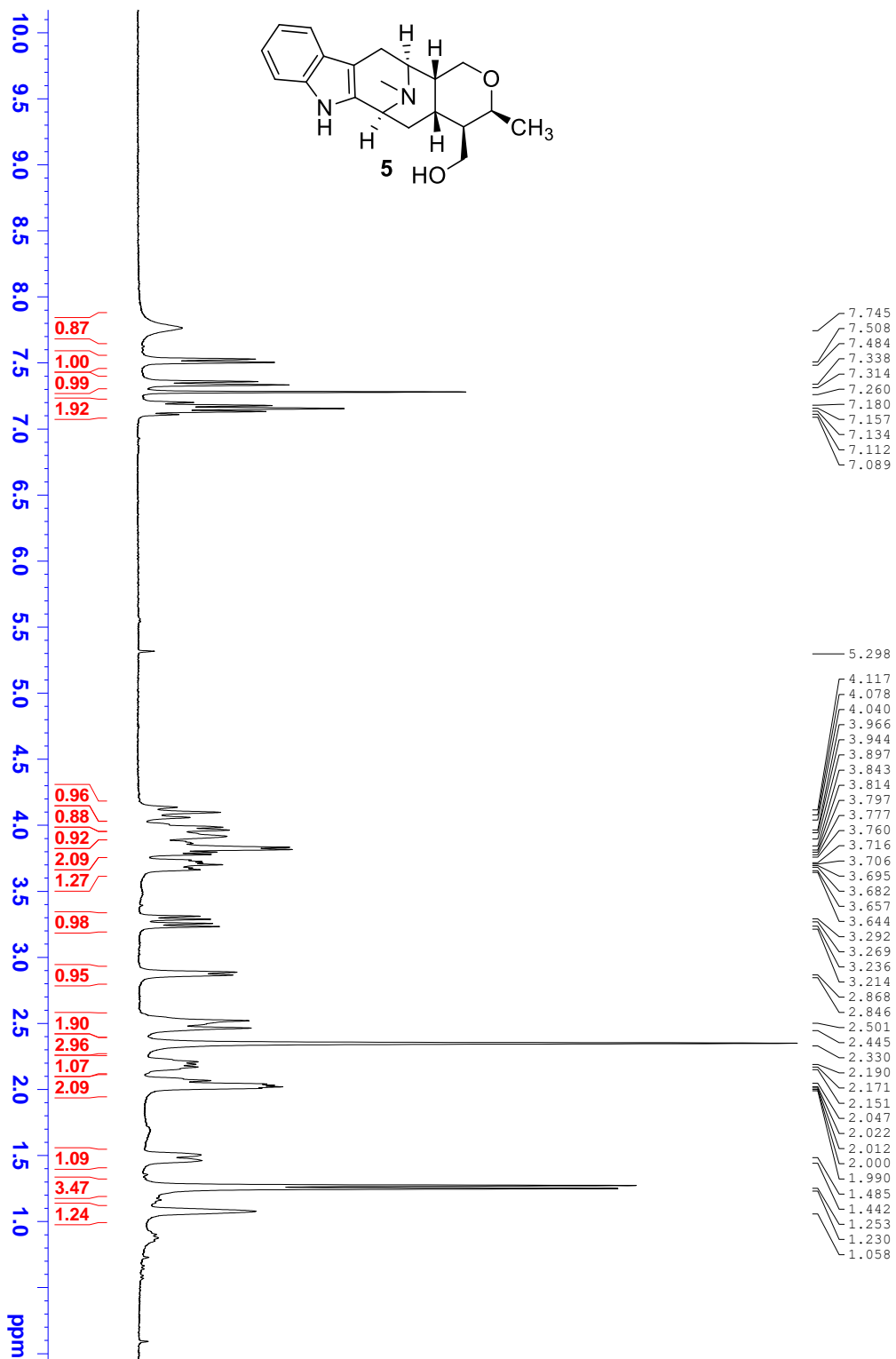
DEPT-135 spectrum of macrocarpine D (4) (75 MHz, CDCl₃)



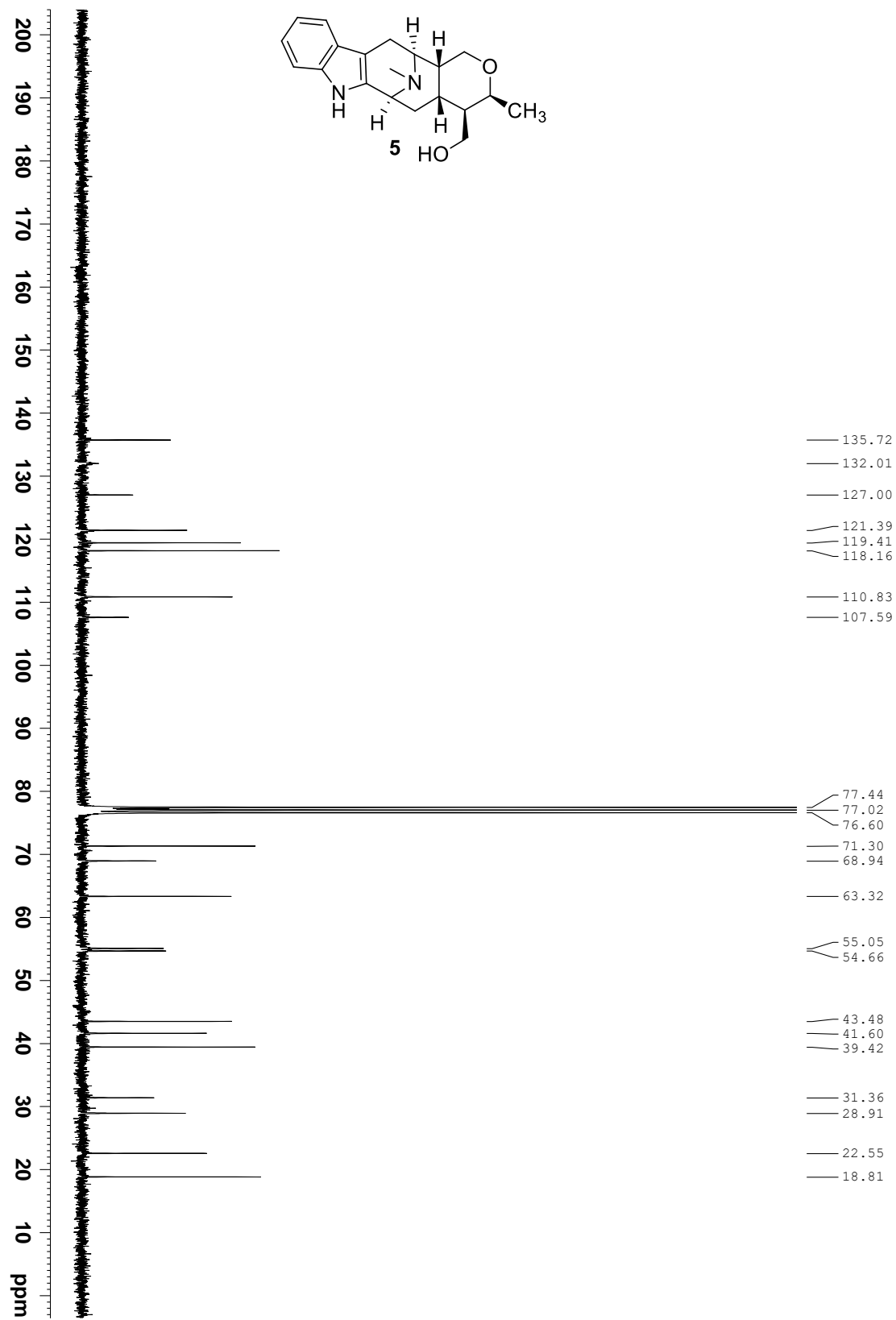
HSQC NMR spectrum of macrocarpine D (4) (300, 75 MHz, CDCl_3)



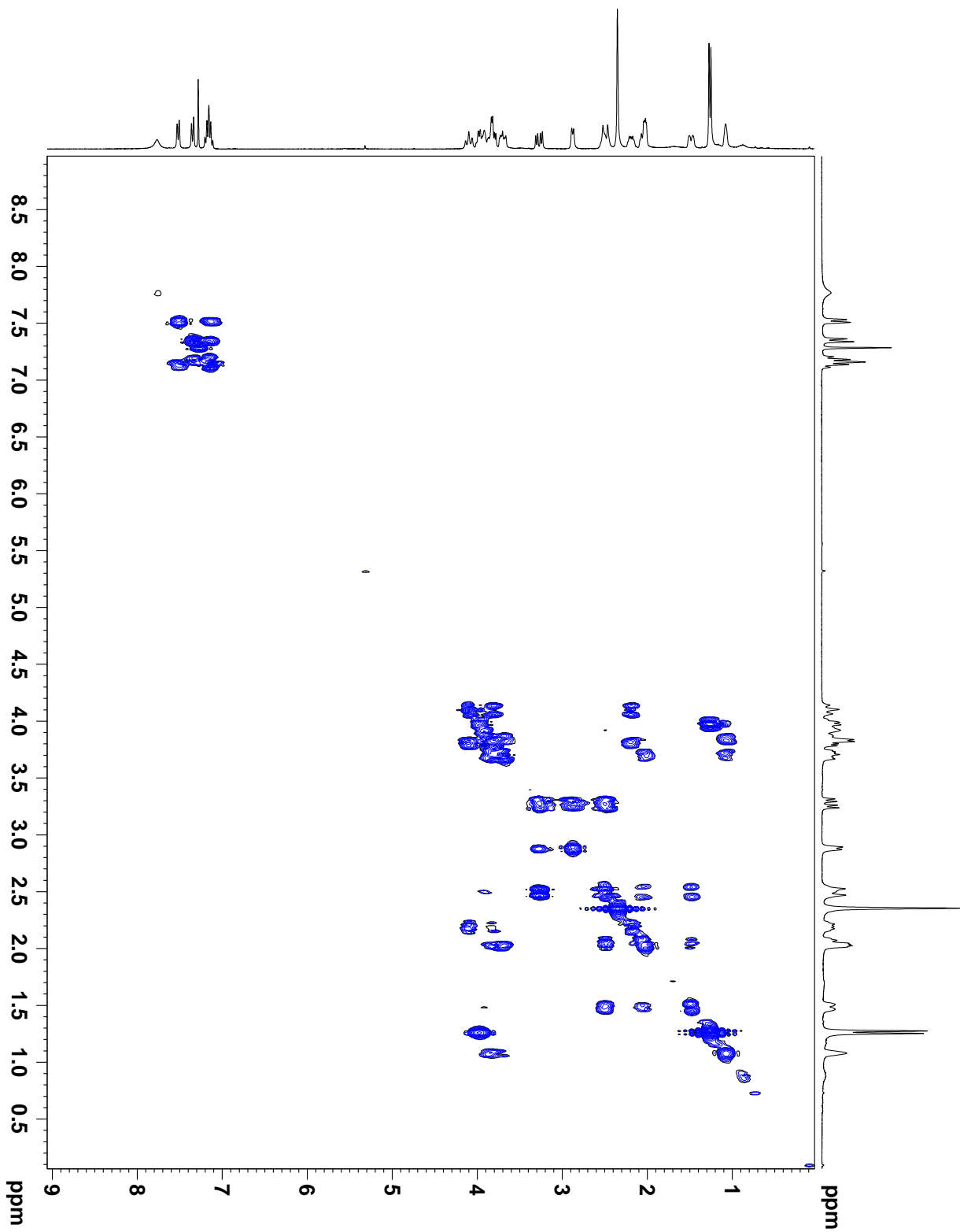
HRMS (ESI) spectrum of macrocarpine D (4)



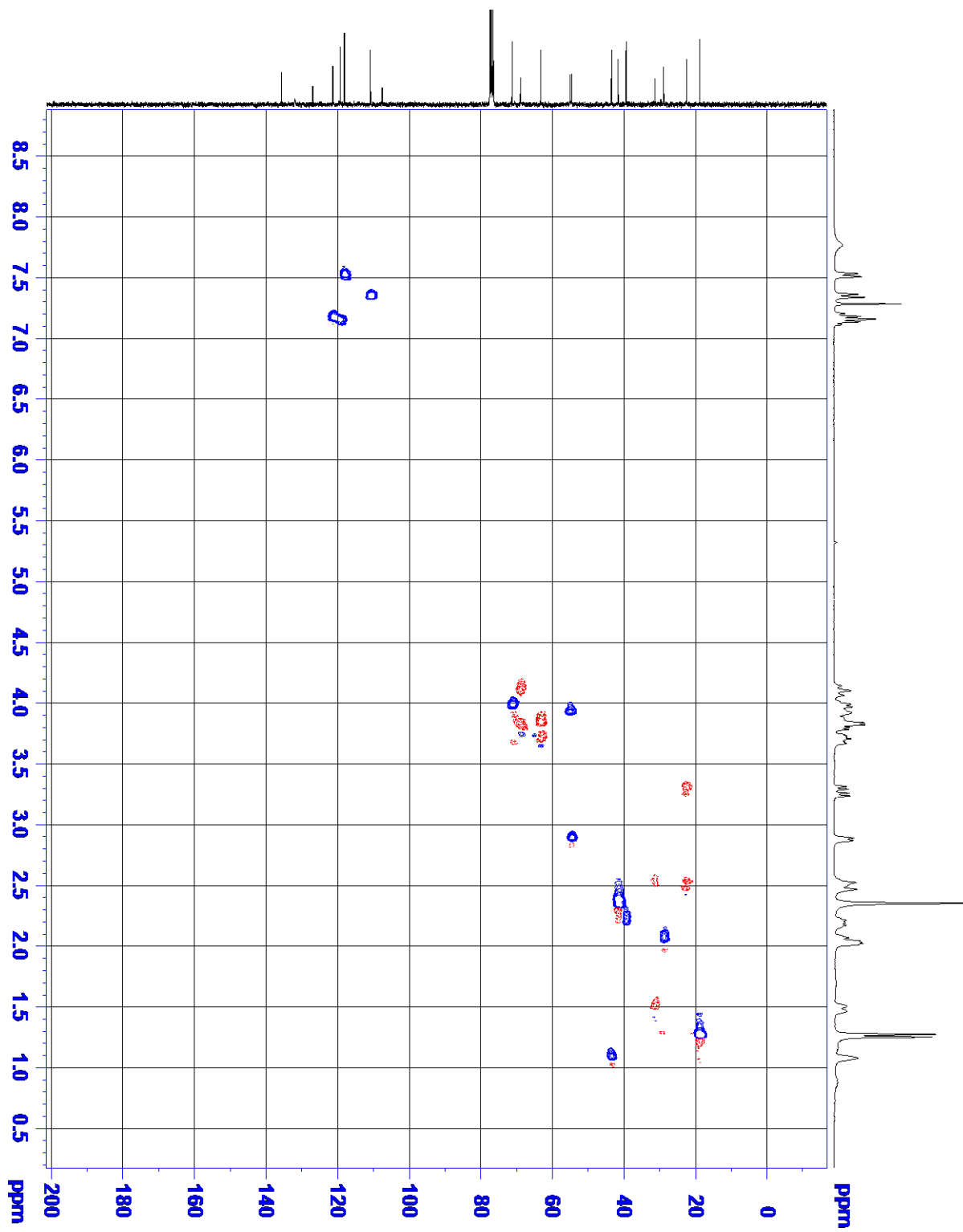
^1H NMR spectrum of macrocarpine E (**5**) (300 MHz, CDCl_3)



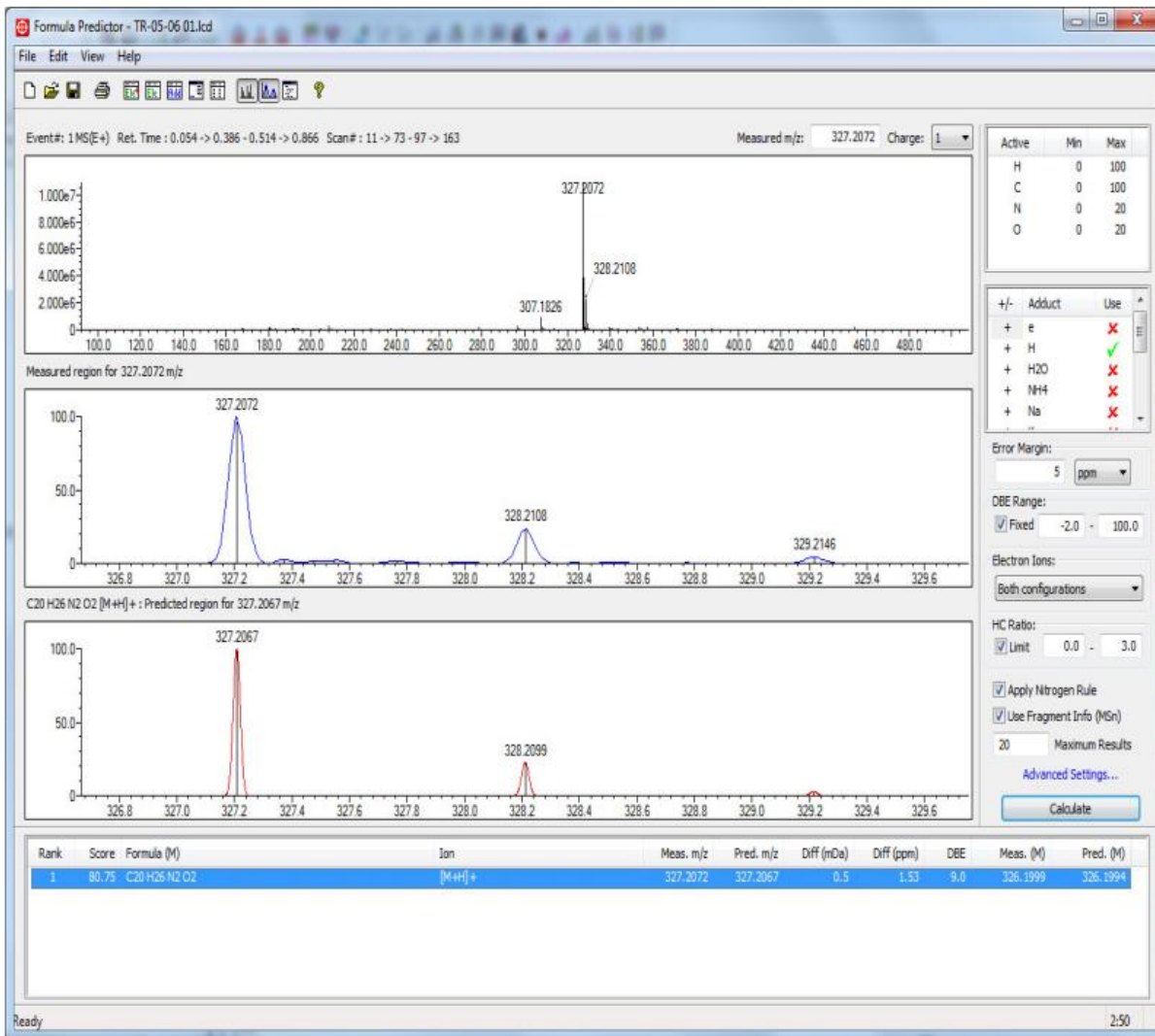
¹³C NMR spectrum of macrocarpine E (5) (75 MHz, CDCl₃)



COSY NMR of macrocarpine E (5) (300 MHz, CDCl₃)



HSQC NMR spectrum of macrocarpine E (5) (300, 75 MHz, CDCl₃)



HRMS (ESI) spectrum of macrocarpine E (5)

VI Appendix D (Chapter 5)

The X-ray crystallographic work was supported by NIDA through Interagency Agreement #Y1-DA1101 with the Naval Research Laboratory (NRL).

Single Crystal X-ray Diffraction Data for Compound **16b**

The single-crystal X-ray diffraction data on compounds **12b**, **16b**, and **25** were collected using Mo K α radiation and a Bruker APEX II area detector at 150 K. Corrections were applied for Lorentz, polarization, and absorption effects. The structures were solved by direct methods and refined by full-matrix least squares on F² values using the programs found in the SHELXL suite (Bruker, SHELXL v2014.7, 2014, Bruker AXS Inc., Madison, WI). The parameters refined included atomic coordinates and anisotropic thermal parameters for all non-hydrogen atoms. The H atoms were included using a riding model. The complete information on data collection and refinement is available in the corresponding sections.

The 0.245 x 0.150 x 0.030 mm³ crystal of **16b** was monoclinic in space group P2₁, with unit cell dimensions a = 9.4487(5) Å, b = 7.3559(4) Å, c = 10.8092(6) Å, $\alpha = 90^\circ$, $\beta = 106.408(2)^\circ$, and $\gamma = 90^\circ$. Data was 99.8% complete to 25.242° θ (~0.83 Å) with an average redundancy of 3.83. The final anisotropic full matrix least-squares refinement on F² with 191 variables converged at R₁ = 0.0379%, for the observed data and wR₂ = 0.0927% for all data.

Table D1. Crystal data and structure refinement for **16b**.

Empirical formula	C ₁₈ H ₁₈ N ₂ O	
Formula weight	278.34	
Temperature	150(2) K	
Wavelength	0.71073 Å	
Crystal system	Monoclinic	
Space group	P2 ₁	
Unit cell dimensions	a = 9.4487(5) Å	a = 90°.
	b = 7.3559(4) Å	b = 106.408(2)°.
	c = 10.8092(6) Å	g = 90°.
Volume	720.68(7) Å ³	
Z	2	
Density (-123°C)	1.283 Mg/m ³	
Absorption coefficient	0.080 mm ⁻¹	
F(000)	296	
Crystal size	0.245 x 0.150 x 0.030 mm ³	
θ range for data collection	3.377 to 30.007°.	
Index ranges	-12 ≤ h ≤ 12, -10 ≤ k ≤ 10, -13 ≤ l ≤ 14	
Reflections collected	8644	
Independent reflections	3900 [R(int) = 0.0237]	
Completeness to θ = 25.242°	99.8 %	
Absorption correction	Semi-empirical from equivalents	
Max. and min. transmission	0.7460 and 0.6948	
Refinement method	Full-matrix least-squares on F ²	
Data / restraints / parameters	3900 / 1 / 191	
Goodness-of-fit on F ²	1.020	
Final R indices [I > 2σ(I)]	R1 = 0.0379, wR2 = 0.0881	
R indices (all data)	R1 = 0.0450, wR2 = 0.0927	
Largest diff. peak and hole	0.228 and -0.205 e.Å ⁻³	

Table D2. Atomic coordinates ($\times 10^4$) and equivalent isotropic displacement parameters ($\text{\AA}^2 \times 10^3$)

for **16b**. $U(\text{eq})$ is defined as one third of the trace of the orthogonalized U^{ij} tensor.

	x	y	z	U(eq)
O(1)	6240(2)	4527(2)	795(2)	37(1)
C(1)	5311(2)	4659(3)	1365(2)	26(1)
C(2)	5016(2)	6411(3)	2021(2)	22(1)
N(3)	3958(2)	6018(2)	2782(2)	20(1)
C(4A)	1354(2)	5151(3)	2582(2)	28(1)
C(4)	2514(2)	5502(3)	1873(2)	24(1)
C(5)	2719(2)	3852(3)	1080(2)	27(1)
C(5A)	1646(3)	3042(4)	188(2)	42(1)
C(6)	4279(2)	3136(3)	1488(2)	25(1)
C(7)	4612(2)	2688(2)	2942(2)	23(1)
C(8)	4560(2)	4483(2)	3692(2)	18(1)
C(9)	6067(2)	5039(2)	4475(2)	18(1)
N(10)	6806(2)	4286(2)	5654(1)	19(1)
C(11)	8183(2)	5102(2)	6064(2)	20(1)
C(12)	9309(2)	4894(3)	7215(2)	25(1)
C(13)	10595(2)	5875(3)	7352(2)	30(1)
C(14)	10762(2)	7052(3)	6381(2)	30(1)
C(15)	9629(2)	7305(3)	5259(2)	26(1)
C(16)	8311(2)	6337(3)	5101(2)	22(1)
C(17)	6937(2)	6280(3)	4101(2)	20(1)
C(18)	6427(2)	7293(3)	2852(2)	23(1)

Table D3. Bond lengths [\AA] and angles [$^\circ$] for **16b**.

O(1)-C(1)	1.210(2)	C(1)-C(6)	1.515(3)
C(1)-C(2)	1.535(3)	C(2)-N(3)	1.491(2)
C(2)-C(18)	1.526(3)	C(2)-H(2)	1.0000
N(3)-C(4)	1.488(2)	N(3)-C(8)	1.500(2)
C(4A)-C(4)	1.526(3)	C(4A)-H(4A)	0.9800
C(4A)-H(4B)	0.9800	C(4A)-H(4C)	0.9800
C(4)-C(5)	1.530(3)	C(4)-H(4)	1.0000
C(5)-C(5A)	1.327(3)	C(5)-C(6)	1.509(3)
C(5A)-H(5A)	0.9500	C(5A)-H(5B)	0.9500
C(6)-C(7)	1.548(3)	C(6)-H(6)	1.0000
C(7)-C(8)	1.557(3)	C(7)-H(7A)	0.9900
C(7)-H(7B)	0.9900	C(8)-C(9)	1.493(2)
C(8)-H(8)	1.0000	C(9)-C(17)	1.364(2)
C(9)-N(10)	1.384(2)	N(10)-C(11)	1.387(2)
N(10)-H(10)	0.8800	C(11)-C(12)	1.398(2)
C(11)-C(16)	1.413(3)	C(12)-C(13)	1.384(3)
C(12)-H(12)	0.9500	C(13)-C(14)	1.404(3)
C(13)-H(13)	0.9500	C(14)-C(15)	1.385(3)
C(14)-H(14)	0.9500	C(15)-C(16)	1.402(3)
C(15)-H(15)	0.9500	C(16)-C(17)	1.436(3)
C(17)-C(18)	1.497(3)	C(18)-H(18A)	0.9900
C(18)-H(18B)	0.9900		
O(1)-C(1)-C(6)	124.24(18)	O(1)-C(1)-C(2)	123.71(18)
C(6)-C(1)-C(2)	112.03(16)	N(3)-C(2)-C(18)	111.58(14)
N(3)-C(2)-C(1)	109.24(15)	C(18)-C(2)-C(1)	112.73(16)
N(3)-C(2)-H(2)	107.7	C(18)-C(2)-H(2)	107.7
C(1)-C(2)-H(2)	107.7	C(4)-N(3)-C(2)	108.52(14)
C(4)-N(3)-C(8)	110.37(14)	C(2)-N(3)-C(8)	108.61(14)
C(4)-C(4A)-H(4A)	109.5	C(4)-C(4A)-H(4B)	109.5
H(4A)-C(4A)-H(4B)	109.5	C(4)-C(4A)-H(4C)	109.5
H(4A)-C(4A)-H(4C)	109.5	H(4B)-C(4A)-H(4C)	109.5
N(3)-C(4)-C(4A)	111.49(15)	N(3)-C(4)-C(5)	109.54(15)
C(4A)-C(4)-C(5)	111.72(16)	N(3)-C(4)-H(4)	108.0
C(4A)-C(4)-H(4)	108.0	C(5)-C(4)-H(4)	108.0
C(5A)-C(5)-C(6)	122.6(2)	C(5A)-C(5)-C(4)	124.9(2)
C(6)-C(5)-C(4)	112.42(16)	C(5)-C(5A)-H(5A)	120.0
C(5)-C(5A)-H(5B)	120.0	H(5A)-C(5A)-H(5B)	120.0
C(5)-C(6)-C(1)	108.41(16)	C(5)-C(6)-C(7)	105.81(15)
C(1)-C(6)-C(7)	107.13(15)	C(5)-C(6)-H(6)	111.7
C(1)-C(6)-H(6)	111.7	C(7)-C(6)-H(6)	111.7
C(6)-C(7)-C(8)	108.75(14)	C(6)-C(7)-H(7A)	109.9
C(8)-C(7)-H(7A)	109.9	C(6)-C(7)-H(7B)	109.9
C(8)-C(7)-H(7B)	109.9	H(7A)-C(7)-H(7B)	108.3
C(9)-C(8)-N(3)	106.81(14)	C(9)-C(8)-C(7)	111.20(14)

N(3)-C(8)-C(7)	111.00(13)	C(9)-C(8)-H(8)	109.3
N(3)-C(8)-H(8)	109.3	C(7)-C(8)-H(8)	109.3
C(17)-C(9)-N(10)	110.55(15)	C(17)-C(9)-C(8)	125.01(16)
N(10)-C(9)-C(8)	124.36(15)	C(9)-N(10)-C(11)	107.78(15)
C(9)-N(10)-H(10)	126.1	C(11)-N(10)-H(10)	126.1
N(10)-C(11)-C(12)	130.32(17)	N(10)-C(11)-C(16)	108.05(15)
C(12)-C(11)-C(16)	121.60(17)	C(13)-C(12)-C(11)	117.59(18)
C(13)-C(12)-H(12)	121.2	C(11)-C(12)-H(12)	121.2
C(12)-C(13)-C(14)	121.46(19)	C(12)-C(13)-H(13)	119.3
C(14)-C(13)-H(13)	119.3	C(15)-C(14)-C(13)	121.00(19)
C(15)-C(14)-H(14)	119.5	C(13)-C(14)-H(14)	119.5
C(14)-C(15)-C(16)	118.64(19)	C(14)-C(15)-H(15)	120.7
C(16)-C(15)-H(15)	120.7	C(15)-C(16)-C(11)	119.61(17)
C(15)-C(16)-C(17)	133.59(18)	C(11)-C(16)-C(17)	106.80(15)
C(9)-C(17)-C(16)	106.78(16)	C(9)-C(17)-C(18)	122.17(16)
C(16)-C(17)-C(18)	131.05(16)	C(17)-C(18)-C(2)	108.96(15)
C(17)-C(18)-H(18A)	109.9	C(2)-C(18)-H(18A)	109.9
C(17)-C(18)-H(18B)	109.9	C(2)-C(18)-H(18B)	109.9
H(18A)-C(18)-H(18B)	108.3		

Table D4. Anisotropic displacement parameters ($\text{\AA}^2 \times 10^3$) for **16b**. The anisotropic displacement factor exponent takes the form: $-2p^2[h^2a^*2U^{11} + \dots + 2hk a^* b^* U^{12}]$

	U11	U22	U33	U23	U13	U12
O(1)	45(1)	37(1)	40(1)	-3(1)	27(1)	-3(1)
C(1)	32(1)	25(1)	22(1)	2(1)	10(1)	-1(1)
C(2)	26(1)	20(1)	21(1)	4(1)	8(1)	0(1)
N(3)	20(1)	18(1)	20(1)	4(1)	5(1)	1(1)
C(4A)	21(1)	28(1)	34(1)	2(1)	5(1)	1(1)
C(4)	23(1)	24(1)	23(1)	6(1)	2(1)	2(1)
C(5)	32(1)	31(1)	18(1)	4(1)	4(1)	-2(1)
C(5A)	39(1)	52(2)	29(1)	-7(1)	-1(1)	-3(1)
C(6)	33(1)	23(1)	21(1)	-3(1)	9(1)	-3(1)
C(7)	26(1)	16(1)	25(1)	2(1)	5(1)	-1(1)
C(8)	19(1)	17(1)	19(1)	3(1)	6(1)	-1(1)
C(9)	20(1)	17(1)	18(1)	-1(1)	6(1)	1(1)
N(10)	18(1)	18(1)	20(1)	1(1)	5(1)	-1(1)
C(11)	18(1)	18(1)	25(1)	-4(1)	8(1)	1(1)
C(12)	24(1)	23(1)	27(1)	-1(1)	4(1)	1(1)
C(13)	21(1)	28(1)	35(1)	-6(1)	1(1)	2(1)
C(14)	19(1)	27(1)	45(1)	-7(1)	10(1)	-4(1)
C(15)	23(1)	22(1)	36(1)	-2(1)	13(1)	-3(1)
C(16)	21(1)	19(1)	26(1)	-3(1)	9(1)	-1(1)
C(17)	21(1)	19(1)	22(1)	-1(1)	9(1)	0(1)
C(18)	27(1)	21(1)	25(1)	4(1)	11(1)	-3(1)

Table D5. Hydrogen coordinates ($\times 10^4$) and isotropic displacement parameters ($\text{\AA}^2 \times 10^3$) for **16b**.

	x	y	z	U(eq)
H(2)	4532	7295	1328	27
H(4A)	1553	3982	3032	42
H(4B)	373	5121	1959	42
H(4C)	1391	6125	3209	42
H(4)	2166	6540	1266	29
H(5A)	1846	1968	-221	51
H(5B)	678	3537	-42	51
H(6)	4396	2044	974	30
H(7A)	5600	2124	3258	27
H(7B)	3872	1818	3080	27
H(8)	3918	4301	4276	22
H(10)	6464	3440	6068	22
H(12)	9197	4109	7878	30
H(13)	11381	5749	8121	36
H(14)	11666	7685	6495	36
H(15)	9742	8117	4610	31
H(18A)	7200	7257	2397	28
H(18B)	6236	8580	3020	28

Table D6. Torsion angles [°] for **16b**.

O(1)-C(1)-C(2)-N(3)	-172.06(18)	C(6)-C(1)-C(2)-N(3)	9.4(2)
O(1)-C(1)-C(2)-C(18)	-47.4(3)	C(6)-C(1)-C(2)-C(18)	134.04(16)
C(18)-C(2)-N(3)-C(4)	169.19(15)	C(1)-C(2)-N(3)-C(4)	-65.48(18)
C(18)-C(2)-N(3)-C(8)	-70.80(18)	C(1)-C(2)-N(3)-C(8)	54.52(18)
C(2)-N(3)-C(4)-C(4A)	-177.73(15)	C(8)-N(3)-C(4)-C(4A)	63.37(19)
C(2)-N(3)-C(4)-C(5)	58.09(18)	C(8)-N(3)-C(4)-C(5)	-60.81(18)
N(3)-C(4)-C(5)-C(5A)	179.5(2)	C(4A)-C(4)-C(5)-C(5A)	55.4(3)
N(3)-C(4)-C(5)-C(6)	3.7(2)	C(4A)-C(4)-C(5)-C(6)	-120.35(18)
C(5A)-C(5)-C(6)-C(1)	126.6(2)	C(4)-C(5)-C(6)-C(1)	-57.5(2)
C(5A)-C(5)-C(6)-C(7)	-118.8(2)	C(4)-C(5)-C(6)-C(7)	57.2(2)
O(1)-C(1)-C(6)-C(5)	-128.7(2)	C(2)-C(1)-C(6)-C(5)	49.9(2)
O(1)-C(1)-C(6)-C(7)	117.5(2)	C(2)-C(1)-C(6)-C(7)	-63.9(2)
C(5)-C(6)-C(7)-C(8)	-63.71(19)	C(1)-C(6)-C(7)-C(8)	51.8(2)
C(4)-N(3)-C(8)-C(9)	174.39(14)	C(2)-N(3)-C(8)-C(9)	55.54(17)
C(4)-N(3)-C(8)-C(7)	53.02(19)	C(2)-N(3)-C(8)-C(7)	-65.83(18)
C(6)-C(7)-C(8)-C(9)	-109.07(17)	C(6)-C(7)-C(8)-N(3)	9.7(2)
N(3)-C(8)-C(9)-C(17)	-24.1(2)	C(7)-C(8)-C(9)-C(17)	97.1(2)
N(3)-C(8)-C(9)-N(10)	159.68(15)	C(7)-C(8)-C(9)-N(10)	-79.1(2)
C(17)-C(9)-N(10)-C(11)	1.5(2)	C(8)-C(9)-N(10)-C(11)	178.14(16)
C(9)-N(10)-C(11)-C(12)	176.16(18)	C(9)-N(10)-C(11)-C(16)	-1.90(19)
N(10)-C(11)-C(12)-C(13)	178.84(18)	C(16)-C(11)-C(12)-	
C(13)	-3.3(3)	C(12)-C(13)-C(14)-	
C(11)-C(12)-C(13)-C(14)	0.6(3)	C(14)-C(15)-C(16)-	
C(15)	1.5(3)	N(10)-C(11)-C(16)-	
C(13)-C(14)-C(15)-C(16)	-1.0(3)	N(10)-C(11)-C(16)-	
C(11)	-1.7(3)	N(10)-C(9)-C(17)-C(16)	-0.4(2)
C(14)-C(15)-C(16)-C(17)	179.0(2)	N(10)-C(9)-C(17)-C(18)	179.24(16)
C(15)	-177.85(16)	C(15)-C(16)-C(17)-C(9)	178.6(2)
C(12)-C(11)-C(16)-C(15)	3.9(3)	C(15)-C(16)-C(17)-	
C(17)	1.62(19)	C(9)-C(17)-C(18)-C(2)	-12.3(2)
C(12)-C(11)-C(16)-C(17)	-176.64(16)	N(3)-C(2)-C(18)-C(17)	45.4(2)
C(8)-C(9)-C(17)-C(16)	-177.08(16)		
C(8)-C(9)-C(17)-C(18)	2.6(3)		
C(11)-C(16)-C(17)-C(9)	-0.7(2)		
C(18)	-1.0(3)		
C(11)-C(16)-C(17)-C(18)	179.63(19)		
C(16)-C(17)-C(18)-C(2)	167.34(18)		
C(1)-C(2)-C(18)-C(17)	-77.99(18)		

Table D7. Hydrogen bonds for **16b** [\AA and $^\circ$].

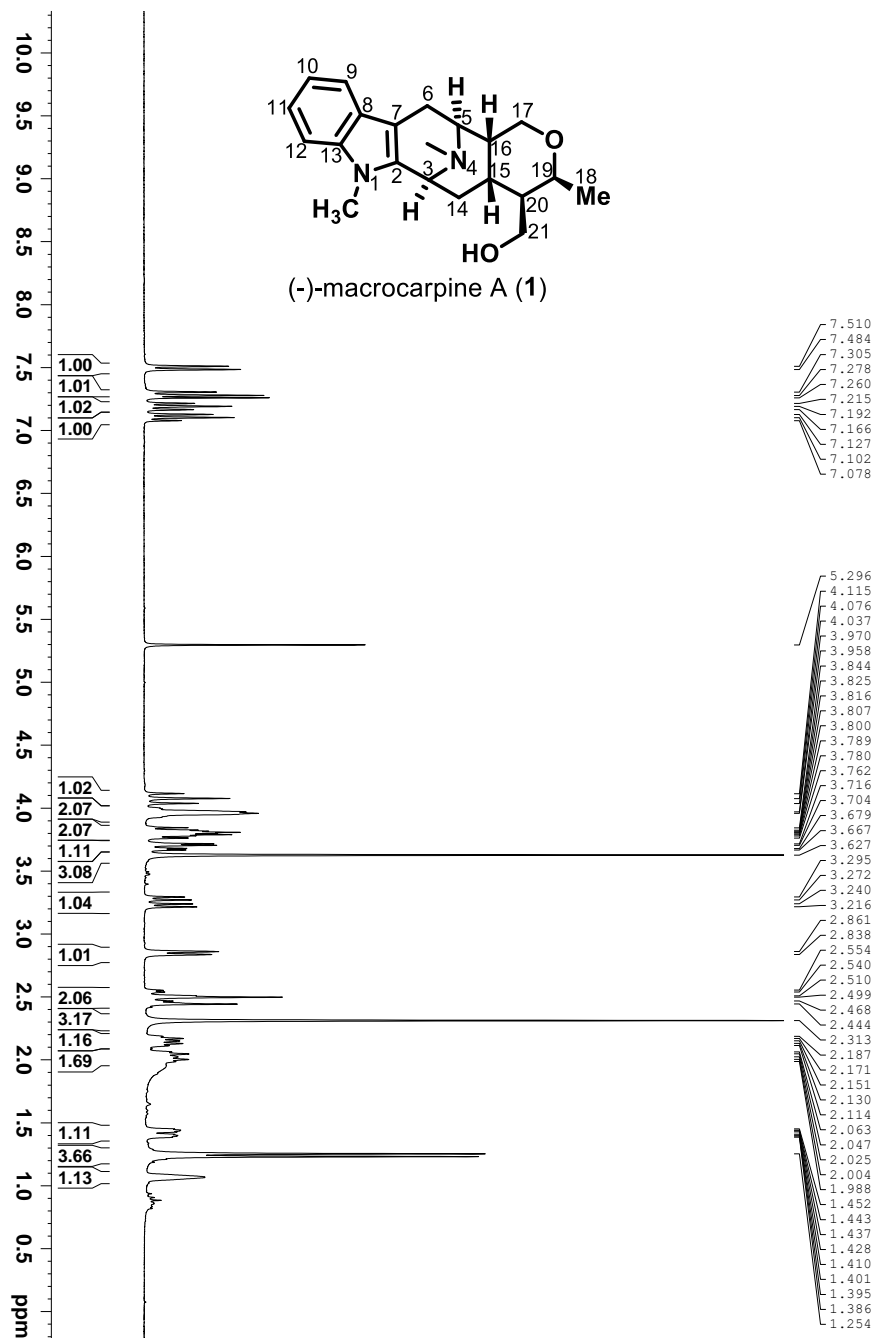
D-H...A	d(D-H)	d(H...A)	d(D...A)	$\angle(\text{DHA})$
N(10)-H(10)...N(3)#1	0.88	2.27	3.138(2)	168.5

Symmetry transformations used to generate equivalent atoms:

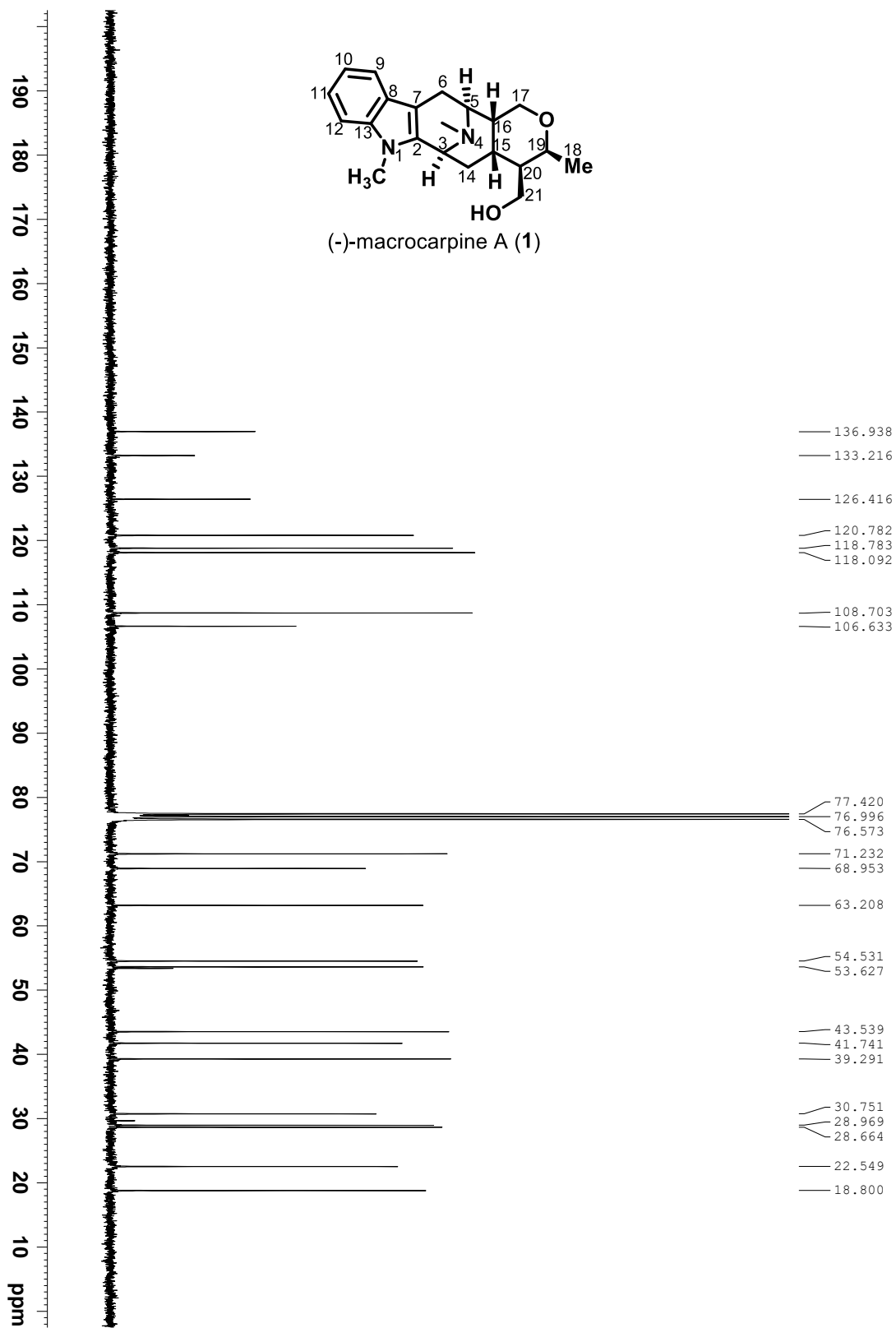
#1 $-x+1, y-1/2, -z+1$

VII Appendix E (Chapter 5)

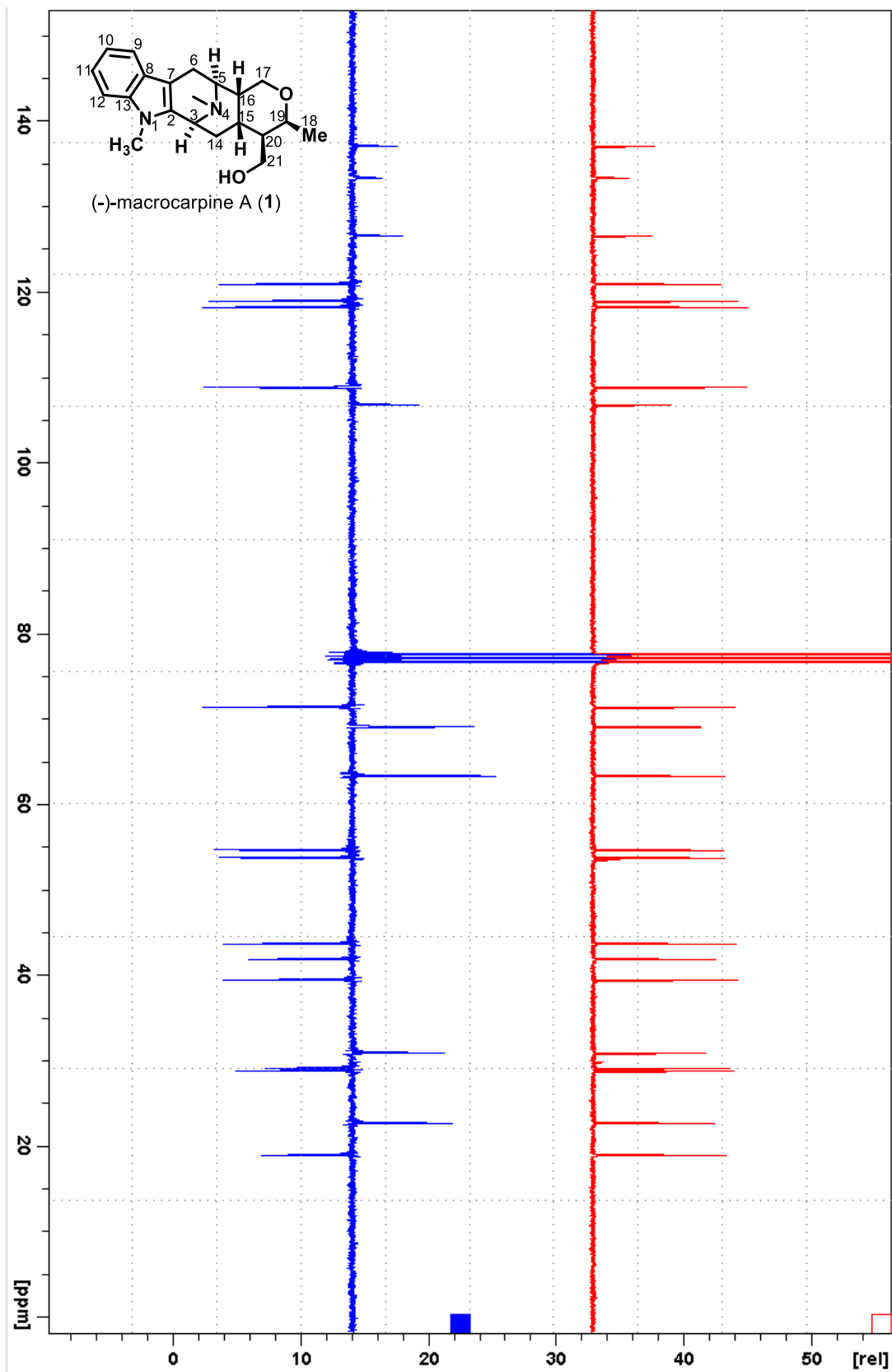
NMR spectra of the synthetic alkaloids 1-5, 8, and 9



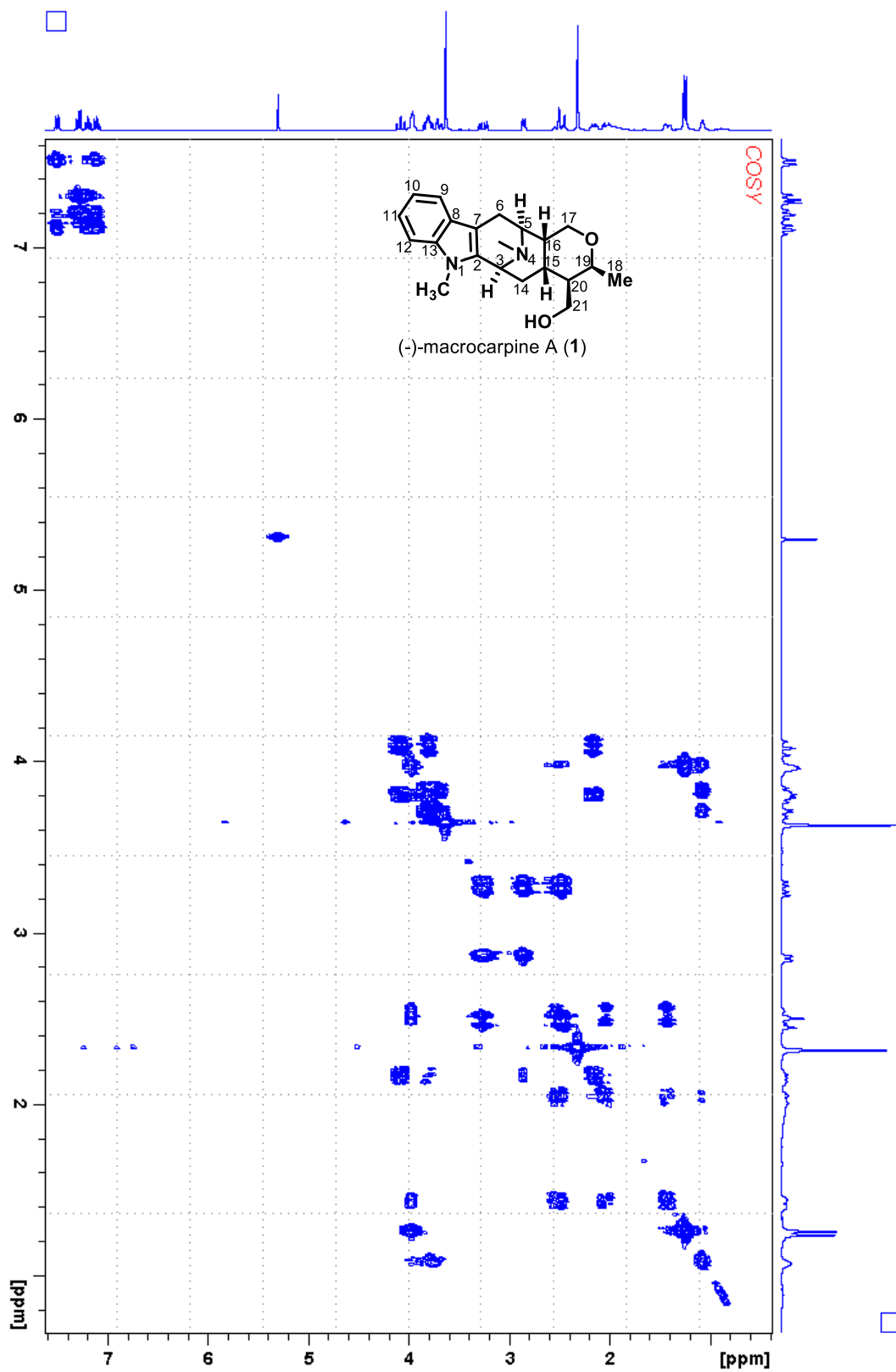
¹H NMR spectrum of macrocarpine A (1) (300 MHz, CDCl₃)



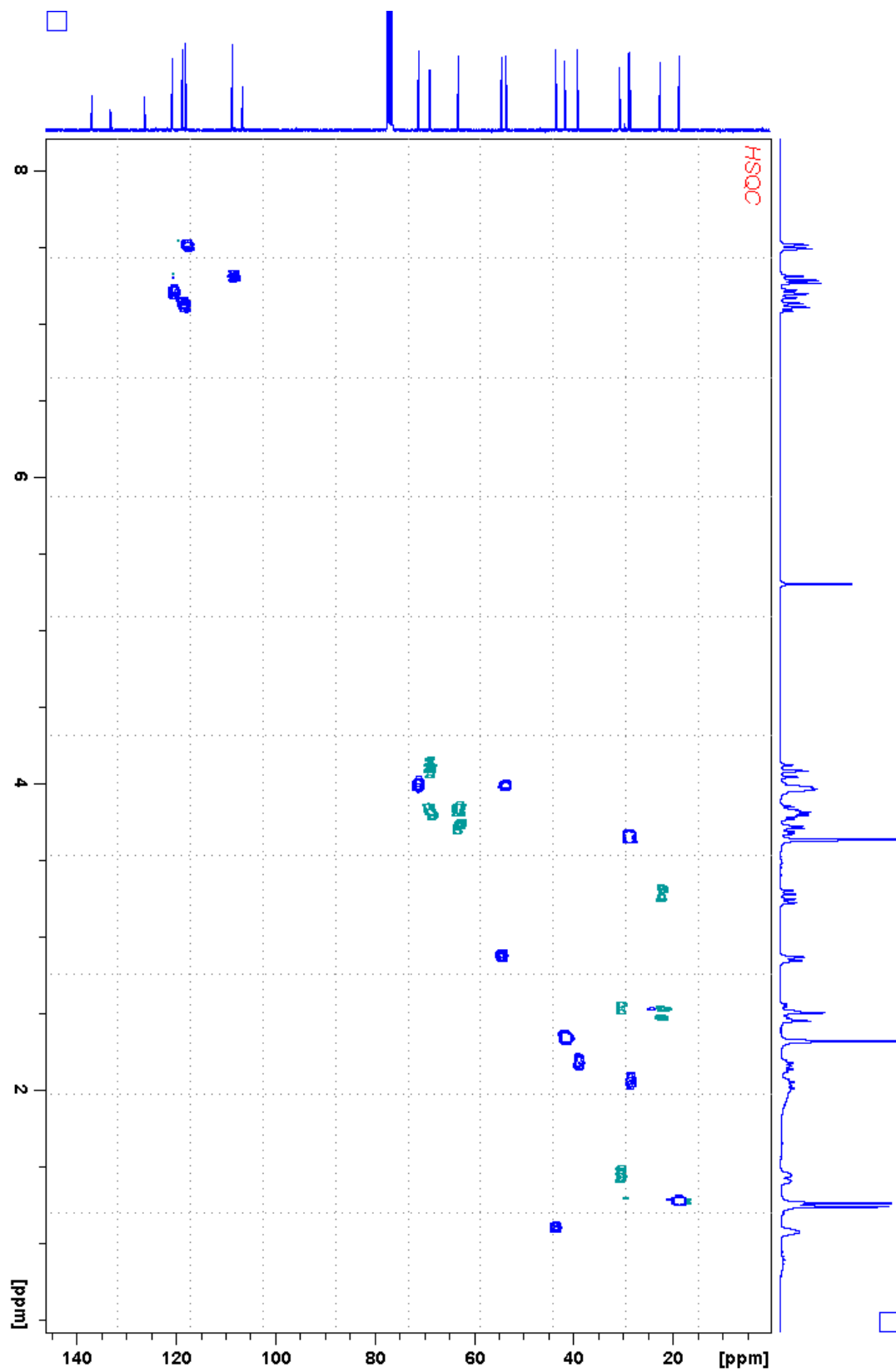
^{13}C NMR spectrum of macrocarpine A (1) (75 MHz, CDCl_3)



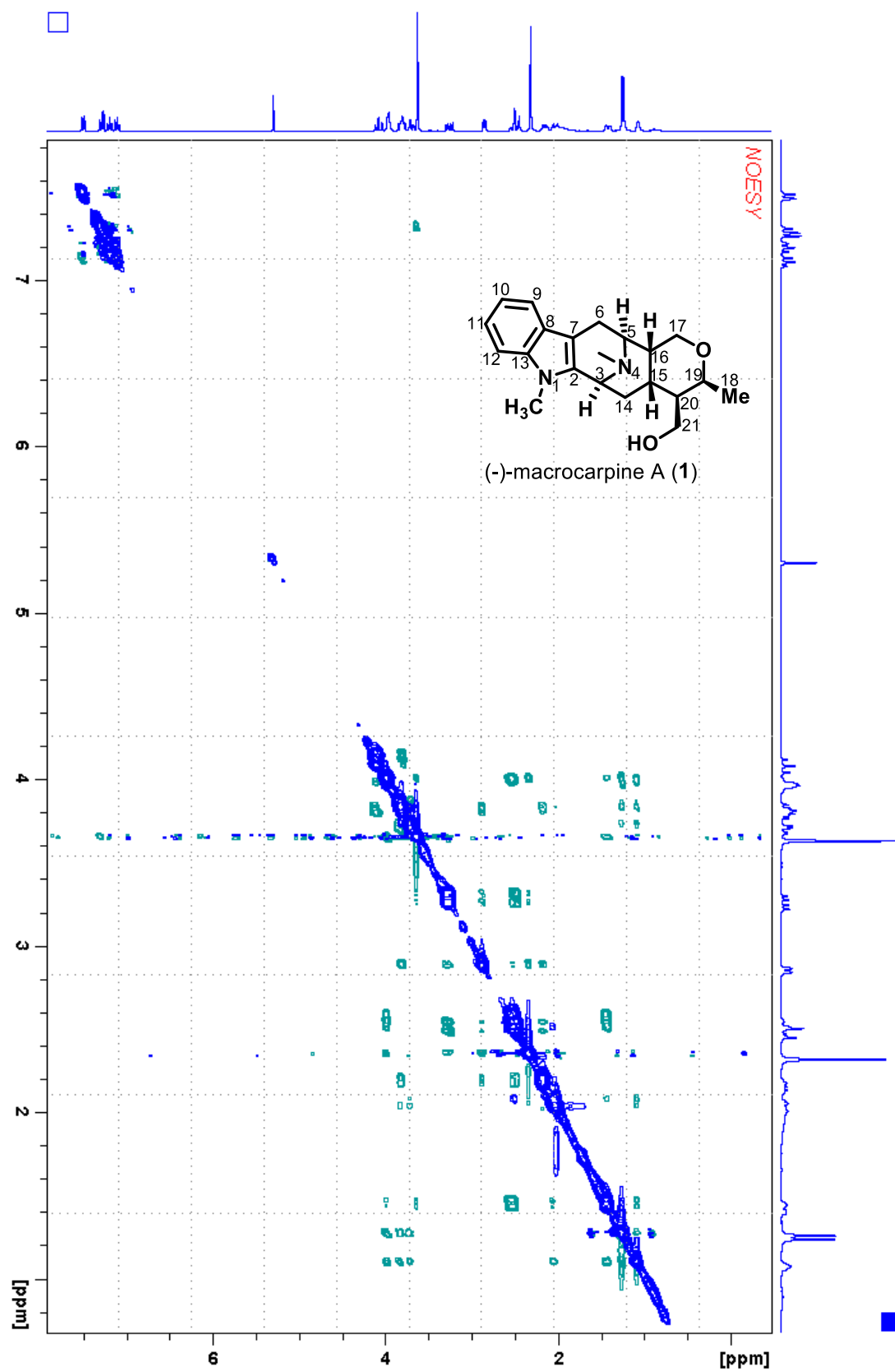
^{13}C vs ^{13}C -APT spectra of 1 (75 MHz, CDCl_3)



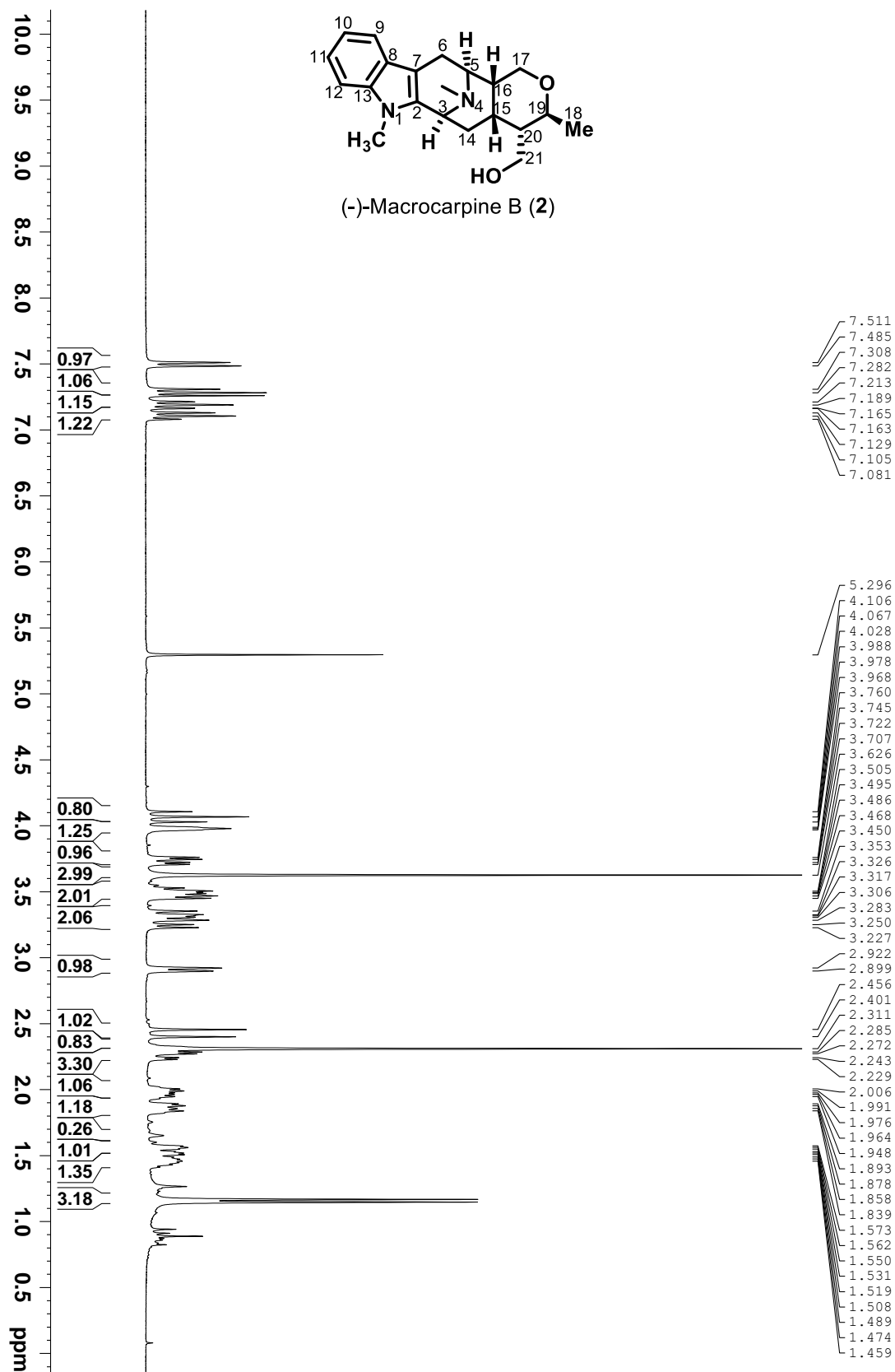
COSY NMR spectrum of macrocarpine A **1** (300 MHz, CDCl₃)



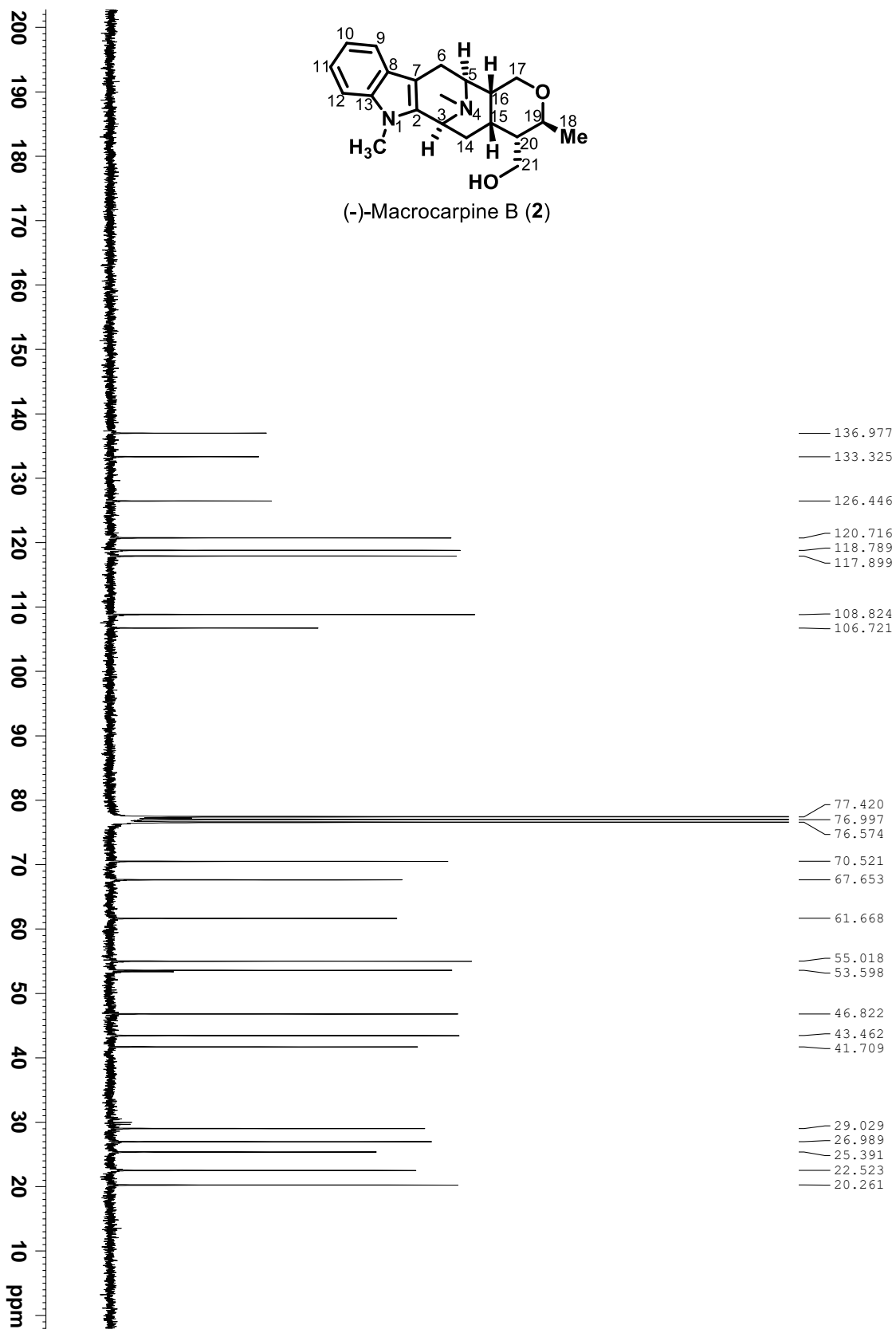
HSQC NMR spectrum of macrocarpine A **1** (300 MHz, 75 MHz, CDCl₃)



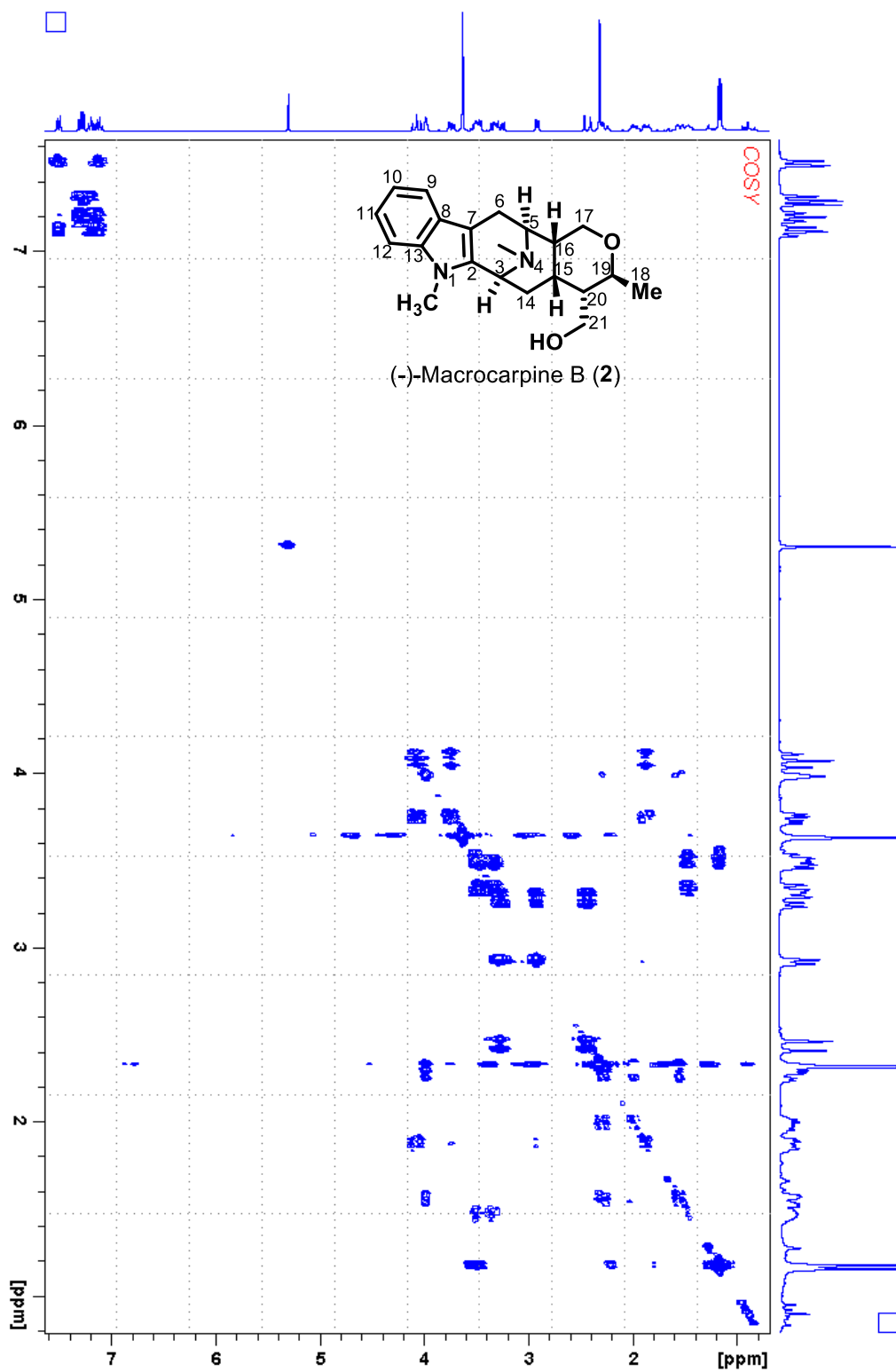
NOESY NMR spectrum of macrocarpine A **1** (300 MHz, CDCl₃)



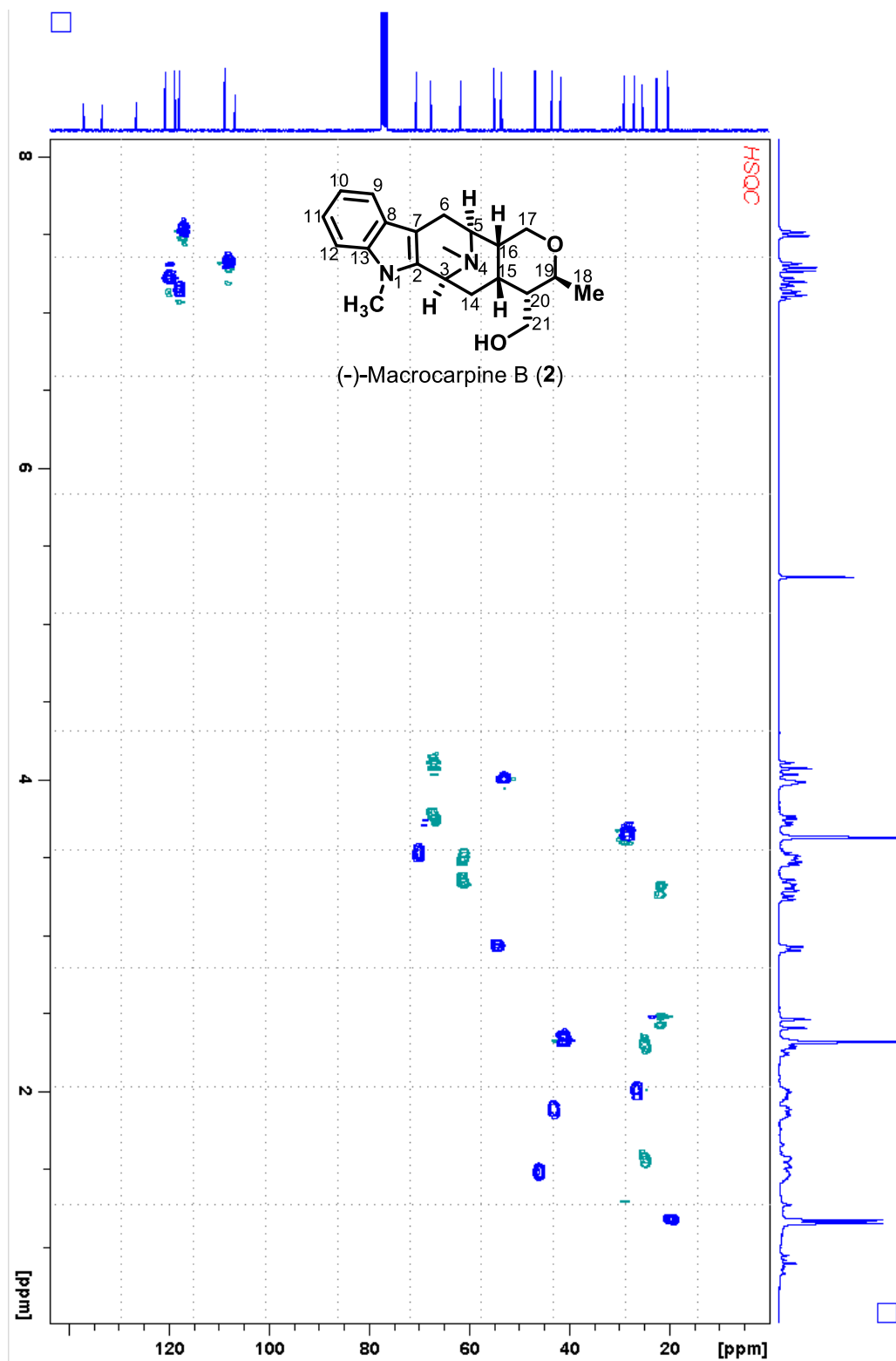
¹H NMR spectrum of macroparpine B **2** (300 MHz, CDCl₃)



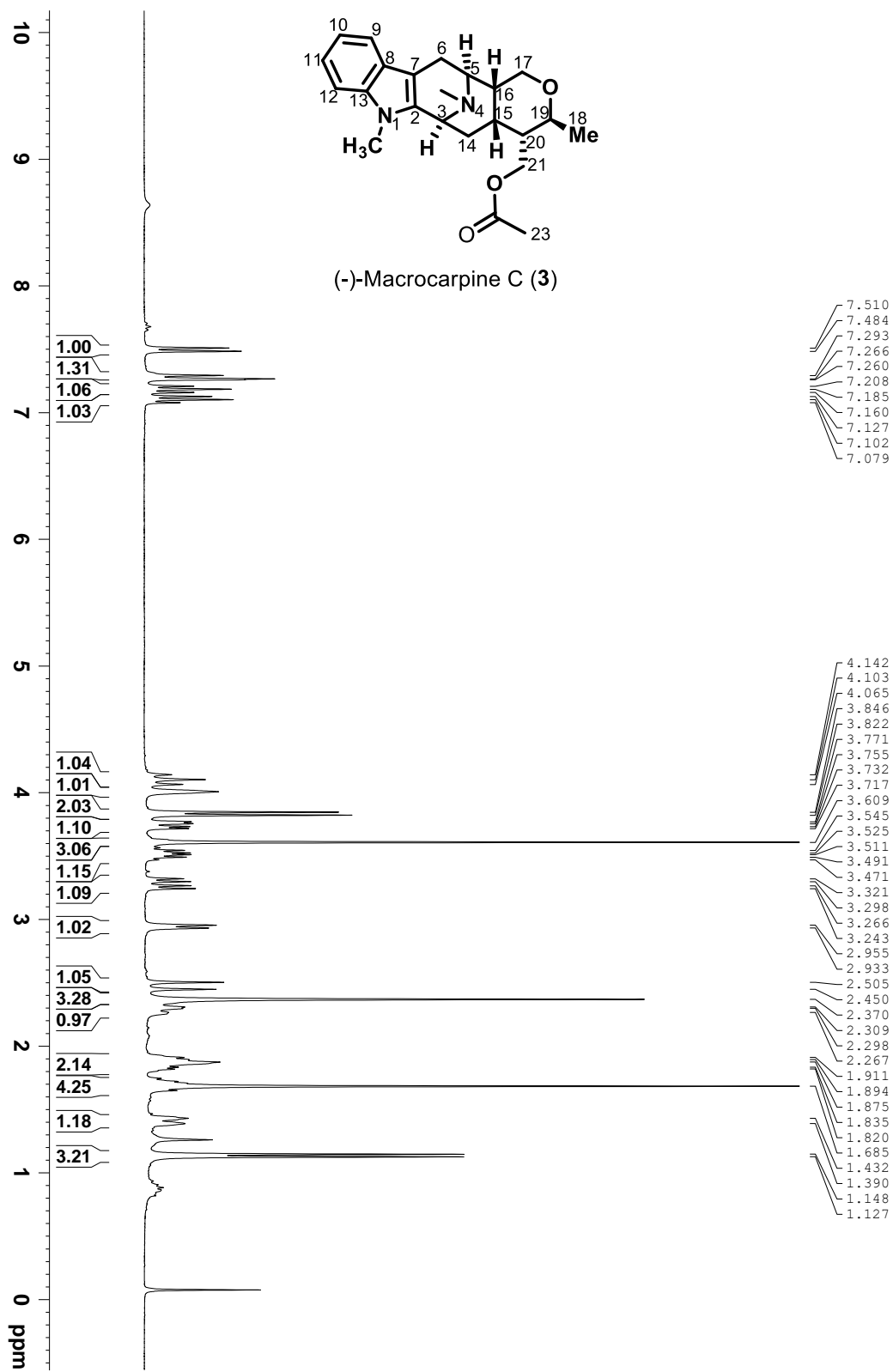
^{13}C NMR spectrum of macrocarpine B **2** (75 MHz, CDCl_3)



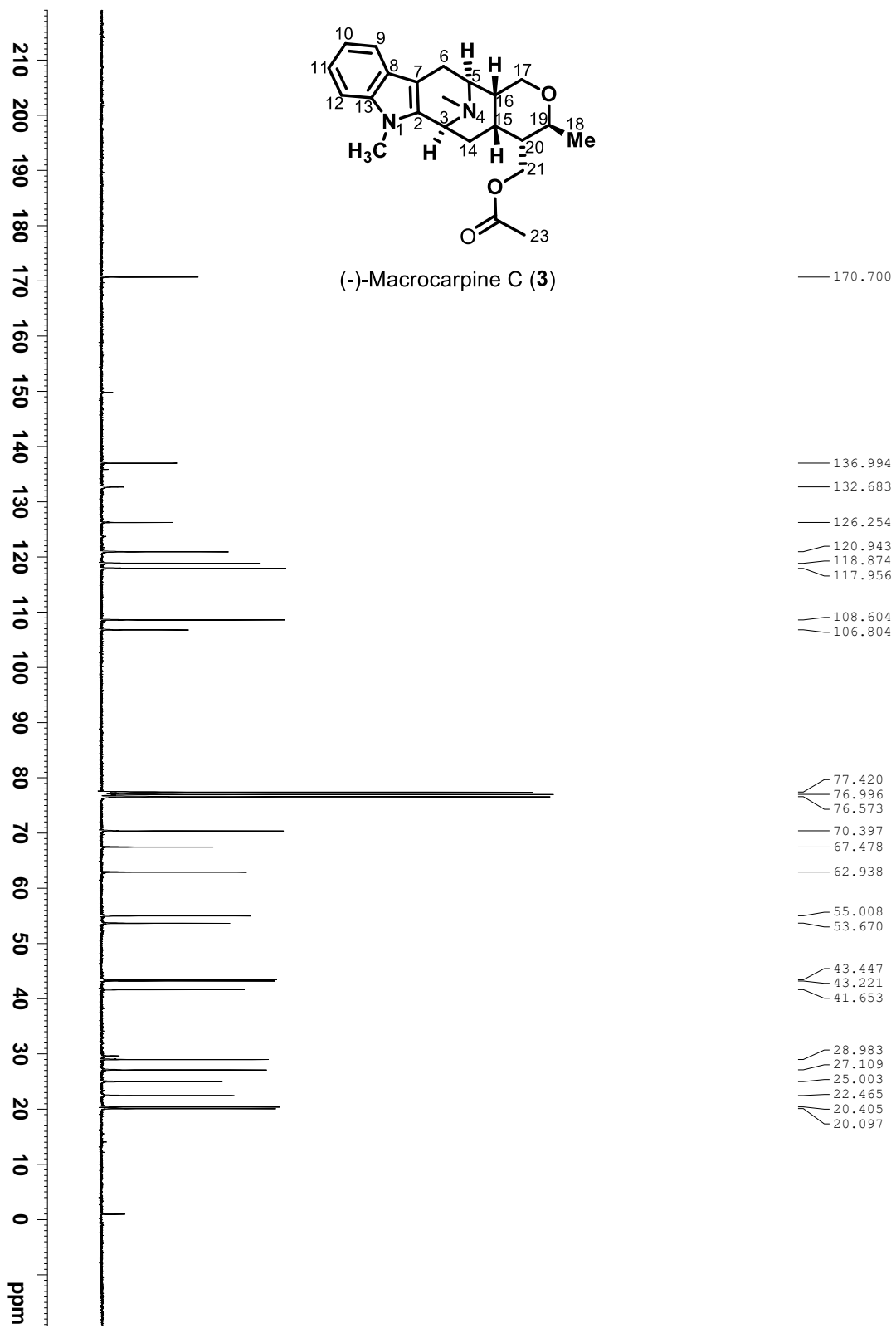
COSY NMR spectrum of macrocarpine B 2 (300 MHz, CDCl₃)



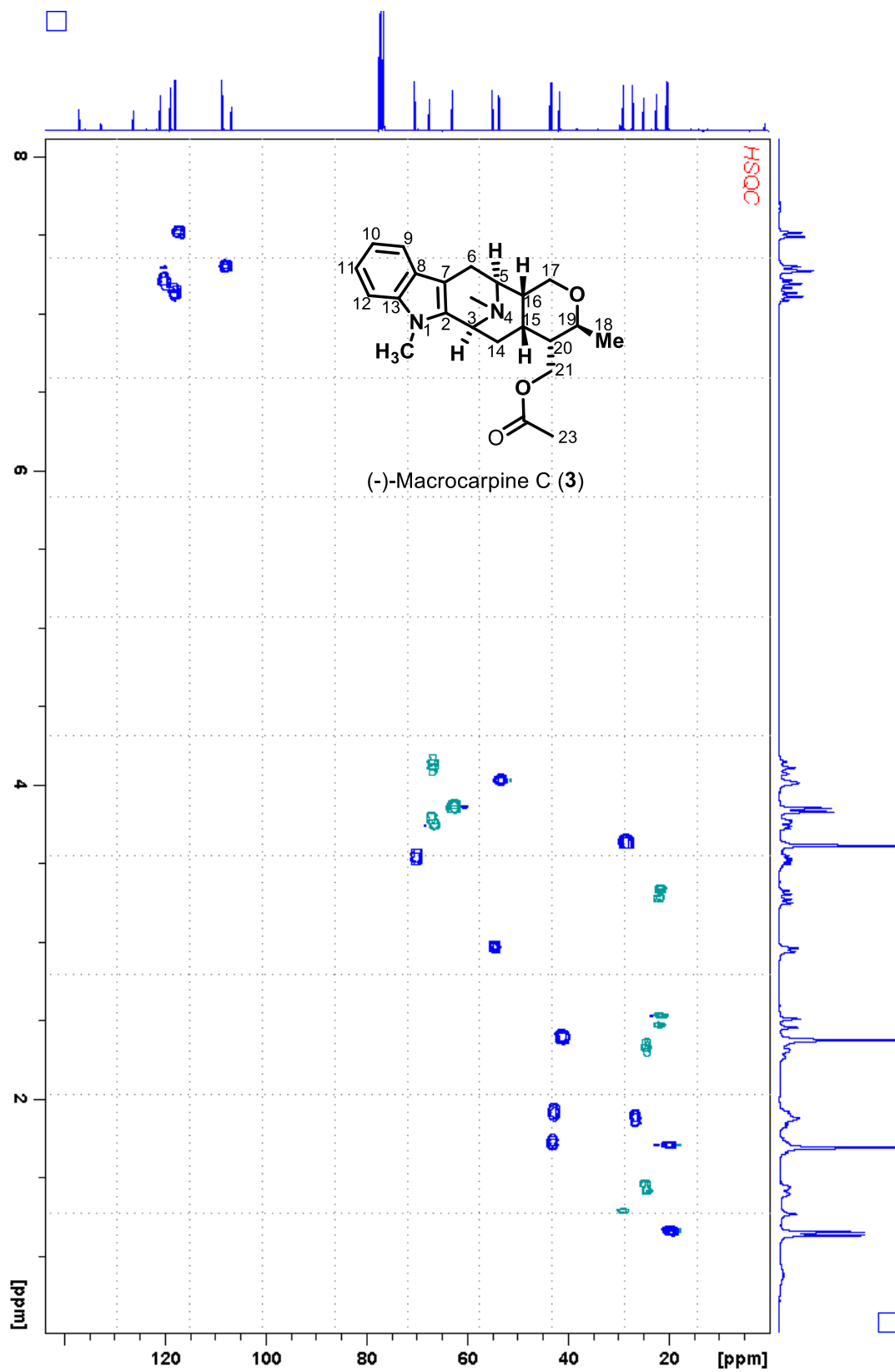
HSQC NMR spectrum of macrocarpine B **2** (300 MHz, 75 MHz, CDCl₃)



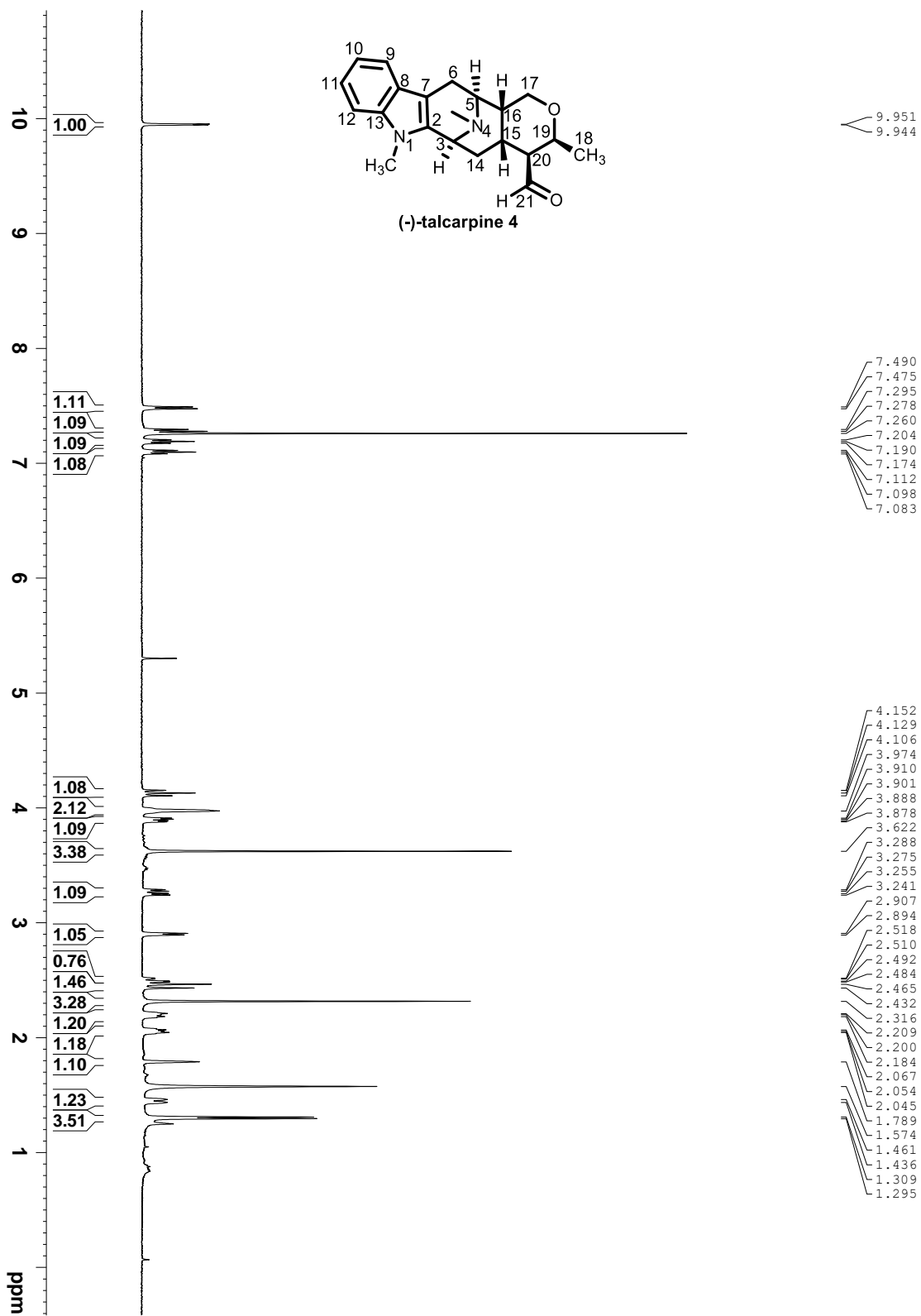
¹H NMR spectrum of macroparpine C **3** (300 MHz, CDCl₃)



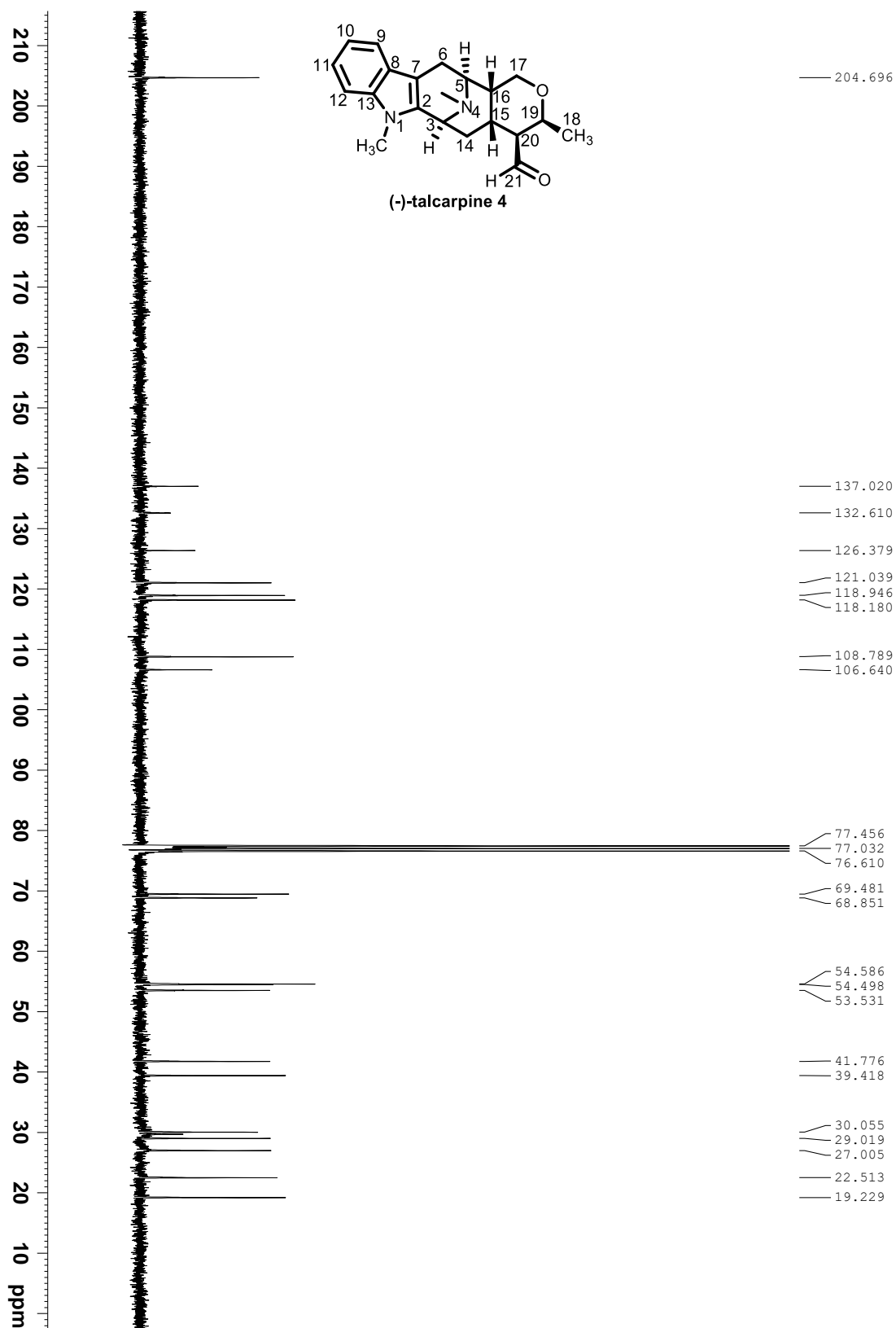
¹³C NMR spectrum of macrocarpine C **3** (75 MHz, CDCl₃)



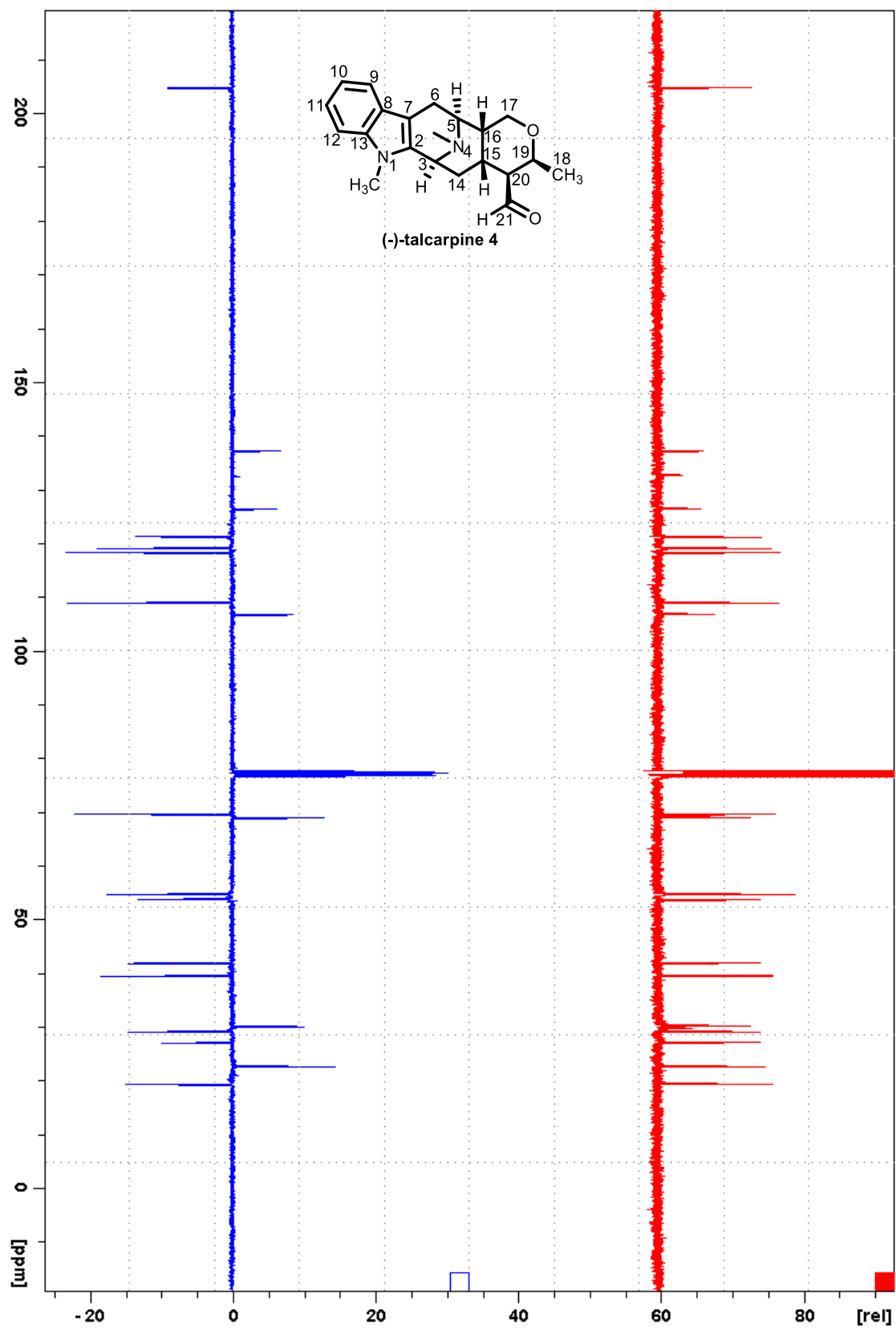
HSQC NMR spectrum of macrocarpine C 3 (300 MHz, 75 MHz, CDCl₃)



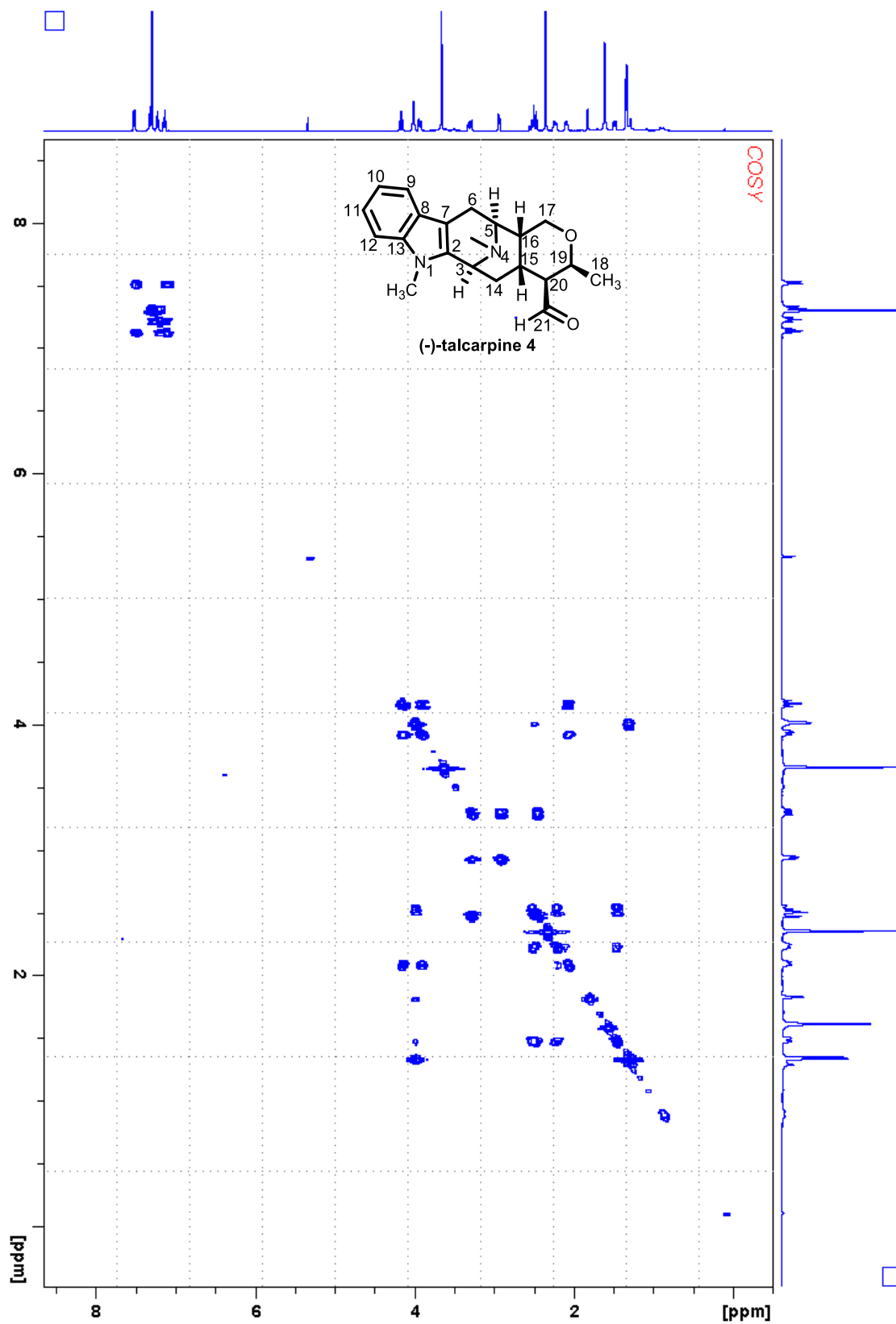
¹H NMR spectrum of talcarpine 4 (500 MHz, CDCl₃)



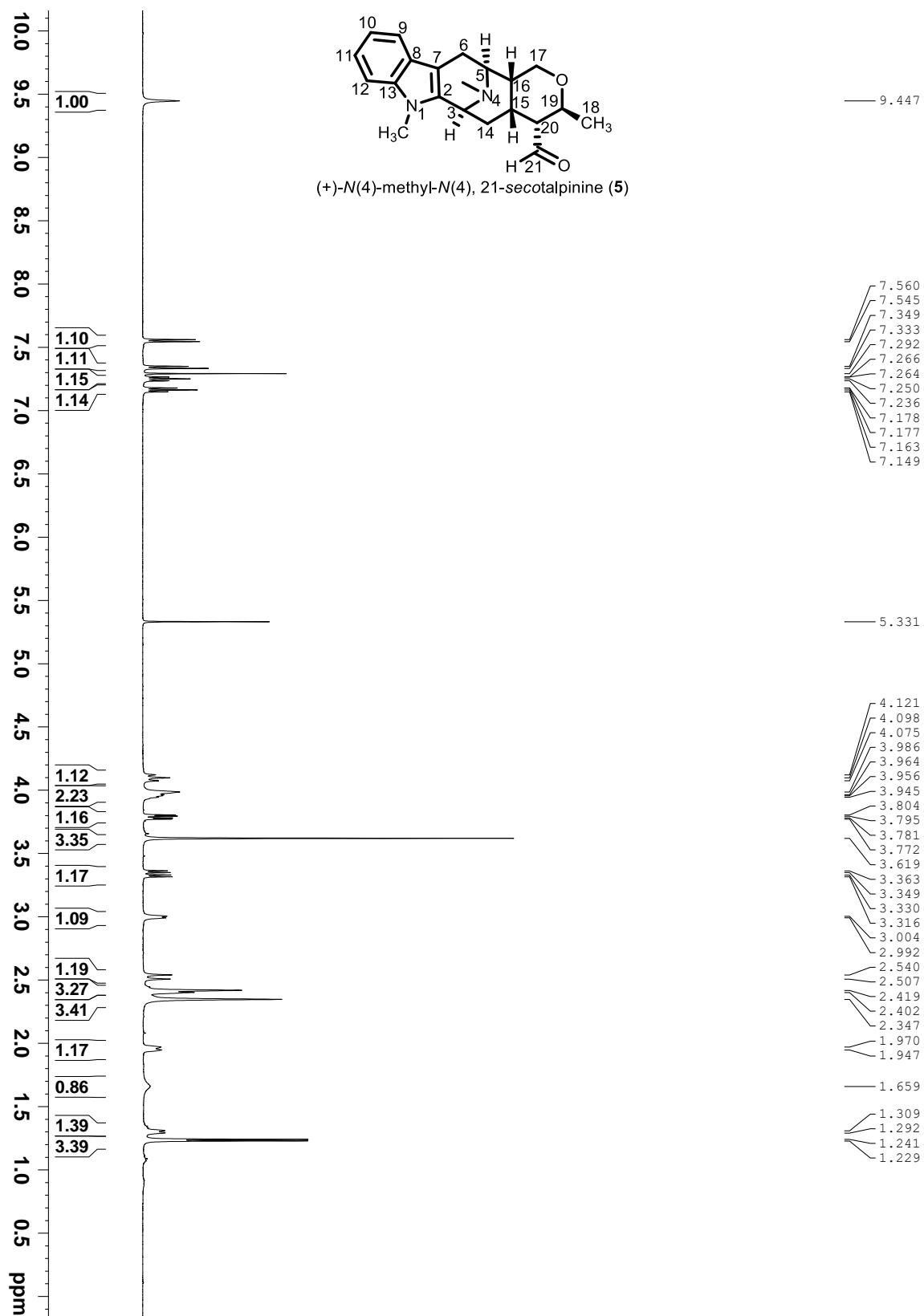
¹³C NMR spectrum of talcarpine 4 (75 MHz, CDCl₃)



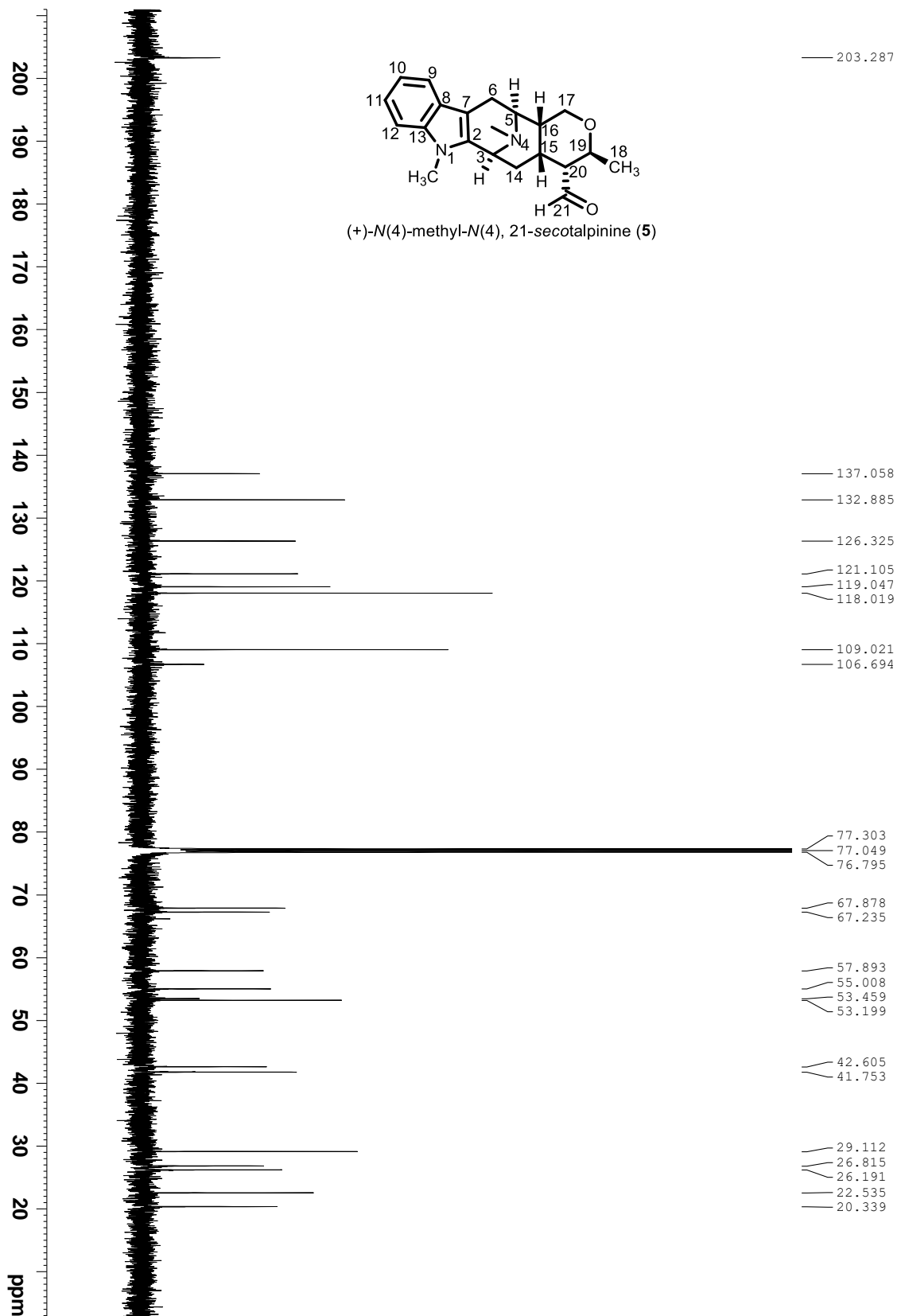
¹³C vs ¹³C-APT NMR spectra of talcarpine 4 (75 MHz, CDCl₃)



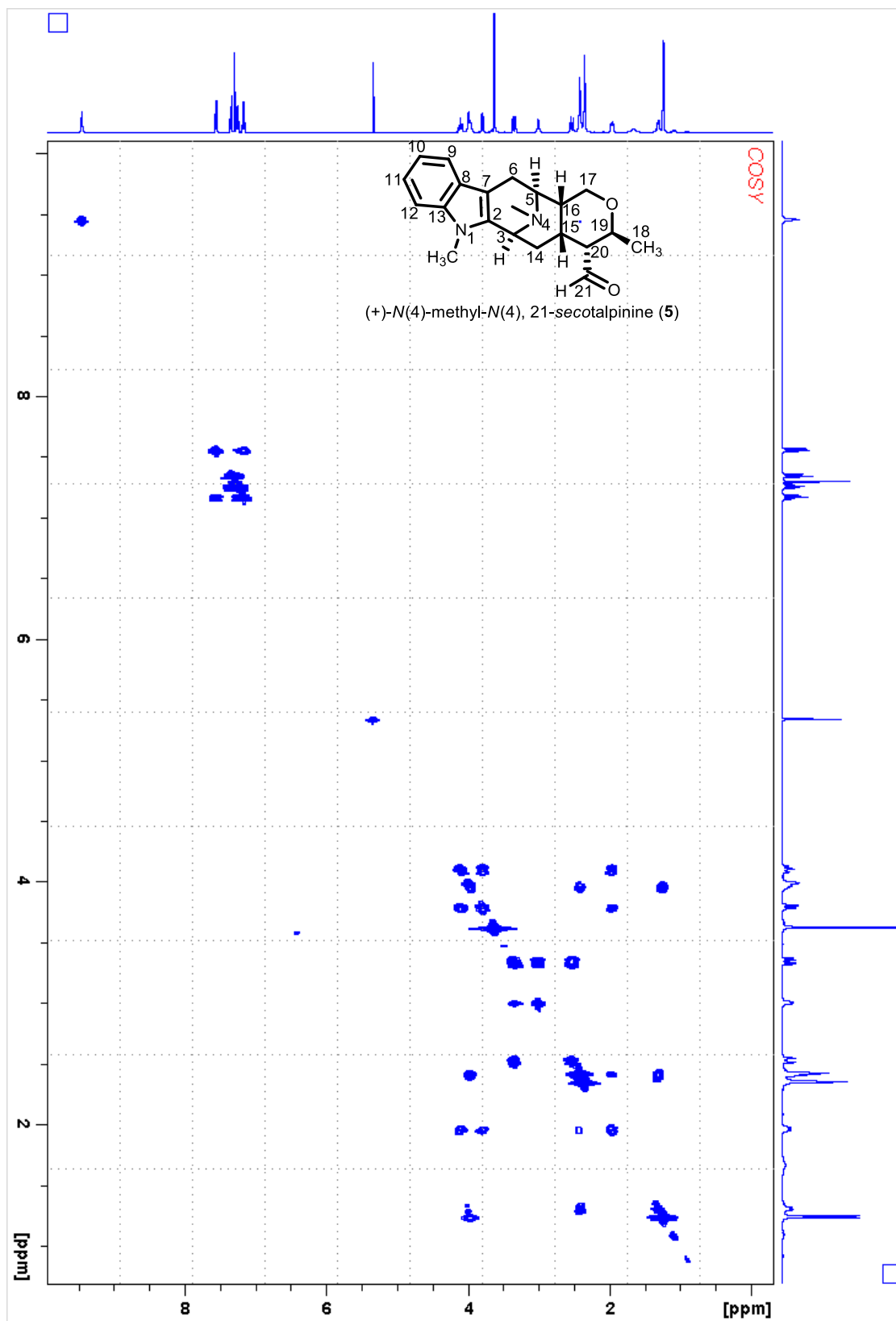
COSY NMR spectrum of talcarpine 4 (300 MHz, CDCl₃)



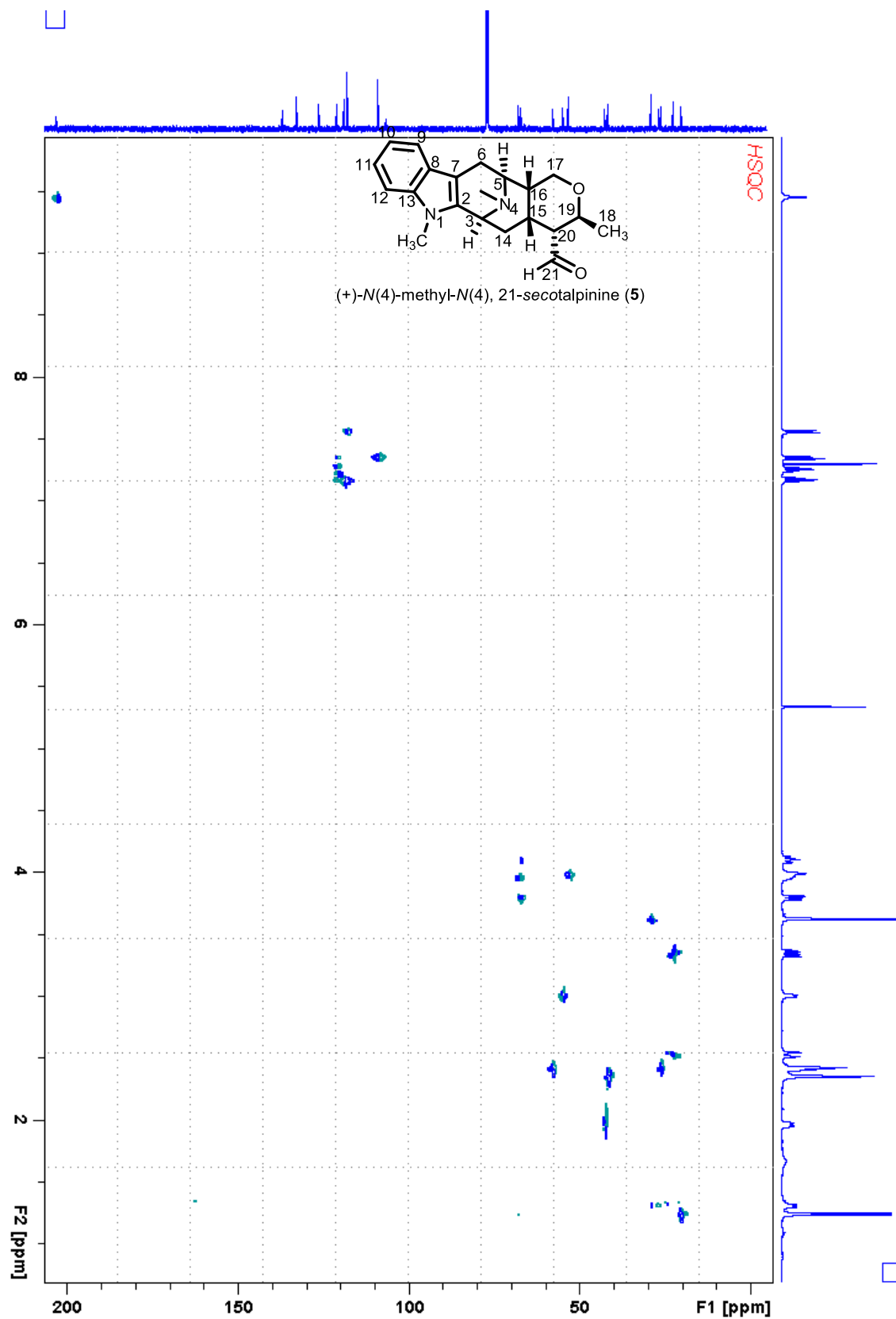
¹H NMR spectrum of **5** (500 MHz, CDCl₃)



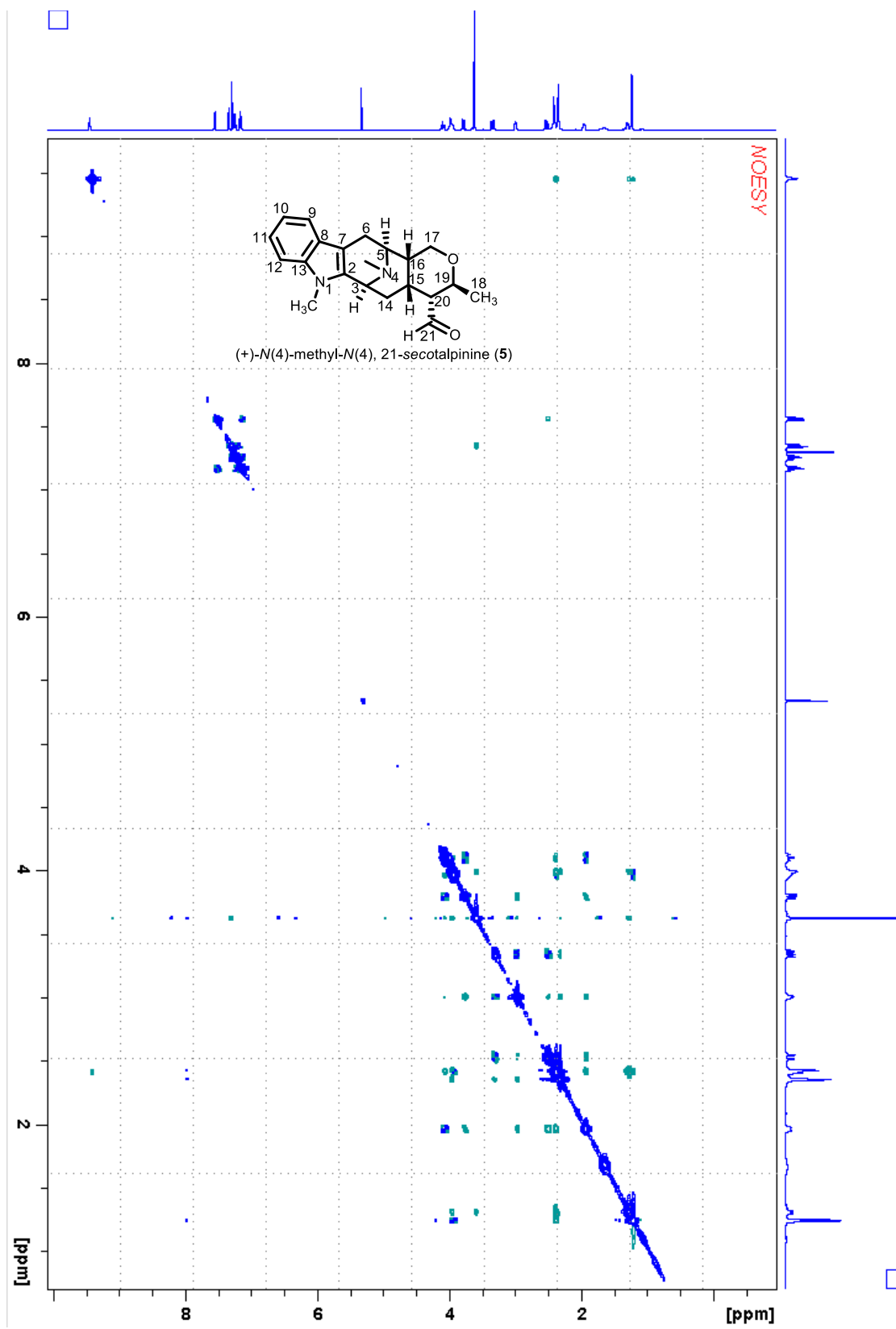
^{13}C NMR spectrum of **5** (125 MHz, CDCl_3)



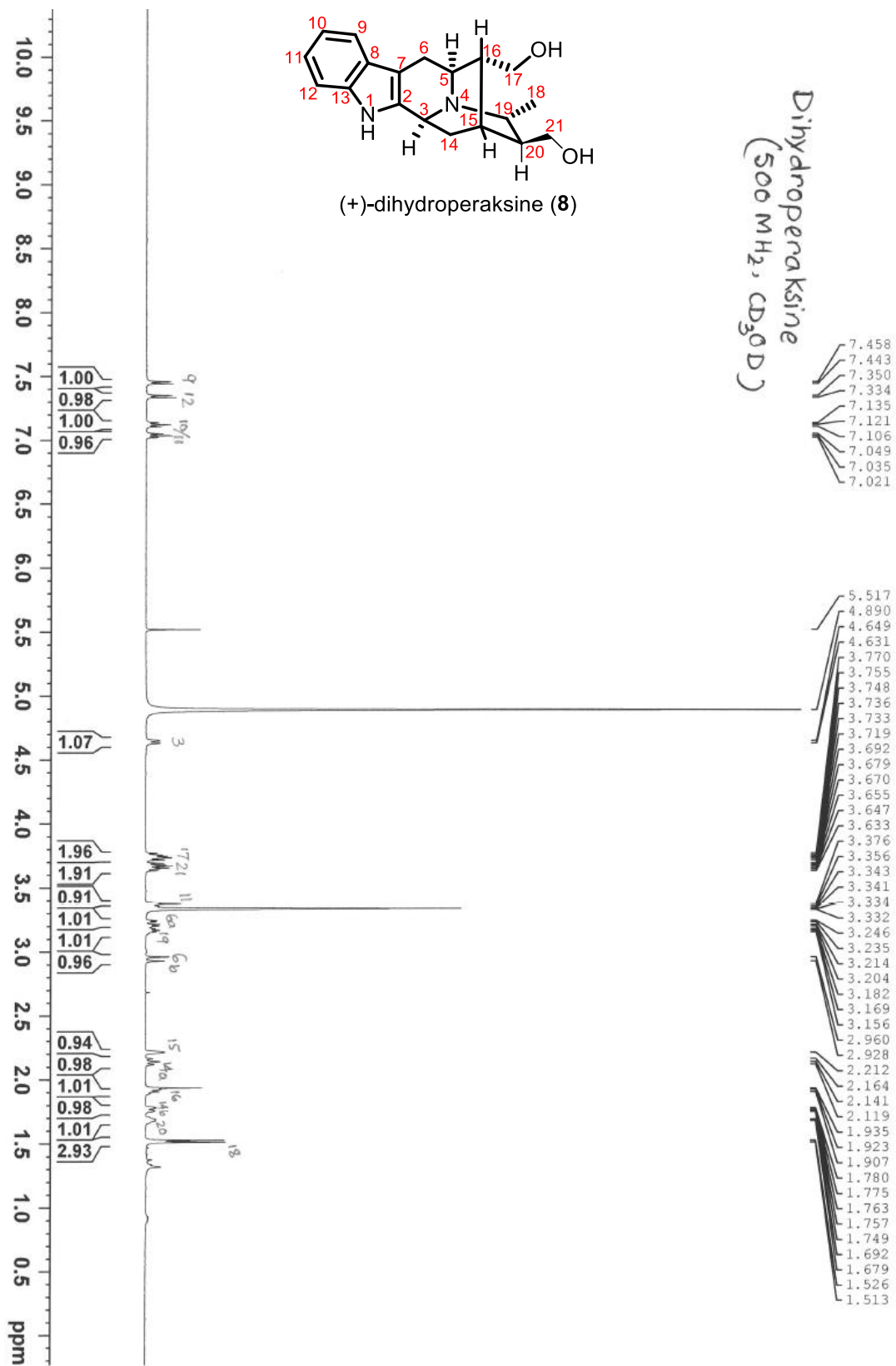
COSY NMR spectrum of **5** (500 MHz, CDCl₃)



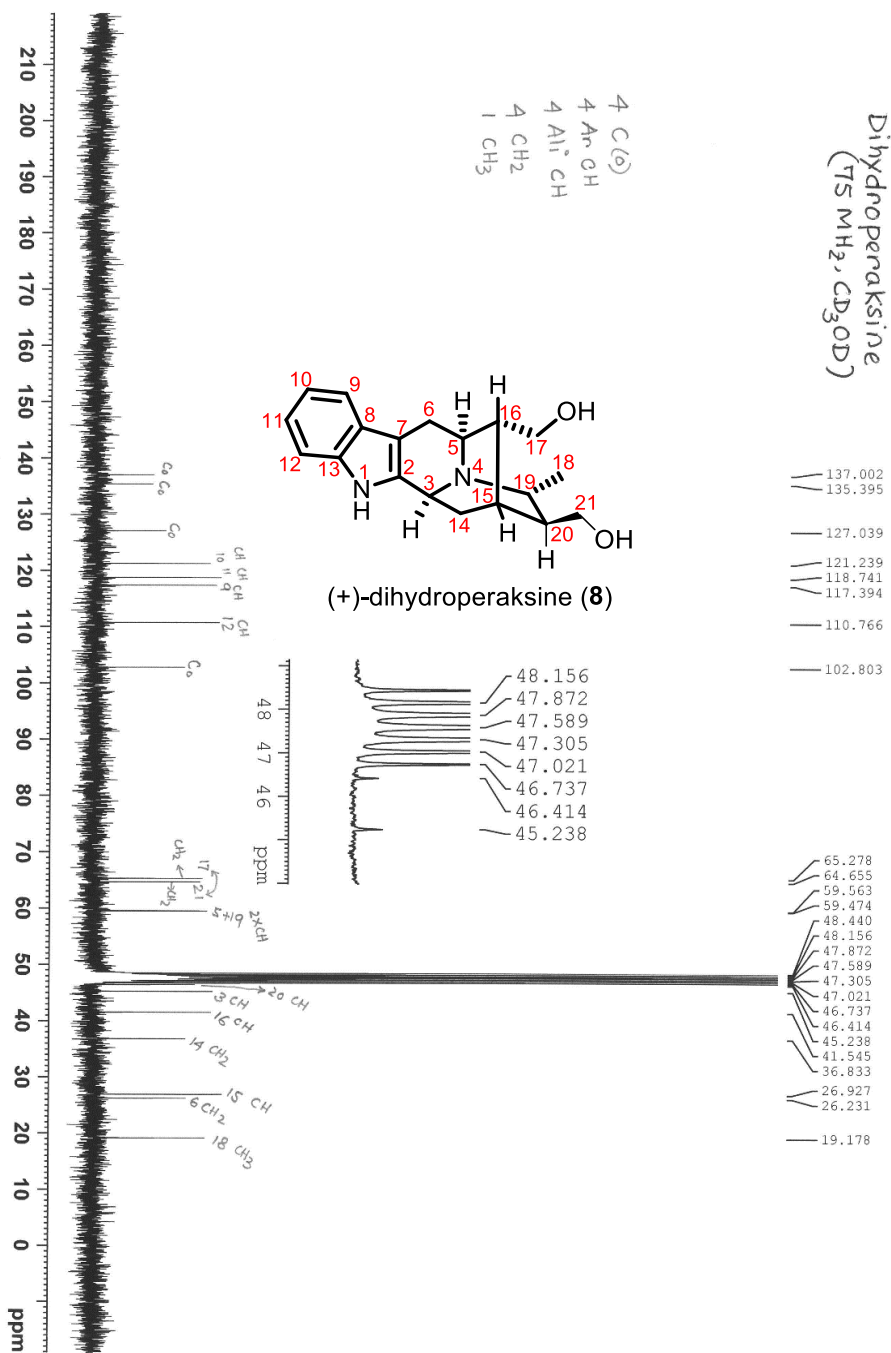
HSQC NMR spectrum of **5** (500 MHz, 125 MHz, CDCl₃)



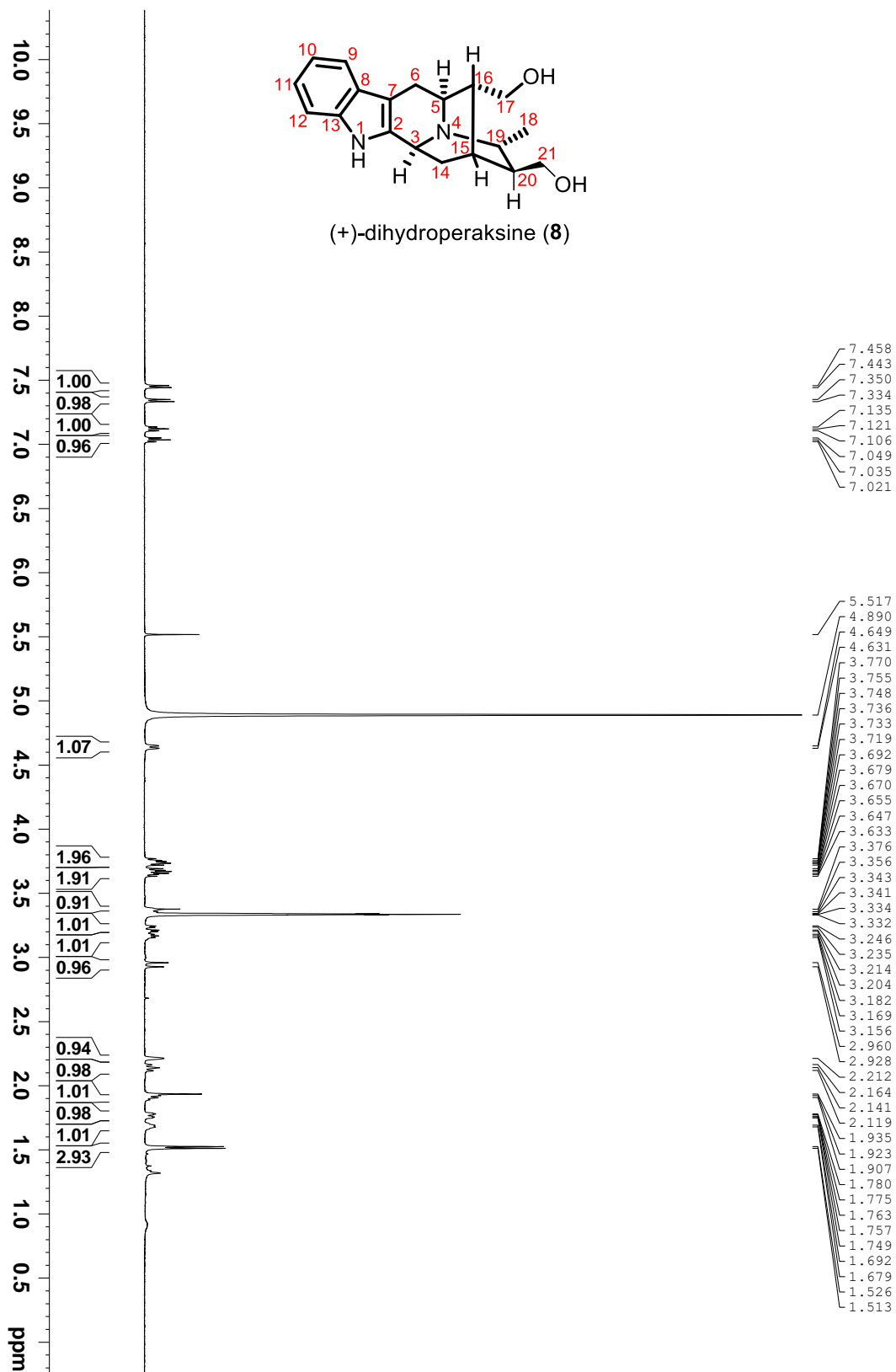
NOESY NMR spectrum of **5** (500 MHz, CDCl₃)



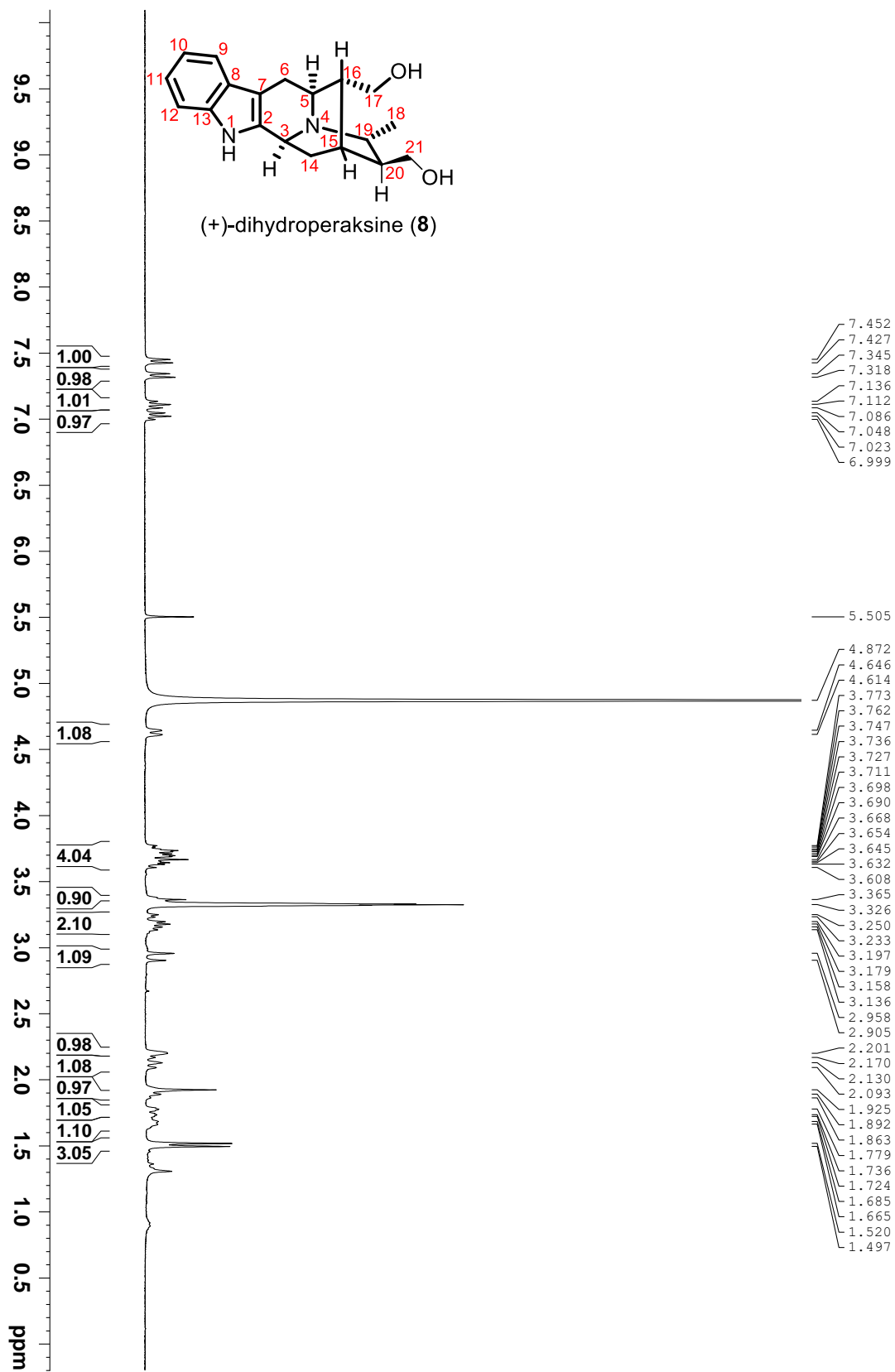
¹H NMR spectrum of (+)-**8** (500 MHz, CD₃OD)



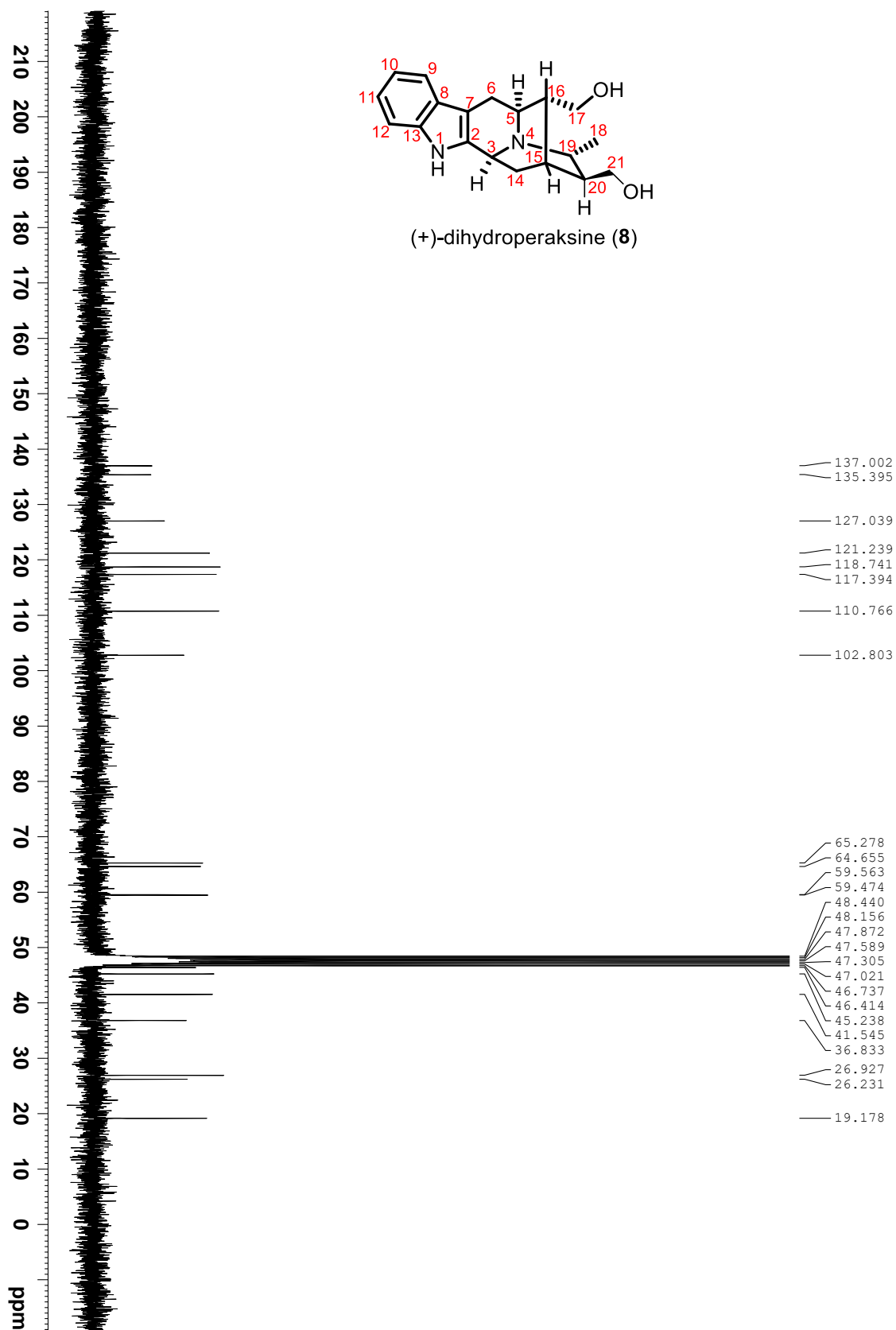
¹H NMR spectrum of (+)-**8** (125 MHz, CD₃OD)



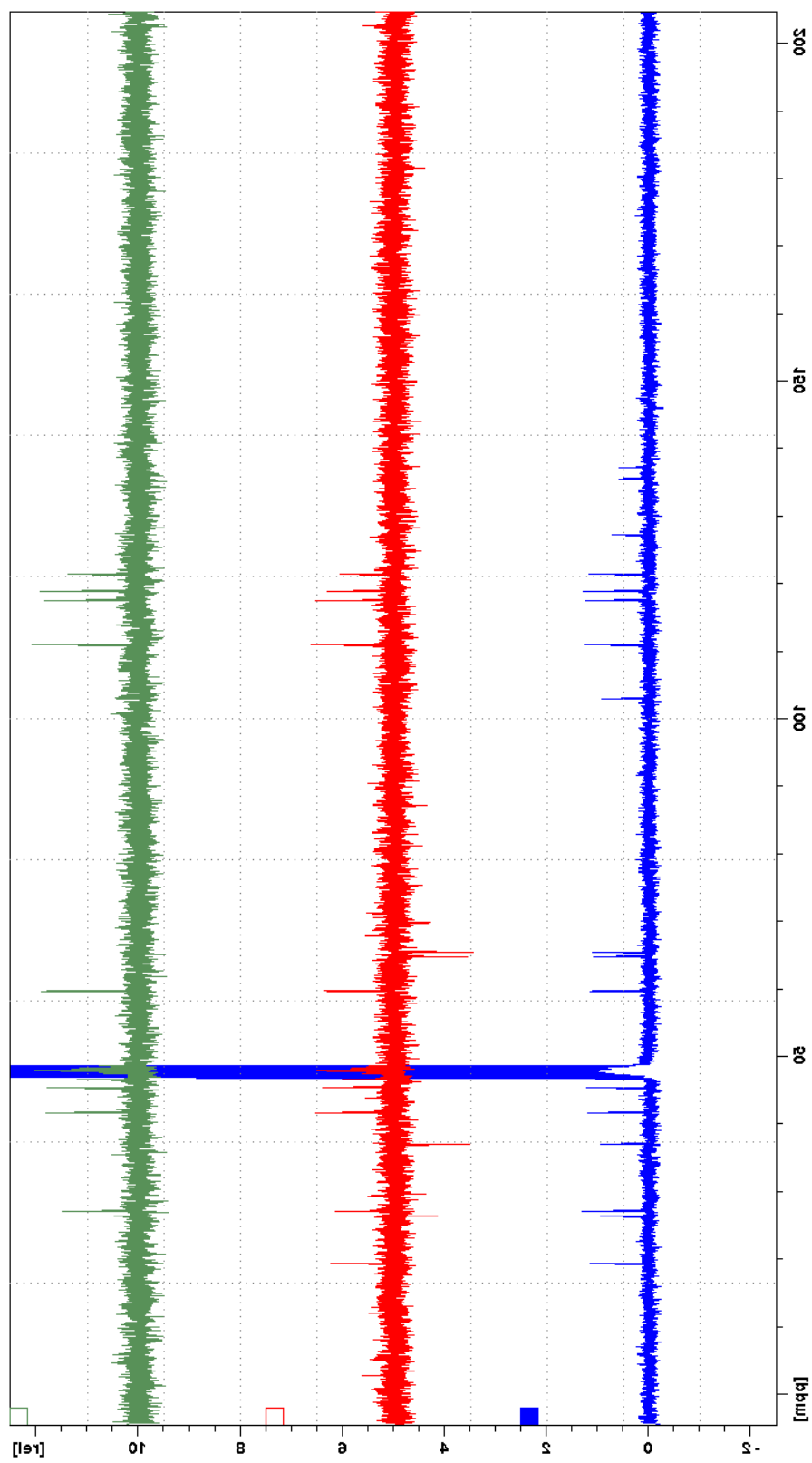
¹H NMR spectrum of (+)-8 (500 MHz, CD₃OD)



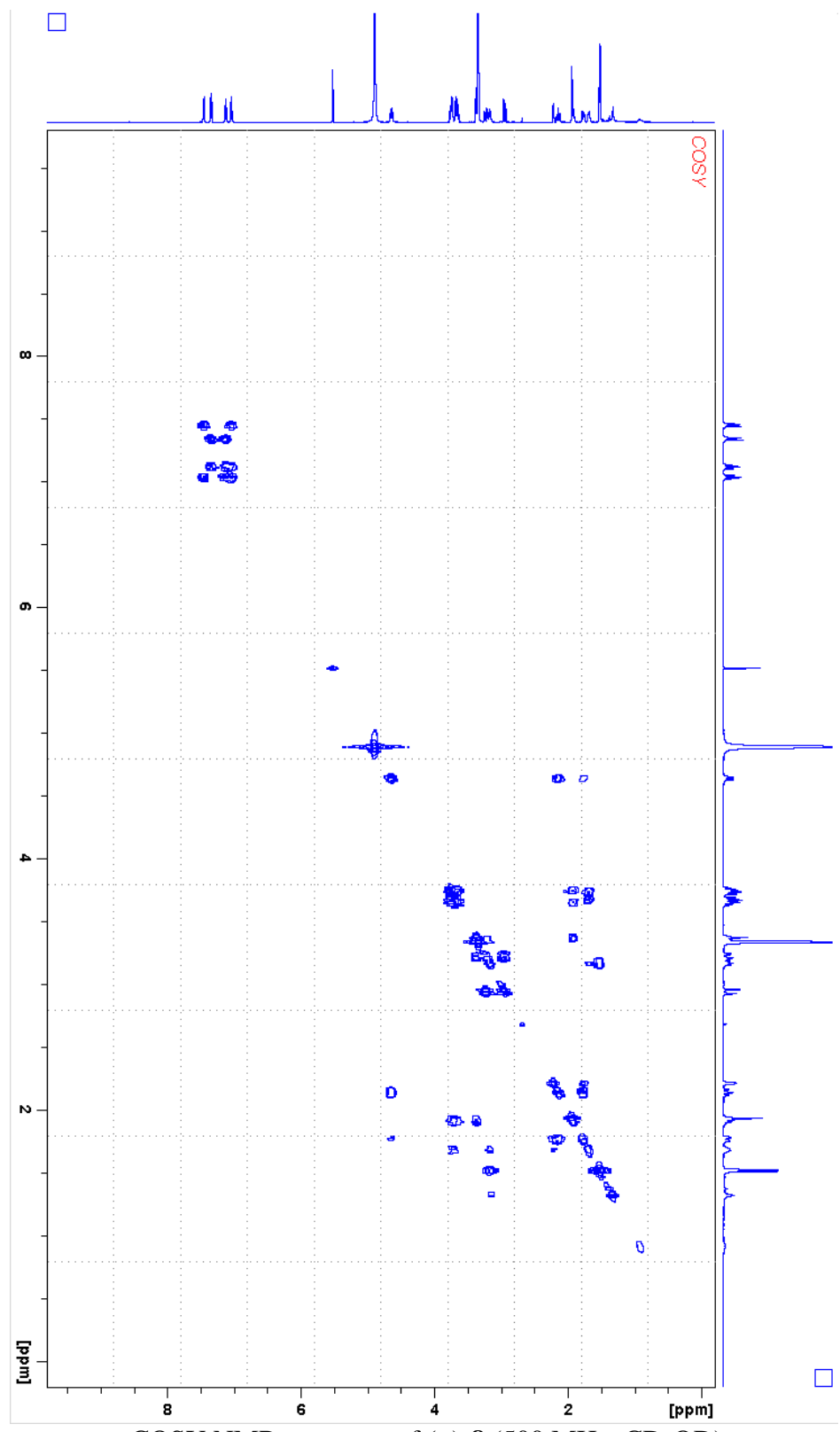
¹H NMR spectrum of (+)-**8** (300 MHz, CD₃OD)



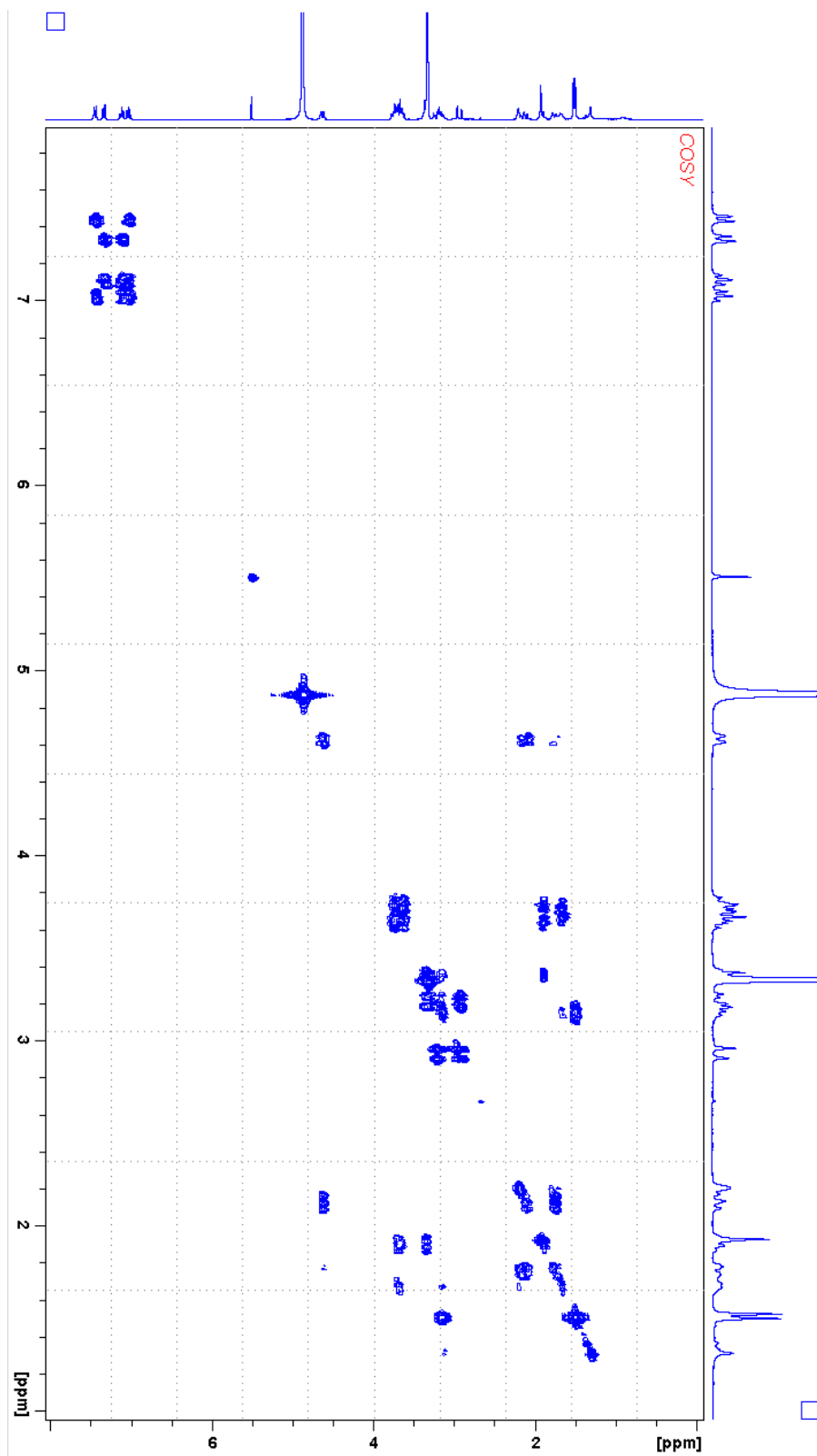
¹³C NMR spectrum of (+)-8 (75 MHz, CD₃OD)



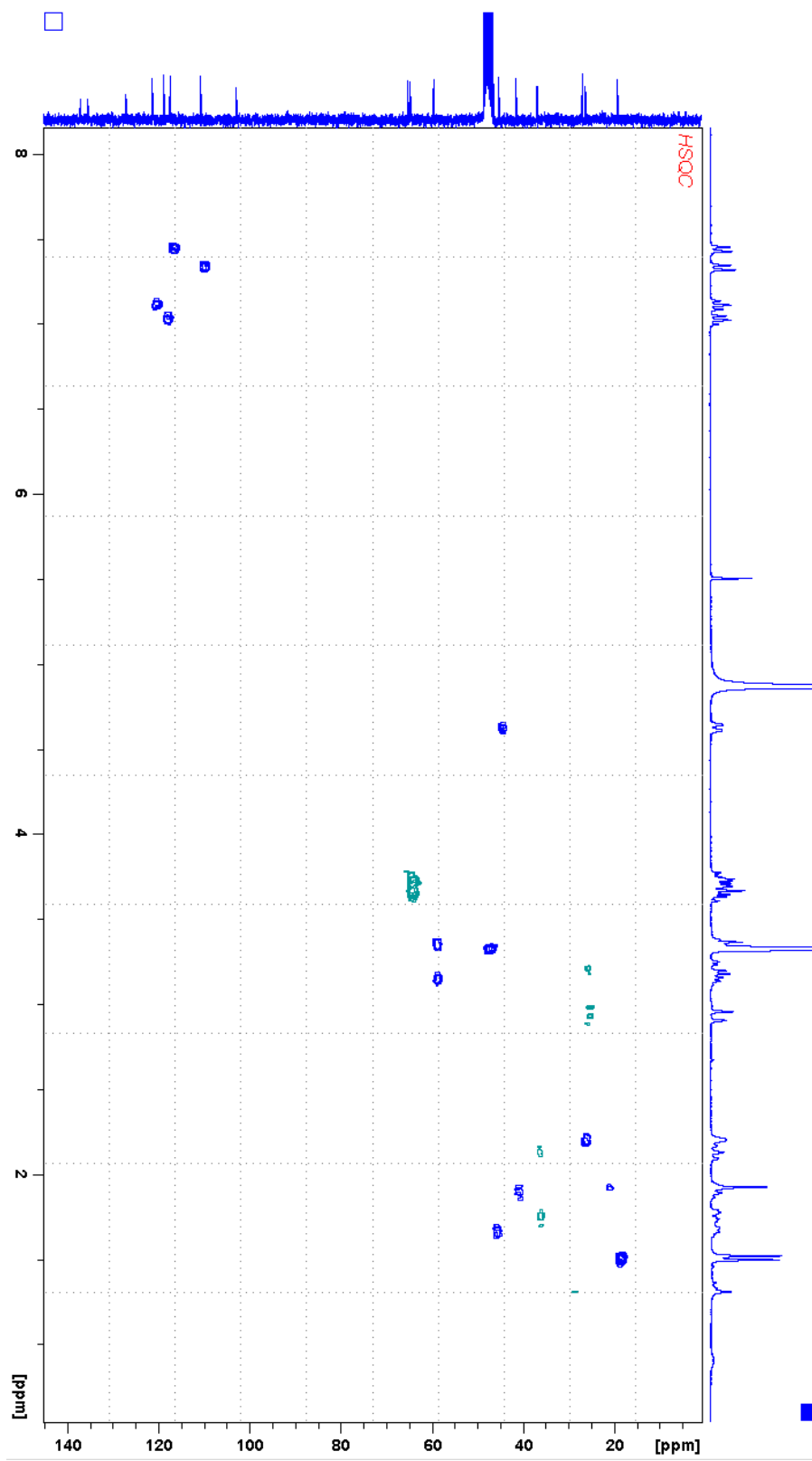
^{13}C NMR vs DEPT-135 and DEPT 90 spectra of (+)-**8** (75 MHz, CD_3OD)



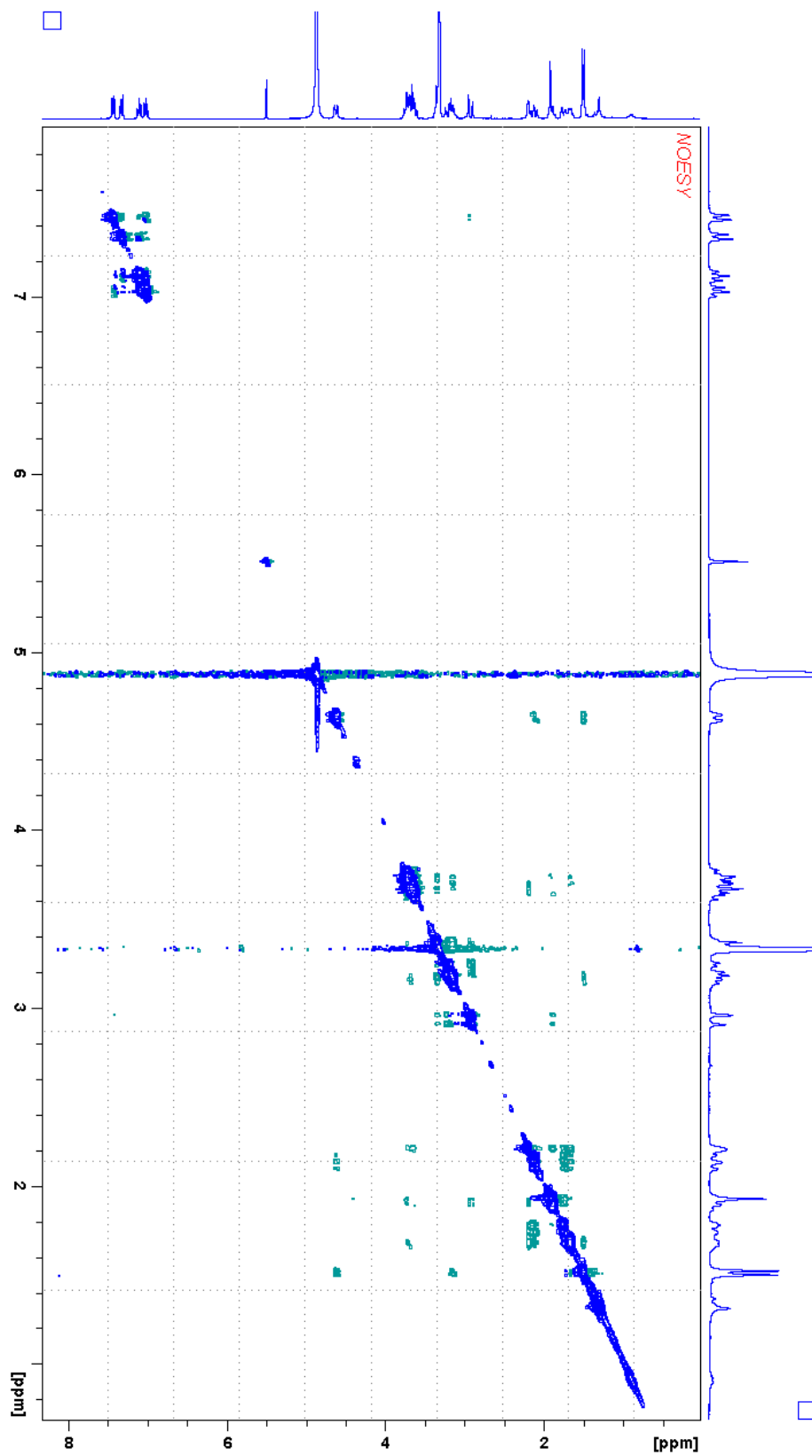
COSY NMR spectrum of (+)-8 (500 MHz, CD₃OD)



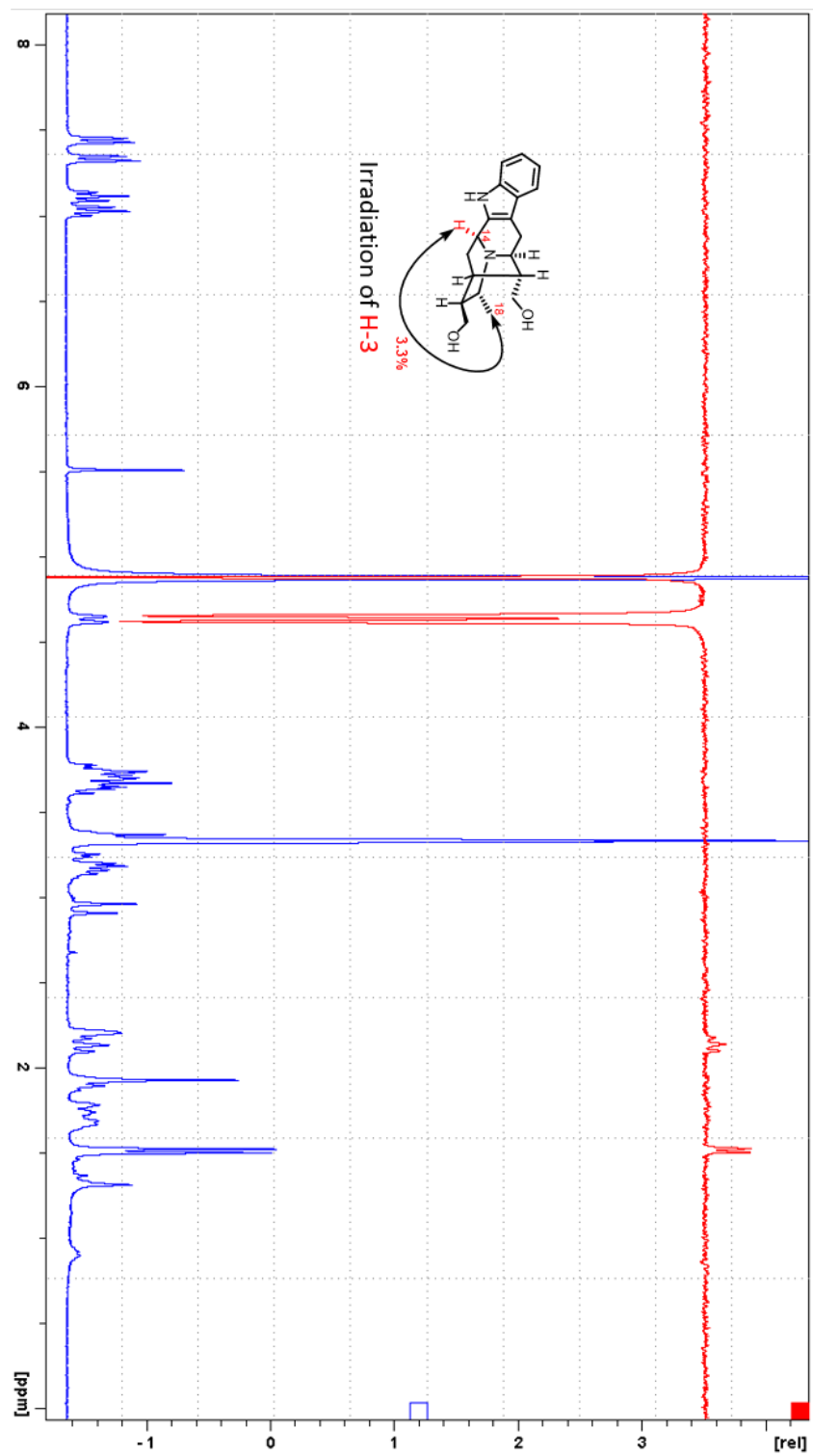
COSY NMR spectrum of (+)-**8** (300 MHz, CD₃OD)



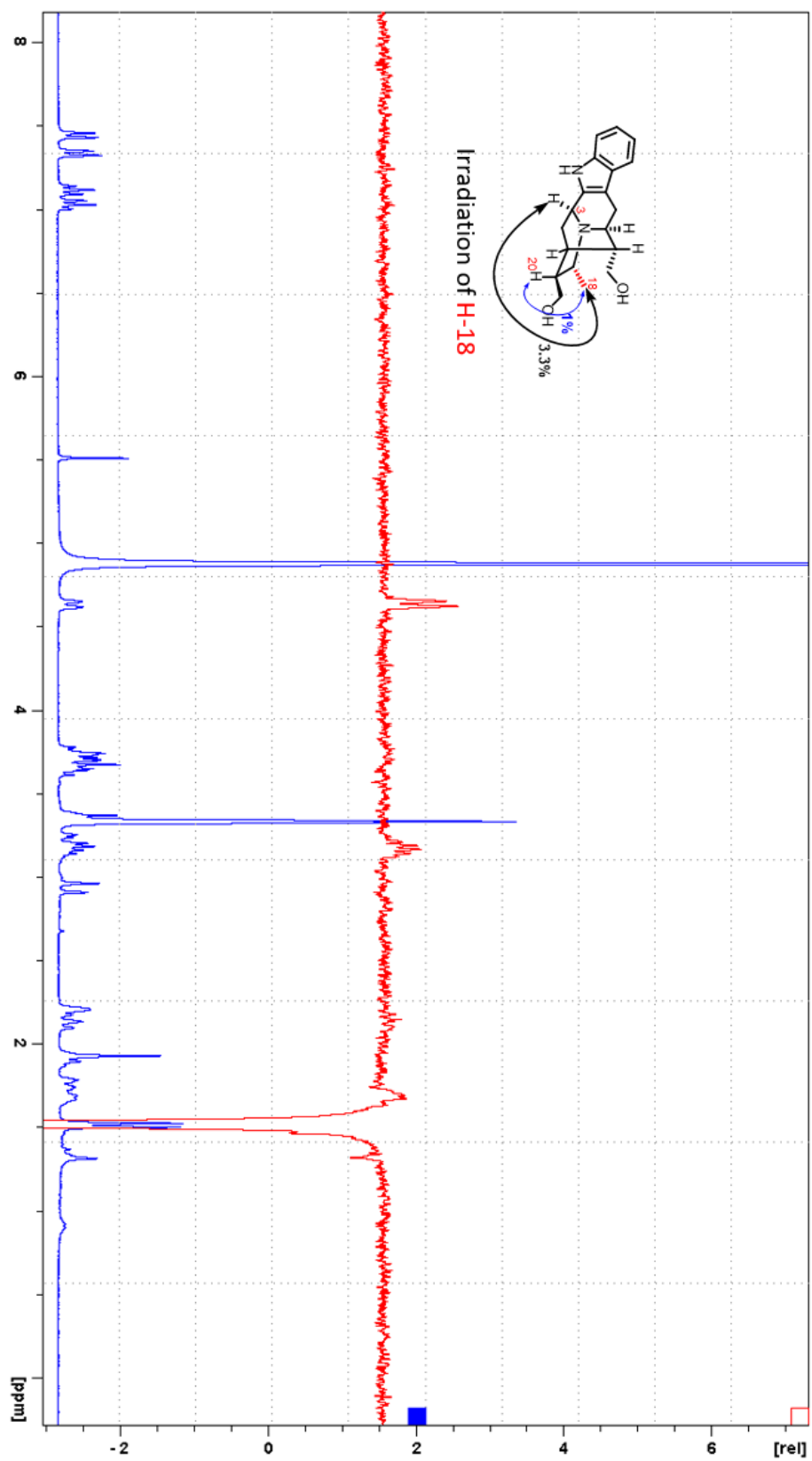
HSQC NMR spectrum of (+)-**8** (300 MHz, 75 MHz, CD_3OD)



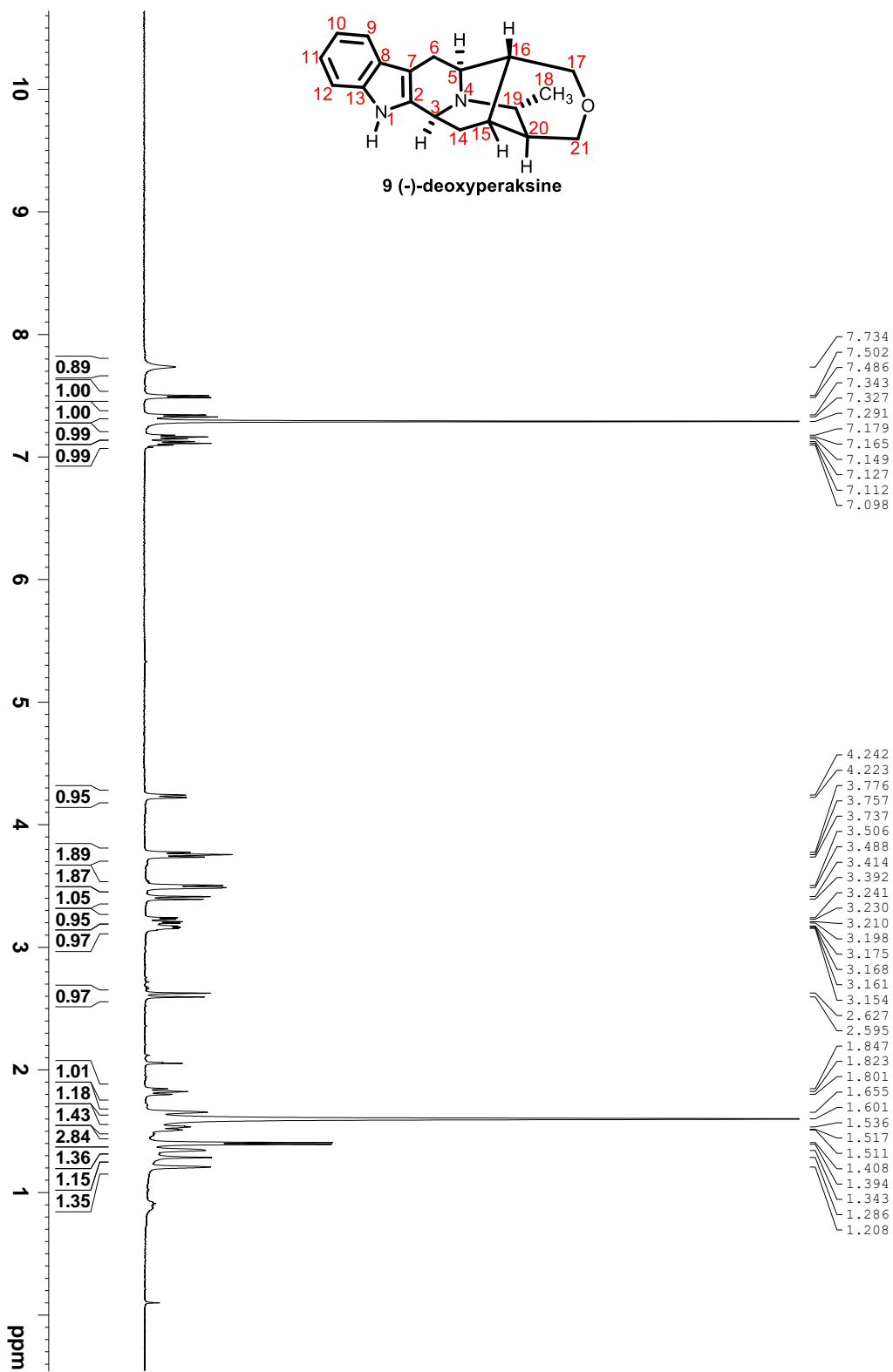
NOESY NMR spectrum of (+)-**8** (300 MHz, CD₃OD)



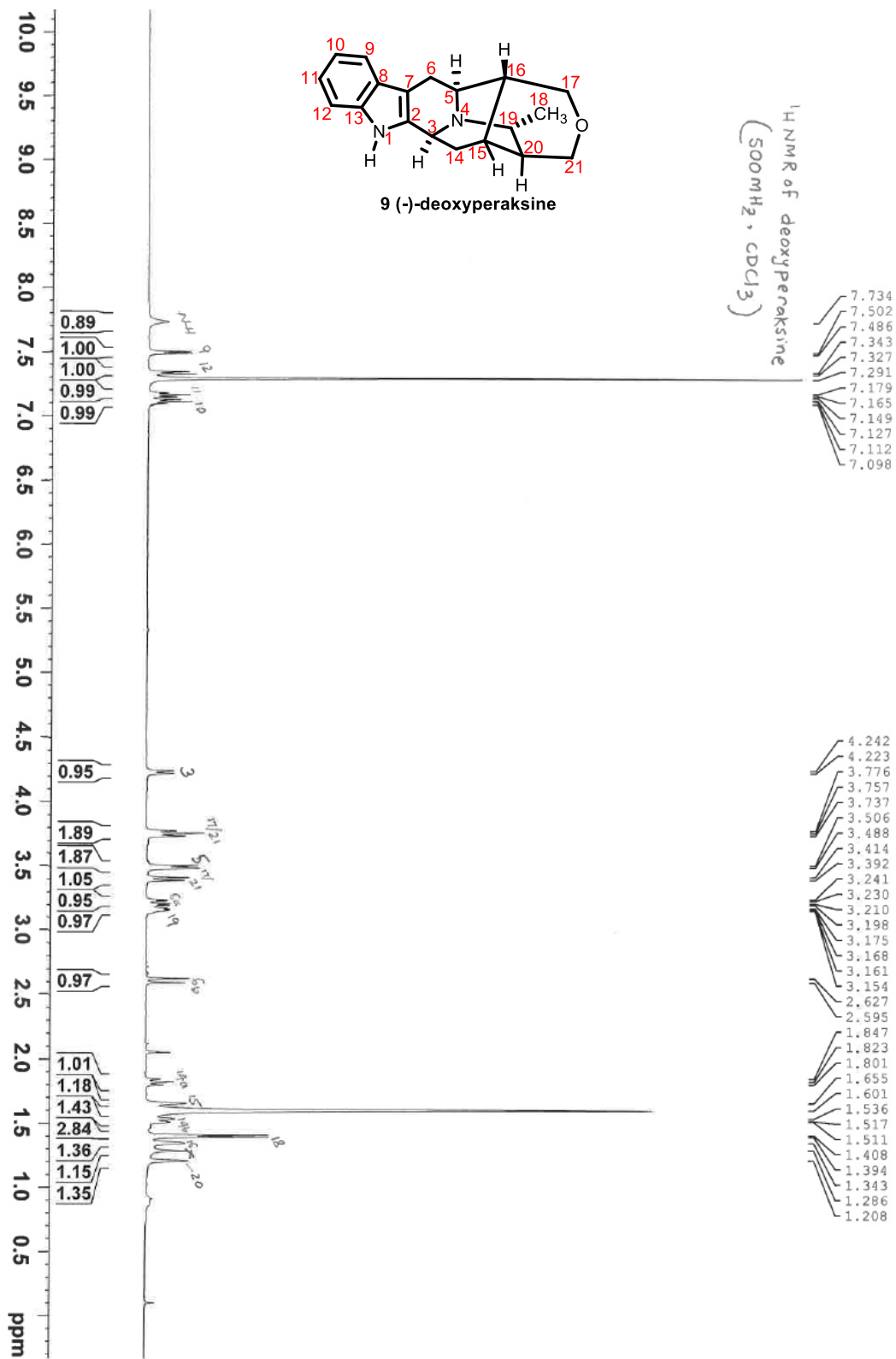
1D-NOE spectra of (+)-**8**, irradiation of H-3 (300 MHz, CD₃OD)



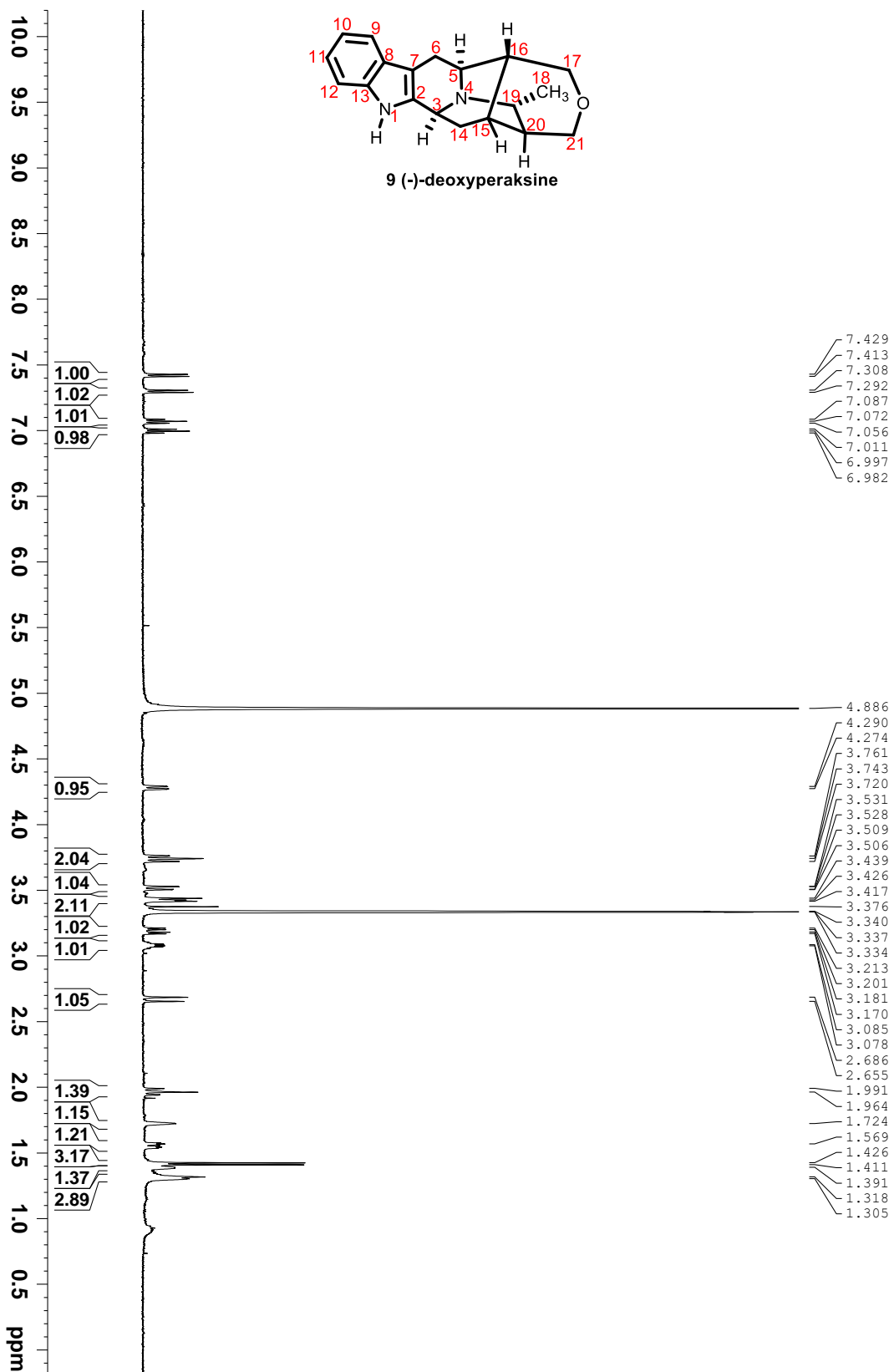
1D-NOE spectra of (+)-8, irradiation of H-18 (300 MHz, CD₃OD)



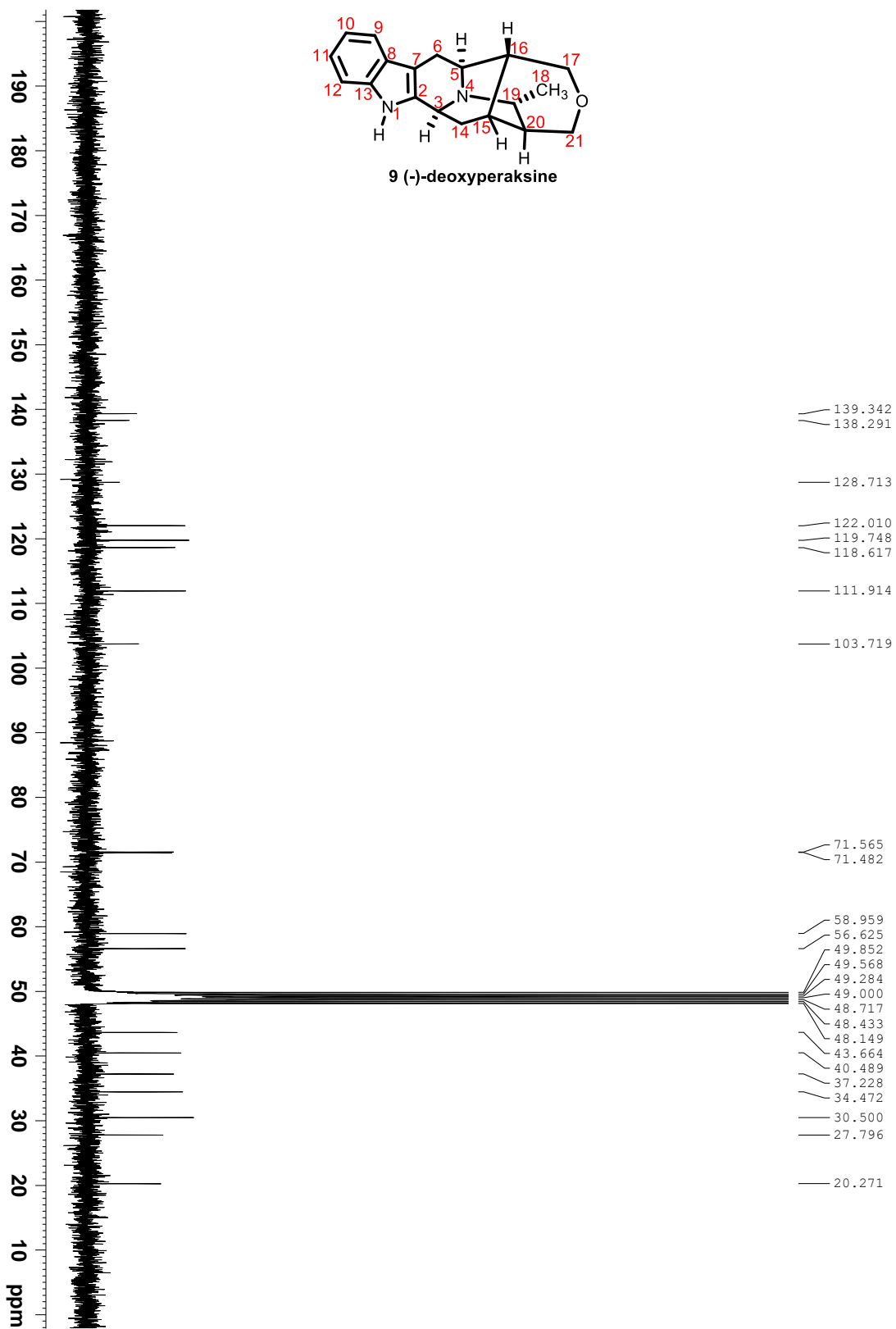
¹H NMR spectrum of (-)-9 (500 MHz, CDCl₃)



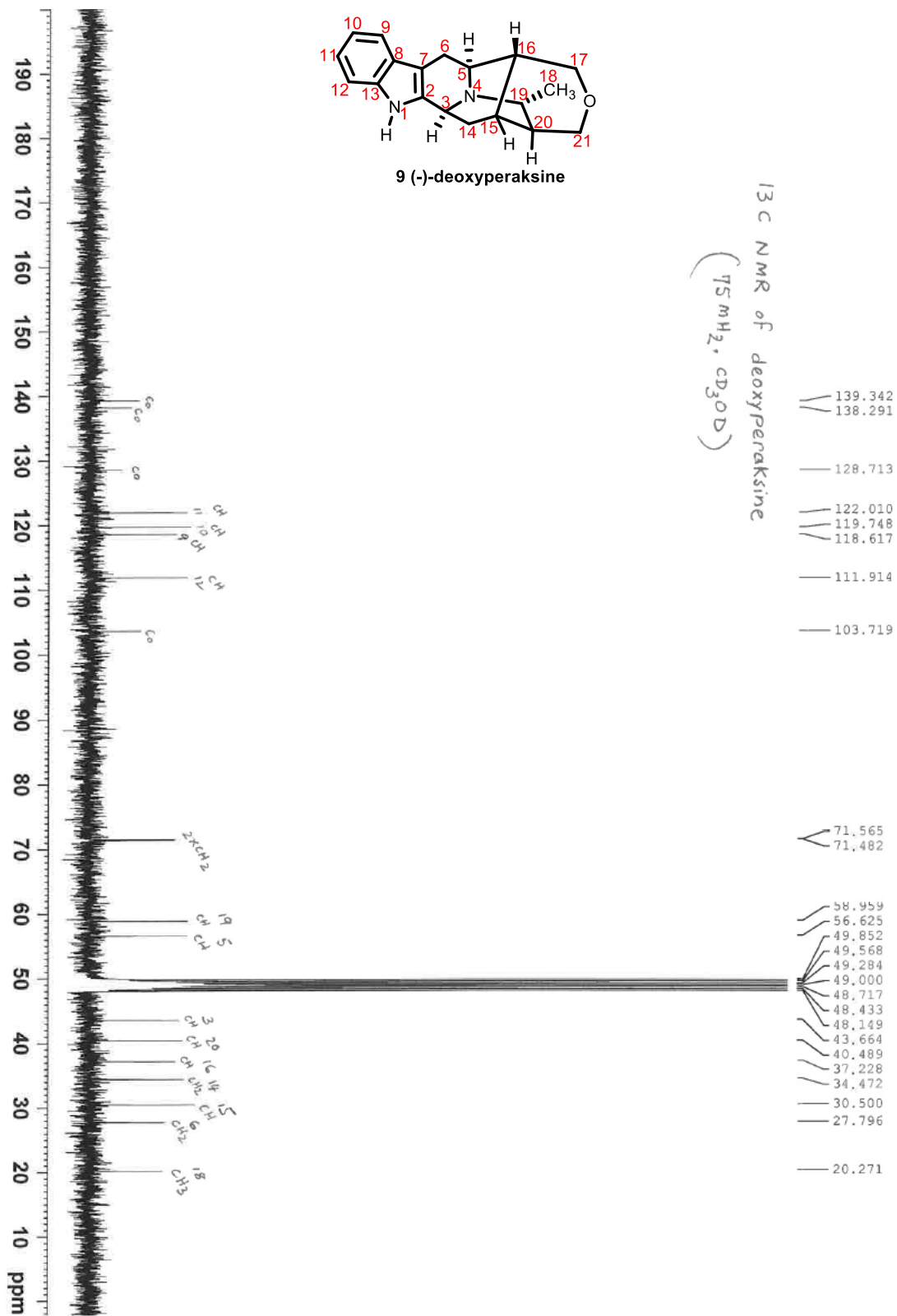
¹H NMR spectrum of (-)-9 (500 MHz, CDCl₃)



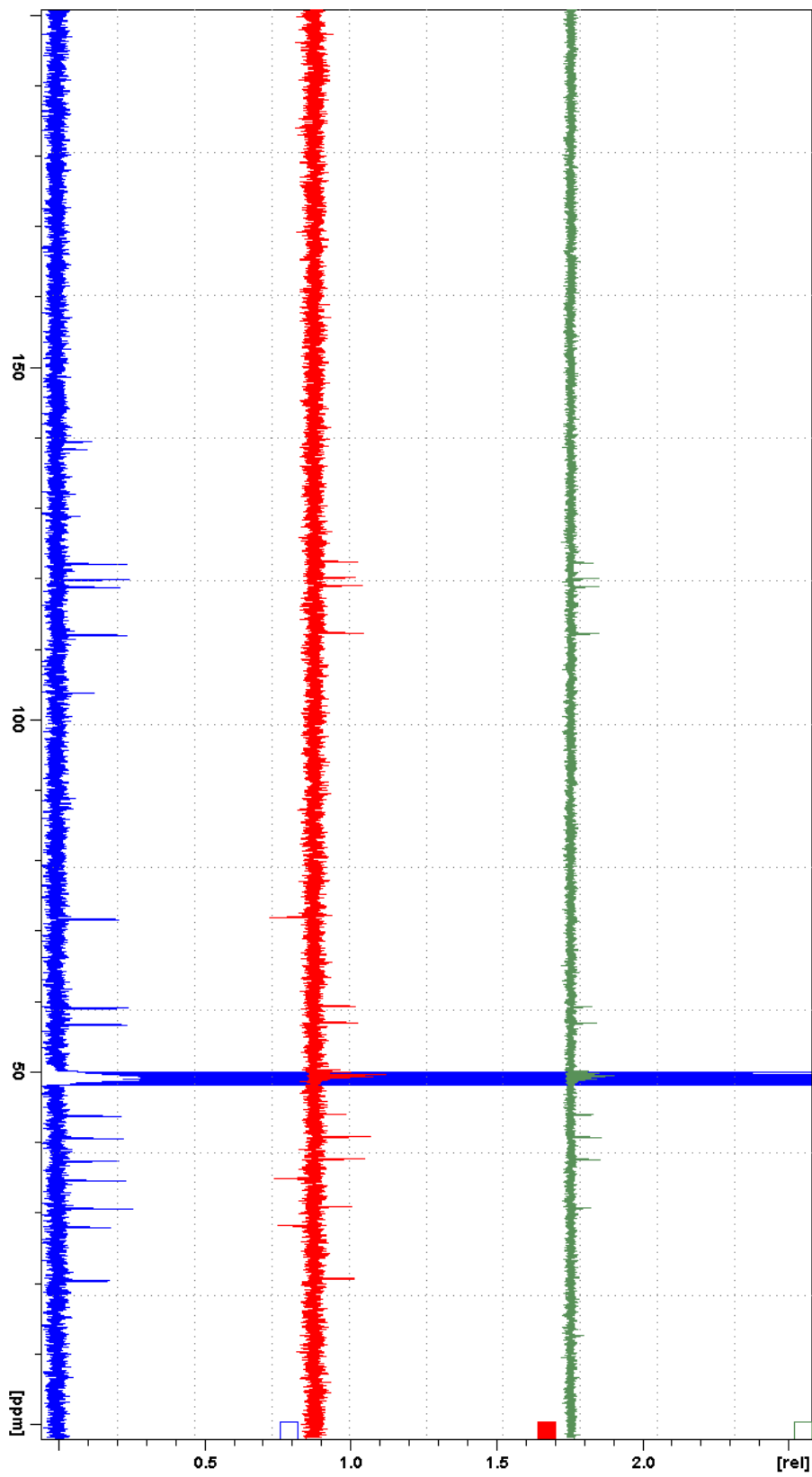
¹H NMR spectrum of (-)-9 (500 MHz, CD₃OD)



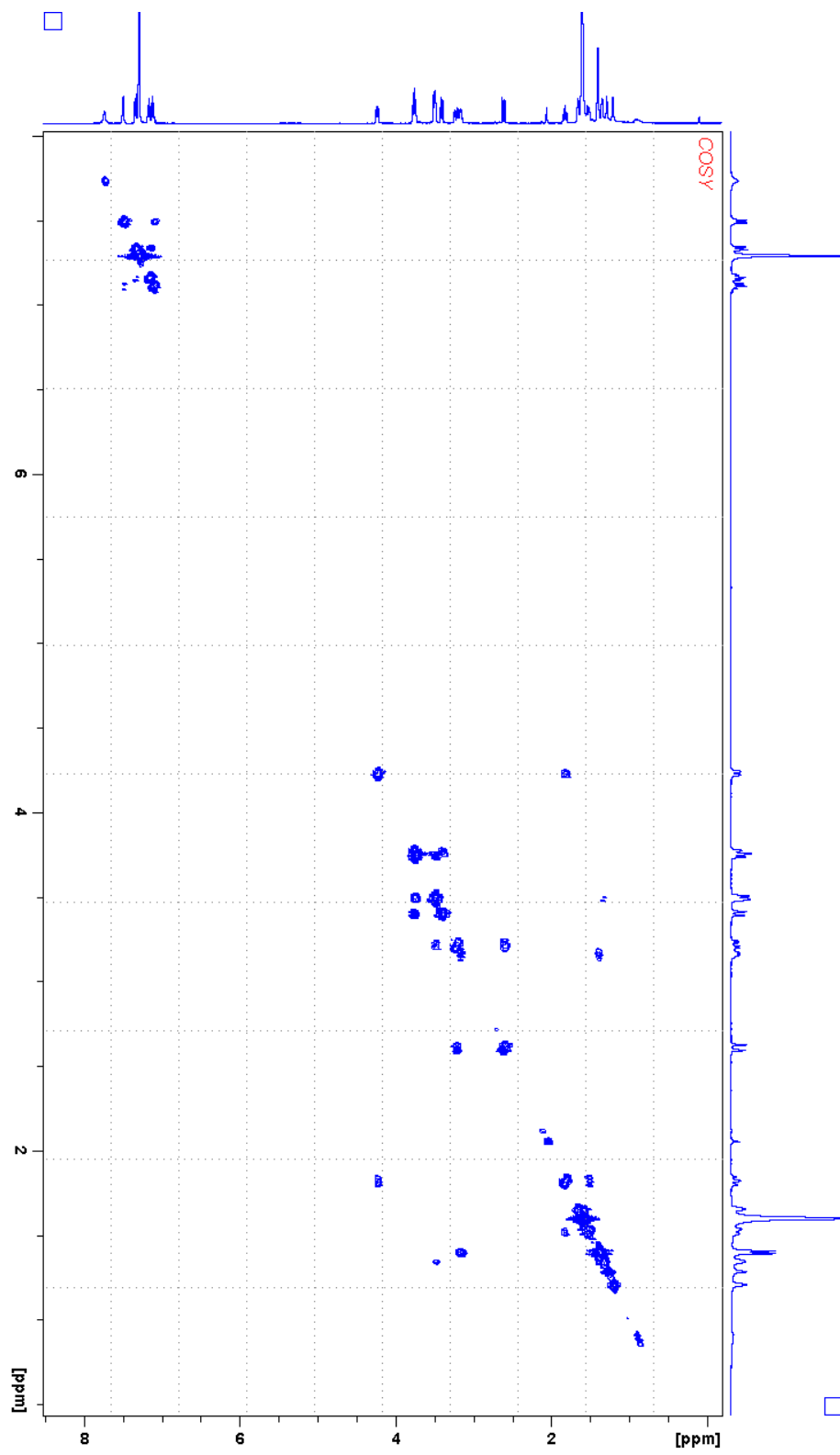
^{13}C NMR spectrum of (-)-**9** (75 MHz, CD_3OD)



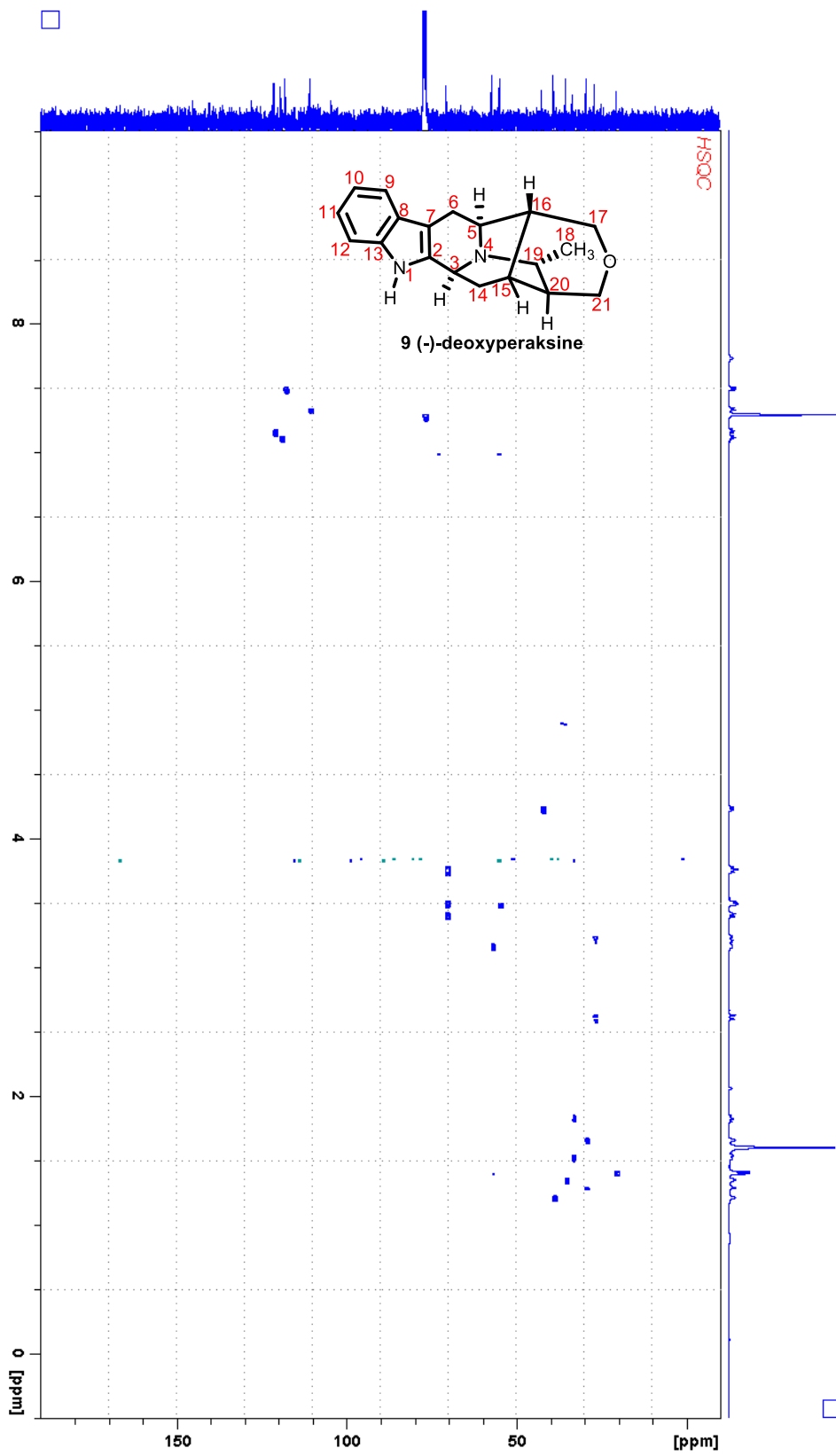
¹³C NMR spectrum of (-)-9 (75 MHz, CD₃OD)



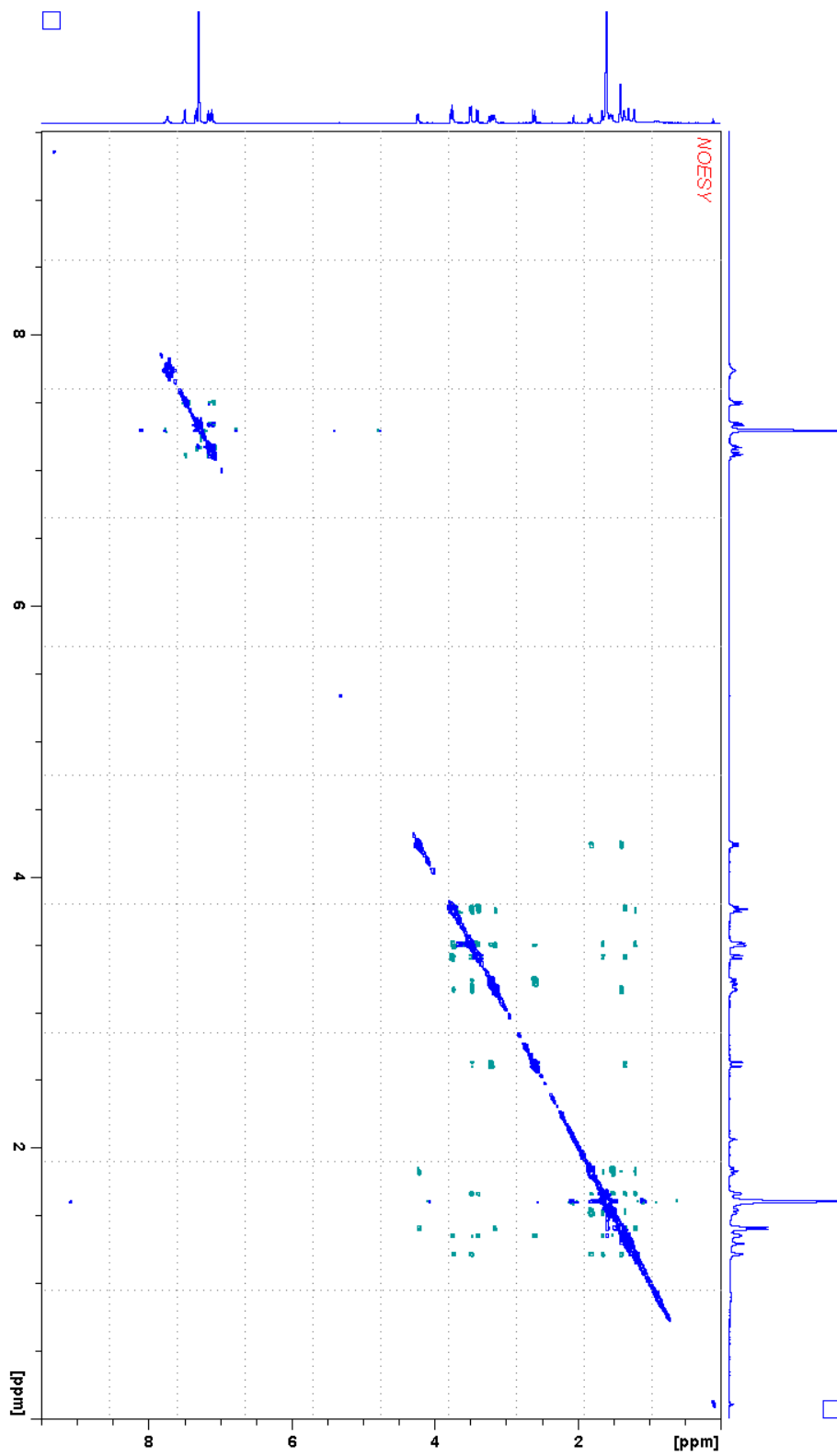
^{13}C vs DEPT 135 and DEPT-90 spectra of (-)-**9** (75 MHz, CD_3OD)



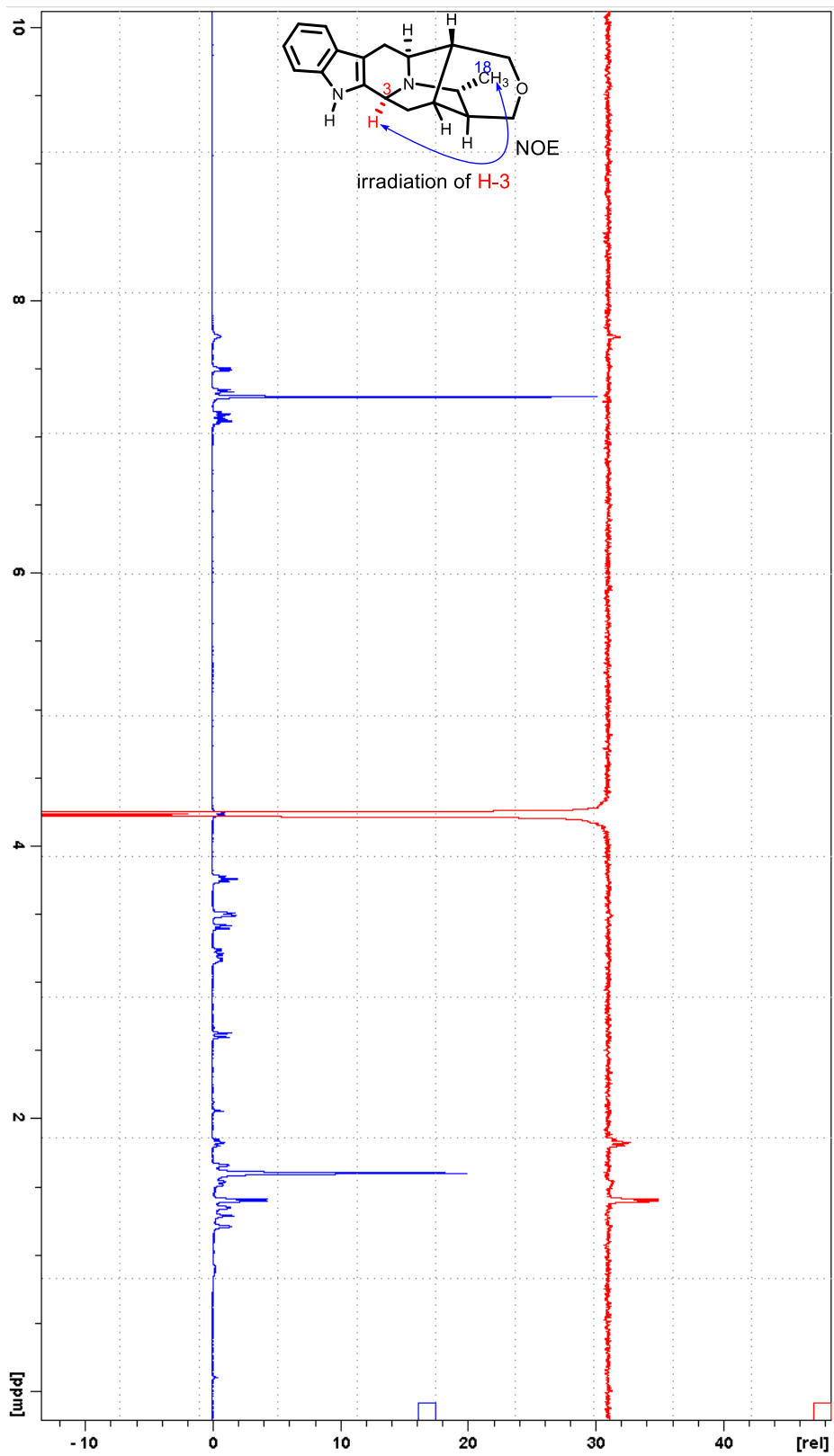
COSY NMR spectrum of (-)-9 (500 MHz, CDCl₃)



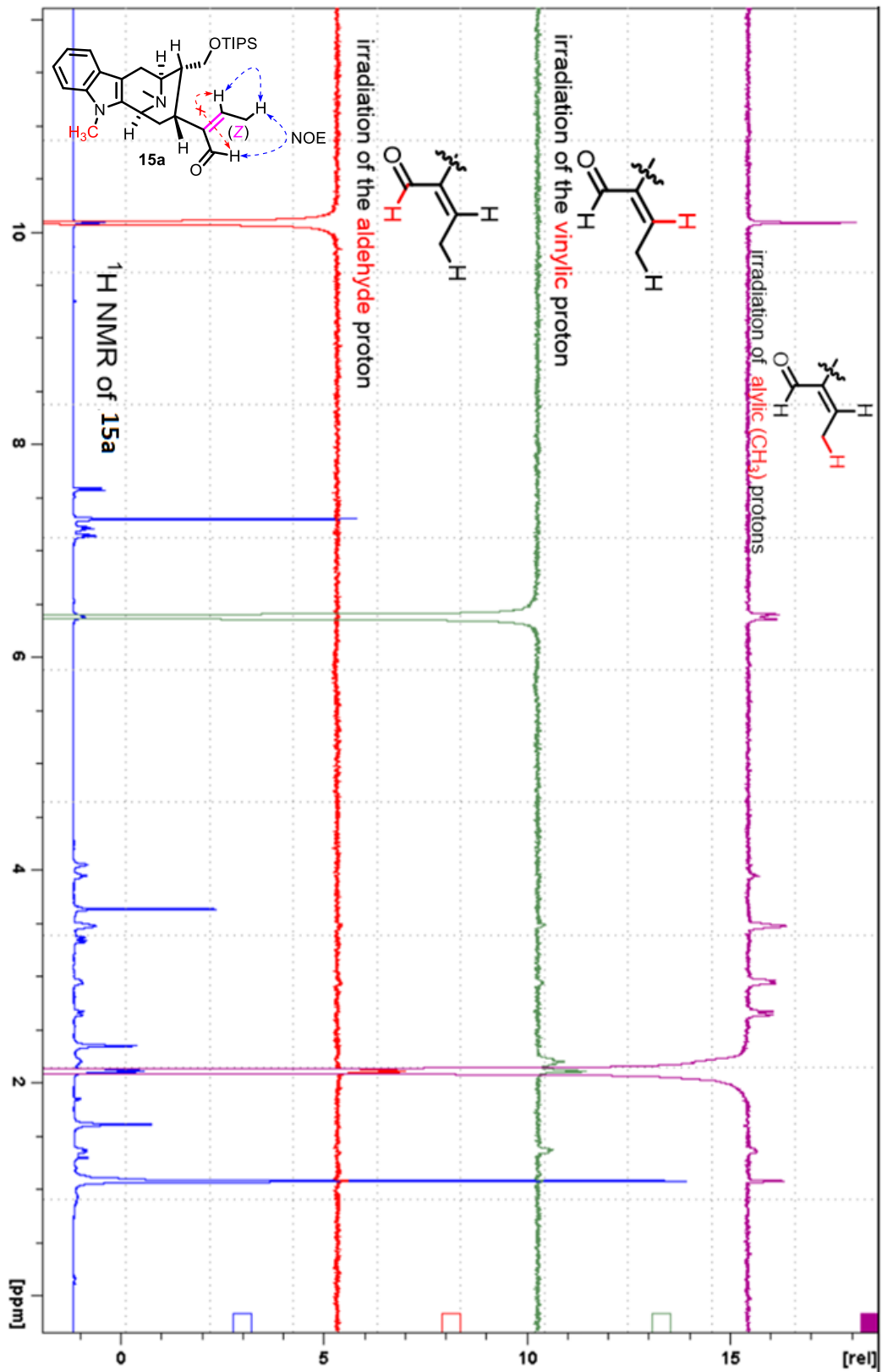
HSQC NMR spectrum of (-)-9 (500 MHz, 125 MHz, CDCl₃)



NOESY NMR spectrum of (-)-**9** (500 MHz, CDCl₃)



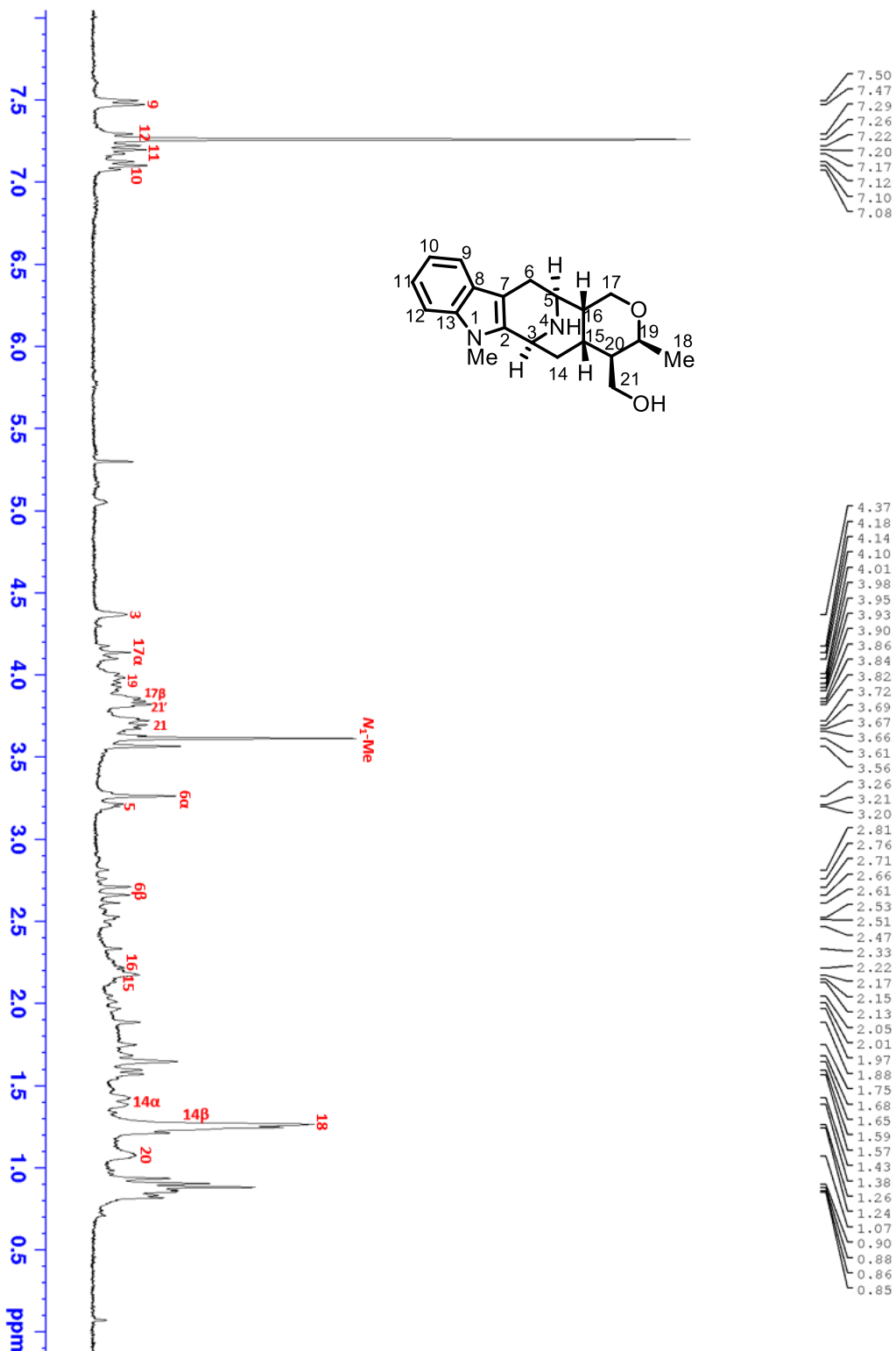
1D NOE NMR Spectrum of (-)-9 to confirm α -configuration of the C-19 methyl function



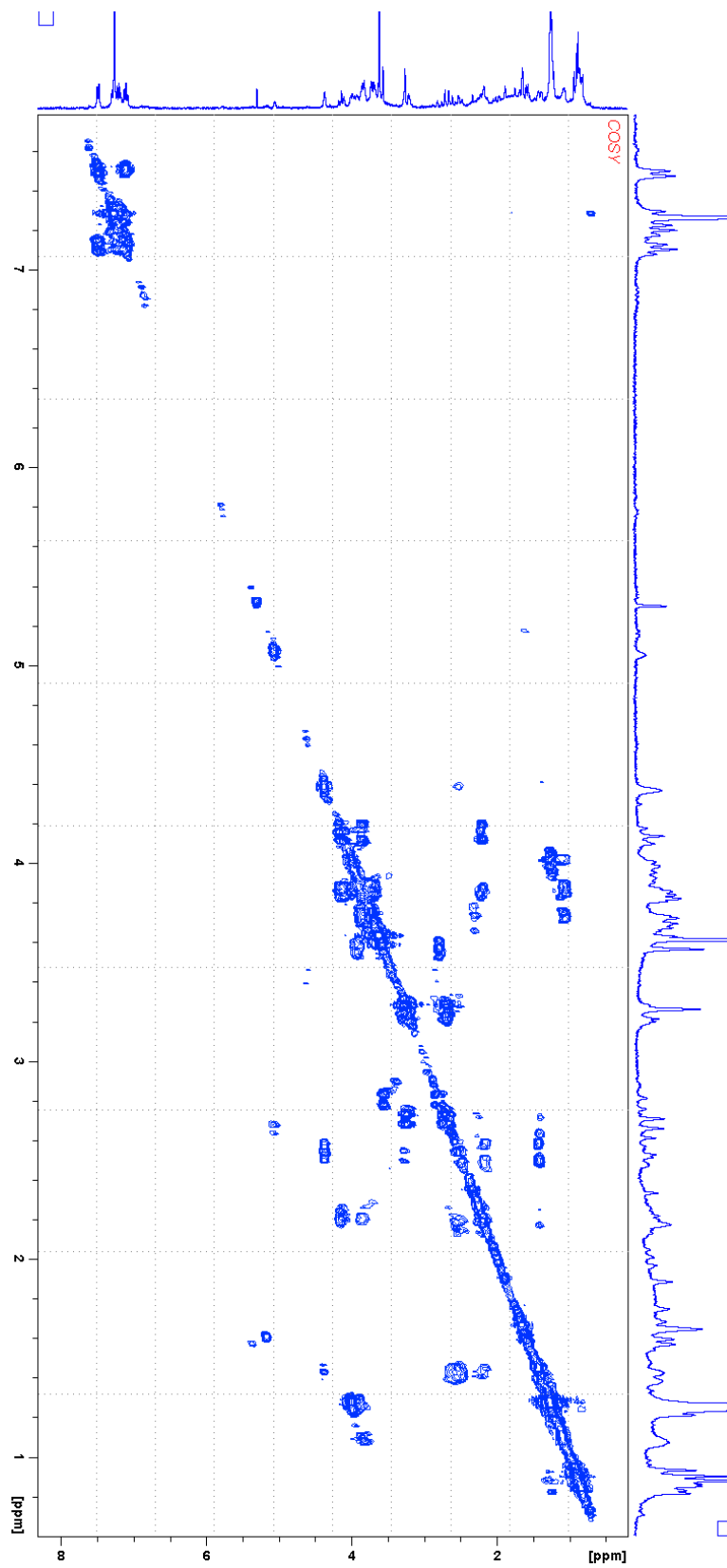
1D NOE spectra of **15a** to confirm the olefin geometry

VIII Appendix F (Chapter 6)

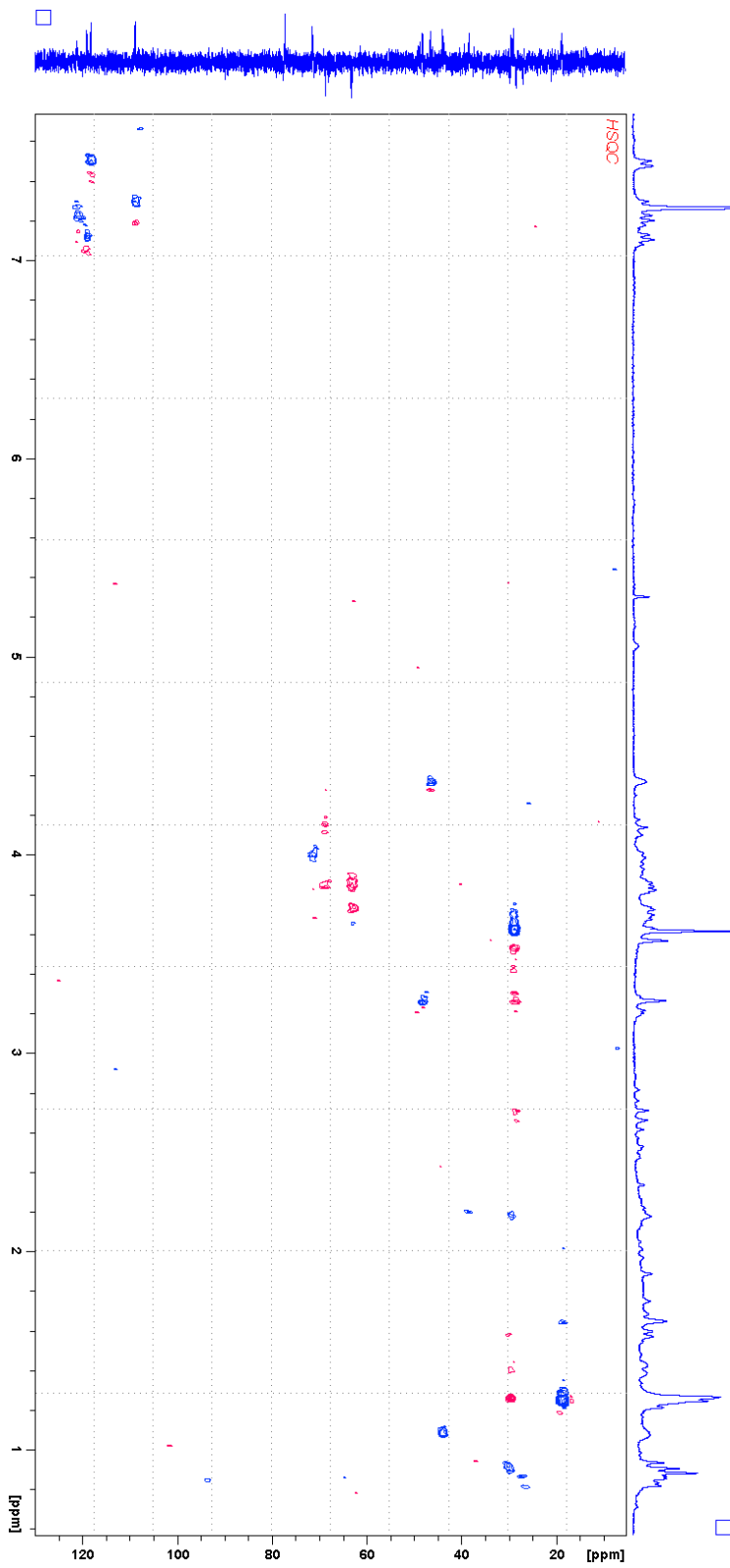
NMR spectra of the synthetic alkaloids 1, 2, 8, 14, and 15



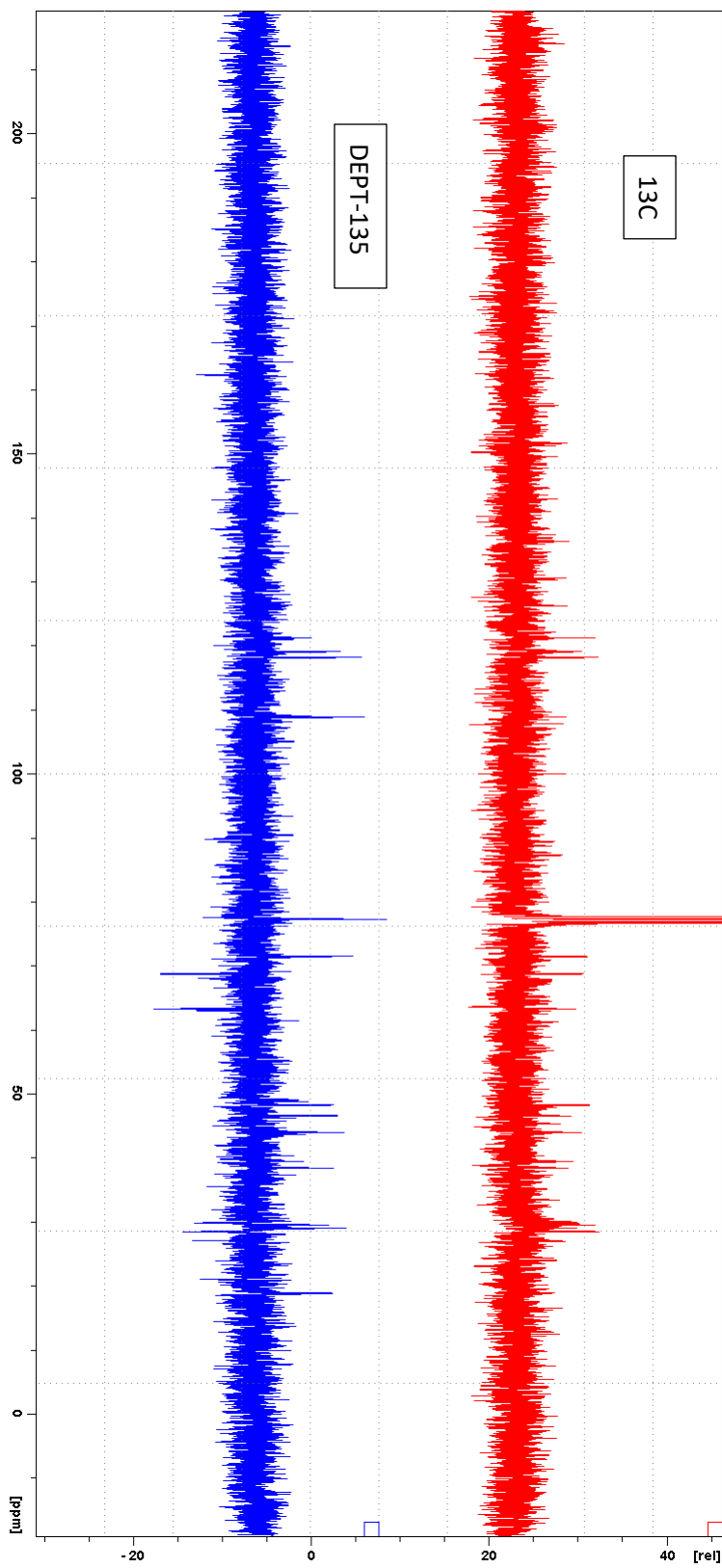
¹H NMR spectrum of macrocarpine F 1 (300 MHz, CDCl₃); Assignment is based on ¹H, DEPT-135, COSY and HSQC NMR correlations



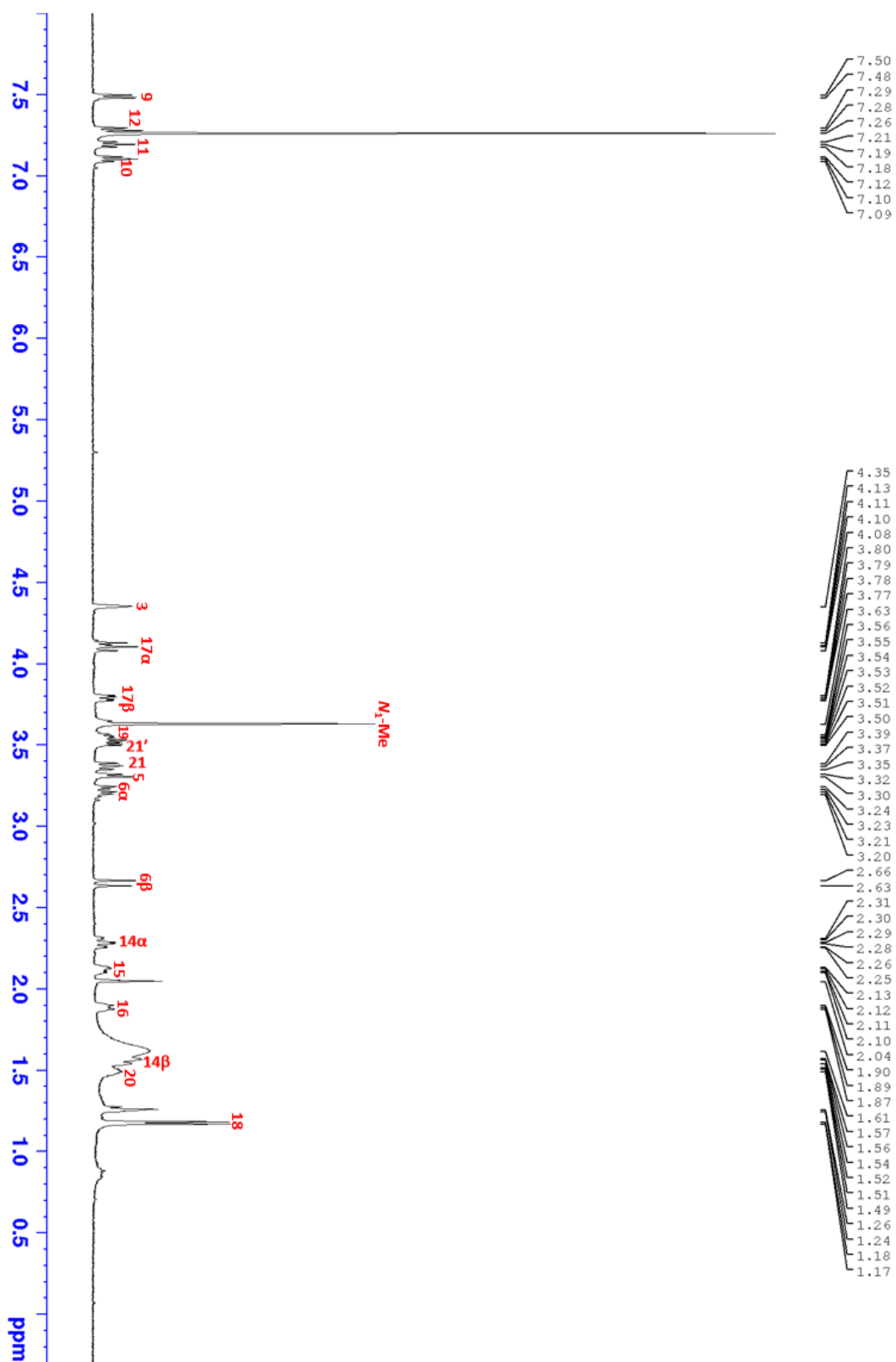
COSY NMR spectrum of macrocarpine F 1 (300 MHz, CDCl₃)



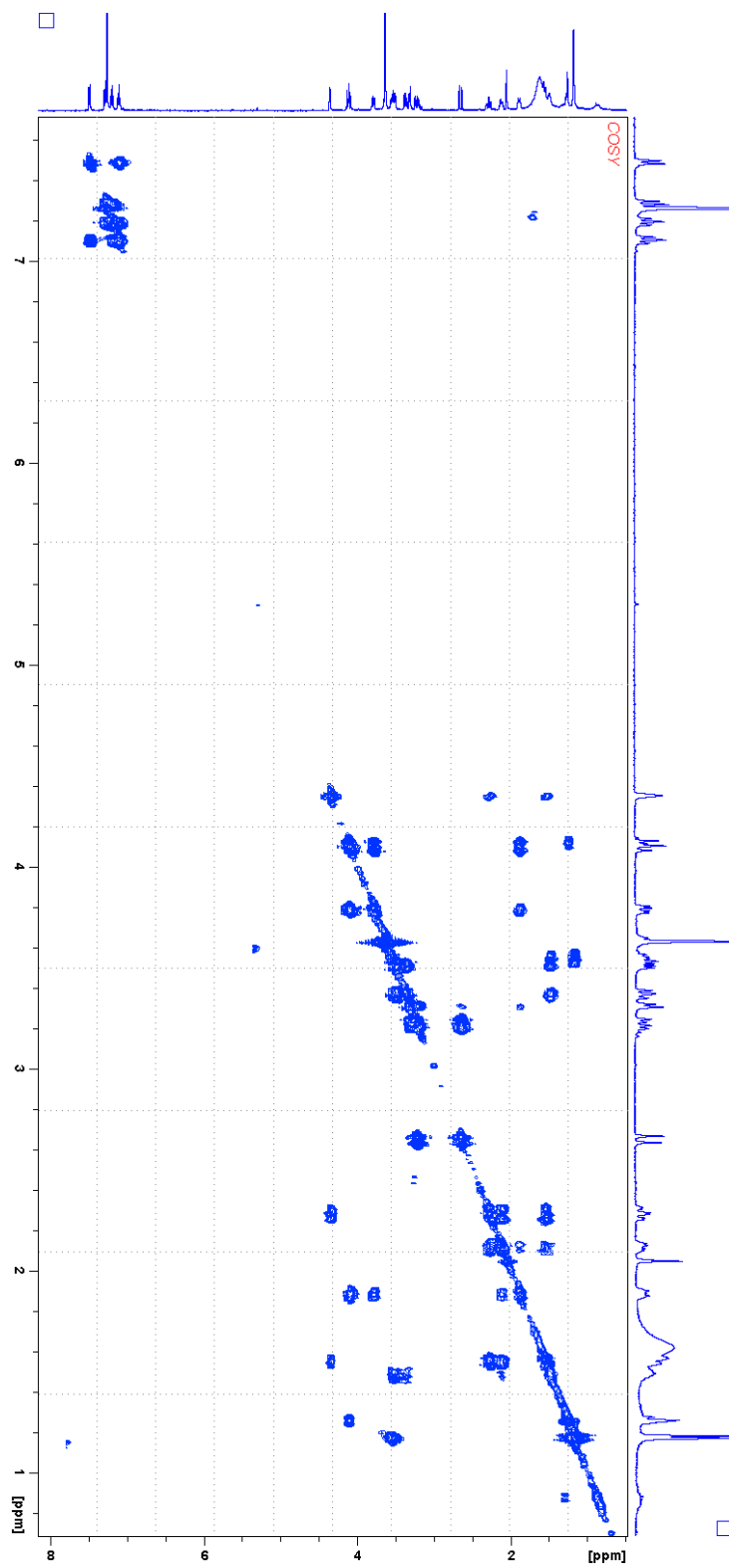
HSQC NMR spectrum of macrocarpine F 1 (300, 75 MHz, CDCl₃)



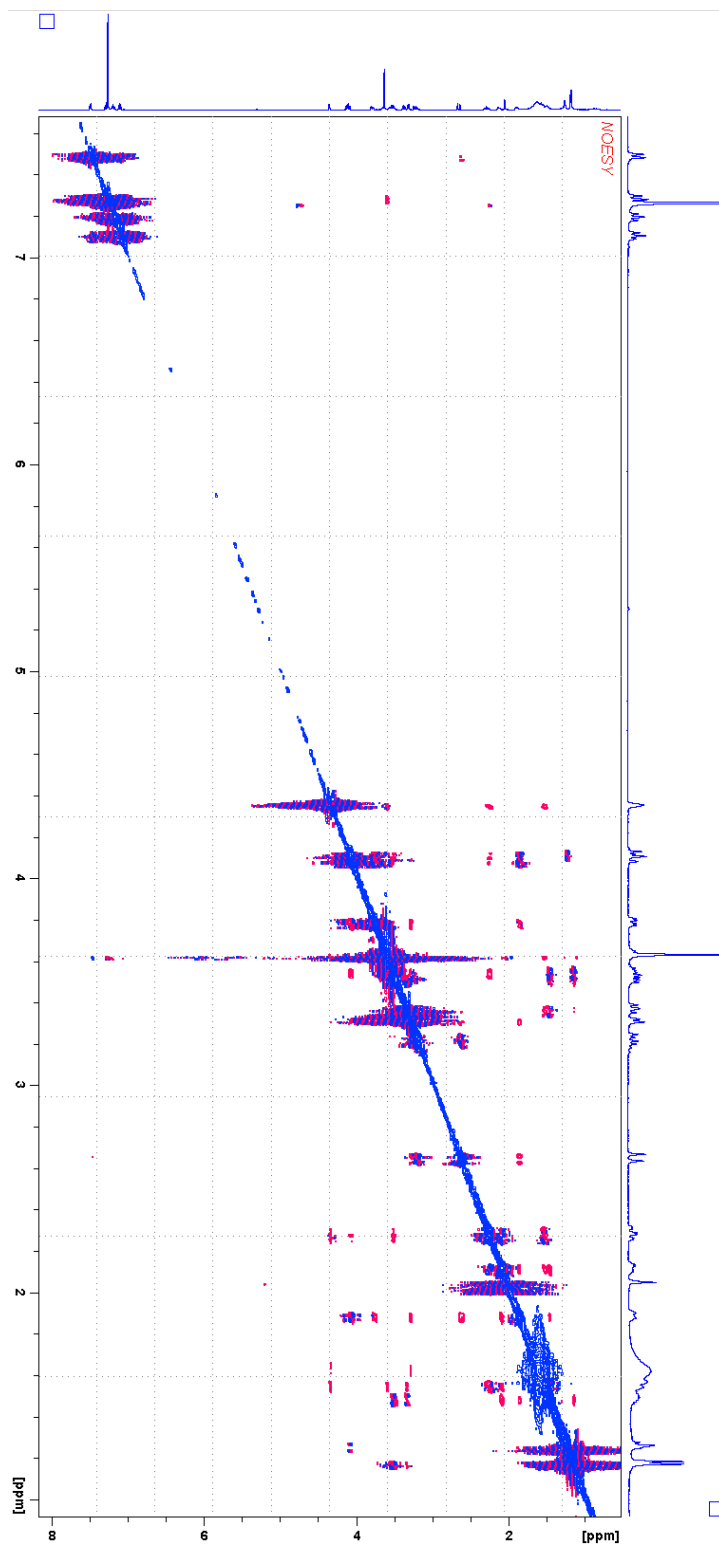
^{13}C and DEPT-135 NMR spectra of macrocarpine F 1 (75 MHz, CDCl_3)



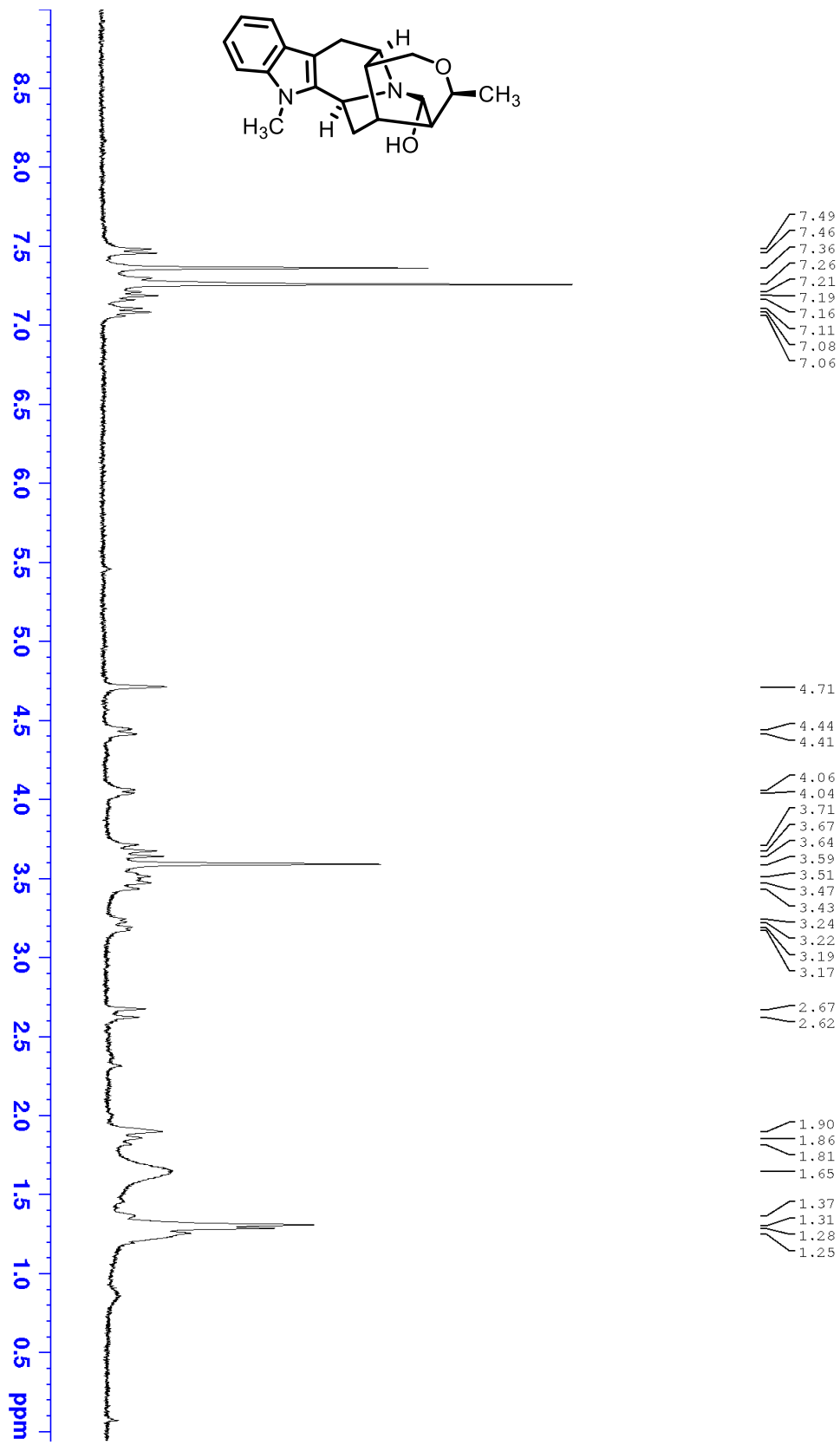
¹H NMR spectrum of synthetic macrocarpine G 2 (500 MHz, CDCl₃)



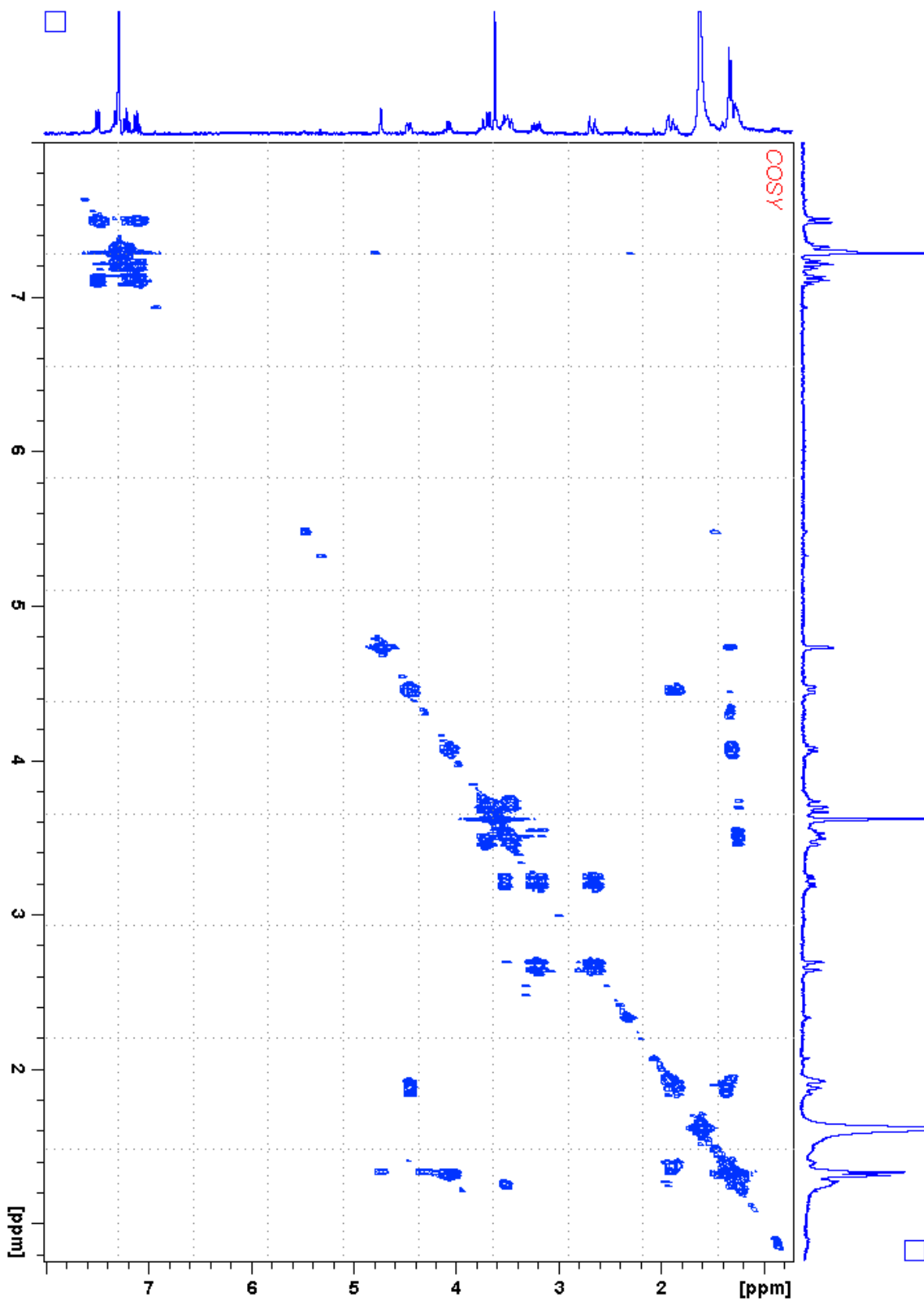
COSY NMR spectrum of synthetic macrocarpine G 2 (500 MHz, CDCl₃)



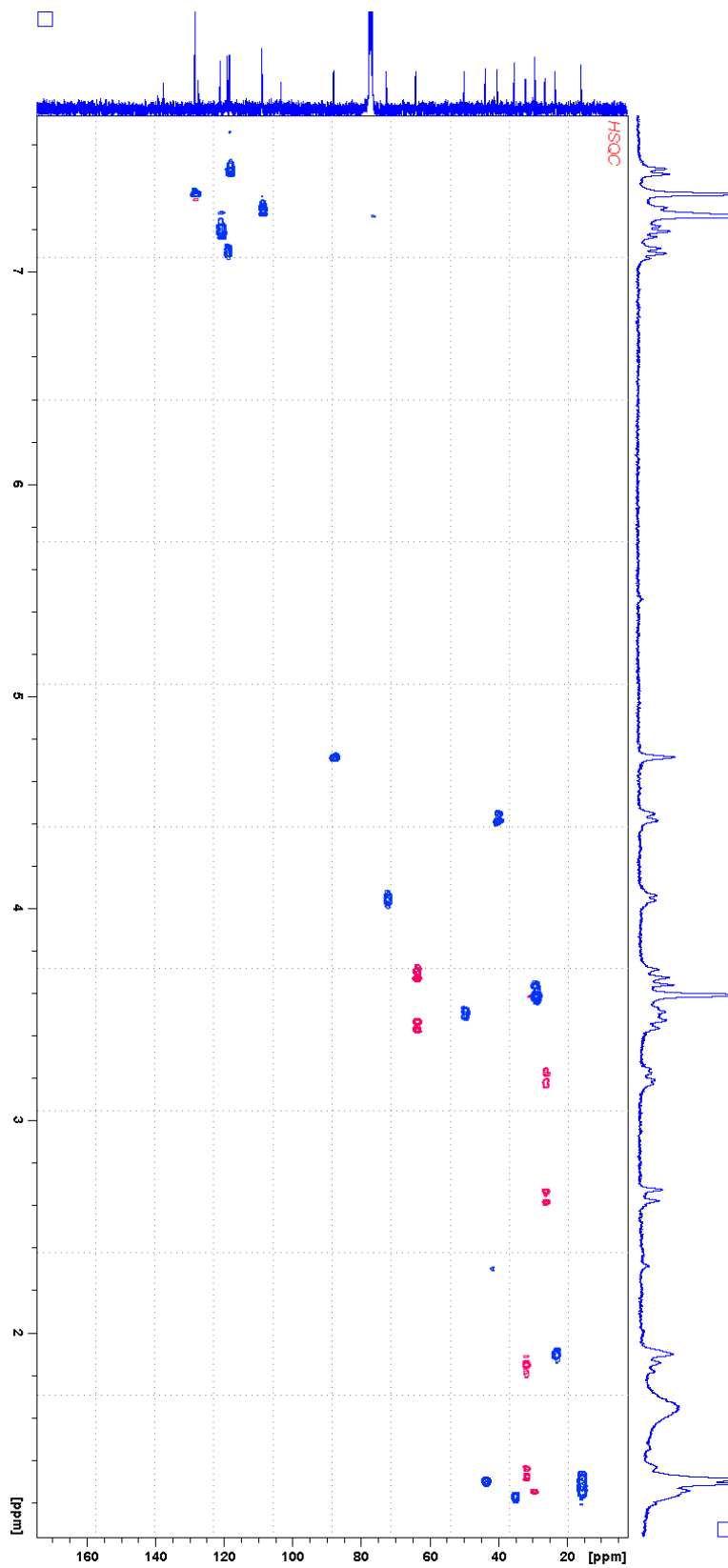
NOESY NMR spectrum of macrocarpine G 2 (500 MHz, CDCl₃)



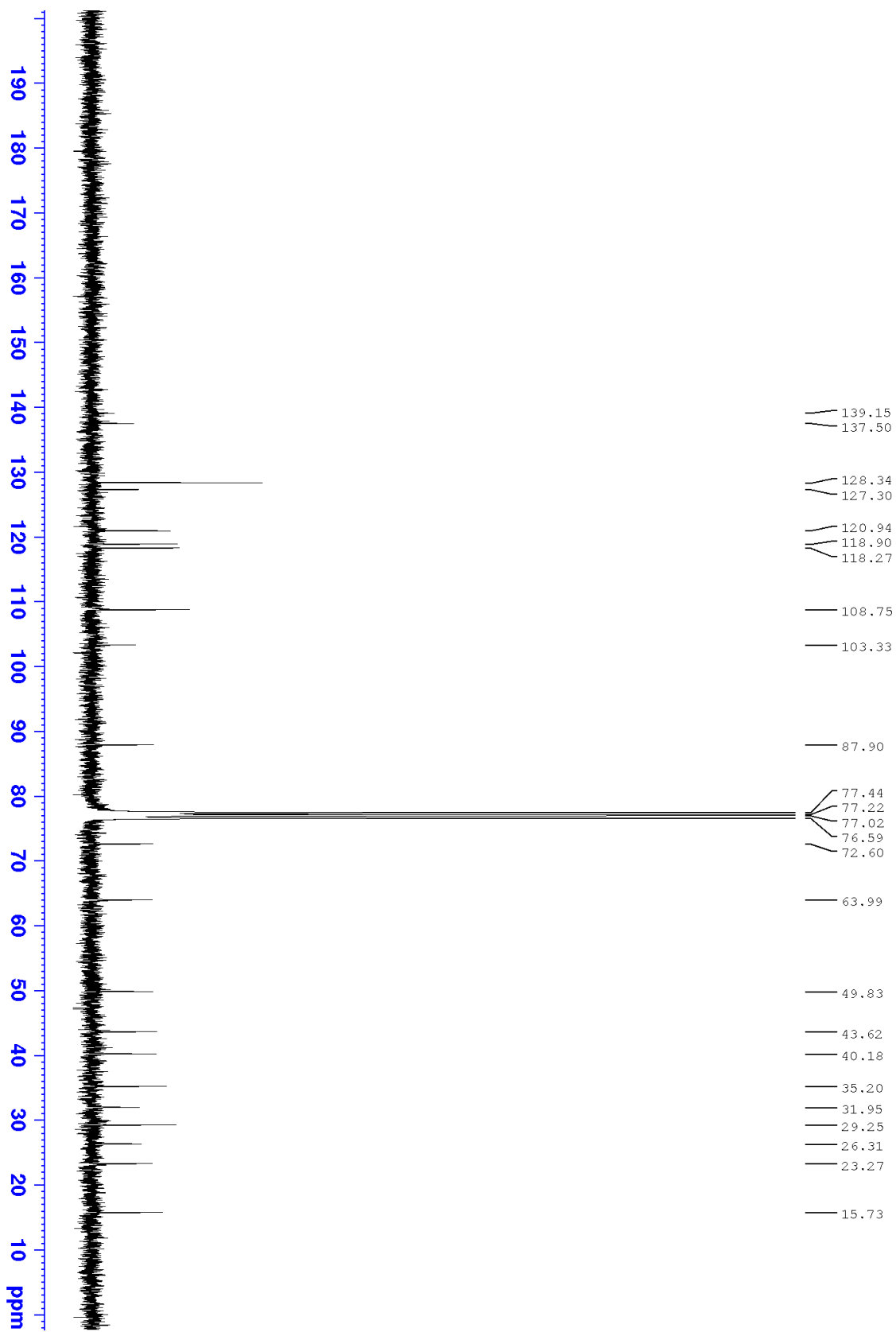
¹H NMR spectrum of talpinine **8** (300 MHz, CDCl₃)



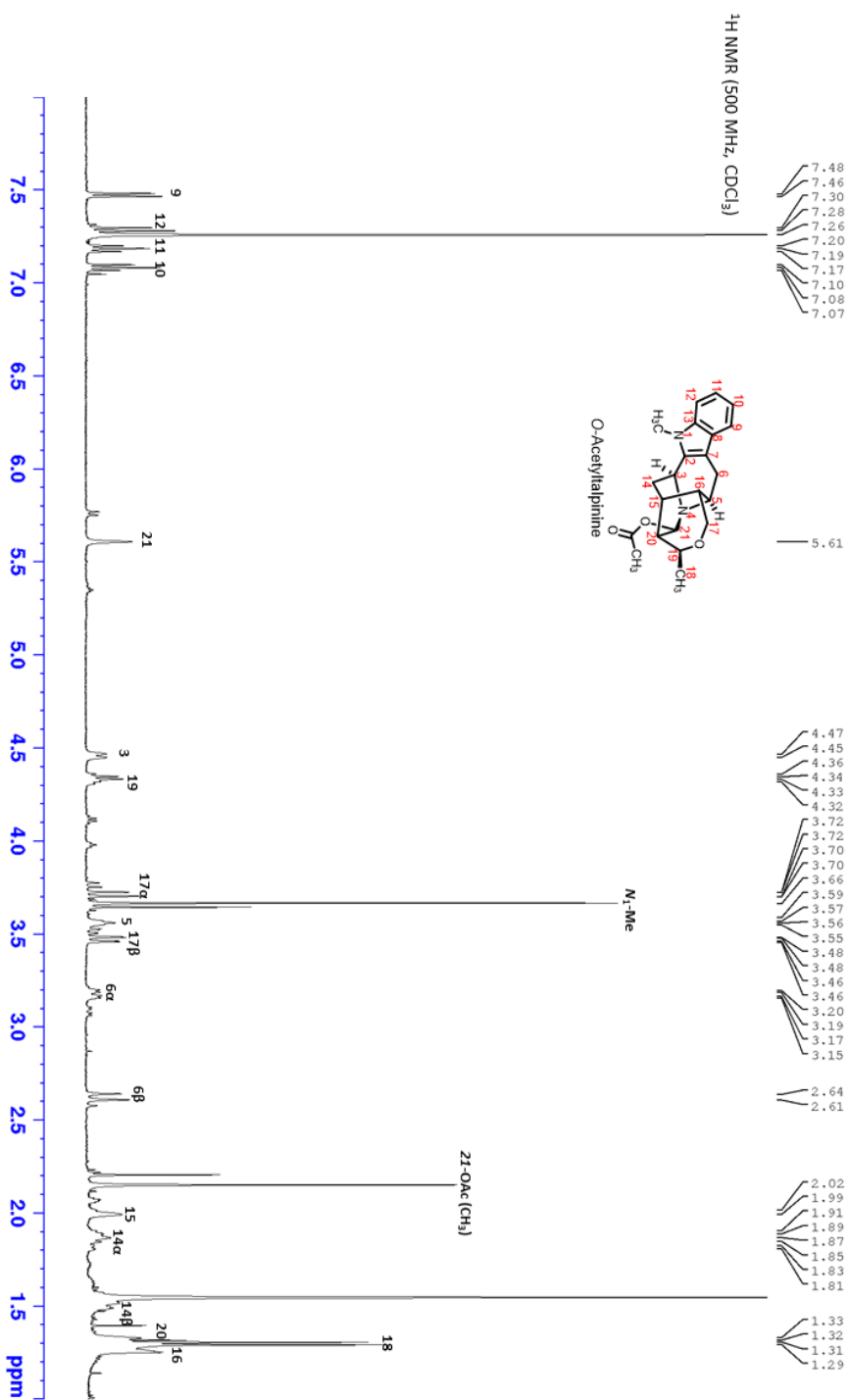
COSY NMR spectrum of talpinine **8** (300 MHz, CDCl₃)



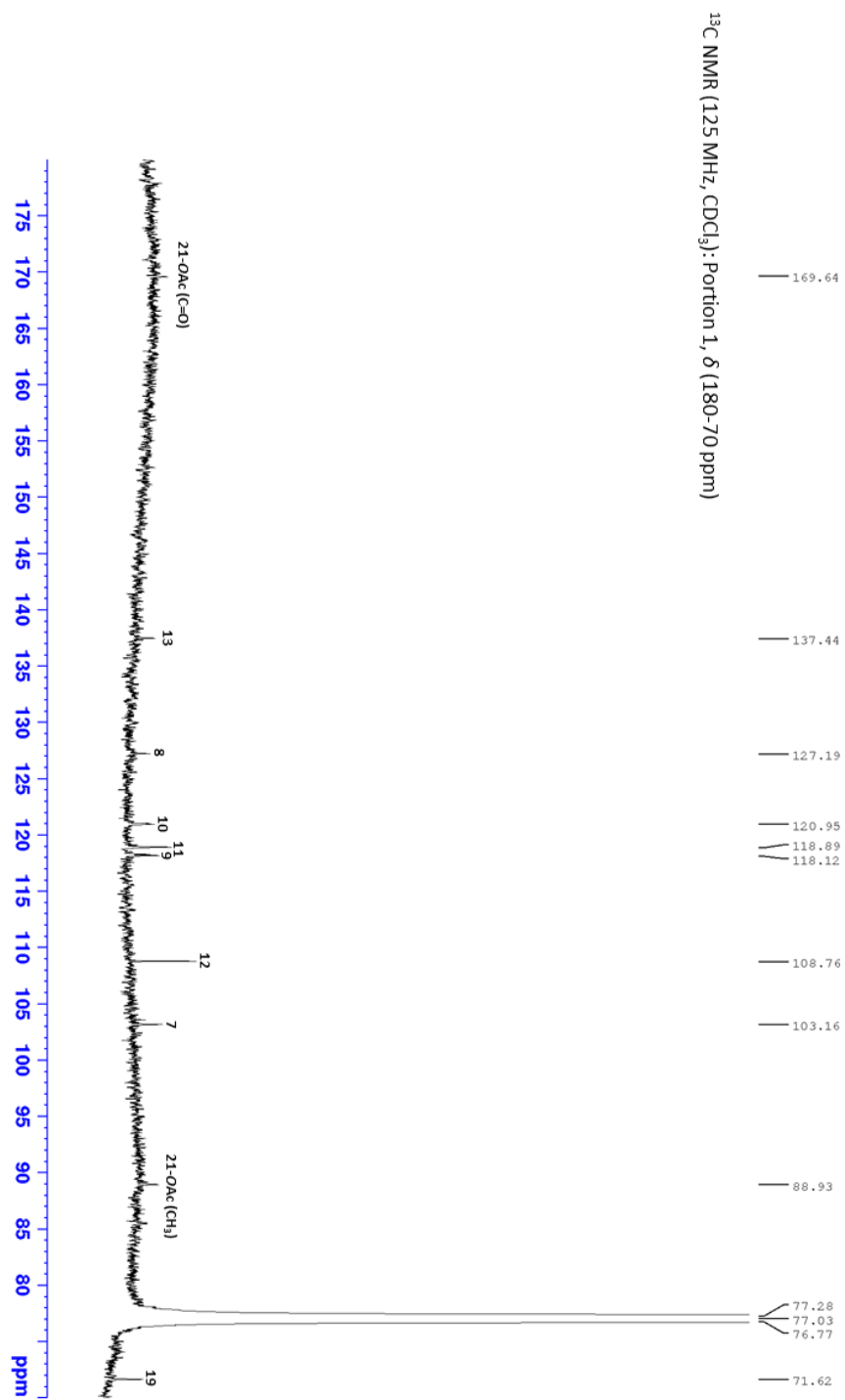
HSQC NMR spectrum of talpinine **8** (300, 75 MHz, CDCl₃)



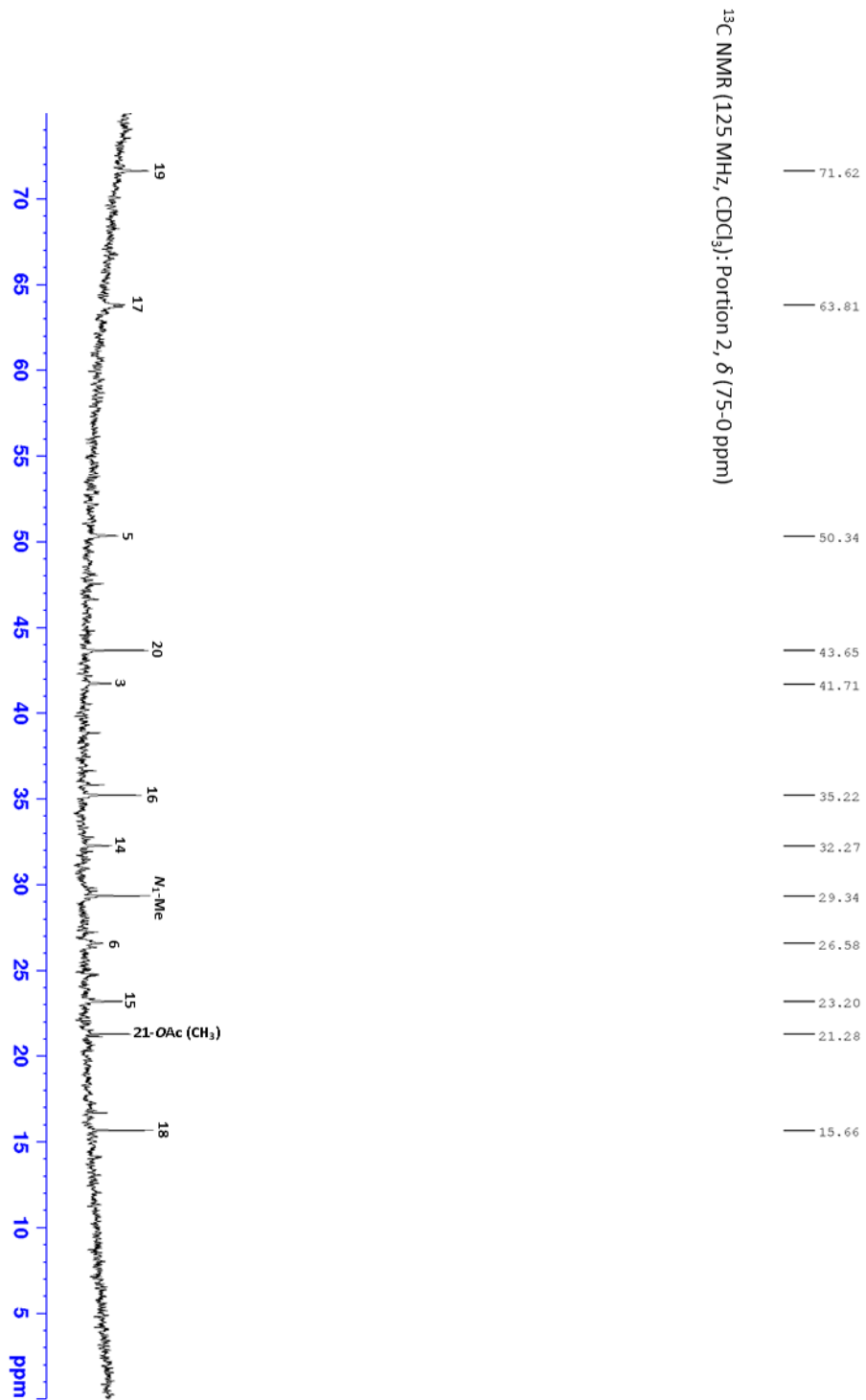
¹³C NMR spectrum of talpinine **8** (75 MHz, CDCl₃)



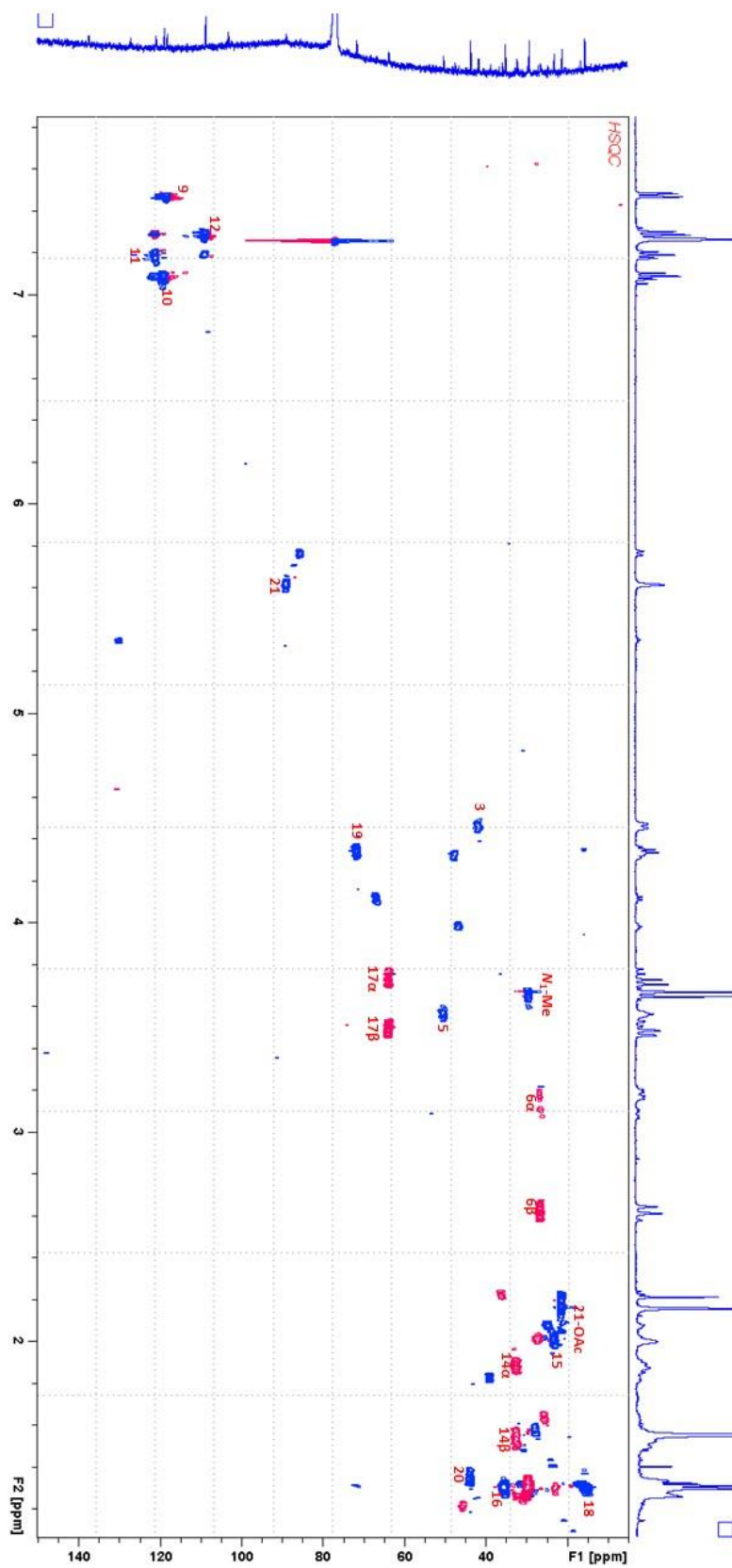
Assigned ¹H spectrum of *O*-acetyltalpinine **14** (500 MHz, CDCl₃). Assignment was based on ¹H, ¹³C and HSQC NMR correlations



^{13}C NMR spectrum δ 180-70 ppm (125 MHz, CDCl_3) of *O*-acetylalpinine **14**
 (Assignment is based on ^1H , ^{13}C and HSQC NMR correlations)



¹³C NMR spectrum δ 75-0 ppm (125 MHz, CDCl₃) of *O*-acetylaltapinine **14**



Assigned HSQC NMR spectrum of *O*-Acetylaltapinine **14** (500, 125 MHz, CDCl_3)

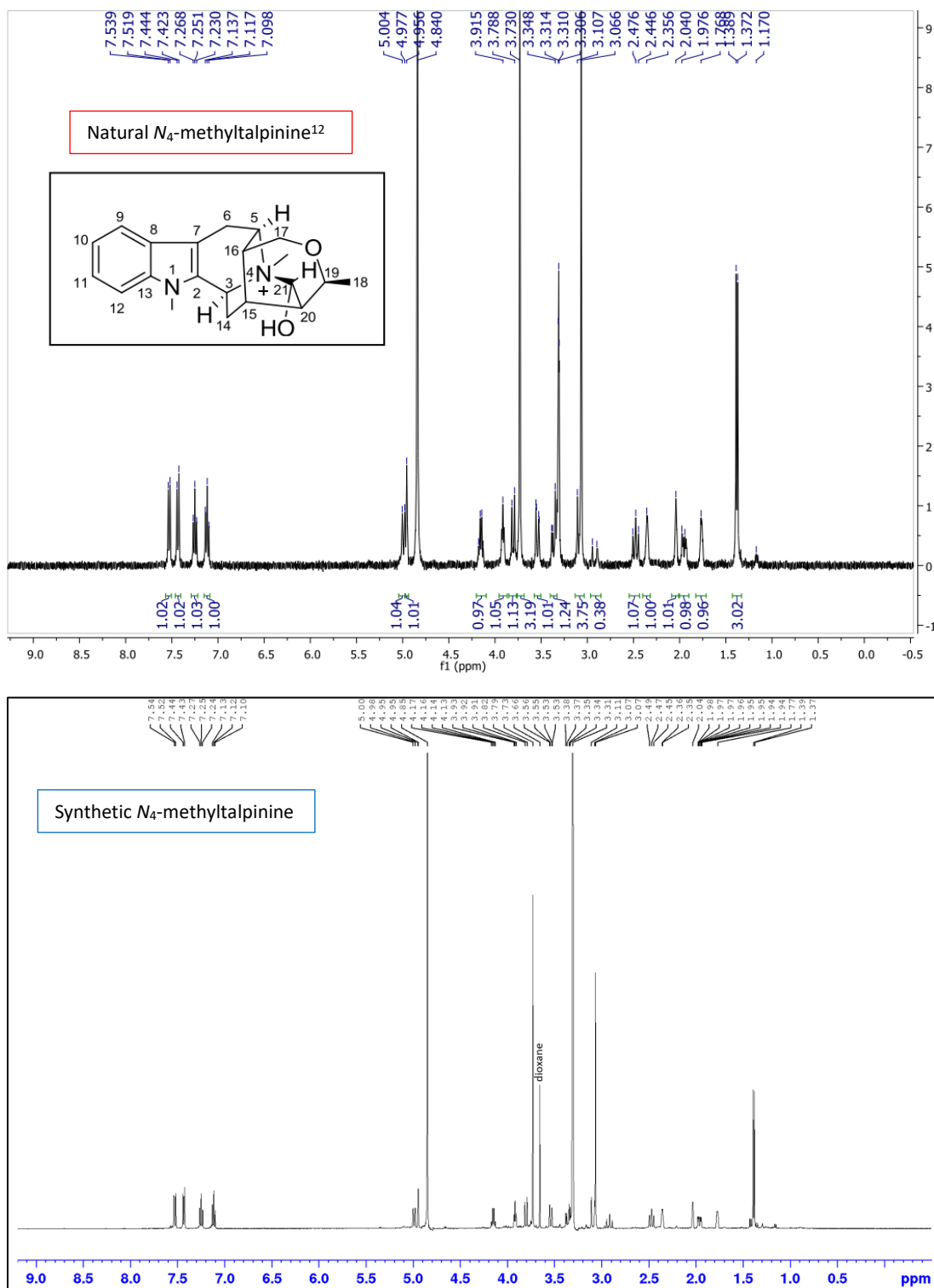
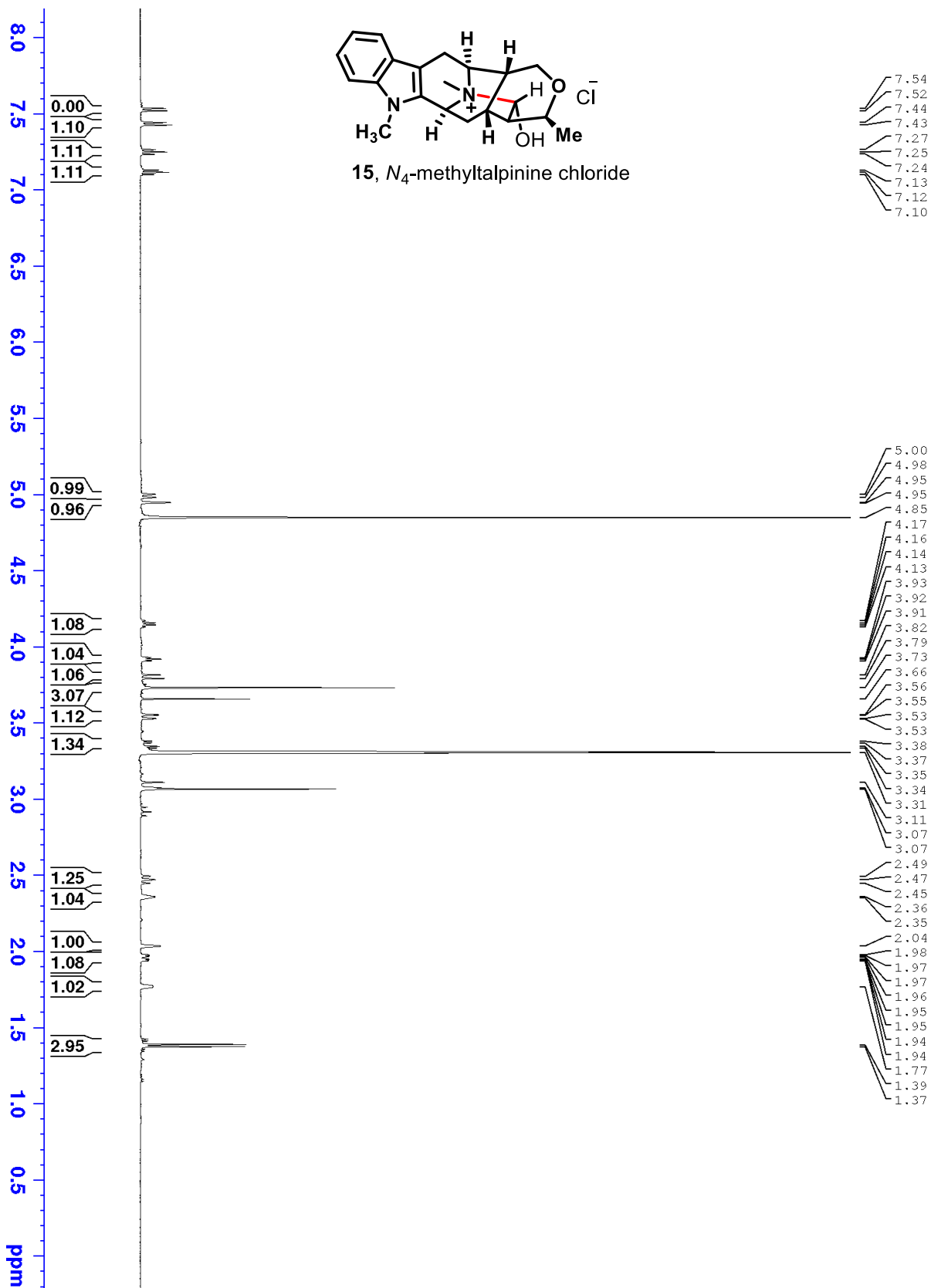
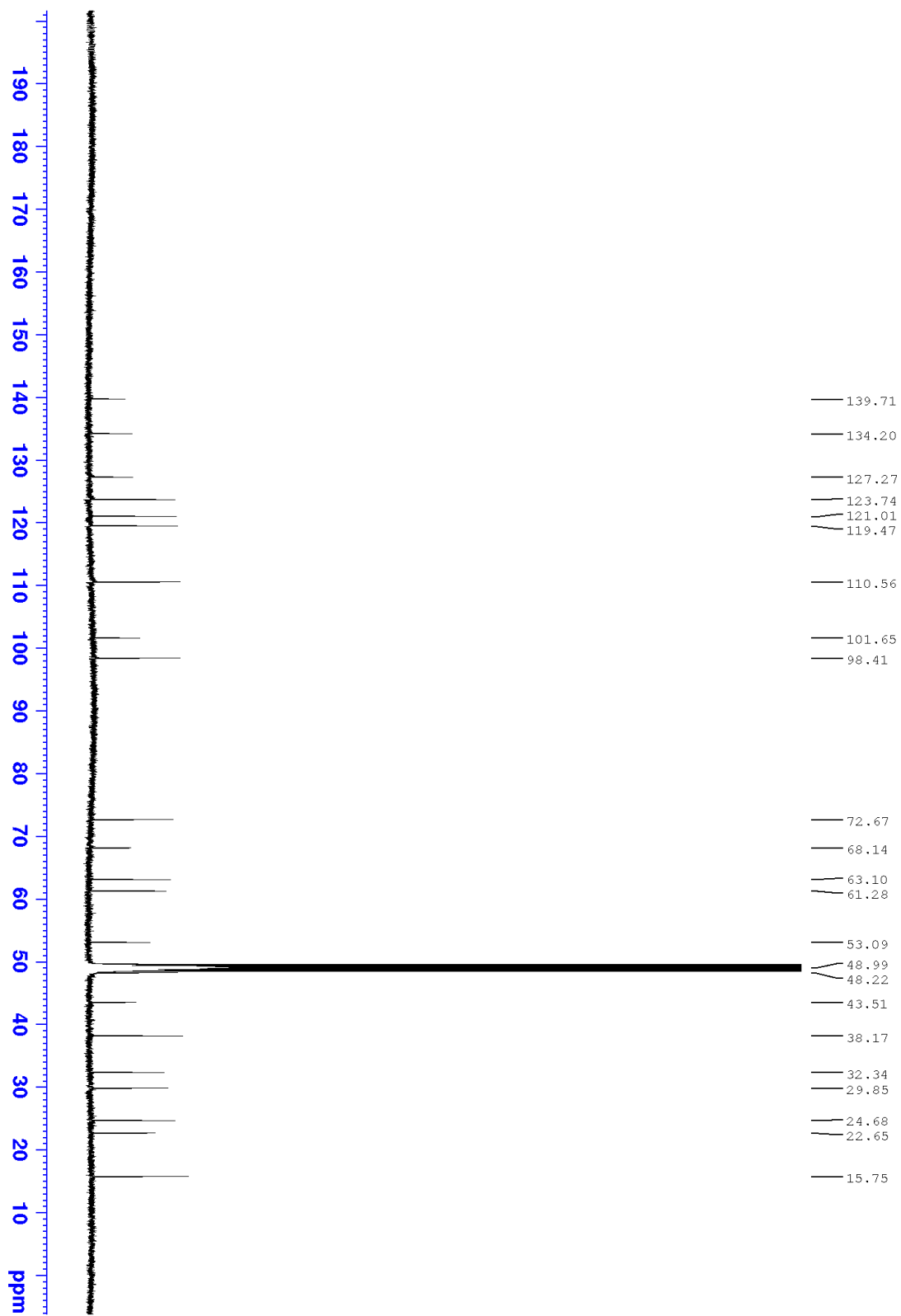


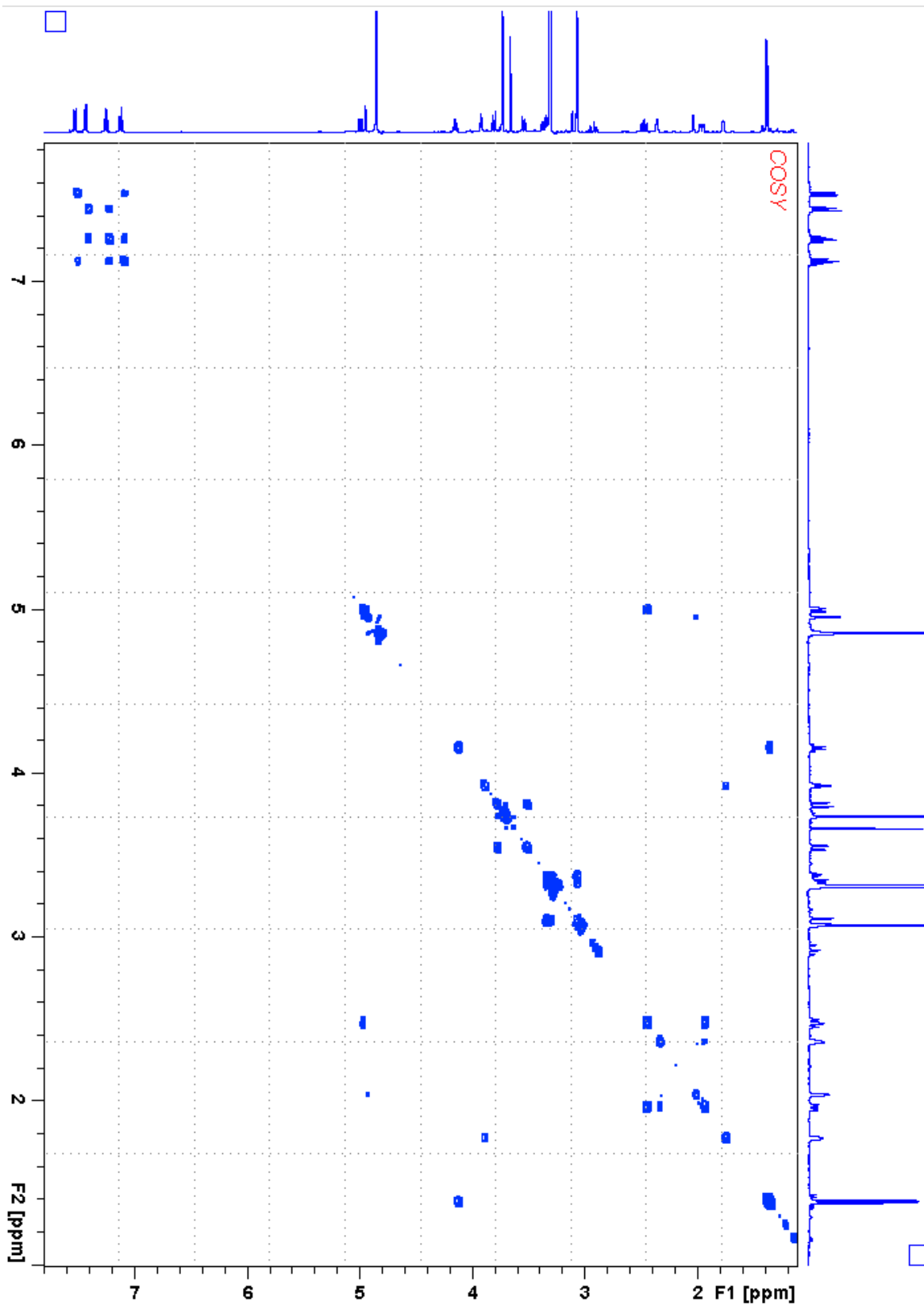
Figure 10. Comparison between the ^1H NMR spectra of natural¹² and synthetic N_4 -methyl talpinine **15**. (Note: The spectrum of natural N_4 -methyltalpinine is reused with permission from Elsevier, License no: 4467260919785, Nov 13, 2018)



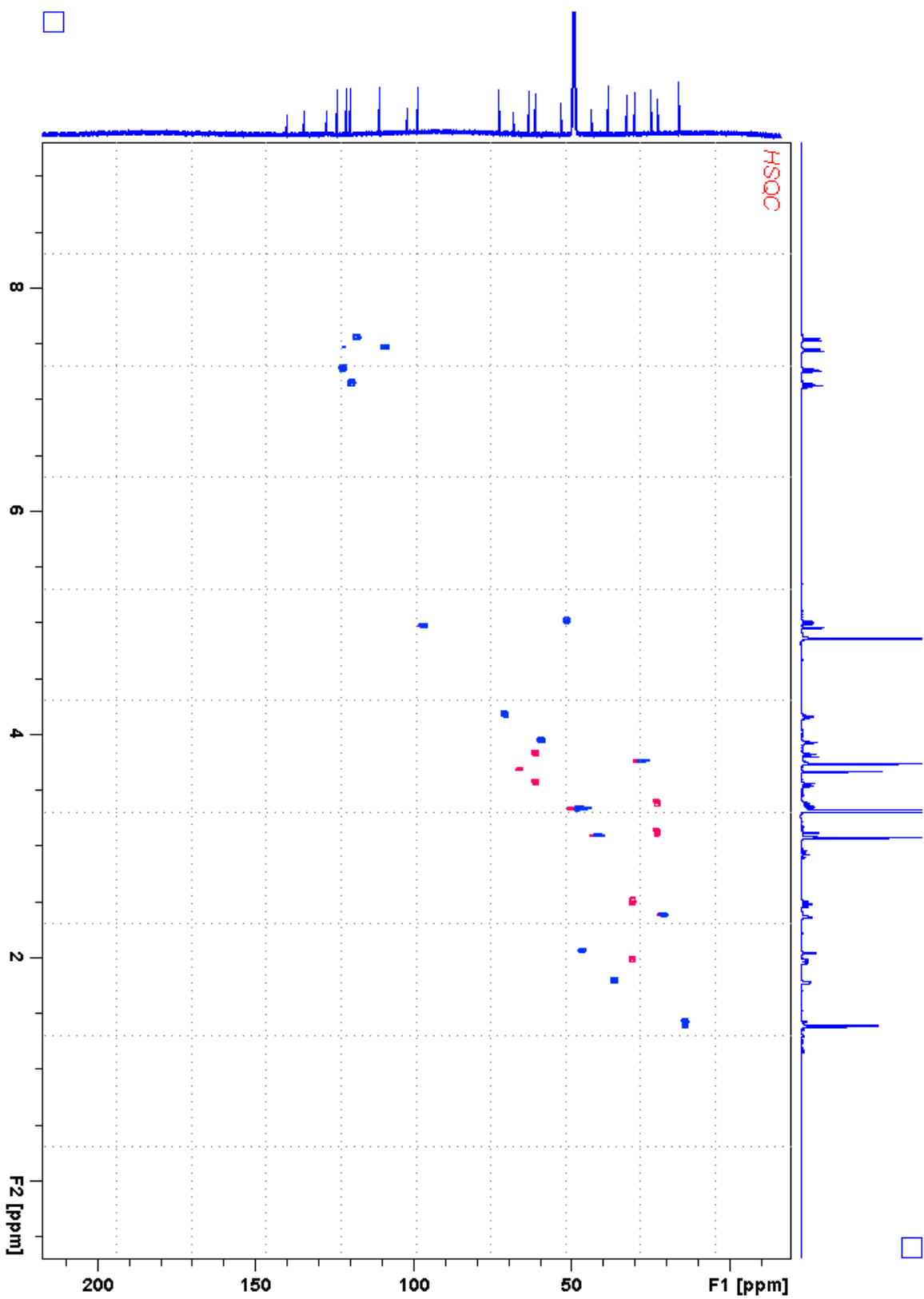
¹H NMR spectrum of synthetic *N*₄-methyltalpinine **15** (500 MHz, CD₃OD)



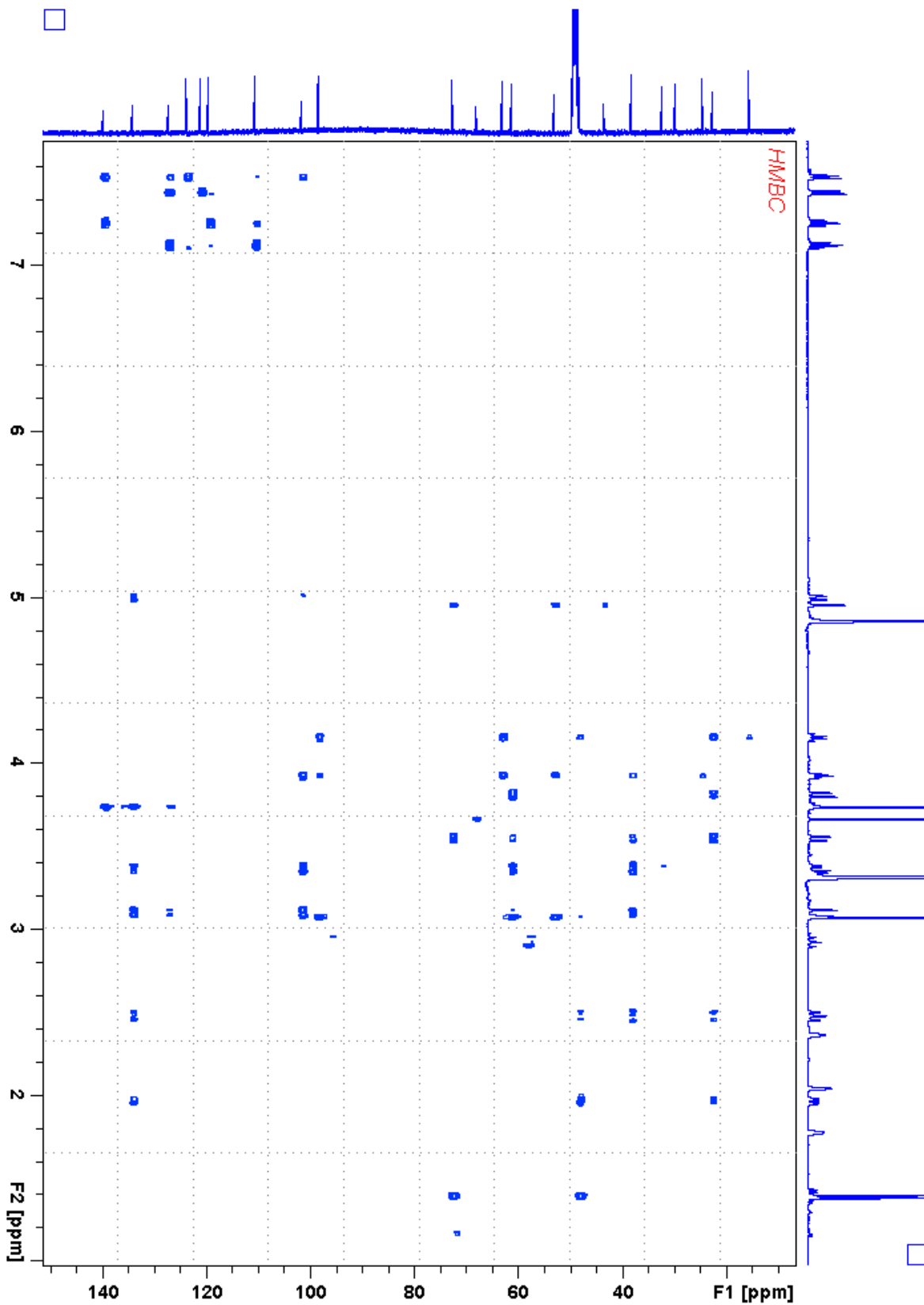
^{13}C NMR spectrum of synthetic N_4 -methyltalpinine **15** (125 MHz, CD_3OD)



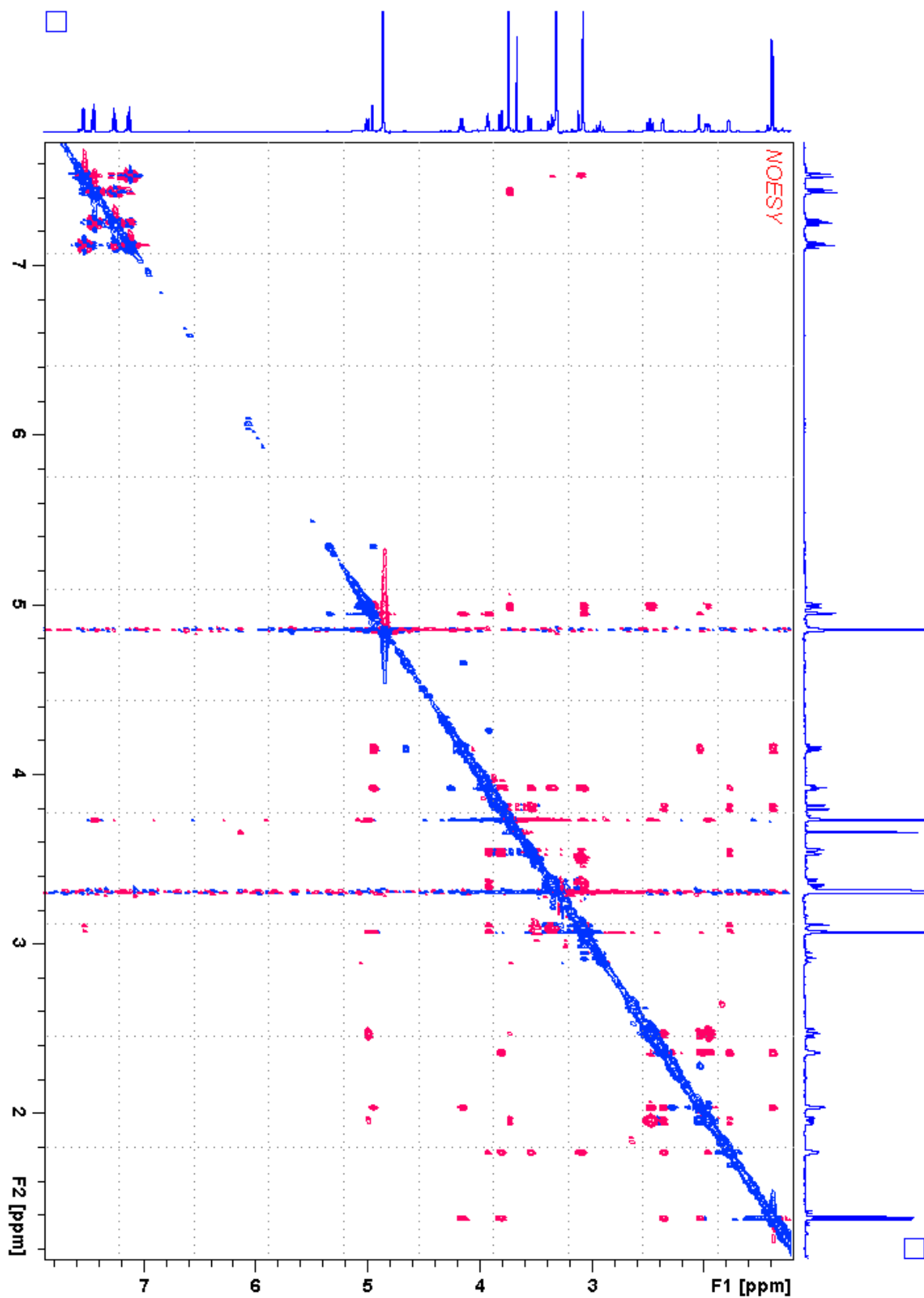
COSY NMR spectrum of synthetic N_4 -methyltalpinine **15** (500 MHz, CD_3OD)



HSQC NMR spectrum of synthetic *N*₄-methyltalpine **15** (500, 125 MHz, CD₃OD)



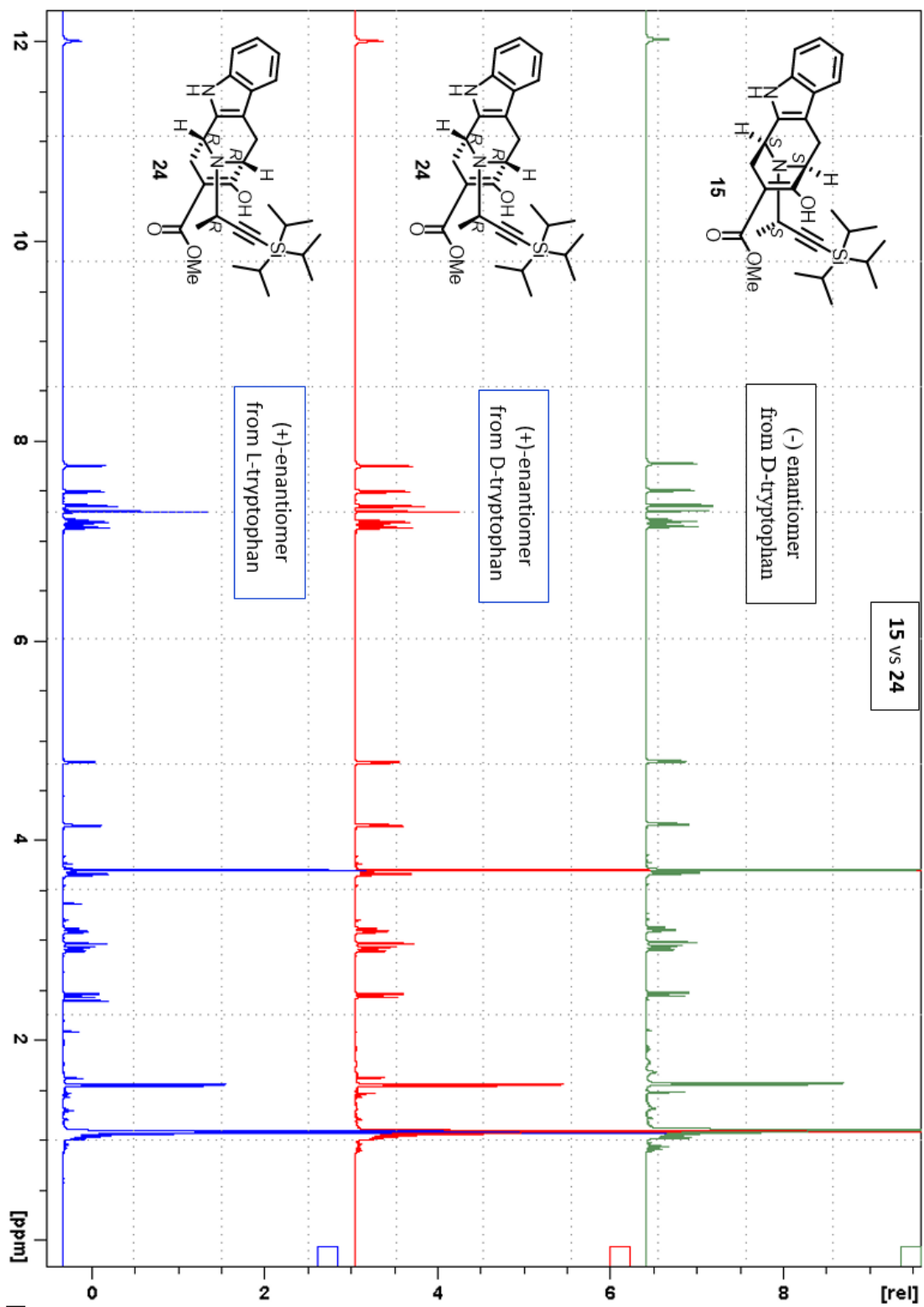
HMBC NMR spectrum of synthetic *N*₄-methyltalpinine **15** (500, 125 MHz, CD₃OD)



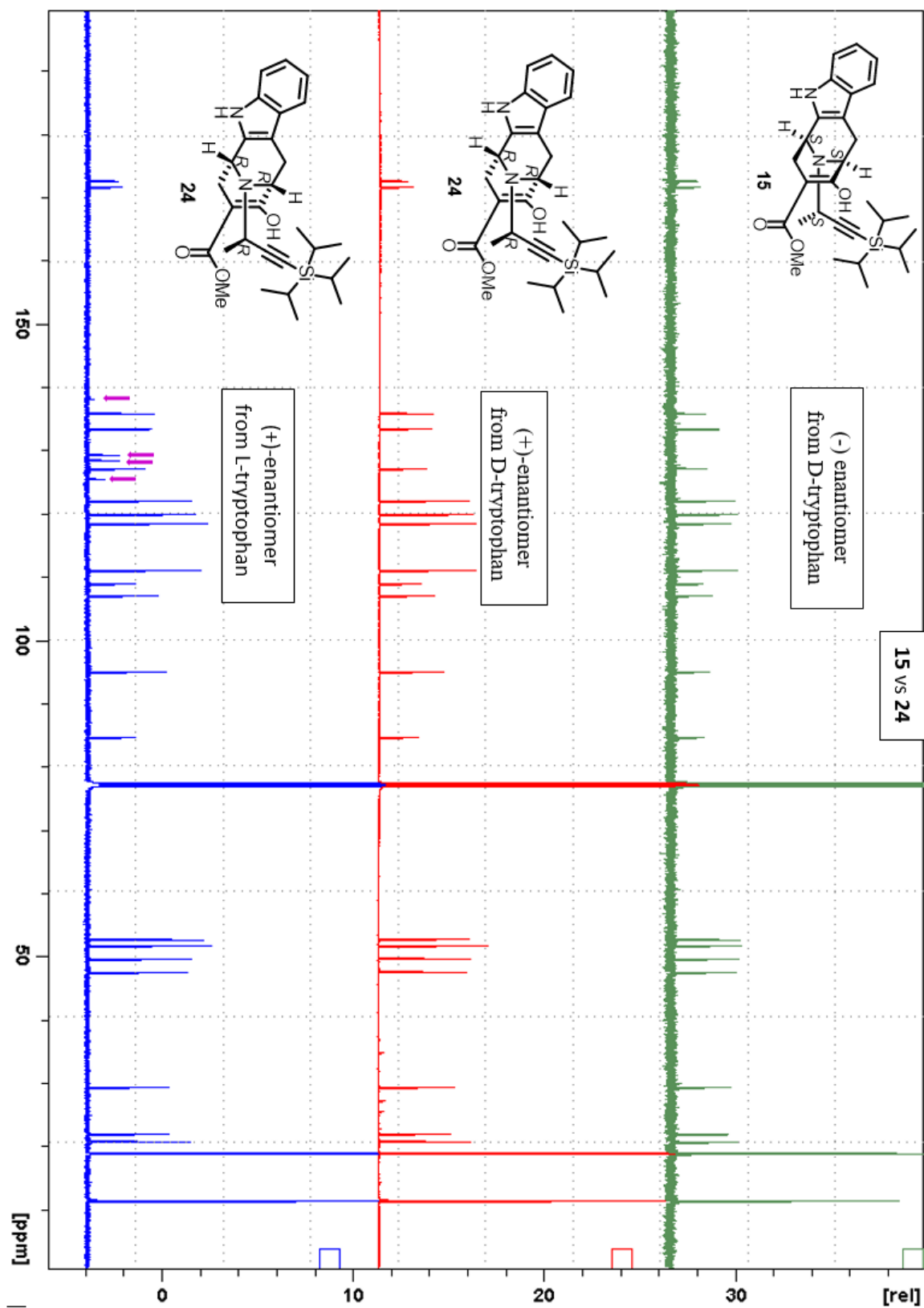
NOESY NMR spectrum of synthetic *N*₄-methyltalpinine **15** (500 MHz, CD₃OD)

IX Appendix G (Chapter 3)

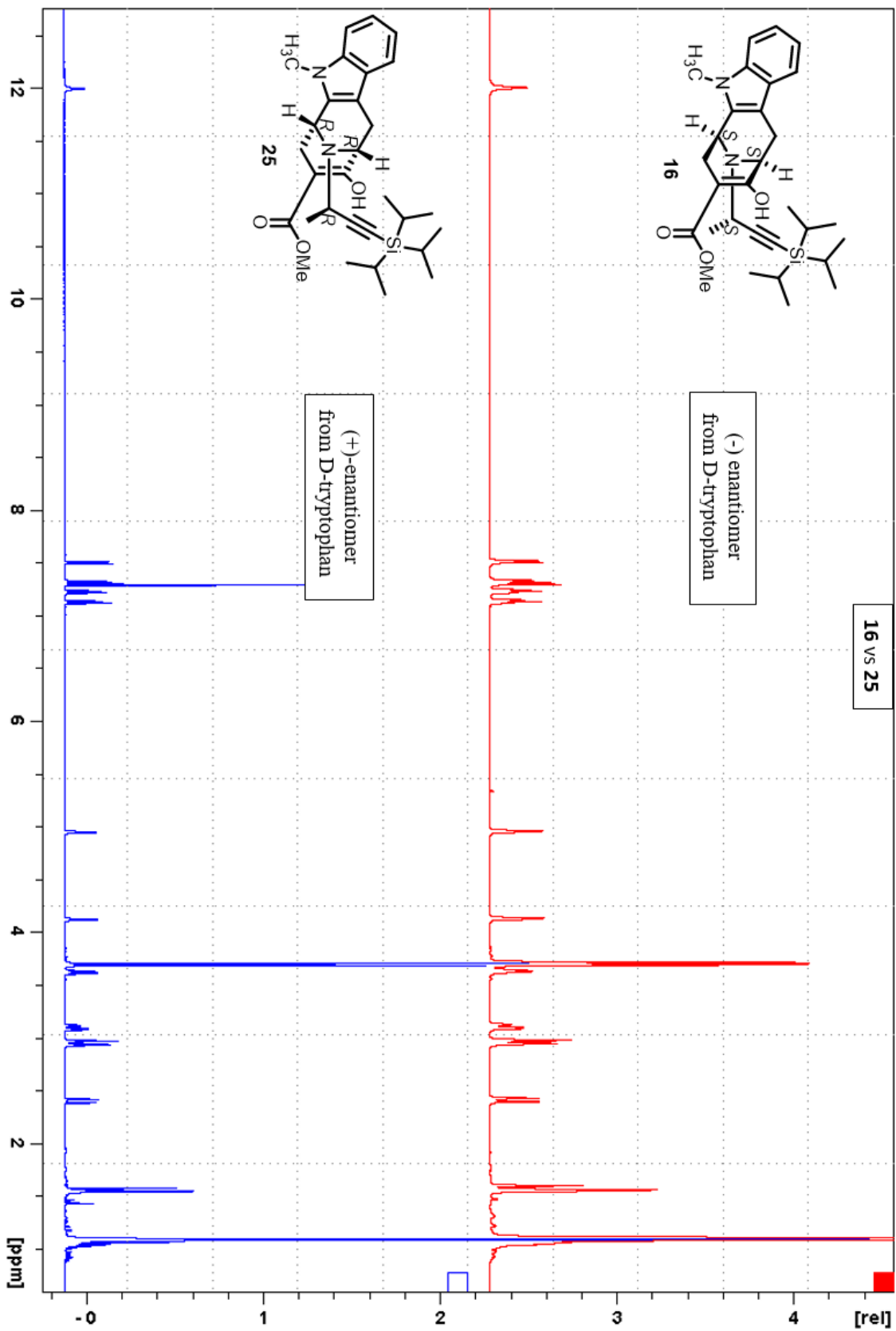
Comparisons between the NMR spectra of the enantiomeric pairs (**15 vs 24**), (**16 vs 25**), (**17 vs 26**), (**18 vs 27**), (**19 vs 29**), (**20 vs 28**), (**21 vs 30**), (**22 vs 31**), and (**23 vs 32**)



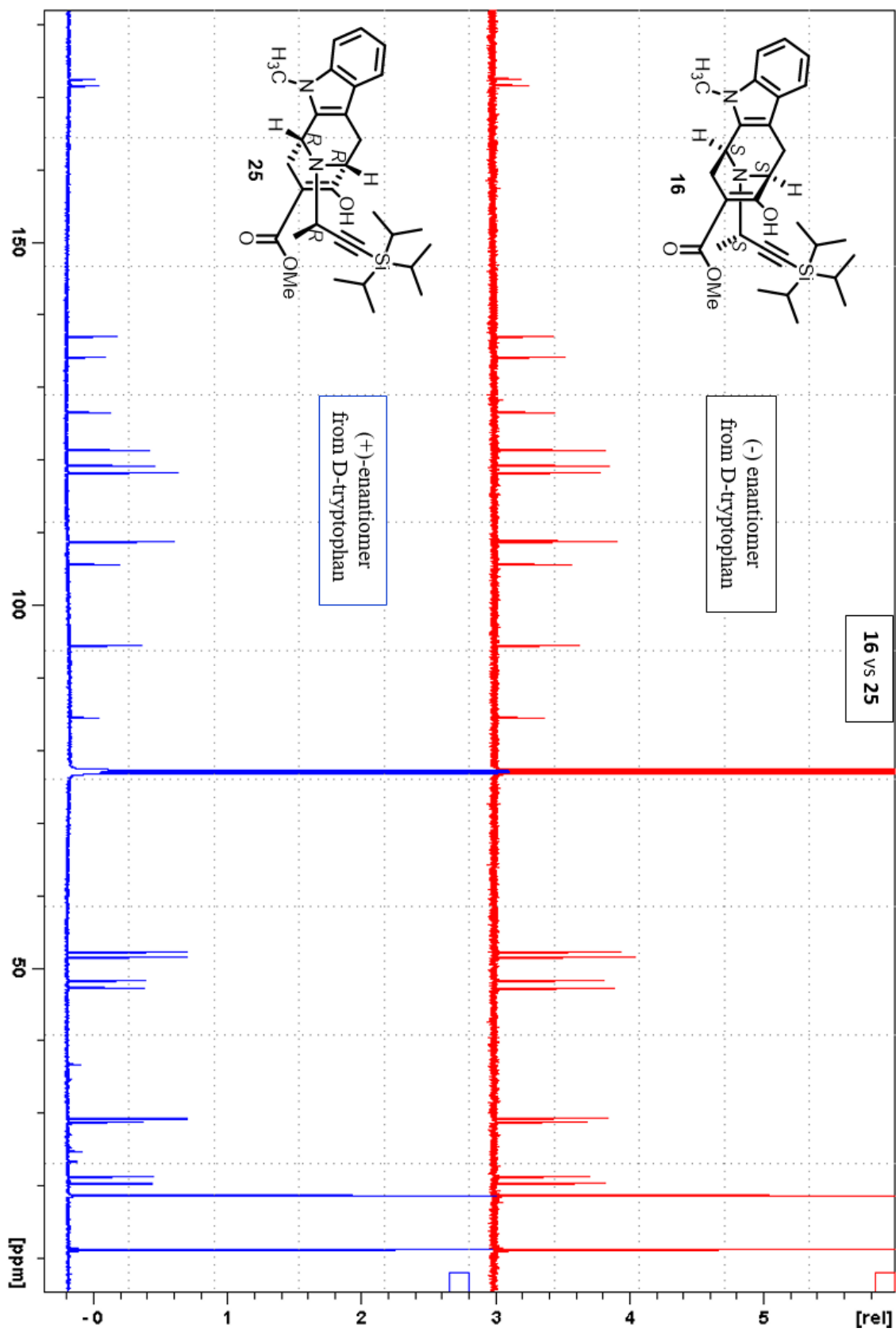
Comparison between the ¹H NMR spectra of (+)-**24** and (-)-**15** (500 MHz, CDCl₃)



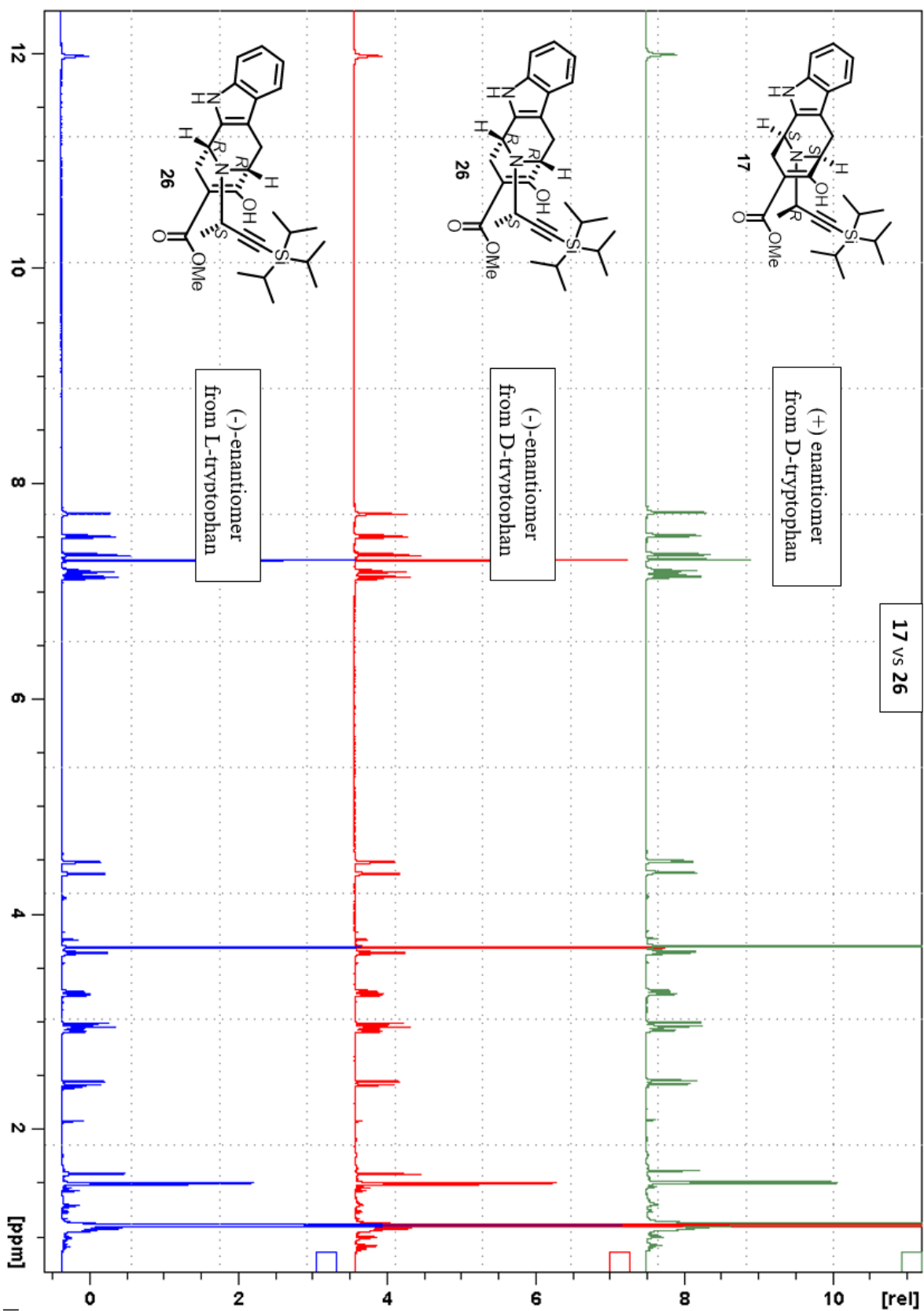
Comparison between the ^{13}C NMR spectra of (+)-**24** and (-)-**15** (125 MHz, CDCl_3) [marked peaks at δ 137.9, 129.1, 128.2, and 125.3 are from residual **toluene**]



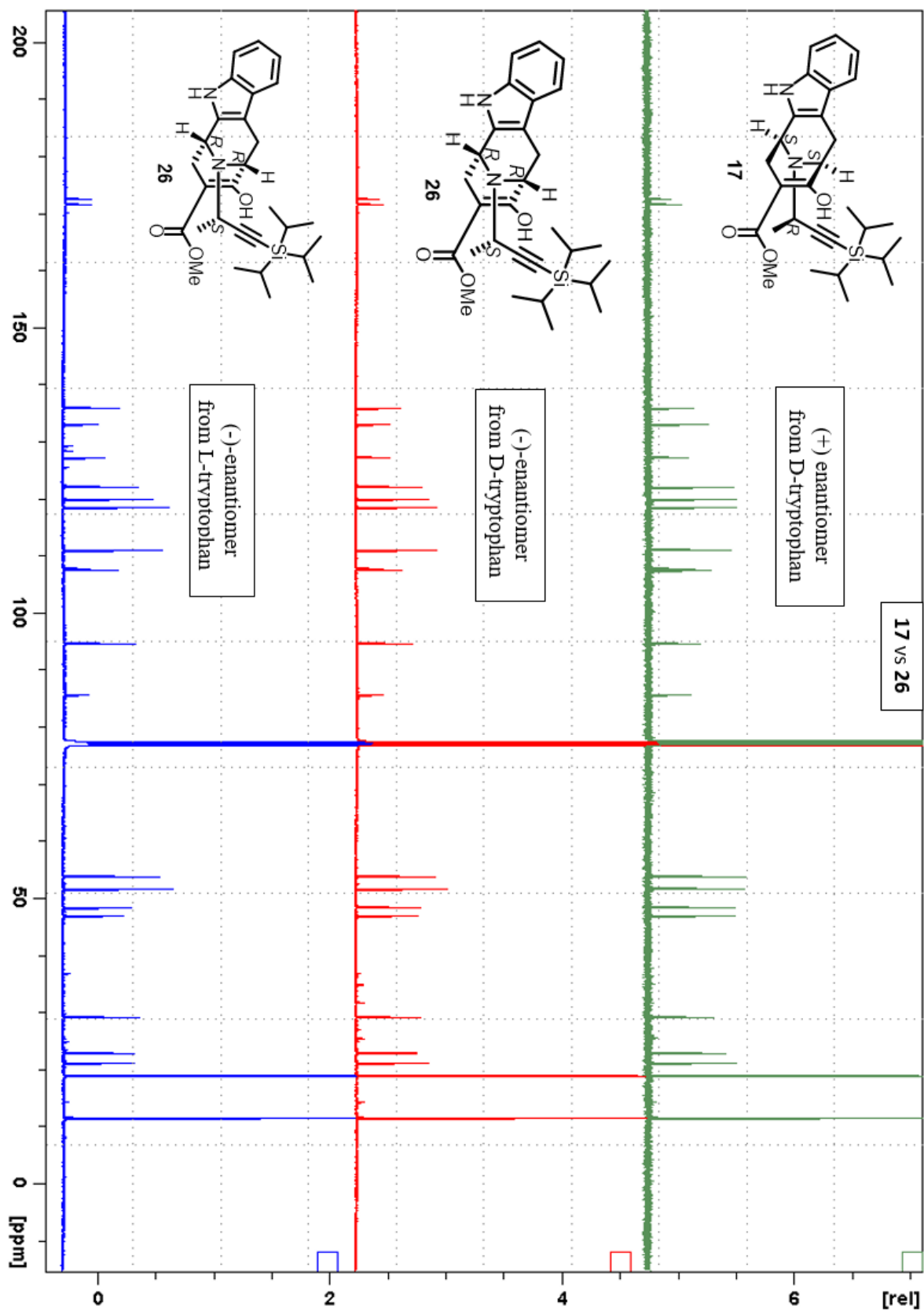
Comparison between the ^1H NMR spectra of (+)-**25** and (-)-**16** (500 MHz, CDCl_3)



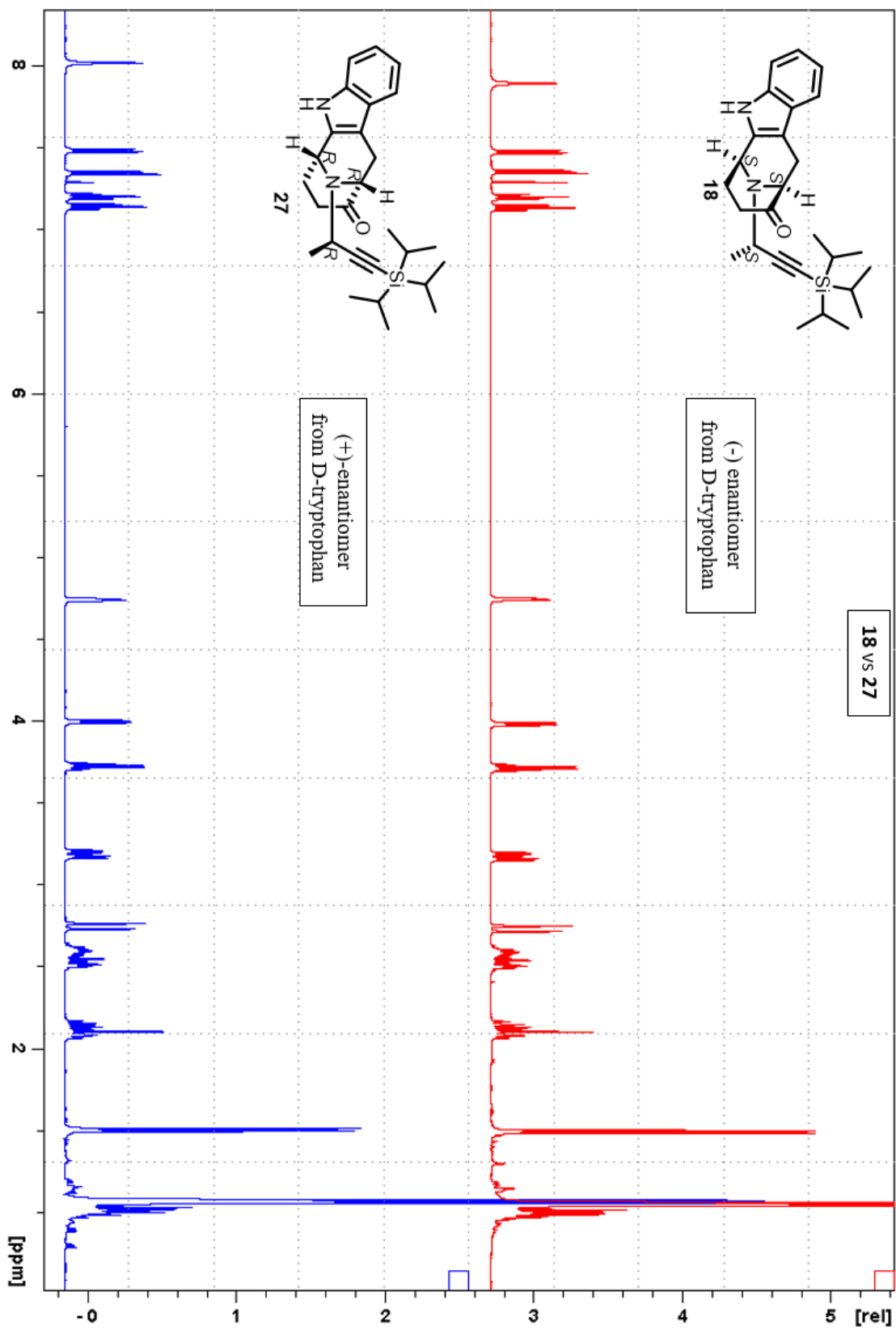
Comparison between the ^{13}C NMR spectra of (+)-**25** and (-)-**16** (125 MHz, CDCl_3)



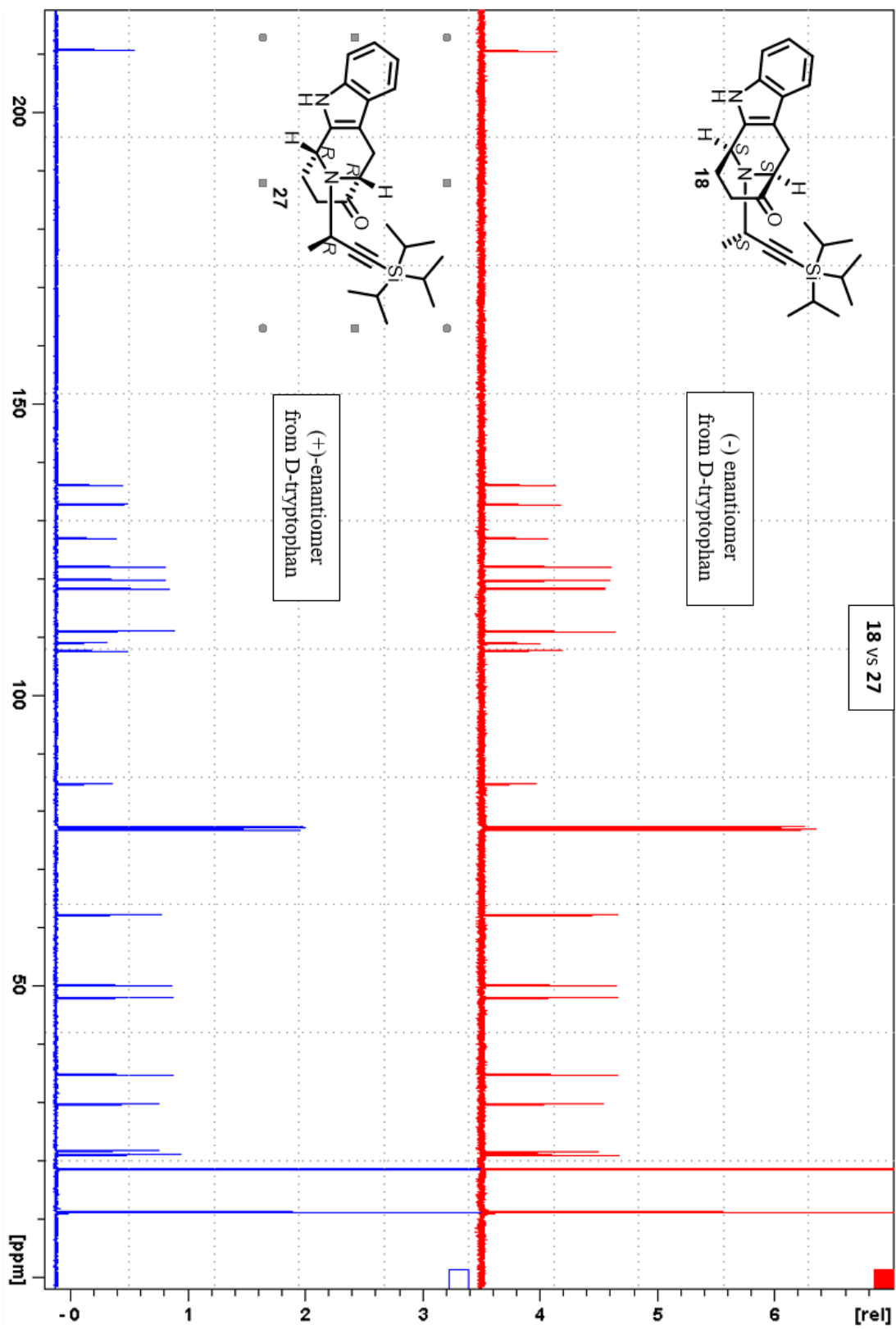
Comparison between the ¹H NMR spectra of (-)-26 and (+)-17 (500 MHz, CDCl₃)



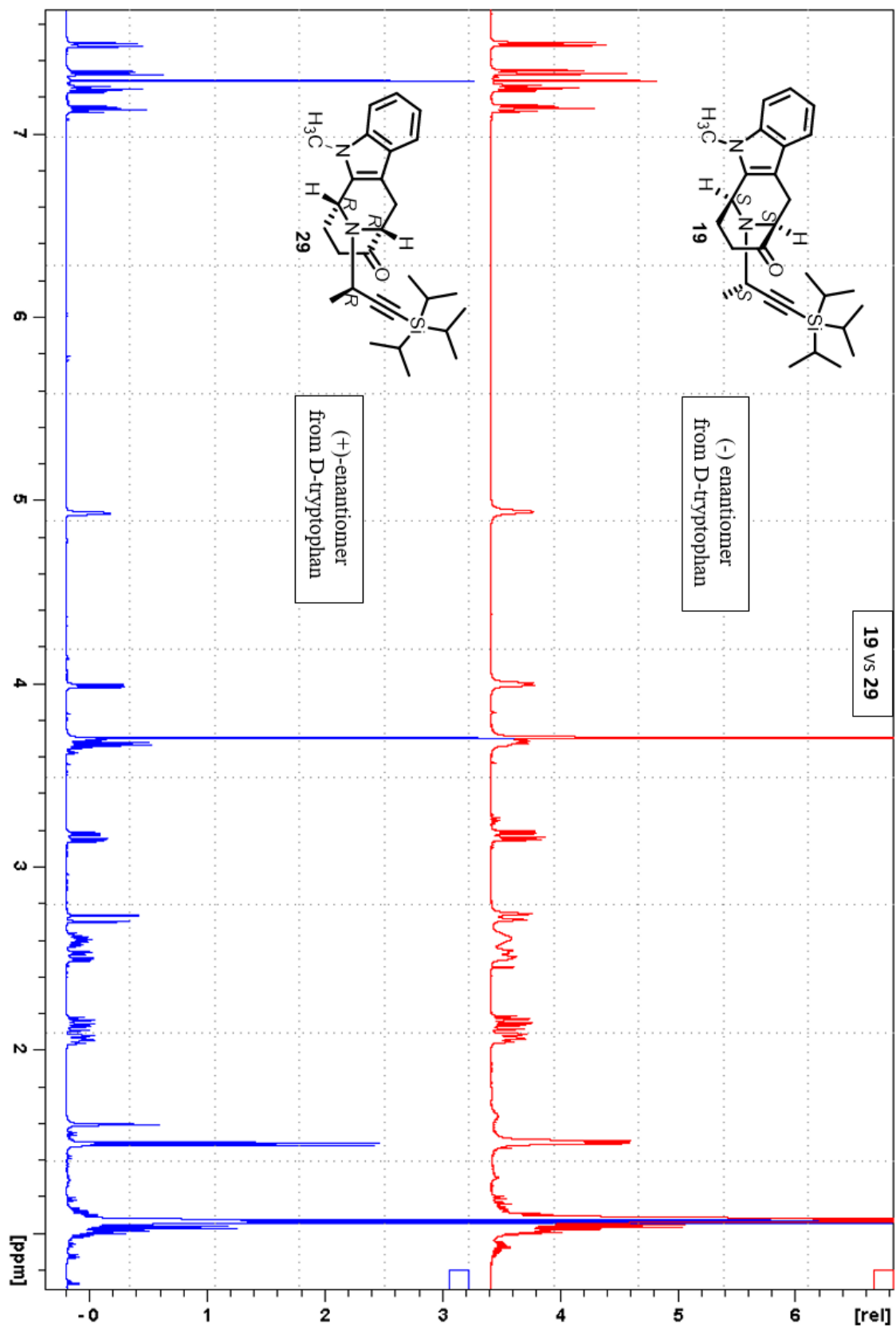
Comparison between the ^{13}C NMR spectra of (-)-26 and (+)-17 (125 MHz, CDCl_3)



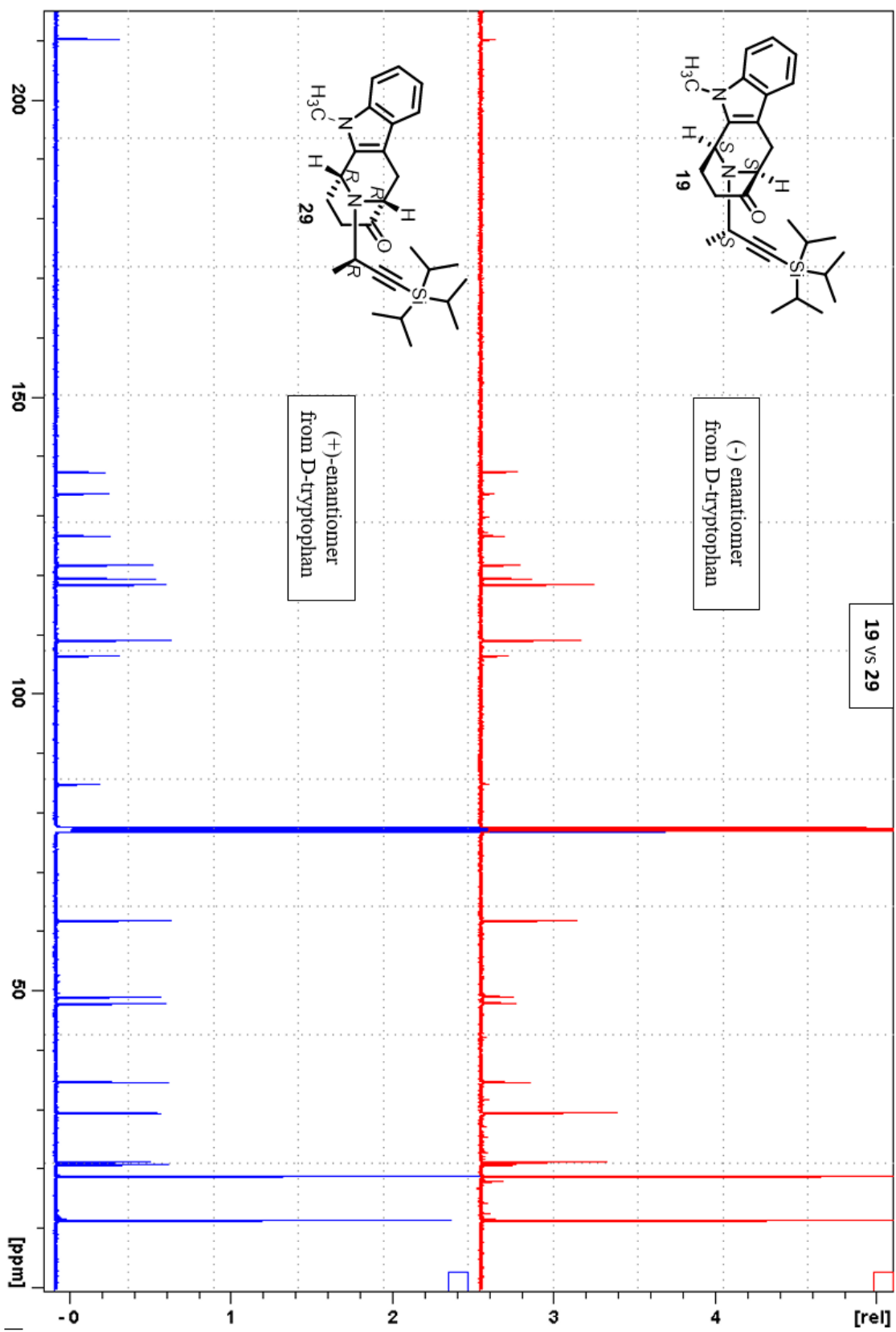
Comparison between the ¹H NMR spectra of (+)-27 and (-)-18 (500 MHz, CDCl₃)



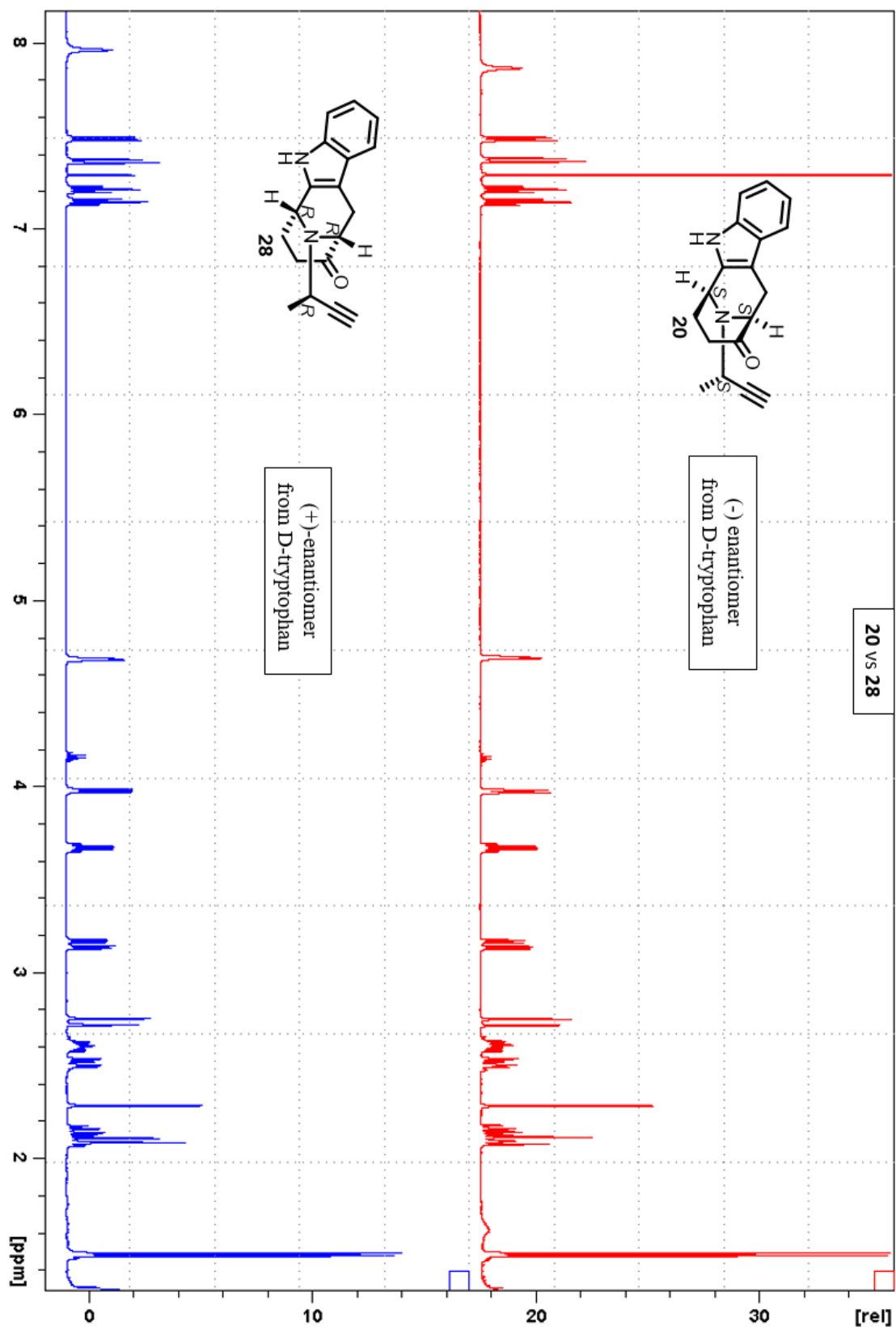
Comparison between the ^{13}C NMR spectra of (+)-**27** and (-)-**18** (125 MHz, CDCl_3)



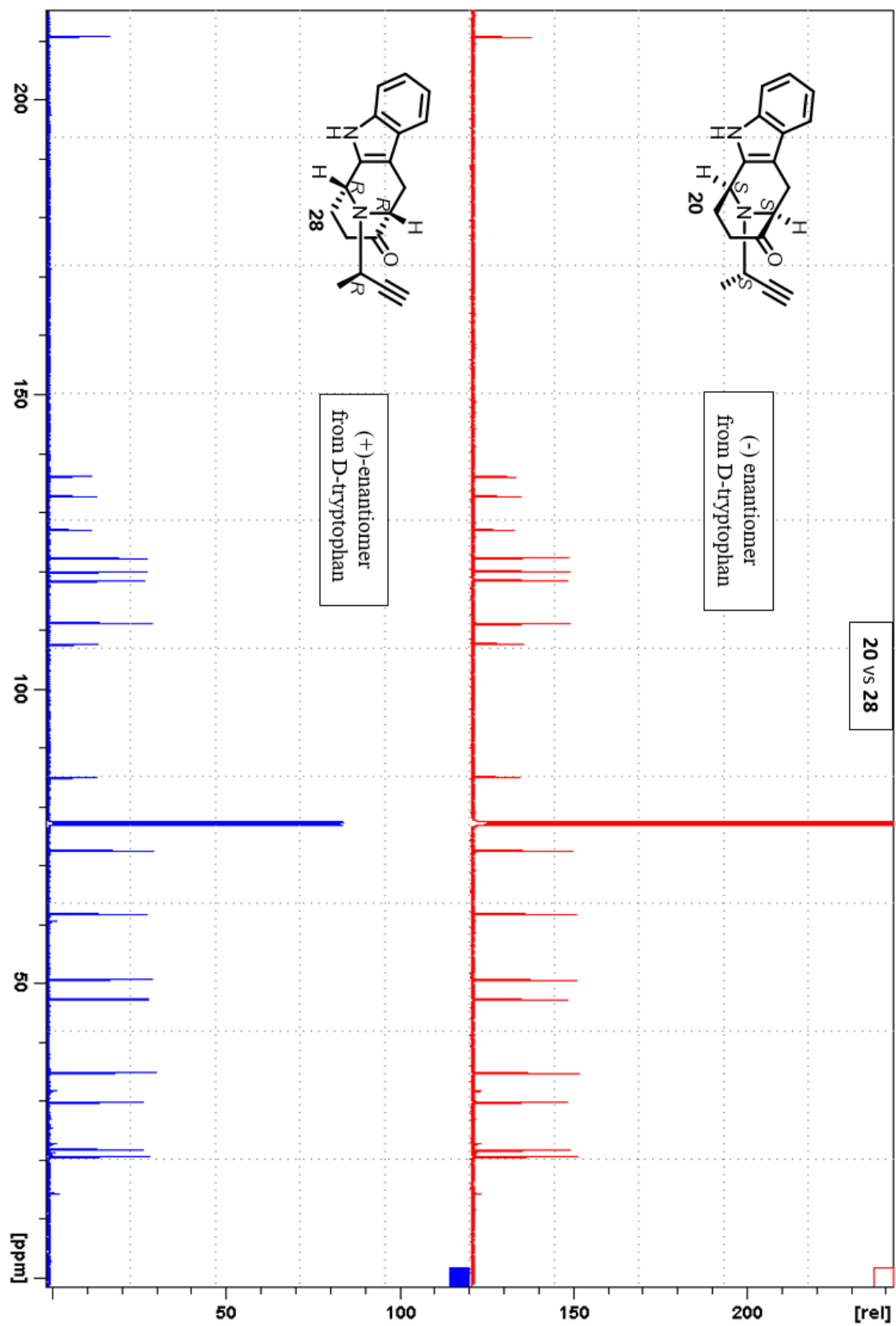
Comparison between the ^1H NMR spectra of (+)-**29** and (-)-**19** (500 MHz, CDCl_3)



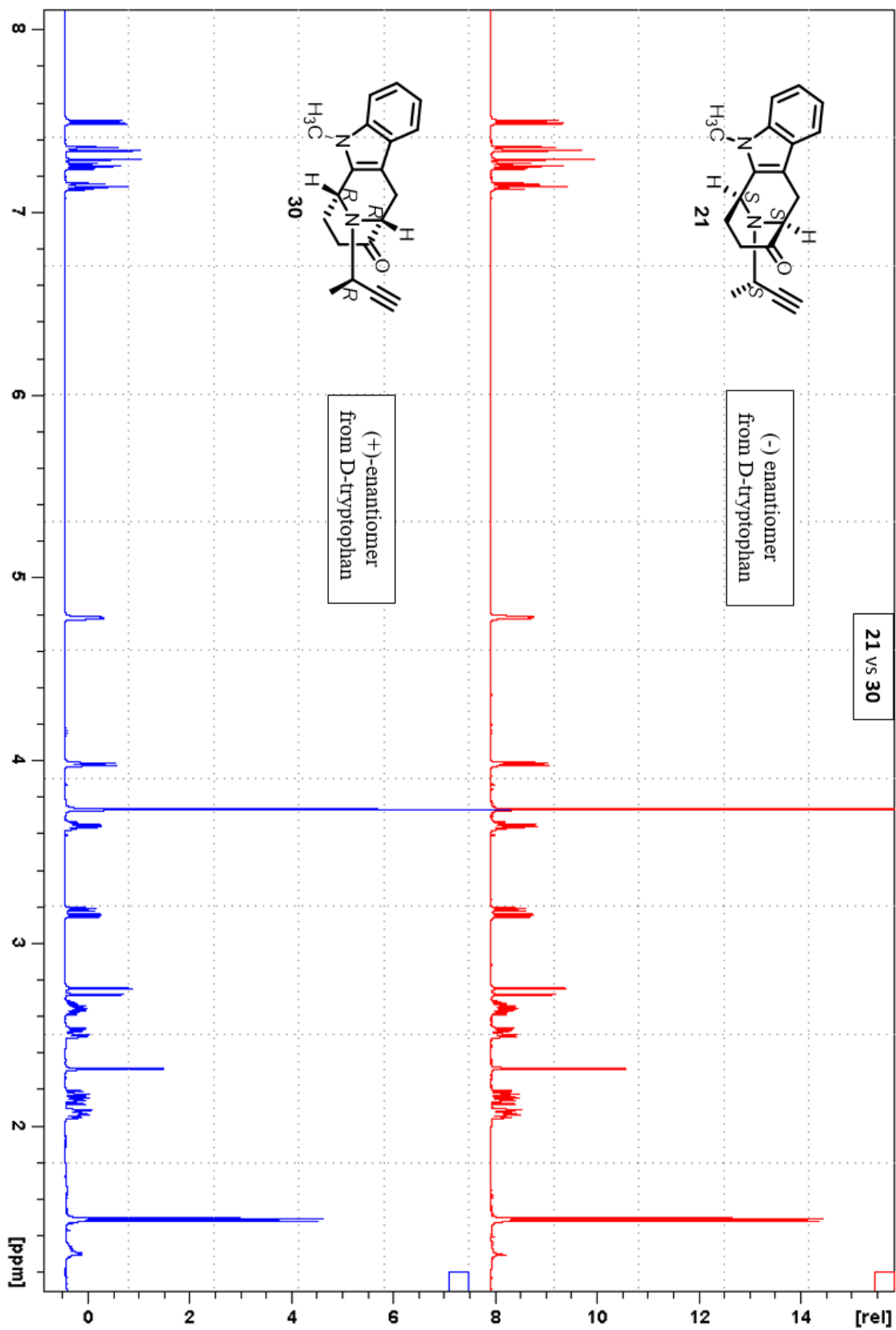
Comparison between the ^{13}C NMR spectra of (+)-**29** and (-)-**19** (125 MHz, CDCl_3)



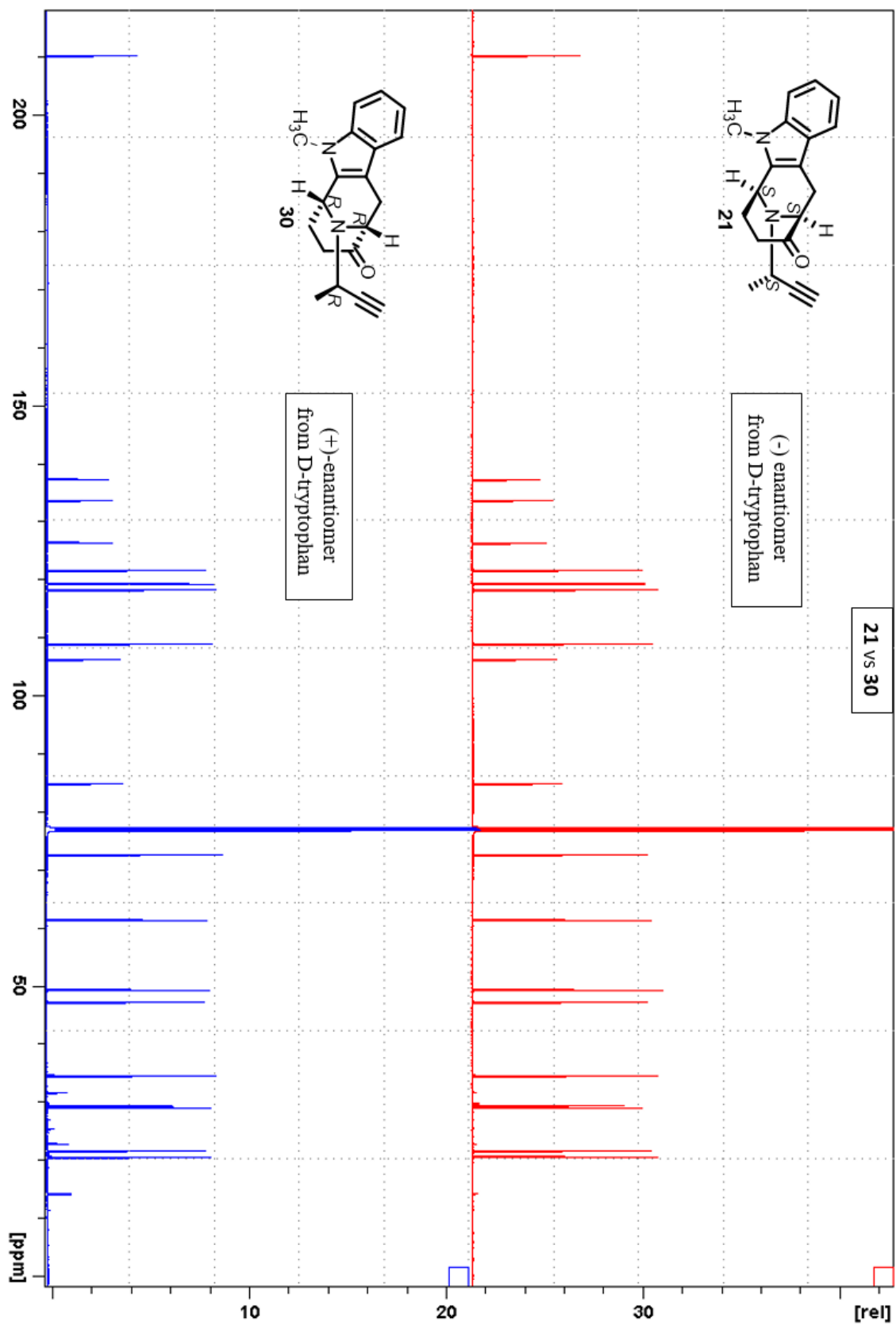
Comparison between the ¹H NMR spectra of (+)-28 and (-)-20 (500 MHz, CDCl₃)



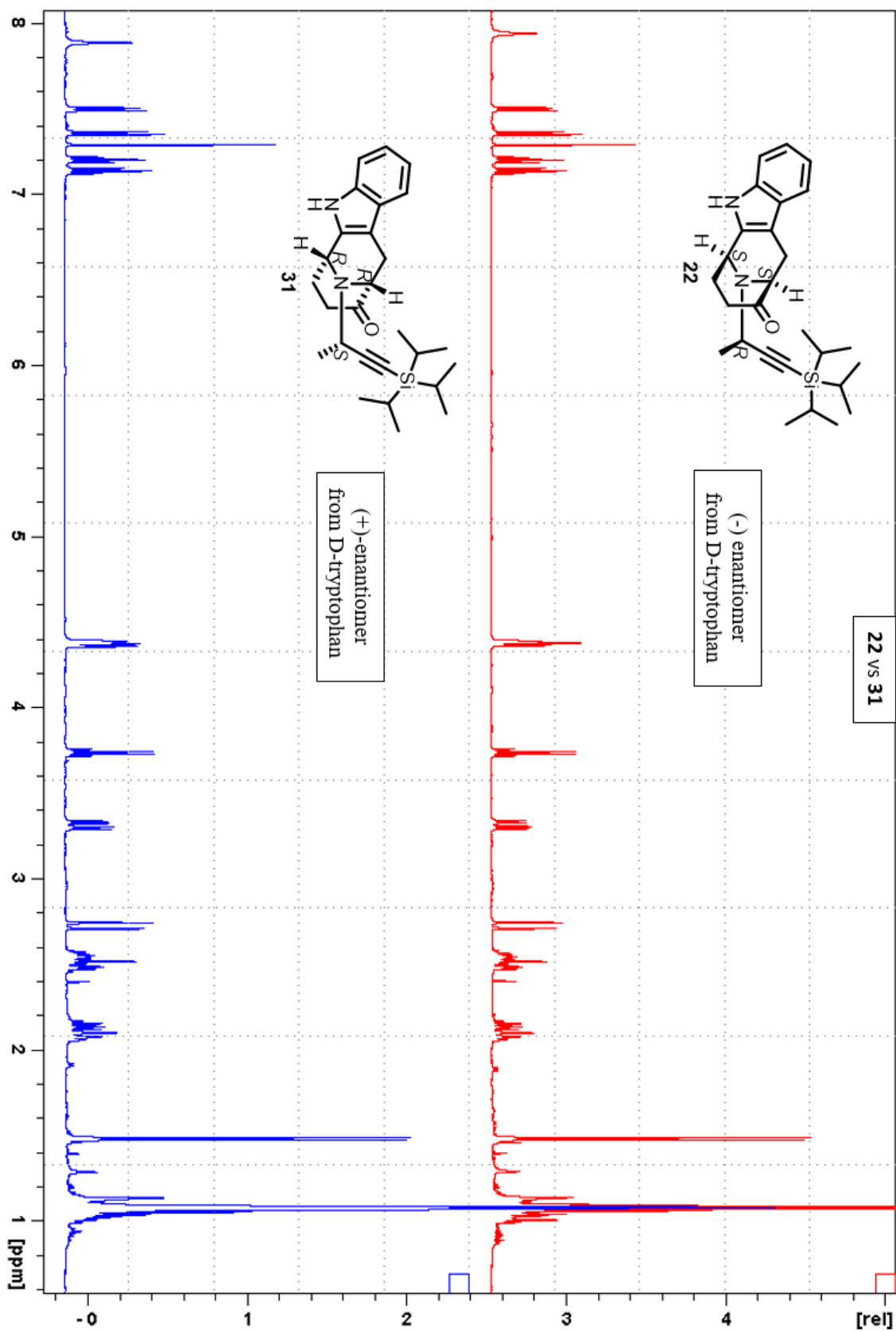
Comparison between the ^{13}C NMR spectra of (+)-**28** and (-)-**20** (125 MHz, CDCl_3)



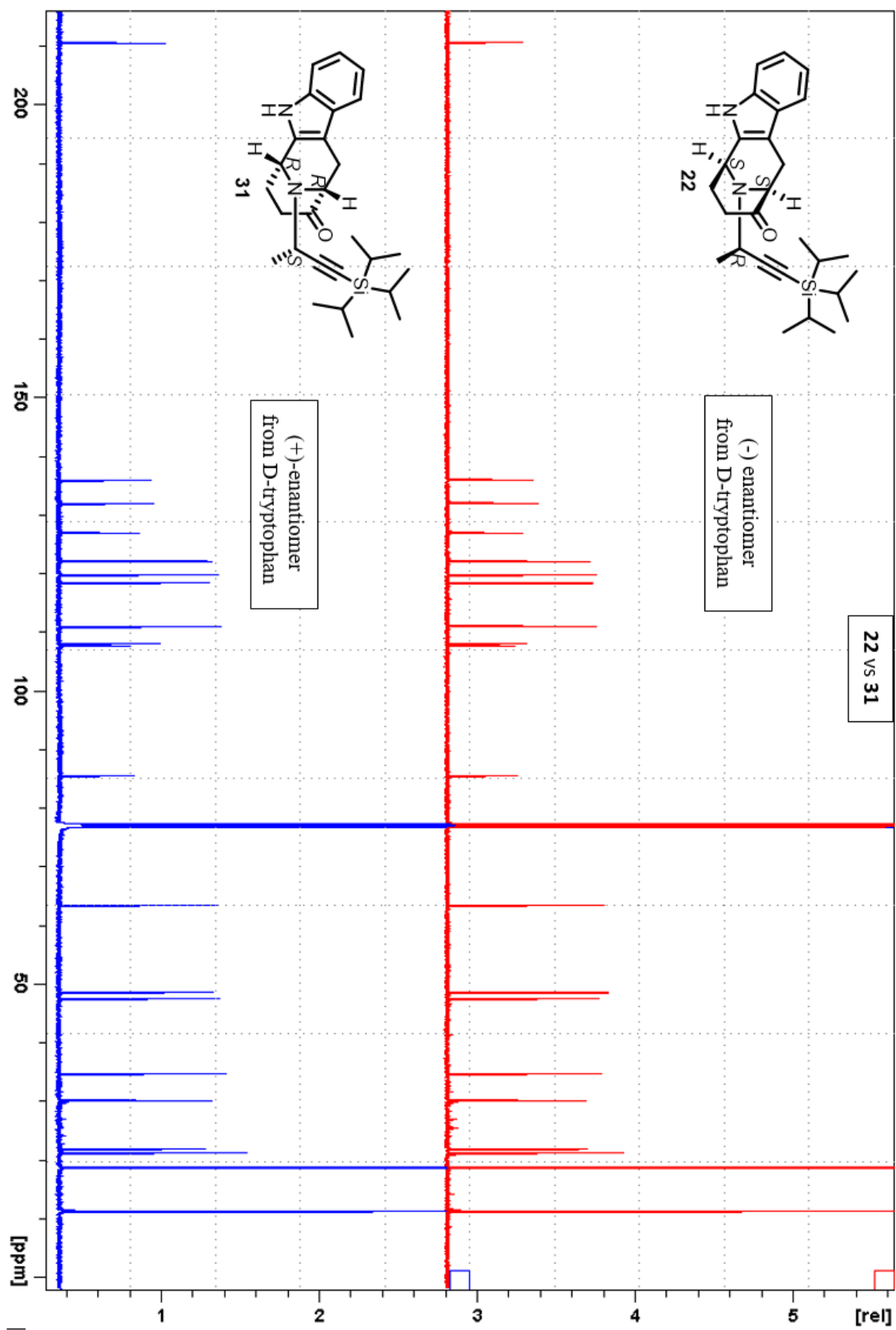
Comparison between the ¹H NMR spectra of (+)-**30** and (-)-**21** (500 MHz, CDCl₃)



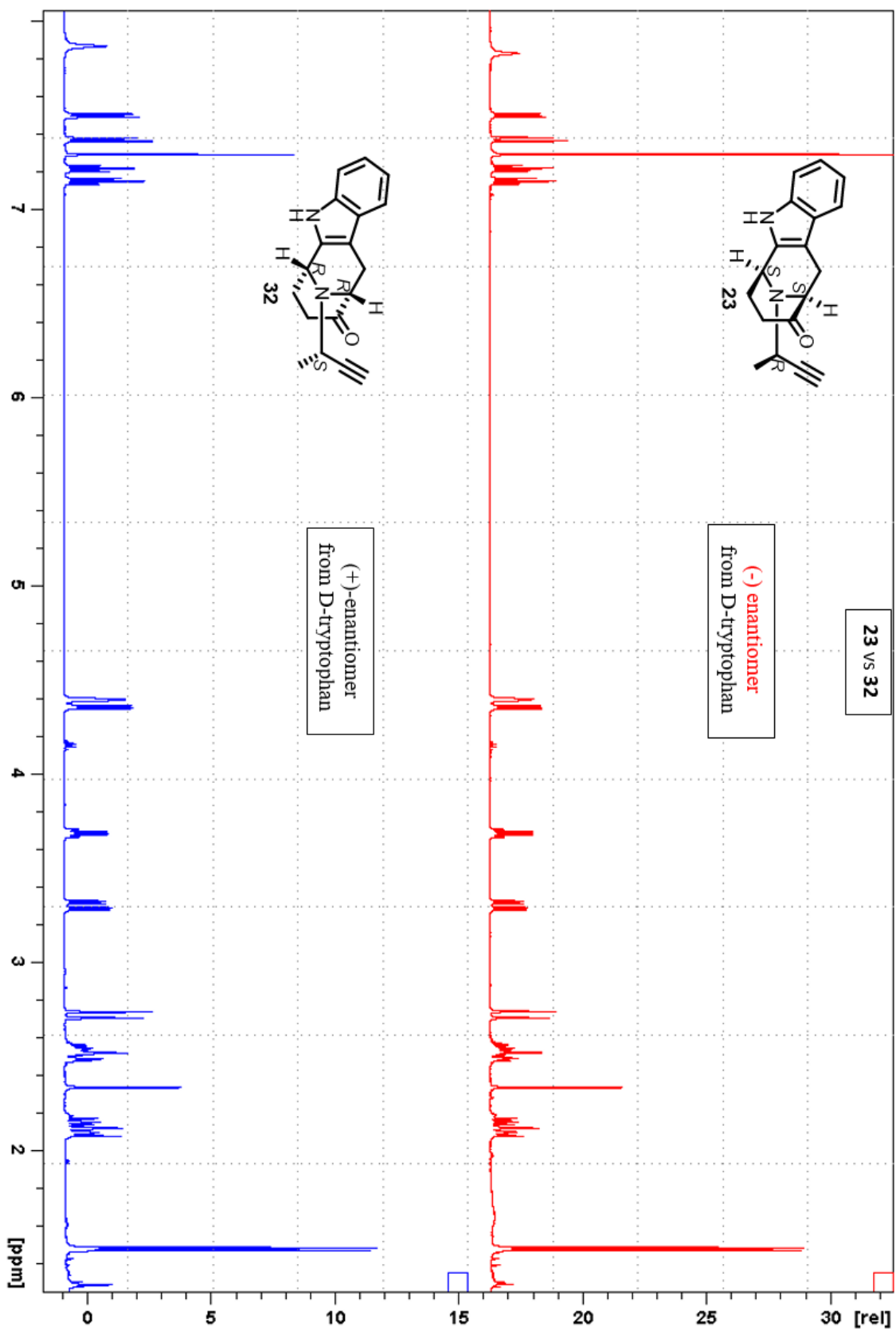
Comparison between the ^{13}C NMR spectra of (+)-**30** and (-)-**21** (125 MHz, CDCl_3)



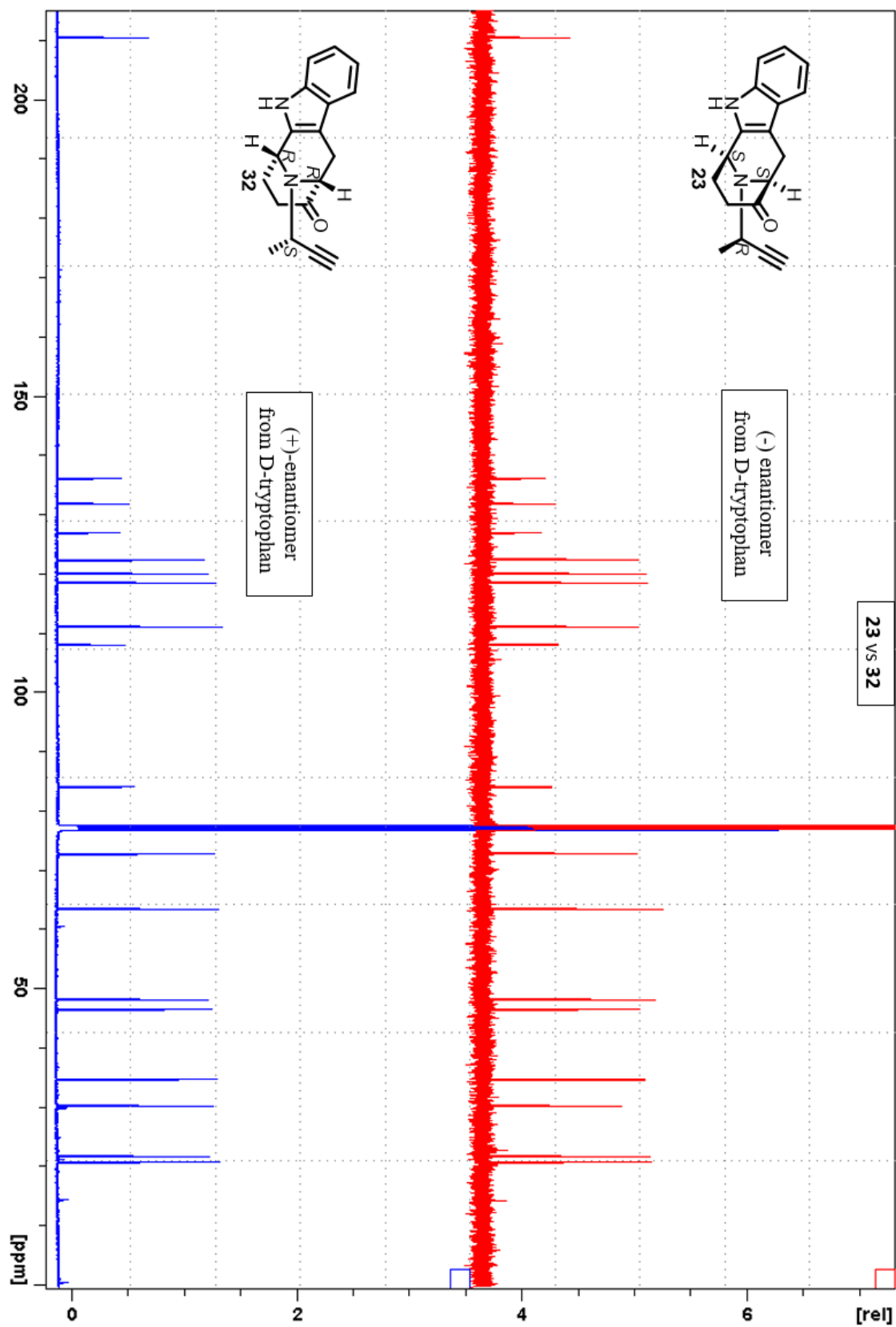
Comparison between the ^1H NMR spectra of (+)-**31** and (-)-**22** (500 MHz, CDCl_3)



Comparison between the ^{13}C NMR spectra of (+)-**31** and (-)-**22** (125 MHz, CDCl_3)



Comparison between the ^1H NMR spectra of (+)-**32** and (-)-**23** (500 MHz, CDCl_3)



Comparison between the ^{13}C NMR spectra of (+)-**32** and (-)-**23** (125 MHz, CDCl_3)

X. CURRICULUM VITAE

Md Toufiqur Rahman

Place of birth: Comilla, Bangladesh

Awards & Travel Grants

- Sosnovsky Award for Excellence in Graduate Research, Department of Chemistry and Biochemistry, UW-Milwaukee, **2018**
- Research Poster Competition Award, *34th H. C. Brown Lectures in Organic Chemistry*, Purdue University, West Lafayette, IN, **April 2017**
- Chemistry Alumni Research Poster Award (UWM Foundation Inc.), *UWM Department of Chemistry & Biochemistry, Awards Day and Symposium*, **2018**
- Chemistry Alumni Research Poster Award (UWM Foundation Inc.), *UWM Department of Chemistry & Biochemistry, Awards Day and Symposium*, **2016**
- Research Poster Prize-3rd Place, 2nd BACABANA Convention, Milwaukee, WI, **2018**
- *Sweden Bangladesh Trust Fund* (Ministry of Education, Bangladesh, **2013**)
- *Chemistry and Biochemistry Graduate Student Council @UWM* Travel Grant, **Spring 2016**
- *UWM Graduate School* Travel Grant (**Spring 2015, Spring 2016, and Spring 2017**)
- *UWM Department of Chemistry and Biochemistry* Travel Grant (**Spring 2015**)
- *Mentoring Travel Award* (**Spring 2016 and Spring 2017**)
- *ACS-Milwaukee* Travel Grant (**Spring 2017**)
- *Chancellor's Graduate Student Award* (received every semester appointed as a TA from 2011-2016)

Education

- **PhD, Organic Chemistry**, University of Wisconsin-Milwaukee (UWM), Milwaukee, WI December, 2018

Advisor: Professor Dr. James M. Cook, FRSC

Dissertation Title:

Part I: “Shorter and Improved Access to the Key Tetracyclic Core of C-19 Methyl Substituted Bioactive Sarpagine-Macroline-Ajmaline Indole Alkaloids via a New Ambidextrous Asymmetric Pictet-Spengler Reaction Beginning from Either D-(+)- or L-(-)-Tryptophan”

Part II: “The Total Synthesis of a Number of Bioactive C-19 Methyl Substituted Macroline-Sarpagine Indole Alkaloids Including Macrocarpines A-G, Talcarpine, *N*(4)-Methyl-*N*(4),21-Secotalpinine, Deoxyperaksine, Dihydroperaksine, Talpinine, *O*-Acetyltalpinine, as well as *N*(4)-Methyltalpinine”

- **MS, Physical Chemistry**, University of Dhaka (DU), Dhaka, Bangladesh 2011
Result: First Class
- **BSc (Honors), Chemistry**, DU, Dhaka, Bangladesh 2009
Result: First Class

Teaching Experience

- University of Wisconsin-Milwaukee: Teaching Assistant: Fall 2011 (General Chem.), Spring 2012 (General Chem.), Fall 2012 (Organic Lab), Spring 2013 (Intro. Biochemistry), Spring 2014 (Intro. Biochemistry), Fall 2017 (Organic Lab), and Spring 2018 (Organic Lab); Research assistant 2014-2017.

Leadership Experience

- *Vice President*, UWM Bangladesh Student Association (BSA) 2015-2017
- *Graduate Student Ambassador*, UWM Research Foundation 2017-2018
- *Peer Mentor*, Department of Chemistry & Biochemistry, UWM 2016 & 2017
- *Founding Member and Elected Organizational Secretary*, Bangladesh Chemical and Biochemical Association in North America (BACABANA) 2016-Present

Professional Affiliations

- American Chemical Society (ACS) 2014- present
- Division of Organic Chemistry (ACS) 2016-Present
- Division of Medicinal Chemistry (ACS) 2018-Present
- American Association for the Advancement of Science (AAAS) 2017-present
- International Society of Heterocyclic Chemistry (ISHC) 2018-present
- Bangladesh Chemical and Biochemical Association in North America (BACABANA) 2016-present

Publications

Papers

- **Rahman, M. T.** and Cook, J. M. “Unprecedented stereocontrol in the synthesis of 1,2,3-trisubstituted tetrahydro- β -carbolines through an asymmetric Pictet-Spengler reaction towards sarpagine-type indole alkaloids” *Eur. J. Org. Chem.* **2018**, 3224-3229. *Very Important Paper*; DOI: <https://doi.org/10.1002/ejoc.201800600>
- **Rahman, M. T.**; Deschamps, J. R.; Imler, G. H.; Cook, J. M., “Total Synthesis of Sarpagine-Related Bioactive Indole Alkaloids” *Chem. Eur. J.* **2018**, 24, 2354-2359. DOI: <https://doi.org/10.1002/chem.201705575>.

- **Rahman, M. T.**; Deschamps, J.; Imler, G. H.; Schwabacher, A.; Cook, J. M., “Total Synthesis of Macropines D and E via an Enolate-Driven Copper-Mediated Cross-Coupling Process: Replacement of Catalytic Palladium with Copper Iodide” *Org. Lett.*, **2016**, *18* (17), pp 4174–4177. DOI: <http://10.1021/acs.orglett.6b01526>
- **Rahman, M. T.**; Tiruveedhula, V. V. N. P. B.; Cook, J. M., “Synthesis of Bisindole Alkaloids from the Apocynaceae Which Contain a Macropine or Sarpagine Unit: A Review” *Molecules*, **2016**, *21*(11), 1525. DOI: 10.3390/molecules21111525
- Stephen, M. R.; **Rahman, M. T.**; Tiruveedhula, V. V. N. P. B.; Fonseca, G. O.; Deschamps, J. R.; Cook, J. M., “Concise Total Synthesis of (–)-Affinisine Oxindole, (+)-Isoalstonisine, (+)-Alstofoline, (–)-Macrogentine, (+)-Na-Demethylalstonisine, (–)-Alstonoxine A, and (+)-Alstonisine” *Chem. Eur. J.* **2017**, *23*, 15805. DOI: <https://doi.org/10.1002/chem.201703572>.
- Zu, N. Z.; Ernst, M.; Trevern, M.; Crene, R.; Wakulchik, M.; Li, X.; Jones, T., M.; Gleason, S. D.; Morrow, D.; Schkeryantz, J. M.; **Rahman, M. T.**; Li, G.; Poe, M. M.; Cook, J. M.; Witkin, J. M., Negative allosteric modulation of alpha 5-containing GABAA receptors engenders antidepressant-like effects and selectively prevents age-associated hyperactivity in tau-depositing mice” *Psychopharmacology*, **2018**, *235*, 1151-1161. DOI: <https://doi.org/10.1007/s00213-018-4832-9>
- K. R. Methuku, X. Li, R. Cerne, S. D. Gleason¹, J. M. Schkeryantz, V. V. N. P. B. Tiruveedhula, L. Golani and G. Li, M.M. Poe, **Md. T. Rahman**, J. M. Cook, J. L.

- Fisher, and J. M. Witkin “An Antidepressant-Related Pharmacological Signature for Positive Allosteric Modulators of $\alpha_{2/3}$ -Containing GABA_A Receptors” *Pharmacol. Biochem. Behav.* **2018**, *170*, 9-13. DOI: <https://doi.org/10.1016/j.pbb.2018.04.009>
- Schwam, W. R.; Polanowski, R.; Dunman, P. M.; Medina-Bielski, S.; Lane, M.; Rott, M.; Lipker, L.; Wescott, A.; Monte, A.; Cook, J. M.; Baumann, D. D.; Tiruveedhula, V. V. N.; Witzigmann, C. M.; Mikel, C.; **Rahman, M. T.**, *Antibiotics*, **2017**, *6* (3), 17. DOI: [10.3390/antibiotics6030017](https://doi.org/10.3390/antibiotics6030017)
 - Hossain, M. U.; **Rahman, M. T.**; Ehsan, M. Q.; “Simultaneous Detection and Estimation of Catechol, Hydroquinone, and Resorcinol in Binary and Ternary Mixtures Using Electrochemical Techniques” *Int. J. Anal. Chem.* Vol 2015 (2015), Article ID 862979, 8 pages. DOI: <http://dx.doi.org/10.1155/2015/862979>
 - **Rahman, M. T.**; Hossain, M. U.; Ehsan, M. Q.; “Electrochemical Behaviour of Dihydroxybenzene Isomers at Glassy Carbon Electrode in Different Electrolytic Media” *J. Bangladesh Acad. Sci.*, **2015**, *39*(2), 135-146. DOI: <http://dx.doi.org/10.3329/jbas.v39i2.25947>
 - **Rahman, M. T.**; Hossain, M. E.; Ehsan, M. Q.; “Spectrophotometric and cyclic voltammetric study of interaction of Fe (iii) with vitamin B3 and vitamin B6” *J. Bangladesh Acad. Sci.*, **2014**, *38*(2), 143-153, DOI: <http://dx.doi.org/10.3329/jbas.v38i2.21339>

- Cassie M. Chandler, Jaren Reeves-Darby, Sherman A. Jones, Guanguan Li, **Md T. Rahman**, James M. Cook, Donna M. Platt "Inverse agonists selective for GABAA receptors containing the $\alpha 5$ subunit attenuate alcohol cue-induced reinstatement and active alcohol self-administration in rats" *Psychopharmacology*, **2018** (Under review)
- Cassie M. Chandler, Jaren Reeves-Darby, Sherman A. Jones, Guanguan Li, **Md T. Rahman**, James M. Cook, Donna M. Platt "Modulation of relapse-like drinking in rats by ligands targeting the $\alpha 5$ GABAA receptor" *Alcoholism: Clinical and Experimental Research*, Submitted
- **Rahman, M. T.**; Cook, J. M.; "The Ambidextrous Pictet-Spengler Reaction: Access to the (+)- or (-)-enantiomers of the Bioactive C-19 Methyl Substituted Sarpagine/-Macroline/Ajmaline Alkaloids from Either D- or L-Tryptophan" (Submitted: *Synthesis*, Nov 2018)

Book Chapter

- **Rahman, M.T.**; Cook, J. M. *In Studies in Natural Products Chemistry* (Bioactive Natural Products); Prof. Atta-ur-Rahman, FRS, Ed.; Elsevier Science Publishers: The Netherlands. (In press)

Contribution Acknowledged

- "Sarpagine and Related Alkaloids," O. Namjoshi; J.M. Cook, in "The Alkaloids," Volume 76, Hans-Joachim Knölker, Editor, Elsevier, N.Y. pp. 64-171 (2016)

Conference Proceedings, Oral, and Posters Presentations

- **Rahman, M. T.**, “Total Synthesis of Sarpagine-Related Bioactive Indole Alkaloids”
Oral presentation at *Nobel Graduate Seminar*, arranged by Milwaukee Institute for Drug Discovery (MIDD) on the occasion of 2016 Chemistry **Nobel Laureate Professor Bernard L. Feringa**’s visit to The UWM Chemistry Department, September, 2017.
- **Rahman, M. T.**; Deschamps, J.R.; Cook, J.M. General strategy for the total synthesis of C-19 methyl substituted sarpagine/macroline indole alkaloids including macrocarpines A-G, peraksine, and dihydroperaksine. **Oral Presentation** (ORGN 654), 253rd ACS National Meeting, San Francisco, CA, April 2017.
- **Rahman, M. T.**; Deschamps, J. R.; Cook, J. M., General Strategy for the Total Synthesis of C-19 Methyl Substituted Sarpagine/Macroline Indole Alkaloids, Poster Presentation, (Poster # 50), **34th H. C. Brown Lectures in Organic Chemistry**, Department of Chemistry, Purdue University, April, 2017.
- **Cook, J. M.**; **Rahman, M. T.**; Proceedings of the 27th Mona Symposium, University of the West Indies, Mona, Kingston, Jamaica, January 8-11, 2018.
- **Cook, J. M.**; **Rahman, M. T.**; Proceedings of the 26th Mona Symposium, Jan 4-7, 2016. University of West Indies, Mona Campus, Jamaica, (Short Paper #1)
- **Cook, J. M.**; **Rahman, M. T.** Proceedings of the Florida Heterocyclic & Synthetic Conference (FloHet 2016), February 2016.
- **Rahman, M. T.**; Deschamps, J. R.; Cook, J. M. 5th ICBS Conference, Madison, WI, October 24-26, 2016 (Poster Presentation, Poster Number 108)

- **Rahman, M. T.**; Deschamps, J. R.; Cook, J. M. 251st ACS National Meeting and Exposition, San Diego, CA, March 13-17, 2016 (Poster Presentation, ORGN 206)
- **Rahman, M. T.**; Deschamps, J. R.; Cook, J. M. 249th ACS National Meeting and Exposition, Denver, CO, March 22-26, 2015 (Poster presentation, ORGN 164)
- **Rahman, M. T.**; Deschamps, J. R.; Cook, J. M. Poster presentation at ACS Milwaukee Meeting, Carrol University, WI, March 31, 2016.
- **Rahman, M. T.**; Deschamps, J. R.; Cook, J. M. Poster Presentation at UWM Department of Chemistry and Biochemistry Awards Day and Symposium, Milwaukee, WI, May 21, 2016.
- **Rahman, M. T.**; Deschamps, J. R.; Cook, J. M. Poster Presentation at UWM Graduate Student Research Symposium, Milwaukee, WI, October 28, 2016.
- Pareek, T.; Overton, J. S.; Rowlett, J. K.; **Rahman, M. T.**; Cook, J. M.; Platt, D. M. CPDD 2019, San Antonio, TX, Abstract 361, Jun 2019.

Major: Organic Chemistry

Minor: Biochemistry